Topics in Stereochemistry, Volume 21

Editors
Ernest L. Eliel
Samuel H. Wilen

JOHN WILEY & SONS

TOPICS IN STEREOCHEMISTRY

VOLUME 21

ADVISORY BOARD

STEPHEN J. ANGYAL, *University of New South Wales, Sydney, Australia*

ALAN R. BATTERSBY, *Cambridge University, Cambridge, England*

GIANCARLO BERTI, *University of Pisa, Pisa, Italy*

F. ALBERT COTTON, *Texas A & M University, College Station, Texas*

JOHANNES DALE, *University of Oslo, Oslo, Norway*

DAVID A. EVANS, *Harvard University, Cambridge, Massachusetts*

MEIR LAHAV, *The Weizmann Institute of Science, Rehovoth, Israel*

JEAN-MARIE LEHN, *Collège de France, Paris, France*

MARIAN MIKOŁAJCZYK, *Centre of Molecular and Macromolecular Studies, Polish Academy of Sciences, Łódź, Poland*

KURT MISLOW, *Princeton University, Princeton, New Jersey*

MICHINORI ŌKI, *Okayama University of Science, Okayama, Japan*

VLADIMIR PRELOG, *Eidgenössische Technische Hochschule, Zurich, Switzerland*

JOHN B. STOTHERS, *University of Western Ontario, London, Ontario, Canada*

HANS WYNBERG, *University of Groningen, Groningen, The Netherlands*

NIKOLAI S. ZEFIROV, *Moscow State University, Moscow, Russia*

TOPICS IN

STEREOCHEMISTRY

EDITORS

ERNEST L. ELIEL
Professor of Chemistry, Emeritus
University of North Carolina
Chapel Hill, North Carolina

SAMUEL H. WILEN
Professor of Chemistry
City College, City University of New York
New York, New York

VOLUME 21



AN INTERSCIENCE® PUBLICATION
John Wiley & Sons, Inc.
NEW YORK / CHICHESTER / BRISBANE / TORONTO / SINGAPORE

This text is printed on acid-free paper.

An Interscience® Publication

Copyright © 1994 by John Wiley & Sons, Inc.

All rights reserved. Published simultaneously in Canada.

Reproduction or translation of any part of this work beyond that permitted by Section 107 or 108 of the 1976 United States Copyright Act without the permission of the copyright owner is unlawful. Requests for permission or further information should be addressed to the Permissions Department, John Wiley & Sons, Inc., 605 Third Avenue, New York, NY 10158-0012.

Library of Congress Catalog Card Number: 67-13943

ISBN 0-471-52120-5

Printed in the United States of America

10 9 8 7 6 5 4 3 2 1

To the memory of
Günther Snatzke

INTRODUCTION TO THE SERIES

It is patently impossible for any individual to read enough of the journal literature so as to be aware of all significant developments that may impinge on his or her work, particularly in an area such as stereochemistry, which knows no topical boundaries. Stereochemical investigations may have relevance to an understanding of a wide range of phenomena and findings irrespective of their provenance. Because stereochemistry is important in many areas of chemistry, comprehensive reviews of high quality play a special role in educating and alerting the chemical community to new stereochemical developments.

The above considerations were reason enough for initiating a series such as this. In addition of updating information found in such standard monographs as *Stereochemistry of Carbon Compounds* (Eliel, McGraw-Hill, 1962) and *Conformational Analysis* (Eliel, Allinger, Angyal, and Morrison, Interscience, 1965; reprinted by American Chemical Society, 1981) as well as others published more recently, the series is intended also to deal in greater detail with some of the topics summarized in such texts. It is for this reason that we have selected the title *Topics in Stereochemistry* for this series.

The series is intended for the advanced student, the teacher, and the active researcher. A background of the basic knowledge in the field of stereochemistry is assumed. Each chapter is written by an expert in the field and, hopefully, covers its subject in depth. We have tried to choose topics of fundamental importance aimed primarily at an audience of inorganic and organic chemists. Yet, many of these topics are concerned with basic principles of physical chemistry and some deal with stereochemical aspects of biochemistry as well.

We are fortunate in having been able to secure the help of an international board of editorial advisors who have been of great assistance by suggesting topics and authors for several chapters and by helping us avoid, insofar as possible, duplication of topics appearing in other, related monograph series. We are grateful to the editorial advisors for this assistance, but the editors and authors alone must assume the responsibility for any shortcomings of *Topics in Stereochemistry*.

E. L. ELIEL
S. H. WILEN

PREFACE

The first of the five chapters in this volume, by E. Vedejs and E. J. Peterson, is concerned with the stereochemistry and mechanism of the Wittig reaction. An earlier chapter on the Wittig reaction, by M. Schlosser, appeared in Volume 5 of this series, 23 years ago. Since then, not only has this extremely useful reaction been most widely applied, but, especially in the last eight years, there has been extensive work on its mechanism, notably by M. Schlosser, by B. Maryanoff and by E. Vedejs himself. This work is not only of great interest in its own right, but also, in as much as it leads to an understanding of the stereochemical course of the Wittig reaction with a wide variety of carbonyl compounds and ylides, it is of substantial importance in organic synthesis. In fact, there are, in this chapter, extensive tabulations of Wittig reactions that will no doubt prove valuable. Even so, and despite a radical change of view concerning betaine intermediates in the Wittig reaction, the last word concerning its general mechanism has apparently not yet been spoken.

The second chapter, on the anomeric effect, by P. P. Graczyk and M. Mikołajczyk, deals with another topic which, though by no means recent in development, has been much in the news in the last few years and has even been reviewed at regular intervals. Nonetheless, we believe that this scholarly and extensive discussion of the effect in its conceptual, theoretical and applied aspects will make an important contribution to the topic and lead to its deeper understanding.

The third chapter, by Helena Dodziuk, deals with unusual saturated hydrocarbons. This chapter is, in the main, an overview of theoretical approaches to a series of "unnatural products"—most of them molecules, real and hypothetical, with considerable strain—with a discussion of important principles and an extensive list of references.

The fourth chapter, by Douglas W. Young, deals with an entirely different topic, namely the steric course of metabolic reactions of α-amino acids. Exploration of the stereochemistry of such reactions generally centers on two questions: Which of two enantiotopic ligands (often enantiotopic hydrogen atoms) is replaced or affected in a biological reaction and how does the configuration of the product relate to the spatial disposition (topicity) of the ligand displaced or affected? Again an earlier chapter by Arigoni and Eliel in Volume 4 of this series (1969) dealt with this topic in a general way

and once more the literature has mushroomed to the point where this timely chapter deals with an extensive and important subset of the examples of 24 years ago.

The last chapter, by M. G. Bures, Y. C. Martin and P. Willett, in contrast, deals with a very recent and novel subject, namely the searching of databases of chemical structures in three dimensions. It is only in the last few years that extensive three-dimensional databases (other than records of molecular structures determined by X-ray crystallography or other techniques) have been constructed. The question, to which much ingenuity has been applied, is how to search such databases for structures with a specific spatial relationship of ligands, for example one believed to be conducive to a desired pharmacological activity. The answer is not easy to come by, especially in view of the fact that many potential candidate molecules display several low-lying energy minima corresponding to different conformations, and the conformation expected to be active may not be the one corresponding to the global energy minimum. This chapter gives an authoritative picture of the present state of the art in this field.

It is with great sorrow that we must report the death, on January 14, 1992, of our advisor Günther Snatzke. Professor Snatzke was not only a personal friend of both of the editors, he was also an unusually active and effective advisor. Several chapters in recent volumes were commissioned at his suggestion; and he himself had planned to contribute a chapter on aspects of circular dichroism to Volume 21. But this was not to be. We dedicate this volume to the memory of Günther Snatzke whom we shall miss.

In conclusion, a more upbeat note: The manuscript of our long expected "Stereochemistry of Organic Compounds" book finally went to the publisher (Wiley) late last year and we expect that the book will appear at about the same time as this volume.

ERNEST L. ELIEL
SAMUEL H. WILEN

Chapel Hill, North Carolina
New York, New York
November 1993

CONTENTS

STEREOCHEMISTRY AND MECHANISM OF THE WITTIG REACTION 1
by E. Vedejs and M. J. Peterson
Department of Chemistry
University of Wisconsin
Madison, Wisconsin

ANOMERIC EFFECT: ORIGIN AND CONSEQUENCES 159
by Piotr R. Graczyk and Marian Mikołajczyk
Department of Organic Sulfur Compounds
Center of Molecular and Macromolecular Studies
Polish Academy of Science
Łódź, Poland

UNUSUAL SATURATED HYDROCARBONS; INTERACTION BETWEEN THEORETICAL AND SYNTHETIC CHEMISTRY 351
by Helena Dodziuk
Institute of Organic Chemistry
Polish Academy of Sciences
Warsaw, Poland

STEREOCHEMISTRY OF METABOLIC REACTIONS OF AMINO ACIDS 381
by Douglas W. Young
School of Chemistry and Molecular Sciences
University of Sussex
Falmer, Brighton, United Kingdom

SEARCHING TECHNIQUES FOR DATABASES OF THREE-DIMENSIONAL CHEMICAL STRUCTURES 467
by Mark G. Bures and Yvonne C. Martin
Computer-Assisted Molecular Design Project
Abbott Laboratories
Abbott Park, Illinois;

and Peter Willett
Krebs Institute for Biomolecular Research and Department of Information Studies
University of Sheffield
Sheffield, United Kingdom

CUMULATIVE TITLE INDEX, VOLUMES 1–21 **513**

SUBJECT INDEX **519**

TOPICS IN STEREOCHEMISTRY

VOLUME 21

Stereochemistry and Mechanism in the Wittig Reaction

E. VEDEJS AND M. J. PETERSON

Department of Chemistry, University of Wisconsin Madison, Wisconsin

I. Introduction
II. Background
III. Characteristics of Phosphorus Ylides
IV. Characterization of Oxaphosphetanes
V. Boundary Conditions for Stereochemical Equilibration of Wittig Intermediates
VI. Oxido Ylide Reactions; Modification of Oxaphosphetane Stereochemistry
VII. Stereochemical Results; Empirical Z:E Data
VIII. Nonstabilized Ylides $Ph_3P{=}CHR$
IX. Lithium Halide Effect on Stereoselectivity
X. Phosphorus Ligand Effects in Reactions of Nonstabilized Ylides
XI. Allylic and Benzylic Ylides
XII. Carbonyl-stabilized Ylides
XIII. Ylide Reactions with Ketones
XIV. Wittig Reactions in Multifunctional Systems
XV. Mechanistic Considerations
XVI. Probes for Electron Transfer
XVII. Probes for Betaine Intermediates
XVIII. Theoretical Considerations
XIX. Transition State Characteristics
XX. Interpretation of Stereochemistry
XXI. Transition State Geometries of Stabilized Ylides
XXII. Miscellaneous Reactions
A. Ketones
B. Reactions of $Ph_3P{=}CHX$
C. Ylides with Unsymmetrically Substituted Phosphorus
D. Lithium Ion Effects
XXIII. Alternative Transition State Models
Acknowledgment
References

Topics In Stereochemistry, Volume 21, Edited by Ernest L. Eliel and Samuel H. Wilen.
ISBN 0-471-52120-5 © 1994 John Wiley & Sons, Inc.

I. INTRODUCTION

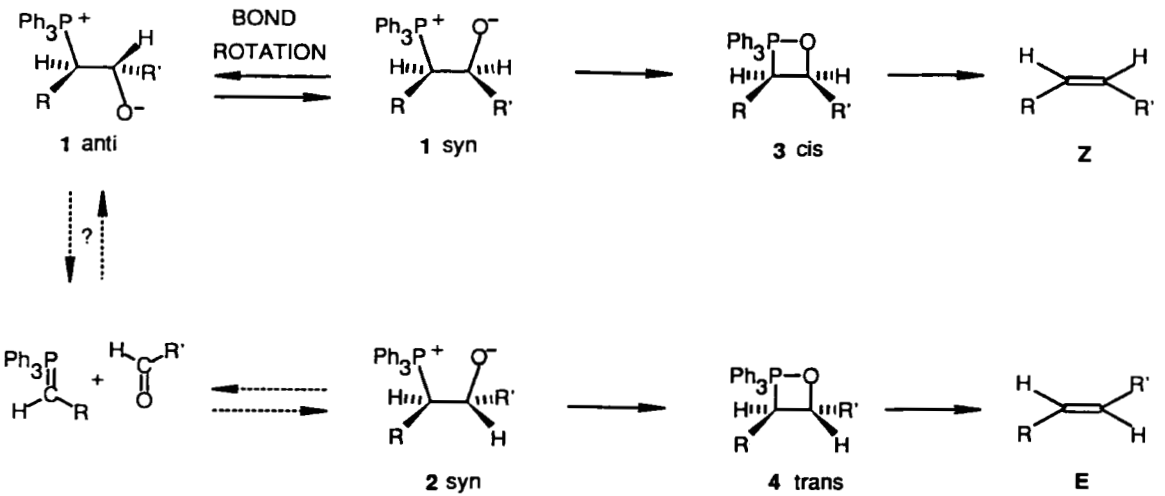
In 1970, a review entitled "The Stereochemistry of the Wittig Reaction" was published in *Topics of Stereochemistry* by M. Schlosser (1). This review was a milestone in early attempts to understand the Wittig mechanism based on a stepwise, ionic process (Scheme 1) (1, 2). The reaction of ylides with aldehydes was believed to involve a partly reversible nucleophilic addition step to generate a betaine intermediate (**1** or **2**). Subsequent decomposition to the alkene was attributed to the formation of oxaphosphetanes **3** or **4**, structures that were assumed to be intermediates of higher energy leading from the betaine to the alkene.

No single research group was responsible for the betaine mechanism. The rationale had evolved from suggestions made by Wittig and Haag (3), House and Rasmusson (4), and Bergelson and Shemyakin (5), and it was adjusted to fit subsequent stereochemical observations by other authors in the secondary literature (1, 2a–e, h). By 1970, it was common practice to explain the (*Z*)-alkene selectivity of nonstabilized ylide reactions ($RCH{=}P(C_6H_5)_3 + R'CHO$) via the initial formation of **1-anti** (2a–e). It was also believed that the (*E*)-olefin selectivity of carbonyl-stabilized ylides was due to increased stereochemical equilibration of intermediates via reversal. If the extent of reversal increases with increasing ylide stabilization by the α-substituent, then kinetically preferred decomposition of the intermediates **2** or **4** might explain increased selectivity for the (*E*)-alkene. These assumptions are summarized in the reaction profile diagram of Figure 1, an illustration that is reproduced directly from the 1970 account.

Some version of this scheme can be found in virtually every organic chemistry textbook through 1990 even though the original version was phrased in very cautious terms. It is worth repeating a paragraph that was appended to the figure:

> Any attempt to rationalize the complex stereochemistry of olefin formation will have to be concerned with the mechanism of the Wittg reaction. Unfortunately many mechanistic details of this reaction have not been satisfactorily elucidated. Thus, it is even uncertain whether the reaction system (ylide plus carbonyl compound) passes, on its way to phosphine oxide and olefin, through an open chain zwitterion, i.e. a betaine, through a cyclic oxaphosphetane, or through both of them consecutively. *The reaction sequence depicted in Figure 1 has no other merit than that of being believed to be the most probable one* (1).

In light of this statement, and of contrary experimental evidence that had already begun to appear by 1970 (1), it may be difficult to understand why the betaine rationale became so widely accepted (2a–e, h). Readers who are interested in the controversies and the complicated chronology of the mechanistic investigations between 1970 and 1990 may want to consult



Scheme 1

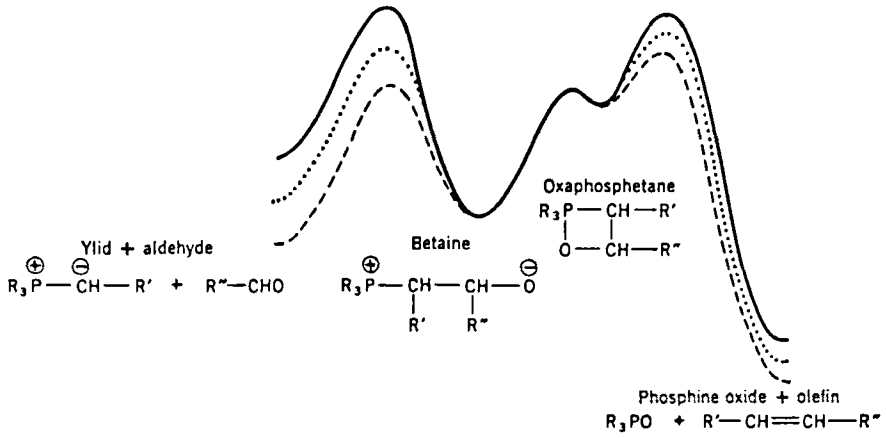


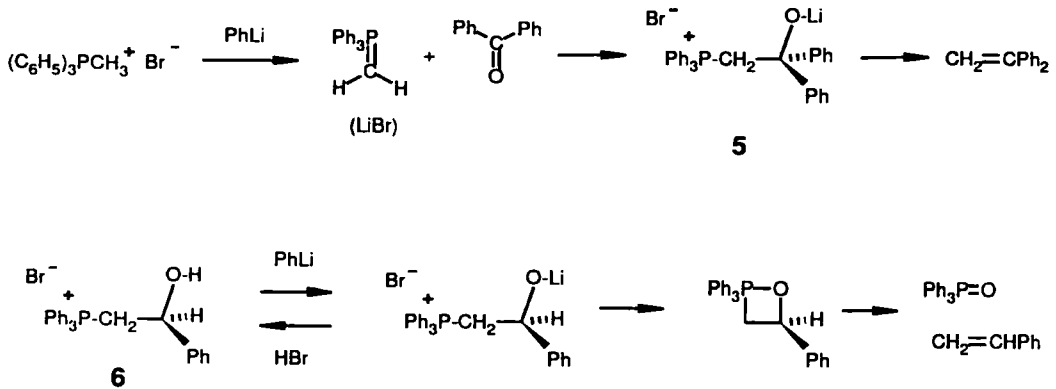
Figure 1. (Assumed) energy profile of the Wittig carbonyl olefination reaction, effected by (——) "reactive", (····) "moderated," or (- - - -) "stable" phosphonium ylids. (In the following figures the hypothetical oxaphosphetane intermediate will be omitted, since it has no further bearing on the discussion.)

another recent review where historical topics are discussed in depth (6). The main thrust of the present review will be to summarize what is currently known about Wittig stereoselectivity and its origins. Historical issues will be included only to the extent necessary to explain how the early observations provided a logical basis for the betaine rationale and how subsequent events required its modification.

II. BACKGROUND

Although a carbonyl olefination reaction using a phosphorus ylide had been reported by Staudinger and Meyer in 1919 (7), Wittig's group was the first to recognize and develop its practical importance. During attempts to prepare pentavalent phosphorus compounds, Wittig and Geissler performed the reaction of phenyllithium with methyltriphenylphosphonium iodide (8). The experiment produced the phosphonium ylide and not the desired pentavalent adduct. When benzophenone was added to characterize the ylide, an unstable intermediate adduct **5** was obtained. Its decomposition to 1,1-diphenylethylene (Scheme 2) occurred over 1.5 days at room temperature, and the key observation with regard to the Wittig olefin synthesis had been made. However, the fact that **5** contains LiBr was not realized until later (9).

Soon after the first brief report, a systematic investigation was published by Wittig and Schöllkopf (10). Three ylides $(C_6H_5)_3P{=}CHR$ were prepared

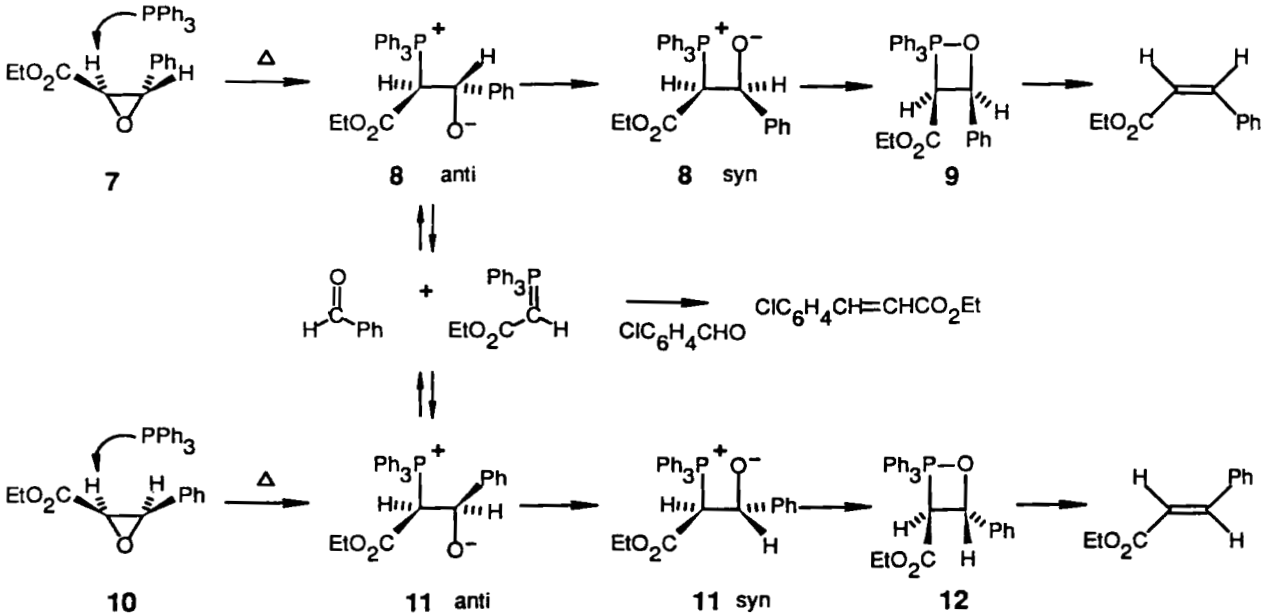

(C6H5)3PCH3+ Br-
PhLi
Ph3P
H
H
(LiBr)
Ph
Ph
O
Br-
O-Li
Ph3P-CH2
Ph
Ph
5
CH2=CPh2
Br-
O-H
Ph3P-CH2
H
Ph
6
PhLi
HBr
Br-
O-Li
Ph3P-CH2
H
Ph
Ph3P
O
H
Ph
Ph3P=O
CH2=CHPh

Scheme 2

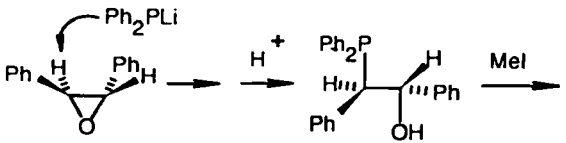
with R = H, Ph, $CH{=}CH_2$, all by the deprotonation of the phosphonium salt with phenyllithium in ether. In several examples, white precipitates appeared upon mixing the ylide and the carbonyl component (benzaldehyde, cyclohexanone, etc.), and the precipitate obtained from $(C_6H_5)_3P{=}CH_2$ with benzaldehyde was characterized as the hydrobromide salt **6**. When this compound was reacted with organolithium bases, the white precipitate reappeared and conversion into styrene could be demonstrated upon warming. The deprotonation experiment suggested not only that betaines generated independently followed the same Wittig reaction course, but also that betaines must be the most stable intermediates along the reaction pathway. Only later was it realized that the precipitated intermediates (lithium halide betaine adducts) do not form in the absence of lithium salts (9), nor do they appear in strongly coordinating solvents (1). Ylides generated using sodium or potassium bases undergo the Wittig reaction without forming precipitates, but this fact was not widely appreciated.

Wittig and Schöllkopf had observed that allylidenetriphenylphosphorane (a "moderated" ylide) reacts with benzaldehyde to give a mixture of the (*E*) and (*Z*)-1-phenylbutadienes, but they did not comment on the Z:E selectivity of nonstabilized ylide reactions. Within a few years, many other groups had explored synthetic applications of Wittig's procedure, and isolated reports of Z-selective olefinations had begun to appear (11). Eventually, Bergelson and Shemyakin (5) were able to show that high Z selectivity can be achieved with $Ph_3P{=}CHCH_3$ generated using NaH in dimethylformamide solution and that other experimental conditions gave lower Z:E ratios. House and Rasmusson (4) also observed changes in Z:E selectivity as a function of experimental variables and found significant solvent effects in the reactions of carbonyl-stabilized ylides. The results were attributed to differing degrees of stereochemical equilibration by the Wittig intermediates.

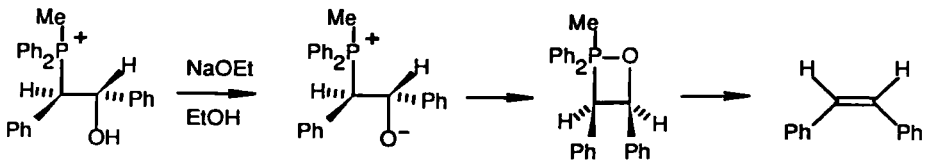
By 1970, several research groups had provided direct evidence to support the hypothesis that Wittig Z:E ratios are influenced by betaine reversal. In each case, the study involved the independent synthesis of a single betaine diastereomer followed by observation of its conversion to alkenes. Thus, Speziale and Bissing (12) found that treatment of ethyl trans-2-phenylglycidate **7** with triphenylphosphine in refluxing ethanol was sufficient to induce the conversion to ethyl cinnamate in good yield (Scheme 3). The trans epoxide **7** gave a mixture of Z:E cinnamate. Only the (*Z*)-isomer is expected if the epoxide reacts by the S_N2 process to give the betaine **8**, followed by cyclization to **9** and syn elimination of the phosphine oxide. Therefore, formation of the (*E*)-cinnamate could be the result of betaine dissociation to benzaldehyde and the ylide with subsequent Wittig recombination. To test this hypothesis, the epoxide deoxygenation was repeated in the presence of excess *m*-chlorobenzaldehyde. The crossover product ethyl *m*-chlorocinnamate was detected


PPh3
EtO2C
Ph
Δ
7
8 anti
8 syn
9
ClC6H4CHO
ClC6H4CH=CHCO2Et
10
11 anti
11 syn
12

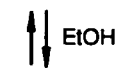
Scheme 3

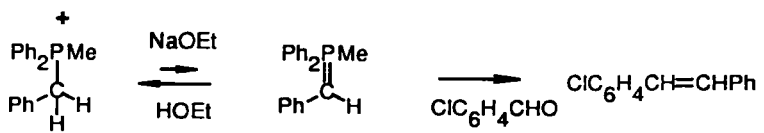


13



14 **15** **16**





18 **17**

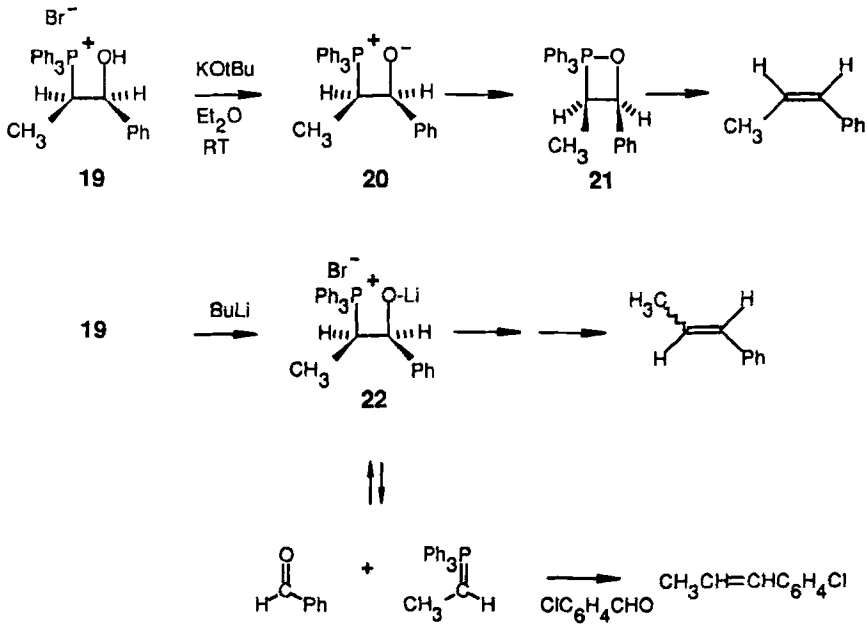
Scheme 4

(34%) together with ethyl cinnamate (66%) derived from decomposition of the original betaine **8** without reversal. In the case of cis-epoxide **10**, only 13% of the crossover product was obtained in refluxing ethanol, an observation that indicates relatively minor reversal by the betaine **11**. This result would be expected if conversion from **11** to the trans-disubstituted oxaphosphetane **12** and then to the *E*-enoate is relatively fast compared to the corresponding sequence from **8** to **9** and then to the (*Z*)-enoate. The evidence was consistent with expectations based on partly reversible formation of betaines.

Shortly after the study of Speziale and Bissing, another important paper appeared that provided even more decisive evidence in favor of betaine reversal (13). Jones and Trippett (13) were able to generate betaines by deprotonation of β-hydroxyphosphonium salts. Thus, reaction of trans-stilbene oxide with sodium diphenylphosphide gave a hydroxyphosphine **13** that could be methylated to afford a crystalline salt **14** (Scheme 4). Deprotonation with sodium ethoxide could then be used to generate the betaine **15**. When this experiment was performed in ethanol with excess *m*-chlorobenzaldehyde added (17 h at 20°C), 45% of the crossover product *m*-chlorostilbene was produced, together with 55% of stilbene (ca. 9:1 Z:E). The crossover experiment shows that betaine diastereomer **15** undergoes extensive retro-Wittig cleavage to the ylide **17** in ethanol at room temperature. Trippett and Jones also found that similar experiments in tetrahydrofuran (THF) afford up to 94% (*Z*)-stilbene, but this experiment did not attract much attention (1, 2).

A third investigation of betaine reversal was reported in 1967 by Schlosser and Christmann (14). The Wittig reaction of benzaldehyde with ethylidenetriphenylphosphorane was quenched at -78°C with HBr, and multiple recrystallizations gave the hydroxyphosphonium salt **19** (Scheme 5). Deprotonation with KO-*tert*-C_4H_9 in ether gave 96–97% (*Z*)-β-methylstyrene, a result that indicates overwhelming retention of stereochemistry from the betaine to the alkene. However, a more extensive series of experiments was performed in the presence of lithium ion. The starting material was less pure (89% **19**; 11% of the diastereomer), but olefin ratios indicated considerable loss of stereochemistry [28–90% (*E*)-alkene, depending on solvent] and reversal of **20** to the ylide and benzaldehyde was established by the crossover test. Schlosser's study demonstrated reversal to a nonstabilized ylide ($Ph_3P{=}CHCH_3$) under low temperature (Li-containing) conditions. On the other hand, it also clearly demonstrated > 95% stereospecific conversion from **19** to the alkene via **21** in the absence of lithium ion (ether solution).

Nearly all of the results available through 1967 could be interpreted to tell a consistent story. Betaines corresponding to carbonyl-stabilized ylides or to benzylic ("moderated") ylides apparently were capable of extensive reversal, at least in hydroxylic solvents. Betaines corresponding to nonstabi-



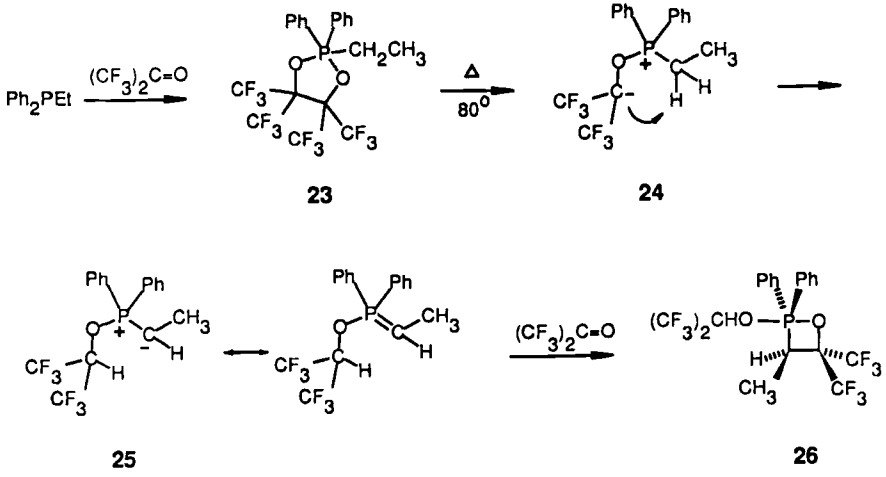
Scheme 5

lized ylides were less inclined to undergo the retro-Wittig cleavage, although they appeared to do so in the presence of lithium ion. Since nonstabilized ylides had been shown to react with high (*Z*)-olefin selectivity while moderated or carbonyl-stabilized ylides gave progressively larger product ratios in favor of (*E*)-alkenes, it was logical to connect the extent of (*E*)-alkene formation with the extent of reversal by the betaine. This hypothetical situation is illustrated in Figure 1. Energy barriers from the ylide to the betaine were assumed to reflect the degree of ylide stabilization, while the energy of the betaine itself was believed to be similar in all three ylide families (nonstabilized, moderated, and stabilized). Figure 1 also assumed that betaine formation is rate determining, that betaine intermediates are more stable than oxaphosphetanes, and that the oxaphosphetane decomposition barriers are reduced somewhat by the presence of an unsaturated group at C_3. This simple and satisfying mechanistic picture represented a broad consensus in 1970 (1, 2).

Nevertheless, evidence had begun to accumulate that could not be easily reconciled with the assumptions inherent in the betaine rationale as summarized in Figure 1. Rüchardt et al. (15) had found a suprising similarity in the reaction rates for $Ph_3P{=}CHCO_2Et$ with various aldehydes in benzene and in acetonitrile. If the mechanism involved rate-determining betaine formation,

then the reaction should be much faster in the solvent having the higher dielectric constant, but no evidence for such a trend was found. Extension of this early work culminated in a detailed study of solvent effects by Aksnes and Khalil (16) for $Ph_3P{=}CHCOPh$ and $O_2NC_6H_4CHO$. They showed conclusively that this Wittig reaction proceeds faster in CCl_4 than in methanol or acetonitrile. Therefore, the transition state (TS) must be less polar than the ylide and carbonyl reactants, a result that cannot be understood via an ionic, stepwise pathway involving rate-determining formation of betaine intermediates. A four-center transition state was proposed to explain the solvent effect. However, the evidence was not decisive because it could not exclude the prior formation of a betaine, followed by rate-determining cyclization to a less stable oxaphosphetane.

A more serious complication for the betaine mechanism arose when it was found that oxaphosphetanes are *more* stable than betaines. The earliest evidence was encountered by Ramirez et al. (17), who found that certain phosphines react with two equivalents of hexafluoroacetone to give 1,3,2-dioxaphospholane derivatives **23** (Scheme 6). These compounds rearrange into unusually stable oxaphosphetanes **26** via fragmentation to **24**, followed by a proton shift to generate an intermediate ylide **25** (17). Shortly thereafter, Vedejs and Snoble (18) used ^{31}P nuclear magnetic resonance (NMR) methods to show that more typical Wittig reactions of nonstabilized ylides $Ph_3P{=}CHR$ also produce oxaphosphetanes and that these intermediates can be easily observed at temperatures below 0°. Since betaines did not accumulate in any of the experiments, their conversion to oxaphosphetanes could not be rate



Scheme 6

determining. These developments did not rule out betaines as transient intermediates in the Wittig reaction, but they proved that betaines could not be lower in energy than oxaphosphetanes.

The relative energies of betaines and oxaphosphetanes suggested in Figure 1 could not be correct, nor could some of the assumptions regarding the relative rates for the formation, reversal, or decomposition of Wittig intermediates that had been advanced. Conversion from nonstabilized ylides and aldehydes into oxaphosphetanes is exothermic, not endothermic, as it had been depicted in Figure 1. Because $Ph_3P{=}CHPh$ or $Ph_3P{=}CHCH{=}CH_2$ also react with unhindered aldehydes at $-78°C$, these reactions likewise can be assumed to form oxaphosphetanes in an exothermic step. Therefore, the activation barrier ΔG^*_{REV} for reversal from **3** (R = alkyl, $CH{=}CH_2$, aryl, Fig. 2) to the ylide and aldehyde is higher than the barrier for oxaphosphetane formation (ΔG^*_{OP}).

Figure 2 illustrates several reaction coordinate diagrams that allow exothermic oxaphosphetane formation. Option **a** (four-center process) and the kinetically equivalent **b** (transient betaine precursor of the oxaphosphetane; two-step mechanism) are consistent with the observation that oxaphosphetanes are formed rapidly and decompose slowly when R = alkyl. Since the barrier ΔG^*_{DEC} for decomposition to the alkene is smaller than ΔG^*_{REV}, there will be little reversal or loss of stereochemistry in option **a**. Reversal should become less likely if the α-substituent R is unsaturated ($CH{=}CH_2$ or aryl), a situation that would decrease ΔG^*_{DEC} by weakening the $P{-}C_3$ bond (reaction profile **c**). If substituents are present that retard the rate of decomposition relative to reversal (as in options **d** or **e**), then oxaphosphetane reversal and equilibration of stereochemistry become possible, as discussed in a later section. However, this behavior has not been demonstrated for members of the $Ph_3P{=}CHR$ ylide family in the absence of lithium salts.

If the above conjectures are correct, then the highly Z-selective Wittig reactions of aldehydes with the nonstabilized ylide $Ph_3P{=}CHCH_3$ should be *more* sensitive to reversal and stereochemical equilibration (reaction profile **a**) than are the relatively nonselective reactions of $Ph_3P{=}CHCH{=}CH_2$ (profile **c**). Most of the experimental evidence needed to reach this conclusion was available in 1973, but there were also some contradictory data. In particular, the Trippett–Jones experiment (Scheme 4) (13) suggested that the Wittig intermediates corresponding to a benzylide reaction ($MePh_2P{=}CHPh$ + PhCHO) might be subject to reversal in protic solvents. It became clear that all of the betaine control experiments and key assumptions that had led to the adoption of Figure 1 as a working model would have to be reevaluated. This process has taken many years and has resulted in a modified view of the Wittig mechanism for the most familiar and synthetically useful reactions (6):

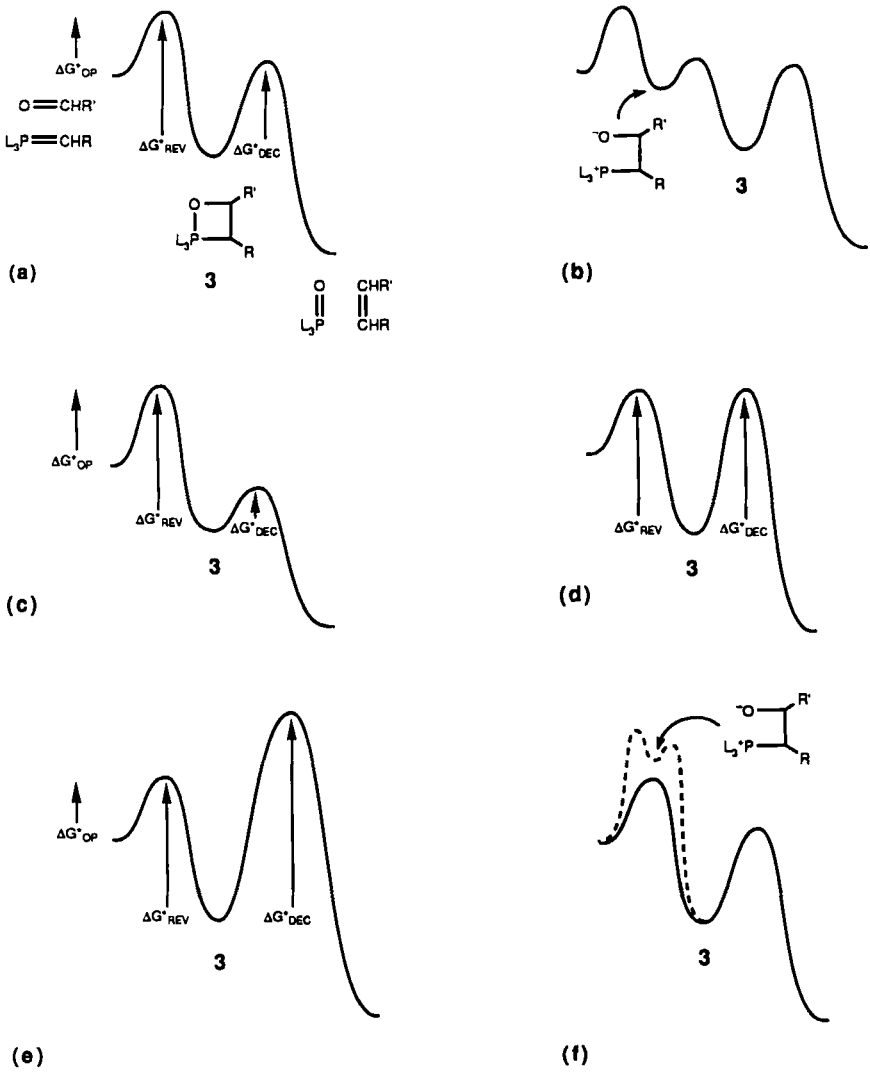


Figure 2. Possible energy profiles of the Wittig carbonyl olefination reaction.

1. Under salt-free, aprotic conditions, ylides $Ph_3P{=}CHR$ (R = alkyl, alkenyl, phenyl) react with aldehydes to produce the oxaphosphetane directly (Fig. 2, options **a** and **c**): four center mechanisms are accessible in all cases (18, 20).
2. The Z:E ratio of alkenes corresponds to the cis–trans ratio of oxaphosphetanes in typical reactions ("kinetic control"). This is true of nonstabi-

lized, moderated, and carbonyl-stabilized ylides (20–22), although there are certain exceptions (22, 23).

3. The oxaphosphetane decomposes by a syn-cycloreversion process to the alkene (18–23).
4. There are no zwitterionic or diradical intermediates having significant lifetimes (6, 21).
5. Betaines are energetically uphill compared to reactants as well as to oxaphosphetanes (illustrated for nonstabilized ylides in Fig. 2, **f**).

The last item (5) may explain why the independent betaine generation control experiments gave contradictory results. If betaines are high-energy species that lie *above* the saddle point leading from the ylide to the oxaphosphetane, then experiments that deliberately generate betaines (Schemes 3–5) may encounter pathways for stereochemical equilibration that are not accessible to typical Wittig reactions.

The chronology of events that resulted in generalizations 1–5 will not be presented in detail because this topic is extensively discussed in another account (6). Complex synthetic applications will be included to the extent necessary to illustrate stereochemical issues. Many other interesting examples are explored in a recent review by Maryanoff and Reitz (2j). The emphasis will be on the typical reactions and on the correlation of stereochemical results. Exceptional cases will be discussed where necessary to illustrate the limitations of current mechanistic models.

III. CHARACTERISTICS OF PHOSPHORUS YLIDES

Carbonyl-stabilized Wittig reagents react slowly with typical aldehydes at room temperature (reaction times of the order of minutes for $Ph_3P{=}CHCO_2Et$ or hours for $Ph_3P{=}CHC(O)R$. The stabilized ylides are resistant to water and to oxygen and can be prepared from the phosphonium salts using aqueous sodium hydroxide or generated *in situ* using diazabicycloundecene (DBU) (21c). By comparison, the nonstabilized or the moderated ylides are much more reactive and are destroyed rapidly by exposure to oxygen or to moisture. Nonstabilized ylides react rapidly with nonhindered aldehydes at $-78°C$ on a time scale of minutes or less (lithium-free conditions; ether solvents). No detailed kinetic studies have been performed to compare ylide reactivity, but qualitative competition experiments indicate that $Ph_3P{=}CHPh$ is ca. five-fold less reactive than the nonstabilized ylide $Ph_3P{=}CHCH_3$ (5c), a modest rate difference that could be due to steric as well as delocalization effects.

Table 1 lists some of the pK_a values that have been measured for phosphonium salts by Bordwell et al. (24a). These values are determined under

TABLE 1
pK_a Values of Selected Phosphonium Salts (24a)

Entry	Salt	pKa (DMSO)
1	$Ph_3P^+–CH_3\ Br^-$	(22.5)[a]
2	$Ph_3P^+–CH(CH_3)_2\ Br^-$	(21.3)[a]
3	$Ph_3P^+–CH_2Ph\ Br^-$	17.4
4	$Ph_3P^+–CH_2SPh\ Cl^-$	14.9
5	$Ph_3P^+–CH(CH_3)CO_2Et\ NO_3^-$	9.3
6	$Ph_3P^+–CH_2CO_2Et\ NO_3^-$	8.5
7	$Ph_3P^+–CH_2C(O)CH_3\ NO_3^-$	7.1
8	$Ph_3P^+–CH_2CN\ NO_3^-$	6.9
9	Ph_3P^+–(fluorenyl) Br^-	6.6
10	$Ph_3P^+–CH_2CHO\ NO_3^-$	6.1
11	$Ph_3P^+–CH_2C(O)Ph\ NO_3^-$	6.0

(a) Approximate value from one-point titration; the ylide appears to be unstable.

aprotic conditions [dimethyl sulfoxide (DMSO) solution] and allow only a qualitative comparison in the ether solvents that are normally used for preparative Wittig reactions. The phosphonium salts are stronger acids in DMSO solution than are simple ketones, aldehydes, or alcohols. Their relative acidity shows the expected dependence on conjugating substituents at the ylide α-carbon, and there is a qualitative correlation between ylide reactivity and phosphonium salt pK_a. However, the influence of α-alkyl substituents does not follow a simple pattern. Alkyl branching in the non-stabilized ylides increases acidity (entry 2 vs. 1), but the pK_a values are not accurately known. Branching in the stabilized ylides has the opposite effect (entry 5 vs. 6) even though sp^2 hybridization should be favored by the presence of the α-carbonyl group. This result could be attributed to an unfavorable steric effect on solvation in the stabilized ylide, but steric interference with ylide delocalization in the crowded Ph_3P enviroment may also play a role.

Another qualitative comparison of ylide reactivity is available from the photoelectron spectra (PES). The first ionization potential for a series of ylides is given in Table 2 (IE_1; corresponding to the removal of an electron from the ylide HOMO) (highest occupied molecular orbital) (24b). Lower

TABLE 2
Photoelectron Ionization Potentials of Selected Ylides (24b)

Entry	Ylide	IE_1(eV)
1	$(CH_3)_3P{=}CH_2$	6.81
2	$(CH_3)_3P{=}CHCH{=}CH_2$	6.20
3	$(CH_3)_3P{=}CHCH{=}CHCH_3$	6.02
4	$(CH_3)_3P{=}CHPh$	6.19
5	$Ph_3P{=}CH_2$	6.62
6	$Ph_3P{=}CHCH_3$	6.15
7	$Ph_3P{=}C(CH_3)_2$	6.04
8	$Ph_3P{=}CHPh$	6.01
9	$Ph_3P{=}CHCH{=}CHCH_3$	5.95

ionization potentials for $Ph_3P{=}CHCH_3$ (6.15 eV) and $Ph_3P{=}CMe_2$ (6.04 eV) compared to $Ph_3P{=}CH_2$ (6.62 eV) suggest that increased α-alkyl substitution facilitates ionization. A change of the ligands on phosphorus from methyl to phenyl has a similar but smaller effect. This trend toward lower ionization potentials would be expected to correlate qualitatively with an increase in ylide reactivity due to a higher energy HOMO level, but the differences among α-substituted ylides are small and could easily be dominated by steric factors.

An extensive collection of both experimental and theoretical evidence suggests that the most accurate description of the ylide is one in which an easily pyramidalized carbanion is stabilized by an adjacent tetrahedral phosphonium center (25–34). These conclusions are supported by NMR studies and X-ray crystal structure determinations. Thus, increased electron density at the α-carbon of nonstabilized ylides is consistent with the upfield chemical shift in the ^{13}C NMR spectrum by comparison with the parent phosphonium salts (Table 3, entries 1–5) (26). However, the chemical shift by itself is not a reliable indicator of ylide structure. This is most clearly seen in some of the conjugated ylides, and also in entry 3, which differs from entry 1 only by the presence of lithium bromide. Both the lithium-free (1) and the lithium-containing ylides (3) have the same ^{13}C chemical shift, but they differ dramatically in the ^{31}P–^{13}C coupling constant. In entry 3, $^1J_{P-C} = 51.9$ Hz is typical of phosphonium phosphorus and supports the

TABLE 3
Chemical Shift and Coupling Constant Values for Representative Triphenylphosphonium Salts and Ylides

Entry	Formula	Salt		Ylide		Reference
		$\delta^{13}C$	$^1J_{CP}$	$\delta^{13}C$	$^1J_{CP}$	
1	$Ph_3P{=}CH_2$	11.4	57.1	-4.1	100.0	26d
2	""			-5.4		26h
3	""			-4.1	51.9[a]	26c
4	$Ph_3P{=}CHCH_3$	17.0	51.6	3.2	110.7	26a
5	$Ph_3P{=}C(CH_3)_2$	21.5	47.0	9.0	121.5	26a
6	$Ph_3P{=}CHPh$	30.3	47.7	28.0	128.0	26a
7	$Ph_3P{=}CHCH{=}CH2$	28.6	49.7	28.7	131.4	26a
8	""			28.2	125.2	26h
9	$Ph_3P{=}CHC(O)CH_3$	40.1	58.8	51.3	108.0	26a
10	$Ph_3P{=}CHCO_2CH_3$	32.9	55.5	29.3	130.0	26b
11	""			29.8		26h
12	$Ph_3P{=}Cp$[b]			78.3	113.1	26b
13	$Ph_3P{=}F$[c]			53.3	128.7	26b

(a) This compound is Ph_3P^+— CH_2Li Br^-
(b) Cyclopentadienylidene
(c) Fluorenylidene

covalent organolithium structure $Ph_3P^{(+)}$—CH_2Li. The salt-free ylide, written for convenience in the inaccurate π-bonded notation $Ph_3P{=}CH_2$ (entry 1) has a larger $^1J_{P-C} = 100$ Hz, (26c) and even larger $^1J_{P-C}$ values are seen for the other ylides in Table 3. More highly substituted ylides have not been reported to form covalent lithium halide adducts analogous to the example of entry 3.

The carbon chemical shift for $Ph_3P{=}CH_2$ (or Ph_3P^+—CH_2^-) of -4.1 ppm (26d) is far from the typical value for sp^2-hybridized carbon and more closely resembles that of methylithium (-13.2 ppm in Et_2O) (27a). On the other hand, the ylide α-carbon (28.7 ppm) in allylidenetriphenylphosphorane is 32 ppm downfield relative to the methylide (26a), an effect that might be

taken to suggest increased sp^2 character and delocalization. However, the allylic ylide chemical shift is virtually identical to that of the precursor allyl phosphonium salt (entry 7). Futhermore, a much larger deshielding effect is seen in a highly ionic allylic carbanion structure such as allylpotassium (52.8 ppm) (27b). Delocalization effects are more apparent in cyclopentadienylidene and fluorenylidene ylides (entries 12, 13). Increased delocalization of anionic charge in the former results in an ylide carbon that is deshielded by 25 ppm relative to fluorenylidenetriphenylphosphorane (26b) (Table 3).

An examination of the $^1J_{C-P}$ coupling constants (Table 3) reveals a large difference between values for ylides (100–130 Hz) and the corresponding salts (47–59 Hz) in all cases (26a). These values are also different from $^1J_{C-P}$ for the $P-C_{phenyl}$ bond, which is approximately the same in both the ylides and the salts (86–92 Hz) (26b). Although the ^{13}C data provide no definitive answers regarding the nature of the ylide bond, these data indicate that ylides cannot be described as typical delocalized sp^2 hybridized carbanions nor can they be viewed simply as localized sp^3 hybridized carbanions. This information points instead to a substantially localized carbanion of intermediate hybridization, stabilized by an adjacent phosphonium center (26–28). Theoretical considerations have reached similar conclusions (29).

The issue of hybridization at the ylide α-carbon has been addressed by several other studies. Low-temperature NMR coalescence experiments indicate that rotation about the ylide C—P bond is virtually unrestricted, suggesting that it retains substantial single-bond character. (The activation barrier for bond rotation is < 8 kcal/mol) (28a). However, a recent crystallographic study by Schmidbaur et al. (30a) on $Ph_3P{=}CH_2$ determined an ylide bond length of 1.700 Å, noticeably shorter than the bond length of the precursor phosphonium salt (1.800 Å) (30a, 31). More importantly, however, this study showed that the hydrogen atoms on the ylide carbon are clearly bent out of the plane formed by the P—C bond ($\angle P-C-H = 116°$, $\angle H-C-H = 119°$). Several other recent crystal structure determinations also show that the ylide α-carbon is partly pyramidalized (isopropylidene and cyclopropylidene phosphorane derivatives) (30b, c). According to ^1H NMR experiments, cyclopropylidenetriphenylphosphorane undergoes rapid pyramidal inversion of the ylide carbon at − 110°C (32). All these data argue against a simple sp^2 hybridized ylide structure and are more consistent with an easily pyramidalized geometry having partial sp^2 character.

Data obtained from crystallographic studies on stabilized ylides present a different picture. Speziale and Ratts (33) showed that the ylide α-carbon of 2-chloro-2-(triphenylphosphoranylidene) acetophenone is planar ($\angle P-C_\alpha-Cl = 118.3°$, $\angle P-C_\alpha-C = 120.2°$, $\angle Cl-C_\alpha-C = 121.1°$). The ylide bond length is 1.736 Å, somewhat longer than in the nonstabilized ylides. These data, along with the C_α—C(O) and C(O)—O bond lengths (1.361 and

1.301 Å, respectively) led these workers to conclude that the stabilized ylide α-carbon is sp^2 hybridized. The ylide electron distribution can be approximated by a charge-separated phosphonium enolate representation.

IV. CHARACTERIZATION OF OXAPHOSPHETANES

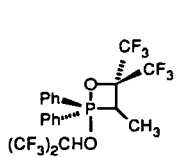
The discovery that oxaphosphetanes are the low-temperature intermediates in representative Wittig reactions was based largely on the observation of characteristic ^{31}P chemical shifts for pentacoordinated phosphorus (19a). Although the phosphorus chemical shifts rule out isomeric, tetravalent phosphorus (betaine) structures, they are not especially informative with regard to other structural details. So far, none of the representative Wittig intermediates has afforded crystals of sufficient quality for X-ray crystal structure determination. However, the unusually stable oxaphosphetane **A**, Table 4 (identical with **26**, Scheme 6), reported originally by Ramirez et al. (17) has been characterized by X-ray methods (34). The crystal structure indicates that phosphorus is at the center of a distorted trigonal bipyramid with the four-membered ring in an apical-equatorial plane with oxygen in the apical position, consistent with geometric constraints and the rules of apicophilicity (35). The oxaphosphetane ring is somewhat puckered (PCCO dihedral angle 8.6°), and its shape is distorted by the differences in bond lengths between the ring atoms (distances in angstroms: P—C_3 = 1.83, P—O = 1.79, C_3—C_4 = 1.52, C_4—O = 1.36). The most striking feature of the molecule is its severe intramolecular crowding. Between the various substituents around the oxaphosphetane ring (not including hydrogens), 27 nonbonded interatomic distances of less than 3.6 Å were found. In addition, the cis relationship between the C_3—CH_3 group and one of the C_4—CF_3 groups results in a geometry for the CF_3 substituent that is far from tetrahedral. The CF_3 group with a trans relationship does not suffer from the same steric interactions and adopts a tetrahedral geometry as expected. This distortion is a result of the eclipsing interactions imposed by the conformation of the oxaphosphetane ring and underscores an exceptionally demanding steric environment. Some of the most important bond distances and bond angles are summarized in Table 4, along with X-ray data for other unusually stable oxaphosphetanes (34). Two of the oxaphosphetane structures summarized in Table 4 (**C**, **D**) have a nearly planar oxaphosphetane, perhaps because they contain an sp^2 hybridized carbon in the four-membered ring. Three others (**A**, **E**, **F**) have varying degrees of ring pucker (PCCO dihedral angles between 4.7° and 9.7°). These distortions from planarity may be due to steric crowding and probably reflect compromises between bond angle strain and nonbonded interactions along the oxaphosphetane ring.

The NMR data collected by the Ramirez (17), Röschenthaler (36),

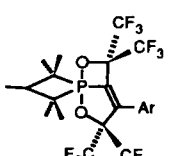
TABLE 4
Oxaphosphetane Crystal Structure Data[a]

Entry	dP-O	dP-C	dC-C	dC-O	∠OPC	∠PCC	∠CCO	∠COP	∠PCCO[b]	Reference
A	1.79	1.83	1.52	1.36	75.5	88.1	100.5	94.8	8.6	34a
B	1.85	1.61	1.48	1.43	71.6	---	---	---	---	34b
C	1.83	1.78	1.51	1.43	73.6	95.4	94.9	95.9	2.9	34c
D	2.01	1.76	1.57	1.39	71.3	98.5	96.1	94.1	0.6	34d
E	1.73	1.81	1.53	1.45	77.4	89.8	95.6	95.7	9.7	34e
F	1.78	1.82	1.55	1.40	75.5	90.2	97.0	97.0	4.7	34f

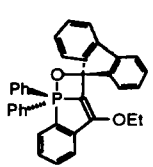
(a) Distances in angstroms, angles in degrees
(b) Dihedral angle



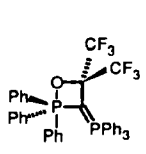
A



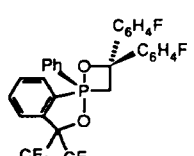
B



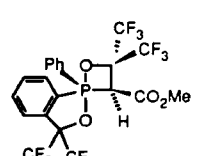
C



D



E



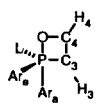
F

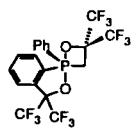
TABLE 5

Nuclear Magnetic Resonance Data of Representative Oxaphosphetanes

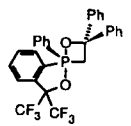
Entry	$\delta^{31}P$:	$\delta^{1}H$:		$\delta^{13}C$:						
	P	$H_3(^2J_{HP})$	$H_4(^3J_{HP})$	$C_3(^1J_{CP})$	$C_4(^2J_{CP})$	$L(^1J_{CP})$	$Ar_e(^1J_{CP})$	$Ar_a(^1J_{CP})$	$C_3Me(^2J_{CP})$	Ref.
E	-36.5	4.37(26) 4.55(20)	---	57.1(110)	75.2(17)	132(147)/137(141)[a]		---	---	34e
F	-36.7	5.25(26)	---	64.4(120)	74.3(14)	130(149)/131(148)[a]		---	---	34f
G	-33.3	4.02(24) 4.32(20)	---							34f
H	-35.8	4.43(26) 4.62(20)	---	56.8(110)	76.0(17)	132(146)/137(142)[a]		---	---	34e
I	-62.9	4.09(16)	3.52(6)	65.2(85)	69.9(16)	---	---	---	11.5(9)	20
J	-62.2	4.56(22)	3.05(2)	59.3(85)	73.5(15)	---	---	---	13.8(9)	20
K	-70.8	3.56(16)	---	60.3(83)	66.9(15)	24.4(96)	148.8(71)[b]	---	21a	
L	-79.2	3.93(17) 2.81(15)[c]	---	54.5(82)	67.3(16)	21.9(98)	134.3(132)	XX[d](<19)	---	21a
M	-61.7	---	3.44(3)	67.0(88)	71.3(16)	137.6(134)	132.2(126)	XX[d](<18)	17.1(5) 21.5(<1)	21b

(a) Assignment uncertain. (b) An averaged value; pseudorotation makes the equatorial and axial sites equivalent. (c) Pseudorotation frozen out at -53 °C. (d) Entries marked XX indicate that the assignment of quaternary aromatic carbons is uncertain. The J value is no larger than the value given in parentheses.

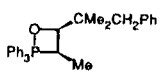




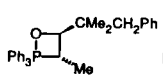
G



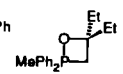
H



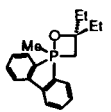
I



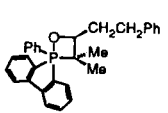
J



K



L



M

Schmidbaur (37), and Okazaki (34e,f) groups on these and other related oxaphosphetane and oxaphospholane systems reveal characteristic spectroscopic features. The ^{31}P chemical shift is similar to that of other pentavalent phosphorus species, coming in the range from $\delta = -10$ to -80 ppm. There is a large change in the magnitude of $^{1}J_{C-P}$, depending upon the apical (10–20 Hz) or equatorial (100–150 Hz) orientation of the coupled carbon. In the ^{1}H NMR spectrum, the hydrogens on C_3, adjacent to phosphorus, are shifted downfield relative to those on oxaphosphetane C_4, adjacent to oxygen. The magnitude of $^{2}J_{H-C-P}$ and $^{3}J_{H-C-C-P}$ follows the usual trend, with the former (15–20 Hz) smaller than the latter (25–30 Hz) (38). This information provides an important relay point between structure types that have been characterized by both NMR and X-ray methods (oxaphosphetanes **E** and **F**) (34e,f) and those that can only be studied by NMR techniques.

The first ^{13}C characterization of an oxaphosphetane prepared by a typical Wittig reaction was reported by Maryanoff et al. (22a). Thus, reaction of butylidenetriphenylphosphorane with benzaldehyde at $-78°C$ (THF; LiBr present) was monitored by ^{31}P NMR. The spectrum contained two singlets at -61.4 and -63.8 ppm that were attributed to the cis and trans oxaphosphetanes, respectively. When this experiment was repeated with ^{13}C-labeled starting materials, the chemical shifts and coupling constants of C_3 and C_4 in both isomers could be determined cis: δC_3, 71.5 ppm ($^{1}J_{C-P} = 85$ Hz), δC_4, 69.2 ppm ($^{2}J_{C-C-P} = 16$ Hz); trans: δC_3, 75.0 ppm ($^{1}J_{C-P} = 84$ Hz), C_4 72.3 ($^{2}J_{C-C-P} = 15$ Hz). In each diastereomer, C_3 shows the large $^{1}J_{C-P}$ coupling constant expected for an equatorially oriented substituent in a trigonal bipyramidal phosphorus environment by analogy to the precedents cited above (36, 37). No other ^{13}C data were reported from this series.

A number of other oxaphosphetanes have now been studied using natural abundance ^{13}C NMR methods, and several representative examples are summarized in Table 5 (21a,b, 39). Selected ^{1}H and ^{31}P NMR data are also included. All of the data are consistent with trigonal bipyramidal oxaphosphetane structures having apical oxygen. The $^{13}C-^{31}P$ coupling constants are especially informative and require that C_3 is in the equatorial location and that oxygen occupies the apical site. Although no definite evidence regarding bond lengths and bond angles is available from the NMR data, these oxaphosphetanes are likely to resemble **26** in steric congestion as well as qualitative geometric features.

V. BOUNDARY CONDITIONS FOR STEREOCHEMICAL EQUILIBRATION OF WITTIG INTERMEDIATES

Oxaphosphetanes are obligatory intermediates in all known aldehyde Wittig reactions (19, 22b). If they decompose stereospecifically to alkenes, then the

final olefin Z:E ratio will be the same as the cis-trans ratio of the oxaphosphetanes (kinetic control). As will be shown, nearly all classes of ylides follow this reactivity pattern. However, there are certain well-defined exceptions to the rule (20, 21c, 22, 23). This section considers experimental tests that can distinguish between oxaphosphetanes that equilibrate and those that do not and tabulates representative examples of stereospecific oxaphosphetane decomposition (Table 6) as well as the known examples of stereochemical equilibration (Table 7).

Several tests are available to determine whether equilibration of stereochemistry occurs in the course of oxaphosphetane decomposition (methods A–E, Scheme 7), but each method has some limitations. In method A, oxaphosphetane diastereomers are prepared independently by deprotonation of the β-hydroxyphosphonium salts **27** or **28** with base (NaHMDS, $NaNH_2$, KO-*tert*-Bu, etc.) (20). If each isomer affords a distinct oxaphosphetane **31** or **32** according to NMR analysis (usually, ^{31}P or ^{1}H), then the solutions are warmed up to the decomposition temperature. Kinetic control is established if stereospecific conversion to the alkenes can be demonstrated from each diastereomer. A less rigorous version of this test is to perform the experiment only with isomer **27**, the precursor of the cis-disubstituted oxaphosphetane **31** (21c). All known examples of significant ($> 5\%$) stereochemical equilibration involve **31** and not the trans-disubstituted isomer **32** (20, 21c). A negative equilibration result with the cis diastereomer **31** can be assumed to apply to **32** as well.

It is also possible to assay stereochemical equilibration directly by monitoring Wittig reactions (Maryanoff et al., method B) (22). One version of this technique depends on resolution of the ^{31}P signals of oxaphosphetane diastereomers using high-field NMR instruments. If two distinct signals can be resolved for **31** and **32** from a Wittig reaction performed at $-40°C$ or below, then the kinetic diastereomer ratio can be determined. If this ratio differs from the empirical Z:E ratio of alkene products, then stereochemical equilibration of intermediates is established. In some cases, the ratio changes well below the temperature threshold for Wittig decomposition to the alkene, and it is possible to monitor equilibration ("stereochemical drift") directly by using NMR methods. More often, the thermal conversion into alkene competes with equilibration of diastereomers (20, 22). Under these circumstances, the diastereomer ratio observed by NMR is altered because one isomer decomposes faster than the other, and NMR evidence by itself is not sufficient to establish interconversion of oxaphosphetane diastereomers. However, any ambiguity can be removed by comparing the initial cis-trans oxaphosphetane ratio with the empirical Z:E ratio of alkenes. Occasionally, ^{31}P or ^{1}H signals of **31** and **32** cannot be resolved due to line broadening in the more hindered isomer **31**. In this case, the isomer ratio can be determined

TABLE 6
Kinetically Controlled Wittig Systems $L_3P{=}CHR + R'CHO$; Minimal Stereochemical Equilibration

	Substitution Pattern:								Alkene	Decomposition	Maximum	
Entry	L_3	R'	R	Reactants	Solvent	Li^+?	Initial Temp.	31:32[a]	Z:E	Temp.	% Equil.[b]	Method
1	Ph_3	C_6H_5	CH_3	**27** + KO*tert*Bu	Et_2O	no	0°	(>98:2)[c]	96:4	0°	4%	A[14]
2	Ph_3	C_6H_5	C_3H_7	**28** + NaHMDS	THF	no	-78°	(<2:98)[c]	<1:99	+23°	1%	A[22a]
3	Ph_3	C_6H_5	C_3H_7	**27** + NaHMDS	THF	no	-78°	(>98:2)[c]	99:1	+23°	1%	A[22a]
4	Ph_3	C_6H_5	C_3H_7	**33** + R'CHO	THF	0.015M	-40°	98:2	97:3	+23°	2%	B[22a]
5	Ph_3	C_5H_{11}	C_3H_7	**33** + R'CHO	THF	0.07M	-40°	---	85:15	+23°	2%	B[22a]
6	Ph_3	CH_2OAc[d]	C_3H_7[d]	**36** + Ph_3P	neat	no	160°	(>95:5)[c]	96:4	+160°	4%	D[44]
7	Ph_3	$PhCH_2(Me_2)C$	CH_3	**28** + NaHMDS	PhMe	no	-70°	<5:95	<1:99	+20°	1%	A[20]
8	Ph_3	$PhCH_2(Me_2)C$	CH_3	**27** + NaHMDS	PhMe	no	-70°	>95:5	>99:1	+20°	1%	A[20]
9	Ph_2Me	$PhCH_2(Me_2)C$	CH_3	**28** + NaHMDS	PhMe	no	-70°	<5:95	<1:99	+20°	1%	A[20]
10	Ph_2Me	$PhCH_2(Me_2)C$	CH_3	**27** + NaHMDS	PhMe	no	-70°	>95:5	>99:1	+20°	1%	A[20]
11	Ph_2Me	C_5H_{11}[d]	CH_3[d]	**34** + MeI	THF	yes	25°	(>98:2)[c]	>99:1	+25°	1%	E[19b]
12	Ph_2Me	C_5H_{11}[d]	CH_3[d]	**35** + MeI	THF	yes	25°	(<2:98)[c]	<1:99	+25°	1%	E[19b]
13	Ph_2Me	C_6H_5	C_6H_5	**27** + NaOEt	THF	no	0°	(>98:2)[e]	96:4	0°	4%	A,C[13]
14	Ph_2Me	C_6H_5	C_6H_5	**34** + MeI	THF	yes	25°	(>98:2)[e]	98:2	+25°	2%	E[19b]
15	Ph_2Me	C_6H_5	C_6H_5	**35** + MeI	THF	yes	25°	(>2:98)[e]	<1:99	+25°	1%	E[19b]
16	Ph_2Me	C_6H_5	C_6H_5	**27** + NaHMDS	THF	no	-78°	(>98:2)[e]	>99:1	-78°	1%	A[43]
17	Ph_2Me	C_6H_5	C_6H_5	**27** + BuLi	THF	yes	-78°	(>98:2)[e]	>99:1	-78°	1%	A[43]
18	Ph_2Me	$PhCH_2(Me_2)C$	CO_2Et	**27** + DBU	EtOH	no	+20°	(>98:2)[e]	98:2[f]	+20°	3%[f]	A,C[21c]
19	Ph_2Me	C_6H_5	CO_2Et	**27** + DBU	EtOH	no	+20°	(>98:2)[e]	99:1[f]	+20°	6%[f]	A,C[21c]
20	Ph_2Me	c-C_6H_{11}	CO_2Et	**27** + DBU	EtOH	no	+20°	(>98:2)[e]	>98:2	+20°	2%	A,C[21c]

	Substitution Pattern:								Alkene	Decomposition	Maximum	
Entry	L_3	R'	R	Reactants	Solvent	Li^+?	Initial Temp.	31:32[a]	Z:E	Temp.	% Equil.[b]	Method
21	Ph_2Me	$Ph(CH_2)_2$	CO_2Et	**27** + DBU	EtOH	no	+20°	(>98:2)[e]	>98:2	+20°	2%	A,C[21c]
22	Ph_2Me	C_6H_5	$CH{=}CH_2$	**34**[g] + MeI	THF	yes[g]	0°	(>95:5)[e]	96:4	0°	<5%[e]	E[45]
23	Ph_2Me	C_6H_{11}	$CH{=}CH_2$	**34**[g] + MeI	THF	yes[g]	0°	(>95:5)[e]	96:4	0°	<5%[e]	E[45]
24	EtDBP[h]	$PhCH_2(Me_2)C$	CH_3	**28** + $NaNH_2$	PhMe	no	-70°	<5:95	<1:99	+20°	1%	A[20]
25	EtDBP[h]	$PhCH_2(Me_2)C$	CH_3	**27** + $NaNH_2$	PhMe	no	-70°	>95:5	>99:1	+20°	1%	A[20]
26	MeDBP[h]	c-C_6H_{11}	$CH{=}CH_2$	**28** + NaHMDS	THF	no	-70°	<5:95	2:98	-40°	2%	A[21c]
27	MeDBP[h]	c-C_6H_{11}	$CH{=}CH_2$	**27** + NaHMDS	THF	no	-70°	>95:5	96:4	-40°	4%	A[21c]
28	MeDBP[h]	c-C_6H_{11}	Ph	**27** + NaHMDS	THF	no	-70°	>95:5	99:1	-20°	1%	A[21c]
29	Et_3	$PhCH_2(Me_2)C$	CH_3	**28** + KO*tert*Bu	THF	no	-70°	<5:95	<1:99	-5°	1%	A,C[20]
30	Bu_3	C_5H_{11}	C_3H_7	**33** + R'CHO	THF	no	-78°	14-20:86-80[i]	10:90	+23°	6-10%[j]	B[22a]
31	Bu_3	c-C_6H_{11}	C_3H_7	**33** + R'CHO	THF	no	-78°	12:88[i]	10:90	+23°	2%	B[22c]

(a) Oxaphosphetane ratio based on ^{31}P or ^{1}H NMR assay at the initial temperature. (b) Sum of equilibration by the betaine as well as the oxaphosphetane unless noted otherwise. (c) Oxaphosphetane ratio not reported. Diastereomeric purity of precursor is given. (d) Arbitrary assignment for R and R'; the regiochemistry of epoxide opening is not known and a mixture of regioisomers can be assumed. (e) Unstable oxaphosphetane decomposes too rapidly to monitor directly. Diastereomeric purity of precursor is given. (f) Alkene ratio from an experiment with ClC_6H_4CHO present in excess to trap any **33** that forms; % equilibration is based on % crossover product. (g) $Ti(iOPr)_4$ is also present in this experiment; the exact diastereomer composition of **34** is not known. (h) DBP= dibenzophosphole; EtDBP= P-ethyldibenzophosphole. (i) NMR assay indicates 14% **31**; low temperature acid quench suggests a larger amount of **31** based on the observed ratio of **27:28**. The experiment also produces a substantial amount of phosphonium enolate species by deprotonation of the aldehyde substrate. (j) The larger value is based on the ratio of **27:28** compared to the olefin Z:E ratio.

TABLE 7
Systems That Undergo (> 10%) Stereochemical Equilibration

Subset 1. Equilibration in Wittig Experiments.

							Initial Observation:		Final Observation:			Maximum % Equilibration:	
Entry	L_3	R'	R	Reactants:	Solvent	Li^+?	Temp.	**31**:**32**	**31**:**32**	Temp.	Z:E Ratio	via **29** and/or **31**	Method
1	Ph_3	C_6H_5	C_3H_7	**33** + R'CHO	THF	1.0M[a]	-40°	72:28[b]	---	---	36:64[c]	36%,[d] > -40°	B[22a]
2	Ph_3	C_6H_5	C_3H_7	**33** + R'CHO	THF	0.4M[a]	-40°	77:23[b]	---	---	55:45[c]	22%,[d] > -40°	B[22a]
3	Ph_3	C_6H_5	$(CH_2)_3CO_2Li$	**33** + R'CHO	THF	0.13M	-45°	89:11[b,e]	20:80[f]	-30°	7:93[c]	82%,[d] > -30°	B[23b]
4	Ph_3	C_6H_5	$(CH_2)_2$-OLi	**33** + R'CHO	THF	0.5M	-80°	31:69[b,g]	6:94	-55°	4:96[c]	>27%,[d,g] > -55°	B[23b]
5	Ph_3	C_5H_{11}	$(CH_2)_3CO_2Li$	**33** + R'CHO	THF	0.13M	-80°	73:27[b]	---	---	42:58[c]	43%,[d] > -80°	B[23b]
6	Et_3	$PhCH_2(Me_2)C$	CH_3	**33** + R'CHO	THF	no	-95°	76:24[b]	<5:95[h]	-5°	10:90[c]	66%, > -60°	B[20]
7	Bu_3	*tert*-C_4H_9	C_3H_7	**33** + R'CHO	THF	no	-55°	40:60[b]	<5:95[h]	-15	4:96[c]	36%, > -55°	B[22a]
8	Bu_3	C_6H_5	C_3H_7	**33** + R'CHO	THF	no	-78°	47:53[b]	2:98[h]	-10°	8:92[c]	39%, > -40°	B[22a]

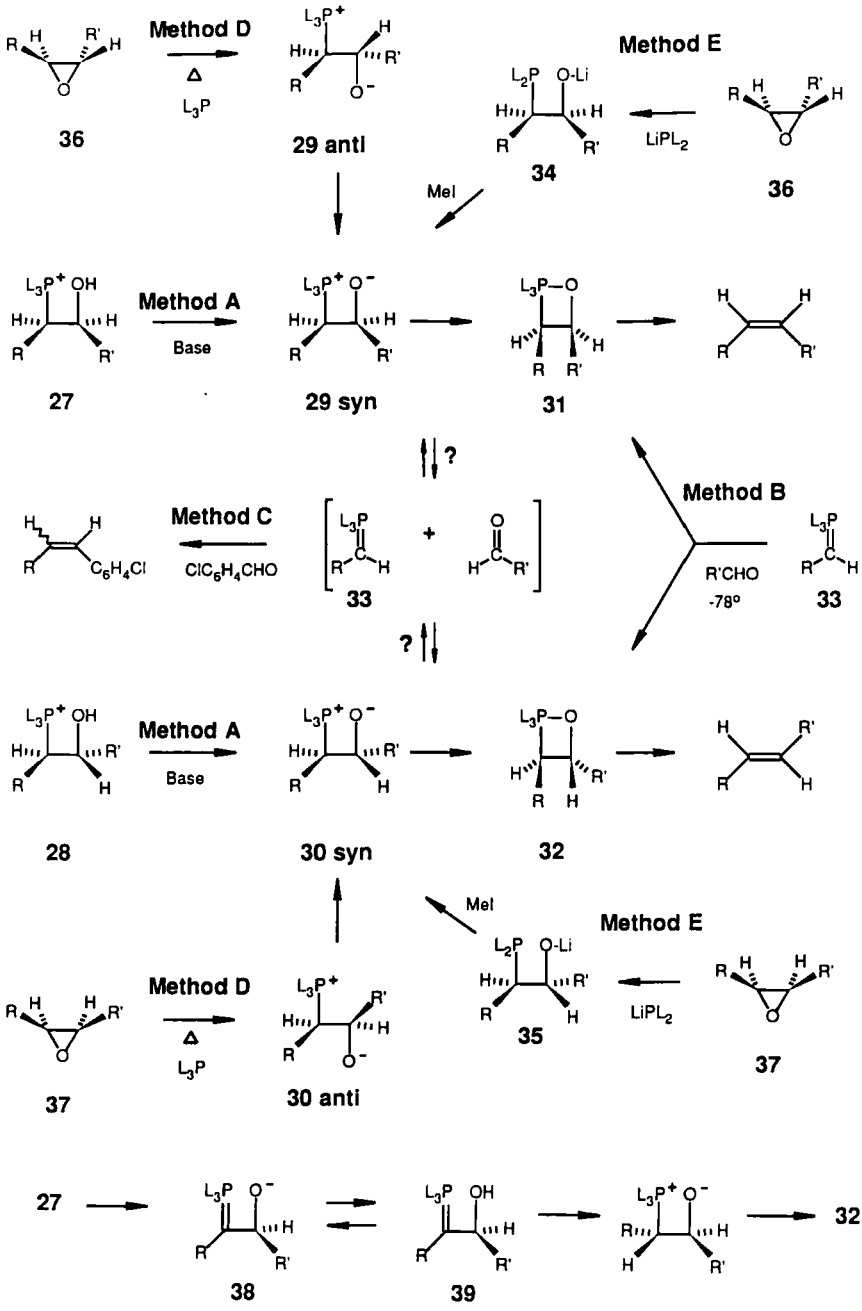
Subset 2. Equilibration in Experiments that Access Oxaphoshetanes via Deliberate Generation of Betaines.

							Initial Observation:		Final Observation:			Maximum % Equilibration:	
Entry	L_3	R'	R	Reactants:	Solvent	Li^+?	Temp.	**31**:**32**	**31**:**32**	Temp.	Z:E Ratio	via **29** and/or **31**	Method
9	Ph_3	C_6H_5	CH_3	**27** + LiOtBu	Et_2O	yes[i]	0°	(89:11)[j]	---	0°	59:41[c]	30%,[d] 0°	A[14]
10	Ph_3	C_6H_5	CH_3	**27** + LiOtBu	tBuOH	yes[k]	25°[l]	(89:11)[j]	---	RT[l]	18:82[c]	71%,[d] RT[l]	A[14]
11	Ph_3	C_6H_5	CO_2Et	**7** + Ph_3P	EtOH	no	20°	(97:3)[m]	---	20°	equil.[n]	20%°, 20°	C[21c]
12	Ph_3	C_6H_5	CO_2Et	**7** + Ph_3P	EtOH	no	78°	(>98:2)[m]	---	78°	equil.[n]	34%°, 78°	C[12]
13	Ph_3	C_6H_5	CO_2Et	**7** + Ph_3P	EtOH	no	100°	(>98:2)[m]	---	100°	equil.[n]	75%°, 100°	C[12]
14	Ph_3	C_6H_5	CO_2Et	**10** + Ph_3P	EtOH	no	78°	(>98:2)[m]	---	78°	equil.[n]	13%°, 100°	C[12]
15	Ph_3	C_6H_5	CO_2Et	**10** + Ph_3P	EtOH	no	100°	(>98:2)[m]	---	100°	equil.[n]	35%°, 100°	C[12]
16	Ph_2Me	C_6H_5	C_6H_5	**27** + NaOEt	EtOH	no	25°	(>98:2)[p]	---	25°	64:36[c]	36-45%,[d,q] 25°	A,C[13]
17	Ph_2Me	C_6H_5	C_6H_5	**27** + NaOEt	EtOH	no	50°	(>98:2)[p]	---	50°	52:48[c]	48%,[d] 50°	A[13]
18	Et_3	$PhCH_2(Me_2)C$	CH_3	**27** + KOtBu	THF	no	-43°	80:20[r]	<5:95[h]	-5°	17:83[c]	20%,-78°; 83%,> -43°	A,C[20]

Subset 3. Induced Reversal of Oxaphosphetanes in the Presence of Additives (Lithium-free Conditions; -78° to 23°).

Entry	L_3	R'	R	Oxaphosphetane(s)	Additive	Solvent	[M] (mol/L)	Z:E $PhCH{=}CHC_3H_7$	% Reversal	Method
19	Ph_3	C_6H_5	C_3H_7	**31**	none	THF	?	99:1[c]	1%	A[22a]
20	Ph_3	C_6H_5	C_3H_7	**31** + **32** (56:44)	**32**	THF	0.02	57:43[c]	<2%	A[23a]
21	Ph_3	C_6H_5	C_3H_7	**31** + **32** (56:44)	**32**	THF	0.1	49:51[c]	14%[s]	A[23a]
22	Ph_3	C_6H_5	C_3H_7	**31**	*p*-ClC_6H_4CHO, 4 mol	THF	0.1	96:4[c]	20%[t]	A,C[23a]
23	Ph_3	C_6H_5	C_3H_7	**31** + **32** (56:44)	*p*-ClC_6H_4CHO, 4 mol	THF	0.1	41:59[c]	31%[s,t]	A,C[23a]
24	Ph_3	C_6H_5	C_3H_7	**31**	*m*-$NO_2C_6H_4CHO$, 3 mol	THF	0.06	>97:3[c]	40%[t]	B,C[39b]
25	Ph_3	C_6H_5	C_3H_7	**31**	*p*-$CH_3C_6H_4CHO$, 3 mol	THF	0.06	>97:3[c]	9%[t]	B,C[39b]

(a) Dissolved salt; [Li^+] is known. (b) Assumed to be the kinetic ratio from the Wittig reaction; in sensitive systems such as entry 3, the ratio of **31**:**32** (and also the % equilibration) may be too low due to oxaphosphetane equilibration that might occur prior to the first observation. (c) Olefin ratio after warming to cause complete decomposition of intermediate oxaphosphetanes. (d) Intermediates were not assayed; upper limit values are based only on the alkene ratio. (e) Reproducibility problems; highest ratio reported is given. (f) Ratio based on diastereomer ratio of **27**:**28** after low temperature quenching with acid. (g) Exceptionally facile equilibration; kinetic ratio of **31**:**32** is probably higher, and so is the extent of equilibration. (h) Not a final equilibrium ratio; **31** is depleted by selective decomposition relative to **32**. (i) Lithium ion *was present, but homogeneous conditions were not demonstrated; [Li^+] is not known; [tBuOH]= 0.3M.* (j) *Starting* **27** *was an 89:11 mixture with* **28**; *ratio of oxaphosphetanes* was not determined in this study. (k) Lithium ion was present, but homogeneous conditions were not demonstrated; [Li^+] is not known. (l) Exact temperature not given; ambient conditions assumed to ensure thawed solvent. (m) Intermediates not assayed; isomeric purity of starting epoxide. (n) Products are isomerized by the Ph_3P reactant; Z:E ratios are not informative. (o) Intermediates not assayed; % equilibration is based on the % crossover with added ClC_6H_4CHO. (p) Intermediates were not assayed; starting **27** was a single diastereomer. (q) Crossover indicates 45% reversal; loss of stereochemistry indicates 36% equilibration in the absence of ClC_6H_4CHO. (r) Partial equilibration prior to first NMR observation indicates betaine reversal; starting **27** was a single diastereomer. (s) Value assumes that only **31** equilibrates. (t) sum of % Z to E conversion + % crossover.


Method D
Δ
L3P
Method E
LiPL2
Mel
Method A
Base
Method C
ClC6H4CHO
Method B
R'CHO
-78°
?
36
29 anti
34
29 syn
27
31
33
28
30 syn
32
30 anti
35
37
38
39

Scheme 7

after quenching with mineral acid at $-78°C$. The resulting mixture of **27** and **28** can be assayed by conventional NMR techniques.

Both of the above techniques can be reinforced by crossover experiments (method C) (12–14, 20, 21c, 22, 23a). An excess of ClC_6H_4CHO (ArCHO) is added to the solution *below the temperature for oxaphosphetane decomposition.* If stereochemical equilibration occurs exclusively by a retro-Wittig process to give the ylide **33**, then an excess of the crossover aldehyde must produce the crossover products. Since **33** would be intercepted by excess ArCHO faster than it can recombine with the original aldehyde, the conversion from one oxaphosphetane diastereomer into the other (i.e., from **31** to **32**) by way of any retro-Wittig mechanism will be suppressed using method C. However, it is essential to prove that the oxaphosphetane has not already decomposed prior to the addition of the crossover aldehyde. Otherwise, there is the risk of a false-negative crossover result.

If the β-hydroxyphosphonium salts **27** and **28** cannot be obtained independently, then it may be possible to resort to a variation of the original Speziale-Bissing technique (12) (method D) to generate the betaines **29** and **30** from the reaction of a phosphine with the trans and the cis epoxides **36** and **37**, respectively. However, this method is the least general and the most difficult to interpret (21c). Few epoxides are sufficiently reactive toward triphenyl phosphine unless the reaction mixture is heated far above the temperatures used in the corresponding Wittig reactions. This is a serious limitation because the degree of stereochemical equilibration increases substantially as the deoxygenation reaction temperature increases (12, 21c). Valid comparisons are possible only if method D can be performed at the same temperature as the corresponding Wittig reaction. Otherwise, the technique will overestimate equilibration of intermediates. The most informative experiments have been performed with phenylglycidate esters (**36** and **37** with $R = CO_2Et$ and $R' = Ph$). Interpretation of the results is complicated because the product enoate esters undergo Z:E equilibration under the conditions of the experiment, and no firm conclusions are possible unless method D is combined with method C (crossover experiment).

Method E is similar to method D in that it relies upon the nucleophilic cleavage of epoxides to generate stereochemically defined betaines. A two-step procedure is employed, starting with the reaction of a lithium phosphide with the cis or trans epoxides (**36** or **37**). The resulting alkoxy phosphines **34** or **35** are converted into betaines by direct alkylation with methyl iodide (19). This contrasts with method A where the betaine is generated by the deprotonation of a β-hydroxyphosphonium salt, and method E may therefore produce a different population of betaine rotamers than does method A. This subtle difference may explain why method E proceeds with higher stereospecificity than does method A in the Trippett–Jones experiment (Table 7; entry 16,

36–45% loss of stereochemistry in ethanol (13); Table 6; entry 14, 2% loss of stereochemistry in THF (19b); see also the discussion pertinent to Scheme 4).

Methods A, D, and E suffer from the inherent limitation that they deliberately generate a betaine as the precursor of the oxaphosphetane. Since there is no assurance that the reaction of an ylide with an aldehyde would involve the same ionic intermediate (19, 21) these control experiments may provide opportunities for stereochemical equilibration that may not be available to the corresponding Wittig reactions. If the oxaphosphetane generated by methods A or E is stable enough to observe directly, then it is usually possible to distinguish between oxaphosphetane equilibration, betaine equilibration, and other mechanisms for loss of stereochemistry (21c). However, this is not possible for oxaphosphetanes that contain unsaturated substituents at C_3 because oxaphosphetane decomposition is fast at $-78°C$ (21c). In these examples, method A (like method D or E) can only establish an *upper limit for equilibration of all of the conceivable intermediates*: betaines, betaine lithium halide adducts, oxaphosphetanes, and so on.

There are some additional potential complications with the control experiments. Loss of stereochemistry in method D can be due to product equilibration induced by the phosphine additive as already mentioned. Furthermore, equilibration in method A or E can occur because of competing (reversible) α-deprotonation to give the oxido ylide **38** or the derived hydroxy ylide **39** (21c). The latter problem can usually be avoided by lowering the temperature or by using a weaker base for the deprotonation of the β-hydroxyphosphonium salt **27** or **28** (21c). Nevertheless, positive equilibration results cannot be attributed to retro-Wittig reaction unless (1) crossover is also demonstrated or (2) labeling results can rule out the intervention of **38** or **39**.

In at least one case, method C detects equilibration while methods A and B do not. Thus, *cis*-oxaphosphetane **31** (Table 7, entry 19; $L_3P = Ph_3P$; $R = C_3H_7$; $R' = Ph$) can be generated as a single isomer (NMR assay) from pure **27** using potassium hexamethyl disilazide (KHMDS), and decomposition gives a 99:1 Z:E ratio of alkenes (22a). This result indicates minimal reversal. Nevertheless, extensive crossover occurs if *p*-ClC_6H_4CHO (22a) or *m*-$NO_2C_6H_4CHO$ (39b) is added, and the presence of **32** decreases stereospecificity ("synergism") (22a, 23c). The system is easily perturbed by the crossover aldehyde or other additives, but the origin of these complicating factors is not at all clear.

Method B (direct monitoring of the Wittig reaction) has the advantage that it produces oxaphosphetanes without necessarily involving betaines and without using additives (ClC_6H_4CHO, etc.) that might perturb the system. The technique is usually reliable when the Wittig reaction is fast at $-78°C$. This method assumes that the first diastereomer ratio observed (**31**:**32**) is the kinetic ratio. The assumption is generally valid (22, 23), but this may not be

easy to prove, especially if the low-temperature Wittig reaction produces a strong exotherm or if the temperature for oxaphosphetane decomposition is unusually low, as in Table 7, entry 16 (20, 21c). Unfortunately, method B cannot be used with carbonyl-stabilized ylides, nor with other families of conjugated ylides such as $Ph_3P{=}CHX$ (X = aryl, alkenyl, etc.) because the corresponding oxaphosphetanes decompose within seconds at $-78°C$. So far, such reactions can only be studied using the betaine generation methods.

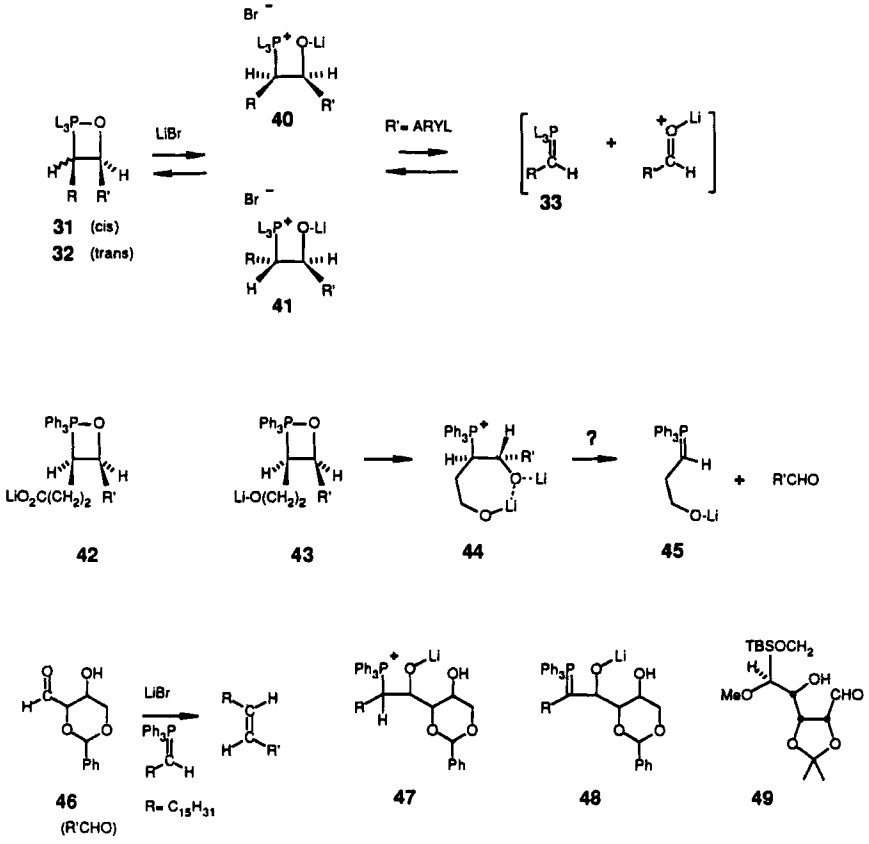
Tables 6 and 7 summarize results from stereochemical equilibration studies performed over the past decade by Maryanoff et al. (22, 23), and Vedejs et al. (20, 21c, 39–42). A few other convincing examples are included to expand the scope of the systems covered. Table 6 lists those examples where control experiments establish at least 90% retention of stereochemistry from intermediates to alkene products. As already discussed, the percentage of equilibration represents the upper limit for loss of stereochemistry from all possible pathways in the control experiments. No attempt has been made to determine whether the minor levels of stereochemical leakage in Table 6 occur at the stage of oxaphosphetanes, betaines, or other potential intermediates. Table 6 includes entries corresponding to all of the principal families of Wittig reagents: nonstabilized ylides (entries 1–12, 24, 25, 29, and 30), benzylic ylides (entries 13–17 and 28), allylic ylides (entries 22, 23, 26, and 27), and ester-stabilized ylides (entries 18–21). The corresponding Wittig reactions must take place under dominant kinetic control.

There are also some examples where significant reversal and stereochemical equilibration of intermediates has been demonstrated in aldehyde Wittig reactions (Table 7, subset 1). Several additional examples of reversal from betaine generation experiments may also be relevant, depending on whether the same betaines play any role in the Wittig process (Table 7, subset 2). The following generalizations follow from the comparison of Tables 6 and 7.

1. Lithium-free Wittig reactions proceed without significant reversal, except for the $Et_3P{=}CHCH_3$ or $Bu_3P{=}CHC_3H_7$ examples with tertiary or aromatic aldehydes (Table 7, entries 6, 7, 8).
2. Intermediates from ylides and aliphatic aldehydes do not undergo reversal (exceptions: Table 7, entries 5–7).
3. Significant reversal occurs only for precursors of (*Z*)-alkenes (compare Table 7, entry 18 and Table 6, entry 29; see also Table 6, entries 7, 8, 9, 10, 24, 25). Exceptions are known at high temperatures: see Table 7, entries 14, 15.
4. Deliberate betaine generation maximizes the risk of reversal. The risk is highest for betaines corresponding to adducts of ArCHO.
5. For Wittig reactions, the risk of reversal is highest for ArCHO in the presence of lithium ion (Table 7, entries 1–5), and for reactions of

ylides containing anionic (alkoxide, carboxylate, amido) substituents with lithium as the counterion. Other risk factors include hydroxylic solvents (compare Table 7, entry 16, with Table 6, entries 13, 14) or high temperature (compare Table 7, entries 12, 13, and Table 6, entry 19).

Reversal correlates with the presence of lithium ion and also with the involvement of betaine species. These two risk factors are interrelated because lithium halides rapidly cleave oxaphosphetane **31** or **32** (Scheme 8) at $-70°C$ resulting in the reversible formation of the betaine lithium halide complexes **40** or **41**, respectively (18b). Donor solvents shift the equilibrium toward the oxaphosphetane by coordinating the lithium halides and thereby promote stereospecific decomposition to the alkenes. If the solvent is not an effective lithium coordinating agent, then **40** and **41** decompose slowly, and the risk of



Scheme 8

reversal will increase. Factors that weaken the C—C bond (unsaturated R or R') promote bond cleavage and stereochemical equilibration via **33**.

Oxaphosphetanes such as **42** or **43**, containing anionic side-chain substituents, are especially sensitive to the lithium ion–catalyzed equilibration mechanisms (Table 7, entries 3, 5). Maryanoff et al. (2j, 22a, 23b) have demonstrated that retro-Wittig cleavage is involved (positive crossover results, method C) and have suggested that the anionic group may facilitate reversal by interacting with the pentavalent phosphorus center in the oxaphosphetane intermediate. This rationale does not explain why lithium bases are more effective than sodium or potassium bases in the E-selective olefinations of oxido ylides. The present authors prefer an alternative explanation where the anionic substituent exerts its influence at oxaphosphetane oxygen. This involves a seven center interaction that is shown in the conversion from **43** to the betaine lithium halide adduct **44** or some equivalent aggregated species. Stereochemical equilibration would then occur via betaine C—C bond cleavage to give the corresponding ylide, followed by the usual recombination process to produce the more stable trans-disubstituted oxaphosphetane.

A variety of anionic ylides reacts with high E selectivity with the reversal-prone aromatic aldehydes. On the other hand, aliphatic aldehyde adducts are more resistant to Li^+-induced betaine equilibration. The γ-oxido ylides appear to have the optimal substitution pattern for betaine reversal, and these reagents afford useful (*E*)-alkene selectivity with aliphatic as well as aromatic aldehydes, results that are tabulated later. Only the aromatic aldehyde example (Table 7, entry 4) has been studied in depth, but it seems safe to conclude that all of the E-selective γ-oxido ylide reactions are dominated by betaine reversal (23b). Other anionic ylides react with aliphatic aldehydes to give lower, less predictable (*E*)-alkene selectivity (for example, Table 7, entry 5; 42:58 Z:E).

There are indications that a hydroxyl group in the carbonyl substrate can also promote E selectivity, as in the reaction of **46** with a nonstabilized ylide ["near-exclusive" (*E*)-alkene product] (46a). A betaine reversal process may be involved here as well, assisted internally by the proximity between the hydroxyl group of the aldehyde fragment and the oxaphosphetane or betaine oxygen (structure **47**) and externally by the deliberate addition of excess lithium bromide to ensure conversion of the oxaphosphetane into **47**. If the conditions are sufficiently basic, stereochemical equilibration might also occur via **48** (reversible deprotonation α to phosphorus in **47**). There are also some examples of E-selective reactions of γ-hydroxy aldehydes (for example, **49** + $Ph_3P{=}CHCHMe_2$; 16:84 Z:E, Li-containing conditions) (46b). Decisive control experiments to probe reversal or mechanistic details in these reactions have not yet been reported.

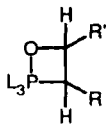
Earlier attempts to understand stereoselectivity overstated the extent of

retro-Wittig reaction (1, 2). Part of the reason was that the early control experiments had concentrated on benzaldehyde-derived adducts, substrates that are especially sensitive to the catalyzed reversal process. Another reason can be traced to the somewhat deceptive control experiments performed at high temperatures or in hydroxylic solvents (12, 13). However, the fundamental difficulty in all of the early studies was that rates of decomposition of isomeric Wittig intermediates could no be measured directly in any example. This resulted in the logical (but incorrect) assumption that trans-disubstituted oxaphosphetanes would have a kinetic advantage in the decomposition step to afford the more stable (*E*)-alkene. If this were so, then any equilibration process that allows access to the trans-disubstituted oxaphosphetanes might explain increased formation of (*E*)-alkene. Conversely, increased (*E*)-alkene selectivity might then be used as a qualitative test for equilibration of intermediates. These generalizations are incorrect, as shown below.

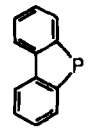
Recent improvements in instrumentation have made possible the direct monitoring of oxaphosphetane diastereomers in the decomposition step, and qualitative half-lives for several cis–trans pairs are now known. Three of the pairs are included in Table 8 (20, 21c). The results show that the cis-disubstituted oxaphosphetanes **51** and **53** decompose at least five times faster compared to the trans diastereomers **50** and **52**, respectively. Earlier, Maryanoff et al. (22a, b) observed a similar, although smaller, trend in some related systems. It is not possible to achieve increased (*E*)-alkene selectivity by preferentially draining off the trans diastereomer in an equilibrium of isomeric oxaphosphetanes. Preferential decomposition can only favor the (*Z*)-alkene isomer because the decomposition of the cis-disubstituted oxaphosphetane has the kinetic advantage (20, 21c, 22a, b)! The reason that interconversion of oxaphosphetane or betaine diastereomers promotes the eventual formation of (*E*)-alkenes is that the trans-disubstituted oxaphosphetanes are *thermodynamically more stable* than the cis diastereomers. This fact has been demonstrated conclusively using NMR methods by Maryanoff et al. [for example, Table 7, entries 7, 8, (22a); see also entries 6 and 18 (20)]. The rates of oxaphosphetane decomposition *do not reflect the stability advantage of (E)- versus (Z)-alkenes.* The transition state for alkene formation must therefore come relatively early along the reaction coordinate for oxaphosphetane decomposition.

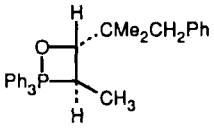
Oxaphosphetanes containing an unsaturated substituent R at C_3 are exceptionally short-lived. Only the unusually stable dibenzophosphole derivatives **52c**, **53c**, and **53b** can be detected, but not even this phosphorus environment provides sufficient stabilization to allow detection of **53d**, the oxaphosphetane that would be formed from an ester-stabilized ylide (21c). Strongly electron-withdrawing substituents are required in addition to a five-membered ring, as in structure **F** (Tables 4 and 5), the first known

TABLE 8
Qualitative $T_{1/2}$ for Oxaphosphetane Decomposition

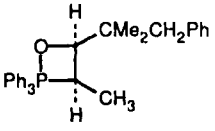


a. R= ALKYL **c.** R= VINYL
b. R= PHENYL **d.** R= CARBOALKOXY

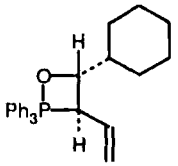
DBP= 



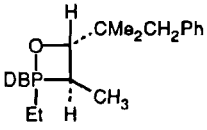
50a 1 h, -3°



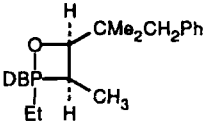
51a <10 min, -3°



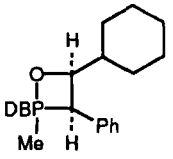
50c <30 sec, -78°



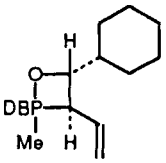
52a 7 h, 65°
minutes, 110°



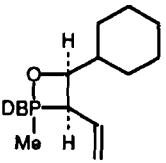
53a 1 h, 55°



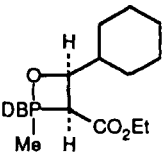
53b 30 min, -20°



52c 30 min, -40°



53c 5 min, -40°



53d <1 min, -78°

oxaphosphetane containing an ester group at C_3 (34f). The oxaphosphetane **F** decomposes to the alkene above 70°C while the C_3-unsubstituted analog **G** (Table 5) must be heated to 200°C to achieve similar rates. Structures **F** and the related **H** (Table 5) are also of interest because their decomposition rates have been investigated in several solvents (34e, f). A 1.3-fold increase in decomposition rate is observed for **H** in acetonitrile versus toluene, while the corresponding ratio for **F** is 15. The solvent effect for **F** is significant, but it is smaller than would be expected if ionic intermediates were involved. The authors suggest an asynchronous cycloreversion process with relatively more bond breaking at $P—C_3$ compared to $O—C_4$ (34e, f). In the analogous adducts of $Ph_3P{=}CHR$, none of the oxaphosphetanes **50b,c,d** and **51b,c,d** has ever been detected because decomposition to the alkene occurs within a fraction of a minute at − 78°C. There is no time for stereochemical equilibration of oxaphosphetanes of this type under typical Wittig conditions. Exceptions to this generalization may be possible in the presence of lithium halides if the salt concentration is high enough to intercept the oxaphosphetane as the lithium halide betaine adduct [**40** or **41**; R = alkenyl or phenyl (47)]. However, there is no evidence for retro-Wittig cleavage or equilibration under lithium-free conditions in the allylic or benzylic ylide reactions, as expected if these reactions follow reaction profile **c** (Fig. 2).

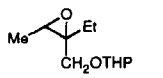
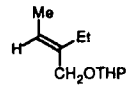
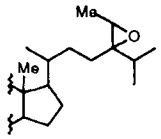
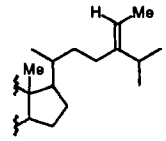
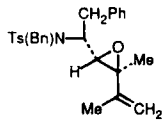
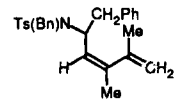
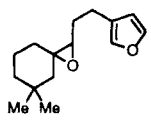
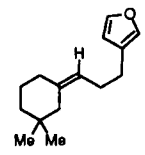
By the same logic, it is unlikely that the stabilized ylide reactions can be influenced by stereochemical equilibration. It would be difficult for any equilibration process to compete with the exceptionally rapid oxaphosphetane decomposition step. Partial loss of stereochemistry does occur in some of the high-temperature control experiments at the betaine stage, as listed in Table 7, but oxaphosphetane decomposition takes place with retention of stereochemistry (Table 6, entries 18–21) (21c).

The observations summarized in Table 8 have important preparative consequences. To achieve the highest possible (*E*)-alkene selectivity in a system that is capable of stereochemical equilibration, it is essential to provide sufficient time for oxaphosphetane equilibration below the decomposition temperature. This is best done by monitoring the diastereomer mixture using NMR methods to establish the temperature thresholds for diastereomer equilibration as well as for alkene formation from the more reactive cis-diastereomer. Once these temperatures are known, equilibration can be allowed to proceed below the temperature for (*Z*)-alkene formation until the optimum ratio of trans–cis oxaphosphetanes is obtained. Subsequent warming completes the optimized E-selective alkene synthesis in an equilibrating system (Table 7).

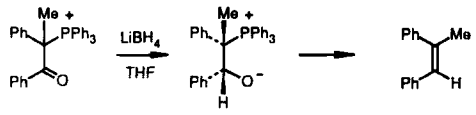
The mechanistic studies discussed so far deal with the Wittig reactions of aldehydes and nearly always focus on the stereochemical aspects of 1,2-disubstituted alkene synthesis. By comparison, little is known regarding

TABLE 9
Stereospecific Decomposition of Trisubstituted Oxaphosphetanes

METHOD E (epoxide + $LiPPh_2$; MeI/THF, 0°-20°)

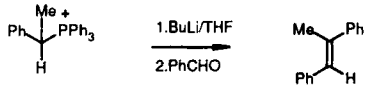
STARTING MATERIAL	Z:E RATIO	PRODUCT	Z:E RATIO	YIELD	REF.
	>98:2		<1:99	60%	19b
	<5:95		>95:5	80%	48
	<5:95		>95:5	60%	49
	15:85		80:20	65%	50

MODIFIED METHOD A; BETAINE GENERATION BY KETOPHOSPHONIUM SALT REDUCTION WITH $LiBH_4$/THF



Z:E RATIO		
89:11	80%	51

COMPARE WITH:



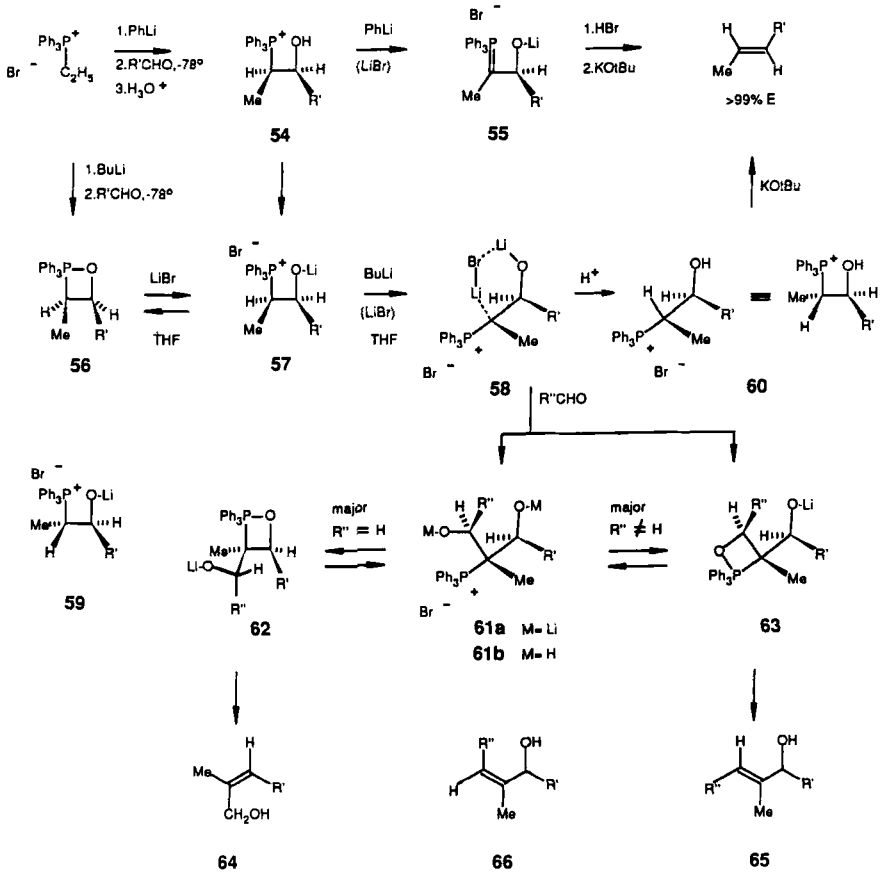
20:80	--	51

trisubstituted alkene synthesis via phosphorus ylides. According to the empirical results given in Table 9, trisubstituted oxaphosphetanes also appear to decompose stereospecifically. Although none of the examples in Table 9 has been studied in depth, there is no reason to believe that the Wittig reactions of ketones are fundamentally different from the extensively studied reactions of aldehydes. Likewise, aldehyde reactions with ylides $L_3P{=}CR_2$ also appear to be unexceptional. In the absence of evidence to the contrary, kinetic control can be assumed in the Wittig synthesis of trisubstituted alkenes, but there is little systematic information to guide the evaluation of lithium ion or equilibration effects.

VI. OXIDO YLIDE REACTIONS; MODIFICATION OF OXAPHOSPHETANE STEREOCHEMISTRY

Loss of oxaphosphetane stereochemistry can take place by deprotonation pathways, provided that the reaction conditions allow the formation of betaine derivatives. The first systematic studies were described by Schlosser et al. between 1965 and 1970 (14, 52, 53). An ylide $Ph_3P{=}CHCH_3$ was generated using an alkyl- or aryllithium base (Scheme 9) and was made to react with an aldehyde at $-78°C$, well below the temperature for alkene formation. Subsequent addition of a second equivalent of the organolithium reagent was performed to generate a β-oxido ylide **55** (originally named a "betaine ylide"), and sequential addition of acid and potassium *tert*-butoxide was then performed to produce (*E*)-alkene of $>99\%$ isomeric purity in the best examples (52, 53). It was also shown that treatment of the stereochemically defined β-hydroxyphosphonium salt **54** (R′ = phenyl) with an excess of the organolithium reagent followed by acid and butoxide as before likewise afforded the (*E*)-alkene (14). At the time that this work was performed, it was not known that **56** is the stable low-temperature intermediate in the Wittig reaction. Accordingly, the above results were attributed to the equilibration of betaines **57** and **59** via **55**. It was assumed that **59** is the more stable isomer and that an equilibrium preference for this betaine is responsible for the E-selective alkene formation.

Subsequent work by Corey et al. (54, 55) has left little doubt that reactions of the oxido ylide **55** are controlled by kinetic, not equilibrium factors. According to these workers, **55** is quenched irreversibly by electrophiles in a geometry that can be approximated by the betaine-lithium halide aggregate **58** (55). Although the actual solution structure of **55**=**58** is very complex according to NMR evidence (56), structure **58** provides a useful guide for stereochemical predictions in the quenching step using protic acids or most other electrophiles, and it also underscores the importance of lithium halides



Scheme 9

in many of the oxido ylide reactions. There has been some confusion on this point, perhaps because the first full paper on oxido ylides specified the use of lithium-free alkylidenetriphenylphosphoranes in the first step, the reaction with an aldehyde, and then used home-made (lithium halide-containing) organolithium reagents for the subsequent deprotonation step to form **55** (53, 57). It is now known that the oxaphosphetane **56** is formed in the first step. Since **56** lacks acidic C—H bonds (56), electrophilic catalysts (Li^+, hydroxylic impurities, etc.) are required to provide access to the more acidic betaine species (for example, **57**). If such catalysts are not provided in sufficient concentration, the deprotonation will not go to completion and high E selectivity will not be achieved. Sodium or potassium cations generally do not

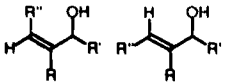
have sufficient Lewis acidity to cleave the oxaphosphetane. Therefore, sodium or potassium bases are not recommended for the E-selective alkene synthesis.

Corey et al.'s (54, 55) study established kinetically controlled oxido ylide trapping in a fascinating series experiments that used carbonyl electrophiles and resulted in the stereoselective synthesis of trisubstituted alkenes. First, it was observed that treatment of **55**=**58** with an aldehyde R″CHO (R″ = alkyl or aryl) produces the alkene **65** as the major product. This isomer corresponds to the formation and selective decomposition of an oxaphosphetane **63**. However, it was also observed that treatment of the dihydroxyphosphonium salt **61b** with two equivalents of methyllithium likewise affords **65** as the major product (93:7 **65**:**66** for R′ = R″ = CH_3) (55). This experiment should generate the oxido betaine **61a**, an intermediate that is capable of forming two different isomeric oxaphosphetanes, **62** as well as **63**. Since the major alkene product **65** is formed via **63**, the preference for one of the two decomposition pathways must be due to differences in stereochemistry at the oxygenated carbons in **61a** and in the derived oxaphosphetanes. Indeed, **63** has the largest oxaphosphetane substituents trans, while in **62** the largest groups are cis. In any event, a diastereomer of **61b** (not shown) was also obtained in small amounts. Treatment of this material with methyllithium afforded **66** as the major alkene. Taken together with the first deprotonation experiment, this result proves that **61a** and **63** decompose under dominant kinetic control and that regiochemistry can be controlled by stereochemistry at the stage of **61a**.

One other experimental result from the Corey et al. study is important for trisubstituted alkene synthesis. When **55**=**58** is quenched with formaldehyde, the stereochemistry of C—C bond formation remains the same as before. However, the regiochemistry of the elimination step no longer favors the second aldehyde added, and the major product is now the allylic alcohol **64** (54). This experiment suggests that both oxaphosphetanes **63** and **62** are in equilibrium with the lithium halide adduct **61a**. Decomposition is controlled by the nature and degree of oxaphosphetane substitution as well as by stereochemistry. In the formaldehyde reaction, these factors combine to favor the trisubstituted alkene (via **62**) over the disubstituted alkene that would be formed via **63** (R″=H). Several examples of trisubstituted alkene synthesis using Corey's method are summarized in Table 10 without further comment because the origins of stereochemistry are not understood in detail, but Corey's model **58** is consistent with the available evidence.

All of the oxido ylide reactions demand the presence of at least one equivalent of lithium halide. This requirement is most easily satisfied when the starting alkylidenetriphenylphosphorane is generated by the conventional butyllithium method from phosphonium salts in THF. Thus, Maryanoff et al. (22a) treated $Ph_3P^+C_4H_9\ Br^-$ sequentially with butyllithium, benzaldehyde, butyllithium, and acid to give **60** (R′ = phenyl; replace Me by propyl) con-

TABLE 10
Examples of Corey Trisubstituted Olefin Synthesis

	YLIDE	1st ALDEHYDE	2nd ALDEHYDE	PRODUCTS			
	Ph_3P=CHR	R'CHO	R''CHO				
Entry	R	R'	R''	Yield	Z : E	Yield	Reference
1	CH_3	CH_3	CH_3	---	7 : 93	65%[a]	55
2	"	Ph	Ph	---	<1 : 99	??	55
3	"	Ph[b]	Ph	---	<1 : 99[c]	74%	54a
4	"	Ph	Ph[b]	---	<1 : 99[d]	74%	54a
5	"	CH_3	C_6H_{13}	---	<1 : 99	67%	54a
6	"	C_6H_{13}	CH_3	---	<1 : 99	67%	54a
7	"	"	C_6H_{13}	---	10 : 90	??	54a
8	"	"	H	73%		---	54a
9	$(CH_2)_2X$[e]	$(CH_2)_2Y$[e]	"	50%		---	54b
10	$(CH_2)_2Z$[e]	"	"	46%		---	54c

(a) The oxido intermediate was isolated as the dihydroxyphosphonium salt. The yield refers to the transformation from this species to products (MeLi/Et_2O @ RT).

(b) 1-Deuteriobenzaldehyde was used.

(c) Deuterium incorporation exclusively at the carbinol carbon.

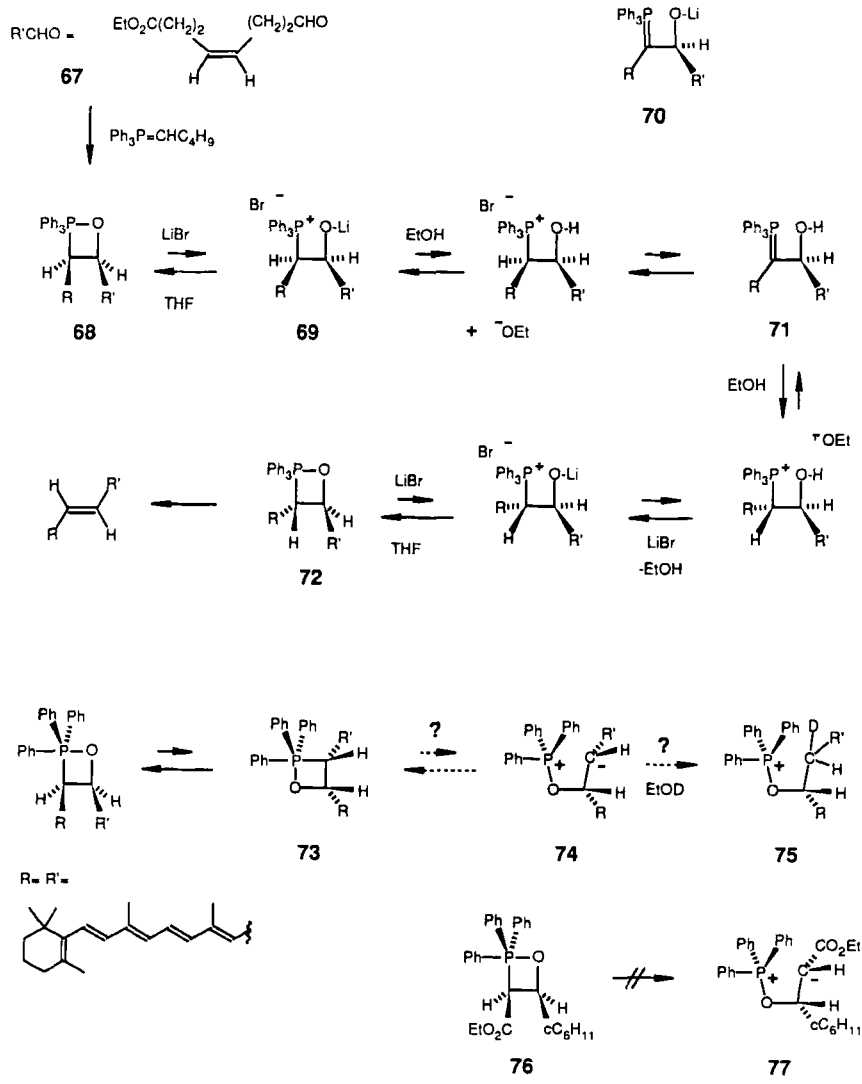
(d) Deuterium incorporation exclusively at the vinyl carbon.

(e) X = CH=C(Me)Et. Y = (Me)C=$CHCH_2$OTHP. Z = CH=$C(Me)_2$.

taining less than 1% of the diastereomer. Similarly, **55** = **58** (R′ = *tert*-Bu) was obtained by adding butyllithium to the mixture of **56** and **57**, and low-temperature quenching with acid gave the β-hydroxyphosphonium salt **60** (unoptimized ca. 9:1 diastereomer ratio) (20). Subsequent reaction of recrystallized **60** with sodium or potassium bases afforded the (*E*)-alkene. This recent variation of the Schlosser–Wittig method may prove simpler experimentally than some of the available alternatives (57), but it requires careful optimization of experimental variables to allow sufficient time, lithium halide, and alkyllithium reagent to drive the deprotonation step to completion. Otherwise, the product alkene will be contaminated by the (*Z*)-isomer due to the presence of residual **56** or **57** in the acid-quenching step.

One additional technique that can modify oxaphosphetane stereochemistry will be mentioned to underscore the subtle relationship between experimental conditions and the mechanistic variations that are possible. Anderson and Henrick have shown that Li^+-containing Wittig intermediates can be partly equilibrated by the addition of alcohols (Scheme 10) (58). Thus, reaction of aldehyde **67** with pentylidenetriphenylphosphorane (generated from the phosphonium bromide using butyllithium) in ether afforded a 78:22 Z:E alkene mixture, typical for a Wittig reaction conducted in the presence of LiBr. When the experimental procedure was altered by adding ethanol to the Wittig intermediate (4.5 h between −78 and −50°C), considerably more of the (*E*)-alkene was formed (31:69 Z:E) (58). Retro-Wittig cleavage was ruled out by suitable crossover experiments. However, the use of deuterated ethanol for the equilibration step afforded alkenes with up to 65% deuterium per mole. These results indicate that an α-deprotonation mechanism must be involved, similar to that deduced for the Schlosser (*E*)-alkene synthesis. However, there are some important differences. As before, LiBr will induce reversible oxaphosphetane ring cleavage to generate the betaine lithium halide adduct **69**. Subsequent α deprotonation might conceivably involve an oxido ylide **70**, but the alternative of β-hydroxy ylide (**71**) formation appears more likely beacuse the conditions are not strongly basic. Assuming that most of the material remains in the oxaphosphetane form (**68** and **72**), the equilibrium is driven by the thermodynamic preference for the trans-disubstituted isomer **72** relative to the cis isomer **68**.

Bestmann (59) also reports one example of partial loss of stereochemistry and deuterium incorporation when an oxaphosphetane is treated with several equivalents of deuterated ethanol at −78°C followed by warming. His explanation invokes pseudorotation of the oxaphosphetane to give the less stable pseudorotamer **73**, followed by reversible C—P bond heterolysis to afford a zwitterion **74**. Loss of oxaphosphetane stereochemistry is attributed to rotation about the C—C bond in **74**. Competing formation of unlabeled alkene is suggested to involve the direct elimination of triphenylphosphine



Scheme 10

oxide from **74**, while the D-labeled alkene is presumed to arise from the deuteration of **74** to give an alkoxyphosphonium salt **75** followed by elimination. Bestmann (59) did not dicuss the hydroxy ylide mechanism for deuterium incorporation, but the experimental conditions appear to be similar to those used by Anderson and Henrick (58). The latter authors make a convincing

case for the hydroxy ylide mechanism as the pathway for deuterium exchange. There is also a considerable body of evidence against stereochemical equilibration via high-energy intermediates such as the Bestmann zwitterion **74**. Several of the examples of stereospecific oxaphosphetane decomposition given in Table 6 should have encountered **74** if such a species is energetically feasible. Thus, the intermediate **76** in a stabilized ylide reaction should have the best opportunity for C—P bond heterolysis to give the stabilized zwitterion **77**. However, the corresponding control experiment in ethanol as well as in THF proceeds without significant loss of stereochemistry (Table 6, entry 20) (21c), and the formation of **77** is ruled out in this example as well as in a number of others (21c).

To summarize the material presented so far, there are four distinct, but mechanistically interrelated pathways for the stereochemical modification of Wittig reaction intermediates:

1. *Lithium Halide–catalyzed Reversal via Betaine Lithium Halide Adducts.* This is the most common mechanism for loss of stereospecificity under Wittig conditions and often contributes to the stereochemical outcome of bezaldehyde reactions in the presence of lithium ion. The process is most facile for ylides containing anionic (alkoxide, carboxylate, or amido) substituents.
2. *Thermal Equilibration of Salt-free cis-Disubstituted Oxaphosphetanes.* Only three examples of this process are known. The reaction appears to occur spontaneously when certain oxaphosphetanes are warmed to temperatures near the decomposition point. Spontaneous equilibration is restricted to oxaphosphetanes derived from P-trialkyl ylides and aromatic or tertiary aliphatic aldehydes. A catalyzed process via betaine derivatives is not ruled out, but there is no direct evidence to implicate catalysis.
3. *Schlosser Synthesis of (E)-alkenes.* In contrast to the first two examples, this process does not involve equilibration of stereoisomers. The Schlosser method establishes stereochemistry in a kinetically controlled quenching reaction of an oxido ylide with acid.
4. *Partial Epimerization of Lithium Halide–containing Oxaphosphetanes by Alcohols.* This process occurs via reversible formation of β-hydroxy ylide intermediates.

A fifth category must be mentioned even though it may have no direct relevance to Wittig alkene synthesis. This is the equilibration of anti betaines under lithium-free conditions that was encountered in early attempts to design control experiments [Speziale and Bissing (12) and Trippett and Jones (13)]. As already discussed, strong evidence is now available that the

corresponding syn betaines as well as the derived oxaphosphetanes decompose without loss of stereochemistry (21c).

Reaction conditions play a critical role in many of the above options for loss of stereochemistry, and factors such as the presence of Lewis acids (i.e., lithium ion), elevated temperatures, and hydroxylic solvents or impurities may well induce partial equilibration. However, the most commonly employed Wittig procedures rely upon inert solvents (ethers, hydrocarbons, DMSO, etc.) and temperatures no higher than 25°C. Under these conditions, significant equilibration is seldom encountered, especially with the simple nonstabilized ylides.

VII. STEREOCHEMICAL RESULTS; EMPIRICAL Z:E DATA

Alkene Z:E ratios from representative Wittig reactions are tabulated in the following sections. The tables begin with reactions of simple carbonyl substrates, organized according to ylide structural types. Reactions involving more complex carbonyl substrates are tabulated last, and these examples are organized according to the carbonyl reactant. An attempt has been made to restrict table entries to reactions where key variables including the phosphonium counterion, solvent, base, and the temperature are specified. This information is not always clearly stated in the original publications, and assumptions were necessary in some of the entries. In a few isolated cases where the results appear to contradict similar experiments in the tables, the Z:E ratios are given in parentheses together with a question mark to alert the reader that the result may not be general or that the experiment may need to be repeated. To make systematic comparisons easier, small subsets of data obtained under comparable conditions have been placed at the end of some of the tables.

VIII. NONSTABILIZED YLIDES $Ph_3P{=}CHR$

Table 11 summarizes many of the representative Wittig reactions of nonstabilized ylides $Ph_3P{=}CHR$ that contain no other functional groups that might influence the stereochemical outcome. The table entries have been compared with relevant control experiments discussed in connection with Tables 6 and 7. In those cases where $> 5\%$ catalyzed or spontaneous equilibration of oxaphosphetane stereochemistry appears likely, the stereochemical results are marked by a double asterisk. Entries for the lithium-containing experiments include a rough estimate of the maximum possible lithium ion concentration. However, the estimate assumes that all of the

TABLE 11

Empirical Alkene Z:E Selectivity in Reactions of Nonstabilized Ylides $Ph_3P{=}CHR$ and Aldehydes R'CHO

Unbranched Ylides.

Entry	R'	R	X⁻	Base	Solvent	Temp	$[Li^+]^a$ (M)	Z : E	Yield	Ref.
1	Et	Et	Br	$NaNH_2$	PhH/pet ether	0°		97 : 3	70%	14
2	Et	Et	Br	K	HMPA	RT		96 : 4	82%	60a
3	Et	Et	??	BuLi	DMF[b]	RT		93 : 7	--	5c
4	Et	Et	Cl	BuLi	DMF	RT		94 : 6	--	5c
5	Et	Et	I	BuLi	DMF	RT		95 : 5	--	5c
6	Et	Et	??	BuLi	PhH[b]	RT		92 : 8	--	5c
7	Et	Et	I	BuLi	PhH	RT	0.33	77 : 23	--	5c
8	Et	$(CH_2)_9OH$	Br	$LiNH(CH_2)_3NH_2$	THF	-78°	0.25	99 : 1	31%	60b
9	Et	$(CH_2)_9OH$	Br	BuLi	THF	-78°	0.25	79 : 21	39%	60b
10	Pr	Pr	Br	$NaNH_2$	PhH/pet ether	0°		95 : 5	78%	14
11	Pr	Pr	Br	$NaNH_2$	Ether	-75°		98 : 2	--	61
12	Pr	Pr	Br	BuLi	Ether	10°	0.20	84 : 16	82%	11e
13	C_5H_{11}	Me	Br	$NaNH_2$	THF	25°		87 : 13	83-95%[c]	62
14	C_5H_{11}	Me	Br	$NaNH_2$	THF	0°		90 : 10	"	62
15	C_5H_{11}	Me	Br	$NaNH_2$	THF	-25°		92 : 8	"	62
16	C_5H_{11}	Me	Br	$NaNH_2$	THF	-50°		94 : 6	"	62
17	C_5H_{11}	Me	Br	$NaNH_2$	THF	-75°		96 : 4	"	62
18	C_5H_{11}	Me	Br	$NaNH_2$	THF	-100°		97 : 3	"	62
19	C_5H_{11}	Et	Br	$NaNH_2$	PhH/pet ether	0°		96 : 4	86%	14
20	C_5H_{11}	Et	Br	$NaNH_2$	THF	-75°		97 : 3	95%	62
21	C_5H_{11}	Et	Br	NaHMDS	THF	-75°		96 : 4	70%	62
22	C_5H_{11}	Et	Br	NaH	DMSO	RT[d]		91 : 9	60%	62
23	C_5H_{11}	Et	Br	BuLi	Ether	-75°	0.50[e]	(50:50?)	81%	62

24	C_5H_{11}	Pr	Br	$NaNH_2$	THF	-75°		98 : 2	--	65
25	C_5H_{11}	Pr	Br	LiHMDS	THF	-78°	0.03	90 : 10	--	23c
26	C_5H_{11}	Pr	Br	LiHMDS	THF	-78°	0.07	85 : 15	--	23c
27	C_5H_{11}	Pr	Br	LiHMDS	THF	-78°	0.25	80 : 20	--	23c
28	C_5H_{11}	Pr	Br	LiHMDS	THF	-78°	0.31	82 : 18	--	23c
29	C_5H_{11}	Pr	Br	LiHMDS	THF	-78°	0.90	78 : 22	--	23c
30	$PhCH_2CH_2$	Me	Br	KHMDS	THF	-78°		94 : 6	92%	20
31	$PhCH_2CH_2$	Me	Br	BuLi	THF	-78°		70 : 30	--	18a
32	Ph	Me	??	$NaNH_2$	THF	-75°		87 : 13	99%	63
33	Ph	Me	Br	$NaNH_2$	Toluene	0°		91 : 9	--	61
34	Ph	Me	Br	$NaNH_2$	PhH/pet ether	0°		87 : 13	98%	14
35	Ph	Me	Br	K	HMPA	RT		86 : 14	55%	60
36	Ph	Me	??	K_2CO_3[f]	THF	66°		85 : 15	96%	64
37	Ph	Me	Br	BuLi	THF	-78°	??	67 : 33**	--	18a
38	Ph	Me	??	BuLi	Ether	-75°	0.40[e]	61 : 39**	68%	63
39	Ph	Et	Br	$NaNH_2$	PhH/pet ether	0°		96 : 4	88%	14
40	Ph	Et	Br	$NaNH_2$	THF	-75°		94 : 6	97%	62
41	Ph	Et	Br	NaHMDS	THF	-75°		85 : 15	97%	62
42	Ph	Et	Br	NaH	DMSO	RT[d]		73 : 27	68%	62
43	Ph	Et	Cl	NaH	DMF	20°		75 : 25	58%	5d
44	Ph	Et	Cl	BuLi	DMF	20°	0.30	73 : 27	52%	5d
45	Ph	Et	Cl	BuLi	PhH	20°	0.30	79 : 21	62%	5d
46	Ph	Et	Cl	BuLi	Ether	20°	0.30	80 : 20	70%	5d
47	Ph	Et	I	BuLi	PhH/Hex[g]	0°		89 : 11	--	5c
48	Ph	Et	I	BuLi	PhH/Hex	0°	??	61 : 39**	--	5c
49	Ph	Et	Br	BuLi	Ether	-75°	0.50[e]	86 : 14	80%	62
50	Ph	Pr	Br	$NaNH_2$	THF	-75°		96 : 4	--	61

TABLE 11 *(Continued)*

Unbranched Ylides.

Entry	R'	R	X⁻	Base	Solvent	Temp	$[Li^+]^a$ (M)	Z : E	Yield	Ref.
51	Ph	Pr	Br	NaHMDS	THF	-78°		91 : 9	52%	23c
52	Ph	Pr	Br	LiHMDS	THF	-78°	0.015	97 : 3	--	23c
53	Ph	Pr	Br	LiHMDS	THF	-78°	0.05	83 : 17**	--	23c
54	Ph	Pr	Br	LiHMDS	THF	-78°	0.10	71 : 29**	--	23c
55	Ph	Pr	Br	LiHMDS	THF	-78°	0.20	64 : 36**	--	23c
56	Ph	Pr	Br	LiHMDS	THF	-78°	0.33	50 : 50**	86%	23b
57	Ph	Pr	Br	LiHMDS	THF	-78°	0.33[h]	84 : 16**	--	23c
58	Ph	Pr	Br	LiHMDS	THF	-78°	0.50	44 : 56**	--	23c
59	Ph	Pr	Br	LiHMDS	THF	-78°	1.00	36 : 64**	--	23c
60	Ph	Pr	Br	LiHMDS	Toluene	-78°	0.21	23 : 77**	51%	23c
61	Ph	Pr	Br	LiHMDS	DMSO	RT	0.33	69 : 31	53%	23c
62	Ph	Pr	Br	LiHMDS	DMSO	RT	1.00	66 : 34	72%	23c
63	Ph	Pr	Br	$NaNH_2$	PhH/pet ether	0°		94 : 6	66%	14
64	p-MeOPh	Pr	Br	$NaNH_2$	PhH/pet ether	0°		91 : 9	80%	14
65	p-MePh	Pr	Br	$NaNH_2$	PhH/pet ether	0°		92 : 8	71%	14
66	p-MePh	n-Bu	Br	$LiNH(CH_2)_3NH_2$	THF	-78°	0.25	97 : 3	43%	60b
67	p-MePh	n-Bu	Br	$NaNH(CH_2)_3NH_2$	THF	-78°		94 : 6	36%	60b
68	p-MePh	$(CH_2)_9OH$	Br	$LiNH(CH_2)_3NH_2$	THF	-78°	0.25	94 : 6	66%	60b
69	p-ClPh	Pr	Br	$NaNH_2$	PhH/pet ether	0°		>99: 1	64%	14
70	$CH_3CH=CH$	$(CH_2)_9OH$	Br	$LiNH(CH_2)_3NH_2$	THF	-78°	0.25	82 : 18	32%	60b
71	$CH_3CH=CH$	$(CH_2)_9OH$	Br	nBuLi	THF	-78°	0.25	79 : 21	32%	60b
72	$CH_2=CHCH=CH$	C_2H_5	Br	NaHMDS	THF	-78°		97 : 3	78%	60d
73	c-C_6H_{11}	Me	Br	KHMDS	THF	-78°		99 : 1	92%	42
74	$PhCH_2(Me)CH$	Me	Br	KO*tert*Bu	THF	-78°		97 : 3	85%	20
75	2-[$(CH_2O)_2CH$]-cyclopropyl[i]	C_4H_9	Br	$NaNH_2$	C_6H_6	RT		92 : 8	--	60c
76	trans-2-vinylcyclopropyl	C_4H_9	Br	nBuLi	ether/pentane	RT	0.2	56 : 44	66%	60e
77	cis-2-($PrCO_2CH_2$)cyclopropyl	C_4H_9	Br	NaHMDS	THF/HMPA	-65°		>99: 1	99%	60f

78	$PhCH_2Me_2C$	Me	Br	KO*tert*Bu	THF	-78°	>99: 1	98%	20
79	tBu	Me	Br	nBuLi	THF	-78°	99 : 1	--	18a
80	tBu	Me	Br	$NaNH_2$	THF	-75°	98 : 2	92%	66
81	tBu	YCH_2[j]	I	nBuLi	THF	-78°	97 : 3	82%	67
82	tBu	YCH_2[j]	I	$NaNH_2$	Ether	RT	97 : 3	50%	67
83	tBu	nC_7H_{15}	Br	NaDMSO	DMSO	RT	98 : 2	--	68
84	$Y(Me)_2C$[j]	Me	Br	MeLi	THF	RT	>95: 5	--	69
85	$Y(Me)_2C$[j]	Me	Br	KHMDS	THF	-78°	99 : 1	98%	20
86	$Y(Me)_2C$[j]	Pr	Br	KHMDS	THF	-78°	98 : 2	--	70
87	$Y(Me)_2C$[j]	YCH_2[j]	Br	NaDMSO	DMSO	RT	>95: 5	--	71
β-Branched Ylides.									
88	YCH_2[j]	iPr	Br	KOtBu	DMF	RT	91 : 9	85%	72
89	YCH_2[j]	iPr	Br	nBuLi	THF	RT	80 : 20	--	72
90	Ph	$c\text{-}C_3H_5$	Br	NaH	THF	RT	66 : 34	75%	73
91	Ph	$c\text{-}C_3H_5$	Br	NaH	DMF	RT	61 : 39	--	73
92	Ph	$c\text{-}C_3H_5$	Br	NaH	PhH	RT	69 : 31	--	73
93	Ph	$c\text{-}C_6H_{11}$	??	??	??	??	(50:50?)	--	75
94	Ph	tBu	I	PhLi	Ether	RT	24 : 76**	84%	76
95	TMSC≡C	$c\text{-}C_6H_{11}$	Br	nBuLi	THF	-78°	95 : 5	85%	74
96	TMSC≡C	$c\text{-}C_6H_{11}$	Br	KHMDS	THF/TMEDA	-78°	98 : 2	76%	74

** Significant (>5%) equilibration of intermediates is likely in this example.

(a) Concentration assuming that all lithium halide remains in solution. (b) Ylide made in benzene and filtered to remove insoluble lithium salts. The benzene was evaporated and replaced by the appropropriate solvent. (c) The same range of yields is reported for all of the entries 11-16. (d) A reaction temperature above the melting point of DMSO is assumed. (e) This concentration is given in a general experimental procedure, and does not always match variables in the original tables. (f) 18-Crown-6 added. (g) Ylide solution made in benzene and filtered; benzene evaporated and replaced by hexane. (h) 1.6 equiv of cryptand-211 was added to the solution to coordinate lithium ion. (i) X= *trans*-2-[1,3-dioxolan-2-yl]. (j) Y = CH_2R (R= variable alkyl chain containing remote functionality).

lithium ion remains in solution when the ylide is prepared, an approximation that will be inaccurate in nonpolar solvents (ether, benzene, toluene, etc.). Unpredictable variations in Z:E ratios among some of the lithium-containing entries may reflect the lack of control over $[Li^+]$ or the presence of precipitated lithium salts. Since the concentration of dissolved lithium ion remains unknown in virtually all cases, contrasting results reported by different research groups should be interpreted with care.

The lithium-free experiments of Table 11 tell a consistent story, one that has changed little compared to the overview presented in 1970 (1). Typical nonstabilized ylides of the $Ph_3P{=}CHR$ family are $>90\%$ selective for the formation of (*Z*)-alkenes at room temperature. The (*Z*)-alkene selectivity increases to $>95\%$ as the reaction temperature is lowered (Table 11, entries 10–18) and is highest for tertiary aldehydes (entries 78–87). Relatively few β-branched ylides have been studied, but the more recent entries appear to follow the usual pattern of (*Z*)-alkene selectivity (entries 88, 95, 96). Somewhat lower Z:E selectivities appear in one study of the cyclopropylcarbinyl member of the β-branched ylide family (entries 90–92) (73), but these experiments involve benzaldehyde as the substrate and employ the relatively inefficient base sodium hydride for ylide generation. These factors may increase the risk of catalyzed equilibration of intermediates. A more recent study reports a typical Z:E ratio of 9:1 in the case of a 2,3-diphenylcyclopropylcarbinyl ylide (salt-free conditions; 2,3-diphenylcyclopropanecarboxaldehyde substrate) (77).

IX. LITHIUM HALIDE EFFECT ON STEREOSELECTIVITY

According to Table 11, high (*Z*)-alkene selectivity is possible for lithium-free aliphatic aldehyde reactions in dimethyl formamide (DMF), DMSO, hexamethylphosphoramide (HMPA), THF, ether, benzene, or hexane. There are some indications that Wittig reactions of benzaldehyde are more sensitive to the nature of the solvent (compare Table 11, entries 33–35, 39, 42), but the effect is small and may also be influenced by differences in temperature. The presence of relatively insoluble, nonelectrophilic metal salts such as NaCl, NaBr, KCl, KBr, or KI also does not exert any significant effect on Z:E ratios in a variety of solvents. On the other hand, the experimental conditions are important when Wittig reactions are performed in the presence of soluble salts or Lewis acids. This situation is encountered when lithium-containing bases are employed to prepare the ylide. Thus, Maryanoff, Reitz et al. (23c) have demonstrated that the Z:E ratio decreases as $[Li^+]$ increases for the reaction of hexanal with $Ph_3P{=}CHC_3H_7$ in THF (Table 11, entries 24–29). Since Z:E selectivity in the aliphatic aldehyde example is kinetically controlled

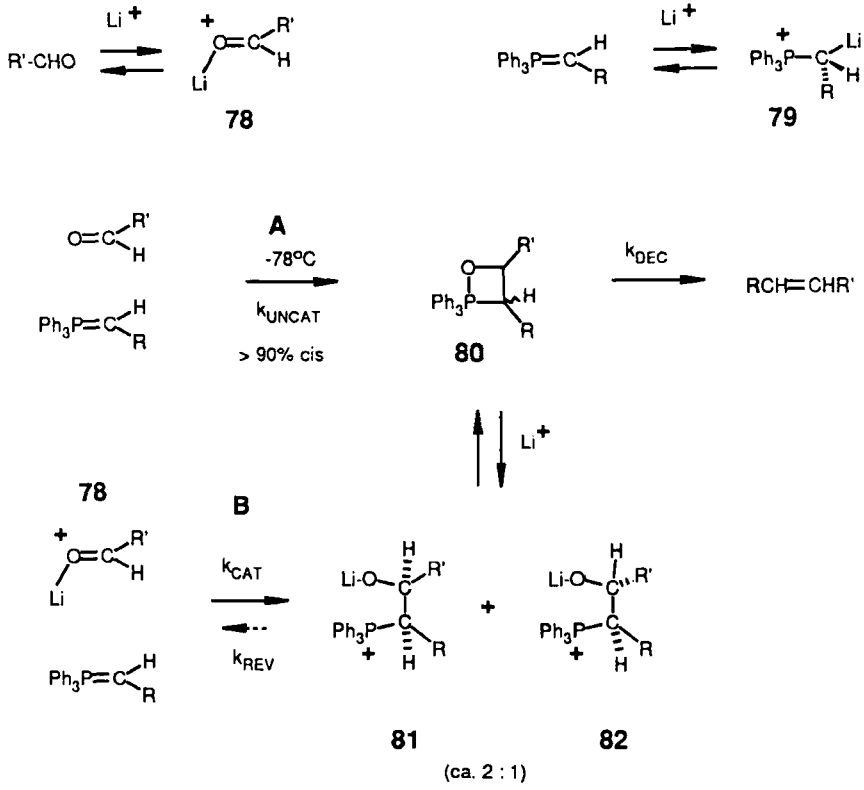
TABLE 12
Effect of Conditions on the Z:E Ratio for the Reaction $Ph_3P{=}CHC_4H_9$ + $EtO_2C(CH_2)_2CH{=}CH(CH_2)_2CHO$ (58)

Entry	Base	Solvent	Temp	Conc[a] (M)	Z : E	Yield
1	nBuLi	Ether	RT	0.10	78 : 22	61%
2	nBuLi	THF	RT	0.14	86 : 14	57%
3	nBuLi	C_6H_6	RT	0.09	87 : 13	49%
4	nBuLi	DMF[b]	RT	0.14	94 : 6	68%
5	NaH	DMF	RT	0.34	94 : 6	59%
6	$NaNH_2$	C_6H_6[c]	0°	0.27	94 : 6	52%
7	tBuOK	THF	RT	0.16	94 : 6	63%

(a) Concentration of the ylide solution before addition of the aldehyde.
(b) The ylide was initially generated in ether, which was removed in vacuo before addition of DMF.
(c) The ylide was initially generated in NH_3. The NH_3 was allowed to boil away and the residue was taken up in benzene. The benzene solution was then refluxed and filtered to produce an ylide solution without any inorganic salts present.

(58, 18b) the result proves that there is a competition between Li^+-catalyzed and Li^+-uncatalyzed mechanisms. Anderson and Henrick (58) have performed a systematic study of the key variables for one pair of reactants (Table 12). Their results show that the lithium-free reaction (Table 12, entries 6, 7) is identical to a lithium-containing reaction (Table 12, entry 4) in DMF. Other polar solvents that act as efficient lithium ion complexing agents are likely to behave in the same way (23c). Similar conclusions had been reached earlier from a comparison of Z:E selectivity data (1). However, Anderson and Henrick (58) also demonstrated that differences in selectivity among some of the entries of Table 12 are due to kinetic factors (negative crossover experiments). Other groups have reported similar findings with aliphatic aldehydes (18b, 23c).

The most dramatic medium effects on alkene Z:E ratios are seen in Wittig reactions of aromatic aldehydes (Table 11, entries 52–62). Maryanoff et al. (23c) have shown that the catalyzed Wittig reaction pathway in the system $PhCHO + Ph_3P{=}CHC_3H_7$ accounts for more than 50% of the total reaction when $[Li^+] >$ ca. 0.15 M in THF. A comparison of results obtained using several different values of $[Li^+]$ allowed an estimate for the stereoselectivity of the lithium-catalyzed reaction component, ca. 2:1 in favor of the cis-



Scheme 11

disubstituted oxaphosphetane. However, some of the empirical alkene ratios (Table 11, entries 56–60) show a much larger trend toward the (*E*)-alkene than would be expected from the influence of $[Li^+]$ on the *kinetic* cis–trans oxaphosphetane ratios. This is because the catalyzed equilibration of oxaphosphetane stereochemistry by reversible formation and cleavage of the betaine lithium halide complex is also dependent on $[Li^+]$. This possibility was already discussed in connection with Schemes 7 and 8, and further details are provided in Scheme 11.

Two different mechanisms for Li^+ catalysis of the Wittig reaction can be envisioned. One possibility involves the formation of a covalent organolithium species **79** from the phosphorus ylide. Such a process appears to take place with ylides of the general structure $L_3P{=}CH_2$ (26c), and this potential mechanism for catalysis cannot be ruled out. However, a different mechanism is more consistent with some of the experimental results. Thus, reactions of

tertiary aldehydes are not influenced by lithium ion (see Table 11, entries 79, 81, 84). If **79** is the intermediate resposible for catalysis (and reduced stereoselectivity) in the unbranched aldehyde reactions, it is difficult to understand why the relatively unreactive tertiary aldehydes would also not benefit from the same catalytic effect. A more plausible mechanism invokes activation of the aldehyde as the Lewis acid complex **78**, a possibility that has long been recognized (1). Sterically hindered aldehydes would be less likely to form complexes of this type, and the absence of a lithium halide effect on stereoselectivity in the reactions of tertiary aldehydes would be easy to understand. Activation of relatively unhindered aldehydes by reversible Lewis acid complexation would explain the stereochemical results as well as the modest rate enhancements reported by Maryanoff (23c) and would be most likely in solvents that do not coordinate lithium ion.

Subsequent reaction of **78** with the ylide results in the diastereomeric betaine halide adducts **81** and **82** (path B), species that are capable of cyclization to the oxaphosphetane. The mechanism for lithium halide catalysis of the Wittig reaction can be regarded as the microscopic reverse of the lithium-catalyzed oxaphosphetane equilibration process discussed earlier. The details would depend on the donor properties of the solvent. Thus, lithium-coordinating solvents would increase the rate of cyclization from **81** and **82** to oxaphosphetane **80** and would also increase the equilibrium concentration of **80**. Conversely, **81** and **82** would be favored in weak donor solvents such as diethyl ether, benzene, etc. With relatively long lifetimes for **81** and **82**, the chances for equilibration of the betaine lithium halide adducts by C—C bond cleavage would increase, especially if unsaturated substituents are present (R or R′ = aryl, alkenyl). The result would be a Wittig reaction with strongly concentration dependent stereoselectivity under lithium-containing conditions, due to the competition between paths **A** and **B**, Scheme 11. Since the catalyzed pathway **B** occurs without much selectivity, no attempt will be made to rationalize the modest 2:1 ratio of **81**:**82** in the only case (R′ = C_6H_5) where this ratio is accurately known (23c).

Some of the most profound lithium ion effects are observed in diethyl ether, benzene, or toluene, and the literature on Wittig reactions under these conditions contains a number of results that appear to be somewhat contradictory. The reason for this lack of consistency may be related to issues of lithium halide or betaine adduct solubility. Thus, Bergelson and Shemyakin et al. (5c, d) were able to show that ylide solutions prepared in benzene behaved differently if they were filtered to remove precipitated salts prior to use (compare Table 11, entries 3 and 4; entries 47 and 48). Later, it was shown that filtered toluene solutions of $Ph_3P{=}CHCH_3$ obtained from the phosphonium bromide using butyllithium contain $< 0.1\%$ bromide according to elemental analysis (18b). Therefore, the dramatic change in the alkene ratio

(23:77 Z:E) observed for the benzaldehyde/$Ph_3P{=}CHC_3H_7$ reaction in toluene (Table 11, entry 60) is almost certainly due to precipitated lithium bromide or the lithium bromide betaine adduct. The reported inverse dependence of Z:E ratios on lithium concentration in toluene is not likely to reflect solution phenomena because the toluene reactions were performed using suspensions, not homogeneous solutions (23c). These experiments cannot be interpreted in detail because they are conducted under heterogeneous conditions, but it is probable that they are influenced by lithium ion catalysis in the C—C bond forming step and also by substantial stereochemical equilibration of intermediates because the starting aldehyde is aromatic. The presence of precipitated salts may also explain the variation in Z:E ratios reported for reactions in diethyl ether (compare Table 11, entries 12 and 23), but further studies are needed before the relationship between stereoselectivity and potentially electrophilic metal salts can be fully understood. In particular, *it will be necessary to control* $[Li^+]$ *and to remove precipitates.* Selectivity data obtained "in the presence" of metal salts cannot be interpreted in detail unless the lithium ion concentration is measured under rigorously homogeneous conditions.

X. PHOSPHORUS LIGAND EFFECTS IN REACTIONS OF NONSTABILIZED YLIDES

Table 13 extends the coverage of stereoselectivity results to a number of different phosphorus environments. As shown in the data subsets at the end of Table 13, modified ylides are available that allow the synthesis of alkenes with $> 95\%$ selectivity for either the (*E*)- or the (*Z*)-alkene. Nearly all of the examples have been studied under lithium-free conditions, and there is little information available regarding metal salt effects on stereoselectivity. As in Table 11, most of the reactions are under kinetic control, with the exception of some of the *P*-trialkyl ylide examples (Table 13, entries 58–63, 65, 67, 71) where equilibration is assumed by analogy to the cases where specific control experiments were performed (entries 56, 60, 61) and also with the possible exception of the unusual ylide $(Me_2N)_3P{=}CHCH_3$ (entry 72). Only one stereochemical result with this ylide is available (20). The relatively basic reagent is not well-behaved with enolizable aldehydes, but the promising result of the example of entry 72 in Table 13 suggests that the problem of (*E*)-alkene synthesis from tertiary aldehydes may have a simple solution.

The results of Table 13 show that Z:E selectivity in phosphorus ylides is strongly influenced by the phosphorus substituents. There is a qualitative trend toward (*E*)-alkene formation as the bulk of phosphorus ligands decreases. However, there are a number of exceptions to the trend (for

example, the *P*-cyclohexyl examples, Table 13, entries 20–22, 65–69) that suggest the involvement of subtle, interdependent steric factors.

In nearly all cases, (*Z*)-alkene selectivity is higher for tertiary than for unbranched aliphatic aldehydes. The combination of a tertiary aldehyde and bulky phosphorus ligands in the ylide usually results in the highest Z:E ratios, except for the cases already mentioned where oxaphosphetane intermediates undergo cis–trans equilibration according to control experiments. The *kinetic oxaphosphetane ratios* follow the general rule that cis selectivity is higher for tertiary than for unbranched aldehydes. If this rule is not reflected in the empirical alkene ratios, then equilibration of intermediates is a distinct possibility.

Table 13 includes several ylide families that afford useful product ratios in favor of the (*Z*)-alkene. However, the original Wittig reagents $Ph_3P{=}CHR$ are preferred for most purposes where (*Z*)-alkenes are desired (Table 11). Selectivities of $> 95\%$ (*Z*)-alkene can be achieved at $-78°C$ for virtually any aliphatic aldehyde. In the event that higher Z selectivity is essential, modified, more hindered ylides of the general formula $Ar_3P{=}CHR$ may have an advantage (Table 13, entries 5–12) (61). However, the selectivity advantage is relatively small.

There are also several nonstabilized ylide families that react with useful (*E*)-alkene selectivity. The most promising reactions to date involve ylides containing phosphorus in a five-membered ring environment such as the dibenzophospholes ("DBP" ylides, Table 13, entries 30–42) (41) or bridged tetrahydrophospholes ("BTP" ylides, entries 48–51) (42b). The DBP ylides are known to react under kinetic control (20, 41) and the analogous BTP ylides presumably do so as well. Both of these (*E*)-alkene selective ylide families should therefore avoid the experimental complications associated with reversible Wittig systems. However, the nonstabilized DBP ylides have the disadvantage that the intermediate oxaphosphetanes are exceptionally stable and must be heated to induce alkene formation (hours at 70°C; minutes at 110°C). Another problem is that only one of the two identical alkyl groups in the precursor phosphonium salt (for example, the ethylidene ylide precursor **87**) is utilized in the Wittig reaction. This factor limits the use of DBP ylides of the general formula **88** to examples where the substituent R is relatively simple and inexpensive.

It has been found that nonstabilized ylides derived from the tetrahydrophosphole nucleus (**90** or **91**) afford oxaphosphetanes that decompose at room temperature. Since **89**, the phosphonium salt precursor of **90**, contains only one alkyl group, BTP ylide **90** can be recommended for E-selective alkene synthesis in cases where the alkyl substituent must be used efficiently. Since the phosphorus environment in **90** is relatively expensive, this family of reagents will not provide a practical solution for large-scale synthesis of

TABLE 13

Phosphorus Ligand Effects on Z:E Selectivity: Nonstabilized Ylides from $L_3P^+CH_2RX^-$ + Aliphatic R'CHO

Entry	R'	L_3P	R	X^-	Base	Solvent	Temp[a]	Z : E	Yield	Ref
1	$PhCH_2CH_2$	Ph_3P	Me	Br	KHMDS	THF	-78°, 25°	94:6	92%	20
2	*c*-C_6H_{11}	Ph_3P	Me	Br	KHMDS	THF	-78°, 25°	99:1	92%	42
3	$PhCH_2(Me)CH$	Ph_3P	Me	Br	KO*tert*Bu	THF	-78°, 25°	97:3	85%	20
4	$PhCH_2Me_2C$	Ph_3P	Me	Br	KO*tert*Bu	THF	-78°, 25°	>99:1	98%	20
5	C_5H_{11}	(*o*-tolyl)$_3$P	CH_3	Br^-	$NaNH_2$	THF	-75°, 25°	98:2	54-97%[b]	61
6	C_6H_5	(*o*-tolyl)$_3$P	CH_3	Br^-	$NaNH_2$	THF	-75°, 25°	95:5	"	61
7	C_3H_7	(*o*-tolyl)$_3$P	C_3H_7	Br^-	$NaNH_2$	THF	-75°, 25°	99:1	"	61
8	C_6H_5	(*o*-tolyl)$_3$P	C_3H_7	Br^-	$NaNH_2$	THF	-75°, 25°	97:3	"	61
9	C_5H_{11}	$(F_2C_6H_3)_3P$	CH_3	Br^-	$NaNH_2$	THF	-75°, 25°	99:1	"	61
10	C_6H_5	$(F_2C_6H_3)_3P$	CH_3	Br^-	$NaNH_2$	THF	-75°, 25°	99:1	"	61
11	C_3H_7	$(F_2C_6H_3)_3P$	C_3H_7	Br^-	$NaNH_2$	THF	-75°, 25°	99:1	"	61
12	C_6H_5	$(F_2C_6H_3)_3P$	C_3H_7	Br^-	$NaNH_2$	THF	-75°, 25°	99:1	"	61
13	$PhCH_2CH_2$	**83b**	CH_3	I^-	$NaNH_2$[c]	THF	-78°, 110°	50:50	75%	20
14	$PhCH_2(CH_3)_2C$	**83b**	CH_3	I^-	$NaNH_2$[c]	THF	-78°, 110°	90:10	60%	20
15	$PhCH_2CH_2$	$EtPh_2P$	CH_3	I^-	KO*tert*Bu	THF	-78°, 20°	30:70	72%	20
16	$PhCH_2(CH_3)CH$	$EtPh_2P$	CH_3	I^-	KO*tert*Bu	THF	-78°, 20°	27:73	76%	20
17	$PhCH_2(CH_3)_2C$	$EtPh_2P$	CH_3	I^-	KO*tert*Bu	THF	-78°, 20°	85:15	85%	20
18	$PhCH_2CH_2$	*i*-$PrPh_2P$	CH_3	I^-	KO*tert*Bu	THF	-78°, 20°	18:82	83%	20
19	$PhCH_2(CH_3)_2C$	*i*-$PrPh_2P$	CH_3	I^-	KO*tert*Bu	THF	-78°, 20°	50:50	98%	20
20	$PhCH_2CH_2$	*c*-$C_6H_{11}Ph_2P$	CH_3	I^-	KO*tert*Bu	THF	-78°, 20°	25:75	58%	78a
21	$PhCH_2(CH_3)CH$	*c*-$C_6H_{11}Ph_2P$	CH_3	I^-	KO*tert*Bu	THF	-78°, 20°	20:80	49%	78a
22	$PhCH_2(CH_3)_2C$	*c*-$C_6H_{11}Ph_2P$	CH_3	I^-	KO*tert*Bu	THF	-78°, 20°	44:56	91%	78a
23	$PhCH_2CH_2$	*tert*-$BuPh_2P$	CH_3	I^-	KO*tert*Bu	THF	-78°, 20°	94:6	74%	20
24	$PhCH_2(CH_3)CH$	*tert*-$BuPh_2P$	CH_3	I^-	KO*tert*Bu	THF	-78°, 20°	98:2	80%	20
25	$PhCH_2(CH_3)_2C$	*tert*-$BuPh_2P$	CH_3	I^-	KO*tert*Bu	THF	-78°, 20°	99:1	96%	20

26	$PhCH_2CH_2$	**84**	CH_3	I^-	$NaNH_2$[c]	THF	-78°, 75°	14:86	77%	80
27	$PhCH_2(CH_3)_2C$	**84**	CH_3	I^-	$NaNH_2$[c]	THF	-78°, 75°	50:50	85%	80
28	$PhCH_2CH_2$	**83d**	CH_3	I^-	$NaNH_2$[c]	THF	-78°, 110°	82:18	31%	20
29	$PhCH_2(CH_3)_2C$	**83d**	CH_3	I^-	$NaNH_2$[c]	THF	-78°, 110°	96:4	92%	20
30	$PhCH_2CH_2$	**83a**	CH_3	I^-	$NaNH_2$[c]	THF	-78°, 110°	5:95	83%	41
31	$PhCH_2$	**83a**	CH_3	I^-	$NaNH_2$[c]	THF	-78°, 110°	4:96	66%	41
32	*c*-C_6H_{11}	**83a**	CH_3	I^-	$NaNH_2$[c]	THF	-78°, 110°	3:97	92%	41
33	$C_9H_{19}(CH_3)CH$	**83a**	CH_3	I^-	$NaNH_2$[c]	THF	-78°, 110°	1.8:98.2	78%	41
34	$PhCH_2(CH_3)_2C$	**83a**	CH_3	I^-	$NaNH_2$[c]	THF	-78°, 110°	10:90	62%	41
35	$PhCH_2CH_2$	**83a**	C_3H_7	I^-	$NaNH_2$[c]	diglyme	-78°, 110°	<5:95	66%	41
36	$PhCH_2$	**83a**	C_3H_7	I^-	$NaNH_2$[c]	THF	-78°, 110°	9:91	64%	41
37	C_6H_5	**83a**	C_3H_7	I^-	$NaNH_2$[c]	THF	-78°, 110°	14:86	75%	41
38	*c*-C_6H_{11}	**83a**	C_3H_7	I^-	$NaNH_2$[c]	THF	-78°, 110°	1.2:98.8	97%	41
39	$C_9H_{19}(CH_3)CH$	**83a**	C_3H_7	I^-	$NaNH_2$[c]	THF	-78°, 110°	0.8:99.2	91%	41
40	$PhCH_2(CH_3)_2C$	**83a**	C_3H_7	I^-	$NaNH_2$[c]	THF	-78°, 110°	8:92	82%	41
41	$PhCH(CH_3)CH$	**83a**	C_3H_7	I^-	$NaNH_2$[c]	THF	-78°, 110°	3:97	84%	41
42	2-($PrCO_2CH_2$)cyclopropyl	**83a**	C_4H_9	Br^-	NaHMDS	THF	-65°, 110°	<1:99	90%	60f
43	$PhCH_2CH_2$	Et_2PhP	CH_3	I^-	KO*tert*Bu	THF	-78°, 20°	36:64	86%	20
44	$PhCH_2(CH_3)_2C$	Et_2PhP	CH_3	I^-	KO*tert*Bu	THF	-78°, 20°	57:43	90%	20
45	$PhCH_2CH_2$	*i*-Pr_2PhP	CH_3	I^-	KO*tert*Bu	THF	-78°, 20°	72:28	57%	20
46	$PhCH_2(CH_3)_2C$	*i*-Pr_2PhP	CH_3	I^-	KO*tert*Bu	THF	-78°, 20°	72:28	98%	20
47	$PhCH_2CH_2$	**86**	CH_3	I^-	KHMDS	THF	-78°, 20°	27:73	34%	42
48	$PhCH_2CH_2$	**85**	CH_3	I^-	KHMDS	THF	-78°, 20°	5:95	78%	42
49	*n*-C_6H_{13}	**85**	CH_3	I^-	KHMDS	THF	-78°, 20°	4:96	70%	42
50	*c*-C_6H_{11}	**85**	CH_3	I^-	KHMDS	THF	-78°, 20°	6:94	75%	42
51	$PhCH_2(CH_3)_2C$	**85**	CH_3	I^-	KHMDS	THF	-78°, 20°	20:80	84%	42
52	*n*-C_6H_{13}	Et_3P[d]	CH_3	--	--	THF	-75°, 25°	33:67	94%	66
53	$PhCH_2CH_2$	Et_3P[d]	CH_3	--	--	THF	-78°, 30°	33:67	53%	20

TABLE 13 *(Continued)*

Entry	R'	L_3P	R	X⁻	Base	Solvent	Temp[a]	Z : E	Yield	Ref
54	$PhCH_2(CH_3)CH$	Et_3P^d	CH_3	--	--	THF	-78°, 30°	23:77	48%	20
55	$(CH_3)_3C$	Et_3P^d	CH_3	--	--	THF	-75°, 25°	10:90[e]	92%	66
56	$PhCH_2(CH_3)_2C$	Et_3P^d	CH_3	--	--	THF	-78°, 30°	10:90	97%	20
57	C_6H_5	Et_3P^d	CH_3	--	--	THF	-75°, 25°	17:83[f]	99%	66
58	p-ClC_6H_5	Et_3P^d	CH_3	--	--	THF	-75°, 25°	4:96[f]	89%	66
59	C_5H_{11}	Bu_3P^d	C_3H_7	--	--	THF	-60°, RT	10:90	--	22a
60	$(CH_3)_3C$	Bu_3P^d	C_3H_7	--	--	THF	-50°, 25°	4:96	--	22a
61	$PhCH_2(CH_3)_2C$	Bu_3P^d	C_3H_7	--	--	THF	-95°, 20°	6:94	98%	20
62	C_6H_5	Bu_3P^d	C_3H_7	--	--	THF	-78°, RT	8:92	--	22a
63	C_6H_5	Bu_3P	$PhthNCH_2$	Br^-	NaH	THF	RT	<5:95	83%	78b
64	$PhCH_2CH_2$	Bu_3P	$PhthNCH_2$	Br^-	NaH	THF	RT	25:75	60%	78b
65	$PhCH_2CH_2$	$(c\text{-}C_6H_{11})_3P$	CH_3	I^-	KO*tert*Bu	THF	-78°, 20°	57:43	20%	78a
66	$PhCH_2(CH_3)CH$	$(c\text{-}C_6H_{11})_3P$	CH_3	I^-	KO*tert*Bu	THF	-78°, 20°	44:56	33%	78a
67	$PhCH_2(CH_3)_2C$	$(c\text{-}C_6H_{11})_3P$	CH_3	I^-	KO*tert*Bu	THF	-78°, 20°	12:88	94%	78a
68	n-C_6H_{13}	$(c\text{-}C_6H_{11})_3P$	CH_2Ph	?	LDA	THF	-78°, 20°	62:38	--	79
69	C_6H_5	$(c\text{-}C_6H_{11})_3P$	CH_2Ph	?	LDA	THF	-78°, 20°	13:87	--	79
70	$PhCH_2CH_2$	$(i\text{-}Pr)_3P$	CH_3	I^-	KO*tert*Bu	THF	-78°, 20°	57:43	29%	78
71	$PhCH_2(CH_3)_2C$	$(i\text{-}Pr)_3P$	CH_3	I^-	KO*tert*Bu	THF	-78°, 20°	27:73	95%	78
72	$PhCH_2(CH_3)_2C$	$(Me_2N)_3P$	CH_3	I^-	KHMDS	THF	-78°, 20°	<2:98[g]	86%	20

Table 13. Selected Reactions of L_3P=CHR with R'CHO (Dominant Kinetic Control; Lithium-free Conditions).

		Subset 1. Unbranched R'.		Subset 2. α-Branched R'		Subset 3. Tertiary R'.	
L_3P	R	Entry	Z:E	Entry	Z:E	Entry	Z:E
Ph_3P	CH_3	1	94:6	2	99:1	4	>99:1
(*o*-tolyl)$_3$P	C_3H_7	5	98:2	--	---	--	---
83b (PhDBP)	CH_3	46	50:50	--	---	14	90:10
$EtPh_2P$	CH_3	15	30:70	16	27:73	17	85:15
i-$PrPh_2P$	CH_3	18	18:82	--	---	19	50:50
c-$C_6H_{11}Ph_2P$	CH_3	20	25:75	21	20:80	22	44:56
tert-$BuPh_2P$	CH_3	23	94:6	24	98:2	25	99:1
83a (RCH_2DBP)	CH_3	30	5:95	33	1.8:98.2	34	10:90
83a	C_3H_7	35	<5:95	38	1.2:98.8	40	8:92
Et_2PhP	CH_3	43	36:64	--	---	44	57:43
i-Pr_2PhP	CH_3	45	72:28	--	---	46	72:28
85 (BTP)	CH_3	48	5:95	50	6:94	51	20:80
Et_3P	CH_3	52	33:67	54	23:77	56	76:24[h]
Bu_3P	C_3H_7	59	10:90	--	---	60	40:60[i]

(a) The temperature for the ylide reaction with the aldehyde is given first, followed by the decomposition temperature.

(b) Specific yields for each example were not given. According to the discussion, yields were close to the higher end of the indicated range for these examples.

(c) The experimental conditions and yield are given as described in ref. 41. However, dibenzophosphole ylides generated using the $NaNH_2$/THF tend to decompose. Better results are usually obtained with KHMDS/THF, or less conveniently, with $NaNH_2$/Et_2O (ref. 39).

(d) The distilled ylide was used; no counterion or metal salts were present.

(e) Stereochemical equilibration is based on control experiments in ref. 20 and 22a.

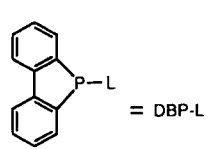
(f) Stereochemical equilibration is based on control experiments in ref. 22a.

(g) No control experiments have been performed. The assumption of stereochemical equilibration is based only on the high empirical E-alkene content compared with reactions of sterically similar ylides.

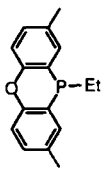
TABLE 13 *(Continued)*

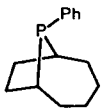
(h) The kinetic ratio of cis:trans oxaphosphetanes is given (see Table 6, entry 2). After equilibration, the empirical alkene ratio is 10:90 Z:E.

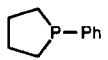
(i) The kinetic ratio of cis:trans oxaphosphetanes is given (see Table 6, entry 3). After equilibration, the empirical alkene ratio is 4:96 Z:E.



= DBP-L







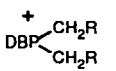
83 **a** L= CH_2R **84** **85** **86**

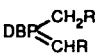
b L= Ph

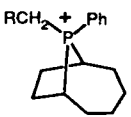
c L= tBu

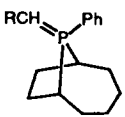
d L= NMe_2

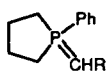
e L= Me











87 R= CH_3 **88** **89** **90** **91**

(*E*)-alkenes until access to the bicyclic ring system can be improved. However, work on this problem is still at an early stage. Future studies should improve access to five-membered phosphorus environments having all of the desirable features: regioselective ylide formation, efficient utilization of the group R, E-selective alkene formation, and relatively facile oxaphosphetane decomposition.

XI. ALLYLIC AND BENZYLIC YLIDES

Benzylidenetriphenylphosphorane derivatives are historically important because their reactions with aromatic aldehydes were explored extensively during the first attempts to understand the Wittig reaction. Unfortunately, the key reaction $Ph_3P{=}CHAr + Ar'CHO$ has proved to be the most difficult to control among all of the known Wittig systems. An inspection of Table 14 reveals inconsistencies in a number of the Z:E ratios when the work of different groups is compared. For example, entries 1–20 all feature the same benzaldehyde and benzylide reactants, but the reported Z selectivity among the lithium-free entries varies from 25% (Table 14, entry 13) to 74% (entry 12), and an even higher Z selectivity of 81% is reported *in the presence* of lithium ion (entry 10). Inconsistencies in the lithium-containing experiments are probably the result of solubility differences caused by variations in the counterion, the solvent, and also the solvent composition (for example, reactions reported in THF with BuLi as base often contain a variable amount of hexane, depending on the concentration of commercial BuLi). Another problem is the practice of reporting reactions "in the presence" of lithium ion. For reproducible results, the concentration of *dissolved* lithium salt would have to be established and precipitates would have to be excluded, but this has rarely been done.

The lithium-free experiments shown in Table 14 also contain surprising discrepancies. Many of these can be traced to experiments that were performed without maintaining positive temperature control. Regrettably, this problem has only recently been identified, and it casts doubt on some of the experimental results reported in Table 14. In contrast to typical nonstabilized ylides, benzylides of the $Ph_3P{=}CHAr$ family react relatively slowly with aldehydes at $-78°C$. Thus, the common technique of combining reactants at $-78°C$ followed by removal of the cooling bath results in a complicated reaction temperature profile that varies according to the reactivity of the aldehyde. The importance of this variable is clear from a comparison of the lithium-free benzaldehyde reactions at 0°C (Table 14, entries 17, 19; 43% Z) and at temperatures below $-70°C$ (entries 18, 20; $62 \pm 3\%$ Z). Another, more striking example of this phenomenon is reported in the reaction

TABLE 14
Z:E Selectivity of Benzylic Ylides from $L_3P^+CH_2ArX^-$ and Aldehydes R'CHO

Entry	R'	L_3P	Ar	X^-	Base	Solvent	Initial Temp.	Z : E	Yield	Ref
1	Ph	Ph_3P	Ph	Cl^-	PhLi	Et_2O	RT	30:70	--	10,5a
2	"	"	"	Br^-	BuLi	THF	RT	60:40	95%	82b
3	"	"	"	Br^-	BuLi	THF	20°	57:43	99%	82c
4	"	"	"	Br^-	BuLi	THF	-98°	68:32	86%	82c
5	"	"	"	Br^-	LiHMDS	THF	0°[a]	61:39	--	82d
6	"	"	"	--	BuLi[b]	C_6H_6	RT	34:66	--	5c
7	"	"	"	--	BuLi/LiBr[c]	C_6H_6	RT	50:50	--	5c
8	"	"	"	Cl^-	BuLi/LiBr[c]	DMF	RT	62:38	--	5c
9	"	"	"	Br^-	LiOEt	EtOH	RT	56:44	82%	82b
10	"	"	"	Cl^-	NaOEt/LiBr	DMF	RT	81:19	--	5a
11	"	"	"	Cl^-	NaOEt	EtOH	RT	53-66:47-34	--	3,5a,82a
12	"	"	"	Cl^-	NaOEt	DMF	RT	74:26	--	5a
13	"	"	"	Cl^-	KOC_4H_9	tert-BuOH	RT	25:75	--	81
14	"	"	"	Cl^-	NaOH	CH_2Cl_2/H_2O	RT	59:41	80%	83
15	"	"	"	Cl^-	$NaNH_2$	C_6H_6	RT	44:56	100%	14
16	"	"	"	--	$NaNH_2$	THF	20°	47:53	95%	63
17	"	"	"	Br^-	NaHMDS	THF	0°[a]	43:57	--	82d
18	"	"	"	Br^-	NaHMDS	THF	-72°[a]	64:36	--	82d
19	"	"	"	Br^-	KHMDS	THF	0°[a]	43:57	92%	82e
20	"	"	"	Br^-	KHMDS	THF	-78°[a]	59:41	61%	82e
21	*p*-MeC_6H_4	Ph_3P	Ph	Br^-	LiHMDS	THF	0°[a]	63:37	--	82d
22	"	"	"	Cl^-	$NaNH_2$	C_6H_6	RT	36:64	88%	14
23	"	"	"	Cl^-	NaOH	CH_2Cl_2/H_2O	RT	44:56	78%	83
24	"	"	"	Br^-	NaHMDS	THF	0°[a]	39:61	--	82d
25	"	"	"	Br^-	KHMDS	THF	0°[a]	29:71	84%	82e

26	"	"	"	Br^-	NaHMDS	THF	-72°[a]	64:36	--	82d
27	"	"	"	Br^-	KHMDS	THF	-78°[a]	64:36	36%	82e
28	*m*-MeC_6H_4	Ph_3P	Ph	Br^-	LiHMDS	THF	0°[a]	59:41	--	82d
29	"	"	"	Br^-	NaHMDS	THF	0°[a]	38:62	--	82d
30	"	"	"	Br^-	NaHMDS	THF	-72°[a]	62:38	--	82d
31	*o*-MeC_6H_4	Ph_3P	Ph	Br^-	LiHMDS	THF	0°[a]	55:45	--	82d
32	"	"	"	Br^-	NaHMDS	THF	0°[a]	37:63	--	82d
33	"	"	"	Br^-	NaHMDS	THF	-72°[a]	57:43	--	82d
34	*p*-$MeOC_6H_4$	Ph_3P	Ph	Br^-	LiHMDS	THF	0°[a]	61:39	--	82d
35	"	"	"	Cl^-	$NaNH_2$	C_6H_6	RT	19:81	84%	14
36	"	"	"	Cl^-	NaOEt	EtOH	RT	<5:>95	--	81
37	"	"	"	Br^-	NaHMDS	THF	0°[a]	39:61	--	82d
38	"	"	"	Br^-	NaHMDS	THF	-72°[a]	60:40	--	82d
39	*m*-$MeOC_6H_4$	Ph_3P	Ph	Br^-	LiHMDS	THF	0°[a]	56:44	--	82d
40	"	"	"	Br^-	NaHMDS	THF	0°[a]	46:54	--	82d
41	"	"	"	Br^-	NaHMDS	THF	-72°[a]	71:29	--	82d
42	*o*-$MeOC_6H_4$	Ph_3P	Ph	Br^-	LiHMDS	THF	0°[a]	68:32	--	82d
43	"	"	"	Br^-	NaHMDS	THF	0°[a]	84:16	--	82d
44	"	"	"	Br^-	NaHMDS	THF	-72°[a]	94:6	--	82d
45	*p*-ClC_6H_4	Ph_3P	Ph	Br^-	LiHMDS	THF	0°[a]	56:44	--	82d
46	"	"	"	Cl^-	$NaNH_2$	C_6H_6	RT	10:90	72%	14
47	"	"	"	Br^-	NaHMDS	THF	0°[a]	44:56	--	82d
48	"	"	"	Br^-	NaHMDS	THF	-72°[a]	63:37	--	82d
49	"	"	"	Br^-	KHMDS	THF	-78°[a]	55:45	86%	82e
50	*m*-ClC_6H_4	Ph_3P	Ph	Br^-	LiHMDS	THF	0°[a]	57:43	--	82d
51	"	"	"	Br^-	NaHMDS	THF	0°[a]	44:56	--	82d
52	"	"	"	Br^-	NaHMDS	THF	-72°[a]	64:36	--	82d
53	*o*-ClC_6H_4	Ph_3P	Ph	Br^-	LiHMDS	THF	0°[a]	64:36	--	82d

TABLE 14 *(Continued)*

Entry	R'	L_3P	Ar	X^-	Base	Solvent	Initial Temp.	Z : E	Yield	Ref
54	"	"	"	Br^-	NaHMDS	THF	0°[a]	86:14	--	82d
55	"	"	"	Br^-	NaHMDS	THF	-72°[a]	92:8	--	82d
56	*p*-$NO_2C_6H_4$	Ph_3P	Ph	Cl^-	NaOH	CH_2Cl_2/H_2O	RT	56:44	72%	83
57	"	"	Ph	Br^-	KHMDS	THF	-78°[a]	62:38	81%	82e
58	Ph	Ph_3P	*p*-MeC_6H_4	Br^-	LiHMDS	THF	0°[a]	57:43	--	82d
59	"	"	"	Br^-	NaHMDS	THF	0°[a]	45:55	--	82d
60	Ph	Ph_3P	*o*-MeC_6H_4	Br^-	LiHMDS	THF	0°[a]	44:56	--	82d
61	"	"	"	Br^-	NaHMDS	THF	0°[a]	31:69	--	82d
62	Ph	Ph_3P	*p*-$MeOC_6H_4$	Br^-	LiHMDS	THF	0°[a]	60:40	--	82d
63	"	"	"	Br^-	NaHMDS	THF	0°[a]	54:46	--	82d
64	Ph	Ph_3P	*o*-$MeOC_6H_4$	Br^-	LiHMDS	THF	0°[a]	41:59	--	82d
65	"	"	"	Br^-	NaHMDS	THF	0°[a]	34:66	--	82d
66	Ph	Ph_3P	*p*-ClC_6H_4	Br^-	LiHMDS	THF	0°[a]	67:33	--	82d
67	"	"	"	Br^-	NaHMDS	THF	0°[a]	57:43	--	82d
68	Ph	Ph_3P	*o*-ClC_6H_4	Br^-	LiHMDS	THF	0°[a]	64:36	--	82d
69	"	"	"	Br^-	NaHMDS	THF	0°[a]	44:56	--	82d
70	*p*-$MeOC_6H_4$	Ph_3P	*p*-$C_6H_4NO_2$	Br^-	BuLi	C_6H_6	RT	26:74	78%	84
71	*p*-$NO_2C_6H_4$	Ph_3P	*p*-$MeOC_6H_4$	Br^-	BuLi	C_6H_6	RT	44:56	--	84
72	*p*-$NO_2C_6H_4$	(*p*-$ClC_6H_4)_3P$	*p*-$MeOC_6H_4$	Br^-	BuLi	C_6H_6	RT	80:20	--	84
73	Ph	(*o*-$MeC_6H_4)_3P$	Ph	Br^-	NaOEt	EtOH	RT	70:30	76%	82b
74	"	"	Ph	Br^-	LiOEt	EtOH	RT	72:28	95%	82b
75	"	"	Ph	Br^-	BuLi	THF	RT	21:79	54%	82b
76	Ph	(*p*-$MeC_6H_4)_3P$	Ph	Br^-	NaOEt	EtOH	RT	42:58	95%	82b
77	"	"	"	Br^-	BuLi	THF	RT	57:43	59%	82b
78	Ph	(*o*-$MeOCH_2OC_6H_4)_3P$	Ph	Br^-	$NaNH_2$	THF	25°	53:47	--	85
79	"	"	"	Br^-	$NaNH_2$	THF	-75°[a]	96:4	91%	85
80	"	"	"	Br^-	$NaNH_2$	THF	-75°	73:27	--	65
81	C_5H_{11}	(*o*-$MeOCH_2OC_6H_4)_3P$	Ph	Br^-	$NaNH_2$	THF	-75°	72:28	--	65

82	"	"	"	Br^-	$NaNH_2$	THF	-75°[a]	84:16	84%	85
83	C_2H_5	Ph_3P	Ph	--	$NaNH_2$	C_6H_6	RT	25:75	83%	63
84	"	"	"	Cl^-	BuLi	C_6H_6	RT	21:79	--	5c
85	"	"	"	I^-	BuLi	C_6H_6	RT	41:59	--	5c
86	"	"	"	Cl^-	NaOEt	DMF	RT	46:54	66%	4b
87	*E*-$C_5H_{11}CH$=CH	Ph_3P	Ph	Br^-	BuLi	Et_2O	0°	30:70	90%	83b
88	$PhCH_2CH_2$	Ph_3P	Ph	Br^-	KHMDS	THF	-78°[a]	25:75	86%[d]	82e
89	$PhCH_2(CH_3)_2C$	Ph_3P	Ph	Br^-	KHMDS	THF	-78°[a]	35:65	1.4%[d]	82e
90	Ph	$MePh_2P$	Ph	Br^-	NaOEt	EtOH	RT	28:72	97%	13
91	"	"	"	Cl^-	KHMDS[b]	THF	-78°[a]	14:86	>90%	39b
92	"	"	"	Cl^-	KHMDS[b]	THF	0°[a]	15:85	>90%	39b
93	"	"	"	Cl^-	KHMDS	THF	-78°	18:82	96%	43
94	"	"	"	Cl^-	BuLi	THF	-78°	66:34	94%	43
95	"	"	"	I^-	BuLi	THF	-78°	63:37	91%	43
96	"	"	"	I^-	NaHMDS	THF	-78°	69:31	96%	43
97	"	"	"	I^-	KHMDS	THF	-78°	19:81	84%	43
98	*p*-MeC_6H_4	$MePh_2P$	Ph	Cl^-	KHMDS	THF	-78°	17:83	84%	43
99	"	"	"	Cl^-	BuLi	THF	-78°	67:33	97%	43
99	*p*-$MeOC_6H_4$	$MePh_2P$	Ph	Cl^-	KHMDS	THF	-78°	17:83	92%	43
100	"	"	"	Cl^-	BuLi	THF	-78°	68:32	81%	43
102	*p*-ClC_6H_4	$MePh_2P$	Ph	Cl^-	KHMDS	THF	-78°	22:78	88%	43
103	"	"	"	Cl^-	BuLi	THF	-78°	54:46	90%	43
104	*p*-$CF_3C_6H_4$	$MePh_2P$	Ph	Cl^-	KHMDS	THF	-78°	24:76	95%	43
105	"	"	"	Cl^-	BuLi	THF	-78°	42:58	92%	43
106	*p*-$NO_2C_6H_4$	$MePh_2P$	Ph	Cl^-	KHMDS	THF	-78°	34:66	89%	43
107	"	"	"	Cl^-	BuLi	THF	-78°	30:70	86%	43
108	$PhCH_2CH_2$	$MePh_2P$	Ph	Br^-	KHMDS	THF	-78°	6:94	87%	42
109	c-C_6H_{11}	$MePh_2P$	Ph	I^-	KHMDS	THF	-78°	8:92	>95%	40

TABLE 14 *(Continued)*

Entry	R'	L_3P	Ar	X	Base	Solvent	Initial Temp.	Z : E	Yield	Ref
110	$(CH_3)_3C$	$MePh_2P$	Ph	Cl^-	KHMDS	THF	-78°	21:79	92%	43
111	"	"	"	Cl^-	BuLi	THF	-78°	50:50	88%	43
112	"	"	"	I^-	KHMDS	THF	-78°	21:79	95%	43
113	"	"	"	I^-	NaHMDS	THF	-78°	69:31	88%	43
114	"	"	"	I^-	BuLi	THF	-78°	63:37	95%	43
115	Ph	$PhCH_2Ph_2P$	Ph	Br^-	KO*tert*Bu$^\oplus$	THF	0°	<1:99	88%	86
116	"	"	"	Br^-	BuLi	THF	20°	15:85	87%	82c
117	"	"	"	Br^-	BuLi	THF	-98°	13:87	86%	82c
118	Ph	$(PhCH_2)_2PhP$	Ph	Br^-	KO*tert*Bu$^\oplus$	THF	0°	5:95	93%	86
119	"	"	"	Br^-	BuLi	THF	20°	32:68	92%	82c
120	"	"	"	Br^-	BuLi	THF	-98°	24:76	81%	82c
121	Ph	Me_2PhP	Ph	Br^-	NaOEt	EtOH	RT	13:87	91%	13
122	Ph	MeEtPhP	Ph	I^-	PhLi	Et_2O	RT	4:96	87%	87a
123	"	"	"	"	NaOEt	EtOH	RT	17:83	>70%	87b
124	Ph	$(PhCH_2)_3P$	Ph	Br^-	KO*tert*Bu$^\oplus$	THF	0°	9:91	97%	86
125	"	"	"	Br^-	BuLi	THF	20°	37:63	100%	82c
126	"	"	"	Br^-	BuLi	THF	-98°	48:52	96%	82c
127	Ph	$(c\text{-}C_6H_{11})_3P$	Ph	Cl^-	NaOEt	EtOH	RT	5:95	92%	88
128	Ph	$(Bu)_3P$	Ph	--	NaOEt	EtOH	RT	9:91	--	89
129	Ph	**83a** (R=Ph; $PhCH_2DBP$)	Ph	Br^-	BuLi	THF	20°	15:85	100%	82c
130	$c\text{-}C_6H_{11}$	**83e** (MeDBP)	Ph	I^-	KHMDS	THF	-78°	3:97	85%	21c

Selected Entries from Table 14.

Subset 1: R'CHO + Ph_3P=CHPh (THF; reaction and acid quench at the specified temperature).[82d,e]

Entries	R'	Z:E (LiHMDS, 0°)[82d]	Z:E (NaHMDS, 0°)[82d]	Z:E (NaHMDS, -72°)[82d]	Z:E (KHMDS, -78°)[82e]
5,17,18,20	Ph	61:39	43:57	64:36	59:41
21,24,26,27	*p*-MeC_6H_4	63:27	39:61	64:36	64:36
28,29,30	*m*-MeC_6H_4	59:41	38:62	62:38	
31,32,33	*o*-MeC_6H_4	55:45	37:63	57:43	
34,37,38	*p*-$MeOC_6H_4$	61:39	39:61	60:40	
39,40,41	*m*-$MeOC_6H_4$	56:44	46:54	71:29	
42,43,44	*o*-$MeOC_6H_4$	68:32	84:16	94:6	
45,47,48,49	*p*-ClC_6H_4	56:44	44:56	63:37	55:45
50,51,52	*m*-ClC_6H_4	57:43	44:56	64:36	
53,54,55	*o*-ClC_6H_4	64:36	86:14	92:8	
57	*p*-$NO_2C_6H_4$				62:38
88	$PhCH_2CH_2$				25:75
89	$PhCH_2(CH_3)_2C$				35:65

TABLE 14 *(Continued)*

Subset 2. Metal Ion (M^+) Concentration Effects in the Reaction of $MePh_2P{=}CHPh$ + ArCHO (-78°).

A. ArCHO = C_6H_5CHO (see entries 91-97).

$[M^+]$	MX	Solvent	Z:E	yield	ref.
0.34[f]	LiCl	90:10 THF:hexane	68:32	89%	43
0.17[f]	"	90:10 THF:hexane	66:34	94%	43
0.05	"	97:3 THF:hexane	71:29	>85%	43
0.05	LiBr	97:3 THF:hexane	70:30	84%	42a
0.04	NaI	THF	60:40[a]	96%	39b
0.015	NaI	THF	43:57[a]	97%	39b
0.01	LiBr	97:3 THF:hexane	45:55	87%	42a
0.005	LiBr	" "	28:72	77%	42a
0.00	--	90:10 THF:hexane	18:82	96%	43

B. ArCHO = p-$NO_2C_6H_5CHO$ (see entries 106,107).

$[Li^+]$	Solvent	Z:E	yield	ref.
0.51[f]	90:10[f] THF:hexane	42:58	89%	43
0.34[f]	" "	36:64	75%	43
0.17[f]	" "	30:70	86%	43
0.00[f,g]	" "	34:66	89%	43

(a) This reaction was quenched at the indicated temperature using aqueous HCl[82d], by pouring into ethereal HCl,[85] or by cannula transfer into precooled MeOH-H_2O/NH_4Cl[82e]. In entries where superscript "a" is not appended to initial temperatures of 0° or lower, it was common practice to allow the reactions to warm to room temperature prior to workup. No assumptions can be made about the actual reaction temperature in those examples.

(b) The solution was filtered to remove precipitated salts.

(c) One equivalent of LiBr was added.

(d) Conversion after 30 min at -78° using 5-fold excess aldehyde; the reaction was quenched into cold aqueous-methanolic NH_4Cl.

(e) The ylide was prepared in toluene, the salts were filtered, and the toluene was evaporated and replaced by THF.

(f) Concentrations are based on reagent volumes and stoichiometry specified in text, tabulated data, and general procedures in ref. 43.

(g) The ylide was generated using the KHMDS method.

of $(o\text{-MeOCH}_2\text{OCH}_2\text{C}_6\text{H}_4)_3\text{P}{=}\text{CHPh}$ with benzaldehyde to give stilbene as summarized in Table 14, entry 79 (96% Z at −75°C) vs. 78 (53% Z at 25°C) (85). An earlier study of the same reaction had reported 73% (*Z*)-stilbene at −75°C, a result that reflects a variable temperature profile in a reaction that was not quenched or forced to completion at −75°C (65). Experiments where quenching methods were used to control temperature are identified in Table 14 by footnote a, appended as a superscript to the reaction temperature variable.

Since the benzylide reactions are unusually sensitive to temperature variations, experiments at "room temperature" are also suspect. Such experiments may be affected by the exotherm of reaction, depending on the reactivity of the aldehyde. Since benzylide reactions have been so common in the literature, they are often published without sufficient experimental detail to establish whether positive temperature control was maintained (82d,e, 85) or whether the temperature was allowed to vary (43). Thus, it will not be possible to interpret many of the results in Table 14 without repeating them. However, Yamataka et al. (82d) have reported a large number of aldehyde experiments where temperature control was maintained by quenching samples into dilute HCl. This information is gathered in Table 14, subset 1, together with several other experiments where reactions were quenched using cannula transfer into cold aqueous-methanolic NH_4Cl (82e). Where comparisons can be made, these methods give consistent results.

As in the nonstabilized ylide reactions, benzylides afford alkenes with increasing Z selectivity as the temperature is lowered (lithium-free conditions). However, the inherent selectivity is lower for the benzylides, and the temperature effect is larger. With the exception of the *ortho*-methoxybenzaldehyde and *ortho*-chlorobenzaldehyde entries in subset 1, the Z:E ratios are similar for a large variety of aromatic aldehydes. There is no simple effect of electron-releasing or electron-withdrawing groups when the temperature variable is controlled.

Subset 1 also shows that the lithium-containing experiments tend to give ca. 60:40 Z:E mixtures with essentially all aromatic aldehydes. This ratio is similar to that determined for the lithium-catalyzed component of the benzaldehyde reaction with $Ph_3P{=}CHC_3H_7$ (23c). Furthermore, nearly the same Z:E ratio is observed in the reaction of $Ph_2MeP{=}CHPh$ with PhCHO when $[Li^+]$ exceeds ca. 0.01 M in THF (Table 14, subset 2) (42a, 43). Catalysis is effective at much lower lithium ion concentrations than in the analogous reactions of nonstabilized ylides (Table 11, entries 52–59) (23c). This is to be expected because the benzylide is inherently less reactive. Lithium ion concentration effects have not been studied systematically for the $Ph_3P{=}$ CHPh entries of subset 1, but the similarity of Z:E ratios suggests that the catalyzed pathway dominates in all of these reactions. The influence of lithium

ion increases the proportion of the (*Z*)-alkene in most of the 0°C entries because the corresponding lithium-free reactions tend to be modestly selective for the (*E*)-alkene. However, lithium ion catalysis can have the opposite effect with aldehydes that are strongly biased toward Z selectivity, as in the *o*-chlorobenzaldehyde and *o*-methoxybenzaldehyde entries of subset 1.

Most of the results summarized in subset 2, Table 14, were obtained without positive temperature control. However, the $MePh_2P{=}CHPh$ reactions are less sensitive to temperature (Table 14, entries 91, 92), and they are relatively fast at $-78°C$ by comparison to analogous $Ph_3P{=}CHPh$ entries. Futhermore, intermediates in the $MePh_2P{=}CHPh$ experiments can be studied by the method of independent betaine generation. These advantages have resulted in consistent Z:E data and a better understanding of experimental variables. Betaines and oxaphosphetanes derived from $MePh_2P{=}CHPh$ are resistant to equilibration in THF whether or not Li^+ is present (19, 43). The Li^+ effects in subset 2 are therefore due to dominant (> 98%) kinetic control. Catalysis is less effective in the *p*-nitrobenzaldehyde case (subset 2), as expected for a mechanism that requires Lewis acid activation of the aldehyde carbonyl group by Li^+. The benzaldehyde reaction can also be catalyzed by Na^+I^- (see entry 96). In contrast to insoluble salts such as NaCl, NaBr, or KI, the relatively soluble NaI is an effective Lewis acid. Further studies are needed to dissect the relative rates and Z:E selectivities of catalyzed versus uncatalyzed pathways. However, judging from the similarity of product ratios (entry 96 vs. 95) the mechanisms for catalysis by NaI and LiBr appear to be closely related.

Several puzzling entries in Table 14 remain to be explained, including reactions where hydroxylic solvents or alkoxide bases are used (entries 11–14). Betaine reversal was demonstrated under hydroxylic conditions in the original Trippet–Jones experiment (Scheme 4) (13), and it is conceivable that interconversion between oxaphosphetanes and betaines could be fast enough in hydroxylic solvents to allow significant betaine reversal to the ylide and aldehyde in some cases. However, there is no clear evidence to implicate stereochemical equilibration of benzylide-derived Wittig intermediates in ether solvents.

Allylic ylides display many of the same trends as do the benzylides (Table 15). In general, there are fewer controversial entries, probably because much of the work has been done under similar conditions. However, none of the experiments have included low-temperature quenching techniques. Only the initial reaction temperature is known in most examples, and temperature effects on Z:E selectivity have not been studied in depth.

Four data subsets are provided, and they tell a consistent story. The benzaldehyde reactions (subset 1) proceed with mediocre selectivity that is not much affected by lithium ion. Selectivity in the Ph_3P series is also poor

TABLE 15

Z:E Selectivity of Allylic Ylides from $L_3P^+CH_2C(R_\beta)=CR_{\gamma Z}R_{\gamma E}X^-$ and Aldehydes R'CHO

Entry	R'	L_3P	R_β	($R_{\gamma Z}$, $R_{\gamma E}$)	X^-	Base	Solvent	Temp[a]	Z : E	Yield	Ref
1	C_6H_5	Ph_3P	H	H, H	Br^-	BuLi	Et_2O	RT	45:55	58%	10,63
2	"	"	"	"	Br^-	BuLi	MeC_6H_5	RT	44:56	68%	92
3	"	"	"	"	BF_4^-	BuLi	THF	RT	56:44	65%[c]	90
4	"	"	"	"	BF_4^-	DBU	THF	65°	56:44	59%[d]	93
5	"	"	"	"	?	$NaNH_2$	THF	20°	66:34	95%	63
6	*n*-C_4H_9	Ph_3P	H	H,H	?	$NaNH_2$	THF	20°	85:15	93%	63
7	$PhCH_2CH_2$	Ph_3P	H	H, H	Br^-	KHMDS	THF	-78°	45:55	80%	42a
8	$(CH_3)_2CH$	Ph_3P	H	H, H	Br^-	BuLi	THF	-78°	72:28	49%	92
9	*c*-C_6H_{11}	Ph_3P	H	H, H	Br^-	BuLi	THF	-78°	53:47	28%	40
10	*c*-C_6H_{11}	Ph_3P	H	H, H	Br^-	KHMDS	THF	-78°	22:78	67%	42a
11	$PhCH_2(CH_3)_2C$	Ph_3P	H	H, H	Br^-	KHMDS	THF	-78°	50:50	21%	42a
12	C_6H_5	Ph_3P	H	H, CH_3	BF_4^-	DBU	MeOH	65°	48:52	19%[e]	90
13	$(CH_3)_2CH$	Ph_3P	H	H, CH_3	BF_4^-	DBU	THF	65°	34:66	37%[f]	92
14	*c*-C_6H_{11}	Ph_3P	H	H, CH_3	Br^-	BuLi	THF	-78°	50:50	41%	47a
15	$PhCH_2CH_2$	Ph_3P	H	H, CH_3	Br^-	BuLi	THF	-78°	49:51	69%	47a
16	$AcO(CH_2)_8$	Ph_3P	H	H, C_2H_5	Br^-	BuLi	DME	--	50:50	--	94
17	"	"	"	"	Br^-	KO*tert*Bu	C_6H_6	--	40:60	--	94
18	"	"	"	"	Br^-	$NaCH_2S(O)Me$	DMSO	--	60:40	--	94
19	C_6H_5	Ph_3P	H	H, C_6H_5	Br^-	BuLi	THF	-78°	48:52	83%	47b
20	"	"	"	"	Br^-	KO*tert*Bu	THF	-78°	75:25	59%	47b
21	*c*-C_6H_{11}	Ph_3P	H	H, C_6H_5	Br^-	BuLi	THF	-78°	54:46	71%	47b
22	"	"	"	"	Br^-	KO*tert*Bu	THF	-78°	30:70	65%	47b
23	$(CH_3)_3C$	Ph_3P	H	H, C_6H_5	Br^-	BuLi	THF	-78°	83:17	32%	47b
24	C_6H_5	Ph_3P	H	CH_3, CH_3	Br^-	BuLi	MeC_6H_5	-78°	61:39	96%	47a
25	"	"	"	"	Br^-	KO*tert*Bu	THF	-78°	78:22	57%	47b

TABLE 15 *(Continued)*

Entry	R'	L_3P	R_β	(R_{fZ}, R_{fE})	X^-	Base	Solvent	Temp[a]	Z : E	Yield	Ref
26	*c*-C_6H_{11}	Ph_3P	H	CH_3, CH_3	Br^-	BuLi	MeC_6H_5	-78°	37:63	59%	47a
27	〃	〃	〃	〃	Br^-	KO*tertBu*	THF	-78°	20:80	60%	47b
28	$PhCH_2CH_2$	Ph_3P	H	CH_3, CH_3	Br^-	BuLi	MeC_6H_5	-78°	55:45	75%	47a
29	$(CH_3)_3C$	Ph_3P	H	CH_3, CH_3	Br^-	BuLi	THF	-78°	>95:5	47%	47b
30	C_6H_5	Ph_3P	CH_3	H, H	Cl^-	BuLi	THF	-78°	31:69	60%	47b
31	〃	〃	〃	〃	Cl^-	KO*tertBu*	THF	-78°	55:45	21%	47b
32	*c*-C_6H_{11}	Ph_3P	CH_3	H, H	Cl^-	BuLi	THF	-78°	10:90	36%	47b
33	$PhCH_2CH_2$	Ph_3P	CH_3	H, H	Cl^-	BuLi	THF	-78°	29:71	45%	47b
34	〃	〃	〃	〃	Cl^-	KO*tertBu*	THF	-78°	39:61	23%	47b
35	C_6H_5	Ph_3P	-($CH_2CH_2CH_2$)-, H		NO_2^-	BuLi	THF	-78°	55:45	63%	47b
36	〃	〃	〃	〃	NO_2^-	KO*tertBu*	THF	-78°	53:47	29%	47b
37	*c*-C_6H_{11}	Ph_3P	-($CH_2CH_2CH_2$)-, H		NO_2^-	BuLi	THF	-78°	27:73	45%	47b
38	C_6H_{13}	Ph_3P	-($CH_2CH_2CH_2$)-, H		NO_2^-	BuLi	THF	-78°	42:58	60%	47b
39	$(CH_3)_3C$	Ph_3P	-($CH_2CH_2CH_2$)-, H		NO_2^-	BuLi	THF	-78°	85:15	44%	47b
40	$PhCH_2(CH_3)_2C$	**83b** (PhDBP)	H	H, H	Br^-	KHMDS	THF	-78°	13:87	97%	40
41	*c*-C_6H_{11}	$MePh_2P$	H	H, H	I^-	BuLi	THF	-78°	33:67	70%	40
42	〃	〃	〃	〃	I^-	LDA	THF	-78°	29:71	66%	40
43	〃	〃	〃	〃	I^-	KHMDS	THF	-78°	<5:95	74%	40
44	〃	〃	〃	〃	I^-	KO*tertBu*	THF	-78°	<5:95	74%	40
45[g]	$R^{1''}CH_2(R^{2''})CH$	$MePh_2P$	H	H, H	Br^-	KO*tertBu*	THF	0°	<5:95	75%	95
46	C_6H_5	$MePh_2P$	CH_3	H, H	I^-	BuLi	THF	-78°	40:60	57%	47a
47	〃	〃	〃	〃	I^-	KO*tertBu*	THF	-78°	33:67	96%	47a
48	*c*-C_6H_{11}	$MePh_2P$	CH_3	H, H	I^-	BuLi	THF	-78°	6:94	57%	47a
49	〃	〃	〃	〃	I^-	KO*tertBu*	THF	-78°	4:96	73%	47a
50	$PhCH_2CH_2$	$MePh_2P$	CH_3	H, H	I^-	BuLi	THF	-78°	30:70	44%	47a
51	〃	〃	〃	〃	I^-	KO*tertBu*	THF	-78°	14:86	92%	47a
52	*c*-[$(CH_2)_5SCH$]	$MePh_2P$	$SiMe_3$	H, H	I^-	KHMDS	MeC_6H_5	-78°	<5:95	75%	40
53	$MeO_2C(CH_2)_4$	$MePh_2P$	H	H, $C(TMSCH_2)$=CHMe	I^-	KHMDS	THF	-78°	<5:95	>65%	96

54	$THPO(CH_2)_6$	$MePh_2P$	H	H, CH_3	I^-	KO*tert*Bu	THF	-18°	2:98	76%	97
55	$THPO(CH_2)_8$	$MePh_2P$	H	H, CH_3	I^-	KO*tert*Bu	THF	-18°	10:90	75%	97
56	$AcO(CH_2)_8$	$MePh_2P$	H	H, C_2H_5	I^-	KO*tert*Bu	THF	-18°	14:86	79%	97
57	$AcO(CH_2)_8$	$MePh_2P$	H	H, C_4H_9	I^-	KO*tert*Bu	THF	-18°	21:79	75%	97
58	$AcO(CH_2)_4$	$MePh_2P$	H	H, C_2H_5	I^-	BuLi	THF	-15°	30:70	61%	97
59	*c*-C_6H_{11}	**83e** (MeDBP)	H	H, H	Br^-	KHMDS	THF	-78°	1:99	82%	21c
60	*c*-C_6H_{11}	$(CH_2{=}CHCH_2)Ph_2P$	H	H, H	Br^-	LDA	THF	-78°	54:46	20%	40
61	〃	〃	〃	〃	Br^-	KHMDS	THF	-78°	20:80	26%	40
62	C_6H_5	$(Me_2C{=}CHCH_2)Ph_2P$	H	CH_3, CH_3	Br^-	BuLi	THF	-78°	16:84	90%	47a
63	*c*-C_6H_{11}	$(Me_2C{=}CHCH_2)Ph_2P$	H	CH_3, CH_3	Br^-	BuLi	THF	-78°	4:96	55%	47a
64	$PhCH_2CH_2$	$(Me_2C{=}CHCH_2)Ph_2P$	H	CH_3, CH_3	Br^-	BuLi	THF	-78°	17:84	80%	47a
65	C_6H_5	$(MeCH{=}CHCH_2)Ph_2P$	H	H, CH_3	Br^-	BuLi	THF	-78°	33:67	76%	47a
66	*c*-C_6H_{11}	$(MeCH{=}CHCH_2)Ph_2P$	H	H, CH_3	Br^-	BuLi	THF	-78°	7:93	61%	47a
67	$PhCH_2CH_2$	$(MeCH{=}CHCH_2)Ph_2P$	H	H, CH_3	Br^-	BuLi	THF	-78°	17:83	89%	47a
68	$PhCH_2CH_2$	**86**	H	H, H	Br^-	KHMDS	THF	-78°	12:88	85%	42a
69	$PhCH_2(CH_3)_2C$	**86**	H	H, H	Br^-	BuLi	THF	-78°	39:61	75%	42a
70	〃	〃	〃	〃	Br^-	KHMDS	THF	-78°	12:88	64%	42a
71	C_6H_5	Bu_3P	H	CH_3, CH_3	Br^-	BuLi	THF	-78°	29:71	82%	47b
72	〃	〃	〃	〃	Br^-	KO*tert*Bu	THF	-78°	22:78	63%	47b
73	*c*-C_6H_{11}	Bu_3P	H	CH_3, CH_3	Br^-	BuLi	THF	-78°	15:85	72%	47b
74	〃	〃	〃	〃	Br^-	KO*tert*Bu	THF	-78°	5:95	61%	47b
75	$(CH_3)_3C$	Bu_3P	H	CH_3, CH_3	Br^-	BuLi	THF	-78°	23:77	61%	47b
76	C_6H_5	Bu_3P	H	H, C_6H_5	Br^-	BuLi	THF	-78°	40:60	92%	47b
77	〃	〃	〃	〃	Br^-	KO*tert*Bu	THF	-78°	42:58	68%	47b
78	*c*-C_6H_{11}	Bu_3P	H	H, C_6H_5	Br^-	BuLi	THF	-78°	18:82	71%	47b
79	〃	〃	〃	〃	Br^-	KO*tert*Bu	THF	-78°	5:95	57%	47b
80	$(CH_3)_3C$	Bu_3P	H	H, C_6H_5	Br^-	BuLi	THF	-78°	37:63	59%	47b
81	C_6H_5	Bu_3P	CH_3	H, H	Cl^-	BuLi	THF	-78°	16:84	75%	47b

TABLE 15 *(Continued)*

Entry	R'	L_3P	R_β	($R_{\gamma Z}$, $R_{\gamma E}$)	X^-	Base	Solvent	Temp[a]	Z : E	Yield	Ref
82	"	"	"	"	Cl^-	KO*tert*Bu	THF	-78°	16:84	35%	47b
83	*c*-C_6H_{11}	Bu_3P	CH_3	H, H	Cl^-	BuLi	THF	-78°	<5:95	54%	47b
84	$PhCH_2CH_2$	Bu_3P	CH_3	H, H	Cl^-	BuLi	THF	-78°	8:92	63%	47b
85	"	"	"	"	Cl^-	KO*tert*Bu	THF	-78°	9:92	41%	47b
86	C_6H_5	Bu_3P	-($CH_2CH_2CH_2$)-, H		NO_2^-	BuLi	THF	-78°	<5:95	82%	47b
87	"	"	"	"	NO_2^-	KO*tert*Bu	THF	-78°	<5:95	41%	47b
88	*c*-C_6H_{11}	Bu_3P	-($CH_2CH_2CH_2$)-, H		NO_2^-	BuLi	THF	-78°	<5:95	80%	47b
89	C_6H_{13}	Bu_3P	-($CH_2CH_2CH_2$)-, H		NO_2^-	BuLi	THF	-78°	8:92	84%	47b
90	$(CH_3)_3C$	Bu_3P	-($CH_2CH_2CH_2$)-, H		NO_2^-	BuLi	THF	-78°	<5:95	67%	47b

Subset 1. Representative Benzaldehyde Reactions.

Entry	L_3P	R_β	($R_{\gamma Z}$,$R_{\gamma E}$)	Li^+-free Z:E	Li^+-ctg Z:E
5,1	Ph_3P	H	H, H	66:34	45:55
12	Ph_3P	H	H, CH_3	48:52	----
20,19	Ph_3P	H	H, C_6H_5	75:25	48:52
25,24	Ph_3P	H	CH_3, CH_3	78:22	61:39
31,30	Ph_3P	CH_3	H, H	55:45	31:69
36,35	Ph_3P	-($CH_2CH_2CH_2$)-, H		53:47	55:45
47,46	$MePh_2P$	CH_3	H, H	33:67	40:60
72,71	Bu_3P	H	CH_3, CH_3	22:78	29:71
82,81	Bu_3P	CH_3	H, H	16:84	16:84

Subset 2. Unbranched Aldehyde (R"CH_2CHO) Reactions .

Entry	L_3P	R_β	($R_{\gamma Z}$,$R_{\gamma E}$)	Li^+-free Z:E	Li^+-ctg Z:E
7	Ph_3P	H	H, H	45:55	---
17,16	Ph_3P	H	H, C_2H_5	40:60	50:50
28	Ph_3	H	CH_3, CH_3	---	55:45
34,33	Ph_3P	CH_3	H, H	39:61	29:71
51,50	$MePh_2P$	CH_3	H, H	14:86	30:70
58,56	$MePh_2P$	H	H, C_2H_5	14:86	30:70
85,84	Bu_3P	CH_3	H, H	9:91	8:92
68	86	H	H,H	12:88	---

Subset 3. α-Branched Aldehyde Reactions.

Entry	L_3P	R_β	($R_{\gamma Z}$,$R_{\gamma E}$)	Li^+-free Z:E	Li^+-ctg Z:E
10,9	Ph_3P	H	H, H	22:78	53:47
22,21	Ph_3P	H	H, C_6H_5	30:70	54:46
27,26	Ph_3P	H	CH_3, CH_3	20:80	37:63
43,41	$MePh_2P$	H	H, H	<5:95	33:67
49,48	$MePh_2P$	CH_3	H, H	4:96	6:94
59	**83e**	H	H, H	1:99	---
79,78	Bu_3P	H	H, C_6H_5	5:95	18:82
74,73	Bu_3P	H	CH_3, CH_3	5:95	15:85

Subset 4. α-Disubstituted (Tertiary) Aldehyde Reactions.

Entry	L_3P	R_β	($R_{\gamma Z}$,$R_{\gamma E}$)	Li^+-free Z:E	Li^+-ctg Z:E
11	Ph_3P	H	H, H	50:50	---
23	Ph_3P	H	H, C_6H_5	---	83:17
29	Ph_3P	H	CH_3, CH_3	---	>95:5
39	Ph_3P	$-(CH_2CH_2CH_2)-$, H		---	85:15
40	**83b** (PhDBP)	H	H, H	13:87	---
69,70	**86**	H	H, H	12:88	39:61
75	Bu_3P	H	CH_3, CH_3	---	23:77
80	Bu_3P	H	H, C_6H_5	---	37:63
90	Bu_3P	$-(CH_2CH_2CH_2)-$, H		---	<5:95

(a) The temperature for mixing the aldehyde and the ylide is given. Reaction times and final temperatures vary with each individual case, but warming to room temperature is commonly done for the low-temperature reactions.

(b) Ylide color was not discharged after 6 h at 20°. A second equivalent of aldehyde was added, and the reaction was terminated after 18 h.

(c) Control experiments show that ca. 10% of the ylide reacts at the γ-carbon under these conditions.

(d) The byproduct 1,5-diphenylpenta-2,4-dien-1-ol, derived from γ-capture of the ylide, was also isolated from this experiment, 26% yield.

(e) The byproduct 1,5-diphenyl-2-methylpenta-2,4-dien-1-ol, derived from γ-capture of the ylide, was also isolated from this experiment, 40% yield.

(f) γ-Capture of the ylide gave 13% of a dienol byproduct.

(g) The abbreviations $R^{1°}$ and $R^{2°}$ indicate unbranched and branched sp^3 carbon substituents, respectively.

with aliphatic aldehydes (subsets 2–4), but better results can be obtained by modifying phosphorus substituents. Thus, allylic ylides of the $MePh_2P$ series afford useful ratios in favor of the (*E*)-alkenes, and exceptional selectivities are possible with the phosphole-derived reagents (Table 15, entries 40, 59, 68, 70). In the E-selective reactions, lithium ion must be avoided because it moderates selectivity in much the same way as in the benzylide examples. Once again, some of the tertiary aldehyde reactions proceed with the highest selectivity for (*Z*)-alkene formation, but few systematic comparisons are available.

One other consistent feature in Table 15 will be mentioned because it has practical implications. Thus, many of the Ph_3P-derived allylic ylide reactions proceed in low yield (entries 11–14, 31, 34, etc.), while the corresponding reactions of $MePh_2P$-derived ylides are relatively efficient. One reason is that allylic ylides are capable of reacting with aldehydes at the γ-carbon to give polar byproducts derived from the initial formation of alkenylphosphonium salts (90). Reduced steric bulk in the $MePh_2P$-derived ylides promotes normal (Wittig) αC—C bonding, and the complication of γ-capture is minimized. As expected from the steric effect, the $MePh_2P$-derived ylides are also more reactive than the Ph_3P analogues, a factor that becomes important with hindered aldehydes. Overall, the $MePh_2P$-derived ylides offer a good compromise of reactivity, practicality, and (*E*)-alkene selectivity. No analogous reagents have been reported for the direct synthesis of (*Z*)-alkenes, and the exceptionally Z-selective environments such as $(o\text{-tolyl})_3P$ (61, 82b) remain to be explored. Less direct phosphorus-based strategies are already available for Z-selective diene synthesis using modified Wittig reagents (91).

XII. CARBONYL-STABILIZED YLIDES

The utility of carbonyl-stabilized ylides for (*E*)-alkene synthesis was recognized in the early 1960s (4b, 5a, 98). Solvent and substituent effects that work against the inherent trend for E selectivity were also noted (4b). Thus, House (4b) reported that the reaction of acetaldehyde with $Ph_3P{=}CHCO_2Me$ produces methyl crotonate with Z:E ratios of 3:97 in dry DMF and 6:94 in CH_2Cl_2. In methanol, two different results were given, 28:72 Z:E after distillation and 38:62 Z:E by direct GLPC (gas liquid partition chromatography) analysis. House (4b) also observed that lithium or magnesium salts reduced E selectivity in DMF, but not in methanol. Similar results were obtained for the reaction of $Ph_3P{=}CHCO_2Me$ with chloroacetaldehyde. This substrate gave relatively more of the (*Z*)-enoate: Z:E = 17:83 (DMF), 29:71 (CH_2Cl_2), and 52:48 (CH_3OH) (4b). Many subsequent studies of stabilized ylides are summarized in Tables 16–19. While the findings follow

TABLE 16

Solvent Effects on Z:E Selectivity of Aldehyde Reactions with $Ph_3P{=}CHCO_2Et$ (42, 99).

		$PhCH_2CH_2CHO$ (1h, RT).			2-FORMYLTETRAHYDROPYRAN (3h, RT).	
Solvent	Entry	Z:E,[a] preformed[b]	Z:E,[a] *in situ*[c]	Entry	Z:E,[a,d] preformed[b]	Z:E,[a,d] *in situ*[c]
MeOH	1	38:62 (87%)[e]	41:59 (91%)	10	75:25 (>95%)	73:27 (92%)
EtOH	2	28:72 (88%)	32:68 (94%)	11	69:31 (85%)	69:31 (96%)
CF_3CH_2OH	3	9:91 (83%)	13:87 (93%)	12	46:54 (89%)	46:54 (86%)
CH_3CN	4	7:93 (87%)	30:70 (86%)	13	11:89 (94%)	52:48 (95%)
CH_2Cl_2	5	4:96 (89%)	25:75 (98%)	14	10:90 (>95%)	50:50 (95%)
DMF	6	5:95 (69%)	20:80 (70%)	15	8:92 (82%)	38:62 (71%)
THF	7	8:92 (96%)	9:91 (95%)	16	8:92 (74%)	22:78 (96%)
CCl_4	8	4:96 (87%)	6:94 (98%)	17	8:92 (63%)	21:79 (93%)
C_6H_6	9	5:95 (89%)	6:94 (91%)	18	14:86 (68%)	24:76 (91%)

(a) Yields determined after chromatography over silica gel; Z:E ratios based on NMR integration of isomer mixtures.

(b) The ylide was purified by recrystallization prior to use.

(c) The ylide was generated *in situ* from the phosphonium bromide and diazabicycloundecene (DBU); the reaction mixture contains 1 equiv of $DBU{+}H^+$ Br^-

(d) Yields based on the starting phosphonium salt. The aldehyde was made by Swern oxidation from the alcohol, and was used in two-fold excess.

(e) Partial ester exchange occurs under the reaction conditions; the product consists of 13% methyl ester and 74% ethyl ester, both having 38:62 Z:E.

TABLE 17

Substituent Effects on Z:E Selectivity of R'CHO Reactions with $L_3P{=}CHCO_2R''$ at Room Temperature

Entry	R''	R'	L_3P	Solvent	Method	Z:E	Yield	Ref
1	Et	C_6H_5	Ph_3P	EtOH	*in situ* NaOEt	15:85	---	98
2	"	"	"	MeOH	*in situ* DBU	25:75	98%	99
3	"	"	"	EtOH	*in situ* DBU	18:82	98%	99
4	"	"	"	CH_2Cl_2	*in situ* DBU	14:86	95%	99
5	"	"	"	THF	*in situ* DBU	4:96	83%	99
6	"	"	"	C_6H_6	*in situ* DBU	3:97	86%	99
7	Me	PhCH=CH	Ph_3P	$CHCl_3$[a]	preformed ylide	14:86[a]	84%	101
8	Et	$PhCH_2(CH_3)_2C$	Ph_3P	EtOH	*in situ* DBU	35:65	5%	21c
9	"	"	"	THF	*in situ* DBU	5:95	3%	21c
10	Et	*c*-C_6H_{11}	Ph_3P	MeOH	*in situ* DBU	32:68[b]	95%	99
11	"	"	"	EtOH	*in situ* DBU	16:84	93%	99
12	"	"	"	CH_2Cl_2	*in situ* DBU	14:86	93%	99
13	"	"	"	CH_2Cl_2	preformed ylide	3:97	76%	99
14	"	"	"	THF	*in situ* DBU	2:98	93%	99
15	Me	*c*-C_6H_{11}	Ph_3P	$CHCl_3$[a]	preformed ylide	5:95[a]	93%	101
16	Et	$PhCH_2CH_2$	Ph_3P	EtOH	*in situ* DBU	32:68	94%	99
17	"	"	"	EtOH	preformed ylide	28:72	88%	99
18	"	"	"	THF	*in situ* DBU	9:91	95%	99
19	"	"	"	THF	preformed ylide	8:92	96%	99
20	"	"	"	C_6H_6	*in situ* DBU	6:94	91%	99
21	"	"	"	C_6H_6	preformed ylide	5:95	89%	99
22	Me	CH_3	Ph_3P	MeOH	preformed ylide	28-38:72-62	38%	4b
23	"	"	"	DME	preformed ylide	3:97	--	4b
24	"	"	"	EtOH	*in situ* NaOEt	27:73	71%	100

25	Et	C_5H_{11}	**83b**	EtOH	*in situ* DBU	54:46	--	99b
26	"	"	"	THF	*in situ* DBU	10:90	--	99b
27	Et	$PhCH_2CH_2$	**83b**	EtOH	*in situ* DBU	47:53	--	99b
28	"	"	"	THF	*in situ* DBU	15:85	--	99b
29	Et	C_6H_5	$MePh_2P$	EtOH	*in situ* DBU	37:63	54%	21c
30	"	"	"	THF	*in situ* DBU	17:83	87%	21c
31	Et	$PhCH_2(CH_3)_2C$	$MePh_2P$	EtOH	*in situ* DBU	58:42	10%	21c
32	"	"	"	THF	*in situ* DBU	22:78	7%	21c
33	Et	*c*-C_6H_{11}	$MePh_2P$	EtOH	*in situ* DBU	35:65	64%	21c
34	"	"	"	THF	*in situ* DBU	15:85	95%	21c
35	"	"	"	THF	*in situ* KHMDS	4:96	88%	21c
36	Et	$PhCH_2CH_2$	$MePh_2P$	MeOH	*in situ* DBU	60:40	88%	42
37	"	"	"	EtOH	*in situ* DBU	50:50	71%	21c
38	"	"	"	THF	*in situ* DBU	19:81	87%	21c
39	Et	$PhCH_2CH_2$	**86**	MeOH	*in situ* DBU	54:46[d]	96%[d]	42
40	"	"	"	CF_3CH_2OH	" "	34:66	83%	42
41	"	"	"	THF	" "	13:87	92%	42
42	Et	$PhCH_2CH_2$	Bu_3P	MeOH	*in situ* DBU	10:90	71%	42
43	"	"	"	THF	*in situ* DBU	5:95	96%	42
44	Et	C_6H_5	Bu_3P	EtOH	*in situ* NaOEt	5:95	---	98
45	Et	C_6H_5	(*n*-$C_6H_{13})_3P$	EtOH	*in situ* NaOEt	2:98	---	98
46	Et	C_6H_5	(*n*-$C_8H_{17})_3P$	EtOH	*in situ* NaOEt	20:80	---	98
47	Et	C_6H_5	(*n*-$C_{10}H_{21})_3P$	EtOH	*in situ* NaOEt	4:96	---	98
48	Et	C_6H_5	(*c*-$C_6H_{11})_3P$	EtOH	*in situ* NaOEt	1:99	---	98

(a) Reflux temperature. (b) Partial transesterification occurs; 53% ethyl ester, 42% methyl ester. (c) The reactants were mixed at room temperature and then refluxed for two hours. (d) Partial transesterification occurs under these conditions (57% methyl esters; 43% ethyl esters).

TABLE 18

Z:E Selectivity of Stabilized Ylides $L_3P{=}CRX + R'CHO$

Entry	CRX	R'	L_3P	Solvent	Temp	Z:E	Yield	Ref
1	CHCHO	n-C_6H_{13}	Ph_3P	C_6H_6	80°	5:95	32%	102
2	CHCHO	$CH_3O_2C(CH_2)_8$	Ph_3P	C_6H_6	80°	5:95	52%	102
3	CHC(O)SEt	c-C_6H_{11}	Ph_3P	$CHCl_3$	61°	4:96	91%	101
4	"	PhCH=CH	Ph_3P	"	"	4:96	87%	101
5	CHCN	$PhCH_2CH_2$	Ph_3P	THF	RT	27:63[a]	94%	42a
6	"	"	Ph_3P	MeOH	RT	63:27[a]	90%	42a
7	CHC(O)Me	$PhCH_2$	Ph_3P	THF	0°	<5:95[b]	89%	103
8	"	$PhCH_2CH_2$	Ph_3P	THF	RT	6:94	84%	42a
9	"	"	Ph_3P	MeOH	RT	16:84	86%	42a
10	"	$Ph(CH_3)CH$	Ph_3P	CH_2Cl_2	40°	<5:95[b]	52%	104
11	CHC(O)Ph	CH_3	Ph_3P	C_6H_6	RT	12:88	>90%	105
12	CHC(O)Ph	CH_3	Ph_3P	EtOH	RT	14:86	>90%	105
13	CHC(O)Ph	C_6H_5CHO	Ph_3P	C_6H_6	80°	12:88	>90%	105
14	CHC(O)Ph	C_6H_5CHO	Ph_3P	EtOH	80°	10:90	>90%	105
15	CHC(O)Ph	CH_3	**83b**	C_6H_6	RT	28:72	>90%	105
16	CHC(O)Ph	CH_3	**83b**	EtOH	RT	21:79	>90%	105
17	CHC(O)Ph	C_6H_5CHO	**83b**	C_6H_6	RT	28:72	>90%	105
18	CHC(O)Ph	C_6H_5CHO	**83b**	EtOH	RT	13:87	>90%	105
19	$C(CH_3)CO_2Et$	p-(i-Pr)$C_6H_5CH_2CH_2$	Ph_3P	THF	RT	<10:90[b]	90%	106
20	"	R"$CH(CH_3)CH_2$	Ph_3P	CH_2Cl_2	40°	5:95	95%	107a
21	"	$Ph(CH_3)CH$	Ph_3P	CH_2Cl_2	RT	5:95	--	108
22	"	"	Ph_3P	MeOH	RT	15:85	--	"
23	$C[(CH_2)_8CH{=}CH_2]CO_2Me$	"	Ph_3P	THF	RT	<1:99	84%	107b
24	" "	n-C_8H_{17}	Ph_3P	THF	RT	<1:99	60%	107b

(a) The ylide was generated *in situ* from the phosphonium bromide with DBU.

(b) Estimated limit based on yield and method of isolation; only one isomer was reported.

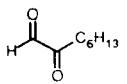
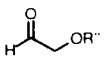
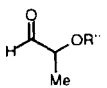
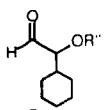
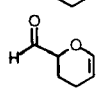
the patterns originally reported by House, some of the more complex substrates (Table 19) display incredible sensitivity to experimental conditions. Structural details in the aldehyde are also important, especially when heteroatom substituents are present (2j). Before considering the most dramatic examples, we will examine two simple aldehyde substrates in detail to evaluate solvent and additive effects.

Table 16 summarizes the solvent dependence of Z:E ratios for the representative reactions of an unbranched alkanal ($PhCH_2CH_2CHO$) and an α-branched, α-alkoxy aldehyde (2-formyltetrahydropyran) (99a). Each entry provides Z:E data for the reaction of crystallized $Ph_3P{=}CHCO_2Et$ as well as for the analogous reaction using an *in situ* method for ylide generation from $Ph_3P^+CH_2CO_2Et\ Br^-$ and the amidine base DBU. The latter technique is included to allow comparisons with other ylides that do not crystallize and that are more easily handled using the *in situ* method (Table 17). It is apparent that the two methods give rather different Z:E ratios due to the variable presence of $DBU{\cdot}H^+Br^-$. Substantial solvent effects are seen with both of the aldehydes, but the α-alkoxy substrate is affected more strongly, and its reactions have a smaller bias for (*E*)-enoate formation. Optimum selectivity for the (*E*)-enoate is obtained under aprotic conditions, and the most reliable conditions employ the least polar solvents. Thus, the selectivity perturbation due to $DBU{\cdot}H^+Br^-$ is smallest in THF, CCl_4, and C_6H_6, probably because the salt precipitates from these solvents. The effect is also small in alcohol solvents where the salt remains in solution, but these reactions are already substantially perturbed by the hydroxylic solvent compared to the aprotic experiments. Reactions performed in CH_3CN, CH_2Cl_2, and DMF are influenced the most by $DBU{\cdot}H^+Br^-$, as shown by entries 4–6 and 13–15 in Table 16. The reaction of 2-formyltetrahydropyran with crystallized $Ph_3P{=}CHCO_2Et$ (CH_2Cl_2, room temperature) is especially sensitive to impurities (use of aldehyde several days after distillation, 17:83 Z:E) and to additives: (1) 0.5 equiv excess $Ph_3P^+CH_2CO_2Et\ Br^-$ added, Z:E = 25:75, (2) 1.1 equiv $C_6H_{11}NH_3^+Cl^-$ added, Z:E = 41:59; (3) 1.2 equiv $C_6H_5CO_2H$ added, Z:E = 2:98; and (4) 1 equiv CH_3CO_2H added, Z:E = 10:90. Stronger acids (for example, pyridinium trifluorosulfonate) protonate the ylide and inhibit the Wittig reaction.

The enhancement of E selectivity by benzoic acid is especially striking. This phenomenon was first reported in 1974 (100b), but little is known regarding its origin. In the examples mentioned above, benzoic acid preferentially catalyzes the E-selective Wittig pathway and does not cause E/Z equilibration of the products (99). Thus, the enhanced (*E*)-enoate selectivity is the result of kinetic control.

Since solvents or additives can promote *either* the E-selective or the Z-selective pathway with $Ph_3P{=}CHCO_2Et$, it is crucial to focus on

TABLE 19
Substituent Effects on Z:E Selectivity; Stabilized Ylides $Ph_3P{=}CRX$ + Aliphatic R'CHO

	Entry	CRX	R''	Solvent	Temp	Z:E	Yield	Ref
	1	$CHCO_2Me$	--	MeOH	RT	52:48	--	4b
	2	"	--	CH_2Cl_2	40°	33:67	57%	4b
	3	$C(CH_3)CO_2tBu$	--	CH_2Cl_2	40°	6:94	86%	109
	4	$CHCO_2Me$	--	CH_2Cl_2	-78° to RT	6:94[a]	84%	110
	5	CHC(O)Me	Bn	THF	RT	<5:95[b]	82%	111a
	6	$C(CH_3)CO_2Et$	Bn	CH_2Cl_2	RT	6:94	74%	111b
	7	"	Bn	"	"	10:90	90%	111c
	8	$CHCO_2Me$	Bn	MeOH	RT	79:21	82%	112
	9	"	Bn	MeC_6H_5	RT	50:50	81%	112
	10	"	Bn	CH_2Cl_2	RT	33:67	80%	112
	11	$C(CH_3)CO_2Et$	Bn	CH_2Cl_2	RT	6:94	--	113a
	12	$C(CH_3)CO_2Et$	MOM	CH_2Cl_2	40°	<10:90[b]	--	113b
	13	$CHCO_2Me$	Bn	$CHCl_3$	61°	25:75	81%	101
	14	CHC(O)SEt	Bn	"	"	9:91	78%	101
	15	$CHCO_2Et$	--	MeOH	RT	75:25[a]	95%	99a
	16	"	--	THF	RT	8:92	74%[c]	99a
	17	$CHCO_2Et$	--	$C_6H_5CH_3$	60°	12:88	80%	114a

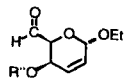
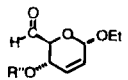
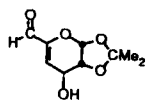
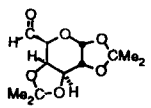
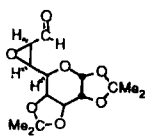
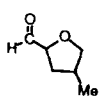
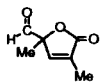
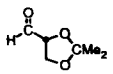
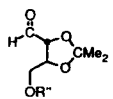
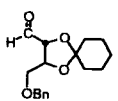
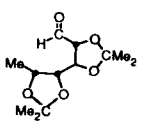
	18	$CHCO_2Et$	--	$C_6H_5CH_3$	60°	10:90	90%	114a
	19	$CHCO_2Me$	OBn	MeOH	RT	>99:1	78%	112
	20	$CHCO_2Me$	OBz	MeOH	RT	>99:1	76%	112
	21	$CHCO_2Me$	OTBS	MeOH	RT	22:78	92%	112
	22	$CHCO_2Me$	--	MeOH	RT	37:63	73%	112
	23	$CHCO_2Me$	--	MeOH	RT	95:5	80%	112
	24	"	"	"	-8°	>99:1	68%	112
	25	"	"	iPrOH	RT	91:9	56%	112
	26	$CHCO_2Me$	--	MeOH	RT	81:19	82%	112
	27	$CHCO_2Et$	--	CH_2Cl_2 ($DBU{\cdot}H^+Br^-$)	RT	50:50[a]	62%	42a
	28	$CHCO_2Et$	--	CH_2Cl_2	RT	<10:90[a,b]	65%	114b
	29	CHC(O)Me	--	CH_2Cl_2	RT	<10:90[a,b]	50%	114b

TABLE 19 *(Continued)*

	Entry	CRX	R''	Solvent	Temp	Z:E	Yield	Ref
	30	C(Me)CHO	--	THF	65°	<10:90[a]	75%	113c
	31	CHCHO	--	$C_6H_5CH_3$	0° (39 h)	2:98	85%	115
	32	$CHCO_2Me$	--	MeOH	RT	88:12	97%	115,116a,b,c
	33	$CHCO_2Et$	-	CH_2Cl_2/H_2O	RT	74:26	88%	116d
	34	"	--	$C_6H_5CH_3$	RT	<5:95[d]	90%	117
	35	CHC(O)Me	--	CH_2Cl_2	RT	50:50	--	118
	36	"	--	$C_6H_5CH_3$	RT	14:86	67%	117,118
	37	$CHCO_2Et$	Bn	MeOH	RT	86:14	94%	115
	38	"	Bn	"	RT	89:11	88%	119
	39	"	Bn	MeOH	65°	80:20	100%	119
	40	"	Bn	CH_2Cl_2	40°	65:35	88%	119
	41	"	Bn	C_6H_6	80°	30:70	83%	119
	42	"	Bn	DMF	RT	27:73	77%	119
	43	"	TBS	CH_2Cl_2	?	32:68	87%	120
	44	$C(CH_3)CO_2Et$	--	C_6H_6	70°	8:92	92%	121
	45	$CHCO_2Me$	--	MeOH	RT	88:12	70%	112

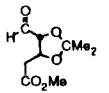
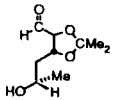
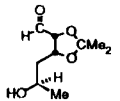
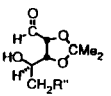
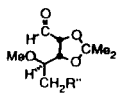
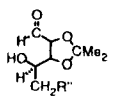
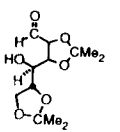
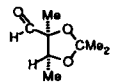
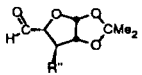
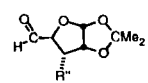
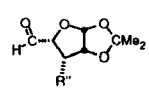
	46	$C(CH_3)CO_2Et$	--	CH_3CN	RT	<10:90[b]	81%	122
	47	CHC(O)SEt	--	$CHCl_3$	61° (add DMAP at RT to equilibrate Z to E)	<5:95	72%	101b
	48	CHC(O)SEt	--	$CHCl_3$	61°	20:80	78%	101b
	49	"	--	"	(add DMAP at RT)	<5:95	"	"
	50	$CHCO_2tertBu$	Br	CH_2Cl_2	25°	91:9	90%	123
	51	$CHCO_2Et$	TBSO	DME	25°	88:12	80%	123
	52	$CHCO_2tertBu$	MOMO	CH_2Cl_2	25°	91:9	95%	123
	53	$CHCO_2Me$	Ph_3CO	CH_2Cl_2	RT	88:12	90%	124
	54	"	"	"	40°	71:29	83%	124
	55	"	"	C_6H_{14}	69°	29:79	86%	124
	56	$CHCO_2tertBu$	MOMO	CH_2Cl_2	25°	5:95	87%	123
	57	$CHCO_2tertBu$	MOMO	CH_2Cl_2	25°	20:80	92%	123
	58	$CHCO_2Et$	Br	CH_2Cl_2	25°	25:75	81%	123
	59	$CHCO_2Et$	--	C_6H_6	80°	<5:95	60%	124

TABLE 19 *(Continued)*

	Entry	CRX	R''	Solvent	Temp	Z:E	Yield	Ref
	60	$C(CH_3)CO_2Et$	--	CH_2Cl_2	40°	<5:95	88%	125
	61	$CHCO_2Et$	MeO	MeOH	RT	92:8	--	126
	62	"	"	$CHCl_3$	"	60:40	--	126
	63	"	"	CCl_4	"	53:47	--	126
	64	"	"	Acetone	"	47:53	--	126
	65	"	"	Hexane	"	46:54	--	126
	66	"	"	Benzene	"	20:80	--	126
	67	"	"	DMF	"	14:86	--	126
	68	$CHCO_2Et$	BnO	MeOH	RT	99:1	80%	125b
	69	"	HO	MeOH	RT	80:20	75%	125b
	70	"	"	CH_3CN	82°	20:80	86%	125c
	71	CHCN	BnO	DMSO	20°	>95:5	46%	127
	72	$CHC(O)CH_3$	MeO	$CHCl_3$	"	30:70	87%	126
	73	"	"	C_6H_6	"	5:95	86%	126
	74	"	"	DMF	"	2:98	78%	126
	75	$CHC(O)CH_3$	Cl	$CHCl_3$	20°	25:75	85%	126
	76	"	"	C_6H_6	"	7:93	79%	126
	77	$CHCO_2Et$	HO	MeOH	RT	74:26	70%	125b
	78	$CHC(O)CH_3$	H	$CHCl_3$ (also C_6H_6, DMF)	20°	<5:95	77%	126
	79	$CHC(O)CH_3$	MeO	$CHCl_3$ (also C_6H_6, DMF)	20°	<5:95	87%	126
	80	$CHCO_2Et$	B. O	CH_3CN	82°	10:90	95%	125c

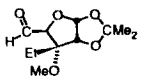
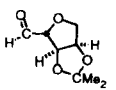
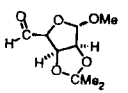
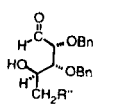
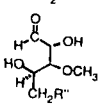
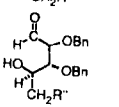
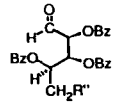
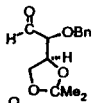
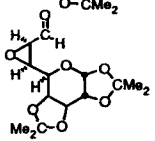
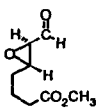
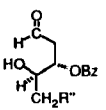
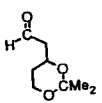
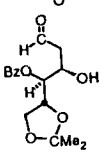
	81	$CHC(O)CH_3$	--	$CHCl_3$	20°	<5:95	88%	126
	82	"	--	C_6H_6	"	<5:95	79%	126
	83	"	--	DMF	"	<5:95	80%	126
	84	$CHC(O)CH_3$	--	$CHCl_3$	20°	38:62	82%	126
	85	"	--	C_6H_6	"	15:85	76%	126
	86	"	--	DMF	"	3:97	79%	126
	87	CHCN	--	DMSO	"	34:67	--	127
	88	"	--	DMSO ($PhCO_2H$)	"	26:74[e]	--	127
	89	"	--	"	"	14:86[f]	61%	127
	90	$CHCO_2Et$	--	MeOH	RT	>99:1	76%	125b
	91	$CHC(O)CH_3$	--	$CHCl_3$	20°	43:57	85%	126
	92	"	--	C_6H_6	"	21:79	88%	126
	93	"	--	DMF	"	4:96	71%	126
	94	$CHCO_2Et$	BnO	DME ($PhCO_2H$)	?	40:60	90%	128
	95	$CHCO_2Me$	BnO	CH_3CN	82°	60:40	90%	129
	96	$CHCO_2Et$	CO_2Me	$C_6H_5CH_3$	25°	<10:90[b]	86%	130
	97	$CHCO_2tertBu$	MOMO	CH_2Cl_2	25°	60:40	87%	123

TABLE 19 *(Continued)*

	Entry	CRX	R''	Solvent	Temp	Z:E	Yield	Ref
	98	$CHCO_2Et$	BzO	DME ($PhCO_2H$)	85°	14:86	96%	131
	99	$CHCO_2CH_3$	--	MeOH	RT	91:9	77%	112
	100	$CHCO_2CH_3$	--	MeOH	RT	81:19	82%	112
	101	CHCHO	--	C_6H_6	80°	<5:95[b]	84%	132
	102	$CHCO_2Et$	BzO	DME ($PhCO_2H$)	85°	17:83	64%	133
	103	$CHC(O)CH_3$	--	CH_3CN	82°	<20:80[b]	57%	134
	104	$CHCO_2CH_3$	--	DME ($PhCO_2H$)	70°	12:88	96%	135

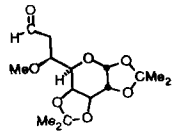
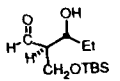
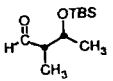
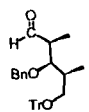
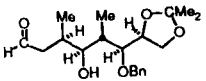
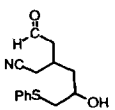
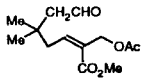
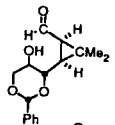
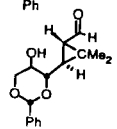
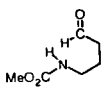
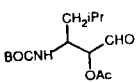
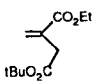
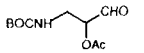
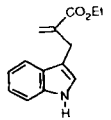
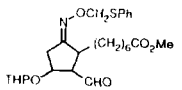
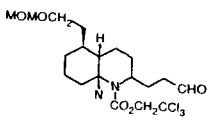
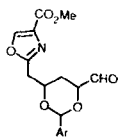
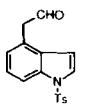
	105	$CHCO_2CH_3$	--	MeOH	RT	56:44	88%	112
	106	$CHCO_2Me$	Bn	$CHCl_3$	61°	3:97	89%	101a
	107	CHC(O)SEt	Bn	$CHCl_3$	61°	3:97	80%	101a
	108	CHC(O)Me	Bn	CH_2Cl_2	40°	33:67	89%	104
	109	$C(CH_3)CO_2Et$	TBS	C_6H_6	70°	<10:90[b]	71%[b]	136
	110	$C(CH_3)CO_2Et$	--	CH_2Cl_2	40°	<1:99	91%	137a
	111	$C(CH_3)CO_2Et$	--	$C_6H_5CH_3$	70°	<5:95	85%	137b
	112	$C(CH_3)CO_2Et$	--	THF	22°	<3:97	52%	138
	113	$C(CH_3)CO_2Et$	--	$C_6H_5CH_3$	45°	<5:95	88%	139
	114	$CHCO_2Et$	--	CH_2Cl_2	RT	11:89	82%	140

TABLE 19 *(Continued)*

	Entry	CRX	R''	Solvent	Temp	Z:E	Yield	Ref
$HSCH_2CHO$	115	$CHCO_2Bn$	--	C_6H_6	60°	<2:98	85%	141a
""	116	$CH(CH_3)CO_2Et$	--	C_6H_6	60°	<5:95	83%	141a
	117		--	CH_2Cl_2/MeOH	reflux	5:1	65%	141b
	118	$C(CH_3)CO_2Et$	--	CH_2Cl_2	RT	<5:95	93%	141c
	119	$C(CH_3)CO_2Et$	--	CH_2Cl_2	RT	11:89	93%	141c
	120	$CHCO_2Et$	--	C_6H_6	105°	6:94	85%	142a
	121		--	CH_2Cl_2	RT	16:84	73%	142b
-- --	122		--	CH_2Cl_2	RT	35:65	70%	142b

	123		--	CH_2Cl_2	RT	14:86	80%	142b
	124	$Bu_3P{=}CHC(O)C_5H_{11}$	--	Et_2O	RT	'E only'	74%	142c
	125	CHCHO	--	$CHCl_3$	reflux	'E only'	75%	142d
	126	CHCHO	--	C_6H_6	reflux	<10:90	77%	142e
	127	$C(CH_3)CN$	--	THF	RT	61:39	54%	142f
	128	""	--	C_6H_6	RT	37:63	54%	142f

(a) Aldehyde generated *in situ* by Swern oxidation; used without purification.

(b) Estimated limits of detection based on yield and isolation method.

(c) Freshly distilled aldehyde was used. Otherwise, the amount of Z enoate was ca. 13-18%.

(d) The aldehyde may contain acetic acid as a byproduct of its preparation; see ref. 116c for further information on the role of acetic acid.

(e) Benzoic acid (stoichiometry: 1 equiv per equiv of ylide and aldehyde) was present.

(f) Stoichiometry: benzoic acid (0.5 equiv), ylide (2 equiv), and aldehyde (1 equiv).

(g) Stoichiometry: benzoic acid (1.0 equiv), ylide (3 equiv), and aldehyde (1 equiv).

experimental details when evaluating (or reporting) Z:E selectivity data. There is a substantial risk that contamination of the aldehyde by the carboxylic acid or by other impurities may influence Z:E ratios by catalysis. In spite of these potential uncertainties, the Z:E ratios collected in Tables 17 and 18 follow consistent patterns to the extent that direct comparisons under identical conditions can be made.

The Wittig reactions of simple aldehydes with a variety of ester-stabilized ylides are summarized in Table 17. Many of these reactions can be performed with high (*E*)-enoate selectivity in ether solvents, but the use of *in situ* ylide generation methods can be problematic unless bases such as NaOEt or KHMDS [$KN(SiMe_3)_2$] are employed. The steric bulk of the aldehyde reactant is not an important factor, nor is the phosphorus substitution pattern under the optimum THF conditions for (*E*)-enoate formation. In contrast to the nonstabilized ylide reactions, there is no dramatic change in Z:E selectivity when the conventional Ph_3P subunit is replaced by derivatives containing a phosphole ring (Table 17, entries 26, 28, 41). However, there are substantial differences in the way that different ylides respond to solvent variations. In general, the *P*-triphenyl derivatives respond strongly to the use of hydroxylic solvents, while the *P*-trialkyl ylides (Table 17, entries 42–48) are relatively insensitive and react with high selectivity for the (*E*)-enoates in ethanol. According to the crossover experiments discussed earlier (Table 6), all of these results are probably due to dominant kinetic control. However, no control experiments have been performed in the *P*-trialkyl series. Futhermore, it is possible that some of the empirical results may be influenced by equilibration of product stereochemistry. This potential complication has been ruled out for the entries of Table 16, but most of the other stabilized ylide examples have not been studied in depth and the possibility of product equilibration has not been tested.

Table 18 summarizes the reactions of several other families of stabilized ylides with simple aldehydes. With the exception of the cyano ylide entries (entries 5, 6), these reactions are consistently selective for the (*E*)-alkene, and the influence of solvents is small by comparison to the ester-stabilized ylides of Table 16 or 17. To the extent that systematic comparisons are possible based on the limited data, the formyl-, acyl-, or phenacyl-stabilized ylides all afford similar product ratios. The α-alkyl ester-stabilized ylides (Table 18, entries 19–24) also react with a consistent preference for the (trisubstituted) (*E*)-alkene in protic or aprotic solvents. No control experiments have been reported for the great majority of examples, and product equilibration is a possibility. Nevertheless, the entries of Table 18 are striking for their consistent E selectivity in a variety of solvents. Apparently, ester- or cyano-stabilized ylides such as $Ph_3P{=}CHCO_2Et$, $Ph_3P{=}CHCN$, and $MePh_2P{=}CHCO_2Et$ (Tables 16, 17, 19) are unique in their sensitivity to solvent changes.

Many reactions of stabilized ylides have been described with aldehydes that contain heteroatom substituents (Table 19). Due to the complexity of the substrates, this table is organized according to the aldehyde reactant and includes a variety of stabilized ylides. The table cites only a few of the more than 200 known reactions of complex aldehydes with $Ph_3P{=}C(CH_3)CO_2R''$ because they all follow the same selectivity pattern as in the simple examples of Table 18. Heteroatom substituents do not alter the usual preference for the (*E*)-trisubstituted enoate. On the other hand, α-heteroatom substitution is clearly important for the reactions of $Ph_3P{=}CHCO_2R''$. These results are covered more thoroughly. Nearly all of the reactions follow the logic of Tables 16–17, but some of the examples are exceptionally selective. Systematic comparisons suggest that remote heteroatoms may enhance or negate the α-alkoxy effect, depending on the details of aldehyde structure.

Most of the α-oxygenated aldehydes in Table 19 display the characteristic trend toward (*Z*)-enoate formation with $Ph_3P{=}CHCO_2R''$ (2j). A simple example of this phenomenon was discussed in connection with Table 16 (2-formyltetrahydropyran entries), but a number of others had been reported much earlier (Table 19, entries 61–93) (126–127). Table 19 also includes the first systematic solvent comparisons (entries 61–67) for an α-alkoxy aldehyde reaction with an ester-stabilized ylide (126). This series of experiments represents the most dramatic known example of solvent effects on selectivity (92:8 Z:E in methanol; 14:86 Z:E in DMF), but the results are qualitatively similar to the solvent study in Table 16. In several other examples, the isomer ratios in methanol are reported to reach synthetically useful levels (> 90%) of the (*Z*)-enoate (Table 19, entries 19, 20, 23–25). However, most of the methanol entries fall in the more typical range of 70–85% (*Z*)-enoate. No similar trend is seen with β- or γ-oxygenated aldehydes (Table 19, entries 102–113) that lack an α-alkoxy group.

Table 19 also includes several remarkable contrasts in selectivity. For example, a γ-hydroxyaldehyde (entry 52) reacts with an exceptionally high 91:9 Z:E ratio in dichloromethane. The corresponding γ-methoxy aldehyde (entry 56) gives a 5:95 Z:E enoate ratio. Assuming a kinetically controlled reaction in each case, the observations show that the normal α-alkoxy effect can be enhanced by the internal γ-hydroxyl group and negated by the γ-methoxy function. However, a small change in relative stereochemistry also appears to negate some of the α-alkoxy effect in aldehydes that contain a free γ-hydroxyl group (entries 57–59). The results suggest the possibility of cooperative effects due to two or more heteroatoms, but it will be necessary to explore simpler model compounds before this hypothesis can be confirmed.

Some of the reactions of $Ph_3P{=}CHC(O)Me$ encounter a similar but smaller cooperative effect that appears to depend on remote stereochemistry. Thus, entries 72 and 75 in Table 19 proceed normally to afford products

containing 70–75% (*E*)-alkene and 25–30% (*Z*)-alkene (chloroform solution), while entries 78, 79, and 81 afford only the (*E*)-isomer (NMR detection limits) under the same conditions. Unfortunately, no experiments have been reported using $Ph_3P{=}CHCO_2R''$ and the same α-alkoxy aldehyde substrates. The closest analogy (entry 77) contains an α-hydroxyl group in the substrate aldehyde, but this reaction appears to proceed normally in methanol and gives a 76:24 Z:E ratio of enoates. These contrasting results, like some of the other entries in Table 19, should be interpreted with care because control experiments were not reported in most of the examples.

Product equilibration is not likely under room temperature reaction conditions, but there are some cases where it has been deliberately used to enhance the (*E*)-enoate selectivity of reactions that otherwise afford mixtures. Entries 47–49 in Table 19 demonstrate that catalytic amounts of *p*-dimethylaminopyridine (DMAP) will induce the Z:E equilibration of α,β-unsaturated thiol esters at room temperature (chloroform solution), resulting in enhanced (*E*)-enoate selectivity (101b). This procedure is not effective with the corresponding oxygen esters, however.

Equilibration may also be involved in some of the reactions of acyl-stabilized ylides such as $Ph_3P{=}CHC(O)CH_3$, or of the formyl analogue $Ph_3P{=}CHCHO$, reagents that tend to produce (*E*)-alkenes in alcohols or halocarbons as well as in the nonpolar, aprotic solvents. These highly stabilized ylides are not very reactive, and extended reaction times increase the risk of Z/E interconversion. On the other hand, product equilibration has been ruled out for at least some of the E-selective reactions of the relatively reactive α-substituted ylide $Ph_3P{=}C(Me)CO_2R''$.

Another way to enhance (*E*)-enoate selectivity of α-alkoxy aldehyde reactions is available, based on the catalytic effect of benzoic acid in ether solvents (99a, 101b, 128, 131). Detailed stereochemical comparisons of catalyzed and uncatalyzed reactions are not available in the examples in Table 19, but entry 98 is reported to benefit significantly by comparison to the uncatalyed process (131). It has not been shown whether benzoic acid catalysis affects the mechanism of C—C bond formation or whether it equilibrates product stereochemistry in this case. The combination of the acid catalyst and the elevated reaction temperature in dimethoxyethane increases the risk of Z:E equilibration. However, in an earlier example discussed in connection with Table 16, the (*E*)-enoate-enhancing effect of benzoic acid is due to kinetic control. It has also been shown that benzoic acid catalysis is more effective in CH_2Cl_2 than in dimethylsulfoxide (99a).

Kinetic control is plausible in many, if not all, of the other E-selective ylide reactions. It follows that the exceptionally solvent- and substrate-dependent reactions of the α-unsubstituted ester-stabilized ylides ($Ph_3P{=}CHCO_2R''$, $Ph_2MeP{=}CHCO_2R''$, etc.) reflect transition state preferences

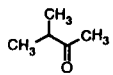
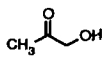
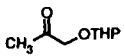
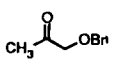
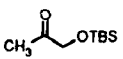
that are unique to this ylide family. Nearly all of the complex examples of Table 19 follow the simpler ester-stabilized ylide precedents of Tables 16–18, provided that comparisons are made in the same solvent. Optimum selectivity for the (*E*)-enoate is seen in ethers or other nonpolar, aprotic solvents, while the highest percentage of (*Z*)-enoate is consistently observed when the reactions are performed in methanol.

XIII. YLIDE REACTIONS WITH KETONES

Wittig reactions of ketones are experimentally more difficult due to diminished carbonyl reactivity and the substantial risk of enolization. These potential problems can be overcome using special experimental techniques to be discussed at the end of this section, but some of the available Z:E selectivity data were obtained from experiments that were not optimized for maximum conversion to the alkene. This situation complicates the interpretation of stereochemical results, especially in those cases where only one product was isolated using chromatography or crystallization (for example, Table 20, entries 58–62, 64–76). If the yield is low, the isolation of a single product does not necessarily prove that the Wittig reaction proceeds with high selectivity for that product. Stereochemical comparisons are further complicated because there is no simple way to prove the geometry of trisubstituted double bonds in complex substrates. Nevertheless, there is a modest amount of reliable data. Table 20 includes most of the reported examples where the basis for stereochemical assignments appears firm, together with a few cases (Z:E ratios in parentheses) that may need to be reinvestigated.

Nonstabilized, lithium-free ylides $Ph_3P{=}CHR$ react with unbranched α-alkoxy ketones to afford the Z-trisubstituted alkenes (Table 20, entries 6–15) (145). The reactions require no special techniques to achieve high conversion because the electronegative α-alkoxy substituent increases ketone reactivity. Alkyl branching α to oxygen reinforces Z selectivity (entry 20), but branching in the α′ position of an α-alkoxy ketone (entry 19) results in a 1:1 mixture (145). This result suggests that an α-alkyl branch point is comparable to an α-alkoxy group in promoting Z selectivity and that the effects are roughly additive. If the same observations also apply to ketones that lack the α-alkoxy substituent, then Z-trisubstituted alkenes should be formed from the reaction of $Ph_3P{=}CHR$ with methyl ketones that also contain a branched alkyl substituent. Indeed, there are several entries that appear to follow this prediction (entries 4, 25, 31). However, there are a number of other ketones where the opposite trend is seen (entries 24, 35, 58–64). Some of the more striking examples of E selectivity (entries 58–64) involve structural

TABLE 20
Z:E Selectivity in Reactions of Ylides from $L_3P^+CH_2RX^-$ with Ketones R'C(O)R"

Ketone	Entry	L_3P	R	X	Base	Solvent	Temp[a]	Z:E	Yield	Ref
	1	Ph_3P	Me	Br^-	BuLi	Et_2O	0°	(10:90)	--	143
	2	Ph_3P	$(CH_2)_2Ph$	Br^-	BuLi (0.2M)	THF	60°	--	<3%	42c
	3	Ph_3P	$(CH_2)_2Ph$	Br^-	KHMDS (0.2M)	THF	60°	73:27	53%	42c
	4	Ph_3P	$(CH_2)_2Ph$	Br^-	KHMDS (0.75M)	THF	20°	81:19	71%	42c
	5	Ph_3P	CO_2Me	(preformed ylide)		CH_3CN (also C_6H_6)	reflux	<20:80	78%	144a
	6	Ph_3P	Me	Br^-	KHMDS	THF/HMPA	-78°	98:2	83%	145
	7	"	"	"	BuLi	THF	-78°	92:8	>85%	145
	8	"	"	"	BuLi	Et_2O	-78°	83:17	>85%	145
	9	"	n-C_3H_7	"	KHMDS	THF/HMPA	-78°	98:2	87%	145
	10	"	i-C_3H_7	"	KHMDS	THF/HMPA	-78°	86:14	45%	145
	11	"	$(CH_2)_2C{=}CH$	"	BuLi	THF/HMPA	-70°	96:4	95%	146
	12	"	"	"	NaOMe	DMF	-70°	92:8	95%	146
	13	Ph_3P	Me	Br^-	KHMDS	THF/HMPA	-78°	92:8	--	145
	14	"	"	"	KHMDS	THF	-78°	89:11	64%	147
	15	"	$(CH_2)_2C{=}CH$	"	NaOMe	DMF	-70°	88:12	89%	146
	16	83a	Me	Br^-	KHMDS	THF	-78°[b]	14:86	42%	147
	17	83a	Me	Br^-	KHMDS	THF	-78°[b]	11:89	43%	147
	18	Ph_3P	CO_2Me	(preformed ylide)		CH_3CN	reflux	"mixture"	<10%	144a

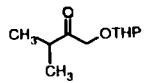
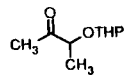
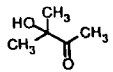
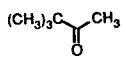
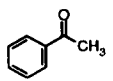
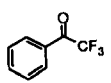
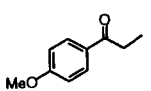
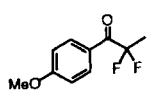
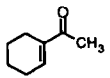
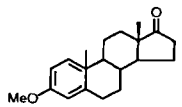
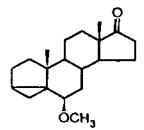
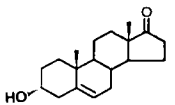
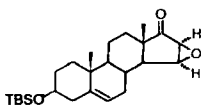
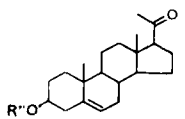
		19	Ph_3P	Me	Br^-	KHMDS	THF/HMPA	-78°	50:50	80%	145
		20	Ph_3P	Me	Br^-	KHMDS	THF/HMPA	-78°	99.5:0.5	>95%	145
		21	Ph_3P	CO_2Me (preformed ylide)			CH_3CN	82°	"E"	23%	144
		22	Bu_3P	"	Br^-	Et_3N	CH_3CN	82°	"E"	46%	"
		24	Ph_3P	C_6H_5	Cl^-	KO*tert*Bu	$C_6H_5CH_3$	105°	<5:95	24%	148
		25	Ph_3P	Me	Br^-	KHMDS	THF	20°	96:4	68%	42c
		26	"	"	"	BuLi	"	"	70:30	47%	42a
		27	85	Me	Br^-	KHMDS	THF	20°	9:91	69%	42c
		28	Ph_3P	CO_2Et (preformed)			C_6H_5Me	70°	44:56	65%	144b
	,2-CH_3	29	Ph_3P	Me	Br^-	$NaCH_2SOMe$	DMSO	RT	63:37	64%	149
	,3-CH_3	30	Ph_3P	Me	Br^-	$NaCH_2SOMe$	DMSO	RT	67:33	74%	149
	,4-CH_3O	31	Ph_3P	n-C_3H_7	Br^-	$NaCH_2SOMe$	DMSO	RT	90:10	71%	150
		32	Ph_3P	CO_2Et (preformed)			C_6H_5Me	50°	90:10	79%	144b
		33	Ph_3P	CO_2Et (preformed)			C_6H_5Me	105°	33:67	47%	144b
		34	Ph_3P	CO_2Et (preformed)			C_6H_5Me	50°	95:5	94%	144b

TABLE 20 *(Continued)*

Ketone	Entry	L_3P	R	X⁻	Base	Solvent	Temp[a]	Z:E	Yield	Ref
	35	**85**	Me	Br^-	KHMDS	THF	20°	2:98	68%	42c
	36	Ph_3P	Me	Br^-	$NaCH_2SOMe$	DMSO	RT	55:45	--	151
	37	Ph_3P	Me	Br^-	KHMDS	THF	20°	14:86	82%	42c
	38	Ph_3P	Me	Br^-	KHMDS	THF	20°	7:93	80%	42c
	39	**83b**	Me	Br^-	KHMDS	THF	20°[b]	15:85	80%	147
	40	**83a**	Me	Br^-	KHMDS	THF	20°[b]	10:90	89%	42c
	41	Ph_3P	Me	Br^-	KHMDS	THF	20°	29:71	38%	42c
	42	**83b**	Me	Br^-	KHMDS	THF	20°[b]	7:93	44%	147
	43	**83a**	Me	Br^-	KHMDS	THF	20°[b]	<2:98	67%	42c
	44	Ph_3P	CO_2Me (preformed ylide)			CH_3CN	82°	<7:93	94%	144a
	45	Ph_3P	Me	Br^-	KHMDS	THF/HMPA	-40°	97:3	86%	152
	46	"	"	"	BuLi	THF	-78°	52:48	55%	152

	47	Ph_3P	Me	Br^-	KHMDS	THF/HMPA	-40°	96:4	90%	152
	48	""	""	""	BuLi	THF	-78°	87:13	61%	152
	49	""	CO_2Me	preformed ylide		CH_3CN	82°	"E"	49%	144a
	50	Ph_3P	Me	Br^-	KHMDS	THF/HMPA	-40°	86:14	65%	152
	51	""	""	""	BuLi	THF	-78°	78:22	77%	152

TABLE 20 *(Continued)*

Ketone	Entry	L_3P	R	X^-	Base	Solvent	Temp[a]	Z:E	Yield	Ref
	52	Ph_3P	Et	Br^-	NaDMSO	DMSO	RT	95:5	85%	153
	53	Ph_3P	Pr	Br^-	NaDMSO	DMSO	RT	96:4	86%	154
	54	Ph_3P	Et	Br^-	tBuOK	THF	RT	95:5	77%	155
	55	Ph_3P	Et	Br^-	tBuOK	THF	RT	95:5	83%	156
	56	Ph_3P	Et	Br^-	LDA	THF	-30°	>"95:5[c]	80%	157
	57	Ph_3P	Et	Br^-	nBuLi	THF	-30°	>"95:5[c]	78%	158
 R"= H	58	Ph_3P	Me	Br	$KOtertC_5H_{11}$	C_6H_6	80°	"E"[d]	75%	159
R"= H	59	"	Et	Br	$KOtertC_5H_{11}$	C_6H_6	80°	"E"[d]	82%	159
R"= H	60	"	iBu	Br	$KOtertC_5H_{11}$	C_6H_6	80°	"E"[d]	67%	159
R"= H	61	"	$(CH_2)_2CH(CH_3)_2$	Br	$KOtertC_5H_{11}$	C_6H_6	80°	"E"[d]	78%	160
R"= THP	62	"	$(CH_2)_2OTHP$	Br^-	$KOtertC_5H_{11}$	C_6H_6	80°	"E"[d]	59%	160
R"= THP	63	"	MeO	Br^-	$KOtertC_5H_{11}$	C_6H_6	80°	20:80	96%	160

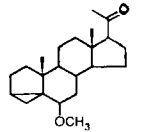
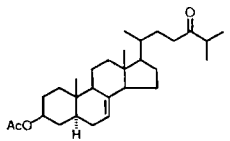
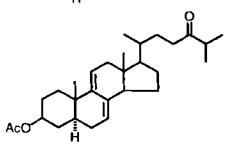
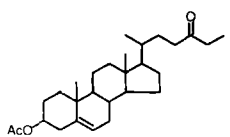
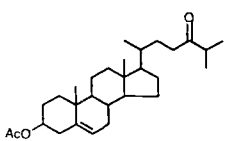
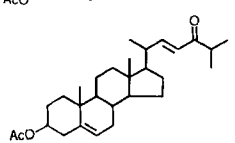
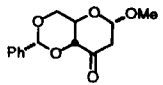
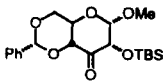
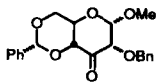
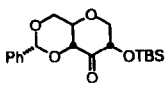
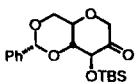
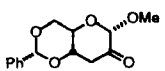
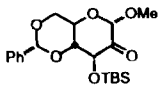
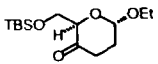
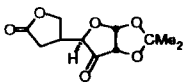
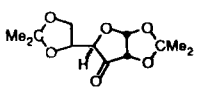
	64	Ph_3P	$(CH_2)_2CH(CH_3)_2$	Br^-	KO*tert*C_5H_{11}	C_6H_6	80°	"E"[b]	100%	160
	65	Ph_3P	Me	Br^-	BuLi	THF	0°	"Z"[d]	41%	161a
	66	Ph_3P	Me	Br^-	BuLi	THF	0°	"Z"[d]	32%	161b
	67	Ph_3P	Me	Br^-	BuLi	Et_2O	35°	"(E?)"[d]	20%	162
	68	Ph_3P	Me	Br^-	BuLi	THF	RT	"Z"[d]	32%	161c
	69	Ph_3P	Me	Br^-	--	--	--	"Z"[d,e]	--	163

TABLE 20 *(Continued)*

Ketone	Entry	L_3P	R	X	Base	Solvent	Temp[a]	Z:E	Yield	Ref
	70	Ph_3P	CO_2Me		(preformed ylide)	CH_3CN	82°	"Z"[d]	90%	164a
	71	Ph_3P	CO_2Me		(preformed ylide)	CH_3CN	82°	"E"[d,f]	76%	164a
	72	Ph_3P	CO_2Me		(preformed ylide)	CH_3CN	82°	50:50	76%	164b
	73	Ph_3P	CO_2Me		(preformed ylide)	CH_3CN	82°	"E"[d,f]	80%	164a
	74	Ph_3P	CO_2Me		(preformed ylide)	CH_3CN	82°	"Z"[d]	80%	164a
	75	Ph_3P	CO_2Me		(preformed ylide)	CH_3CN	82°	"E"[d,g]		164a

	76	Ph_3P	CO_2Me	(preformed ylide)	CH_3CN	82°	"E"[d,g]	90%	164a
	77	Ph_3P	CO_2Me	(preformed ylide)	CH_3CN	82°	"E"	70%	165
	78	Ph_3P	CO_2Me	(preformed ylide)	CH_3CN	82°	mixture	78%	166
	79	Ph_3P	CO_2Me	(preformed ylide)	CH_3CN	82°	27:73	82%	167

(a) The temperature for mixing of reactants is given. Subsequent warming to room temperature completes the process.

(b) After the reagents were combined at the low temperature, the mixture was heated to 100° to induce oxaphosphetane decomposition.

(c) The priority rules change the Z:E designation compared to entry 55. There is no change in product geometry with respect to the steroid backbone in entries 55-57.

(d) Only one product was reported, but the procedure involves separation of products by chromatography or crystallization. Z:E ratio data cannot be deduced from the details as provided.

(e) The product methyl group is Z to the double bond of starting material. Alkene geometry is opposite to that observed for the saturated analog (entry 68).

(f) The same major stereoisomer is observed as in entry 70. The Z:E nomenclature is somewhat confusing in this case.

(g) The same major stereoisomer is observed as in entry 74. The Z:E nomenclature is somewhat confusing in this case.

assignments that are based largely on the assumption that the ^1H NMR methyl chemical shift in the (*Z*)-trisubstituted alkene will be shifted approximately 0.1 ppm to a higher field compared to the (*E*)-isomer. Independent confirmation of selectivity would be helpful here, but the precedents cited are convincing (159, 160). Apparently, the influence of α-alkyl branch points in the ketone reactions is much more sensitive to overall structural details than in the aldehyde reactions. Small structural changes can have large and unpredictable consequences on selectivity. Thus, 2-methylcyclohexanone (entry 37) forms the ethylidene derivative with a Z:E ratio of 14:86 while the corresponding reaction of 2-methylcyclopentanone (entry 36) is nonselective (Z:E 55:45; both experiments under lithium-free conditions) (42, 151).

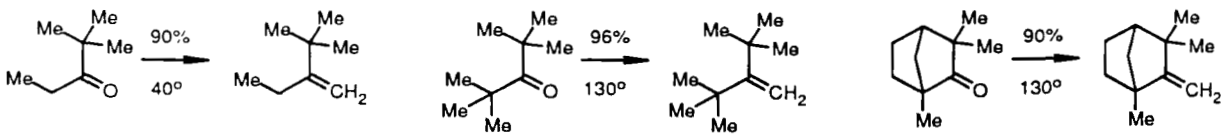
The phosphole reagents follow a more consistent trend for (*E*)-trisubstituted alkene formation (Table 20, entries 16, 17, 27, 35, 39, 40, 42, 43) (42, 147). The stereochemical preference is inverted by comparison to the conventional $Ph_3P{=}CHR$ reactions for the α-alkoxy ketones, for several enone examples (entries 16, 17, 27, 35), and for some of the α-alkyl branched ketones. This trend is similar to the E-selectivity pattern seen in the aldehyde reactions with phosphole-derived ylides, but more systems must be studied before reliable generalizations are possible.

Several of the stabilized ylide reactions with ketones also follow consistent patterns. Thus, α-hydroxy ketones afford (*E*)-enoates (Table 20, entries 5, 21, 22, 44) (144), while most of the α-alkoxy derivatives favor the (*Z*)-isomers (entries 70, 74) (164). There is at least one exception in the α-alkoxy series where the (*E*)-enoate is favored (entry 77) (165), and there are several cases of puzzling selectivity with α,α′-dialkoxy ketone substrates (entries 71, 72, 74) (164). As in many of the ketone Wittig entries, the observations are interesting and high selectivity is often possible. However, the results appear specific to a given class of substrates, and there are insufficient data to establish general trends.

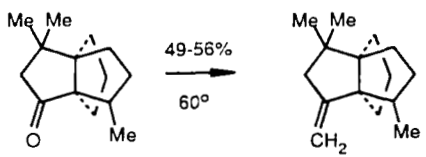
As already mentioned, ketone Wittig reactions are complicated by low carbonyl reactivity and by enolization in the case of nonstabilized ylides. The level of difficulty increases with increasing steric hindrance in the reactants, but experimental solutions are available even for the most extreme cases (159, 168–171). A discussion of the key variables is included below, partly to dispel the notion that the Wittig approach is not practical for hindered, enolizable ketones and partly to guide future stereochemical studies of the ketone reactions.

Enolization in ketone Wittig reactions can usually be attributed to the use of lithium-containing ylide solutions. Thus, 3-methyl-2-butanone reacts rapidly with $Ph_3P{=}CHCH_3$/LiBr to form a precipitate, and prolonged heating produces only traces of the alkene (Table 20, entry 2). When the same

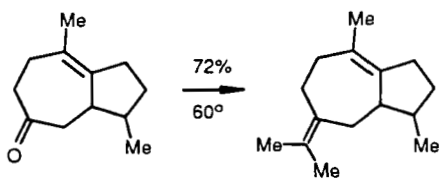
PROCEDURE A;[168] SLURRY OF $Ph_3P{=}CH_2$ + tBuOH:



PROCEDURE B;[159,169] 0.8M $Ph_3P{=}CH_2/C_6H_6$:



PROCEDURE C;[170] 0.8M $Ph_3P{=}CMe_2$/DMSO



Scheme 12

experiment is performed using 0.2 M KHMDS as the base to generate the ylide, the ylide color fades over a period of hours at 60°C and the alkene is formed normally (entry 3) (42). Since the rate-determining step (reaction of the ylide with the ketone) is bimolecular, the reaction shows the expected strong dependence on concentration. Thus, significant improvement is observed using 0.75 M ylide solution (entry 4), and the reaction proceeds at room temperature. The concentration variable is crucial for highly hindered ketones, and extraordinary measures must be taken to maximize the reaction rate. In the most impressive recent technique, the ylide is prepared using KO-*tert*-C_4H_9 in ether or benzene, followed by removal of nearly all of the volatile solvents by distillation [method A, Scheme 12; Fitjer et al. (168)]. Addition of the ketone is performed at elevated temperatures without added solvent, a technique that ensures the highest possible ylide concentration and that permits the use of drastic temperatures as high as 130°C. The Fitjer method is a more extreme variant of the first optimized procedure for ketone olefination [Table 20, entries 58–60; Piraux et al. (159), see methed B, Scheme 12]. In the original procedure, a large excess of the ylide (as much as 7 equivalents) was used and the ketone was added at elevated temperatures. However, the ylide solutions (prepared using sodium *tert*-amylate in benzene or toluene) may have been less concentrated (approx 0.8–1.0 M) (159, 160, 169). By comparison, typical aldehyde olefinations proceed at convenient rates using a small excess of the ylide at concentrations as low as ca. 0.05 M. Method C, Scheme 12, (ca. 0.8 M ylide in DMSO prepared using KO-*tert*-C_4H_9; 60°C reaction temperature) has been used for tetrasubstituted alkene synthesis with $Ph_3P{=}CMe_2$ (170) and a similar procedure has been recommended for the methylenation of hindered ketones containing nearby quaternary carbon (171). Tetrasubstituted alkenes are notoriously difficult to make by the Wittig method (172), although there are several other successful examples under lithium-free conditions (63, 173). However, enolization is the dominant or exclusive pathway when *lithium-containing* $Ph_3P{=}CMe_2$ is reacted with simple ketones such as cyclohexanone (18b).

It is not clear whether enolization is avoided under the lithium-free, high-concentration conditions, or whether it occurs reversibly enough to permit eventual conversion of the ketone to the alkene. However, the most successful procedures involve alkoxide bases (159, 168–170) or require the presence of excess phosphonium salt (171). Proton exchange and reversible enolate formation are likely under these conditions, and aldol condensation pathways would also be reversible when potassium or sodium bases are used. Thus, excellent yields of alkenes are possible with the most hindered substrates, provided that other pathways for irreversible enolate decomposition are not available.

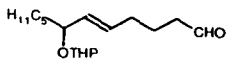
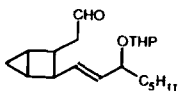
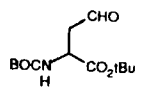
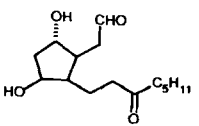
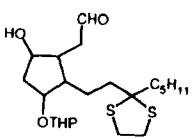
XIV. WITTIG REACTIONS IN MULTIFUNCTIONAL SYSTEMS

The last compilation of empirical data (Table 21) contains selected examples from a variety of reactions where the stereochemical results may be influenced by one or more additional functional groups in the ylide or carbonyl reactants. The first two categories (ylides containing anionic carboxylate or alkoxide substituents) have already been mentioned in connection with the issue of reversibility in Wittig reactions (see Scheme 8). In general, aromatic aldehydes or α,β-unsaturated aldehydes react with useful (*E*)-alkene selectivity with these reagents, provided that lithium ion is present. Unbranched aliphatic aldehydes afford Z:E mixtures under lithium-containing conditions (Table21, entries 21, 33), but further optimization may be possible. Thus, an α-methyl aldehyde (entry 31) affords a synthetically useful product ratio of 15:85 Z:E. Anionic β-amido ylides are similar in behavior to the oxido ylides, and E-selective reactions are observed with the reversal-prone aromatic or tertiary aliphatic aldehydes (entries, 61–64). Under lithium-free conditions, the oxido ylides tend to produce unpredictable Z:E mixtures. However, the lithium-free carboxylate ylides react with normal (excellent) Z selectivity (entries 4–9).

It is likely that the (*E*)-alkene selective reactions of anionic ylides are due to equlibration of the betaine lithium halide adduct as discussed earlier. However, the balance is delicate and small structural changes can have surprising consequences. Thus, Corey's stereospecific *trisubstituted* alkene synthesis via β-oxido ylides (Table 10) is clearly under dominant kinetic control, even though lithium ion is present and aromatic aldehydes can be used as the substrates (54, 55). The only obvious difference between the intermediates of Table 10 and oxido ylide examples such as entry 11 in Table 21 is that the latter must decompose via a disubstituted oxaphosphetane while the stereospecific reactions in Table 10 involve trisubstituted analogues. Apparently, the higher degree of oxaphosphetane substitution favors decomposition relative to equilibration. There are few easy and safe generalizations in this field. Each system must be evaluated in detail before rationales can be recommended.

A few systematic comparisons can be made for the reactions of simple aldehydes with α-heteroatom-substituted ylides. The normal Z-selectivity pattern of the $Ph_3P{=}CHX$ series decreases from X = iodine to bromine to chlorine or fluorine (Table 21, entries. 44–57). There may be a similar decrease in selectivity with decreasing atomic number from α-sulfide to α-ether substituents (compare entries 40–43 with 35–37). Unfortunately, no direct comparisons have been made, and there are very few examples involving reactions of simple aliphatic aldehydes RCH_2CHO with either the α-alkoxy or the α-alkylthio ylides. It is too early for detailed generalizations, but the

TABLE 21
Wittig Reactions with Multifunctional Reactants on Unusual Functional Groups

Carbonyl Reactant	$L_3P^+CH_2R$	Entry	X^-	Base	Solvent	Temp	Z:E	Yield	Ref
Carboxylate ylides:									
PhCHO	$Ph_3P^+(CH_2)_4CO_2H$	1	Br^-	2eq LiHMDS	THF	RT	13:87	74%	23b
"	" "	2	Br^-	2eq KOtBu	THF	RT	35:65	81%	23b
n-$C_8H_{17}CHO$	" "	3	Br^-	2eq LiHMDS	THF	RT	73:27	??	23b
	" "	4	Br^-	2eq NaDMSO	DMSO/THF	RT	'Z only'	??	174
	" "	5	Br^-	2eq NaDMSO	DMSO	RT	'Z only'	74%	175
	" "	6	Br^-	2eq LiHMDS	THF/HMPA	-78°	'Z only'	46%	176
	" "	7	Br^-	2eq KOtBu	THF	RT	'Z only'	59%	177
	" "	8	Br^-	2eq KHMDS	THF	RT	'Z only'	75%	178

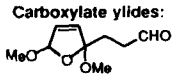
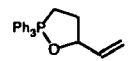
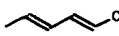
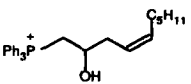
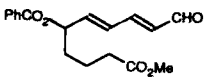
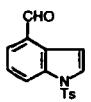
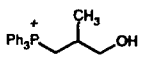
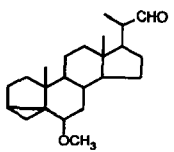
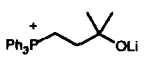
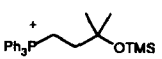
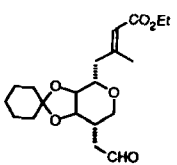
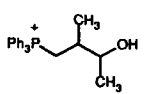
Carboxylate ylides: 	$Ph_3P^+(CH_2)_4CO_2H$	9	Br^-	2eq NaDMSO	DMSO	???	'Z only'	85%	179
Carbonyl Reactant	**$L_3P^+CH_2R$**	**Entry**	**X^-**	**Base**	**Solvent**	**Temp**	**Z:E**	**Yield**	**Ref**
Oxido Ylides:									
PhCHO	$Ph_3P^+CH_2CH_2OH$	10	Br^-	2eq LiHMDS	THF	RT	28:72	14%	180
"	"	11	Br^-	2eq BuLi	THF	RT	3:97	??	180
"	$Ph_3P^+CH_2CH_2CH_2OH$	12	Br^-	2eq LiHMDS	THF	RT	4:96	80%	180
"	"	13	Br^-	2eq KOtBu	THF	RT	44:56	34%	180
"	$[Ph_3P^+CH_2CH_2CH_2O^-]^a$	14	--	----	THF	reflux	73:27	50%	180
"	"	15	--	1eq LiHMDS	THF	RT	6:94	83%	180
"	$Ph_3P^+(CH_2)_4OH$	16	Br^-	2eq LiHMDS	THF	RT	15:85	??	180
"	"	17	Br^-	2eq KOtBU	THF	RT	54:46	??	180
"	$Ph_2P^+(CH_2CH_2OH)CH_2Ph$	18	Br^-	2eq BuLi	THF/HMPA	-78°	15:85	87%	181
"	$Ph_3P^+CH_2CH{=}CHCH_2OH$	19	Br^-	2eq BuLi	THF	-78°	60:40	54%	182
"	"	20	Br^-	2eq KHMDS	THF	-78°	83:17	35%	182
$n\text{-}C_5H_{11}CHO$	$Ph_3P^+CH_2CH_2CH_2OH$	21	Br^-	2eq LiHMDS	THF	RT	42:58	82%	180
"	$[Ph_3P^+CH_2CH_2CH_2O^-]^a$	22	--	----	THF	reflux	88:12	63%	180
"	"	23	--	1eq LiHMDS	THF	RT	48:52	77%	180
"	$Ph_3P^+(CH_2)_4OH$	24	Br^-	2eq LiHMDS	THF	RT	77:23	??	180

TABLE 21 *(Continued)*

Carbonyl Reactant	$L_3P^+CH_2R$	Entry	X^-	Base	Solvent	Temp	Z:E	Yield	Ref
Oxido Ylides:									
$n\text{-}C_5H_{11}CHO$	$Ph_3P^+CH_2CH{=}CHCH_2OH$	25	Br^-	2eq BuLi	THF	-78°	87:13	80%	183
〃	〃	26	Br^-	2eq KHMDS	THF	-78°	95:5	60%	183
$n\text{-}C_6H_{13}CHO$		27	--	1eq LiHMDS	THF	-23°	46:54	56%	184
		28	Br^-	2eq BuLi	THF/HMPA	-78°	'E only'	78%	185
	- -	29	Br^-	2eq BuLi	THF/HMPA	-78°	'E only'	25%	185
		30	Br^-	2eq BuLi	THF	-78°	8:92	80%	186
		31	Br^-	1eq BuLi	THF	0°	15:85	75%	187
		32	Br^-	1eq BuLi	THF	0°	85:15	??	187
		33	Br^-	2eq BuLi	THF	-78°	40:60	??	188

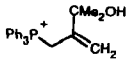
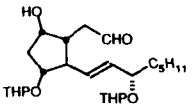
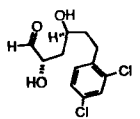
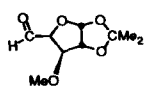
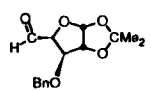
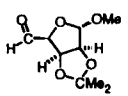
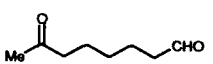
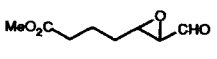
Oxido Ylides:									
PhCHO		34	Br^-	KO*tert*Bu	*tert*BuOH	RT	"Z only"[c]	60%	189
Carbonyl Reactant	**$L_3P^+CH_2R$**	**Entry**	**X^-**	**Base**	**Solvent**	**Temp**	**Z:E**	**Yield**	**Ref**
α-Alkoxy Ylide:									
PhCHO	$Ph_3P^+CH_2OCH_2CH_2SiMe_3$	35	Cl^-	NaH	DMSO	20°	50:50	70-80%	190a
	$Ph_3P^+CH_2OMe$	36	Cl^-	$MeSOCH_2Na$	DMSO	15°	40:60	61%	190b
	"	37	Cl^-	KO*tert*Bu	THF	0°	36:64	87%	190c
Carbonyl Reactant	**$L_3P^+CH_2R$**	**Entry**	**X^-**	**Base**	**Solvent**	**Temp**	**Z:E**	**Yield**	**Ref**
β-Alkoxy Ylide:									
PhCHO	$Ph_3P^+CH{=}CHOEt$[b]	38	Br^-	NaOEt	THF	RT	95:5	86%	191
$C_5H_{11}CHO$	$Ph_3P^+CH{=}CHOEt$[b]	39	Br^-	NaOEt	THF	RT	92:8	72%	191
Carbonyl Reactant	**$L_3P^+CH_2R$**	**Entry**	**X^-**	**Base**	**Solvent**	**Temp**	**Z:E**	**Yield**	**Ref**
α-Alkylthio Ylides:									
	$Ph_3P^+CH_2SPh$	40	??	??	DMSO/DMF	??	67:33	60%	192
	$Ph_3P^+CH_2SMe$	41	Cl^-	NaH	DMSO	20°	68:32	41%	127
	$Ph_3P^+CH_2SMe$	42	Cl^-	NaH	DMSO	20°	55:45	53%	127
	$Ph_3P^+CH_2SMe$	43	Cl^-	NaH	DMSO	20°	89:11	70%	127

TABLE 21 *(Continued)*

Carbonyl Reactant α-Halo Ylides:	$L_3P^+CH_2R$	Entry	X^-	Base	Solvent	Temp	Z:E	Yield	Ref
PhCHO	$Ph_3P^+CH_2F$	44	I^-	PhLi	THF	-78°	50:50	65%	193a
$C_5H_{11}CHO$	"	45	I^-	PhLi	THF	-78°	45:55	55%	193a
PhCHO	$Ph_3P^+CH_2Cl$	46	Cl^-	KO*tert*Bu	*tert*BuOH	RT	54:46	81%	193b
$n\text{-}C_8H_{17}CHO$	"	47	Cl^-	KO*tert*Bu	*tert*BuOH	RT	56:44	45%	193b
2-methylcyclohexanone	"	48	Cl^-	KO*tert*Bu	*tert*BuOH	RT	8:92	89%	193b
$PhSeCH_2CHO$	"	49	Cl^-	BuLi	THF	-30°	40:60	??	193c
PhCHO	$Ph_3P^+CH_2Br$	50	Br^-	KO*tert*Bu	THF	-78°	83:17	71%	194a
"	$Ph_3P^+CHBr_2$[d]	51	Br^-	BuLi	THF	-60°	49:51	44%	194b
$PhCH_2CH_2CHO$	$Ph_3P^+CH_2Br$	52	Br^-	KO*tert*Bu	THF	-78°	86:14	47%	194a
$(CH_3)_3CCHO$	$Ph_3P^+CHBr_2$[d]	53	Br^-	BuLi	THF	-60°	98:2	6%	194b
6-methylhept-5-en-2-one	$Ph_3P^+CH_2Br$	54	Br^-	KO*tert*Bu	THF	-60°	25:75	81%	194c
$c\text{-}C_6H_{11}CHO$	$Ph_3P^+CH_2I$	55	Br^-	NaHMDS	THF	-78°	92:8	72%	195
	$Ph_3P^+CH_2I$	56	Br^-	NaHMDS	THF	-78°	95:5	74%	195
	$Ph_3P^+CH_2I$	57	Br^-	NaHMDS	THF/DMF	-78°	97:3	45%	196
Carbonyl Reactant β-Cyano Ylide:	$L_3P^+CH_2R$	**Entry**	X^-	**Base**	**Solvent**	**Temp**	**Z:E**	**Yield**	**Ref**
PhCHO	$[Ph_3P + CH_2{=}CHCN]$[b]	58	--	--	*tert*BuOH	175°	15:85	85%	197
$n\text{-}C_3H_7CHO$	$[Ph_3P + CH_2{=}CHCN]$[b]	59	--	--	*tert*BuOH	175°	92:8	75%	197

Amino and Amido Ylides:

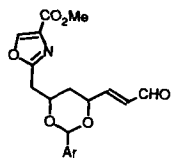
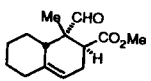
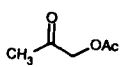
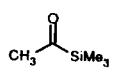
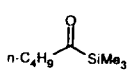
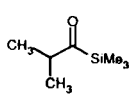
PhCHO	$Ph_3P^+CH_2CH_2NMe_2$		60	Br^-	1eq LiHMDS	THF	RT	31:69	70%	180
"	$Ph_3P^+CH_2CH_2NH_2$		61	Br^-	2eq BuLi	THF	RT	18:82	??	180
"	$Ph_3P^+CH_2CH_2NHBn$		62	Br^-	2eq BuLi	THF	RT	29:71	73%	198
i-PrCHO	$Ph_3P^+CH_2CH_2NHBn$		63	Br^-	2eq BuLi	Et_2O	RT	80:20	57%	198
t-BuCHO	"		64	Br^-	2eq BuLi	Et_2O	RT	18:82	88%	198
$PhCH_2CH_2CHO$	$Bu_3P^+CH{=}CH_2$ + phthalimide[b]		65	Br^-	NaH	THF	23°	25:75	60%	78b
PhCH=CHCHO	"	"	66	Br^-	NaH	THF	23°	17:83	95%	78b
	"	"	67	Br^-	NaH	THF	23°	35:65	26%	199
	"	"	68	Br^-	NaH	THF	23°	'E only'	51%	199
	$Ph_3P^+CH_2CH_2NMe_2$		69	Br^-	NaHMDS	$C_6H_5CH_3$	23°	'Z only'	81%	200
	$Ph_3P^+CH_2CH(Me)NMe_2$		70	Br^-	NaHMDS	$C_6H_5CH_3$	23°	'Z only'	82%	200
	$Ph_3P^+CH_2CH_2NBu_2$		71	Br^-	KHMDS	THF/HMPA	-78°	99:1	??	201

TABLE 21 *(Continued)*

Carbonyl Reactant	$L_3P^+CH_2R$	Entry	X^-	Base	Solvent	Temp	Z:E	Yield	Ref
Silicon and Tin in Wittig reactions:									
PhCHO	$Ph_3P^+CH_2CH_2SiMe_3$	72	I^-	MeLi	THF	RT; reflux	36:64	63%	202
"	$Ph_3P^+CH_2CH_2SnMe_3$	73	I^-	LDA	THF	RT; reflux	5:95	70%	202
"	$(o\text{-tolyl})_3P^+CH_2CH_2SiMe_3$	74	Br^-	BuLi	THF	0°	79:21	76%	203
$n\text{-}C_6H_{13}CHO$	$Ph_3P^+CH_2CH_2SiMe_3$	75	I^-	MeLi	THF	RT; reflux	25:75	71%	202
"	$Ph_3P^+CH_2CH_2SnMe_3$	76	I^-	LDA	THF	RT; reflux	30:70	98%	202
$PhCH_2CH_2CHO$	$(o\text{-tolyl})_3P^+CH_2CH_2SiMe_3$	77	Br^-	BuLi	THF	0°	96:4	82%	203
$c\text{-}C_6H_{11}CHO$	"	78	Br^-	BuLi	THF	0°	96:4	82%	203
	$Ph_3P^+C_2H_5$	79	Br^-	BuLi	THF	-78°	96:4	82%	204
	$Ph_3P^+CH_2OMe$	80	Cl^-	*tert*BuLi	THF	-78°	78:22	50%	204
	$Ph_3P^+C_4H_9$	81	Br^-	BuLi	THF	-78°	98:2	41%	204
	$Ph_3P^+C_2H_5$	82	Br^-	BuLi	THF	-78°	98:2	37%	204

Allylic Ylides:

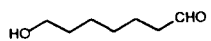
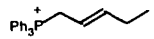
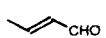
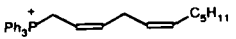
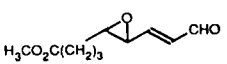
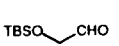
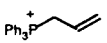
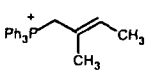
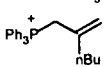
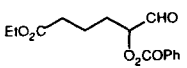
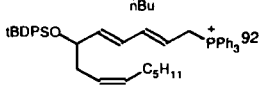
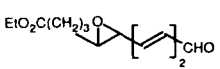
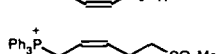
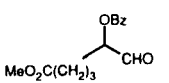
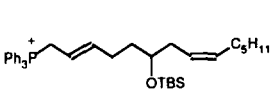
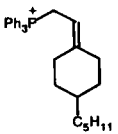
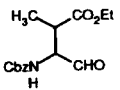
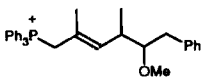
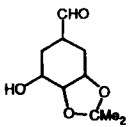
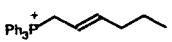
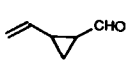
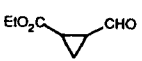
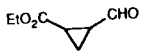
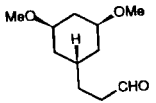
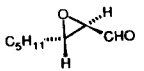
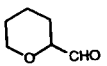
		83	Br^-	BuLi	THF	-30°	50:50	??	205
"	"	84	Br^-	KOtBu	THF	-30°	52:48	??	205
"	"	85	Br^-	KOtBU	toluene	-30°	47:53	??	205
		86	Br^-	KOtBu	DMF	-30°	40:60	??	205
		87	MsO^-	LDA	THF/HMPA	-95°	>95:5	??	183
	"	88	MsO^-	LDA	THF/HMPA	-95°	mixture	25%	183
		89	Br^-	BuLi	THF	-78°	87:13	70%	206
"		90	Br^-	BuLi	THF	-78°	82:18	53%	206
"		91	Br^-	BuLi	THF	-78°	71:29	61%	206
		92	Br^-	BuLi	THF/HMPA	-100°	70:30	88%	207
		93	Br^-	LiHMDS	THF/HMPA	-78°	'Z only'	56%	208
		94	Br^-	BuLi	THF/HMPA	-78°	82:18	76%	209

TABLE 21 *(Continued)*

Carbonyl Reactant **Allylic Ylides:**	$L_3P^+CH_2R$	Entry	X^-	Base	Solvent	Temp	Z:E	Yield	Ref
		95	Br^-	BuLi	THF/HMPA	-78°	90:10	30%	210
		96	Br^-	BuLi	DME	RT	'E only'	43%	211
		97	Br^-	BuLi	THF	0°	20:80	75%	212

Carbonyl Reactant **Propargylic Ylides:**	$L_3P^+CH_2R$	Entry	X^-	Base	Solvent	Temp	Z:E	Yield	Ref
PhCHO	$Ph_3P^+CH_2C{\equiv}CSiMe_3$	98	Br-	BuLi	THF	-78°	27:73	54%	213
$c\text{-}C_6H_{11}CHO$	$Ph_3P^+CH_2C{\equiv}CSiMe_3$	99	Br-	BuLi	THF	-78°	<9:91	56%	213
$CH_3(CH_2)_9CHO$	$Ph_3P^+CH_2C{\equiv}CSiMe_3$	100	Br-	BuLi	THF	-78°	19:81	61%	214
	$Ph_3P^+CH_2C{\equiv}CC_2H_5$	101	Br^-	LiOEt	DMF	RT	36:64	51%	215
	$Ph_3P^+CH_2C{\equiv}CH$	102	Br^-	$NaNH_2$	C_6H_6	0°	90:10	20%	216
	$Ph_3P^+CH_2C{\equiv}CH$	103	Br^-	NH_3	$EtOH/NH_3$	-70°	80:20	40%	216

Propargylic Ylides:

	$Ph_3P^+CH_2C{\equiv}CC_2H_5$	104	Br^-	$NaNH_2$	C_6H_6	0°	85:15	25%	216
	$Ph_3P^+CH_2C{\equiv}CC_2H_5$	105	Br^-	NH_3	$EtOH/NH_3$	-70°	55:45	40%	216
	$Ph_3P^+CH_2C{\equiv}CSiMe_3$	106	Br-	BuLi	THF	-78°	10:90	82%	217
	" "	107	Br-	BuLi	THF	-78°	<9:91	80%	213
	" "	108	Br-	BuLi	THF	-78°	42:58	60%	218
	" "	109	Br-	BuLi	THF	0°	26:74	90%	218

(a) The phosphonium salt is generated thermally from the more stable cyclic oxaphospholane tautomer.

(b) Conjugated addition occurs to generate the ylide *in situ*.

(c) The E stereochemistry was assigned in ref. 193 but the Z-isomer appears more likely, based on the reported 12 Hz vicinal coupling constant for the styrene hydrogens.

(d) The ylide is formed by halogen metal exchange, not by deprotonation.

Z selectivity of $Ph_3P{=}CHX$ increases qualitatively as the electronegativity of X decreases and the volume of X increases.

Ylides that contain neutral heteroatom substituents at the β or γ positions react with normal selectivity for the (*Z*)-alkene. Two of these examples deserve special mention because they provide indirect solutions to difficult stereochemical problems. In the first example, the β,β-dialkoxy ylide $Ph_3P{=}CHCH(OC_2H_5)_2$ can be generated by the conjugate addition of ethoxide ion to the alkenylphosphonium salt $Ph_3P^+CH{=}CHOEt$(191). Subsequent reaction with an aldehyde affords the (*Z*)-alkene acetal, and controlled acid-catalyzed hydrolysis leads to the α,β-unsaturated aldehyde with $>90\%$ Z selectivity (Table 21, entries 37, 38). This two-step sequence provides a Z selective alternative to the Wittig reaction of the corresponding stabilized ylide $Ph_3P{=}CHCHO$, a process that is highly E selective. The method is also interesting because it uses a conjugate addition approach to generate the ylide *in situ* from an alkenylphosphonium salt. Another example of the *in situ* method is illustrated in Table 21, entries 65–68, using the conjugate addition of the phthalimide anion to alkenylphosphonium salts (78b, 199). With $Bu_3P^+CH{=}CH_2$ as the starting salt, moderate selectivity for the (*E*)-alkene is possible in the reaction with unsaturated aldehydes, as in other reactions that use the modified P-trialkyl phosphorus environment.

Another indirect Wittig sequence can be used to prepare 1,3-dienes with selectivity for the formation of a Z-disubstituted C=C bond. This technique complements the highly E selective reactions of reagents such as $Ph_2MeP{=}CHCH{=}CHR$ (Table 15). Thus, treatment of a hindered tertiary aldehyde with a β-dialkylamino ylide $Ph_3P{=}CHCH_2NMe_2$ affords the allylic amine with the expected $>99\%$ Z geometry (Table 21, entry 56). Subsequent conversion to the *N*-oxide (MCPBA oxidation) followed by thermal Cope elimination results in a conjugated diene with retention of the Z geometry that was established in the Wittig step ($>60\%$ overall) (200). A direct Wittig reaction of the tertiary aldehyde with $Ph_3P{=}CHCH{=}CH_2$ was also attempted, but no diene products were formed, perhaps because the allylic ylide can react at the less hindered γ-carbon with the bulky aldehyde (90).

Table 21 also includes reactions of allylic and propargylic ylides with relatively complex aldehydes (entries 83–109). These examples involve a wide range of experimental conditions, and the Z:E ratios are more variable than for the simpler entries of Table 15. Several of the reactions are surprisingly Z selective (for example, Table 21, entries 93, 95, 102, 104) by comparison with simpler analogues, and the results appear to be strongly influenced by lithium ion. Overall, the situation is reminiscent of the benzylide reactions of Table 14 where large variations in reported Z:E ratios were noted because the results were obtained using a variety of experimental conditions.

There are also some examples of silicon- and tin-containing Wittig reactions

TABLE 22

Kinetic *cis–trans* Selectivity at the Oxaphosphetane Stage for Reaction of Ylides with Aldehydes or Ketones

Entry	Ylide	1° R'CHO	3° R'CHO	ArCHO	$R_SC(O)R_L$	$R_SC(O)CH_2OR''$
1	$Ph_3P{=}CHCH_3$, THF/-78°	96:4	>99:1	94:6	VARIABLE	>95:5[a]
2	$Ph_3P{=}CHCH_3$, Et_2O/LiBr, 0°	84:16	>99:1	(60:40)[b]	VARIABLE	84:16[a]
3	*tert*$BuPh_2P{=}CHCH_3$, THF/0°	94:6[a]	99:1[a]	--	--	--
4	$EtPh_2P{=}CHCH_3$, THF/-78°	30:70	85:15	--	--	--
5	*c*-$C_6H_{11}Ph_2{=}CHCH_3$, THF/-78°	25:75[a]	44:56[a]	--	--	--
6	$Et_3P{=}CHCH_3$, THF/-78°	33:67	76:24 (10:90)[b]	(17:83)[b]	--	--
7	$Bu_3P{=}CHC_3H_7$, THF/-78°	10:90	40:60 (4:96)[b]	77:23 (8:92)[b]	--	--
8	EtDBP=$CHCH_3$, THF/-78°	5:95	10:90	--	<30:70	15:85
9	$Ph_3P{=}CHPh$, THF/-78°	25:75[c]	35:65[c]	59:41[c]	--	--
10	$MePh_2P{=}CHPh$, THF/-78°	6:94[c,d]	21:79[c,d]	18:82[c,d]	--	--
11	$Ph_3P{=}CHCH{=}CH_2$, THF/-78°	45:55[c]	50:50[c]	66:34[c]	--	--
12	$MePh_2P{=}CHCMe{=}CH_2$, THF/-78°	14:86[c,d]	--	33:67[c,d]	--	--
13	$Ph_3P{=}CHCO_2Et$, THF/RT	8:92[c]	5:95[c]	4:96[c]	--	VARIABLE
14	$Ph_3P{=}CHCO_2Et$, MeOH/RT	38:62[c]	--	25:75[c]	--	--
15	$MePh_2P{=}CHCO_2Et$, THF/RT	19:81[c,d]	22:78[c,d]	17:83[c,d]	--	--

(a) The oxaphosphetane cis:trans ratio is based on the isolated alkene Z:E ratio, assuming kinetic control by analogy to related systems.

(b) The value in parentheses is the empirical Z:E ratio of alkenes after oxaphosphetane decomposition. Equilibration of diastereomers competes with oxaphosphetane decomposition in this case.

(c) The oxaphosphetane cis:trans ratio cannot be measured due to rapid decomposition to the alkene. The empirical Z:E ratio is given.

(d) Dominant kinetic control is proved by independent betaine generation experiments.

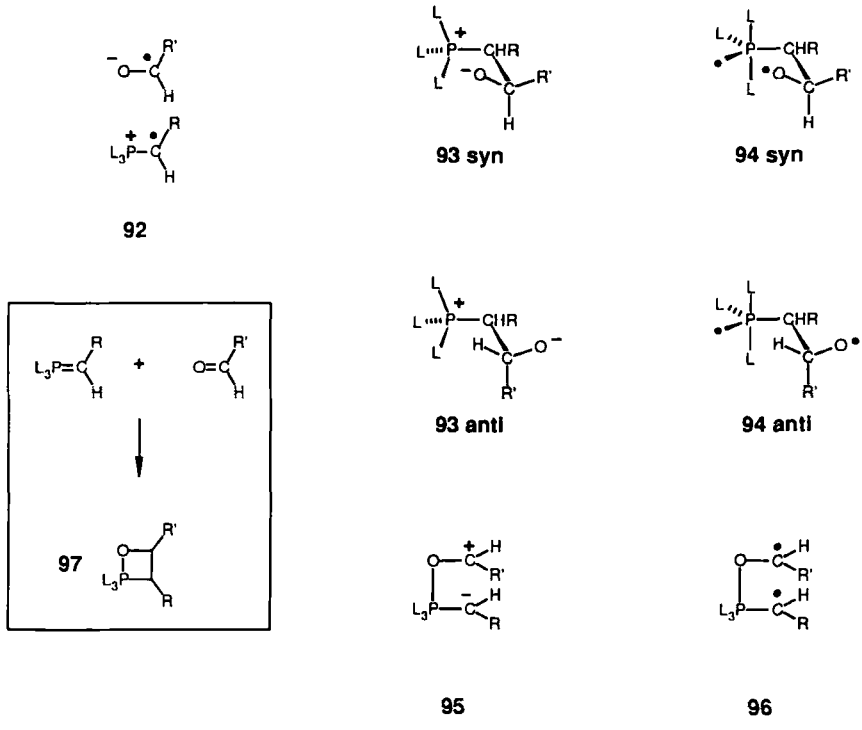
in Table 21. The acyl silane olefinations (entries 79–82) (200) are analogous to the ketone reactions of Table 20, and they follow the same preference for (*Z*)-alkene formation as do the simplest α-branched acyclic ketones (Table 20, entry 4). However, the selectivity is higher and it is not clear whether a simple analogy can be made. Each new functional group environment has its own characteristic combination of steric and conformational factors. Fortunately, only a few of these perturbations are large enough to modify the fundamental trends in kinetic selectivity that have been encountered in previous tables.

Many different research groups have contributed to the collection of empirical data in Tables 6–21. In some cases where the results do not fit overall trends, there are differences between similar experiments due to troublesome experimental or structural variables. A few of the "misfits" are probably due to uncertain structural assignments, and many of the others correlate with experimental procedures in which the concentration of electrophilic byproducts or contaminants (lithium ion, hydroxyl groups, protic or Lewis acids) is not controlled. There are also some misfit cases among the reactions of unsymmetrical ketones, and in reactions where allylic, benzylic, or propargylic ylides are employed. However, the great majority of cases are "well behaved" and follow general patterns that are summarized in Table 22 and are discussed in the section on interpretation of stereoselectivity trends.

XV. MECHANISTIC CONSIDERATIONS

The history of mechanistic ideas in the Wittig reaction has been reviewed in detail (6), and only the essential features will be mentioned here. With a few exceptions as noted in Table 22, preparatively important Wittig reactions are performed under conditions where alkene Z:E ratios are within 5% of the cis–trans oxaphosphetane ratios. Therefore, stereochemistry is established in the TS leading to the oxaphosphetane. The TS options can be classified into two general categories: (1) four-center pathways (partial bonding between both pairs of atoms, P—O as well as C—C, in the TS) or (2) two-center pathways (partial bonding between one pair of atoms in the TS). For purposes of our discussion, partial bonding will be defined as *any* stabilizing interaction between eventual oxaphosphetane ring atoms in the TS. This is intended as a broadly inclusive definition of both the four-center (cycloaddition) and the two-center categories.

Several mechanistic variations might be possible under either of the main options (1 or 2). For example, the four-center process might involve a direct conversion from the P=C and the C=O reactants into the oxaphosphetane (asynchronous cycloaddition) (18, 59, 66, 219, 220). In this case, there would be no other intermediates and no energy minima between the reactants and



Scheme 13

the oxaphosphetane. Similarly, the two-center pathway might involve direct conversion from the reactants into potential intermediates **93**–**96** (Scheme 13) (5a). However, the reaction could also proceed via an electron transfer (ET) pathway that requires initial formation of the radical ion pair **92,** (221–223) followed by two-center bonding to give **93**–**96** or four-center bonding to afford the oxaphosphetane **97**.

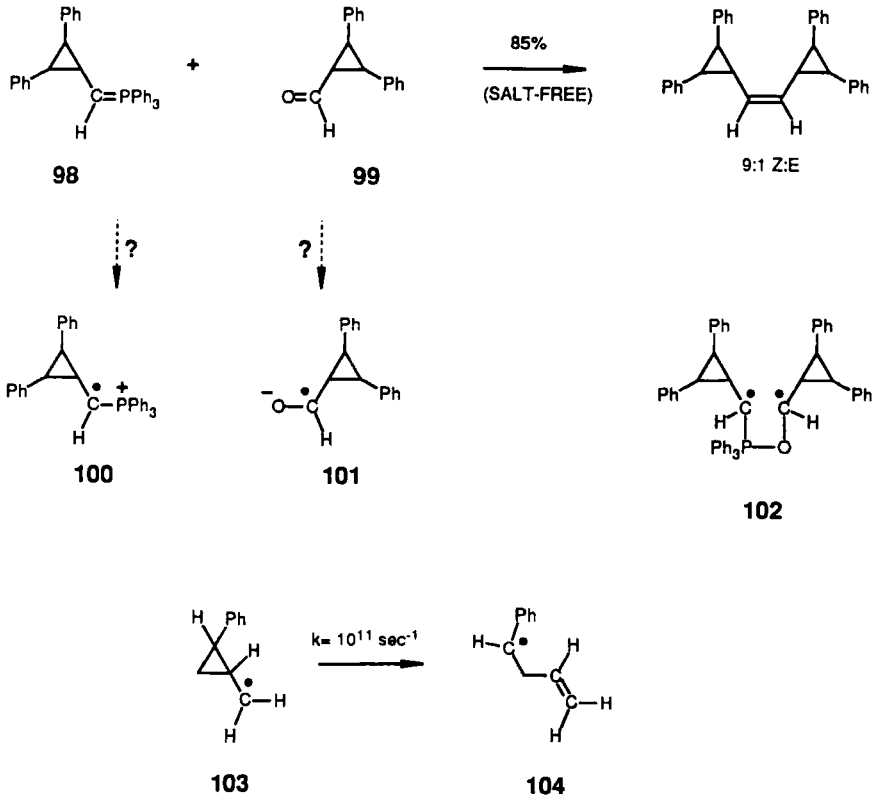
Structures **93 syn** or **93 anti** are the low- and high-energy forms of the hypothetical salt-free betaine intermediate that was proposed in early rationales (1, 2a–h) as was the P—O bonded zwitterion **95** (5a). The diradical representations **94** and **96** have appeared more recently (221, 222), but the apparent difference between zwitterion and diradical notations may be misleading. One electronic representation is simply the excited singlet state of the other, and decay of the higher energy singlet to the ground-state singlet will probably be too fast for any experimental distinction. Based on the electronegativity difference between oxygen and phosphorus, **93** is a better approximation of the hypothetical singlet ground-state species than **94,** but both the zwitterionic and diradical representations contribute to the actual structure of 1,4-diradi-

caloids (224). Thus, **93** (**94**) will have a partial negative charge on oxygen and the corresponding positive charge on phosphorus. For convenience, only the zwitterionic representation **93** will be used in the remainder of this discussion.

The potential intermediate **93 syn** cyclizes rapidly to the more stable oxaphosphetane according to the control experiments described earlier. The corresponding two-center TS may therefore be difficult to distinguish from the four-center TS leading directly to an oxaphosphetane. On the other hand, **93 anti** is clearly distinct in terms of geometry and has the maximum charge separation among all of the hypothetical species **93–96** because of the electronegativity difference between oxygen and phosphorus. The same conclusion applies if **93 anti** is an intermediate or if it serves only as a TS. Thus, high dielectric solvents would be predicted to accelerate the Wittig reaction, and solvent effects on stereoselectivity would be expected. Stabilized ylide reactions do respond to changes in the solvent (see Tables 16–19), but these reactions are not accelerated in high dielectric solvents. To the contrary, Aksnes and Khalil have shown that the reaction of *p*-nitrobenzaldehyde with $Ph_3P{=}CHCO_2Et$ is faster in CCl_4 ($k_{rel} = 58$) or cyclohexane ($k_{rel} = 12$) than in acetonitrile ($k_{rel} = 9$) or DMF ($k_{rel} = 1$) (16)! Similar results have been obtained more recently with aliphatic aldehyde substrates (see Table 25) (99a). In the case of nonstabilized ylides, the effect of solvent on reaction rate has not been studied systematically, but there are abundant data regarding stereoselectivity (Table 11). Variations in the solvent from benzene or ether/pentane to THF–HMPA, DMF, or DMSO cause no significant change in the Z:E ratios of product alkenes under conditions of kinetic control. This is not the pattern expected if the stereochemistry-determining step involves **93 anti** as an intermediate or as a competing TS. The experimental evidence is not compatible with these mechanistic options.

XVI. PROBES FOR ELECTRON TRANSFER

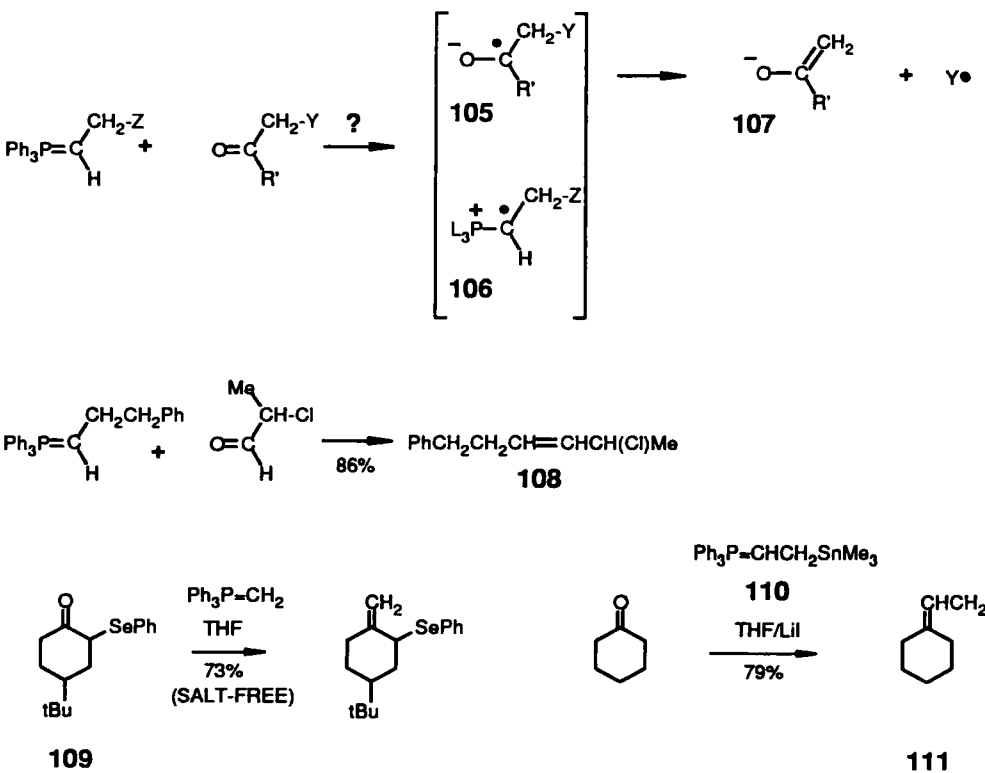
The ET mechanisms invoke intermediates having radical ion as well as diradicaloid character. If the Wittig reaction involves species such as **92** or **95** (**96**), then reactions with suitable test substrates can be used to evaluate this mechanistic possibility. One of the most sensitive radical probes is the 2-phenylcyclopropylcarbinyl system **103** (Scheme 14; $k_{clvg} > 10^{11}\ s^{-1}$ to give **104**) (225a). In the closest Wittig analogy, Castellino and Bruice (77) have reported that the reaction of the 2,3-diphenylcyclopropyl derivatives **98** and **99** affords the alkene in 85% yield (9:1 Z:E). The P—O bonded diradicaloid species **102** cannot play a significant role in this process. Similarly, the radical ions **100** and **101** are not likely to survive and should undergo ring cleavage if they are formed (225b). Many other Wittig reactions of cyclopro-



Scheme 14

pylcarbinyl substrates are known, and no case of radical ring cleavage has been found so far (226).

Carbonyl compounds containing α-heteroatom substituents are sensitive probes for the intervention of radical anion intermediates **105** (Scheme 15) (227). According to Tanner (227), the α-haloacetophenone ketyl (**105**; R′ = phenyl) undergoes exceptionally fast radical elimination to **107** (Y = Br or Cl, $k_{clvg} > 10^9\,s^{-1}$, Y = sulfur or oxygen, $k_{clvg} = 10^6$–$10^8\,s^{-1}$). Rate constants have not yet been determined for aliphatic analogues (**105**, R′ = alkyl or H), but the radical elimination reactions should be at least as fast due to increased localization of spin density at carbonyl carbon. Since many Wittig reactions with α-heteroatom substituted carbonyl reactants appear in Tables 16–21, the absence of side reactions due to potential radical anion intermediates argues against the ET pathway. The α-halo acetophenone system studied by Tanner (227) would be the most convincing test case, but it is not a good Wittig


Ph3P=C(CH2-Z)H
O=C(CH2-Y)R'
?
105
106
107
+ Y•
Ph3P=C(CH2CH2Ph)H
Me
CH-Cl
O=CH
86%
PhCH2CH2CH=CHCH(Cl)Me
108
SePh
tBu
Ph3P=CH2
THF
73%
(SALT-FREE)
109
Ph3P=CHCH2SnMe3
110
THF/LiI
79%
CHCH2SnMe3
111

Scheme 15

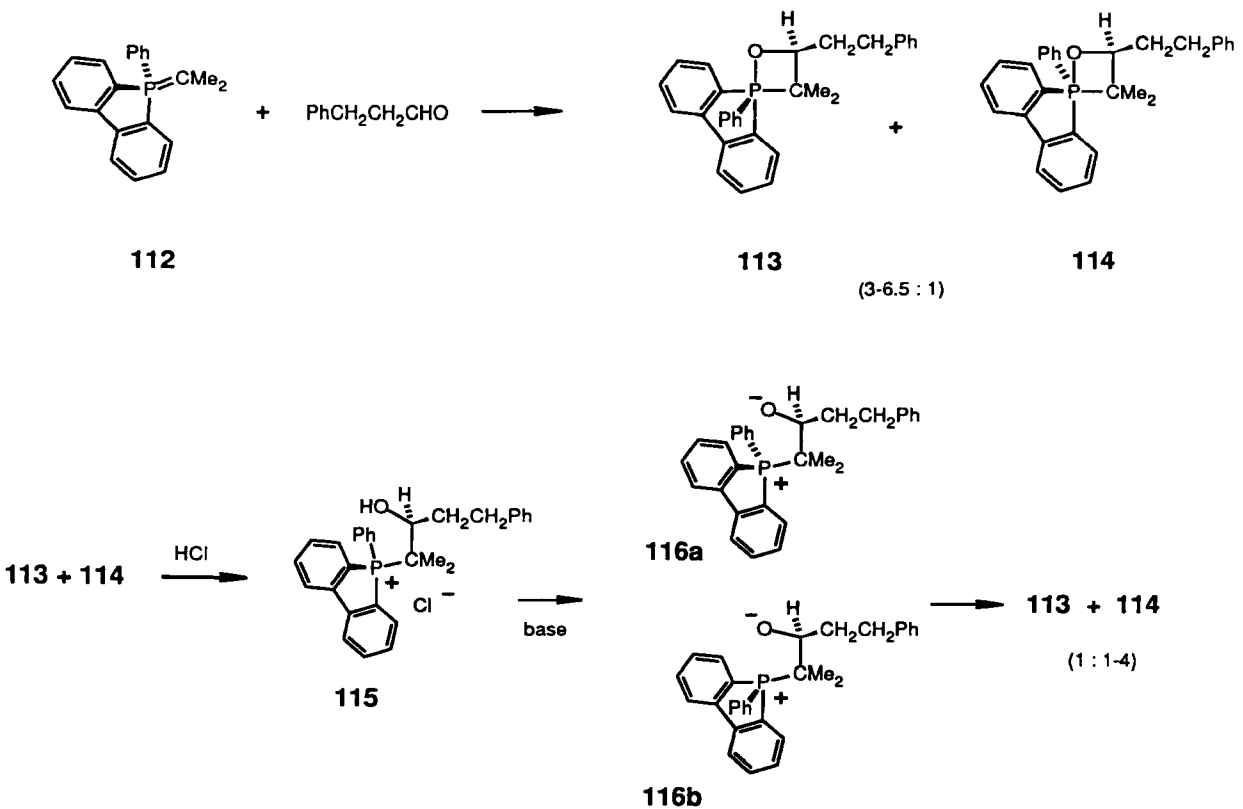
substrate due to competing enolization (42). The α-chloropropionaldehyde reaction with $Ph_3P{=}CH(CH_2)_2Ph$ is the closest known analogy, and this Wittig reaction proceeds normally to afford **108** (> 80% yield) (42a). Similarly, the α-seleno ketone **109** reacts smoothly with $Ph_3P{=}CH_2$ to give the allylic selenide (228). A potential radical leaving group $Z = SnMe_3$ might also be expected to intercept **106**, the radical cation partner in an ET pathway. However, there are no indications that C—Sn bond cleavage occurs when **110** is used for the Wittig synthesis of allyl stannanes such as **111** (202).

There are some examples among the reactions of unreactive ketone substrates where competing radical ion decomposition reactions can be detected (221, 223). Yamataka et al. (223b, c) report that *m*-iodobenzophenone affords 5% of iodine-free products along with 54% of the expected alkene upon reaction with isopropylidenetriphenylphosphorane at 0°C. Under the same conditions, the ortho-iodo isomer gives no Wittig alkene and undergoes ca. 15% deiodination to afford benzophenone. Loss of iodide may well involve an ET pathway and a radical anion (ketyl) intermediate [$k_{clvg} = \sim 10^6\ s^{-1}$ for *m*-iodobenzophenone ketyl] (227). This evidence does not prove that the ketyl intermediate is on the Wittig pathway, but kinetic isotope effects to be discussed later are consistent with ET (223).

If ET intermediates play any role in representative aldehyde or ketone Wittig reactions, they are too short-lived for detection by the fastest available radical or radical anion clocks. This is conceivable if the geometry of the radical ion pair resembles that of an oxaphosphetane with partially developed bonds (223c). Such a scenario fits within the broad definition of a four-center mechanism and allows little (if any) distinction between the geometry of stereochemistry-determining TS that invoke ET versus those that do not. More precise distinctions may have theoretical significance, but they will not influence the stereochemical issues that are of concern in this review.

XVII. PROBES FOR BETAINE INTERMEDIATES

Ionic mechanisms based on betaine intermediates or TS are difficult to reconcile with the absence of solvent effects on lithium-free nonstabilized ylide reactions (Table 12) or reactivity–selectivity considerations (15). Also, there is no apparent reason why the reactants should prefer to form a high-energy intermediate such as **93** when the direct conversion to a more stable oxaphosphetane **97** is possible. Orbital symmetry should not interfere with the four-center process since phosphorus can provide 3*d* orbitals of appropriate symmetry for a 2*s* + 2*s* cycloaddition. Nevertheless, the betaine mechanism has persisted in the literature because there was no direct evidence against the formation of **93** as a transient intermediate until recently (229).


Ph
CMe2
+
PhCH2CH2CHO
H
CH2CH2Ph
O
P
CMe2
Ph
+
112
113
114
(3-6.5 : 1)
113 + 114
HCl
HO
Cl −
base
116a
116b
113 + 114
(1 : 1-4)
115

Scheme 16

The experimental test that distinguishes the stepwise and four-center mechanisms is described in Scheme 16.

The Wittig reaction of the dibenzophosphole ylide **112** (Scheme 16) affords two oxaphosphetane diastereomers **113** and **114** in a ratio of ca. 3–6.5:1 at −95°C (229). The diastereomers can be interconverted by pseudorotation, a process that is most easily visualized using a two-stage Ugi turnstile mechanism. In the first stage, a "trio" consisting of the two dibenzophosphole C—P bonds and the P-phenyl C—P bond is rotated 120°, while the "duo" (consisting of the oxaphosphetane P—O and P—C bonds) is rotated 180°. This process is repeated in the second stage and results in the interconversion of **113** and **114** (229). Interconversion of the pseudorotamers is slow at −95°C, but it occurs at a convenient rate above −70°C to give an eventual equilibrium ratio of 1.8:1 of **113**:**114**. The initial ratio of pseudorotamers from the Wittig experiment has no specific mechanistic significance, but it can be compared to the ratio of **113**:**114** from an independent experiment to generate the betaine. Thus, deprotonation of the β-hydroxyphosphonium salt **115** affords a very different ratio: 1:1–4 of **113** and **114**, depending on the solvent and the base employed. It does not matter whether a syn betaine or an anti betaine is generated by deprotonation because the pseudorotamer ratio reflects the population of syn-betaine rotamers **116a** and **116b** at the instant of cyclization to the oxaphosphetane. Since the initial isomer ratio from the betaine generation experiment is different from the equilibrium ratio, and even more different from the ratio of **113**:**114** obtained from reaction of the ylide **112** with hydrocinnamaldehyde, the Wittig reaction cannot proceed to the oxaphosphetane by way of the betaine as a dominant pathway. This experiment rules out 1,4-diradicaloid intermediates (betaines or 1,4-diradicals; **93** or **94**, Scheme 13) having significant lifetimes.

XVIII. THEORETICAL CONSIDERATIONS

Many attempts have been made to evaluate the Wittig TS by computational methods, as summarized in Tables 23 (calculated oxaphosphetane geometries) and 24 (calculated TS geometries). Energy minima for four-center TS have been identified, but there are no reports of accessible energy minima corresponding to any of the hypothetical intermediates **92**–**96**. The *ab initio* theoretical treatments have focused on the model reaction $H_3P{=}{=}CH_2 + HCHO$ and have not addressed stereochemical issues due to the complexity of ylides that have realistic substituents at phosphorus (see Table 24) (230). Some attempts to incorporate *P*-alkyl or *P*-aryl groups in semiempirical calculations have also been reported ($L_3P{=}CHCH_3$; L = H, Me, Ph) (230c, h, i). Recent MNDO studies conclude that four-center TS geometries would be nearly

TABLE 23
Geometries Calculated for Hypothetical Oxaphosphetanes

Entry	Method	d P-O	d P-C	d C-C	d O-C	∠OPC	∠PCC	∠CCO	∠COP	Ref.
$HCHO + H_3P{=}CH_2$										
1	4-31G	1.933	1.917	1.541	1.422	72.3	92.2	100.1	95.4	230c
2	STO-3G	1.888	1.937	1.548	1.427	73	--	--	--	230b
3	4-31G*	1.757	1.843	1.533	1.399	75.9	89.0	98.0	--	230d
4	DZ + P	1.749	--	1.524	--	--	--	--	--	230e
5	MMX87	1.83	1.79	1.53	1.42	73.2	94.5	94.3	96.8	230f
6	MNDO	1.73	1.85	1.54	1.38	76.4	87.6	98.2	97.7	230f
7	MNDO	1.73	--	1.546	--	--	--	--	--	230e
8	PM3	1.83	--	1.522	--	--	--	--	--	230e
9	PM3	1.83	1.90	1.52	1.40	73.3	90.0	99.5	97.2	230f
10	3-21G	1.83	1.92	1.55	1.44	74.3	90.1	98.6	97.1	230b
$(CH_3)_3CCHO + (CH_3)_3P{=}CHCH_3$										
cis										
10	MMX	1.67	1.84	1.53	1.42	73.5	89.0	90.7	99.7	230f
11	MNDO	1.77	1.94	1.56	1.38	72.6	86.6	96.6	99.6	230f
trans										
12	MMX	1.67	1.82	1.53	1.41	70.9	93.0	92.4	96.5	230f
13	MNDO	1.76	1.94	1.56	1.38	72.9	88.1	97.0	101.6	230f

planar for several combinations of phosphorus and aldehyde substituents, including the $Ph_3P{=}CHCH_3 + CH_3CHO$ example (Table 24, entries 13 and 14) (230h, i). According to these studies, the four-center cis TS has nearly the same ring geometry as the trans TS, and the latter is favored by ca. 1 kcal/mol, contrary to the experimental result (cis TS favored by ca. 2 kcal/mol). Changes in phosphorus substituents from phenyl to methyl do not substantially alter the MNDO geometries or the predicted relative stabilities of cis versus trans precursors. Since these results are not consistent with experimental selectivity trends, Yamataka et al. (230h) and Mari, McEwen et al. (230g, i) have suggested that the mechanism of the reaction may not involve a four-center TS. Another possibility is that the semiempirical methods may not be parametrized correctly to deal with TS that include carbon, oxygen, and phosphorus. Until the MNDO-based techniques can be shown to predict TS geometries and barriers in simpler problems involving pentavalent phosphorus species, their conclusions will be difficult to evaluate.

According to X-ray evidence (Table 4), the oxaphosphetane ring is somewhat distorted from planarity when both C_3 and C_4 are sp^3 hybridized. Thus, oxaphosphetanes **A** and **E** (Table 4) have dihedral angles of 8.6° and 9.7°, respectively, along the PC_3–C_4O axis, values that indicate significant ring puckering to relieve nonbonded interactions. The NMR evidence also suggests a distorted oxaphosphetane ring (Table 5). The ^1H–^{31}P coupling constant for the P—C_3—C_4—H subunit of 3,4-disubstituted oxaphosphetanes varies depending on stereochemistry. Thus, the cis diastereomer has the larger three bond coupling between C_4—H and phosphorus ($^3J_{P-C-C-H} = 5$–11 Hz) compared to the trans-disubstituted oxaphosphetane ($^3J_{P-C-C-H} = 1$–2 Hz), as in Table 5, entry **G** (cis), $^3J = 6$ Hz; entry **H** (trans), $^3J = 2$ Hz (20). A large variation in ^1H–^{31}P coupling ($^3J_{P-C-C-H}$) is not expected in a nearly planar oxaphosphetane having eclipsed C_3 and C_4 substituents because there would be no significant change in the corresponding dihedral angle. Evaluation of the geometric parameters derived from the computations (Table 23, entries 10–13) suggests PC_3–C_4O dihedral angles of ca. 20°. None of this evidence proves that oxaphosphetanes are puckered under typical solution conditions. Thus, variations in ^3J values for the P—C_3—C_4—H segment could be due to bond angle distortion in the exocyclic C—H bonds as well as to ring puckering. In either case, the evidence suggests that there is sufficient ring flexibility to respond to the steric demands of substituents. The subsequent discussion assumes that the same conclusion will apply to early TS where the four-center geometry should be flexible due to a longer, partially developed P—O bond.

It is hoped that future semiempirical computational attempts to explore the stereochemical problem will evaluate pentavalent phosphorus parameters in a setting where there are fewer unknowns. One relevant test would be to

TABLE 24
Calculated Transition State Geometries

Entry	Method	d P-O	d P-C	d C-C	d O-C	∠OPC	∠PCC	∠CCO	∠COP	Ref.
HCHO + $H_3P{=}CH_2$:										
1	4-31G*	2.649	1.736	2.079	1.239	73.9	93.9	108.4	--	230d
2	3-21G*	2.633	--	2.124	--	--	--	--	--	230e
3	MNDO	3.130	--	2.176	--	--	--	--	--	230e
4	PM3	2.839	--	1.907	--	--	--	--	--	230e
5	DZ + P	2.726	--	1.912	--	--	--	--	--	230e
6	STO-3G	2.724	1.879	1.914	1.289	67	--	--	--	230b
MeCHO + $H_3P{=}CHMe$:										
Entry	Method	d P-O	d P-C	d C-C	d O-C	∠OPC	∠PCC	∠CCO	∠COP	Ref.
cis										
7	MNDO	2.972	1.770	2.014	1.251	61.2	105.7	104.7	80.0	230h
8	3-21G	2.742	1.829	2.251	1.251	74.1	92.6	105.3	80.0	230h
9	MNDO-PM3	2.48	--	2.14	--	--	--	--	--	230i
trans										
10	MNDO-PM3	2.57	--	2.11	--	--	--	--	--	230i
MeCHO + $Me_3P{=}CHMe$:										
cis										
11	MNDO	3.2	--	2.00	--	--	110	107	--	220b

trans										
12	MNDO	2.884	1.764	2.033	1.251	64.6	104.5	105.5	83.3	230h
13	3-21G	2.784	1.818	2.264	1.247	73.8	93.2	106.1	86.5	230h
MeCHO + Ph_3P=CHMe:										
cis										
14	MNDO	3.229	1.821	2.056	1.248	56.6	112.3	106.8	78.5	230h
15	MNDO-PM3	2.63	--	1.96	--	--	--	--	--	230i
trans										
16	MNDO	3.248	1.934	2.035	1.248	55.3	114.4	106.4	79.2	230h
17	MNDO-PM3	2.73	--	2.00	--	--	--	--	--	230i
NCCHO + Ph_3P=CHMe:										
cis										
18	MNDO-PM3	2.86	--	1.98	--	--	--	--	--	230i
19	MNDO=PM3	2.93	--	2.00	--	--	--	--	--	230i

calculate the relative stabilities of oxaphosphetane pseudorotamers. Another test would be to calculate the pseudorotation barriers in oxaphosphetanes. Both the isomer ratios and activation barriers for interconversion are known in several cases (229, 231). These parameters should be sensitive to torsional factors and substituent effects, variables that are especially important in the congested Wittig TS.

XIX. TRANSITION STATE CHARACTERISTICS

The extent of bond formation in the TS can be probed using kinetic isotope effects and Hammett σ, ρ correlations. Yamataka et al. (223b) have measured the Hammett ρ values for the isopropylidenetriphenylphosphorane reaction with substituted benzaldehydes and benzophenones. The benzaldehyde reactions are complete within seconds at $-78°C$ and competition experiments indicate that $\rho = +0.59$. This value reflects a small rate advantage for the more electron deficient aldehydes. On the other hand, $Ph_3P{=}C(CH_3)_2$ discriminates quite well among substituted benzophenones in a relatively slow reaction (time scale of hours at 0°C), $\rho = +1.40$ (223a). The larger ρ value corresponds to a greater degree of C—C bond forming in the TS, and this conclusion is supported by a large kinetic isotope effect (KIE), $k_{12}/k_{14} = 1.053$ for benzophenone. Large values for $\rho = +2.77$ and $k_{12}/k_{14} = 1.06$ are also reported for the reaction of $Ph_3P{=}CHPh$ with substituted benzaldehydes (lithium-free conditions, 0°C) (82d).

A negligible KIE is observed for the $PhCHO + Ph_3P{=}CMe_2$ example ($k_{12}/k_{14} = 1.003$), and $\rho = +0.59$, as already mentioned. Even smaller KIE and ρ values are reported for lithium-free $Ph_3P{=}CHC_3H_7$: $\rho = +0.2$ at 0°C ($k_{12}/k_{14} = 0.998$) and $\rho = -0.25$ at $-78°C$ ($k_{12}/k_{14} = 0.993$) (223c). In an earlier study, $\rho = +1.1$ had been found for $ArCHO + Ph_3P{=}CH_2$ and $Ph_3P{=}CHCH_3$ (232a). There may be some discrepancy between the two studies, perhaps due to differences in reversal induced by excess ArCHO, but the Yamataka results indicate a very early TS, or a TS that lacks C—C bonding. A possible explanation has been proposed by Yamataka et al. (223c). Small KIE values for the reaction of $PhCHO + Ph_3P{=}CHR$ are consistent with rate-determining ET, followed by rapid collapse of the radical ion pair (**92**, Scheme 13). For the $Ph_2C{=}O + Ph_3P{=}CMe_2$ example, $k_{12}/k_{14} = 1.053$ and $\rho = +0.59$ can be explained by rate-determining radical ion pair collapse (223), while the large KIE ($k_{12}/k_{14} = 1.06$) and $\rho(+2.77)$ for the $Ph_3P{=}CHPh$ reactions can be attributed to a cycloaddition process (82d). Lithium ion decreases both the $\rho(+1.38)$ and k_{12}/k_{14} (1.05) values for $Ph_3P{=}CHPh +$ PhCHO, suggesting a faster reaction and an earlier TS (82d). This is consistent with the pronounced effect of lithium ion on benzylide Z:E ratios (Table 14).

The more reactive ylides discriminate less well among the aldehydes in competition experiments (ρ, KIE), in accordance with the reactivity–selectivity principle (RSP) (15b, 233). Thus, both the KIE and ρ values could be small. However, Yamataka et al. (223c) question the validity of the RSP in an ET sequence. Their arguments depend on the interpretation of KIE and σ, ρ data for the PhCHO or $Ph_2C{=}O$ reactions, some of which are partially reversible. These reactions also cover a wide range of reactivity. It would be reassuring to have better model reactions for comparison, but it is not clear what experiment would be decisive. Objections to ET mechanisms based on the radical anion clock experiments discussed earlier may also not be decisive because of differences in the counterions. Futhermore, radical clock evidence against ET is available for aliphatic (not aromatic) aldehydes.

In the case of ester–stabilized ylide reactions, the ρ values are predictably large (+ 2.3 to + 2.9) (12a, 15b, 232b). Giese and co-workers (15b, 233) have noted that the RSP is not obeyed in the reactions of $Ar_3P{=}CHCO_2Et$ with substituted benzaldehydes as the ylide reactivity is varied. The more reactive ylides tend to be more selective in this series. This behavior was cited as strong evidence for a four-center mechanism with substantial rehybridization at both pairs of interacting atoms (P—O as well as C—C). According to Giese et al., an apparent violation of the RSP is possible in a four-center process because substituents can have opposing effects on the two developing bonds. Thus, substituents that help the developing C—C bond may retard formation of the P—O bond. As mentioned in the preceding paragraph, nonstabilized ylides do appear to obey the RSP. In these reactions, the TS is earlier and bond formation is less advanced. If the P—O bond is considerably less developed than the C—C bond (asynchronous four-center TS) then reactivity and selectivity for nonstabilized ylides would be controlled primarily by those factors that affect the C—C bonding process, and the influence of P—O bonding would be small.

From the above discussion, P—O bonding lags behind C—C bonding in the TS of nonstabilized ylide reactions, and phosphorus geometry must be close to tetrahedral in an early TS. Carbon rehybridization would be more advanced, but the ylide α-carbon should be closer to tetrahedral geometry than the aldehyde carbon. This conclusion follows from the observation that the ylide α-carbon is partly pyramidalized in the ground state, as deduced from NMR and X-ray evidence discussed earlier.

Further insight into structural details of possible TS depends on the correlation of stereochemical trends tabulated earlier and summarized in Table 22. Stabilized ylide reactions with simple aldehydes favor the trans-selective pathway. As discussed in connection with Table 7, the trans-disubstituted oxaphosphetanes are thermodynamically more stable than the cis diastereomers, and the same preference should be felt in the late TS of

stabilized ylide reactions. However, in this series the stereochemical result is not very sensitive to phosphorus substituents, nor to structural details of the ylide stabilizing group (ester, acyl, formyl, etc.) when the reaction is performed in nonpolar solvents. Apparently, the oxaphosphetane-like TS is too rigid to respond much to changes in the phosphorus environment, and 1,2-interactions along the developing C—C bond are dominant.

Reactive ylides such as $L_3P{=}CHR$ (R = alkyl, alkenyl, aryl) are much more sensitive to the phosphorus environment and to steric or stereoelectronic constraints near the carbonyl group. Thus, 3° aldehydes consistently react with higher cis selectivity compared to unbranched aldehydes with all families of reactive ylides. Selectivity is lower when the ylide contains relatively compact substituents at the α-carbon (MeS, MeO, Cl, F, $CH_2{=}CH$, etc.). This behavior indicates that the accumulation of steric bulk in the early TS of nonstabilized ylide reactions contributes to cis selectivity at the oxaphosphetane stage. However, the shape of substituents is important as well as their bulk, and changes in the bond angles of phosphorus ligands can have striking consequences (see Table 13). The empirical observations are consistent with a congested, substrate dependent TS but one that retains considerable flexibility due to the long P—O bond. The subsequent discussion of TS models is based on the detailed interpretation of substituent effects presented in 1989 by Vedejs and Marth (219). Salient features of some other proposals will be considered briefly later on.

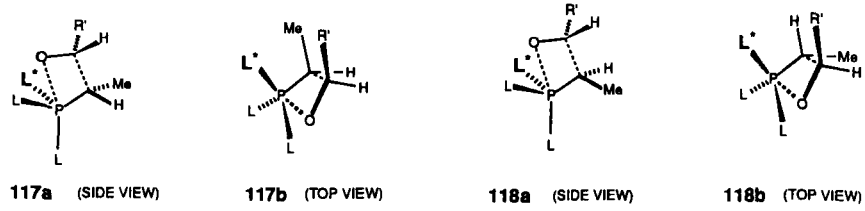
XX. INTERPRETATION OF STEREOCHEMISTRY

In contrast to cycloadditions involving all-carbon reactants, the four-center TS for the Wittig reaction must accommodate a tetrahedral atom (phosphorus) with major steric demands in all three dimensions. Thus, *planar* four-center transition states **117** and **118** (Scheme 17) are destabilized by the gauche interaction between the developing P—O bond with two phosphorus ligands, and also by a 1,3-interaction between the aldehyde alkyl group R′ and the nearby phosphorus ligand (marked L* to simplify comparison of different perspective drawings). In addition, **117** also suffers from an eclipsing 1,2-interaction along the developing C—C bond, especially if the aldehyde R′ group is tertiary.

In principle, the 1,3-interaction can be relieved by enforcing unnatural exocyclic bond angles at ylide phosphorus or at aldehyde carbon. If this is done without altering the planar arrangement of interacting C=P and C=O subunits, then at least four limiting structures **119–122** are possible that differ in subtle structural features. Bond angle distortions at the ylide α-carbon might also be beneficial, but these options have not been illustrated. Geo-

EARLY TRANSITION STATE OPTIONS; PLANAR 4-CENTER GEOMETRIES.

cis: trans:



117a (SIDE VIEW) **117b** (TOP VIEW) **118a** (SIDE VIEW) **118b** (TOP VIEW)

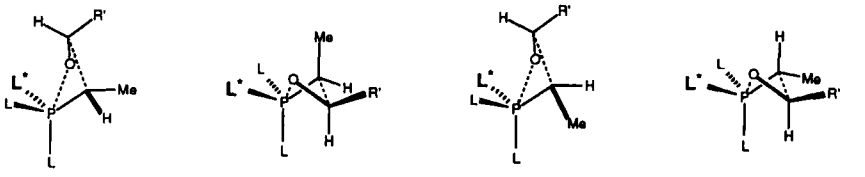
cis: trans: cis: trans:



119 **120** **121** **122**

EARLY TRANSITION STATE OPTIONS; PUCKERED GEOMETRIES.

cis: trans:



123a (SIDE VIEW) **123b** (TOP VIEW) **124a** (SIDE VIEW) **124b** (TOP VIEW)

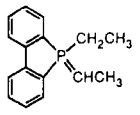
Scheme 17

metries **119** (cis) and **120** (trans) are obtained by compressing the tetrahedral phosphorus bond angles, while **121** (cis) and **122** (trans) are generated by forcing apart the aldehyde alkyl and oxygen substituents. Structures **121** and **122** require unrealistic bond angle distortions for the strongest bond (carbonyl) in the activated complex and appear unlikely. Structures **119** and **120** are more plausible, but they resemble oxaphosphetanes and are more appropriate as models for advanced TS. On the other hand, such geometries would be reasonable for reactive ylides (early TS) if two or more phosphorus ligands are constrained in a ring that enforces small L—P—L* bond angles.

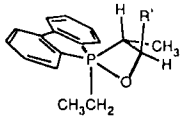
Another way to reduce 1,3-interactions is to pucker the developing four-membered ring, as shown in the somewhat exaggerated drawings **123** and **124**. This perturbation may interfere with efficient overlap, but it relieves 1,2- as well as 1,3-interactions. The aldehyde substituent is far from the phosphorus ligands in both of the puckered TS models, but the cis (**123**) TS is favored over the trans (**124**) TS because of smaller 1,2-interactions between the ylide α-CH_3 substituent with R′, and with the adjacent phosphorus substituent. The 1,2-interactions depend on the dihedral angle along the $R'C_4$–C_3Me axis, and this angle is larger in **123** compared to **124**, depending on the extent of ring puckering. Structure **123** also has minimal 1,2- and 1,3-interactions compared to the planar four-center TS model analogue **117**. It is harder to evaluate the possible TS candidates **118**, **120**, and **124** for the trans-selective reaction component. The compromise between steric effects and bond angle distortion may vary for some of the different phosphorus environments. Geometries similar to the planar TS structure **120** would be best for relatively advanced TS (reactions of $Ph_3P{=}CHR$ with hindered ketones; stabilized ylide reactions) while TS models **124** or **118** should be preferred for the minor, trans-selective pathway of reactive ylides $Ph_3P{=}CHR$.

Nonplanar TS geometries in the $Ph_3P{=}CHR$ reactions are favored by α-branching in the aldehyde substituent R′ because the 1,3-interactions become increasingly important. However, the steric constraints decrease carbonyl reactivity and work against an early TS. The result is a consistent but relatively small trend toward the cis-selective pathway for the reaction of tertiary aldehydes with a variety of ylides. Heteroatom branching at the α-carbon has a similar effect on selectivity. In this case, the steric constraints may be smaller, but there are new constraints due to the need to minimize lone-pair or dipole–dipole interactions. There are fewer conformational options for the carbonyl component in the TS, and the result is an increase in the importance of 1,3-interactions. Since α-heteroatom substituents in the carbonyl reactant will also increase carbonyl reactivity, there will be a trend toward an earlier, more puckered TS. The combination of conformational constraints and increased reactivity results in higher selectivity for the cis-disubstituted oxaphosphetane.

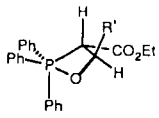
Aldehydes and phosphole-derived nonstabilized ylides react with a kinetic preference for the (*E*)-alkene (Table 13). Since the phosphole ring constrains bond angles for two of the three phosphorus ligands, ylide **125** will preferentially react via the TS geometry **126** (Scheme 18; similar to **119** or **120**). The role of 1,3-interactions is reduced, especially if the third phosphorus ligand (the ethyl group in **126**) is compact. There is little steric advantage for a puckered geometry, and the phosphole-derived ylides react via a planar four-center TS. Even though the TS is relatively early, the TS geometry resembles a planar oxaphosphetane and the trans-selective pathway is favored because 1,2-



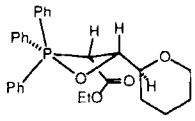
125



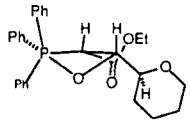
126



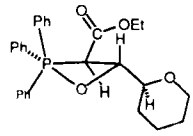
127



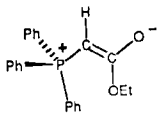
128a



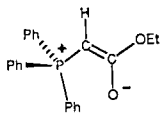
128b



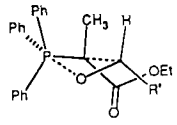
128c



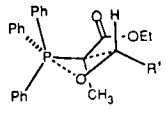
129 anti



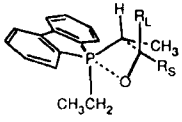
129 syn



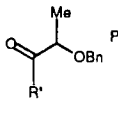
130



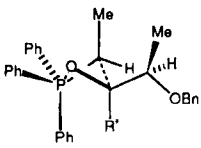
131



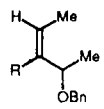
132



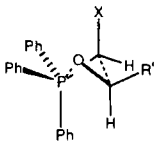
133



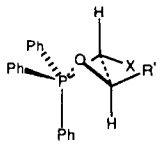
134



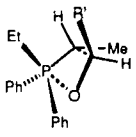
135



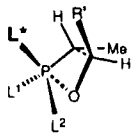
136



137



138



139

Scheme 18

interactions are dominant. However, trans selectivity is easily degraded when bulkier substituents are present at phosphorus (**124** with L = Ph, NMe_2, etc.) due to increased 1,3-interactions (20).

XXI. TRANSITION STATE GEOMETRIES OF STABILIZED YLIDES

Increased P—O bonding in the TS favors more nearly planar four-center TS geometries, as in the stabilized ylide case **127.** Since phosphorus is closer to trigonal bipyramidal geometry, the 1,3-interactions are relieved and 1,2-interactions control selectivity. The normal thermodynamic advantage for the trans-disubstituted oxaphosphetane is felt in the product-like transition state, and the (*E*)-alkene is the major product. Because the TS is relatively rigid, the result is not much affected by changes in the phosphorus ligands, in contrast to the nonstabilized ylide reactions. Essentially all of the carbonyl stabilized ylides react with a preference for (*E*)-alkene formation in aprotic solvents.

Several aspects of the stabilized ylide reactions are not well understood. Reactions conducted in solvents such as CH_2Cl_2, acetonitrile, or DMF are sensitive to Lewis acid or protic acid additives as discussed in connection with Tables 16 and 17. Most of these effects tend to erode E selectivity, but carboxylic acid additives preferentially catalyze the E-selective pathway (99a). No convincing explanation can be offered for this phenomenon. The solvent effects encountered in Tables 16–19 are also difficult to explain, but some progress toward understanding them has been made. Dramatic solvent effects are seldom seen for the stabilized ylide families $L_3P{=}CHX$ (X = acyl, CHO) or the more highly substituted analogues such as $Ph_3P{=}C(Me)CO_2Et$. In contrast, the solvent plays an important role for the closely related ylides $Ph_3P{=}CHCO_2R''$ or $Ph_2MeP{=}CHCO_2R''$ (Tables 16–19). Stabilized ylides are more extensively solvated in the ground state compared to the four-center Wittig TS. The activation parameters are therefore sensitive to the extent of TS desolvation, as shown by a detailed study of the reaction between *p*-nitrobenzaldehyde and $Ph_3P{=}CHC(O)Ph$ (16). The activation entropy in methanol is relatively favorable (−14.3 eu) compared to CCl_4 (−35.1 eu) due to extensive TS desolvation in methanol (16). However, the reaction is faster in CCl_4 because the activation enthalpy is much lower, 8.9 kcal/mol versus 16.2 kcal/mol in methanol. This large difference in activation enthalpies arises because the polar reactants are stabilized by solvation in methanol.

Similar activation parameters have been determined for the reaction of $Ph_3P{=}CHCO_2Et$ with two representative aldehydes, hydrocinnamaldehyde and 2-formyltetrahydropyran (99a). As shown in Table 25, this study has also defined the individual activation parameters for the Z-selective and the E-selective pathways. The activation entropy is more favorable in methanol

TABLE 25
Activation Parameters for R'CHO Reactions with $Ph_3P{=}CHCO_2Et$[99]

R'	solvent	Z:E	k_{OBS} ($L mol^{-1} sec^{-1}$)	$\Delta G_Z^{\ddagger}$ [a] (kcal/mol)	$\Delta G_E^{\ddagger}$ [a] (kcal/mol)	$\Delta H_Z^{\ddagger}$ (kcal/mol)	$\Delta H_E^{\ddagger}$ (kcal/mol)	$\Delta S_Z^{\ddagger}$ (eu)	$\Delta S_E^{\ddagger}$ (eu)
$PhCH_2CH_2$	THF	8:92	0.004	22.2	20.8	9.5	9.5	-43	-38
""	CH_2Cl_2	4:96	0.047	21.2	19.3	8.6	8.6	-42	-36
""	MeOH	38:62	0.062	19.7	19.4	15.7	15.7	-13	-12
2-THP	THF	8:92	0.0028	22.4	21.0	9.8[b]	9.8	-42	-38
""	CH_2Cl_2	10:90	0.13	20.0	18.7	9.3[b]	9.3	-39	-32
""	MeOH	75:25	0.074	19.2	19.8	14.9	14.9	-14	-16

(a) $\Delta G^{\ddagger}$ calculated at 298 °K. (b) Freshly distilled aldehyde gives temperature-invariant Z:E ratios, resulting in identical $\Delta H_Z^{\ddagger}$ and $\Delta H_E^{\ddagger}$. If the aldehyde is not freshly distilled, temperature-variant ratios in the range of 12:88 to 17:83 Z:E are obtained, the apparent values of $\Delta G_Z^{\ddagger}$ and $\Delta H_Z^{\ddagger}$ become smaller, and the apparent $\Delta S_Z^{\ddagger}$ changes accordingly.

than in THF or CH_2Cl_2 due to more extensive TS desolvation while the activation enthalpy is lower in the aprotic solvents. In the case of hydrocinnamaldehyde, activation enthalpy is the same for either the Z-selective or the E-selective pathways and activation entropy is responsible for E selectivity in the aprotic solvents and also for the solvent effect on Z:E ratios. Solvation is relatively unimportant in THF or CH_2Cl_2 and the more flexible (less sterically congested) TS_E is entropically favored, presumably because a larger number of low-energy conformers is available. In methanol, ground-state solvation is more important, and extensive TS desolvation results in a more favorable activation entropy for both the Z-selective and the E-selective pathways. The interpretation of small activation entropy differences becomes increasingly subjective. However, similar values for activation enthalpy and entropy for the E- versus the Z-selective pathways in methanol suggest that the extent of desolvation is comparable for both TS_E and TS_Z. Apparently, the conformational flexibility advantage of TS_E is smaller in methanol, perhaps due to some effect of specific solvation.

The 2-formyltetrahydropyran reactions follow a similar pattern in the aprotic solvents. Activation entropy favors TS_E, although by a smaller margin than in the hydrocinnamaldehyde experiments. The entropy term also controls selectivity in methanol, but now the Z-selective pathway is favored. As before, this is the result of a subtle interplay between desolvation and flexibility factors, and no detailed interpretation is possible. However, the Z selectivity arises from a combination of factors, and not from any specific stabilizing effect of methanol solvation in TS_Z. The latter phenomenon should have resulted in an enthalpic advantage and an entropic penalty, but neither is observed in methanol. In summary, the α-oxygen substituent in the aldehyde promotes a small trend in activation entropy toward (*Z*)-enoates in the aprotic solvents and a larger trend in methanol. A similar solvent effect is seen with most, if not all of the aliphatic aldehydes, but it is largest in the case of α-alkoxy aldehydes. As discussed in connection with Table 19, the combination of solvent and α-alkoxy effects can be further amplified by a syn β-alkoxy group. Although the result in methanol can be astonishing (see Table 19, entries 19, 20, 24, 68, 90; 99:1 Z:E), it requires only an additional advantage of ca. 3 entropy units for TS_Z over TS_E by comparison with the 2-formyltetrahydropyran example in Table 25.

There are many TS geometries to consider for the reaction of $Ph_3P{=}CHCO_2Et$ with 2-formyltetrahydropyran, and three limiting cases **128a–c** have been illustrated in Scheme 18, all with the ether oxygen pointed away from aldehyde oxygen to minimize unfavorable dipole and lone-pair interactions. The cis-selective options **128a** and **128b** differ in the orientation of the ester group, corresponding to the anti and syn forms of the ylide (**129**). In methanol, it is likely that **128a** or **128b** would benefit from solvation effects

that minimize unfavorable interactions among the α-alkoxy, ester, and oxaphosphetane oxygens. The TS_Z rotamer **128a** corresponds to the more polar ylide rotamer **129 anti,** the isomer that is likely to be the most highly solvated ground-state species. For simplicity, only one conformer **128c** is shown for TS_E, the dominant pathway in THF or CH_2Cl_2. Structure **128c** corresponds to the less polar ylide rotamer **129 syn** which should be favored in THF or CH_2Cl_2, but conformers derived from **129 anti** should also be accessible because the ylide rotamers interconvert on the NMR time scale. Other rotamers of the tetrahydropyranyl unit are by no means ruled out, and there are many potential variables. There is no experimental basis for further speculations at this time.

Several other features of the stabilized ylide reactions deserve additional study. For example, it is not clear why the selectivity of the α-substituted ylides $Ph_3P{=}C(Me)CO_2R''$ for E-trisubstituted enoates is so similar to the selectivity of $Ph_3P{=}CHCO_2R''$ for the E-disubstituted enoates (nonpolar aprotic solvents). Apparently, an oxaphosphetane-like TS prefers to have the electron-withdrawing ester group trans to the aldehyde R′ group (**131**). If a donor–acceptor interaction is involved in this preference, then it would be easier to understand the high E selectivity of some of the other stabilized ylides in Tables 18 and 19 (for example, $Ph_3P{=}CHCHO$). However, steric arguments are also possible. Geometries similar to **130** [(*Z*)-enoate precusor] will be destabilized by eclipsing interactions between the ester group and the adjacent R′, methyl, and P—Ph substituents. The alternative puckered TS structure **131** [(*E*)-enoate precursor] allows the ester function to turn away from the aldehyde oxygen, from the eclipsing interaction with methyl, and to avoid the *P*-phenyl groups. A similar puckered geometry does not help **130** because of increased electrostatic repulsion between aldehyde and ester oxygens. This latter issue does not arise for analogous nitrile-stabilized ylides such as $Ph_3P{=}C(CH_3)CN$, and the reaction with an unbranched aldehyde proceeds nonselectively (Table 19, entries 127–128, Z:E = 61:39 in THF; Z:E = 37:63 in benzene) (142f). Once again, there are no reported examples where direct comparisons have been made using the same carbonyl substrate and reaction conditions, and further data are needed to establish a general trend.

XXII. MISCELLANEOUS REACTIONS

A. Ketones

No consistent selectivity pattern has emerged from the reactions of alkyl-branched ketones with $Ph_3P{=}CHR$. The phosphole-derived ylides behave more predictably, and their tendency to form the (*E*)-alkenes via **132** fits well

with their general reactivity pattern in the aldehyde series. The same stereochemical outcome is seen with the α-alkoxy ketones in the small number of examples studied so far. In the $Ph_3P{=}CHR$ series, the ketone reactions appear to be more sensitive to structural details and to remote steric effects (Table 20). Selectivity patterns are different for cyclohexanones versus cyclopentanones, and the 17-keto steroid examples are exceptionally selective for (*Z*)-alkene formation (Table 20, entries 48–53). In contrast, an α-dialkylcyclohexanone reacts with modest 29:71 selectivity for the (*E*)-alkene (entry 37). The α-alkoxy ketones **133** follow a consistent pattern, probably because they are considerably more reactive than alkyl-branched analogues due to the inductive effect of oxygen. Relatively early more flexible TS such as **134** are possible, and the Z-trisubstituted alkenes **135** predominate.

B. Reactions of $Ph_3P{=}CHX$

This category includes the α-alkylthio, α-alkoxy, and α-haloylides (Table 21), and also the allylic and benzylic ylides (Tables 14 and 15), most of which are reactive at −78°C and marginally selective. The Z:E ratio tends to increase with increased reactivity of either reactant (earlier TS). When the substituent X is an sp^2-hybridized alkenyl or aryl group, the 1,2-interactions in **137** can be minimized in conformations where the plane of the sp^2 carbon is parallel to the carbonyl plane. The energy difference between **136** and **137** becomes smaller, and oxaphosphetane formation is nonselective. When the spatial requirements of X increase, selectivity tends to increase as well. Thus, α-alkylthio ylides are more Z selective than their oxygen counterparts, and $Ph_3P{=}CHI$ is the most highly cis-selective member of the halogen series (Table 21, entries 40–57). Electronegativity may also play a role by decreasing reactivity when X is F or Cl (more productlike TS). These results follow a self-consistent pattern, but the interpretation must be viewed with caution because very few systematic comparisons have been reported.

C. Ylides with Unsymmetrically Substituted Phosphorus

Transition state models become increasingly complicated for reactions of several ylides that contain two different ligands at phosphorus (Table 22, entries 3–5). There will be new ways to reduce 1,3-interactions, depending on which group occupies the position corresponding to L* in TS such as **139**. There is a qualitative trend toward E selectivity when one or more of the P-phenyl groups of $Ph_3P{=}CHCH_3$ is replaced by ethyl (Table 22, entry 4 vs. entries 1, 3; see also Table 13) because **138** has reduced 1,3-interactions compared to **139** with L* = phenyl. However, the trans-selective TS **138** is no longer favored when R′ is a tertiary alkyl group because of the resulting

increase in 1,3-interactions, and Wittig reactions of $Et_3P{=}CHCH_3$ or $EtPh_2P{=}CHCH_3$ with tertiary aldehydes become modestly cis selective under conditions of kinetic control.

Only a few results are available in the case of ylides $L_3P{=}CHX$ that are structurally biased toward planar four-center geometries (similar to **126** or **138**; DBP or RPh_2P phosphorus environments). Allylic or benzylic ylides of both types show the expected trend for trans-disubstituted oxaphosphetanes and the corresponding (*E*)-alkenes, as do allylic ylides of the $Bu_3P{=}CHX$ family. To date, no ylides with α-heteroatom substituents have been studied in any of the trans-selective phosphorus environments.

There are several examples of ligand-induced selectivity trends where no simple argument is adequate. For example, replacement of one of the phenyl groups of $Ph_3P{=}CHCH_3$ by a cyclohexyl substituent (Table 22, entry 5) results in an ylide with decreased selectivity, contrary to what would be expected from the relative bulk of cyclohexyl versus phenyl groups. The shapes of phosphorus substituents are at least as important as steric bulk. Furthermore, the balance between 1,2- and 1,3-interactions depends on the conformational properties of all of the nearby substituents because the steric effects are highly interactive in the congested environment. Ultimately, the key ligand L* controls the 1,3-interactions, but neither the identity nor the orientation of L* can be assigned with confidence in most of the examples where phosphorus contains two different ligands.

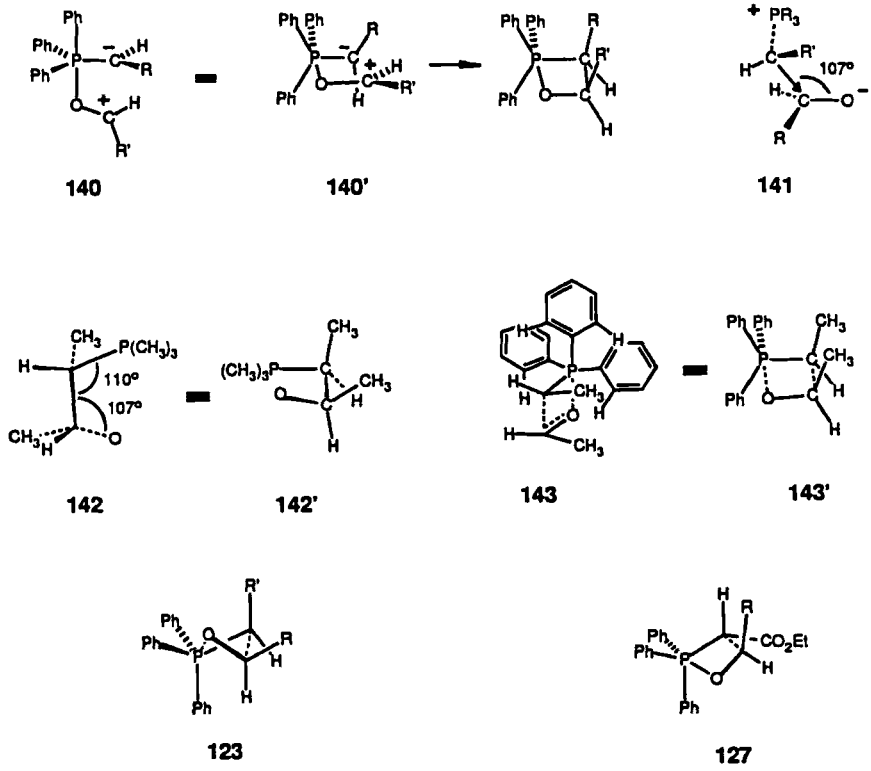
D. Lithium Ion Effects

The stereoselectivity trends have been discussed earlier (Scheme 11), and only the conclusions will be repeated here. In general, the lithium effect reduces the selectivity of all classes of ylides, including those that are inherently trans selective. In the case of aliphatic aldehydes, the phenomenon is attributed to reaction via a competing pathway that involves Lewis acid catalysis at carbonyl oxygen. The catalyzed pathway is not very sensitive to phosphorus ligands or other substituent effects, but it shows the expected strong dependence on lithium ion concentration. Catalysis is especially important for aromatic aldehyde reactions because lithium ion also can catalyze the equilibration of the intermediate oxaphosphetanes via betaine lithium halide adducts. This process accounts for the variable selectivity that has been reported in some of the earlier literature. Since substrate enolization is also enhanced by the presence of lithium ion, many of the complications that arise in preparative Wittig reactions can be avoided by using lithium-free techniques. The NaHMDS or KHMDS/THF conditions can be recommended for preparative as well as mechanistic work. The lithium-catalyzed pathway resembles the original betaine mechanism (1), with the important difference

that the eventual conversion from reactants to the oxaphosphetane is exothermic, not endothermic.

XXIII. ALTERNATIVE TRANSITION STATE MODELS

The literature contains many other attempts to explain the cis selectivity of $Ph_3P{=}CHR$ reactions, several of which are briefly summarized in Scheme 19. Schneider's model **140** is interesting in the historical context because it shows that cis selectivity can be explained via the Bergelson–Shemyakin diradicaloid **95/96** (5) if the interaction between the aldehyde and the ylide occurs in a geometry where the aldehyde plane is perpendicular to the ylide plane (234). If there is a significant activation barrier for ring closure, then **140** would be converted into the cis-disubstituted oxaphosphetane via the least hindered configuration-determining transition state. On the other hand, if the barrier



Scheme 19

to ring closure is small as would be expected for the exothermic process, then ΔG^* for the competing ring closure pathways may be too small to allow the necessary $\Delta\Delta G^*$ of ca. 2 kcal/mol in favor of the cis pathway. Although P—O bonded diradicaloids are inconsistent with the experiments of Scheme 14 and some of the kinetic isotope data, Schneider's model is a logical predecessor of Schemes 17 and 18 because of its use of nonparallel C=O and P=C subunits to explain stereochemistry. In the context of Scheme 17, structure **140** illustrates another way to use bond angle distortion to avoid 1,2- and 1,3-interactions. Like most of the early rationales, Schneider's model implicitly assumes that cis selectivity is a fundamental property of phosphorus ylides.

Bestmann (59, 220) proposed that cis selectivity would result from approach of the ylide along the sp^3 bond angle trajectory at the C=O group, illustrated in the original publications by the drawing **141**. Deviations from cis selectivity were attributed to oxaphosphetane equilibration via pseudorotation to **73** and reversible heterolysis of the P—C_3 bond to a zwitterion **74** (Scheme 10). Specific TS models were not illustrated, with the exception of a cis-selective structure **142** derived from MNDO calculations that indicated a stability advantage for the trans-selective TS (not illustrated). Since an advantage for **142** was expected according to the trajectory argument, Bestmann drew no final conclusions regarding the origins of cis-selectivity. The closest known experimental analogy to the hypothetical TS model **142** is the reaction of $Et_3P{=}CHCH_3$ with unbranched aldehydes, a process that is modestly trans selective (see Table 13). However, the result depends on the aldehyde substituent R′, and cis selectivity predominates with a tertiary aldehyde under kinetically controlled conditions (Table 22, entry 6; see also Table 13).

Another TS model was proposed by Schlosser and Schaub (66) as illustrated by structure **143**. This model explicitly recognizes the importance of phosphorus substituents, but it invokes a dominant *P*-phenyl "propeller" effect that requires kinetic cis selectivity for all $Ph_3P{=}CHR$ as well as $Ph_3P{=}CHX$ reactions and kinetic trans selectivity for reactions of ylides that do not contain the "propeller". The formation of trans alkenes from ylides $Ph_3P{=}CHX$ would have to be due to equilibration. None of these generalizations is consistent with Table 22 or with the control experiments that demonstrate kinetically controlled decomposition of a variety of oxaphosphetanes.

In Schemes 17 and 18, the lithium-free Wittig reactions of Table 22 are interpreted on the basis of a kinetically controlled four-center mechanism. No single TS geometry can be used for all of these diverse reactions, but qualitative models for several of the limiting situations have been suggested. The TS models correlate a large amount of data, but they are intuitive models that are not precise in terms of geometry. Indeed, some of the models have been drawn to exaggerate subtle structural differences for purposes of illustration. Interpretation of TS models can be difficult in cases where there is no

simple way to estimate the steric bulk of the substituents. It is well known that steric comparisons based on *A* values are not reliable in systems other than cyclohexanes because the magnitude of lateral interactions depends on the environment (235). The selectivity of ylides $Ph_3P{=}CHX$ correlates well within sets of related substituents X that have similar shapes and electronic structure (Table 21: MeS > MeO in the ability to promote cis selectivity; similarly, I > Br > Cl). On the other hand, comparisons between groups that differ in symmetry, hybridization, or polarity are risky. Indicators of steric bulk that measure the spatial requirements of the interacting rotamers (phosphorus ligands as well as X) may be better suited for this purpose than conventional *A* values (235).

When the various TS models are drawn using a perspective that emphasizes the similarities (structures **140′**, **142′**, **123′**, **143′**, and **127**), it becomes clear that the geometric differences are often small compared to the differences in terminology. Our "intuitive resolution" may not be sufficient to distinguish geometric options in borderline cases, and there may be other variants that are theoretically reasonable. However, to have predictive value, any distinction between four- and two-center mechanisms must be based on differences in geometry in the stereochemistry-determining TS. Transition state geometry is the only factor that controls stereochemistry in a kinetically controlled reaction. The path taken by the reactants to the competing TS cannot influence relative TS stability or affect the stereochemical outcome. For that reason, it will not be critical to know whether the asymmetric cycloaddition terminology (four-center process) is precise in the theoretical sense, as long as the TS geometry includes all four of the eventual oxaphosphetane atoms within conceivable bonding distance.

It is too early to decide whether semiempirical computations can successfully evaluate TS models such as **117–124** given the current level of precision. This situation is likely to change as the theoretical methods refine their phosphorus parameters and their ability to mimic solvation effects. Table 22 provides many opportunities to test computational TS predictions. Selectivity in the Wittig reaction depends on substituents, not on some fundamental property of phosphorus ylides. Thus, any successful theoretical analysis of the selectivity issue will need to explain the substituent-induced differences in kinetic Z:E ratios.

Several practical problems also remain to be solved in the Wittig reaction. An efficient way to recycle the starting phosphines would be especially useful, but little progress on this problem has been reported. With regard to the reagents, there are several ylide categories that need further development. Desirable goals include inexpensive, E-selective nonstabilized ylides, and stabilized ylides that react with consistently high Z selectivity. Several mechanistic issues also need further study, especially in the area of reaction

kinetics and thermochemistry. No detailed kinetic studies have been reported for the reactive ylides, and no information is available regarding activation entropy and enthalpy contributions to the cis- versus trans-selective TS. Much also remains to be learned about the energy profiles (Fig. 1 or 2) that have often been used in the discussion of Wittig mechanisms. For example, it is still not known whether the conversion from stabilized ylides to oxaphosphetanes is exothermic or endothermic. There also are large gaps in our knowledge of the origin of solvent effects in the ester-stabilized ylide reactions. On the other hand, much has been learned about selectivity trends and about the issue of equilibration. Typical Wittig reactions are under kinetic control, and the remarkable selectivity patterns are largely due to the highly interactive steric effect of substituents near the developing bonds of a congested four-center TS.

ACKNOWLEDGMENT

One of us (E. V.) expresses thanks to a number of colleagues who have contributed to the understanding of mechanistic and theoretical aspects of the Wittig problem over many years. Special thanks are due to F. A. Weinhold, S. F. Nelsen, and H. J. Reich. The authors are also grateful to B. Maryanoff, R. Okazaki, and H. Yamataka for providing copies of several manuscripts prior to publication and to the National Science Foundation for financial support.

REFERENCES

1. Schlosser, M. *Top. Stereochem.* **1970**, *5*, 1.
2. (a) Trippett, S. *Quart. Rev.* **1963**, *17*, 406. (b) Maercker, A. *Org. React.* **1965**, *14*, 270. (c) Trippett, S. *Pure Appl. Chem.* **1964**, *9*, 255. (d) Bergelson, L. D.; Shemyakin, M. M. *Pure Appl. Chem.* **1964**, *9*, 271. (e) Johnson, A. W. *Ylide Chemistry*; Academic Press: New York, **1966**. (f) Reucroft, J.; Sammes, P. G. *Quart. Rev.* **1971**, *25*, 135. (g) Zhdanov, Yu. A.; Alexeev, Yu. E.; Alexeeva, V. G. *Adv. Carbohyd. Chem. Biochem.* **1972**, *27*, 227. (h) Gosney, I; Rowley, A. G. In *Organophosphorus Reagents in Organic Synthesis*, Cadogan, J. I. G., Ed.; Academic Press: New York (1979). (i) Becker, K. B. *Tetrahedron* **1980**, *36*, 1717. (j) Maryanoff, B. E.; Reitz, A. B. *Chem. Rev.* **1989**, *89*, 863. (k) Johnson, A. W.; *Ylides and Imines of Phosphorus*, Wiley; New York, 1993.
3. Wittig, G.; Haag, W. *Chem. Ber.* **1955**, *88*, 1654.
4. (a) House, H. O. ; Rasmusson, G. H. *J. Org. Chem.* **1961**, *26*, 4278. (b) House, H. O.; Jones, V. K.; Frank, G. A. *J. Org. Chem.* **1964**, *29*, 3327.
5. (a) Bergelson, L. D.; Shemyakin, M. M. *Tetrahedron* **1963**, *19*, 149. (b) Bergelson, L. D.; Shemyakin, M. M. *Angew. Chem., Int. Ed. Engl.* **1964**, *3*, 250. (c) Bergelson, L. D.; Barsukov,

L. I.; Shemyakin, M. M. *Tetrahedron* **1967**, *23*, 2709. (d) Bergelson, L. D.; Vaver, V. A.; Barsukov, L. I. Shemyakin, M. M. *Tetrahedron Lett.* **1964**, 2669.

6. Vedejs, E.; Peterson, M. J. "A History of Mechanistic Ideas in the Wittig Reaction". in *Advances in Carbanion Chemistry*, Vol. 2; Snieckus, V., Ed.; Jai pr, Greenwich CN 1994.
7. Staudinger, H.; Meyer, J. *Helv. Chem. Acta* **1919**, *2*, 635.
8. Wittig, G.; Geissler, G. *Liebigs Ann. Chem.* **1953**, *580*, 44.
9. Fliszar, S. F.; Hudson, R. F.; Salvadori, G. *Helv. Chim. Acta* **1963**, *46*, 1580.
10. Wittig, G.; Schöllkopf, U. *Chem. Ber.* **1954**, *87*, 1318.
11. (a) Bohlman, F.; Inhoffen, E.; Herbst, P. *Chem. Ber.* **1957**, *90*, 1661. (b) Pommer, H. *Angew. Chem.* **1960**, *72*, 817. (c) Wailes, P. C. *Chem. Ind.* **1958**, 1086. (d) Butenandt, A.; Hecker, E.; Hopp, M.; Koch, W. *Liebigs Ann. Chem.* **1962**, *658*, 42. (e) Hauser, C. F.; Brooks, T. W.; Miles. M. L.; Raymond, M. A.; Butler, G. B. *J. Org. Chem.* **1963**, *28*, 372.
12. (a) Speziale, A. J.; Bissing, D. E. *J. Am. Chem. Soc.* **1963**, *85*, 3878. (b) Bissing, D. E.; Speziale, A. J. *J. Am. Chem. Soc.* **1965**, *87*, 2683.
13. Jones, M. E.; Trippett, S. *J. Chem. Soc. (C)* **1966**, 1090.
14. Schlosser, M.; Christmann, K. F. *Justus Liebigs Ann. Chem.* **1967**, *708*, 1.
15. (a) Rüchardt, C.; Panse, P.; Eichler, S. *Chem. Ber.* **1967**, *100*, 1144. (b) Giese, B.; Schoch, J.; Rüchardt, C. *Chem. Ber.* **1978**, *111*, 1395.
16. (a) Aksnes, G.; Khalil, F. Y. *Phosphorus* **1972**, *2*, 105. (b) Aksnes, G.; Khalil, F. Y. *Phosphorus* **1973**, *3*, 37, 79, 109; see also Maccarone, E.; Perrini, G. *Gazz. Chim. Ital.* **1982**, *112*, 447 for a more recent discussion.
17. Ramirez, F.; Smith, C. P.; Pilot J. F. *J. Am. Chem. Soc.* **1968**, *90*, 6722, 6726.
18. (a) Vedejs, E.; Snoble, K. A. J. *J. Am. Chem. Soc.* **1973**, *95*, 5778. (b) Vedejs, E.; Meier, G. P.; Snoble, K. A. J. *J. Am. Chem. Soc.* **1981**, *103*, 2823.
19. (a) Vedejs, E.; Snoble, K. A. J.; Fuchs, P. L. *J. Org. Chem.* **1973**, *38*, 1178. (b) Vedejs, E.; Fuchs, P. L. *J. Am. Chem. Soc.* **1973**, *95*, 822.
20. Vedejs, E.; Marth, C. F.; Ruggeri, R. *J. Am. Chem. Soc.* **1988**, *110*, 3940.
21. (a) Vedejs, E.; Marth, C. F. *J. Am. Chem. Soc.* **1989**, *111*, 1519. (b) Vedejs, E.; Marth, C. F. *J. Am. Chem. Soc.* **1990**, *112*, 3905. (c) Vedejs, E.; Fleck, T. J. *J. Am. Chem. Soc.* **1989**, *111*, 5861.
22. (a) Maryanoff, B. E.; Reitz, A. B.; Mutter, M. S.; Inners, R. R.; Almond, H. R., Jr.; Whittle, R. R.; Olofson, R. A. *J. Am. Chem. Soc.* **1986**, *108*, 7664. For the preliminary accounts, see Reitz, A. B.; Mutter, M. S.; Maryanoff, B. F. *J. Am. Chem. Soc.* **1984**, *106*, 1873; Maryanoff, B. E.; Reitz, A. B.; Mutter, M. S.; Inners, R. R.; Almond, H. R., Jr. *J. Am. Chem. Soc.* **1985**, *107*, 1068. (b) A detailed overview of the findings of Maryanoff is provided in Ref. 2j. (c) Maryanoff, B. E.; Reitz, A. B.; Graden, D. W.; Almond, H. R., Jr. *Tetrahedron Lett.* **1989**, *30*, 1361.
23. (a) Maryanoff, B. F.; Reitz, A. B. *Tetrahedron Lett.* **1985**, *26*, 4587. (b) Maryanoff, B. E.; Reitz, A. B.; Duhl-Emswiler, B. A. *J. Am. Chem. Soc.* **1985**, *107*, 217. Preliminary accounts: Maryanoff, B. E.; Duhl-Emswiler, B. A. *Tetrahedron Lett.*, **1981**, *22*, 4185; Maryanoff, B. E.; Reitz, A. B.; Duhl-Emswiler, B. A. *Tetrahedron Lett.*, **1983**, *24*, 2477. (c) Reitz, A. B.; Nortey, S. O.; Jordan, A. D.; Mutter, M. S.; Maryanoff, B. E. *J. Org. Chem.* **1986**, *51*, 3302.
24. (a) Bordwell, F. G. and coworkers unpublished results. The authors thank Professor Bordwell for permission to cite these results. (b) Vincent, M.; Schaefer, H.; Schier, A.; Schmidbaur, H. *J. Am. Chem. Soc.* **1983**, *105*, 3806 and references therein.
25. (a) Ostoja Starzewski, K. A.; Bock, H. *J. Am. Chem. Soc.* **1976**, *98*, 8486. (b) Perry, W. B.; Schaaf, T. F.; Jolly, W. L. *J. Am. Chem. Soc.* **1975**, *97*, 4899.

26. (a) Albright, T.; Gordon, M.; Freeman, W.; Schweizer, E. *J. Am. Chem. Soc.* **1976**, *98*, 6249. (b) Gray, G. *J. Am. Chem. Soc.* **1973**, *95*, 7736. (c) Albright, T.; Schwiezer, E. *J. Org. Chem.* **1976**, *41*, 1168. (d) Yamamoto, Y.; Schmidbaur, H. *J. Organomet. Chem.* **1975**, *97*, 479. (e) Ostoja Starzewski, K. A.; Tom Dieck, H. *Phosphorus* **1976**, *6*, 177. (f) Schmidbaur, H.; Buchner, W.; Scheutzow, D. *Chem. Ber.* **1973**, *106*, 1251. (g) Issleib, K.; Lischewski, M.; Zschunke, A. *Org. Magn. Resonance* **1973**, *5*, 401. (h) Schlosser, M.; Jenny, B.; Schaub, B. *Heteroatom Chem.* **1990**, *1*, 151. (i) Albarella, J. P.; Katz, T. J. *J. Org. Chem.* **1978**, *43*, 4338. (j) Bestmann, H. J.; Snyder, J. P. *J. Am. Chem. Soc.* **1967**, *89*, 3936. (k) Randall, F. J.; Johnson, A. W. *Tetrahedron Lett.* **1968**, *18*, 2841. (l) Crouse, D. M.; Wehman, A. T.; Schweizer, E. E. *J. Chem. Soc., Chem. Commun.* **1968**, 866. (m) Snyder, J. P. *Tetrahedron Lett.* **1971**, *12*, 215.

27. (a) Mckeever, L. D.; Waack, R.; Doran, M. A.; Baker, E. B. *J. Am. Chem. Soc.* **1969**, *91*, 1057. (b) O'Brien, D. H.; Hart, A. J.; Russell, C. R. *J. Am. Chem. Soc.* **1975**, *97*, 4410.

28. (a) Schlosser, M.; Liu, Z. *Tetrahedron Lett.* **1990**, *31*, 5753. (b) See Ref. 26h.

29. Hoffmann, R.; Boyd, D. B., Goldberg, S. Z. *J. Am. Chem. Soc.* **1970**, *92*, 3929. Rank, A.; Allen, L. C.; Mislow, K. *Angew. Chem., Int. Ed. Engl.* **1970**, *9*, 400. Bernardi, F.; Csizmadia, I. G.; Mangini, A.; Schlegel, H. B.; Wangbo, M. H.; Wolfe, *S. J. Am. Chem. Soc.* **1975**, *97*, 2209. Lehn, J. M.; Wipff, G. *J. Am. Chem. Soc.* **1976**, *98*, 7498. Lischka, H. *J. Am. Chem. Soc.* **1977**, *99*, 353, 1977. Trinquier, G.; Malrieu, J. P. *J. Am. Chem. Soc.* **1979**, *101*, 7169. Strich, A. *Nouv. J. Chim.* **1979**, *3*, 105. Eades, R. A.; Gassman, P. G.; Dixon, D. A. *J. Am. Chem. Soc.* **1981**, *103*, 1066. Vincent, M. A.; Schaefer, H. F. I.; Schier, A.; Schmidbaur, H. *J. Am. Chem. Soc.* **1983**, *105*, 3806. Dixon, D. A.; Smart, B. E. *J. Am. Chem. Soc.* **1986**, *108*, 7172. Streitwieser, A.; Rajca, A.; McDowell, R. S.; Glaser, R. *J. Am. Chem. Soc.* **1987**, 109, 4184. Yates, B. F.; Bouma, W. J.; Radom, L. *J. Am. Chem. Soc.* **1987**, *109*, 2250. Nguyen, M. T.; Hegarty, A. F. *J. Chem. Soc. Perkin Trans. 2* **1987**, 47. Francl, M. M.; Pellow, R. C.; Allen, L. C. *J. Am. Chem. Soc.* **1988**, *110*, 3723. Bachrach, S. M. *J. Org. Chem.* **1992**, *57*, 4362.

30. (a) Schmidbaur, H.; Jeong, J.; Schier, A.; Graf, W.; Wilkinson, D.; Müller, G.; Krüger, K. *New J. Chem.* **1989**, *13*, 341. (b) Schmidbaur, H.; Schier, A. S.; Frazao, C. M. F.; Müller, G. *J. Am. Chem. Soc.* **1986**, *108*, 976. (c) Schmidbaur, H.; Schier, A.; Neugebauer, D. *Chem. Ber.* **1983**, *116*, 2173. (d) An earlier X-ray determination suggested a planar ylide carbon: Bart, J. C. J. *J. Chem. Soc. B* **1969**, 350. (e) Other X-ray studies: Mak, T. C. W.; Trotter, J. *Acta Crystallogr.* **1965**, *18*, 81. Stephens, F. S. *J. Chem. Soc.* **1965**, 5640, 5658. Speziale, A. J.; Ratts, K. W. *J. Am. Chem. Soc.* **1965**, *87*, 5603. Ammon, H. L.; Wheeler, G. L.; Watts, P. H., Jr. *J. Am. Chem. Soc.* **1973**, *95*, 6158. Lingner, U.; Burzlaff, H. *Acta Crystallogr.* **1974**, *30B*, 1715. Cameron, A. F.; Dincanson, F. D.; Freer, A.A.; Armstrong, V. W.; Ramage, R. *J. Chem. Soc. Perkin Trans. 2* **1975**, 1030. Trablesi, H.; Rouvier, E.; Cambon, A.; Jaulmes, S. *J. Fluor. Chem.* **1988**, *39*, 1.

31. Averaged values: Allen, F.; Kennard, O.; Watson, D.; Brammer, L.; Orpen, A.; Taylor, R. *J. Chem. Soc., Perkin Trans. 2* **1987**, S1.

32. Schmidbaur, H.; Schier, A.; Milewski-Mahrla, B.; Schubert, U. *Chem. Ber.* **1982**, *115*, 722.

33. Speziale, A. J.; Ratts, K. W. *J. Am. Chem. Soc.* **1965**, *87*, 5603.

34. (a) Ul- Haque, M.; Caughlan, C. N.; Ramirez, F.; Pilot, J. F.; Smith, C. P. *J. Am. Chem. Soc.* **1971**, *93*, 5329. Other solid-state evidence: (b) Aly, H. A. E.; Barlow, J. H.; Russell, D. R.; Smith, D. J. H.; Swindles, M.; Trippett, S. *J. Chem. Soc., Chem. Commun.* **1976**, 449. (c) Bestmann, H. J.; Roth, K.; Wilhelm, E.; Bohme, R.; Burzlaff, H. *Angew. Chem., Int. Ed. Engl.* **1979**, *18*, 876. (d) Birum, G. H.; Matthews, C. N. *J. Chem. Soc. Chem. Commun.* **1967**, 137. (e) Kawashima, T.; Kato, K.; Okazaki, R. *J. Am. Chem. Soc.* **1993**, *114*, 4008. (f) Kawashima, T.; Kato, K.; Okazaki, R. *Angew. Chem., Int. Ed. Engl.* **1993**, *32*, 869. The authors thank Prof. Kawashima for a preprint of this paper.

35. (a) Westheimer, F. H. *Acc. Chem. Res.* **1968**, *1*, 70. (b) Ramirez, F. Acc. Chem. Res. **1968**, *1*, 168. (c) Muetterties, E. L.; Mahler, W.; Schmutzler, R. *Inorg. Chem.* **1968**, *2*, 613.

36. (a) Gibson, J. A.; Röschenthaler, G. V.; Wray, V. *J. Chem. Soc. Dalton Trans.* **1977**, 1492. (b) Gibson, J. A.; Röschenthaler, G. *J. Naturforsch. B* **1977**, *32*, 599. (c) Allwörden, U.; Tseggai, I.; Röschenthaler, G. V. *Phos. Sulfur* **1984**, *21*, 177.

37. (a) Schmidbaur, H.; Stühler, H.; Buchner, W. *Chem. Ber.* **1973**, *106*, 1243. (b) Schmidbaur, H.; Buchner, W.; Köhler, F. H. *J. Am. Chem. Soc.* **1974**, *96*, 6208. (c) Schmidbaur, H.; Holl, P. *Chem. Ber.* **1976**, *109*, 3151. (d) Schmidbaur, H.; Holl, P. *Chem. Ber.* **1979**, *112*, 501. (e) Schmidbaur, H.; Holl, P. *Naturforsch B* **1978**, *33*, 489. (f) Schmidbaur, H.; Holl, P. *Naturforsch B* **1978**, *33*, 572.

38. Gorenstein, D. G. *Progr. NMR Spectrosc.* **1983**, *16*, 1.

39. (a) Marth, C. F. Ph.D. dissertation, University of Wisconsin, 1989. (b) Vedejs, E.; Loža, E. unpublished results.

40. Fleck, T. J. Ph.D. dissertation, University of Wisconsin, 1990; Vedejs, E.; Fleck, T. J., unpublished results.

41. Vedejs, E.; Marth, C. F. *Tetrahedron Lett.* **1987**, *28*, 3445.

42. (a) Peterson, M. J. Ph.D. dissertation, University of Wisconsin, 1992. Vedejs, E.; Peterson, M. J., unpublished results. (b) Vedejs, E.; Peterson, M. J. *J. Org. Chem.* **1993**, *58*, 1985, (c) Vedejs, E.; Cabaj, J.; Peterson, M. J. *J. Org. Chem.* **1993**, *58*, 6509.

43. Ward, W. J., Jr.; McEwen, W. E. *J. Org. Chem.* **1990**, *55*, 493.

44. Garcia Martinez, A.; Oliver Ruiz, M.; Contelles, J. L. M. *Synthesis* **1986**, 125.

45. Ikeda, Y.; Ukai, J.; Ikeda, N.; Yamamoto, H. *Tetrahedron* **1987**, *43*, 723.

46. (a) Schmidt, R.; Zimmermann, P. *Tetrahedron Lett.* **1986**, *27*, 481. (b) Chida, N.; Tobe, T.; Ogawa, S. *Tetrahedron Lett.* **1991**, *32*, 1063.

47. (a) Vedejs, E.; Huang, W. F. *J. Org. Chem.* **1984**, *49*, 210. (b) Tamura, R.; Saegusa, K.; Kakihana, M.; Oda, D. *J. Org. Chem.* **1988**, *53*, 2723.

48. Nicotra, F.; Toma, L. *Gazz Chim. Ital.* **1980**, *110*, 579.

49. Pyne, S. G.; Hensel, M. J.; Fuchs, P. L. *J. Am. Chem. Soc.* **1982**, *104*, 5719.

50. Masaki, Y.; Hashimoto, K.; Serizawa, Y.; Kaji, K. *Bull. Chem. Soc. Jpn.* **1984**, *57*, 3476.

51. Belletire, J. L.; Namie, M. W. *Sym. Comm.* **1983**, *13*, 87.

52. Schlosser, M.; Christmann, K. F. *Angew. Chem.* **1966**, *5*, 126.

53. Schlosser, M.; Christmann, K. F.; Piskala, A. Chem. Ber. **1970**, *103*, 2814.

54. (a) Corey, E. J.; Yamamoto, H. *J. Am. Chem. Soc.* **1970**, *92*, 226, 352. (b) Corey, E. J.; Yamamoto, H. *J. Am. Chem. Soc.* **1970**, *92*, 6636. (c) *id., ibid.*, **1970**, *92*, 6637.

55. Corey, E. J.; Ulrich, P.; Venkateswarlu, A. *Tetrahedron Lett.* **1977**, 3231.

56. Vedejs, E.; Meier, G. P. *Angew. Chem., Int. Ed.* **1983**, *22*, 56.

57. Schlosser, M.; Tuong, H. B.; Schaub, B. *Tetrahedron Lett.* **1985**, *26*, 311. Schaub, B.; Blaser, G.; Schlosser, M. *Tetrahedron Lett.* **1985**, *26*, 307.

58. Anderson, R. J.; Henrick, C. A. *J. Am. Chem. Soc.* **1975**, *97*, 4327.

59. Bestmann, H. J. *Pure & Appl. Chem.* **1979**, *51*, 515.

60. (a) Bestmann, H. J.; Stransky, W. *Synthesis* **1974**, 798. (b) Grandjean, D.; Pale, P.; Chuche, J. *Tetrahedron* **1991**, *47*, 1215.

61. Schaub, B.; Jeganathan, S.; Schlosser, M. *Chimia* **1986**, *40*, 246.

62. Schlosser, M.; Schaub, B.; de Oliveira-Neto, J.; Jeganathan, S. *Chimia* **1986**, *40*, 244.

63. Schlosser, M.; Schaub, B. *Chimia* **1982**, *36*, 396.
64. Boden, R. M. *Synthesis* **1975**, 784.
65. Jeganathan, S.; Tsukamoto, M.; Schlosser, M. *Synthesis* **1990**, 109.
66. Schlosser, M.; Schaub, B. *J. Am. Chem. Soc.* **1982**, *104*, 5821.
67. Coates, R.; Johnson, M. *J. Org. Chem.* **1980**, *45*, 2685.
68. Corey, E. J.; Kwiatkowski, G. *J. Am. Chem. Soc.* **1966**, *88*, 5653.
69. Salomon, R.; El Sanadi, N. *J. Am. Chem. Soc.* **1975**, *97*, 6214.
70. Hentschel, S., University of Wisconsin-Madison, unpublished results.
71. Corey, E. J.; Hamanaka, E. *J. Am. Chem. Soc.* **1967**, *89*, 2758.
72. Gannett, P. M.; Nagel, D. L.; Reilly, P. J.; Lawson, T.; Sharpe, J.; Toth, B. *J. Org. Chem.* **1988**, *53*, 1064.
73. Schweizer, E.; Thompson, J.; Ulrich, T. *J. Org. Chem.* **1968**, *33*, 3082.
74. Carey, S. C.; Aratani, M.; Kishi, Y. *Tetrahedron Lett.* **1985**, *26*, 5887.
75. G. Heublein, private communication, cited in Ref. 1, p. 16.
76. Seyferth, D.; Singh, G. *J. Am. Chem. Soc.* **1965**, *87*, 4156.
77. Castellino, A. J.; Bruice, T. C. *J. Am. Chem. Soc.* **1988**, *110*, 7512. For the optimized reaction, see He, G.-X.; Bruice, T. C. *J. Am. Chem. Soc.* **1991**, *113*, 2747.
78. (a) Vedejs, E.; Ruggeri, R. unpublished results. (b) Meyers, A. I.; Lawson, J. P.; Carver, D. R. *J. Org. Chem.* **1981**, *46*, 3119.
79. Bernstein, P. R.; Snyder, D. W.; Adams, E. J.; Krell, R. D.; Vacek, E. P.; Willard, A. K. *Med. Chem.* **1986**, *29*, 2477. (b) Bernstein, P. R. cited in Maryanoff, B. E.; Reitz, A. B. *Chem. Rev.* **1989**, *89*, 863: Ref. 175b, p. 889.
80. Vedejs, E.; Marth, C. F. *J. Am. Chem. Soc.* **1988**, *110*, 3948.
81. Wheeler, O. H.; Battle de Pabon, H. N. *J. Org. Chem.* **1965**, *30*, 1473.
82. (a) Drehfahl, G.; Lorenz, D.; Schnitt, G. *J. Prakt. Chem.* **1964**, *23*, 143. (b) Allen, D. W. *J. Chem. Res. Synop.* **1980**, 384. (c) McKenna, E. G. *Tetrahedron Lett.* **1988**, *29*, 485. (d) Yamataka, H.; Nagareda, K.; Ando, K.; Hanafusa, T. *J. Org. Chem.* **1992**, *57*, 2865. (e) Vedejs, E.; Loža, E. unpublished results.
83. (a) Märkl, G.; Merz, A. *Synthesis* **1973**, 295. (b) Underiner, T. L.; Goering, H. *J. Org. Chem.* **1991**, *56*, 2563.
84. Johnson, A. W.; Kyllingstad, V. L. *J. Org. Chem.* **1966**, *31*, 334.
85. Schlosser, M.; Tsukamoto, M. *Synlett* **1990**, 605.
86. Bandmann, H.; Bartik, T.; Bauckloh, S.; Behler, A.; Brille, F.; Heimbach, P.; Louven, J-W.; Ndalut, P.; Preis, H.-G.; Zeppenfeld, E. *Z. Chem.* **1990**, 30, 193.
87. (a) McEwen, W. E.; Kumli, K. F.; Blade-font, A.; Zanger, M.; VanderWerf, C.A. *J. Am. Chem. Soc.* **1964**, *86*, 2378. (b) Trippett, S.; Smith, D. J. H. *J. Chem. Soc., Chem. Commun.* **1972**, 191.
88. Bestmann, H. J.; Kratzer, O. *Chem. Ber.* **1962**, *95*, 1894.
89. Schlosser, M.; Christmann, K. F.; Müller, G., unpublished results cited in Ref. 1.
90. Vedejs, E.; Fuchs, P. L.; Bershas, J. P. *J. Org. Chem.* **1973**, *38*, 3626. This paper contains an incorrect 1:3 Z:E ratio for Table 15, entry 3. The correct value is 1.3:1 Z:E.
91. Corey, E. J.; Desai, M. C. *Tetrahedron Lett.* **1985**, *26*, 5747. Yamamoto, H.; Ikeda, Y.; Ukai, J.; Ikeda, N. *Tetrahedron* **1987**, *43*, 723.
92. Bershas, J. P. Ph.D. dissertation, University of Wisconsin, 1975.
93. Fuchs, P. L. Ph.D. dissertation, University of Wisconsin, 1971.

94. (a) Henrick, C.A. *Tetrahedron* **1977**, *33*, 1845. (b) Goto, G.; Shima, T.; Masuya, H.; Masuoka, Y.; Hiraga, K. *Chem. Lett.* **1975**, 103.

95. Corey, E. J.; Magriotis, P. A. *J. Am. Chem. Soc.* **1987**, *109*, 287.

96. Vedejs, E.; Ahmad, S. *Tetrahedron Lett.* **1988**, *29*, 2291.

97. Huang, W.; Zhu, J.; Xiao, W.; Deng, Y. *Phosphorus Sulfur Silicon and the Related Elements*, **1989**, *46*, 99.

98. Bissing, D. E. *J. Org. Chem.* **1965**, 30, 1296.

99. (a) Vedejs, E.; Donde, Y.; Peterson, M. J. unpublished results. (b) Vedejs, E.; Khumbat, B., unpublished results.

100. (a) Allen, D. W.; Ward, H. *Z. Naturforsch.* **1980**, *35B*, 754. (b) Buchanan, J. G.; Edgar, A. R.; Power, M. J.; Theaker, P. D. *Carbohydr. Res.* **1974**, *38*, C22.

101. Keck, G. E.; Boden, E. P.; Mabury, S. A. *J. Org. Chem.* **1985**, *50*, 709. (b) Keck, G. E.; Boden, E. P.; Wiley, M. R. *J. Org. Chem.* **1989**, *54*, 896.

102. Bestmann, H. J.; Vostrowski, O.; Paulus, H.; Billmann, W.; Stransky, W. *Tetrahedron Lett.* **1977**, *18*, 121.

103. Roush, W. R.; Straub, J. A.; Brown, R. J. *J. Org. Chem.* **1987**, *52*, 5127.

104. Heathcock, C. H.; Kiyooka, S.; Blumenkopf, T. A. *J. Org. Chem.* **1984**, *49*, 4214.

105. Wilson, I. F.; Tebby, J. C. *J. Chem. Soc., Perkin Trans. 1* **1972**, 2713.

106. Ho, T. L. *Syn. Commun.* **1981**, *11*, 605.

107. (a) Honda, M.; Katsuki, T.; Yamaguchi, M. *Tetrahedron Lett.* **1984**, *25*, 3857. (b) Marshall, J. A.; DeHoff, B. S.; Cleary, D. G. *J. Org. Chem.* **1986**, *51*, 1735.

108. Nagaoka, H.; Kishi, Y. *Tetrahedron* **1981**, *37*, 3873; footnote 7 and table on p. 3888.

109. Sotter, P. L.; Hill, K. A. *Tetrahedron Lett.* **1975**, *16*, 1679.

110. Ireland, R. E.; Norbeck, D. W. *J. Org. Chem.* **1985**, *50*, 2198.

111. (a) Gossauer, A.; Suhl, K. *Helv. Chim. Acta* **1976**, *59*, 1698. (b) Garner, P.; Park, J. M.; Rotello, V. *Tetrahedron Lett.* **1985**, *26*, 3299. (c) Marshall, J. A.; Grote, J.; Shearer, B. *J. Org. Chem.* **1986**, *51*, 1633.

112. Valverde, S.; Martin-Lomas, M.; Herradon, B.; Garcia-Ochoa, S. *Tetrahedron* **1987**, *43*, 1895.

113. (a) Bernardi, A.; Cardani, S.; Scolastico, C.; Villa, R. *Tetrahedron* **1988**, *44*, 491. (b) Harrison, D. M.; Quinn, P. *Tetrahedron Lett.* **1983**, *24*, 831. (c) Still, I. W. J.; Drewery, M. J. *J. Org. Chem.* **1989**, *54*, 290.

114. (a) Adams, J.; Frenette, R.; Belley, M.; Chibante, F.; Springer, J. P. *J. Am. Chem. Soc.* **1987**, *109*, 5432. (b) Srikrishna, A.; Krishnan, K. *J. Org. Chem.* **1989**, *54*, 3981.

115. Katsuki, T.; Lee, A. W. M.; Ma, P.; Martin, V. S.; Masamune, S.; Sharpless, K. B.; Tuddenham, D.; Walker, F. J. *J. Org. Chem.* **1982**, *47*, 1373.

116. (a) Minami, N.; Ko, S. S.; Kishi, Y. *J. Am. Chem. Soc.* **1982**, *104*, 1109; footnote 10. (b) Matsunaga, H.; Sakamaki, T.; Nagaoka, H.; Yamada, Y. *Tetrahedron Lett.* **1983**, *24*, 3009. (c)Mulzer, J.; Kappert, M. *Angew. Chem., Int. Ed. Engl.* **1983**, *22*, 63; Angew. Chem. Suppl. **1983**, 23. Häfele, B.; Jäger, V. *Liebigs Ann. Chem.* **1987**, 85. (d) Hubschwerlen, H. *Synthesis* **1986**, 962.

117. Leonard, J.; Mohialdin, S.; Swain, P. A. *Synth. Commun.* **1989**, *19*, 3529.

118. Leonard, J.; Ryan, G. *Tetrahedron Lett.* **1987**, *28*, 2525.

119. Tabusa, F.; Yamada, T.; Suzuki, K.; Mukaiyama, T. *Chem. Lett.* **1984**, 405.

120. Iida, H.; Yamazaki, N.; Kibayashi, C. *J. Org. Chem.* **1987**, *52*, 3337.

121. Shishido, K.; Takahashi, K.; Oshio, Y.; Fukumoto, K. *Heterocycles* **1988**, *27*, 495.

122. Georges, M.; Tam, T. E.; Fraser-Reid, B. *J. Org. Chem.* **1985**, *50*, 5747.

123. Webb, T. H.; Thomasco, L. M.; Schlachter, S. T.; Gaudino, J. J.; Wilcox, C. S. *Tetrahedron Lett.* **1988**, *29*, 6823.

124. Lopez Herrera, F. J.; Pino Gonzalez, M. S.; Nieto Sampedro, M.; Dominguez Aciego, R. M. *Tetrahedron* **1989**, *45*, 269.

125. (a) Bowden, M. C.; Patel, P.; Pattenden, G. *Tetrahedron Lett.* **1985**, *26*, 4793. Hatakeyama, S.; Matsui, Y.; Suzuki, M.; Sakurai, K.; Takano, S. *Tetrahedron Lett.* **1985**, *26*, 6485. (b) Prakash, K. R. C.; Rao, S. P. *Tetrahedron Lett.* **1991**, *32*, 7473. (c) Tulshian, D.; Doll, R. J.; Stansberry, M. F.; McPhail, A. T. *J. Org. Chem.* **1991**, *56*, 6819.

126. Tronchet, J.; Gentile, B. *Helv. Chim. Acta* **1979**, *62*, 2091.

127. Tronchet, J. M. J.; Baehler, B.; Eder, H.; Le-Hong, N.; Perret, F.; Poncet, J.; Zumwald, J.-B. *Helv. Chim. Acta* **1973**, *56*, 1310.

128. See Ref. 100b for the first report. Other early work using stabilized ylides and aldose derivatives generally encountered cyclization products derived from Michael addition of a hydroxyl group to the enoate. This process obscures the geometry of the initially formed enoates: see Zhdanov, Yu. A.; Alexeev, Yu. E.; Alexeeva, V. G. *Adv. Carbohyd. Chem. Biochem*, **1972**, *27*, 227.

129. Ohrui, H.; Jones, G. H.; Moffatt, J. G.; Maddox, M. L.; Christensen, A. T.; Byram, S. K. *J. Am. Chem. Soc.* **1975**, *97*, 4602.

130. Nicolaou, K. C.; Pavia, M. R.; Seitz, S. P. *Tetrahedron Lett.* **1979**, *20*, 2327.

131. Corey, E. J.; Clark, D. A.; Goto, G.; Marfat, A.; Mioskowski, C.; Samuelsson, B.; Hämmarström, S. *J. Am. Chem. Soc.* **1980**, *102*, 1436.

132. Rokach, J.; Young, R. N.; Kakushima, M.; Lau, C.-K.; Seguin, R.; Frenette, R.; Guindon, Y. *Tetrahedron Lett.* **1981**, *22*, 979.

133. Marriott, D. P.; Bantick, J. R. *Tetrahedron Lett.* **1981**, *22*, 3657.

134. Masoni, C.; Deschenaux, P.-F.; Kallimopoulos, T.; Jacot-Guillarmod, A. *Helv. Chim. Acta* **1989**, *72*, 1284.

135. Corey, E. J.; Goto, G. *Tetrahedron Lett.* **1980**, *21*, 3463.

136. Thomas, E. J.; Whitehead, J. W. F. *J. Chem. Soc., Perkin Trans. 1* **1989**, 507.

137. (a) Evans, D. A.; Sjogren, E.; Bartoli, J.; Dow, R. L. *Tetrahedron Lett.* **1986**, *27*, 4957. (b) Evans, D. A.; Dimare, M. *J. Am. Chem. Soc.* **1986**, *108*, 2476.

138. Mulzer, J.; Autenrieth-Ansorge, L.; Kirstein, H.; Matsuoka, T.; Münch, W. *J. Org. Chem.* **1987**, *52*, 3784.

139. Roush, W. R.; Brown, B.; Drozda, S. *Tetrahedron Lett.* **1988**, *29*, 3541.

140. Takano, S.; Shimazaki, Y.; Ogasawara, K. *Heterocycles* **1989**, *29*, 2101.

141 (a) Bunce, R. A.; Pierce, J. D. *Tetrahedron Lett.* **1986**, *27*, 5583. (b) Boeckman, R. K.; Alessi, T. R. *J. Am Chem. Soc.* **1982**, *104*, 3216. (c) Fitsimmons, B. J.; Fraser-Reid, B. *Tetrahedron* **1984**, *40*, 1279.

142. (a) Nagasaka, T.; Yamamoto, H.; Hayashi, H.; Watanabe, M.; Hamaguchi, F. *Heterocycles* **1989**, *29*, 155. (b) Shue, Y. K.; Carreray, G. M.; TuFano, M. D.; Nadzan, A. M. *J. Org. Chem.* **1991**, *56*, 2107. (c) Finch, N.; Della Vecchia, L.; Fitt, J. J.; Stephani, R.; Vlattas, I. *J. Org. Chem.* **1973**, *38*, 4412. (d) Overman, L. E.; Lesuisse, D.; Hashimoto, M. *J. Am. Chem. Soc.* **1983**, *105*, 5373.

143. Dusza, J. *J. Org. Chem.* **1960**, *25*, 93.

144. (a) Garner, P.; Ramakanth, S. *J. Org. Chem.* **1987**, *52*, 2630. (b) Eguchi, T.; Aoyama, T.; Kakinuma, K. *Tetrahedron Lett.* **1992**, *33*, 5545.
145. Sreekumar, C.; Darst, K.; Still, W. C. *J. Org. Chem.* **1980**, *45*, 4260.
146. Inoue, S.; Honda, K.; Iwase, N.; Sato, K. *Bull. Chem. Soc. Jpn.* **1990**, *63*, 1629.
147. Vedejs, E.; Cabaj, J. unpublished results.
148. Zimmerman, H. E.; Heydinger, J. A. *J. Org. Chem.* **1991**, *56*, 1747.
149. Hornback, J. M.; Barrows, R. D. *J. Org. Chem.* **1982**, *47*, 4285.
150. James, B.; Pattenden, G. *J. Chem. Soc., Perkin Trans. 1* **1976**, 1476.
151. Wovkulich, P.; Uskokovic, M. *J. Org. Chem.* **1982**, *47*, 1600.
152. Koreeda, M.; Patel, P.; Brown, L. *J. Org. Chem.* **1985**, *50*, 5910.
153. Krubiner, A.; Oliveto, E. *J. Org. Chem.* **1966**, *31*, 24.
154. Krubiner, A.; Gottfried, N.; Oliveto, E. *J. Org. Chem.* **1968**, *33*, 1715.
155. Schmuff, N.; Trost, B. *J. Org. Chem.* **1983**, *48*, 1404.
156. Midland, M., Kwon, Y. *Tetrahedron Lett.* **1982**, *23*, 2077.
157. Marino, J.; Abe, H. *J. Am. Chem. Soc.* **1981**, *103*, 2907.
158. Takahashi, T.; Ootake, A.; Tsuji, J. *Tetrahedron* **1985**, *41*, 5447.
159. Schmit, J. P.; Piraux, M.; Pilette, J. R. *J. Org. Chem.* **1975**, *40*, 1586.
160. Schow, S. R.; McMorris, T. C. *J. Org. Chem.* **1979**, *44*, 3760.
161. (a) Sucrow, W.; Radüchel, B. *Chem. Ber.* **1969**, *102*, 2629. (b) Littmann, W.; Sucrow, W. *Chem. Ber.* **1969**, *102*, 1607. (c) Sucrow, W.; van Nooy, M. *Liebigs Ann. Chem.* **1982**, 1897.
162. Ohtaka, H.; Morisaki, M.; Ikekawa, N. *J. Org. Chem.* **1973**, *38*, 1688.
163. (a) Fryberg, M.; Oehlschlager, A. C.; Unrau, A. M. *Tetrahedron* **1971**, *27*, 1261. (b) Kozikowski, A. P.; Xia, Y.; Reddy, E. R.; Tückmantel, W.; Hanin, I.; Tang, X. C. *J. Org. Chem.* **1991**, *56*, 4636.
164. (a) Tulshian, D. B.; Tsang, R.; Fraser-Reid, B. *J. Org. Chem.* **1984**, *49*, 2349. (b) Fraser-Reid, B.; Tsang, R.; Tulshian, D. B.; Sun, K. M. *J. Org. Chem.* **1981**, *46*, 3767, footnote 10.
165. Tulshian, D. B.; Fraser-Reid, B. *Tetrahedron* **1984**, *40*, 2083.
166. Georges, M.; Tam, T. F.; Fraser-Reid, B. *J. Org. Chem.* **1985**, *50*, 5747.
167. Tadano, K.; Idogaki, Y.; Yamada, H.; Suami, T. *J. Org. Chem.* **1987**, 52, 1201.
168. Fitjer, L.; Quabeck, U. *Syn. Commun.* **1985**, *15*, 885.
169. Smith, A. B.; Jerris, P. J. *J. Org. Chem.* **1982**, *47*, 1845.
170. Oppolzer, W.; Wylie, R. D. *Helv. Chim. Acta.* **1980**, *63*, 1198.
171. Sampath, V.; Lund, E. C.; Kundsen, M. J.; Aimstead, M. M.; Schore, N. E. *J. Org. Chem.* **1987**, *52*, 3595.
172. Moss, R. A.; Chen, E. Y. *J. Org. Chem.* **1981**, *46*, 1466. McGuire, H. M.; Odom, H. C.; Pinder, A. R. *J. Chem. Soc., Perkin Trans. 1* **1974**, 1879.
173. Baldwin, S. W.; Gawley, R. E. *Tetrahedron Lett.* **1975**, *16*, 3969. For synthesis of a tetrasubstituted alkene using $Ph_3P{=}CBr_2$ see Wilson, S. R.; Mao, D. T. *J. Am. Chem. Soc.* **1978**, *100*, 6289.
174. Kienzle, F. *Helv. Chim. Acta* **1980**, *63*, 563.
175. Steliou, K.; Poupart, M. A. *J. Org. Chem.* **1989**, *54*, 5128.
176. Wernic, D.; DiMaio, J.; Adams, J. *J. Org. Chem.* **1989**, *54*, 4224.
177. Wicha, J.; Marczak, S. *Synth. Commun.* **1989**, *19*, 633.
178. Blair, I.; Prakash, C.; Saleh, S.; Taber, D. F. *Synth. Commun.* **1989**, *19*, 245.

179. Floyd, M. B. *J. Org. Chem.* **1978**, *43*, 1641.
180. Maryanoff, B. E.; Reitz, A. B.; Duhl-Emswiler, B. A. *J. Am. Chem. Soc.* **1985**, *107*, 217.
181. Bonbia, B.; Mann, A.; Bellamy, F. D.;Mioskowski, C. *Angew. Chem. Int. Ed. Engl.* **1990**, *29*, 1454.
182. Hosoda, A.; Taguchi, T.; Kobayashi, Y. *Tetrahedron Lett.* **1987**, *28*, 65.
183. Corey, E. J.; Clark, D. A.; Goto, G.; Marfat, A.; Miokowski, C. *J. Am. Chem. Soc.* **1980**, *102*, 1436.
184. Enholm, E. J.; Satici, H.; Prasad, G. *J. Org. Chem.* **1990**, *55*, 324.
185. Corey, E. J., Marfat, A.; Hoover, D. J. *Tetrahedron Lett.* **1981**, *22*, 1587.
186. Kozikowski, A. P.; Chen, Y. Y.; Wang, B.; Xu, Z. B. *Tetrahedron* **1984**, *40*, 2345.
187. Salmond, W. G.; Barta, M. A.; Havens, J. L. *J. Org. Chem.* **1978**, *43*, 790.
188. Kozikowski, A. P.; Schmiesing, R. J.; Sorgi, K. L. *J. Am. Chem. Soc.* **1980**, *102*, 6577.
189. Garbers, C. F.; Malherbe, J. S.; Schneider, D. F. *Tetrahedron Lett.* **1972**, *13*, 1421.
190. (a) Schönauer, K.; Zbiral, E. *Tetrahedron Lett.* **1983**, *24*, 753. (b) Nidy, E. G.; Johnson, R. A. *J. Org. Chem.* **1975**, *40*, 1415. (c) Newton, R. F.; Wadsworth, A. H. *J. Chem. Soc., Perkin Trans. 1* **1982**, 823.
191. Bestmann, H. J.; Roth, K.; Ettlinger, M. *Angew. Chem.* **1979**, *91*, 748.
192. Lee, T. J. *Tetrahedron Lett.* **1985**, *26*, 4995.
193. (a) Schlosser, M.; Zimmerman, M. *Synthesis* **1969**, 75; *Chem. Ber.* **1971**, *104*, 2885. (b) Miyano, S.; Izumi, Y.; Fujii, K.; Ohno, Y.; Hashimoto, H. *Bull. Chem. Soc. Jpn.* **1979**, *52*, 1197. (c) Lerouge, P.; Paulmin, C. *Tetrahedron Lett.* **1984**, *25*, 1983.
194. (a) Matsumoto, M.; Kuroda, K. *Tetrahedron Lett.* **1980**, *21*, 4021. (b) Smithers, R. H. *J. Org. Chem.* **1978**, *43*, 2833. (c) Pattenden, G.; Robson, D. C. *Tetrahedron Lett.* **1987**, *28*, 3751.
195. Stork, G.; Zhao, K. *Tetrahedron Lett.* **1989**, *30*, 2173.
196. Bestmann, H. J.; Rippel, H. C.; Dostalek, R. *Tetrahedron Lett.* **1989**, *30*, 5261.
197. McClure, J. D. *Tetrahedron Lett.* **1967**, *8*, 2401.
198. Linderman, R. J.; Meyers, A. I.*Tetrahedron Lett.* **1983**, *24*, 3043.
199. Meyers, A. I.; Lawson, J. P.; Walker, D. G.; Linderman, R. J. *J. Org. Chem.* **1986**, *51*, 5111.
200. Corey, E. J.; Desai, M. C. *Tetrahedron Lett.* **1985**, *26*, 5747.
201. Donetti, A.; Cereda, E.; Attolini, M.; Bellora, E. *Tetrahedron Lett.* **1982**, *23*, 2219.
202. Seyferth, D.; Wursthorn, K. R.; Mammarella, R. E. *J. Org. Chem.* **1977**, *42*, 3104.
203. Iio, H.; Ishii, M.; Tsukamoto, M.; Tokoroyama, T. *Tetrahedron Lett.* **1988**, *29*, 5965.
204. Soderquist, J. A.; Anderson, C. L. *Tetrahedron Lett.* **1988**, *29*, 2425.
205. Ideses, R.; Shani, A. *Tetrahedron* **1989**, *45*, 3523.
206. Shibousaki, M.; Sodeoka, M.; Yamada, H. *J. Am. Chem. Soc.* **1990**, *112*, 4906.
207. LeMerrer, Y.; Gravier-Pelletier, C.; Micas-Languin, D.; Mestre, F.; Dureault, A.; Depezay, J. C. *J. Org. Chem.* **1989**, *54*, 2409.
208. Delorme, D.; Girard, Y.; Rokach, *J. J. Org. Chem.* **1989**, *54*, 3635.
209. Yadagiri, P.; Lumin, S.; Falck, J. R.; Karara, A.; Capdevila, J. *Tetrahedron Lett.* **1989**, *30*, 429.
210. Vidal, J. P.; Escale, R.; Niel, G.; Rechencq, E.; Girard, J. P.; Rossi, J. C. *Tetrahedron Lett.* **1989**, *30*, 5129.
211. Namikoshi, M.; Rinehart, K. L.; Dahlem, A. M.; Beasley, V. R.; Carmichael, W. W. *Tetrahedron Lett.* **1989**, *30*, 4349.
212. Hanessian, S.; Sakito, Y.; Dhanoa, D.; Baptistella, L. *Tetrahedron* **1989**, *45*, 6623.

213. Corey, E. J.; Ruden, R. A. *Tetrahedron Lett.* **1973**, 1495.

214. Streinz, L.; Saman, D.; Konecny, K.; Romanuk, M. *Collect. Czech. Chem. Commun.* **1990**, *55*, 1555.

215. Jaenicke, M. P.; Akintobi, T.; Marner, F.-J. *Liebigs Ann. Chem.* **1973**, 1252.

216. Akintobi, T.; Jaenicke, L.; Marner, F.-J.; Waffenschmidt, S. *Liebigs Ann. Chem.* **1979**, 986.

217. Grieco, P.; Lis, R.; Zelle, R. E.; Finn, J. *J. Am. Chem. Soc.* **1986**, *108*, 5908.

218. Bentley, R.; Higham, C.; Jenkins, J.; Jones, E.; Thaller, V. *Perkin I* **1974**, 1987.

219. Vedejs, E.; Marth, C. F. *J. Am. Chem. Soc.* **1988**, *110*, 3948.

220. (a) Bestmann, H. J. *Pure Appl. Chem.* **1980**, *52*, 771. (b) Bestmann, H. J.; Vostrowsky, O. *Top. Curr. Chem.* **1983**, *109*, 85.

221. Olah, G. A.; Krishnamurthy, V. V. *J. Am. Chem. Soc.* **1982**, *104*, 3987.

222. (a) McEwen, W. E.; Beaver, B. D.; Cooney, J. V. *Phosphorus Sulfur* **1985**, *25*, 255. (b) McEwen, W. E.; Ward, W. J. *Phosphorus Sulfur* **1989**, *41*, 393.

223. (a) Yamataka, H.; Nagareda, K.; Takai, Y.; Sowada, M.; Hanafusa, T. *J. Org. Chem.* **1988**, *53*, 3877. (b) Yamataka, H.; Nagareda, K.; Hanafusa, T.; Nagase, S. *Tetrahedron Lett.* **1989**, *30*, 7187. (c) Yamataka, H.; Nagareda, K.; Takatsuka, T.; Ando, K.; Hanafusa, T.; Nagase, S. *J. Am. Chem. Soc.* **1993**, *115*, 8571.

224. Salem, L.; Rowland, C. *Angew. Chem., Int. Ed. Engl.* **1972**, *11*, 92.

225. (a) Newcomb, M.; Manek, M. B. *J. Am. Chem. Soc.* **1990**, *112*, 9662. (b) Tanko, J. M.; Drumright, R. E. *J. Am. Chem. Soc.* **1990**, *112*, 5362.

226. (a) Selected cyclopropyl carboxaldehyde examples: Cupas, C.; Watts, W.; Schleyer, P. *J. Chem. Soc., Chem. Commun.* **1964**, 2503. Brown, J. M. *J. Chem. Soc., Chem. Commun.* **1967**, 638. Ullenius, C.; Ford, P. W.; Baldwin, J. E. *J. Am. Chem. Soc.* **1972**, *94*, 5910. (b) 2,2-dimethyl-3-phenylcyclopropane carboxaldehyde: Zimmerman, H. E.; Baeckstrom, P.; Johnson, T.; Kurtz, D. W. *J. Am. Chem. Soc.* **1974**, *96*, 1459. 2-Methyl-2-ethyl-3,3-diphenylcyclopropanecarboxaldehyde: Zimmerman, H. E.; Robbins, J. D.; McKelvey, R. D.; Samuel, C. J.; Sousa, L. R. *J. Am. Chem. Soc.* **1974**, *96*, 4630. (c) 2-Cyano-3,3-dimethylcyclopropanecarboxaldehyde: Matsuo, T.; Mori, K.; Matsui, M. *Tetrahedron Lett.* **1976**, *17*, 1979. (d) 2-Carboethoxy-3,3-dimethylcyclopropanecarboxaldehyde: Crombie, L.; Doherty, C. F.; Pattenden, G. *J. Chem. Soc. C* **1970**, 1076. (e) Heldeweg, R. F.; Hogeveen, H.; Schudde, E. P. *J. Org. Chem.* **1978**, *43*, 1912. (f) Cyclopropylcarbinylidenetriphenylphosphorane: Schweizer, E. E.; Thompson, J. G.; Ulrich, T. A. *J. Org. Chem.* **1968**, *33*, 3082. Teraji, T.; Moritani, I.; Tsuda, E.; Nishida, S. *J. Chem. Soc. C* **1971**, 3252. Tarakanova, A.; Baranova, S.; Pekhk, T.; Dogadin, O.; Zefirov, N. *Zh. Org. Khim.* **1987**, *23*, 515.

227. Tanner, D. D.; Chen, J. J. Chen, L.; Luelo, C. *J. Am. Chem. Soc.* **1991**, *113*, 8074.

228. Vedejs, E.; Rodgers, J. D.; Wittenberger, S. J. *Tetrahedron Lett.* **1988**, *29*, 2287.

229. Vedejs, E.; Marth, C. F. *J. Am. Chem. Soc.* **1990**, *112*, 3905.

230. (a) Trindle, C.; Hwang, J. T.; Carey, F. *J. Org. Chem.* **1973**, *38*, 2664. (b) Höller, R.; Lischka, H. *J. Am. Chem. Soc.* **1980**, *102*, 4632. (c) Bestmann, H. J.; Chandrasekhar, J.; Downey, W. J.; Schleyer, P. R. *J. Chem. Soc. Chem. Commun.* **1980**, 978. (d) Volatron, F.; Eisenstein, O. *J. Am. Chem. Soc.* **1987**, *109*, 1. (e) Rzepa, H. S. *J. Chem. Soc., Perkin Trans. 1* **1989**, 2115. (f) Mari, F.; Lahti, P. M.; McEwen, W. E. *Heteroatom Chem.* **1990**, *1*, 255. (g) Mari, F.; Lahti, P. M.; McEwen, W. E. Heteroatom Chem. **1991**, *2*, 265. (h) Yamataka, H.; Hanafusa, T.; Nagase, S.; Kurakake, T. *Heteroatom Chem.* **1991**, *2*, 465. (i) Mari, F.; Lahti, P. M.; McEwen, W. E. *J. Am. Chem. Soc.* **1992**, *114*, 813.

231. Vedejs, E.; Marth, C. F. *J. Am. Chem. Soc.* **1989**, *111*, 1519.

232. (a) Schlosser, M.; Piskala, A.; Tarchini, C.; Huynh B. T. *Chimia* **1975**, *29*, 341. Piskala, A.; Rehan, A. H.; Schlosser, M. *Collect. Czech. Chem. Commun.* **1983**, *48*, 3539. (b) Kuchar, M.; Kakac, B.; Nemecek, O.; Kraus, E.; Holubek, J. *Collect. Czech. Chem. Commun.* **1973**, *38*, 447. Isaacs, N. S.; Abed, O. H. *Tetrahedron Lett.* **1986**, *27*, 995; these authors also report activation volumes that are consistent with a cycloaddition process although this option was not considered. Donxia, L.; Dexian, W.; Yaozhong, L.; Huaming, Z. *Tetrahedron* **1986**, *42*, 4161.

233. Giese, B. *Angew. Chem., Int. Ed. Engl.* **1977**, *16*, 125.

234. Schneider, W. P. *J. Chem. Soc., Chem. Commun.* **1969**, 785.

235. Förster, H.; Vögtle, F. *Angew. Chem., Int. Ed. Engl.* **1977**, *16*, 429.

ADDENDUM

The following references appeared after completion of the tables. They describe the unusually Z-selective ylides $[o\text{-}(CH_3OCH_2O)C_6H_4]_3P{=}CHX$, X = halogen, methoxy, or carboethoxy. The latter exhibits enhanced Z-selectivity in methanol.

Zhang, X.; Schlosser, M. *Tetrahedron Lett.* **1993**, *34*, 1925.
Patil, V.; Schlosser, M. *Synlett.* **1993**, 125.

Anomeric Effect: Origin and Consequences

PIOTR P. GRACZYK AND MARIAN MIKOŁAJCZYK

Department of Organic Sulfur Compounds, Center of Molecular and Macromolecular Studies, Polish Academy of Science, Łódź, Poland

I. Introduction
II. What Does *Anomeric Effect* Mean?
  A. Classical Definition of Anomeric Effect by Lemieux: Generalized Anomeric Effect
  B. Classical Approach to Evaluation of Magnitude of Anomeric Effect
  C. Franck's Proposal
  D. Application of Franck's Method to Evaluation of Magnitude of Anomeric Effect in Acyclic Molecules
  E. Bidirectionality of Anomeric Effect: Exo and Endo Anomeric Effects
    1. "Bidirectional" Approach
    2. "Nondirectional" Approach
  F. Enthalpic Anomeric Effect
  G. Solvent Effects
  H. Energy of Bond Separation Reactions
  I. Reverse Anomeric Effect
III. Origin of Anomeric Effect
  A. Classical Approaches
    1. Electrostatic Interactions
    2. Solvent-induced Anomeric Effect
    3. Double Bond–No Bond Resonance
    4. Rabbit Ear Effect
    5. Energy Decomposition Scheme
    6. Molecular Mechanics Calculations
  B. Quantum Chemical Approaches
    1. Energy Component Analysis
    2. Fourier Component Analysis of Potential Function
    3. Initial MO-based Approach to Double Bond–No Bond Resonance
    4. Anomeric Effect in Light of Perturbational Molecular Orbital (PMO) Theory
    5. Interpretation of Anomeric Effect with the Aid of Natural Bond Orbital Analysis
    6. Anomeric Effect in Terms of σ Conjugation
    7. Anomeric Effect as a Result of σ-Electron Delocalization Controlled by Orbital Phase

Topics In Stereochemistry, Volume 21, Edited by Ernest L. Eliel and Samuel H. Wilen.
ISBN 0-471-52120-5 © 1994 John Wiley & Sons, Inc.

8. Other General Explanations of Anomeric Effect
9. Special Cases
   a. n_F–$\pi^*_{C=O}$ and n_F–n_O Interactions
   b. $3p$–$3d$ Interaction
   c. $\pi_{C=O}$–$3d_S$ Interaction
   d. σ_{C-X}–$\pi^*_{C=O}$ and $\pi_{C=O}$–σ^*_{C-X} Interactions

IV. Consequences of the Anomeric Effect
   A. Anomeric Effect and Energy
      1. Kinetic Anomeric Effect
         a. n_Y–σ^*_{C-X} Negative Hyperconjugation and Conformational Adjustment
         b. $\sigma_{C(2)-Y}$–$\sigma^*_{C(2)-X}$ and $\sigma_{C(2)-X}$–$\sigma^*_{C(2)-Y}$ Hyperconjugations
         c. Overlap Repulsion
      2. Anomeric Effect and Rotational Barriers
   B. Anomeric Effect and Structure
      1. Bond Lengths and Angles
      2. Anomeric Effect and Electron Density
      3. Spectroscopic Implications of Anomeric Effect
         a. Chemical Shifts
         b. Coupling Constants
         c. Stretching Frequencies and Conformational Equilibrium Isotope Effects

V. Anomeric Effect in Y—C—P System (Y = O, S, Se)
   A. Magnitude of Anomeric Effect
   B. Nature of Anomeric Effect in Y—C—P System (Y = O, S, Se)
      1. Thermodynamic Implications of Anomeric Effect in Y—C—P System (Y = O, S, Se)
      2. Molecular Mechanics- and Molecular Orbital-derived Implications of Anomeric Effect in Y—C—P System (Y = O, S, Se)
      3. X-Ray Crystallographic Implications of Anomeric Effect in Y—C—P System (Y = O, S, Se)
      4. Spectroscopic Implications of Anomeric Effect in Y—C—P System (Y = O, S, Se)
      5. Kinetic Implications of Anomeric Effect in S—C—P System
      6. Anomeric Effect in Y—C—P System (Y = O, S, Se): Summary

Symbols and Abbreviations

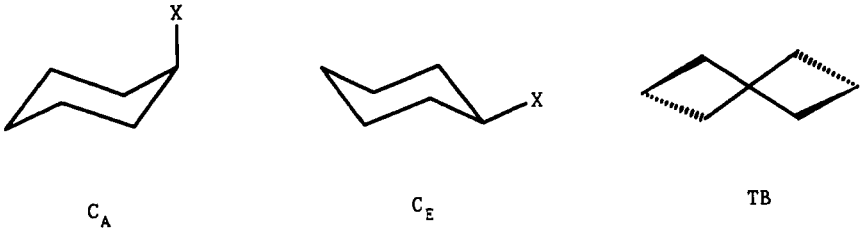
References

I. INTRODUCTION*

Conformational analysis originated about 100 years ago as the result of the pioneering suggestion by Sachse (1) that six-membered saturated rings are not planar but exist in puckered shapes, such that all the valence angles are tetrahedral. He realized that two forms of cyclohexane free of angle strain are possible (now they are called *chair C* and *twist-boat* TB conformers) and

*A glossary of symbols and abbreviations used in this chapter is found at the end of the text (p. 336).

that two monosubstituted chairs could exist (they correspond to *axial* C_A and *equatorial* C_E conformers). Initial work by Mizushima et al. (2) on the conformation of 1,2-dihaloethanes and by Hermans (3) dealing with the effect of structure on the reactivity of some dioxolane derivatives did not have immediate impact on the organic chemical community of the 1920s, 1930s, and 1940s (4). Conformational analysis as a branch of theoretical chemistry was spurred on to rapid development only in 1950, when Barton (5) pointed out various chemical and physical consequences of the axial and equatorial attachment, respectively, of substituents in a cyclohexane ring.



Today, conformational analysis has pervaded chemical thinking so deeply that one can find the keyword *conformation* over 10,000 times in each volume of *Chemical Abstracts*. The search for new conformational effects and their explanations is a part of conformational studies. The anomeric effect is one of those effects.

Though numerous reviews (6–18) on the anomeric effect have been published during the past several years, certain problems should still be discussed and the importance of well-established interactions reevaluated. This chapter is intended to focus the attention of readers on such problems. In this context we present the appropriate results both taken from the literature and based on our own work.

II. WHAT DOES *ANOMERIC EFFECT* MEAN?

The main difference between conformers C_A, C_E, and TB is physical in nature: their energies are different. It is generally accepted (19a, 20a) now that a monosubstituted cyclohexane **1** at equilibrium usually exists in two discrete conformations **1a** (C_A) and **1e**† (C_E) differing in free energy by ΔG°_C and separated by a free energy barrier $\Delta G^{\neq}_{AE}$ (Figure 1). The free energy of the TB conformation is about 22–23 kJ/mol (1 cal = 4.186 J) larger than that of

† For the sake of simplicity axial isomers will usually be denoted in this review as "a" and equatorial as "e", provided the conformation about the exocyclic C—X bond is unimportant.

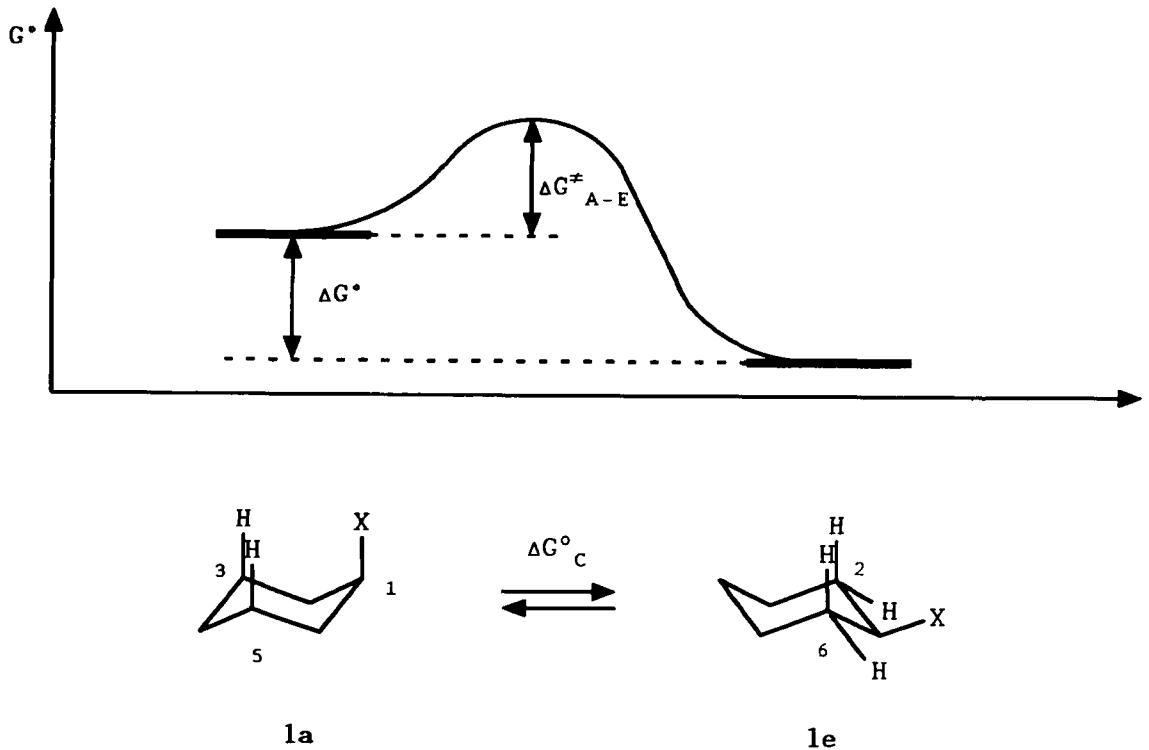


Figure 1. Conformational interconversion of monosubstituted cyclohexane derivatives **1** (twist-boat intermediates disregarded).

C, and therefore the amount of TB at 298 K is negligible (about 0.1%) (20a). Conformers **1e** are more stable than **1a** ($\Delta G_C^\circ < 0$) as a rule [though not without exceptions[†] (21)]. For instance, free energy difference ΔG_{300}° for simple alkyl groups X = Me, Et, *i*-Pr (Figure 1) is equal to -7.28, -7.49, and -9.25 kJ/mol, respectively (22). The equatorial preference of the alkyl groups and the decrease of ΔG_{300}° on going from X = Me to Et to *i*-Pr has been rationalized (perhaps in oversimplified fashion, see Section II.F) in terms of the "steric bulk" or "size" of the substituent X. Thus **1a** is more destabilized than **1e**, and the equilibrium should lie on the side of **1e.** For easily polarizable atoms the interaction mentioned above may, however, be moderated by *London attraction* (19b). Nevertheless, simple consideration of steric interactions permits us to *expect* that equatorial conformers should be more stable than axial ones, and this relation should be correct for six-membered rings other than cyclohexane as well.

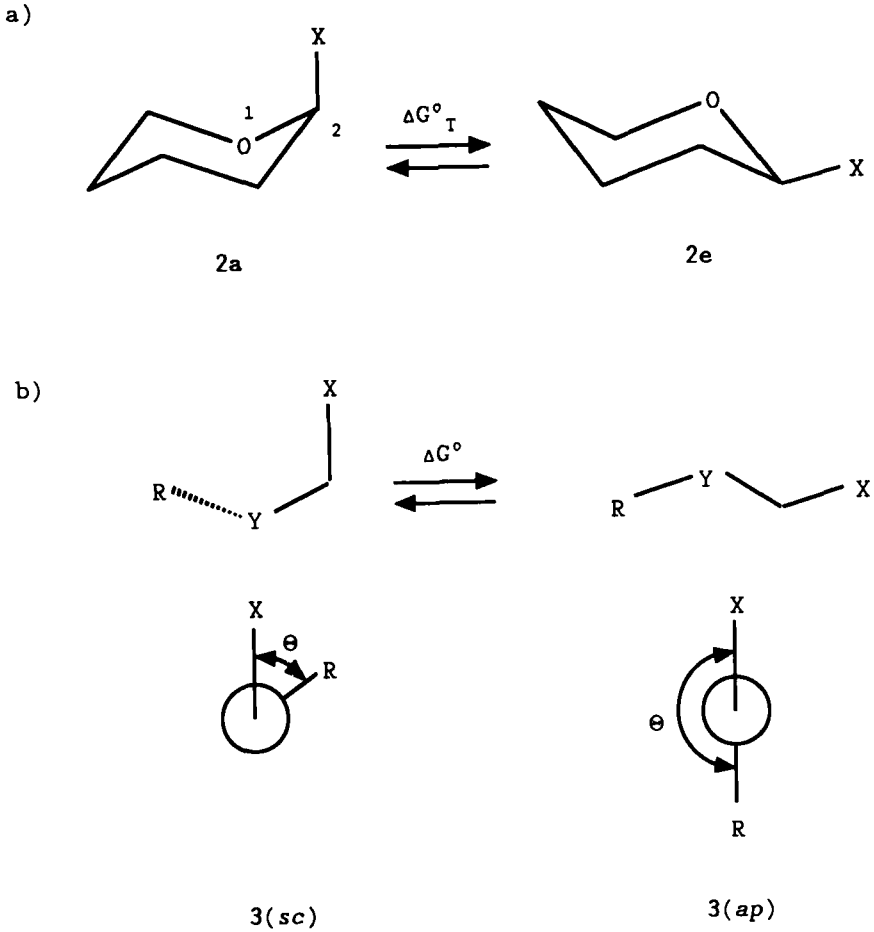
A. Classical Definition of Anomeric Effect by Lemieux: Generalized Anomeric Effect

Whenever our *expectation* based on certain theory faces an unexplained exception, we speak of such an exception as an "effect" (23). Thus, when Lemieux and Chü (24) found α-anomers (axial) of D-glucose derivatives to be more stable than β ones (equatorial), they coined (25) the term *anomeric effect* for this exceptional behavior. This term has therefore a purely phenomenological meaning and does not *per se* reflect on the origin of the phenomenon.

The anomeric effect is quite general. It is usually defined (6) in terms of the preference of electronegative (26) substituent X at the anomeric center of pyranoses for the axial orientation (Scheme 1a, $\Delta G_T^\circ > 0$). This orientation corresponds to a *synclinal (gauche)* arrangement of X—C(2)—O—C(6) bonds[‡] in **2** (Scheme 1). Indeed, analogous preferences for synclinal *sc* conformation in various acyclic compounds of type R—Y—C—X (**3**) were found (6) and termed the *generalized anomeric effect* by Lemieux (27), Eliel (28), and Bailey and Eliel (29). Following usual practice, however, in this

[†] Recent semiempirical molecular orbital calculations by Graczyk (unpublished results) on various compounds containing the C—C—C—X^+ (X = OH_2, NH_3, SH_2, PH_3) system show a predominant axial preference in cyclohexanes containing a strongly electron-withdrawing, X = OH_2 group.

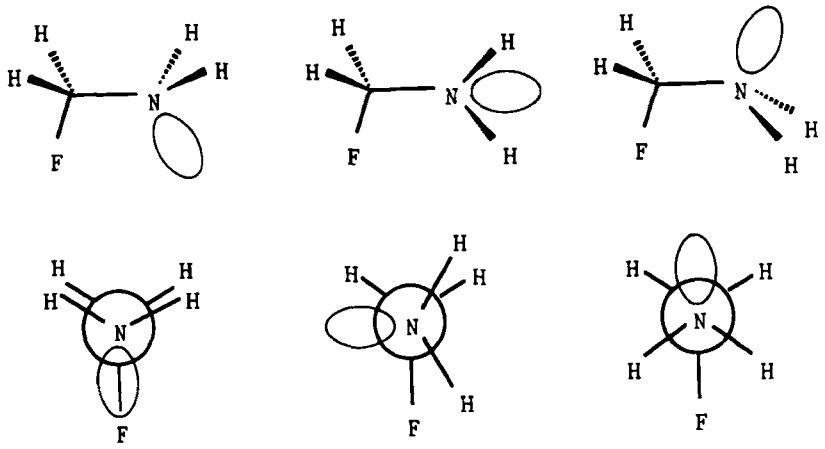
[‡] Two numbering systems are used in this review. According to the first, which is based on the nomenclature of heterocyclic systems, the anomeric carbon atom is denoted as C(2) (number in parentheses). If carbohydrate convention is applied, this carbon atom becomes C1, and the number is not in parentheses.



Scheme 1

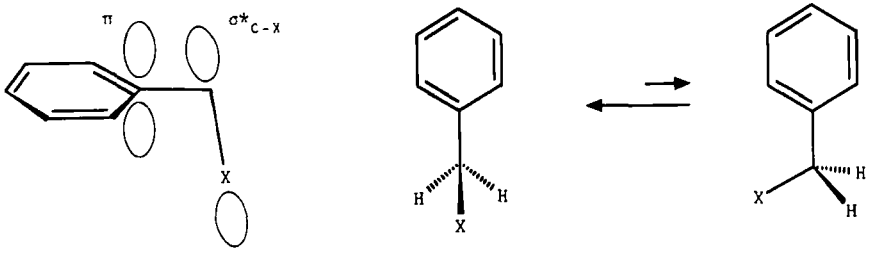
chapter the generalized anomeric effect will be referred to simply as anomeric effect.

Four other so-called anomeric effects are also found in the literature, based, however, on etiological (meaning connected with an origin) grounds. All of them are rationalized in terms of the concept of negative hyperconjugation, which is usually regarded as a source of the anomeric effect (see Sections III.B.4 and III.B.5). Thus, the preference for the synperiplanar (*sp*) arrangement of a lone electron pair and a C—F polar bond (which affords an antibonding σ^* orbital) over the orthogonal (*og*) one in fluoromethylamine (**4**) has been termed the *syn anomeric effect* by Irwin et al. (30). An analogous



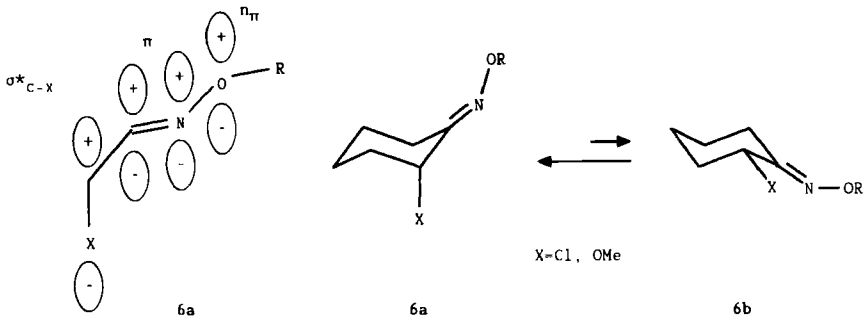
4(sp) 4(og) 4(ap)

preference for the antiperiplanar (*ap*) conformation over the *og* one was called the *anti anomeric effect*. The preference for the conformation **5a** in which the C—X [X = Cl, SH, SMe, S(O)Me, SO_2Me] bond of benzylic derivatives **5** is perpendicular to the plane of the phenyl ring (Scheme 2) was termed the *benzylic anomeric effect* by Penner et al. (31) and explained as due to the π–σ^*_{C-X} negative hyperconjugation. The term *vinylogous anomeric effect* was coined by Denmark and Dappen (32, 33) to describe the axial preference of α-chloro- and α-methoxycyclohexanone oximes and oxime derivatives **6** (Scheme 3). This effect was also postulated by Curran and Suh (34) to account for accelerated Claisen rearrangements of carbohydrate glycals, but in the opinion of Box (15) this is not supported by the relevant X-ray data.



5a 5a 5b

Scheme 2



Scheme 3

B. Classical Approach to Evaluation of Magnitude of Anomeric Effect

What should then be the magnitude of ΔG°_{T} (Scheme 1a) to allow us to say if we deal (or not) with an anomeric effect? The answer should be based on the phenomenological meaning of the term. Our *expectations* were based on steric grounds, and therefore the anomeric effect should be considered as an *excess* of axial preference over the preference determined by steric factors only.

The first attempt to define the magnitude of the anomeric effect was by Eliel et al. (19c) and by Anderson and Sepp (35). They assumed that steric interactions of a given X in a cyclohexane ring remain almost unchanged when the latter is replaced by a pyranose (or tetrahydropyran) ring. Thus, steric interactions $\Delta G^{\circ}_{H(st)}$ are set equal to ΔG°_{C} (Figure 1), and the magnitude of anomeric effect ΔG°_{AE} is given as the difference between the axial–equatorial free energy difference in a pyranose, ΔG°_{T}, or generally, heteroane, ΔG°_{H}, and that for the same substituent in a cyclohexane ring ΔG°_{C}.

$$\Delta G^{\circ}_{AE} = \Delta G^{\circ}_{H} - \Delta G^{\circ}_{H(st)} \quad \text{where} \quad \Delta G^{\circ}_{H(st)} = \Delta G^{\circ}_{C} \qquad [1]$$

Scientists performing molecular orbital (MO) calculations usually consider the magnitude ΔE_{AE} of the anomeric effect as the positive difference of the potential energy E_{ap} of *antiperiplanar* (*ap*) and E_{sc} of *synclinal* (*sc*) conformers (36):

$$\Delta E_{AE} = E_{ap} - E_{sc} \qquad [2]$$

This approach, though simple, is somewhat misleading because it does not correspond to the original definition of the anomeric effect, that is, *increased* preference for the *sc* conformation. It does not take into account

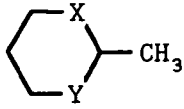
the preference due to steric reasons and hence ΔE_{AE} can tell nothing about the magnitude of the anomeric effect in the classical sense of this notion. Moreover, it may imply the presence of a *reverse anomeric effect* ($\Delta E_{AE} < 0$) in cases where in fact there is no anomeric effect [as in ethyl methyl ether (7)] or there is a *normal anomeric effect* (e.g., in the O—C—NH_2 system; see Sections II.C and II.I).

Irwin et al. (30) took into account several criteria for estimating the relative strength of the *syn* anomeric effect in fluoromethylamine (4), that is, molecular energy stabilization, changes in bond lengths, energy difference between coplanar (*sp* and *ap*) and orthogonal (*og*) conformations, and differences in activation or bond-breaking energies (kinetic criterion). Interestingly, the *syn* effect is comparable to the *anti* one as far as the lengthening of the C—F bond is concerned, or, according to Irwin et al. (30), even greater when C—F bond dissociation energies are compared (calculated bond dissociation energy in the *syn* structure is ca. 21 kJ less than that in the *anti* one).

C. Franck's Proposal

Equation (1) was widely applied in this form for almost 15 years, and it was the main cause of numerous misunderstandings and erroneous interpretations. For instance, it suggested the existence of a reverse anomeric effect for the carbomethoxy group in a tetrahydropyran ring (37) while the opposite is actually true, that is, there is a normal anomeric effect (38). The main weakness of Eq. [1], as was already pointed out by Eliel and Giza (39), is the assumption that steric interactions in a heterocycle are the same as in the analogously substituted cyclohexane. Usually, the distances between axial X and 1,3-syn-axial hydrogens increase or decrease as the result of changes in bond

TABLE 1
Conformational Free Energy Differences ΔG° and Factors F_G for Methyl Group in Selected Heteroanes



X	Y	ΔG° (kJ/mol)	F_G[a]	Temperature (K)	Reference
O	O	−16.65	2.29	298	40
CH_2	O	−11.95	1.64	163	41
CH_2	NH	−10.34	1.42	[b]	42
CH_2	CH_2	−7.28	1.00	300	43
S	S	−7.42	1.02	342	44
Se	Se	−4.36	0.60	147	45

[a]Calculated as $F_G = \Delta G^\circ_H / \Delta G^\circ_C$; assumed to be equal to F_H (see Section II.F).
[b]Not stated.

lengths and angles when C(2) and/or C(6) of cyclohexane are replaced by heteroatoms Y or (and) Z. This, in turn, is reflected in the ΔG° values for axial–equatorial interconversion of a methyl group connected to the anomeric carbon atom of various six-membered rings (Table 1). Although the data refer to different temperatures, the trend is evident: the ΔG° values become more negative on going to oxygen heteroanes indicating a substantial increase in steric hindrance. In contrast, the appropriate ΔG° value for the 1,3-diselenane ring, $\Delta G^\circ_{Me} = -4.36$ kJ/mol, is more positive than in cyclohexane, $\Delta G^\circ_{Me} = -7.27$ kJ/mol, suggesting a diminished steric hindrance. It is then clear that while Eq. [1] can be satisfactorily applied for 1,3-dithiane derivatives (where ΔG°_{Me} is about the same as in cyclohexane), it completely fails for 1,3-diselenanes, tetrahydropyrans, and especially for 1,3-dioxanes.

In order to obtain a more "realistic" value of the anomeric effect, $\Delta G^\circ_{H(st)}$ in Eq. [1] has been replaced by the difference of potential energy ΔE_{class} obtained by semiempirical calculations based on classical mechanics with the assumption of invariability of entropy on going from *ap* to *sc* conformations. The calculation methods vary in their complexity from a simple estimate of steric energy by atom–atom potentials (46, 47) on the one hand to highly sophisticated molecular mechanics calculations (48) on the other.

The first to propose a rather simple way to overcome these difficulties was Franck (49), who linearly correlated free energies of "inert" substituents in cyclohexane, ΔG°_C, and tetrahydropyran [at C(2)], ΔG°_T. He found that if such a substituent is transferred from cyclohexane to the anomeric C(2) carbon in tetrahydropyran, ΔG°_C increases about 1.53 times (Eq. [3]) simply because of the increase in steric hindrance. Thus

$$\Delta G^\circ_{T(st)} = F_G \times \Delta G^\circ_C + C \qquad [3]$$

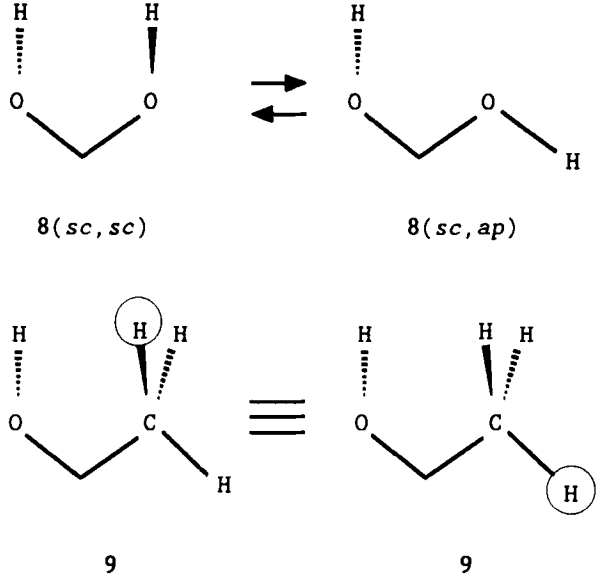
where $F_G = 1.53$ for tetrahydropyran (G in the subscript means that F_G is based on ΔG° values). Franck (49) calculated $C = 0.08$ kJ/mol, but C should actually be zero ($C = 0$) because of his assumption that the steric "size" of a hydrogen is the same in both heteroane (tetrahydropyran) and cyclohexane (if $\Delta G^\circ_C = 0$ then $\Delta G^\circ_T = 0$).

This approach allowed Franck (49) to show that methylamino (MeHN—) and dimethylamino (Me_2N—) groups exhibit weak normal anomeric effects when attached to the anomeric carbon atom of the tetrahydropyran ring. Although he was later criticized by Booth and Khedhair (50) for inadequate experimental data, even their ΔH° values unquestionably support Franck's conclusion.

One could ask: What is the magnitude of the anomeric effect if *two* heteroatoms Y are present in a molecule, for example, in $(R—Y)_2C—X$? Should the anomeric effect be divided by 2? In the opinion of Tschierske

et al. (38) the anomeric effect in $(R—Y)_2C—X$ system is twice as large as that for a single R—Y—C—X fragment. Therefore, the observed anomeric effect for the whole system should be divided by 2. As discussed by Juaristi et al. (51), the results on the tetrahydropyran versus the 1,3-dioxane series rather suggest a "saturation" of the effect. On the other hand, the anomeric effect of alkylthio substituents in dithianes is stronger than that in tetrahydrothiopyrans, but by less than a factor of 2 (51).

The choice of "inert" substituents for the correlation carried out by Franck was arbitrary. Perhaps only alkyl groups can be considered to some extent inert. The inclusion of vinyl, ethynyl, and hydroxymethyl groups in the calculation of the slope (Eq. [3]) appears to be unjustified. It must also be added that neither the classical definition (Eq. [1]) nor Franck's approach can be applied for estimation of the magnitude of the anomeric effect in very simple molecules [e.g., methanediol (**8**)] since the replacement of the rotating oxygen atom in the **8** (*sc*, *sc*) and **8** (*sc*, *ap*) conformers of methanediol by a methylene group leads to indistinguishable molecules of ethanol (**9**, see Scheme 4). This would suggest that steric interactions do not undergo any change, which is not true.



Scheme 4

Franck assumed a linear relation between $\Delta G^{\circ}_{T(st)}$ (or generally in a heteroane $\Delta G^{\circ}_{H(st)}$) and ΔG°_{C} values. In fact, the relationship is more complex. Let us look at cyclohexane and 1,3-dithiane. For the former $\Delta G^{\circ}_{C(Me)} = -7.28$

and for the latter $\Delta G^{\circ}_{D(Me)} = -7.42$ kJ/mol; hence Franck's factor is equal to $F_{G(Me)} = -7.42/-7.28 = 1.019$. This would suggest that the methyl group experiences a slightly more congested steric environment in 1,3-dithiane than in cyclohexane, contrary to expectation based on larger C—S than C—C bond lengths and flattening of 1,3-dithiane ring. When *tert*-butyl groups are considered, $\Delta G^{\circ}_{C(t\text{-}Bu)} = -20.5$ kJ/mol in cyclohexane and $\Delta G^{\circ}_{D(t\text{-}Bu)} = -11.4$ kJ/mol in 1,3-dithiane (44), and $F_{G(t\text{-}Bu)} = -11.4/-20.5 = 0.556$, now in agreement with anticipation. One should also note that a hydrogen atom experiences the same steric interactions in cyclohexane and in 1,3-dithiane rings (one of Franck's assumptions, *vide supra*). Hence, factor $F_{G(H)}$ based on hydrogen is equal to 1.

Now let us plot F_G values for H, Me, and *t*-Bu groups (in 1,3-dithiane), which are perfectly inert, as a function of ΔG°_{C} of the substituent (Figure 2). It is clear that factors F_G for substituents of intermediate size between that

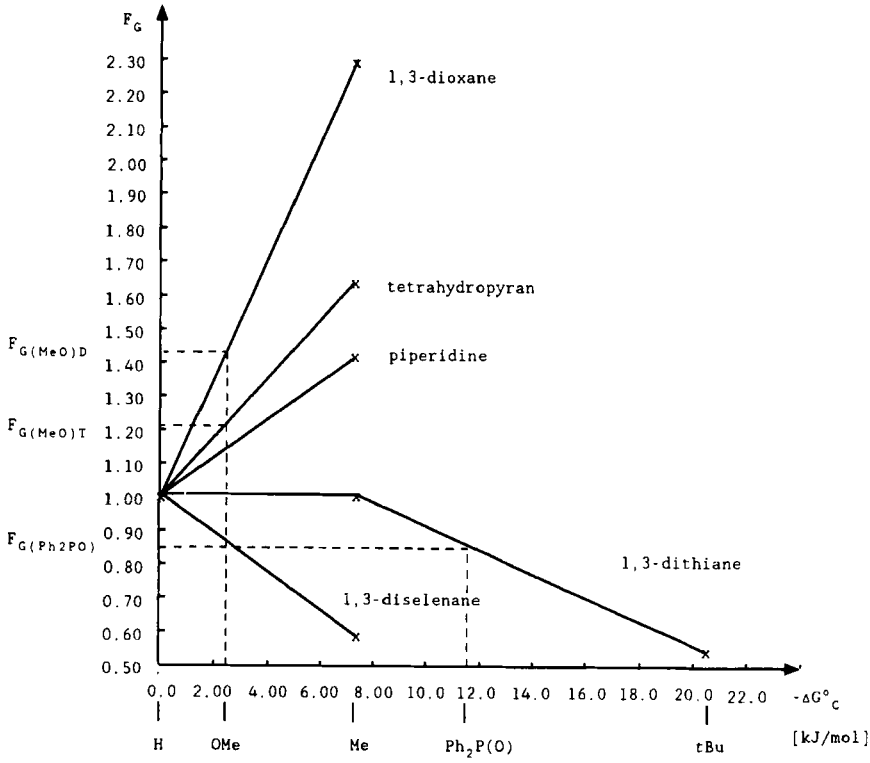


Figure 2. Determination of F_G factors for MeO and $Ph_2P(O)$ groups in some six-membered rings.

TABLE 2
Conformational Free Energy ΔG°, Enthalpy ΔH°, and Entropy ΔS° Differences for Selected Substituents in Certain Six-membered Rings[a]

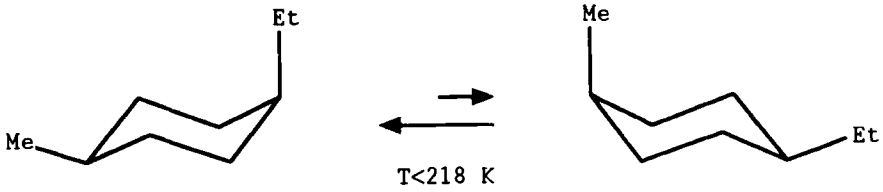
	Cyclohexane				Heterocycle[b]			
Group	ΔG°_C	ΔH°_C	ΔS°	Reference	ΔG°_H	ΔH°_H	ΔS°	Reference
t-Bu	−20.5			44	−11.4[c]			44
OMe	−2.4[d]	−3.0	−1.8	52	3.32[d]	0.17	−10.5	50
$Ph_2P(O)$	−11.5[d]	−8.2	10.9	53	1.57[d]	5.71	13.8	54

[a]Units of ΔG° and ΔH° are kJ/mol and of ΔS° are J/mol/K; substituents are connected to the C(2) atom of a heterocycle.
[b]For *t*-Bu and $Ph_2P(O)$, 1,3-dithiane; for OMe, tetrahydropyran.
[c]At 342 K.
[d]Calculated for $T = 300$ K based on ΔH° and ΔS° values.

of H, Me, and *t*-Bu are different from factors F_G for these reference groups. Let us consider, for instance, the $Ph_2P{=}O$ group, which is of intermediate size between that for Me and *t*-Bu [$\Delta G^\circ_C = -11.46 \pm 0.38$ kJ/mol (53), see Table 2]. If one assumes that F_G is a linear function of ΔG°_C, the linear interpolation between the F_G values for the methyl and *t*-butyl groups affords $F_{G(Ph_2PO)} = 0.87$ for the $Ph_2P{=}O$ group at C(2) in a 1,3-dithiane ring (see Figure 2).

By the same token one may find a dependence of F_G factors on ΔG°_C for other heterocycles, namely 1,3-dioxane, tetrahydropyran, piperidine, and 1,3-diselenane (see Figure 2). Unfortunately, since ΔG°_H values for reference groups in these rings are available for the Me group only (see Table 1), an interpolation of F_G can be performed only for substituents smaller than the methyl group. For instance, for the MeO group in tetrahydropyran an interpolation between F_G values for H ($F_G = 1.00$) and Me ($F_G = 1.64$) gives $F_{G(MeO)T} = 1.21$ (cf. Figure 2). Thus, in contrast to what is usually assumed, steric interactions experienced by the MeO group increase only by a factor of 1.2 on going from cyclohexane to tetrahydropyran. Even on going to 1,3-dioxane they increase only by a factor of 1.43 (!). Therefore, the anomeric effects calculated so far for the MeO group in the tetrahydropyran ring assuming $F_G \cong 1.5$ should be considered to be overestimated by ca. 0.8 kJ/mol. Of course, for groups larger than methyl an interpolation of F_G in 1,3-dioxane, tetrahydropyran, and 1,3-diselenane cannot be performed, and F_G must be assumed to be equal to F_G for the methyl group in the particular heterocycle.

Any interpolation of F_G is based on a certain order of ΔG°_C values (order of size of substituents). Unfortunately, the usually assumed order of ΔG°_C is not perfectly constant. For the ethyl group in cyclohexane at 300 K we have $\Delta G^\circ_{C(Et)} = -7.49$ kJ/mol (22); that is, the ethyl group prefers the equatorial



10a 10e

Scheme 5

position by 0.21 kJ/mol more than methyl at room temperature. However, a low-temperature nuclear magnetic resonance (NMR) study of *cis*-1-ethyl-4-methylcyclohexane (**10**) showed (22) that the conformation with axial ethyl, **10a**, is preferred below 218 K (Scheme 5; see also Section II.F). Therefore, the factor F_G for a particular substituent should not be considered constant but is actually a function of the special properties of the substituent, for example, rotational possibilities resulting in entropy differences (see also Section II.F). This suggests that Franck's method provides only an *approximate* measure of the magnitude of the anomeric effect.

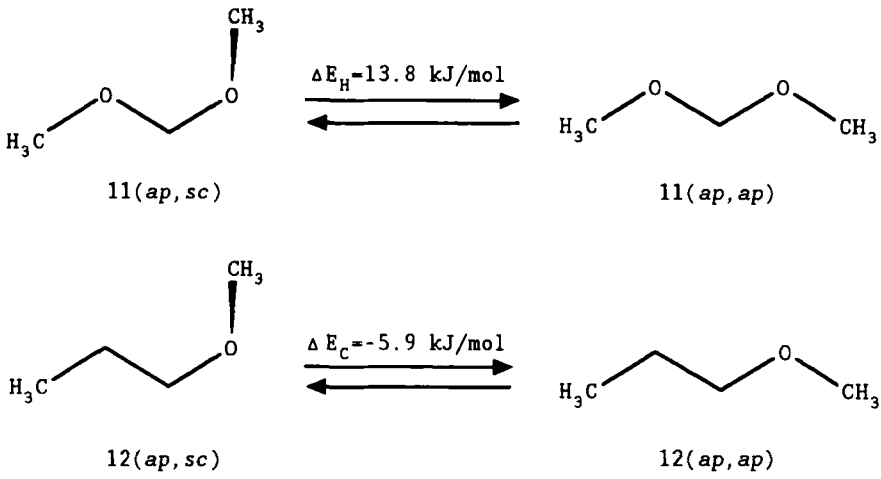
Recently, Juaristi and Cuevas (55) presented an application of Franck's methodology based on temperature-independent enthalpy ΔH° values (see Section II.F., Eqs. [17] and [18]) to estimate the enthalpic contribution to the C—S—C—P(O) anomeric effect as $\Delta H^\circ_{AE} = 14$ kJ/mol [11 kJ/mol in ΔG°_{AE} terms (56), but see also Section V.A].

D. Application of Franck's Method to Evaluation of Magnitude of Anomeric Effect in Acyclic Molecules

In the case of acylic compounds one faces another difficulty in estimating the magnitude of the anomeric effect. Let us consider conformational equilibria for *ap, sc* and *ap, ap* conformers of dimethoxymethane (**11**) and methyl propyl ether (**12**) (Scheme 6) following an approach presented by Wiberg and Murcko (57). They calculated (57) *ab initio* (6–31G*) energy difference between conformers *ap, ap* and *ap, sc* of **11** as $\Delta E_H = 13.8$ kJ/mol. In order to quantify the magnitude of the generalized anomeric effect (or simply anomeric effect) for a single *sc* fragment of **11** an *ab initio* (6–31G*) energy difference ΔE_C for methyl propyl ether (**12**) was computed (57): $\Delta E_C = -5.9$ kJ/mol. The magnitude of the anomeric effect in ΔE_{AE} terms was then calculated (57) according to the equations

$$\Delta E_{AE} = \Delta E_H - \Delta E_{st} \qquad [4]$$

$$\Delta E_{st} = F \times \Delta E_C \qquad [5]$$



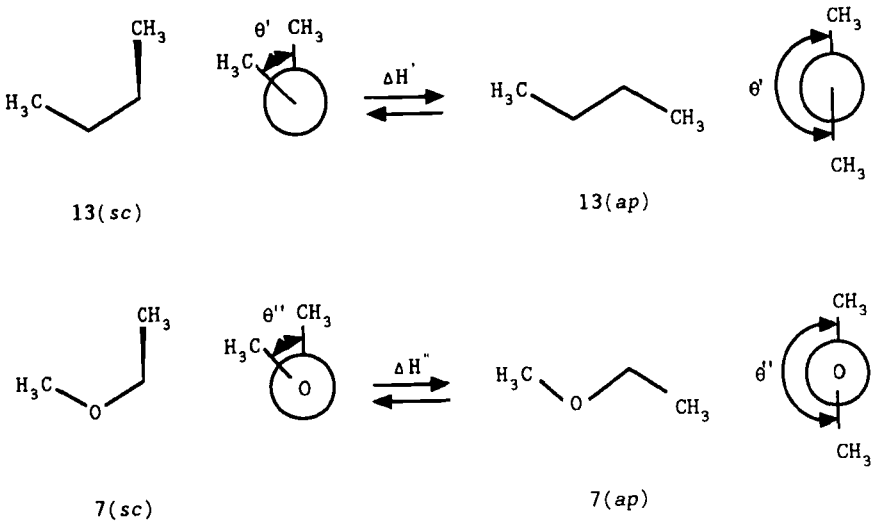
Scheme 6

(cf Eqs. [1] and [3]; ΔE instead of $\Delta G°$) as $\Delta E_{AE} = 22.6$ kJ/mol using Franck's tetrahydropyran–cyclohexane factor $F = 1.5$.

From the methodological point of view, a different F factor derived from the correlation of energies of relevant acyclic compounds should have been used. The anomeric carbon atom in **11** is secondary, whereas in 2-substituted tetrahydropyrans it is tertiary. The introduction of a third substituent at the anomeric carbon may result in a change of preferred conformation (58, 59), appropriate angles (60), and the magnitude of the anomeric effect (61), thus making cyclic models inadequate for the calculation presented above.

Let us consider equilibria pictured for relevant acyclic compounds in Scheme 7. If one takes into account the experimental energy differences $\Delta H' = -3.7 \pm 0.1$ kJ/mol for *n*-butane (**13**) (62) and $\Delta H'' = -6.3 \pm 0.8$ kJ/mol for ethyl methyl ether (**7**) (63), the F_H factor is calculated to be 1.7 ± 0.3. This factor is correct for the methyl group but should be somewhat smaller for MeO. An interpolation of F_H assuming that F_H is a linear function of $\Delta G_C^{\circ\dagger}$, according to the procedure described in Section II.C, affords $F_H = 1.23$ for a OMe group connected to the $CH_3O—CH_2$ system. Therefore, $\Delta E_{AE} = \Delta E_H - 1.23 \times \Delta E_C = 21.1$ kJ/mol. Because in the *sc* conformers of **13** and **7** the appropriate torsion angles Θ' (20b) and Θ'' (64) (see Scheme 7) are both equal to about 70°, one may conclude that the geometries of **13** and **7** are very close, and the obtained factor, $F = 1.23$, should be treated as a more reliable value than that applied by Wiberg and Murcko ($F = 1.5$) (57).

[†]The use of ΔG_C° values instead of ΔH_C° seems to be justified because the relevant entropy differences $\Delta S°$ for H and Me are negligible (see Section II.F.).



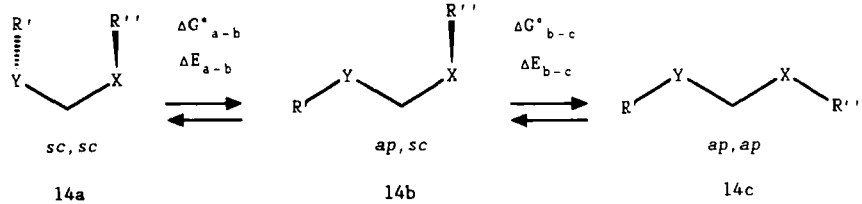
Scheme 7

Consequently, their approach led to a slight (by ca. 1.5 kJ/mol) overestimation of the anomeric effect ΔE_{AE}.

E. Bidirectionality of Anomeric Effect: Exo and Endo Anomeric Effects

1. *"Bidirectional" Approach*

In 1979 Lemieux et al. (65) suggested that the *exo anomeric effect* (see below) is stronger for the equatorial (β) anomers than for the axial (α) ones. A quantitative approach to this problem was subsequently presented by Praly and Lemieux (66). Let us look more carefully at equilibria in the R′—Y—CH_2—X—R″ system **14** (Scheme 8). If X and Y are atoms that allow an anomeric effect to operate, one has two possible contributing anomeric effects: one related to the preference for the *sc* arrangement of the X—C bond, and the second dealing with the conformation around the C—Y bond. The



Scheme 8

magnitudes of these effects in ΔG° terms are $\Delta G^\circ_{AE(a)X}$ for the C—X bond and $\Delta G^\circ_{AE(a)Y}$ for the C—Y bond in **14a** and $\Delta G^\circ_{AE(b)X}$ for the C—X bond in **14b**.

Let us examine equilibrium **14a** $\rightleftarrows$ **14b**. If only steric effects operated, the free energy difference for this process would be $\Delta G^\circ_{a-b(st)}$. However, anomeric effects influence the equilibrium. Substrate **14a** is stabilized by two partial anomeric effects $\Delta G^\circ_{AE(a)X}$ and $\Delta G^\circ_{AE(a)Y}$ while **14b** is stabilized by only one: $\Delta G^\circ_{AE(b)X}$. The free energy change for the reaction **14a** $\rightleftarrows$ **14b**, ΔG°_{a-b}, should then be given by Eq. [6]:

$$\Delta G^\circ_{a-b} = \Delta G^\circ_{a-b(st)} + \Delta G^\circ_{AE(a)X} + \Delta G^\circ_{AE(a)Y} - \Delta G^\circ_{AE(b)X} \quad [6]$$

$$\Delta G^\circ_{AE(a-b)} = \Delta G^\circ_{AE(a)X} + \Delta G^\circ_{AE(a)Y} - \Delta G^\circ_{AE(b)X} \quad [7]$$

Because no anomeric effect exists in **14c**, the relevant anomeric effect in **14b**, $\Delta G^\circ_{AE(b)X}$, is given by

$$\Delta G^\circ_{AE(b)X} = \Delta G^\circ_{b-c} - \Delta G^\circ_{b-c(st)} \quad [8]$$

According to Eq. [1], the magnitude of the anomeric effect found experimentally for the R′—Y—CH_2—X—R″ system as a whole, $\Delta G^\circ_{AE(a-b)}$, is represented by Eq. [7] as a difference of appropriate anomeric effects for the C—X and C—Y bonds. Usually $\Delta G^\circ_{AE(a)X} < \Delta G^\circ_{AE(b)X}$ because of competition between anomeric interactions around the C—X and C—Y bonds in **14a** (65,66). This is why the anomeric effect found for a molecule as a *whole* can take positive or negative values depending on the relative magnitudes of *all* the anomeric effects in Eq. [7]. Consequently, nothing can be said about magnitudes of individual anomeric effects in either segment of **14a** (66). On the other hand, for **14b**, $\Delta G^\circ_{AE(b)X}$ can be determined exactly if the **14b** $\rightleftarrows$ **14c** equilibrium is evaluated.

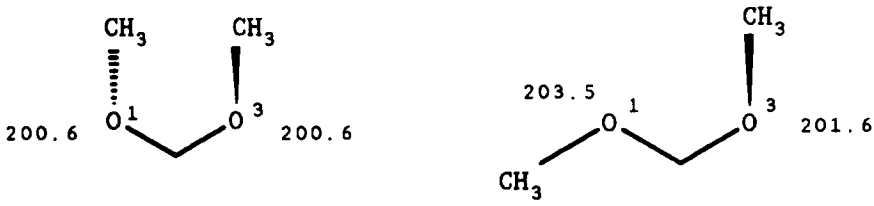
Analogous reasoning may be performed based on *ab initio* accessible ΔE values (see Scheme 8). The anomeric effect $\Delta E_{AE(a-b)}$ will be given by

$$\Delta E_{AE(a-b)} = \Delta E_{AE(a)X} + \Delta E_{AE(a)Y} - \Delta E_{AE(b)X} \quad [9]$$

where

$$\Delta E_{AE(b)X} = \Delta E_{b-c} - \Delta E_{b-c(st)} \quad [10]$$

The idea of competition between the anomeric interactions is strongly supported by an *ab initio* study (67) on proton affinities of oxygens in the *sc*, *sc* and *ap*, *sc* conformers of dimethoxymethane (**11**) (Figure 3). Deslongchamps (7a) suggested that oxygens involved in n_O–σ^*_{C-O} hyperconjugative interaction should be less basic than those not so engaged. Indeed, proton

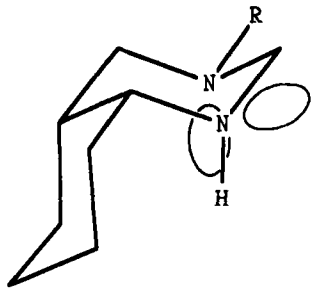


11(*sc*, *sc*) 11(*ap*, *sc*)

Figure 3. Proton affinities for oxygens in **11** (data from ref. 67).

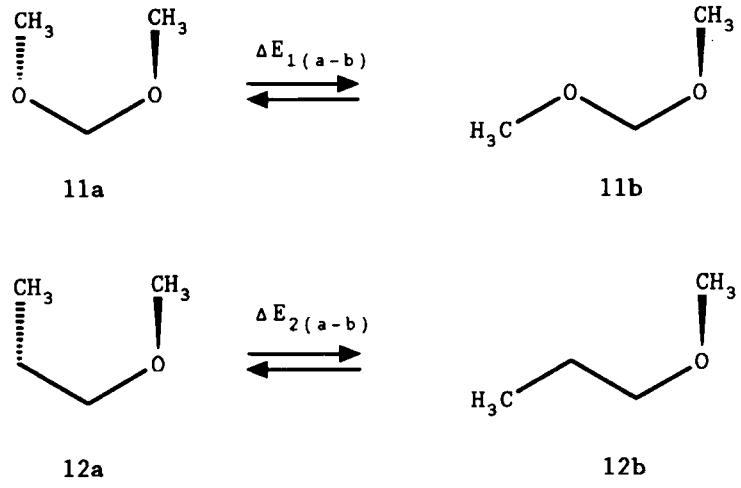
affinities of O(1) and O(3) in the *sc*, *sc* conformer, which both participate in the n_O–σ^*_{C-O} hyperconjugative interaction are the same (67). In the *ap*, *sc* conformer the competition cannot occur, and the proton affinity of the non engaged O(1) is larger than that of the only oxygen, O(3), participating in the n_O–σ^*_{C-O} interaction (67).

When the C—Y bond is a part of a ring, then $\Delta G^\circ_{AE,X}$ describes the *exo* anomeric effect (6a) and $\Delta G^\circ_{AE,Y}$ the *endo anomeric effect* following a suggestion by Booth and Khedhair (50). It must be noted, however, that Booth et al. (68) also extended the latter term to cases where both X and Y are members of the same ring, for example, in *cis*-decahydroquinazoline **15**; note that for this compound the term *exo* anomeric effect does not apply.



15

Praly and Lemieux (66) have estimated the *exo* anomeric effect to be 1.66 times as strong for β-anomers (*ap*, *sc*; here competition between anomeric effects cannot operate) as for α ones (*sc*, *sc*). In order to evaluate the corresponding relation between anomeric effects in an acyclic system, let us return to dimethoxymethane (**11**, Scheme 9). The anomeric effect ΔE_{AE} for the *ap*, *sc* conformer of **11**, calculated to be 21.1 kJ/mol (cf. Scheme 6),



Scheme 9

corresponds exactly to $\Delta E_{AE(b)X}$ (Eq. [10]). To find the anomeric effect, $\Delta E_{AE(a)}$, for a single *sc* fragment of the *sc*, *sc* conformation of **11**, one should examine processes shown in Scheme 9 (cf. Schemes 6 and 8) where $\Delta E_{1(a-b)}$ and $\Delta E_{2(a-b)}$ correspond to energy changes on going from the *sc*, *sc* to the *ap*, *sc* conformers of **11** and **12**, respectively. Wiberg and Murcko (57) computed the *ab initio* energy difference $\Delta E_{1(a-b)}$ as 10.12 kJ/mol (in reasonable agreement with the experimental (59) energy difference of 10.5 ± 0.8 kJ/mol). It should be pointed out that the *sc* conformation of the O—C—C—C fragment in **12** is unexpectedly *more stable* (57) than the *ap* one by $\Delta E_{2(a-b)} = +1.92$ kJ/mol.† If we then use a factor *F larger* than 1 (as for the *ap*, *sc* → *ap*, *ap* interconversion of **11**, *vide supra*) to correct $\Delta E_{2(a-b)}$ according to Eq. [5] in order to obtain the part of the energy change due to steric causes, $\Delta E_{1(a-b)st}$, we surprisingly find an *increase* of the preference for the *sc* arrangement when $Y = CH_2$ (Scheme 8) is replaced by an oxygen atom. This is rather difficult to reconcile with one's intuition that steric hindrance should increase as a result of the shorter C—O (as compared to the C—C) bond. For the sake of simplicity let us assume $F_E = 1$. Then, according to Eq. [9],

$$10.12 = 1.92 + \Delta E_{AE(a)Y} + \Delta E_{AE(a)X} - 23.8 \qquad [11]$$

†This unexpected conformational behavior may be considered as an effect arising from more effective σ_{C-H}-σ^*_{C-O} than σ_{C-C}-σ^*_{C-O} hyperconjugation. Recent semiempirical MO calculations by Graczyk (unpublished results) suggest that the magnitude of this effect may exceed 10 kJ/mol in compounds containing the C—C—C—OH_2^+ system.

For the symmetrical (C_2) *sc, sc* conformation of **11**, $\Delta E_{AE(a)Y} = \Delta E_{AE(a)X} = \Delta E_{AE(a)}$ and

$$\Delta E_{AE(a)} = 0.5(21.1 + 10.12 - 1.92) = 14.6\,\text{kJ/mol} \qquad [12]$$

The relative magnitude of the anomeric effects in the *ap, sc* and *sc, sc* conformers of **11** is then 21.1/14.6 = 1.44, in rather good agreement with the ratio of 1.66 estimated previously for cyclic systems (66) (*vide supra*).

The calculation presented above was based on the assumption that anomeric interactions that refer to C—X and C—Y bonds are equal in the *sc, sc* conformer because of symmetry. Usually, however, this is not the case and one can estimate exactly only the anomeric effect $\Delta E_{AE(b)X}$. Even if all other data in Eq. [9] are available, one can only compute the sum $\Delta E_{AE(a)Y} + \Delta E_{AE(a)X}$. Thus, in general, the exo anomeric effect according to the definition of Praly and Lemieux can be established exactly for the *ap, sc*

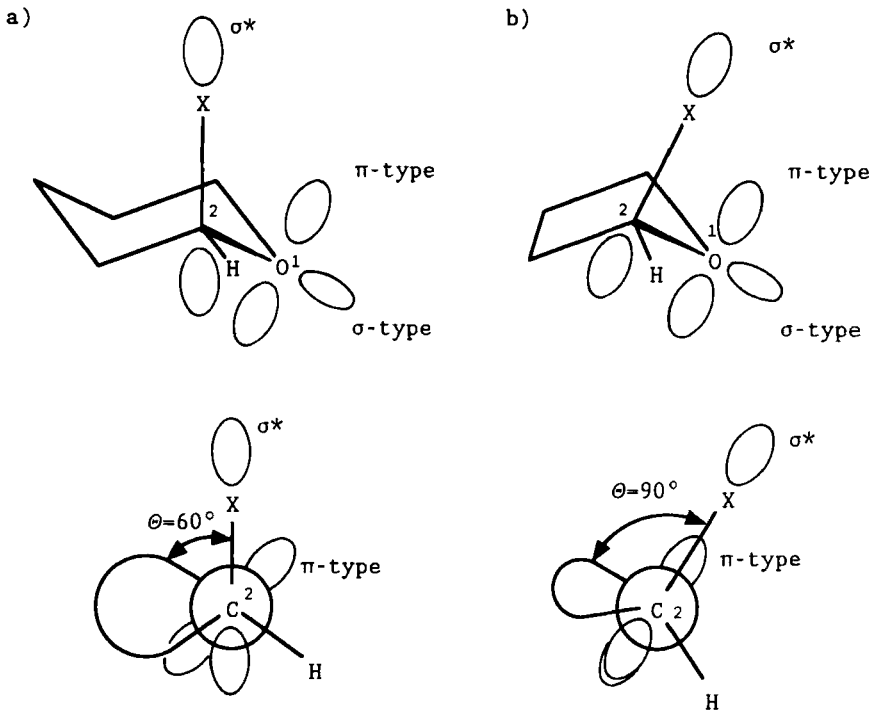
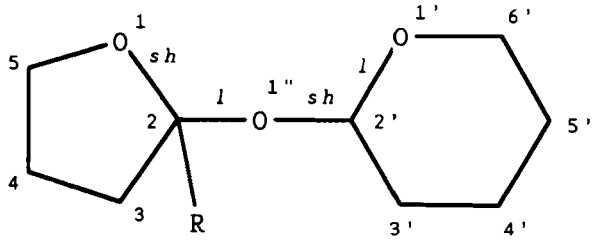


Figure 4. Endo n_O–σ^*_{C-X} hyperconjugative interactions in 2-substituted (a) tetrahydropyran and (b) tetrahydrofuran.

conformers only (it is equivalent to that expressed by Eq. [4]). Nevertheless, this approach has a great interpretative power.

If $R' \neq R''$, $\Delta G^{\circ}_{AE(a)X}$ (Eqs. [6] and [7]) may even be smaller than anticipated on the basis of simple competition between two anomeric effects in the *sc*, *sc* conformer. Such a situation occurs when Y = oxygen is part of a six-membered (e.g., tetrahydropyranyl) ring (Figure 4a; see also Sections III.B.4 and IV.B.1). Since oxygen lone pairs are not equivalent, the arrangement of the π-type lone pair of endocyclic oxygen and the σ^* orbital of the exocyclic C—X bond is not optimal for participation in n–σ^* interaction [C(6)—O(1)—C(2)—X torsion angle $\Theta = 60°$]. Therefore the endo anomeric effect is weak. In contrast, the exo effect is much stronger than the endo one because anomeric interactions in the former are less constrained thanks to the relative freedom of the substituent to attain the optimal rotational arrangement about the exocyclic C—X bond. In five-membered (tetrahydrofuranyl) rings endo interactions are much more effective (Figure 4b, $\Theta = 90°$, the π lone pair and σ^* orbital are collinear) and the difference in strength of the *exo* and *endo* anomeric effects is less (see Section IV.B.1)†.

The competition between the anomeric effects in C—O—C—O—C system is evidenced by the effect of anomeric interactions in disaccharides **16** on bond lengths about the anomeric carbons C(2) and C(2'). The statistical analysis of 677 C—O—C—O—C fragments taken from the Cambridge Crystallographic Database showed (69) that, in hindered $\alpha\alpha'$ structures **16** (R ≠ H) with the C5—O1—C2—O1″ and C2—O1″—C2′—O1′ torsion angles close to 90°, a specific alternation between short (*sh*) and long (*l*) C—O bond lengths occurs (see Figure 5). Since strong anomeric hyper-



16

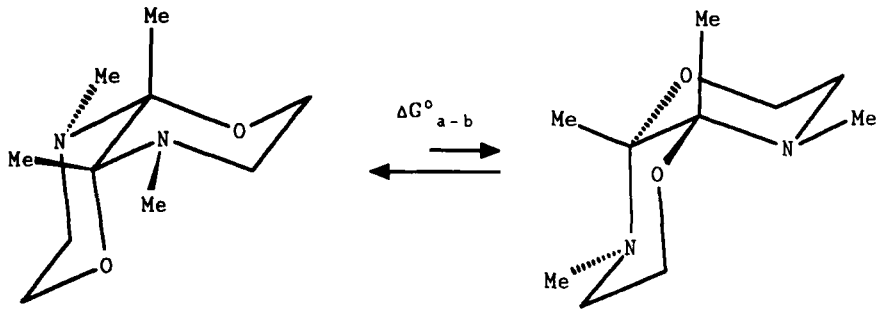
Figure 5. Short (*sh*) and long (*l*) bonds in disaccharides **16**.

†The importance of orientation of the lone electron pairs on nitrogen (involved in anomeric interaction in H—N—C—O systems) for the strength of the anomeric effect about the C—O bond is discussed for compound **83** in Section II.I.

conjugative interactions are reflected in a shortening of the donor–carbon bond (see Section IV.B.1), the observed results can be interpreted in terms of a dominant *endo* anomeric effect in the furanose ring (short C2—O1 and long C2—O1″ bond) and a dominant *exo* anomeric effect for the pyranose ring (short O1″—C2′ and long C2′—O1′ bonds). Moreover, they support the nonequivalence of oxygen lone electron pairs with π-type pair participating most effectively in the hyperconjugative interaction.

Large differences in the magnitude of the endo and exo anomeric effects can also be anticipated for different heteroatoms (which both possess lone pairs) connected to the same central atom, as in 2-aminotetrahydropyrans (**2**, X = N <). Due to a much stronger donor ability of nitrogen lone pairs compared to those on oxygen [the lone pair on nitrogen is higher lying in energy than the lone pair on oxygen by 170 kJ/mol (70)], the *exo* effects about the C—N bond ($\Delta G^{\circ}_{AE(a)X}$ and $\Delta G^{\circ}_{AE(b)X}$ in Eq. [7]; X = N) are much stronger than the *endo* one (about the C—O bond; $\Delta G^{\circ}_{AE(a)Y}$ in Eq. [7]; Y = O). Therefore, the observed anomeric effect for the whole system, $\Delta G^{\circ}_{AE(a-b)}$, is mainly dependent on the difference between $\Delta G^{\circ}_{AE(a)N}$ and $\Delta G^{\circ}_{AE(b)N}$. Because $\Delta G^{\circ}_{AE(a)N} < \Delta G^{\circ}_{AE(b)N}$ (lack of competition between anomeric effects in **14b**; Scheme 8), the observed anomeric effect $\Delta G^{\circ}_{AE(a-b)}$ should be small or even reversed, as is observed (50, 71, 72). This is why amino groups at C(2) in a tetrahydropyran ring were suspected to exhibit the so-called reverse anomeric effect (8, 50, 70) (see Section II.I). However, Franck (49) showed that a small anomeric effect is in fact exhibited by the 2-aminotetrahydropyran system.

An elegant manifestation of the importance of the relative strength of the exo and endo anomeric interactions was presented by Alcaide et al. (73) based on 1,5-dioxa-4,8-diazadecalin **17** (Scheme 10). Owing to the expected



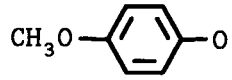
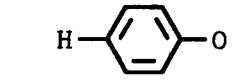
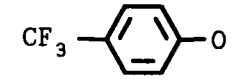
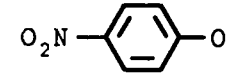
17a 17b

Scheme 10

large difference between the strengths of $n_O-\sigma^*_{C-N}$ and $n_N-\sigma^*_{C-O}$ negative hyperconjugation, compound **17** exists preferentially in conformation **17a** with the oxygen in axial and nitrogen atoms in equatorial positions. The authors estimated (73) $\Delta G^\circ_{a-b} = 3.7$ kJ/mol at 298 K for this equilibrium and interpreted this quantity as a free energy difference between two $n_N-\sigma^*_{C-O}$ and $n_O-\sigma^*_{C-N}$ interactions in **17**.

As may be expected based on the hyperconjugative origin of the anomeric effect (see Sections III.B.4 and III.B.5), the relative strength of the *endo* and *exo* anomeric interactions should be influenced by changes in electronegativity of X and/or Y (Scheme 8). Thus, an increase in electronegativity of X should lead to a decrease of donor properties of X and/or an increase of acceptor abilities of the antibonding σ^*_{C-X} orbital. As a consequence the *endo* anomeric interactions are stronger and $\Delta G^\circ_{AE(a)X}$ and $\Delta G^\circ_{AE(b)X}$ in Eq. [7]

TABLE 3
Conformational Equilibria in Variously Substituted Tetrahydropyrans (Scheme 1a)

Compound No.	X	ΔG°_H (kJ/mol)	Reference
18	$ClCH_2CH_2O$	3.1[a]	74
19	Cl_2CHCH_2O	5.0[a]	74
20	Cl_3CCH_2O	7.5[a]	74
21	CH_3CH_2O	0.38[b]	75
22	FCH_2CH_2O	0.49[b]	75
23	F_2CHCH_2O	0.56[b]	75
24	F_3CCH_2O	0.74[b]	75
25		1.7[c]	76
26		2.3[c]	76
27		2.5[c]	76
28		2.9[c]	76

[a] Neat, at 311 K.
[b] In CD_2Cl_2, calculated from ΔH° and ΔS° values for 273 K.
[c] In CF_2Br_2/CD_2Cl_2 (92/8) at 156 K.

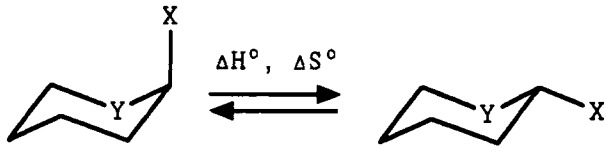
must decrease, while $\Delta G^{\circ}_{AE(a)Y}$ increases. Finally, one should observe an increase in $\Delta G^{\circ}_{AE(a-b)}$ and an increase in the preference for the *sc*, *sc* arrangement.

The above relationship has indeed been observed for 2-substituted tetrahydropyrans (Y = O, X = variable). The relevant data are collected in Table 3. It is clear that the ΔG°_{H} values increase with the increasing number of electron-withdrawing substituents (Cl or F) at the β-carbon of the ethyl group (compounds **18–20** and **21–24**). An analogous order connected with the increasing electron-withdrawing character of the substituent was found (76) for 2-aryloxytetrahydropyrans (compounds **25–28**).

An extreme possibility for the anomeric effect is one-directionality. Such a situation occurs when there is no competition between the anomeric effects, that is, when both $\Delta G^{\circ}_{AE(a)X}$ and $\Delta G^{\circ}_{AE(b)X}$ are equal to zero. Then $\Delta G^{\circ}_{AE(a-b)} = \Delta G^{\circ}_{AE(a)Y}$ (cf. Eq. [7]) and the observed anomeric effect for a molecule is equal to the *endo* anomeric effect. If one takes into account only the hyperconjugative origin of the anomeric effect (see Sections III.B.4 and III.B.5), this would happen for substituents X lacking a lone electron pair α to the anomeric carbon atom (e.g., X = COOR). Such substituents offer a great opportunity to study the importance of the *endo* anomeric interactions

TABLE 4

Thermodynamic Parameters for Equilibria in Selected 2-substituted Heteroanes **29–34**[a] and Relevant Anomeric Effect ΔH°_{AE}



Compound No.	Y	X	ΔH° (kJ/mol)	ΔS° (J mol^{-1} deg^{-1})	ΔH°_{AE}[b] (kJ/mol)
29[c]	CH_2	COOMe	−5.20 ± 0.63	−2.6 ± 3.3	0
30[c]	O	COOMe	−7.1 ± 1.0	−18.8 ± 6.1	0.5
31[c]	NH	COOMe	−2.26 ± 0.29	3.0 ± 1.5	4.5
32[d]	CH_2	C≡N	−0.762 ± 0.030	0.00 ± 0.17	0
33[e]	O	C≡N	1.51 ± 0.29	−3.5 ± 1.6	2.3
34[e]	NH	C≡N	9.3 ± 2.3	24. ± 11.	10.1

[a] From ref. 42.

[b] Calculated based on Eqs. [17] and [18].

[c] In Ether/toluene-d_8 (3:1; v/v).

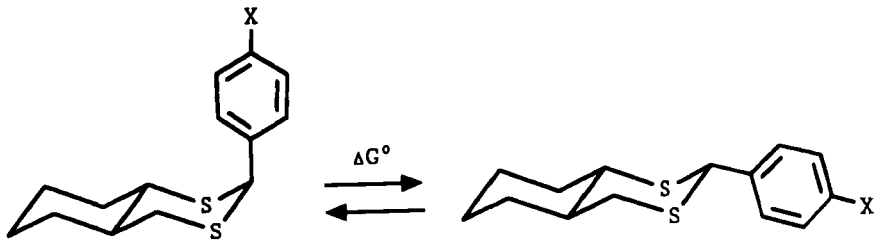
[d] In $CFCl_3$, data taken from ref. 77.

[e] In $CFCl_3/CDCl_3$ (85:15; v/v).

in their "pure" form. This has recently been done by Booth et al. (42) in ΔH° terms for 2-carbomethoxy and 2-cyanotetrahydropyrans and piperidines **29–34** (Table 4). The relevant steric interactions were estimated (42) based on cyclohexane derivatives (compounds **29** and **32**). However, the conclusion of Booth et al. (42) that for **30** one can observe an increased preference for the equatorial conformation [in contrast to the results of Tschierske et al. (38)] is not supported by the data presented. Application of Franck's methodology (Section II.F, Eq. [18]) to the estimation of the relevant steric interactions $\Delta H^\circ_{H(st)}$ experienced by X = COOMe in the tetrahydropyran system affords $\Delta H^\circ_{H(st)} = -5.20 \times 1.46 = -7.59$ kJ/mol, assuming a factor F_H of 1.46 (see Section II.F). Therefore, the observed equatorial preference of X = COOMe in a tetrahydropyran ring (−7.1 kJ/mol) is smaller than that expected based on steric interactions (−7.59 kJ/mol), in qualitative agreement with the results of Tschierske et al. (38). The difference, equal to $-7.1 - (-7.59) = 0.5$ kJ/mol, reflects the magnitude of the *endo* anomeric effect in the O—C—COOMe system in ΔH°_{AE} terms (see Eq. [17], Section II.F). By the same token we calculated other ΔH°_{AE} values and placed them in the last column of Table 4 (F_H values for **31**, **33**, and **34** were taken from Section II.F). It is evident that the *endo* anomeric effect involving Y = NH as a donor is stronger than that for Y = O, as expected (see Section III.B.4). A comparison of compounds **30** with **33** and **31** with **34** shows that the cyano group participates in the anomeric interactions more effectively than the carbomethoxy group.

It should be added that one-directionality of the anomeric interactions could be responsible in part for a strong anomeric effect in 1,3-dioxane derivatives containing COOEt [$\Delta G^\circ_{AE} = 9.4$ kJ/mol (38)] and $Ph_2P(O)$ [$\Delta G^\circ_{AE} = 19.7$ kJ/mol (78), see also Section V.A] groups bonded to the C(2) atom of the 1,3-dioxane ring. When a group attached to C(2) participates in an interaction that destabilizes the equatorial isomer, as has been suggested by us (79) for Y—C(2)—P=Z (Y = O, S; Z = O, S, Se) anomeric interactions (see Section V.B), the $\Delta G^\circ_{AE(b)X}$ value is negative, which enhances the observed axial preference.

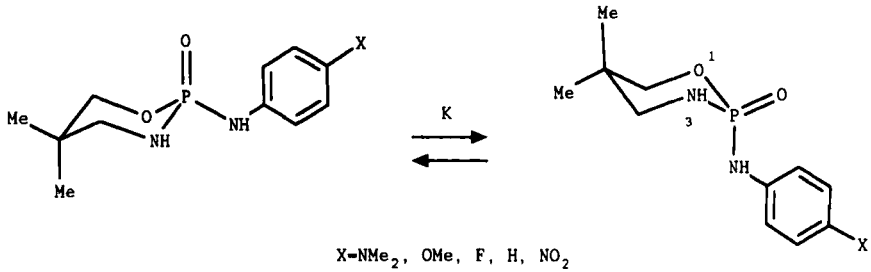
The reasoning presented above has usually been applied as a test for the hyperconjugative origin of the anomeric interactions investigated. Thus, the linear increase in free energy ΔG° for the equilibrium in 2-*para*-substituted aryl-1,3-dithiadecalins **35** (Scheme 11) with the Hammett constant σ_P (which describes electron-withdrawing properties of X) was interpreted in terms of n_S–σ^*_{C-C} negative hyperconjugation, with the antibonding σ^*_{C-C} orbital of the anomeric carbon–aryl carbon bond in **35a** as an acceptor (80). A linear dependence between log K (K = equilibrium constant) and σ_P for **36** (Scheme 12) was also interpreted by Bentrude et al. (81) in terms of a predominance of the *endo* anomeric effect involving overlap of the endocyclic N(3) and



35a 35e

X = OMe, Et, H, Cl, CN, NO_2

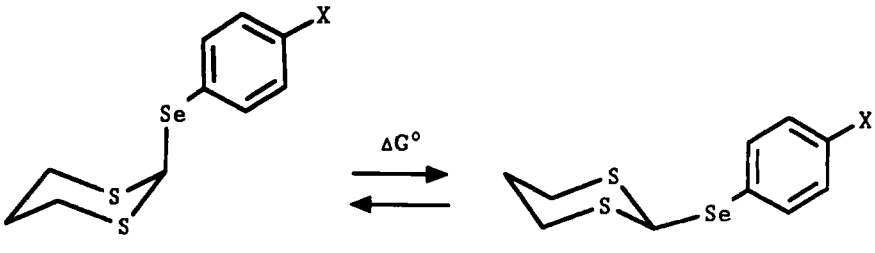
Scheme 11



X=NMe_2, OMe, F, H, NO_2

36a 36b

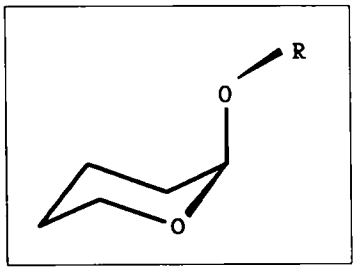
Scheme 12



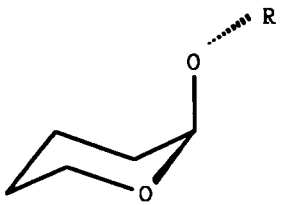
37a 37e

X = NMe_2, OMe, Me, H, F, Cl, CF_3, NO_2

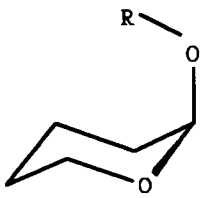
Scheme 13



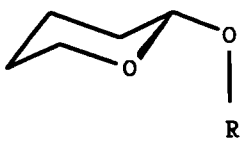
38(*sc*,*sc*)



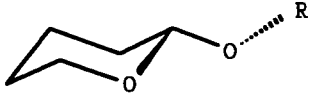
38(*sc*,*ap*)



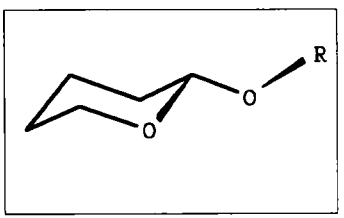
38(*sc*,*-sc*)



38(*ap*,*sc*)



38(*ap*,*ap*)



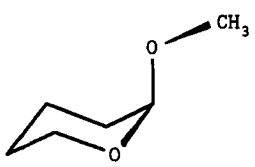
38(*ap*,*-sc*)

O(1) lone electron pairs with the σ^*_{P-N} orbital of the axial P—N bond in **36b**. An analogous approach enabled Pinto et al. (82–84) to argue for a stabilizing hyperconjugative interaction n_S–σ^*_{C-Se} as being responsible for the conformational behavior in 2-arylseleno-1,3-dithianes **37** (Scheme 13). The ΔG° values increased (84) from 2.0 kJ/mol for $X = NMe_2$ to 3.8 kJ/mol for $X = NO_2$.

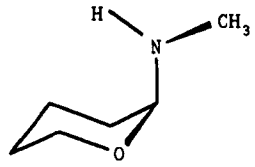
2. *"Nondirectional" Approach*

Usually, however, the *exo* anomeric effect is defined (6a, 65) as a preference for the *gauche* conformation about the exocyclic C—OR bond in the O—C—O—R system of 2-alkoxytetrahydropyrans **38** [i.e., **38** (*sc*, *sc*) and **38** (*ap*, $-sc$) are the energetically preferred species], or generally as the preference for the *gauche* conformation about the exocyclic C—XR bond in a Y—C—X—R system (where Y and C are part of a ring).

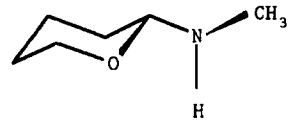
This problem was studied in detail by Booth et al. (85) for solutions of 2-methoxytetrahydropyran (**39**) and 2-methylaminotetrahydropyran (**40**) by means of NMR methods. In the case of the axial OMe group the results unequivocally showed a predominance of the **39** (*sc*, *sc*) conformer. The presence of the *sc*, *ap* rotamer was confirmed, but its relative abundance could not be estimated. In the equatorial conformer the major rotamer was shown to be the *ap*, $-sc$ one. The second, minor isomer was found to be the *ap*, *sc* one, but its proportion was again not stated. Similar results were obtained for 2-alkoxytetrahydropyran derivatives by Touboul and Dana (86) by means of infrared spectra (see Section IV.B.3.c), though the presence of the *ap*, *sc* conformation was not supported.



39(*sc*, *sc*)



40(*sc*, *sc*)



40(*ap*, -*sc*)

When a methylamino group was situated equatorially, Booth et al. (85) found that the preferred species was **40** (*ap*, $-sc$) having the nitrogen lone pair antiperiplanar to the endocyclic C(2)—O bond ($-sc$ arrangement of the O—C—N—C system). For the axial methylamino group the preferred rotamer **40** (*sc*, *sc*) also had the *gauche* arrangement of the O—C—N—C

system with the nitrogen lone electron pair antiperiplanar to the C(2)—O bond.

According to the structure correlation method (87), a distribution of sample points corresponding to observed crystal structures will tend to concentrate in low-lying regions of the potential energy surface. Thus, the energetic superiority of the synclinal arrangement about the exocyclic carbon–oxygen bond has been strongly supported by statistical analysis of carbohydrate structures. Cosse-Barbi and Dubois (60) showed that for 174 fragments taken from 178 axial pyranosides the O—C1—O—R torsion angle [O(1)—C(2)—O—R according to the heterocyclic convention] varies in the range from 54° to 125° (mean 77.0°, σ 19.4°), while for 121 fragments taken from 127 equatorial forms this angle varies from 54° to 105° (mean 77.2°, σ 18.8°).

A more rigorous treatment of the data retrieved from the Cambridge Structural Database by Schleifer et al. (88) confirmed, in general, the results of Cosse-Barbi and Dubois (60). In the whole population of 212 structures they found (after selection and rejection of *sc*, $-sc$, 1,3-dioxane and 1,3-dioxolane derivatives) 119 *sc*, *sc*, 90 *ap*, $-sc$, and 3 *ap*, *ap* fragments. Interestingly, the two statistical analyses here presented did not support the importance of the *ap*, *sc* conformation of the C—O—C—O—R system suggested by Booth et al. (85). It should be added that Schleifer et al. (88) did not find any correlation between bond lengths and angles with the magnitude of the O—C1—O—R dihedral angle. Therefore, their earlier hypothesis (89) concerning a dependence of the strength of the *exo* anomeric effect on the orientation of the n_π lone electron pair of endocyclic oxygen was not supported. This may be due, perhaps, to an insufficient database, since in the case of furanoses, high-level *ab initio* calculations (90) revealed that the lengths of the exocyclic C1—O and C1—H1 bonds vary in length, depending on their disposition with respect to the lone-pair orbitals of the ring oxygen.

It must be noted that the observed preference for the *sc*, *sc* and *ap*, $-sc$ arrangements could also be expected solely on steric grounds, assuming that the interaction between exocyclic OR group and endocyclic oxygen is less stringent than that with the C(3)H_2 methylene group [Figure 6; *sc*, $-sc$ and *ap*, *sc* conformers were rejected based on *gauche* interactions with both O(1) and CH_2]. Indeed, the concept of the *exo* anomeric effect with respect to the conformation about the exocyclic C—O bond has recently been criticized by Kishi's group (91–95) who showed a similarity in a conformational behavior between *O*-glycosides and *C*-glycosides (CH_2—R instead of O—R). On the other hand, the completely different conformational behavior of spiro ether **41** compared with that of spiro ketal **42**, which can be considered good models for *C*- and *O*- glycosides, respectively, led Deslongchamps and Pothier (96a) to the conclusion that the preferred occurrence of the above-discussed

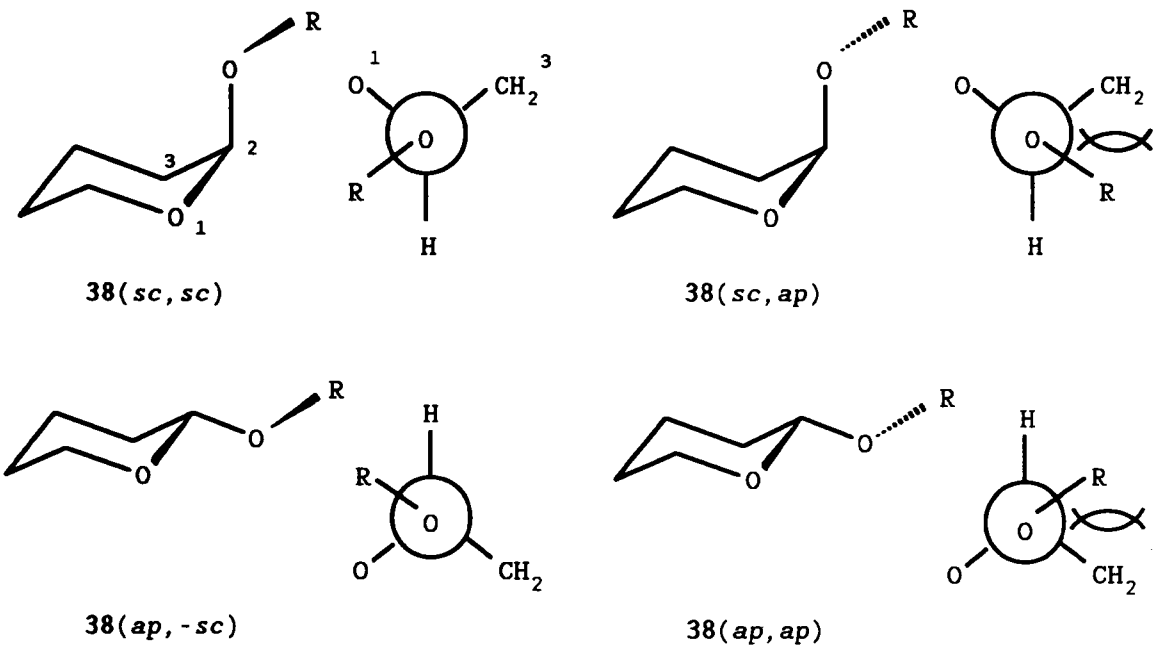
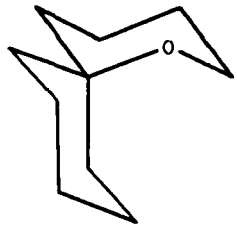
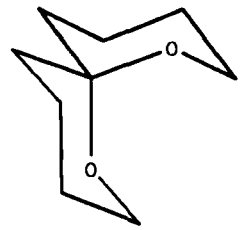


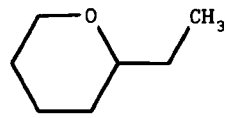
Figure 6. Steric interactions in 2-alkoxytetrahydropyrans **38**.



41

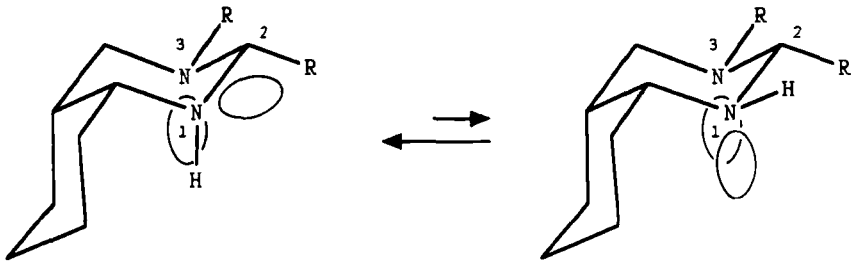


42



43

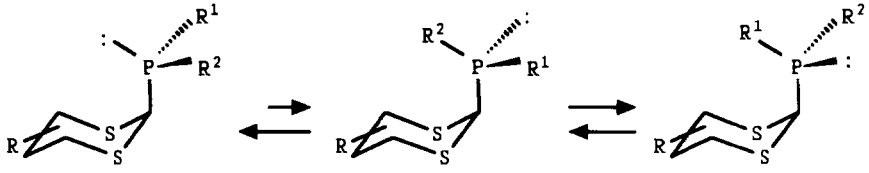
rotamers in α- and β-*O*-glycosides must result from a combination of steric and stereoelectronic (more precisely hyperconjugative) effects. Tvaroška and Bleha (13) noted that 2-ethyltetrahydropyran (**43**) should serve as a benchmark to assess steric interactions inherent in the *exo* anomeric effect, but the detailed conformational energetics of this molecule have not been available. It must be added that based on the preferred conformation of the two decahydroquinazolines **15** (Scheme 14; R = H, Me), namely **15a** in which N(1)—H is axial and the N(1) lone pair is equatorial, Booth et al. (68) concluded that the n_N–σ^*_{C-N} hyperconjugative interaction in **15a** can outweigh steric repulsions experienced in **15a** by the axial N(1)—H hydrogen. Unfortunately, they did not take into account the rabbit ear effect (see Section III.A.4) which could be, at least in part, responsible for destabilization of **15e.**



15a 15e

Scheme 14

The importance of steric factors in conformational behavior about the axial carbon–heteroatom bond was seen by us (54, 96b) in axial 2-phosphino-1,3-dithianes **44** (Scheme 15) whose rotational isomerism was studied by NMR methods. We had expected that if the *exo* anomeric interactions in the C—S—C—P(:) system were strong, the preferred rotamers should be T^+



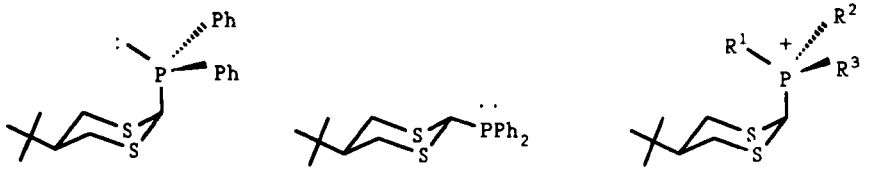
44(G) 44(T^+) 44(T^-)

R^1, R^2 = Ph, Me

R = H, 5,5-Me_2, tBu, *cis*-4,6-Me_2

Scheme 15

and T^- having R^2 or R^1 located over the 1,3-dithiane ring. Surprisingly, we found in the ^1H NMR spectrum of **45a** that the shielding effect of the phenyl group(s) is not observed, and therefore both phenyl groups must be located *exo* [as in the rotamer **45a**(G)]. In particular, in **45a** the chemical shift of the *t*-Bu protons is $\delta_{t\text{-Bu}}$ 0.92 ppm, while in its epimer **45e** and in the parent, unsubstituted 5-*t*-butyl-1,3-dithiane (**47**) it is equal to δ 0.87 (in CD_2Cl_2) and 0.92 (in $CDCl_3$) ppm, respectively (54). On the other hand, in all salts, **46a,** in which at least one R is phenyl, shielding by 0.3 ppm is actually observed; for example, for $R^1 = R^2 = Me$, $R^3 = Ph$ the chemical shift of *t*-Bu group $\delta_{t\text{-Bu}}$ is equal to 0.59 ppm, thus suggesting the *endo* position of the phenyl group. Of course, when $R^1 = R^2 = R^3 = Me$, $\delta_{t\text{-Bu}}$ is not influenced and is 0.91 ppm. The lack of the shielding effect of the phenyl group can also be observed for other nuclei in the C(4)—C(5)—C(6) region (54, 96b).



45a(G) 45e 46a

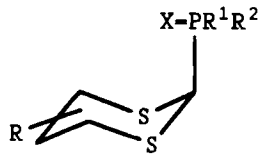
R^1, R^2, R^3 = Ph, Me

Very strong support for the conclusions presented above, which were based on the shielding effect of phenyl rings, is provided (54, 96b) by the coupling constant $^3J_{C(4,6)-P}$ in the ^{13}C NMR spectra of axial 2-phosphino-1,3-

dithianes **44** (R^1, R^2 = Ph, Me). Interestingly, this coupling constant is large (ca. 7–8 Hz), in contrast to that in the relevant axial 2-phosphoryl-1,3-dithianes **48** (54, 97) and 2-phosphonio-1,3-dithianes **46a** (54, 98), which is equal to zero. This observation may be attributed to the presence of the phosphorous lone electron pair in **44** being located *endo;* it is due to the orientational effect of this pair on the C—P coupling. It was demonstrated both experimentally (99–102) and theoretically (103, 104) that the P lone pair is an efficient spin information transmitter. Thus, because of the spatial proximity of the P and C(4,6) atoms in **44**(G), the magnitude of the coupling seems to be governed by through-space interaction, which should be of a maximum for the lone pair lying over the 1,3-dithiane ring.



47



48

X=O, S, Se

R^1, R^2 = Ph, OMe, OEt, OCH_2CF_3

Thus, the *exo* anomeric effect is not manifested in the C—S—C—P(:) system, in contrast to what has been observed for the C—O—C—N system by Booth et al. (85) (**40**, *vide supra*). This finding has serious consequences, insofar as the origin of the anomeric effect in this system is concerned. They will be discussed in Section V.B.1.

It must be added that 2-phosphino-1,3-dithianes **44** provide a very interesting example of noncompetitive hyperconjugative anomeric interactions in a system where both heteroatoms Y = S and X = P (Scheme 8) possess lone electron pairs. In the equatorial conformer the *endo* interactions cannot operate, while in the axial one the exo effect is not manifested.

A quantitative approach to the exo anomeric effect, $\Delta G^\circ_{AE(exo)}$, in **14** (Scheme 8) should be based on Eq.[1]. Thus, the exo anomeric effect in **14a** is equal to

$$\Delta G^\circ_{AE(a)exo} = \Delta G^\circ_{a-b} - \Delta G^\circ_{a-b(st)} \qquad [13]$$

and in **14b** it is

$$\Delta G^\circ_{AE(b)exo} = \Delta G^\circ_{b-c} - \Delta G^\circ_{b-c(st)} \qquad [14]$$

A comparison of Eqs. [13] and [14] with Eqs. [6] and [8], respectively, shows that

$$\Delta G^{\circ}_{AE(a)exo} = \Delta G^{\circ}_{AE(a)X} + \Delta G^{\circ}_{AE(a)Y} - \Delta G^{\circ}_{AE(b)X} \quad [15]$$

and

$$\Delta G^{\circ}_{AE(b)exo} = \Delta G^{\circ}_{AE(b)X} \quad [16]$$

Therefore, the two definitions of the *exo* anomeric effect are equivalent as far as the effect in the *ap*, *sc* conformer is concerned but are different for the *sc*, *sc* conformer. In particular, since $\Delta G^{\circ}_{AE(a)X} < \Delta G^{\circ}_{AE(b)X}$ (due to a competition of anomeric interactions in **14b**), the $\Delta G^{\circ}_{AE(a)exo}$ value should always be smaller than $\Delta G^{\circ}_{AE(a)Y}$.

Finally, it must be noted that the conformational behavior characteristic of the *exo* anomeric effect could be reproduced not only by MO calculations but also using molecular mechanics methods, as was shown by Navio and Molina (105) for twelve 2-alkoxytetrahydropyran derivatives **38** (Figure 6) (see Section III.A.6).

F. Enthalpic Anomeric Effect

A simple theoretical consideration of possible destabilizing interactions in axial and equatorial conformers of ethyl- and isopropylcyclohexane (**1**, X = Et, *i*-Pr, respectively) as well as the results of isomerization of the appropriate 1,3- and 1,4-dialkylcyclohexanes led Allinger and Hu as early as in 1962 to the conclusion that the free energy difference ΔG° for ethyl (106) and isopropyl (107) groups in cyclohexane should not differ markedly from that for the methyl group. This conclusion was subsequently supported (108) by a calculation using a modified Westheimer method. Soon, the Allinger group improved the calculations and found (109) that the enthalpy differences ΔH° *increase* on going from Me to Et to *i*-Pr (see Table 5) in a trend opposite to that expected on the basis of the "size" of a substituent. They also predicted (109) that the magnitude of the enthalpy change is more than compensated for by an opposing entropy change on passing from Me to Et to *i*-Pr. Therefore, at 298 K, the relevant ΔG° values should *decrease* on going from Me to Et to *i*-Pr. Interestingly, both the ΔH° and ΔG° values for the *t*-Bu group (which both are equal to -22.6 kJ/mol) are very low, in agreement with expectation based on the very large size of this group.

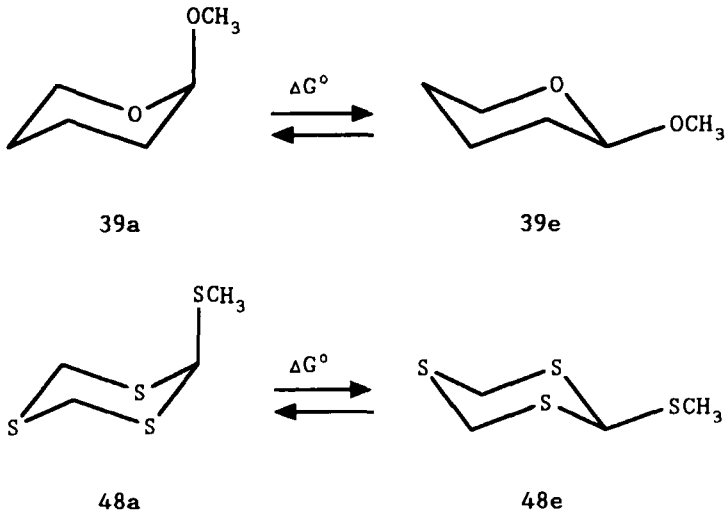
In 1980 Booth and Everett (22) confirmed the prediction of Allinger et al. (109) and showed experimentally that the relative equatorial preference of alkyl groups in a cyclohexane ring depends on temperature because of large dif-

TABLE 5
Calculated Thermodynamic Data for Conformational Equilibrium in Alkylcyclohexanes 1

X	ΔH° (kJ/mol)	ΔS° (J/mol/K)	ΔG°_{298} (kJ/mol)	ΔG°_{40} (kJ/mol)
Me	−7.41	0	−7.41	−7.41
Et	−7.07	2.55	−7.83	−7.17
i-Pr	−5.86	9.12	−8.58	−6.22
t-Bu	−22.6	0	−22.6	−22.6

From ref. 109; see Figure 1.

ferences in entropy, ΔS°, between Me, Et, and *i*-Pr. Thus, while at room temperature the equatorial preference increases in the order Me < Et < *i*-Pr, it is reversed below about 40 K.† Two years later Booth et al. (110) found that for the **39a** ⇄ **39e** equilibrium (Scheme 16) ΔG° is largely determined by the $T\Delta S^\circ$ rather than the ΔH° term. In order to eliminate temperature-dependent entropy-based contributions to the anomeric effect, Booth and Khedhair (50) proposed to evaluate the anomeric effect in ΔH°_{AE} terms (Eq. [17]; ΔH° instead



Scheme 16

†See Table 5. According to these data (109), the reversal should occur somewhere just above 130 K.

of ΔG° in Eq. [1]) and presented an application of this approach to simple tetrahydropyran derivatives:

$$\Delta H^\circ_{AE} = \Delta H^\circ_{H} - \Delta H^\circ_{H(st)} \quad \text{where } \Delta H^\circ_{H(st)} = \Delta H^\circ_{C} \qquad [17]$$

Booth and Khedhair (50) suggested that the smaller entropy, $\Delta S^\circ = -11.3$ J/mol/K, of the equatorial conformer stems from a stronger *exo* anomeric effect in **39e**. Interestingly, if oxygen is replaced by sulfur as in **48a** $\rightleftarrows$ **48e** the entropy of the equatorial conformer is *larger* (111) by $\Delta S^\circ = 16.7 \pm 8.4$ J/mol/K. This diversity of ΔS° values implies that consistency between ΔS° and the strength of anomeric effect is fortuitous and is best explained in terms of solvent–solute interactions (66), although the increased C—OMe bond order (resulting in less rotational freedom) in the equatorial conformer due to the stronger *exo* anomeric effect was invoked as well (89). Still, the proposal by Booth et al. (42, 50, 110, 112) to use temperature-independent enthalpy (ΔH°) instead of free energy (ΔG°) differences to estimate the magnitude of anomeric effects seems to be justified. Appreciable entropy effects can affect the "steric size" at different temperatures (71).

The approach originated by Booth is becoming increasingly accepted (12, 18, 113). Booth et al. have recently presented an estimation of the enthalpic anomeric effect in 2-methoxytetrahydropyran (**39**) (p. 186), 2-(2′,2′,2′-trifluoroethoxy)tetrahydropyran (**24**) (112) (Table 3), and carbomethoxy (COOMe) and cyano (CN) derivatives of tetrahydropyran (**30** and **33**, respectively, Table 4) and piperidine (**31** and **34**, respectively) (42). Unfortunately Franck's suggestion (Section II.C) has been overlooked in this endeavor, and ΔH°_{AE} values have been evaluated (42, 50, 71, 112) according to Eq. [17].

Very recently Juaristi and Cuevas (55) estimated the enthalpic contribution ΔH°_{AE} to the S—C—P(O) anomeric effect following Franck's method (according to Eq. [17], $\Delta H^\circ_{H(st)}$ given by Eq. [18]; see also Section II.C):

$$\Delta H^\circ_{H(st)} = F_H \times \Delta H^\circ_{C} \qquad [18]$$

It must be noted, however, that the factor $F = 0.60$ was determined based on the free energy ΔG° values for the *t*-butyl group. Neither was factor F_H based on ΔH° values ($F_H = 0.99$, *vide infra*) nor was any interpolation of F performed.

An analogous treatment to that presented in Section II.C can be performed in order to estimate the necessary F_H values. Since for the reference groups, H, Me, and *t*-Bu , the relevant entropy differences ΔS° are practically equal to zero (*vide supra*), $\Delta G^\circ \cong \Delta H^\circ$ and $F_G \cong F_H$. However, the relation between the size of substituents [e.g., $Ph_2P(O)$, OMe, COOMe, CN] based on ΔH°_C values (where known) is different from that based on ΔG°_C values (see

Table 2). Hence, an interpolation for these groups will afford factors F_H that differ from F_G.

An application of the $\Delta G_C^\circ \cong \Delta H_C^\circ$ values collected in Table 1 and ΔH_C° from Table 2 ($\Delta G_C^\circ \cong \Delta H_C^\circ$ was assumed for *t*-Bu) as well as ΔH_C° from Table 4 enabled us to calculate the following factors F_H:

For $Ph_2P(O)$ in 1,3-dithiane	$F_H = 0.99$ (cf. Figure 7)
For CN in tetrahydropyran	$F_H = 1.07$
For CN in piperidine	$F_H = 1.04$ (cf. Figure 7)
For COOMe in tetrahydropyran	$F_H = 1.46$ (cf. Figure 7)
For COOMe in piperidine	$F_H = 1.30$ (cf. Figure 7)

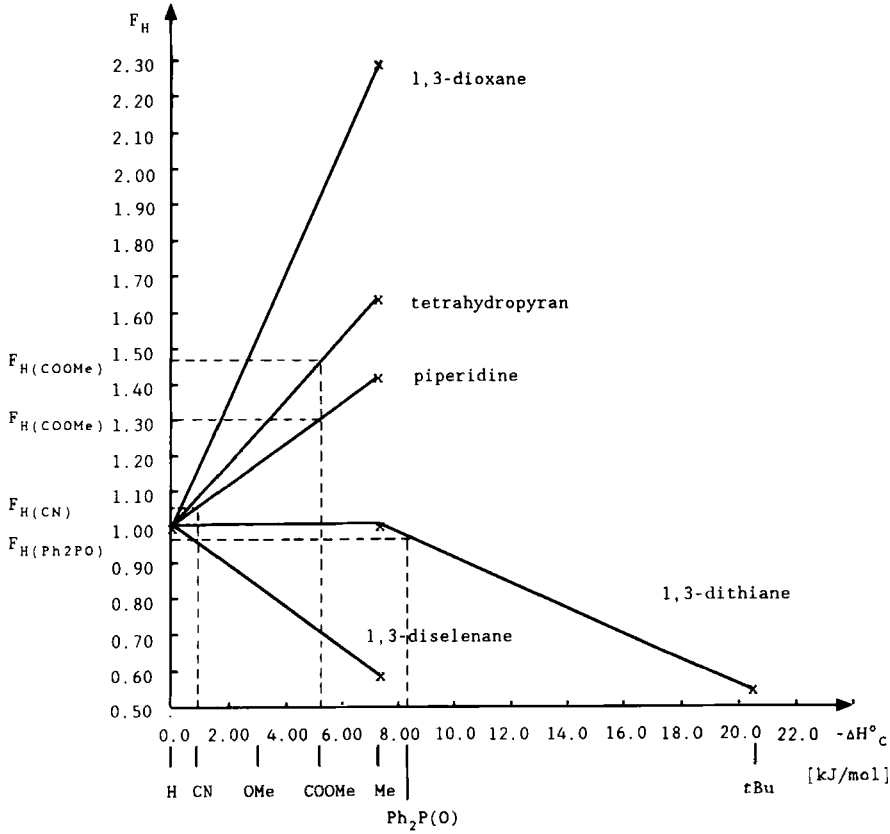


Figure 7. Determination of F_H factors for CN, COOMe, and $Ph_2P(O)$ groups in some six-membered rings.

Several examples of this approach are presented in Section II.E (Table 4). A larger number of conformational equilibria studied in ΔH° terms are collected in reference 18.

G. Solvent Effects

Extensive experimental studies, including low-temperature NMR, infrared, Raman, and microwave spectroscopy, of solvent effects on conformational equilibria have been well documented and reviewed previously (114). Several attempts to compute (9, 13, 114, 115) or correlate (116–120) solvent effects have appeared in the literature and have been described elsewhere. Interestingly, according to Walkinshaw (121), the overriding factor in determining the anomeric equilibrium for aldopyranoses is the relative hydrophilicity (defined as a measure of the probability that a solute–water hydrogen bond will form) of the two anomeric isomers. The energy gain in forming sugar–water hydrogen bonds outweighs both the intramolecular van der Waals and electronic effects (121). Recently, Navio and Molina (105), while evaluating the applicability of different versions of MM2, found that the energetic preference for the axial position decreased with increasing solvent polarity. The same trend is supported by quantum mechanical calculations (122–124). Interestingly, Kysel and Mach (124) found that a polar medium stabilizes the *ap, ap* conformation more than the *sc, sc* one by 28 kJ/mol in methanediol (**8**), by 31 kJ/mol in methoxymethanol (**49**), and by 12 kJ/mol in silanediol (**50**). Thus, the magnitude of the solvent effect on the observed conformational behavior may be comparable to the magnitude of intramolecular stereoelectronic interactions, which are of the order of 15 kJ/mol (see Eq. [15]).

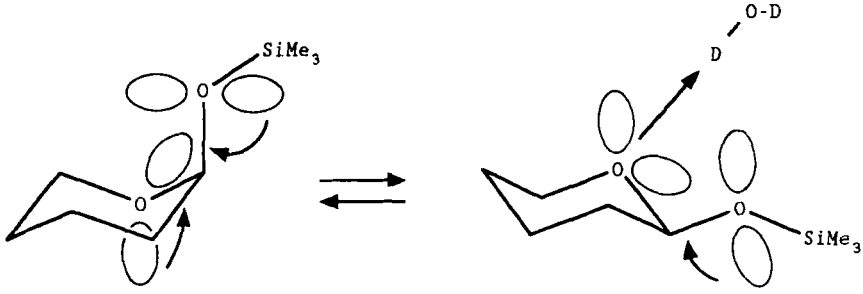


49 **50**

Let us focus on molecules **14a** and **14b** (Scheme 8) in which an anomeric effect (in ΔG° or ΔH° terms) is possible in the vapor phase. Usually, the dipole moment of **14a** is less than that of **14b** (125–128). Since the more polar form is stabilized in solution (114, 128) [as a rule, with several exceptions (29, 129); *vide infra*] it may happen that the anomeric effect (i.e., increased preference for **14a**) disappears in solution or may even change its sense (from $\Delta G^\circ_{AE} > 0$ to $\Delta G^\circ_{AE} < 0$). Such a possibility has been supported by quantum chemical calculations for dimethoxymethane (128). It was shown that, while in CCl_4 solution dimethoxymethane (**11**) exists almost exclusively as the most stable *sc, sc* conformer, in aqueous solution almost exclusive occurrence of the *ap, ap* conformation may be expected. Hence, all considerations regarding the presence, magnitude, or origin of the anomeric effect must take

solvent effects into account. Thus, it would seem that the anomeric effect should be evaluated in the vapor phase, as was postulated for conformational equilibria in general by Zefirov and Somoshin (130). This approach, based on the extrapolation of solution data ($\varepsilon > 1$) to $\varepsilon = 1$ (vapor phase), is becoming increasingly accepted (38, 131).

Two contrasting concepts (i.e., qualitative interpretations) of the influence of solvent on the anomeric effect are found in the literature, depending on whether the authors stress the delocalization or the electrostatic nature of the anomeric effect (128). The first approach assumes that polar solvent can interact with the lone-pair orbitals of, for example, oxygen and hence influence the intramolecular hyperconjugative interactions in which they participate. An elegant presentation of this idea was made by Praly and Lemieux (66). They attributed the increasing population of **51e** with the increasing proton donor abilities of solvent (water) for hydrogen bond formation between the endocyclic oxygen and a water molecule (see Scheme 17). This would decrease



51a 51e

Scheme 17

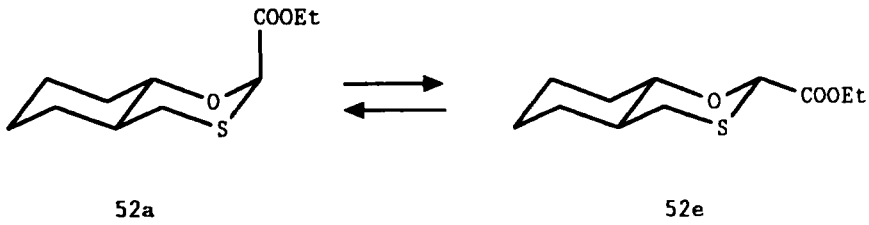
the energy of the σ^*_{O-C} orbital of the endocyclic C—O bond, increase its acceptor ability, and strengthen the exo anomeric interactions. Because of competition of the *exo* and *endo* anomeric interactions (see Section II.E), the overall equatorial preference should be expected to increase, as observed experimentally (66). Such a point of view seems to be strongly supported by the fact that the polar solvent CD_3CN provides an equilibrium with nearly the same population of **51e** as does much less polar solvent $CDCl_3$ (66).

In contrast to the above interpretation, Booth et al. (112) assumed preferred hydrogen bonding with the exocyclic oxygen atom, which enabled them to explain an *increase* in the axial preference (in $\Delta H°$ terms) of 2-alkoxytetrahydropyrans **24** and **39** on going from ether/toluence to ether/methanol solvent. This assumption seems to be supported by an increase in $\Delta S°$ on

passing from the aprotic to the protic medium. Stronger bonding of methanol to the axial exocyclic oxygen than to the equatorial one (the charge at the former should be larger thanks to the *endo* negative hyperconjugation; see proton affinities, Figure 3, Section II.E) should lead to a reduction of entropy of the axial conformer, as observed ($\Delta S^{\circ}_{ax-eq} = 1.6 \pm 2.1$ J/mol/K) (112). Booth et al. (112) attributed the differences between water- (*vide supra*) and methanol-induced conformational changes to unique hydrogen-bonding behavior of water.

It is clearly seen that the effect of stronger hydrogen bonding is not obvious (neglecting steric changes involved). On the one hand, hydrogen bonding between a hydrogen donor and an endocyclic oxygen atom occurs preferably in the equatorial conformer (cf. Figure 3), which should enhance the equatorial preference [as observed by Praly and Lemieux (66)]. On the other hand, however, hydrogen bonding with the exocyclic oxygen atom should be most effective in the axial conformer. This, in contrast, should increase the axial preference [as observed by Booth et al. (112)]. The actual influence of hydrogen-bonding solvents on the conformation of a molecule seems to depend on the relative importance of these two factors.

It should be added that the importance of solvent influence on the conformation about the C—COOEt exocyclic bond for the overall conformational preference of the carboethoxy group in the 1,3-oxathiadecalin derivative **52** (Scheme 18) was recently confirmed by Tschierske et al. (38).

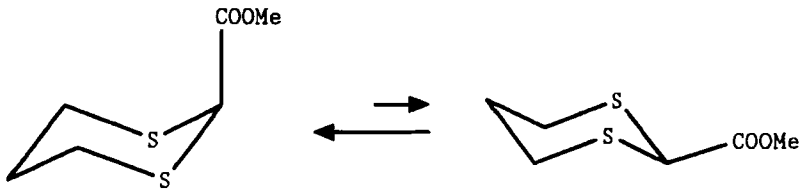


52a **52e**

Scheme 18

The second approach emphasizes the influence of solvent as a polar dielectric on mutual interactions of dipoles of bonds and lone pairs inside a molecule. However the influence of solvent on chemical equilibria may be due to specific solvent–solute interactions (66, 116) which are not accounted for by a purely electrostatic approach.

Thus, Juaristi et al. (51) observed that whereas the solvent effects at room temperature for 2-carbomethoxy-1,3-dithiane (**53**) agree with the anticipated trend, low-temperature ΔG° measurements show an opposite relationship, that is, the amount of axial species **53a** (Scheme 19) increases with increasing

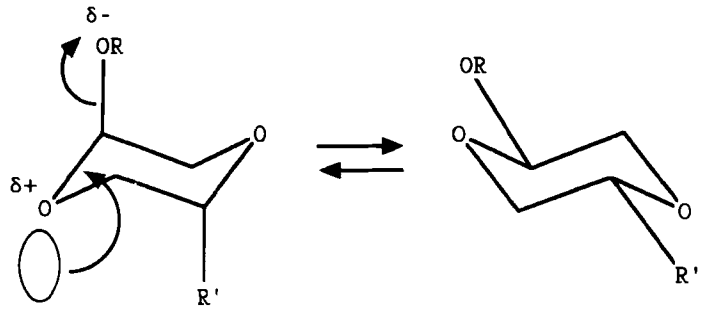


53a 53e

Scheme 19

solvent polarity. The marked contrast between ambient- and low-temperature conformational behavior was suggested by Juaristi et al. (51) to originate from a *solvent compression effect* (132, 133). According to this proposal, the population of the conformer with a smaller molar volume (usually the axial one) should increase with the more polar solvent due to higher internal pressure by the solvent at low temperatures.

Similar disagreement concerning the influence of a polar medium on the population of the more polar conformer of 2,5-disubstituted (R′ = OR; Scheme 20) and monosubstituted (R′ = H) 1,4-dioxanes **54** was observed by



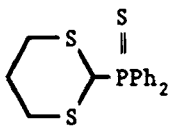
54a 54e

Scheme 20

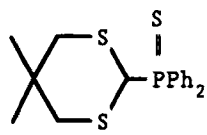
Fuchs et al. (129). They suggested that when the molecular dipoles of the axial and equatorial conformers are of similar magnitude, the more polar double bond–no bond structure, resulting from hyperconjugative interactions in the axial conformer, **54a** (see Scheme 20), will be stabilized in the more polar solvent. This hypothesis would support the importance of the hyperconjugative origin of the anomeric effect. The appearance of a large proportion of the axial conformers of 2-(arylseleno)-1,3-dithianes **37** (Scheme 13), even in

polar medium, led Pinto et al. (84) to a similar conclusion, namely that dipole–dipole interactions do not have a dominating influence on the conformation of **37**, and other electronic factors are important.

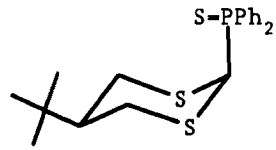
In the course of our studies on the anomeric effect in the C—S—C—P system we also become interested in the influence of solvent on the pertinent conformational equilibria in the hope that solvent effects could shed light on the origin of the observed anomeric effect. As models for our study 2-diphenylthiophosphinoyl-1,3-dithianes **55** and **56** were chosen (54). Confor-



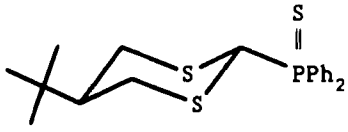
55



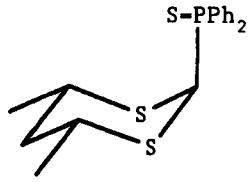
56



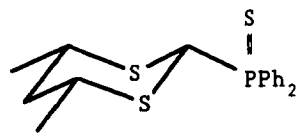
57a



57e



58a



58e

mational equilibrium constants $K_{a \rightleftarrows e}$ and the related ΔG° values obtained (54) by the weighted average method (134) with γ-effects in ^{13}C NMR spectra as the conformational probe are collected in Table 6.

As expected on the basis of least polarity, the greatest axial preference is observed in benzene-d_6. Surprisingly, the largest amount of the equatorial conformer can be found in dichloromethane-d_2 and chloroform-d. Solvents which are usually considered as "polar" (CD_3CN and DMSO-d_6) unexpectedly enhance the axial preference in **55** and **56**. This effect is especially pronounced for dimethyl sulfoxide solutions. Therefore, it is clearly seen that the conformational preference of a $Ph_2P{=}S$ group in a 1,3-dithiane ring is strongly dependent on solvent and this dependence is not stemming from "polarity" of the solvent but, perhaps, is due to specific solvent–solute interactions (54).

The conclusions presented above are strongly supported by the data (54) from equilibration of diastereomeric **57a**, **57e**, **58a**, and **58e** in various solvents.

TABLE 6

γ-Effect Values, Related Equilibrium Constants K_{a-e}, and Free Energy Differences ΔG°_{296} for Solutions of **55** and **56** in Various Solvents[a]

Solvent	γ-Effect[b] (ppm)		K_{a-e}		ΔG°_{296} (kJ/mol)	
	55	**56**	**55**	**56**	**55**	**56**
C_6D_6 ($\varepsilon = 2.28$)	−3.29	−3.14	0.26	0.30	3.31	2.96
$CDCl_3$ ($\varepsilon = 4.81$)	−1.51	−1.57	1.00	0.91	0.00	0.23
CD_2Cl_2 ($\varepsilon = 9.08$)	−1.38	−1.54	1.07	0.96	−0.17	0.10
C_6D_6:CD_3OD = 6:4 (v/v)[c]	−2.34	−2.28	0.60	0.62	1.26	1.18
DMSO-d_6 ($\varepsilon = 36$)	−2.39	−2.49	0.63	0.59	1.14	1.30
CD_3CN ($\varepsilon = 37.5$)	−1.30	−1.37	0.82	0.86	0.49	0.37

[a] Based on data in ref. 54.
[b] in ^{13}C NMR spectra at 75.47 MHz; the C(4,6) chemical shifts in the reference dithianes were determined in appropriate solvent.
[c] $\varepsilon = 14.4$ assuming additivity of ε.

The appropriate equilibrium constants K and free energy differences ΔG° are presented in Table 7. The most striking finding is that the replacement of a benzene–methanol ratio of 6:4 (v/v) solution by anhydrous ethanol results in an *increase* in ΔG° for **57** from 2.08 to 2.66 kJ/mol and a *decrease* in ΔG° from 1.69 to 1.22 kJ/mol in the case of **58**. Thus, the influence of a solvent must not be considered solely in terms of "polarity", a term that is

TABLE 7

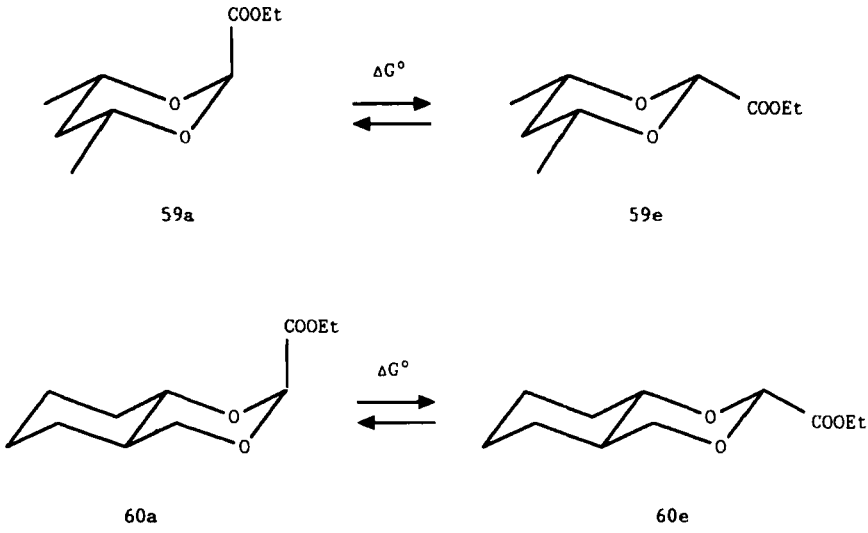
Results of Equilibration of **57** and **58** in Various Solvents at 293 K[a]

Solvent	K_{a-e}		ΔG° (kJ/mol)	
	57	**58**	**57**	**58**
i-PrOH	0.339	[b]	2.64 ± 0.19	[b]
EtOH 100%	0.336	0.606	2.66 ± 0.24	1.22 ± 0.14
EtOH 95%	0.379	0.806	2.36 ± 0.17	0.52 ± 0.40
DMSO-d_6	0.370	[b]	2.42 ± 0.19	[b]
MeOH	0.498	0.990	1.70 ± 0.17	0.02 ± 0.15
C_6H_6:MeOH[c]	0.425	0.500	2.08 ± 0.17	1.69 ± 0.15

[a] Data from ref. 54.
[b] Not determined.
[c] 6:4 (v/v).

very imprecise (116, 118, 120). It is clear that specific interactions between solvent and solute should be taken into account, the more so because they are not the same for the very similar compounds **57** and **58**. Obviously, the nature of the axial preference is almost the same for **57** and **58**. Hence, solvent studies cannot be expected to reveal the nature of the observed anomeric effect.

It must be stressed that ΔG° values for **57** and **58** in the same solvent (e.g., MeOH or EtOH 95%) can differ by more than 1.5 kJ/mol. Such differences seem to arise from different solvent effects on the two equilibria under scrutiny (despite the very similar structure of **57** and **58**). This point of view is strongly supported by the fact that the relevant ΔH° and ΔS° values for **57** and **58** are also different. They are 5.19 ± 0.23 kJ/mol and 10.6 ± 0.7 J/mol/K for **57** and 5.71 ± 0.12 kJ/mol and 13.8 ± 0.4 J/mol/K for **58**, respectively, in 6:4 (v/v) benzene–methanol solution (54). We also observed analogous differences between the equilibria in other derivatives of 1,3-dithianes (54, 98). Support for the hypothesis presented above comes from the work of Tschierske et al. (38), who showed that ΔG° values for dioxanes **59** and **60** (Scheme 21) differ



Scheme 21

by more than 1 kJ/mol in CH_2Br_2 solution. However, extrapolation of the ΔG° values for **59** and **60** to $\varepsilon = 1$ following the method of Zefirov and Samoshin (130) gave (38) identical free energy differences in vacuum, ΔG°_{vac}, equal to 2.1 kJ/mol. It is then clear that the difference between ΔG° for **59** and **60** stems from the solvent effect. Therefore, we would like to point out that

one *should not* expect† the same preference of a substituent connected to the anomeric carbon atom of various homologous heteroanes (e.g., **55**, **56**, **57**, and **58**), in contrast to what is usually done (135) (see especially footnote 22 in ref. 136).

A reversed dependence of the axial preference on solvent polarity, which is sometimes regarded as a proof for the reverse anomeric effect, is discussed together with our results on phosphonio-1,3-dithianes in Section II.I.

H. Energy of Bond Separation Reactions

Estimating the magnitude of the anomeric effect as an additional preference for the *sc* conformation is difficult for several reasons detailed above. Therefore, once the stabilizing character of the $n_Y-\sigma^*_{C-X}$ interaction invoked as the origin of anomeric effect (see Section III.B) had been recognized, scientists began to evalute the energy of the *group (bond) separation reaction* (138, 139) described by the *isodesmic* equation

$$X—AH_2—Y + AH_4 \rightleftharpoons H_3A—X + H_3A—Y + \Delta E_{IS} \qquad [19]$$

The enthalpy change of this process for A = carbon is also called the *methyl stabilization energy*. This reaction measures the energy of substitutent interactions (X with Y) in the $Y—AH_2—X$ system in relation to the reference compounds H_3AX and H_3AY. For instance, for difluoromethane (**61**, Table 8) this reaction is very endothermic, suggesting strong stabilizing interaction between two fluorine atoms.

The isodesmic method has been widely applied in an *ab initio* approach (72, 141–148). The energy ΔE_{IS} (Eq. [19]) is considered a measure of the magnitude of the anomeric effect (18, 141, 144, 146, 147, 149) and/or negative hyperconjugation (145, 148) or specific stabilization due to σ conjugation (142). It must be stressed at this point, however, that the group separation reaction does *not* provide a quantitative measure either for the effect of negative hyperconjugation (see further discussion) or for the anomeric effect and σ conjugation. Does $\Delta E_{IS} = 0$ mean that we do not have anomeric effect and/or that negative hyperconjugation and/or σ conjugation do not operate? Of course not. A good example of such a situation can be found in the work

†This problem is also related to that of a reasonable selection of a conformational probe for estimation of conformational equilibria using the weighted average method. A simple testing procedure for conformational probes was demonstrated by Graczyk (54b). It must be added that any differences in conformational homogeneity between **57** and **58** have been shown to be unimportant as far as the determination of the axial preference of the $Ph_2P{=}S$ group by equilibration is concerned (137).

TABLE 8
Bond Separation Energies ΔE_{IS} (Eq. [19]) for Compounds X—AH_2—Y (**61–65**)

Compound No.	X	A	Y	ΔE_{IS} (kJ/mol)
61	F	C	F	60.0[a]
62	Cl	C	Cl	−2.4[a]
63	Br	C	Br	+3.7[a]
64	I	C	I	−15.2[a]
65	Cl	C	SH	−5.4[b]

[a] ΔE_{IS} corresponds to ΔH°_{298} and vapor phase. Calculated on the basis of data taken from ref. 140 (see text).
[b] Calculated *ab initio* (141) for the *sc* conformer.

(141) of Schleyer's group. For the most stable *sc* conformer of chloromethanethiol (**65**) ΔE_{IS} is negative (Table 8). This would suggest that there is no anomeric effect in the S—C—Cl system whereas the contrary is true (6b, 150). The explanation is very simple. As was stated in the original paper (138), the energy changes in isodesmic reactions measure deviations from additivity of bond energies. In particular, the isodesmic reaction measures the *sum* of all interactions between the separate fragments X and Y in relation to the sum of all interactions between X (or Y) and H in the products. Since the initial molecular orbital calculations were (for obvious reasons) applied to interactions between first-row elements for which ΔE_{IS} is strongly positive, the importance of *destabilizing* interactions has been underestimated.

Let us concentrate our attention on dihalogenomethanes **61–64** (Table 8). The enthalpies of relevant isodesmic reactions were calculated on the basis of standard enthalpies of formation $\Delta H^{\circ}_{298(gas)}$. It is apparent that while in the case of difluoromethane the positive ΔH°_{IS} is mainly due to stabilizing interactions between two fluorines (or, less likely, to destabilizing interactions between H and F), for diiodomethane the negative ΔH°_{IS} results from destabilizing interactions between two iodines (or stabilizing interactions between H and I). Dichloro- and dibromomethane have ΔH°_{IS} close to zero since for them the stabilizing and destabilizing interactions are balanced (see Section III.B for discussion concerning CF_4).

Let us come back to chloromethanethiol (**65**, Table 8) and assume, for the sake of simplicity, that X(Y)–H interactions are negligible [in general this is not true; the importance of n_Y–σ^*_{C-H} interactions has been pointed out recently by Reed and Schleyer (143)]. Since for both the *sc* and *ap* conformers of **65** the bond separation energies, ΔE°_{IS}, are negative (−5.4 and −14.6 kJ/mol, respectively), it is evident that the preference (by 9.2 kJ/mol) for the *sc* over

the *ap* arrangement of the H—S—C—Cl fragment cannot be attributed in a straightforward manner to stabilizing interactions between sulfur and chlorine.

There are two extreme possibilities. The first one is that both conformers, *sc* and *ap*, of **65** are destabilized equally and the difference in energy between them is due to a larger countervailing stabilization of the *sc* conformer. The second possibility is that both conformers are destabilized but the destabilization of the *ap* conformer is greater than that of *sc*. The latter case would correspond to the *"rabbit ear" effect* (see Section III.A.4). *Ab initio* molecular orbital calculations (70) show that the total energy difference between the *sc* and *ap* conformers of **65** (11.1 kJ/mol, cf. 9.2 kJ/mol in ref. 141) is close to the difference in magnitudes of *stabilizing* (negative hyperconjugation) orbital interactions (i.e., 11.7 kJ/mol), thus pointing at the first of the above possibilities. Therefore, *though* ΔE°_{IS} *is negative, there really is an anomeric effect resulting from negative hyperconjugation in* **65**.

A similar conclusion may be drawn for methanedithiol, $HSCH_2SH$ (**66**). The calculated (141) $\Delta E^{\circ}_{IS} = 0.4$ kJ/mol for the *sc*, *sc* conformer of **66** is very small but indicates a slight predominance of stabilizing over destabilizing interactions between two sulfur atoms. On the other hand, for the *sc*, *ap* conformer $\Delta E^{\circ}_{IS} = -3.9$ kJ/mol; thus destabilizing interactions between two sulfurs prevail. Thus, the difference in energy $\Delta E^{\circ} = 4.3$ kJ/mol between *sc*, *sc* and *sc*, *ap* conformers of **66** arises from *both* stabilizing and destabilizing interactions. This conclusion is strongly supported by the fact that the outer C—S bond lengths in orthothiocarbonate $(PhS)_4C$ (151) are significantly shorter than the inner ones, in contrast to the expectation based on the stabilizing n_S–σ^*_{C-S} negative hyperconjugation (see Section IV.B.1, Figure 55). Indeed, recently Salzner and Schleyer (148) showed that —S—C—Se— and —Se—C—Se— anomeric interactions originate from several factors, contrary to earlier statements by Pinto et al. (45, 82–84, 152). It must thus be stressed that a one-sided view of the nature of the anomeric effect as being solely due to stabilizing interactions in the *sc*, *sc* conformation of **14** (Scheme 8) seems to be oversimplified [even though it usually leads to the correct conclusion as to the relative stability of isomers (7b)].

We would like to point out that there is no qualitative discrepancy between MO calculations (141, 153, 154) and experiment (6b, 51, 113) when one deals with the magnitude of anomeric interactions in an S—C—S system, in contrast to suggestions (12, 45, 83, 84, 113, 155) concerning the work (141) of Schleyer's group. The calculated energy difference between the *sc*, *ap* and *sc*, *sc* conformers of methanedithiol (**66**) ranges from 4.3 kJ/mol (141) to 7.5 kJ/mol (154) to 9.04 kJ/mol (153). Experimental studies on various more sterically hindered systems containing the S—C—S moiety afford $\Delta G^{\circ}_{173K} =$ 2.7, 3.2, 3.8 kJ/mol (51), $\Delta G^{\circ} = 1.7$ kJ/mol (6b), and $\Delta G^{\circ}_{186K} = 0.5$, 2.1 kJ/mol

(113) depending on the nature of substituents, temperature, and solvent. The agreement is surprisingly good if one takes into account that the calculated values correspond to energies in the vapor phase, a temperature of 0 K, and configurations in which the nuclei are fixed (138). The only reason for the misunderstanding mentioned above may be the predilection of most workers to use ΔE_{IS} values as a measure of anomeric interactions. In fact, the plot of ΔE_{IS} (Figure 8) as a function of the energy difference ΔE_{a-b} (see Scheme 8) between *ap* and *sc* conformers of various Y—C—X systems (data from Table 9) shows the lack of any acceptable correlation. Though ΔE_{a-b} is not equivalent to the magnitude of the anomeric effect $\Delta E_{AE(a-b)}$ (see Eq. [9]), it seems rather improbable that the involvement of ΔE_{AE} or partial anomeric effects

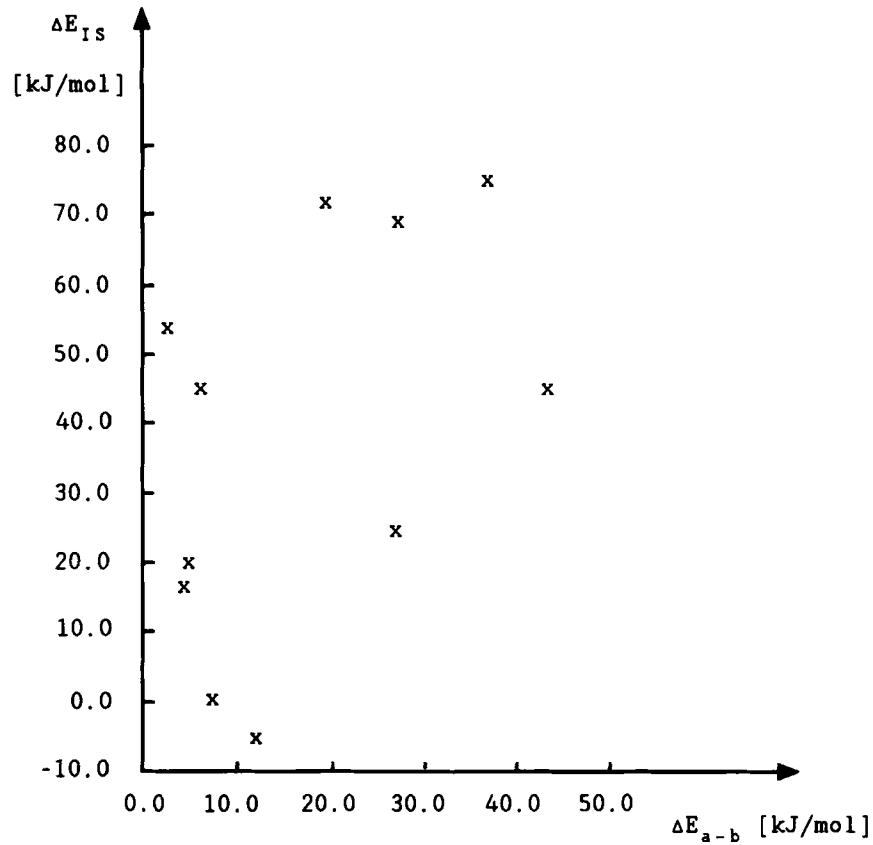


Figure 8. Plot of energies ΔE_{IS} (Eq. [19]) of isodesmic reactions as a function of ΔE_{a-b} (Scheme 8). Data from Table 9.

TABLE 9

Ab initio Energy Differences ΔE_{a-b} between **14a** and **14b** (Scheme 8) and Corresponding Bond Separation Energies ΔE_{IS} for **14a**[a]

X	Y	ΔE^{b}_{a-b} (kJ/mol)	ΔE^{c}_{IS} (kJ/mol)	X	Y	ΔE^{b}_{a-b} (kJ/mol)	ΔE^{c}_{IS} (kJ/mol)
N	N	6.69	44.4[d]	O	S	4.02	19.7
N	S	4.52	17.6	S	Cl	12.34	−5.4
N	O	2.97	53.1	O	O	18.87	72.8
N	Cl	43.10	43.9	O	Cl	26.65	24.3
S	S	7.53	0.4	F	O	27.03	67.8
S	O	3.86	19.7	F	N	37.87	73.6

[a]According to Eq. [19]. All R are hydrogen atoms.
[b]Data from ref. 154 except for X=Y=N.
[c]from ref. 141.
[d]from ref. 156.

(analogous to the *exo* and *endo* effects; right side of Eq. [9]) would improve the correlation dramatically.

The decomposition of ΔE_{IS} into parts corresponding to stabilizing negative hyperconjugation ΔE_D and destabilizing interaction between geminal substituents ΔE_L will be presented in Section III.B.5. It reveals that while stabilizing hyperconjugative interactions ΔE_D increase on passing from difluoromethane (**61**) to trifluoromethane, CHF_3 (**67**) to tetrafluoromethane, CF_4 (**68**), the relevant ΔE_{IS} values *decrease*, thus proving that the sense of ΔE_{IS} and that of stabilizing interactions can even be *opposite*. Hence it seems reasonable to discuss ΔE_{IS} in more general terms of *geminal group interactions* (157a).

Recently, Wiberg and Rablen (157b) have stressed that negative hyperconjugation is not needed to explain the energetic superiority of multiple fluorine substitution in polyfluoromethanes; consideration of electrostatics may well account for both the changes in energy and the changes in C—F bond lengths (see Secs. III.B.5 and IV.B.1).

It must be added that Hati and Datta (149) have recently examined various bond separation reactions in terms of "hardness" (158) η defined by

$$\eta = \tfrac{1}{2}(\mathrm{IP} - \mathrm{EA}) \qquad [20]$$

where IP = ionization potential of species
EA = electron affinity of species

They concluded that the driving force behind all reactions in which anomeric effects are believed to be operative is the generation of the hardest possible species. For instance, for the reaction between methane (**69**) and difluoromethane (**61**),

$$\underset{\eta = 10.3}{\underset{\textbf{69}}{CH_4}} + \underset{7.84}{\underset{\textbf{61}}{CH_2F_2}} \rightleftharpoons 2\underset{9.4}{CH_3F} + \Delta H^\circ_{IS} \qquad [21]$$

a large positive ΔH°_{IS} (Table 8) stems from the hardness of **69** ($\eta = 10.3$).

Recently, the approach to the anomeric effect based on Eq. [19] has been criticized by Leroy et al. (159) as not reflecting properly the stabilization (or destabilization) of geminally substituted species. They proposed a new quantity—*thermodynamic stabilization energy* (SE)—which, unlike the methyl stabilization energy, is independent of the reference system. It is defined by

$$SE = \Delta H^\circ_a - \sum N_i E_i \qquad [22]$$

where ΔH°_a = enthalpy of atomization of considered species
E_i = standard energy of i bond
N_i = number of i bonds

The anomeric effect AE is defined by

$$AE = SE - SE_{ref} \qquad [23]$$

as a difference between the stabilization energy SE of a studied molecule [e.g., 2-methoxytetrahydropyran (**39**, SE = 10.7 kJ/mol)] and that of a reference system, SE_{ref} [i.e., tetrahydropyran (**70**, $SE_{ref} = -7.4$ kJ/mol)]. Thus, the anomeric effect AE = 18.1 kJ/mol in this case. For acyclic molecules the anomeric effect AE is equal to SE. Of course, this definition of the anomeric effect, like that involving bond separation energies (Eq. [19]), has nothing to do with the definition based on the relative energies of conformers (Eq. [1]).

The SE and AE values calculated (159) for some methane derivatives are collected in Table 10 together with the relevant ΔE_{IS} values. It is clearly seen that stabilization energies vary from negative to positive. The largest stabilization takes place for tetramethoxymethane (**72**). Interestingly, the stabilization energy SE (which is equal to AE) for methanedithiol (**66**) is negative. This would mean that the reverse anomeric effect is operative, which is not true (*vide supra*). Therefore, the definition of the anomeric effect given by Leroy et al. (159) is misleading. On the other hand, the authors appreciated the impor-

TABLE 10
Thermodynamic Stabilization Energies SE, Bond Separation Energies ΔE_{IS}, and Anomeric Effect AE for Selected Methane Derivatives

Compound		ΔE_{IS}	SE	AE
No.	Formula	(kJ/mol)	(kJ/mol)	(kJ/mol)
8	$HO—CH_2—OH$	65.6	25.4	25.4
11	$MeO—CH_2—OMe$	54.7	18.2	18.2
61	CH_2F_2	58.6	13.9	13.9
62	CH_2Cl_2	−15.6	−24.5	−24.5
66	$HS—CH_2—SH$	−1.2	−8.7	−8.7
71	$(MeO)_3CH$	128.6	34.9	34.9
72	$(MeO)_4C$	214.7	42.2	42.2
73	$H_2N—CH_2—NH_2$	33.2	10.2	10.2

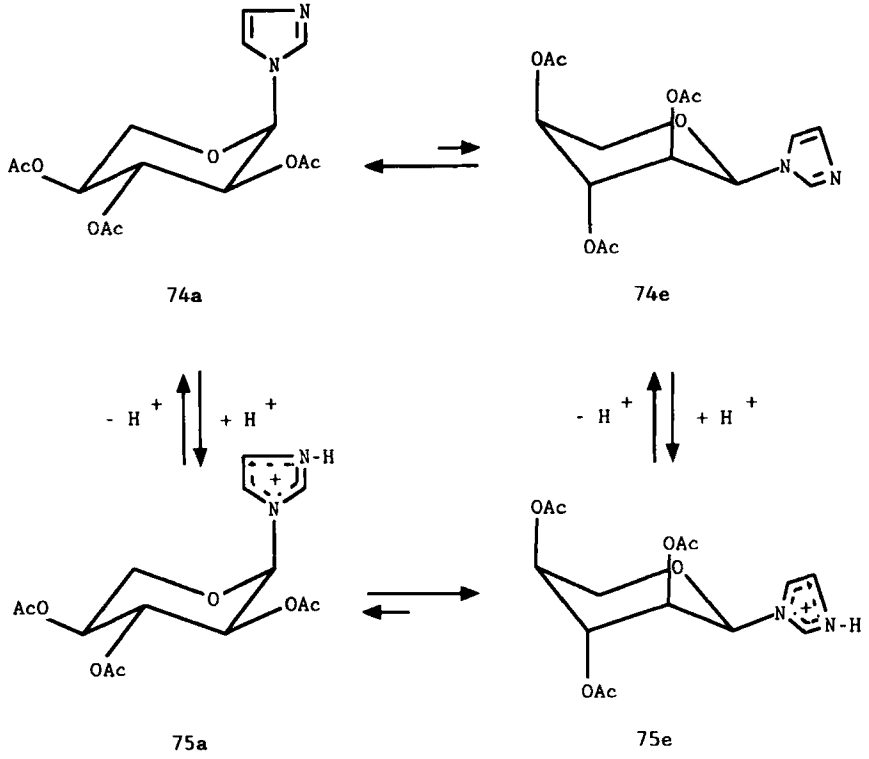
From ref. 159.

tance of destabilizing interactions in methane derivatives. Their approach seems to better reflect the energetic consequences of geminal group interactions. It must be added that their concept of thermodynamic stabilization energy SE enabled Leroy et al. (159) to interpret .he influence of captodative substitution on the properties of a rather wide spectrum of molecules and radicals.

I. Reverse Anomeric Effect

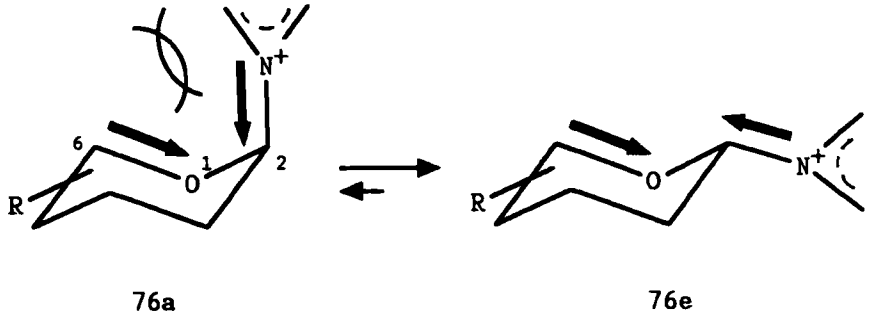
The term *reverse anomeric effect* was introduced in 1965 by Lemieux and Morgan (160) to describe the additional tendency of a substituent bearing positive charge to occupy the equatorial position at the anomeric carbon of a pyranose ring. The most spectacular manifestation of this effect was provided (161) by the protonation of α-D-xylopyranosylimidazole **74**, as shown in Scheme 22. The imidazole group attached to the anomeric carbon atom in **74** is mainly axial. However, after protonation with trifluoroacetic acid in chloroform-*d* to afford **75**, it tends to be situated almost exclusively equatorially, forcing the three acetoxy groups into the axial orientation. Such a marked shift in conformational equilibrium toward **75e** cannot be explained solely on steric grounds. Because the disappearance of a conformational effect (here, the anomeric effect of the imidazole group) is usually accounted for in terms of the operation of another conformational effect (23), this phenomenon has been termed the reverse anomeric effect.

The reverse anomeric effect was initially explained on the basis of electrostatic interactions by Lemieux (27). The enhanced equatorial preference



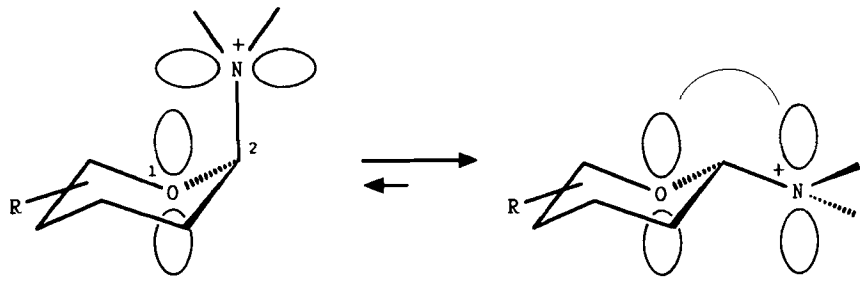
Scheme 22

of the imidazolium (or pyridinium) groups in **76** (Scheme 23) is due to interactions between dipoles of the C(6)—O and N—C(2) bonds, which are the most destabilizing in **76a**, which contains a positively charged substituent in the axial position.



Scheme 23

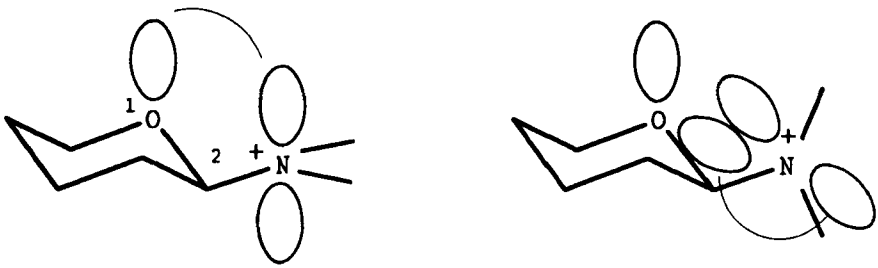
Finch and Nagpurkar (162) presented an alternative picture of a stabilization of the equatorial conformer **76e** based on an interaction between the *p*-type lone pair of the ring oxygen atom and the $e_{2u}\pi^*$ antibonding orbital of the aromatic system of the imidazolium or pyridinium group (see Scheme 24). This interaction can occur in **76e** where the aromatic ring and the C(2)—O bond are coplanar. Such an arrangement is not possible in the alternative axial conformation **76a**.



76a **76e**

Scheme 24

Box based his explanation (8, 14) of the reverse anomeric effect on the lone-pair interaction model analogous to that presented earlier by Finch and Nagpurkar (*vide supra*). The observed conformational behavior is a result of an interplay of stabilizing and destabilizing interactions. The former consist of attractive, stabilizing interactions between the lone pairs of the O(1) oxygen and the electron deficient σ^*, or π^*, orbitals of a substituent, which are favorable in **76e**, as shown in Figure 9. The normal steric requirements of



76e

Figure 9. Stabilizing orbital interactions in equatorial 2-ammoniotetrahydropyrans **76e** (according to ref. 8).

the substituent would also lead to preference for the equatorial postion. Of course, the usual n–σ^* hyperconjugative interactions, which favour the axial arrangement, are present in **76a** too, but they are less important than the sum of the previously discussed factors (14).

Recent *ab initio* calculations (at the 6–31G** level) by Grein and Deslongchamps (163) on protonated species $H_nXCH_2Y^+H_n$ (X and Y = O and/or N) revealed that the most stable species are usually not those having maximum number of possible hyperconjugative interactions (see Figure 10). Conformers of this type are among the least stable ones, for example, **77d**. Furthermore, in the case of **79** and **80** the lowest energy species were those without any hyperconjugative stabilization, that is, **79c** and **80a**, which is in line with the prediction based on the concept of the reverse anomeric effect. Grein and Deslongchamps (163), in order to account for these results, proposed an energy decomposition scheme. The energy of conformers was considered to be a sum of the following parameters:

- r Steric component reflecting 1,3-diaxial H–H repulsive interactions, equal to ca. 4 kJ/mol
- l Electrostatic component for 1,3-diaxial lone pair-lone pair repulsion, equal to ca. 4 kJ/mol
- h Reflecting stabilizing 1,3-diaxial H-lone pair interaction (intramolecular "hydrogen bonding"), equal to ca. -4 kJ/mol
- e Electronic energy component, applicable when a lone pair is antiperiplanar to a polar bond; for an oxygen lone pair $e_O = -8$ kJ/mol, for a nitrogen lone pair $e_N = -10$ kJ/mol

This scheme applied to uncharged systems allowed the authors to estimate the relative energies of conformers in rather good agreement with those obtained by *ab initio* calculations. However, for the charged systems **79c** and **80a**, which were the most stable species (in agreement with expectation based on the reverse anomeric effect), it was necessary to introduce an extra stabilization factor v ($v_N = -21.0$ kJ/mol and $v_O = -16.8$ kJ /mol for **79c** and **80a**, respectively). This led Grein and Deslongchamps (163) to the conclusion that the reverse anomeric effect is a stabilizing electronic effect. In their opinion (163) the reverse anomeric effect is a result of an electrostatic attraction between lone electron pairs of atom X and the positive charge of atom Y as pictured for **79c** (X = Y = N) in Figure 11. Interestingly, while the correction v_O was necessary to match the energy of **80a**, it was not applied in **77a** for unknown reasons. It was also not introduced for **78b**. This suggests that the energy decomposition scheme proposed by Grein and Deslongchamps (163) is oversimplified and their conclusions concerning the nature of the reverse

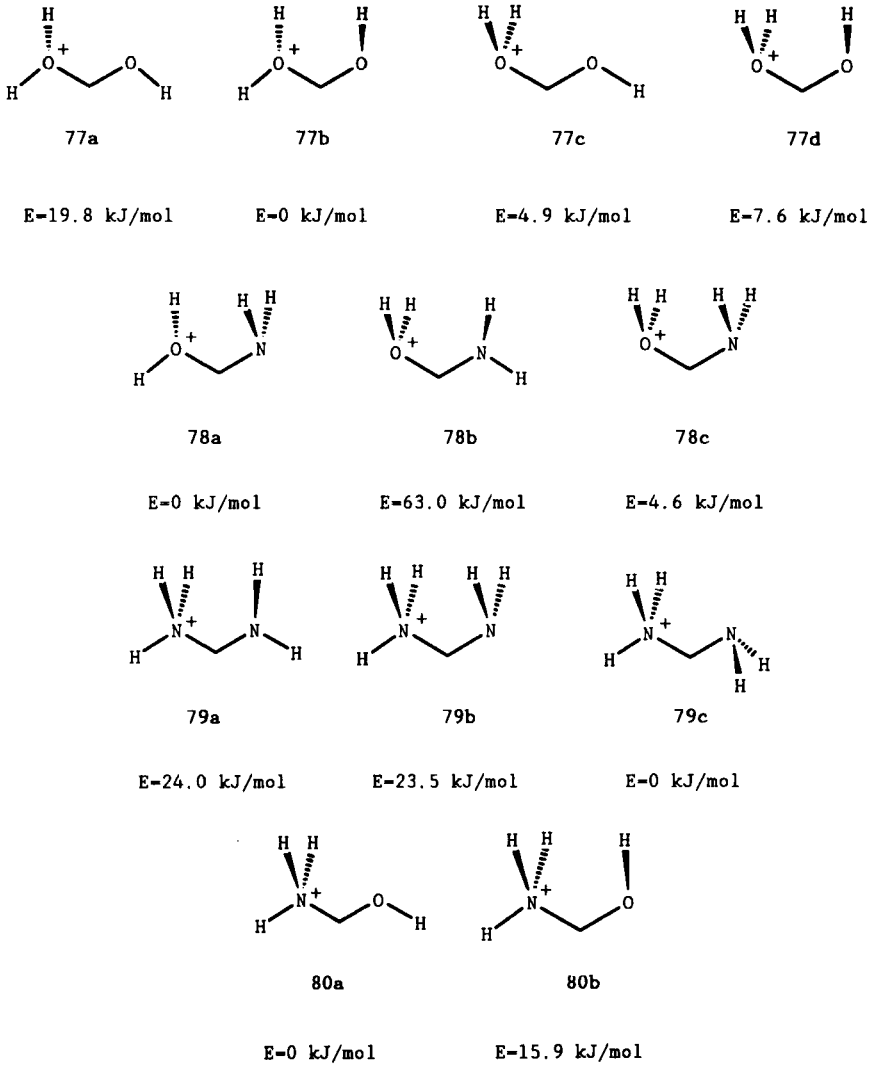
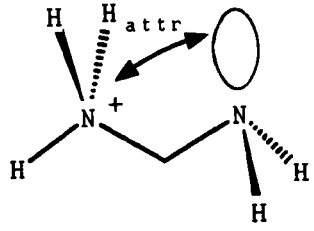


Figure 10. Ab initio relative energies of some $XH_m—CH_2—YH_n^+$ (X, Y = O, N) systems **77–80**. Data taken from ref. 163.

anomeric effect are disputable. It seems quite possible that unlike in uncharged species the assumption that the magnitude of particular energy components does not depend on the compound studied is not valid, especially insofar as the electronic energy components are concerned. Perhaps a larger number of factors should also be taken into account, for example, hyperconjugations



79c

Figure 11. Attractive interactions (*attr.*) in **79c** as a source of the reverse anomeric effect.

involving σ bonds as donors and sp^3-type lone pairs of protonated oxygen atom [the latter interaction was assumed to be negligible by the authors (163)]. In the light of the results of Irwin et al. (30), which are discussed in Section IV.B.1, species with a lone pair of the sp^3 type seem to exhibit stronger anomeric effects than those with a π lone pair [cf. the results of Woods et al. (164), *vide infra*]. Interestingly, when hyperconjugative interactions are not outweighed by 1,3-diaxial repulsions between hydrogen atoms, as in **77b** and **78a**, the most preferred conformations are exactly those reflecting the generalized anomeric effect and expected on the basis of the n_O–σ_{C-O^+} and n_N–σ_{C-O^+} hyperconjugative interactions, respectively. On the other hand, the situation in solution can become even more complicated, since the solvation of OH_2^+(NH_3^+) and OH (NH_2) groups is not identical, and the relation between energies of particular conformers can thus be altered.

The conformational behavior of the protonated methanediol molecule was also studied by Woods et al. (164) with various *ab initio* and semiempirical methods. In contrast to the results of Grein and Deslongchamps (163), the lowest energy species was always found to be **77c**; this would suggest that the n_{O^+}–σ^*_{C-O} negative hyperconjugation is more effective than the n_O–$\sigma^*_{C-O^+}$ one. The energies of **77a**, **77b**, and **77d** were found (at HF/6–31G* level) to be larger by 28.1, 7.1, and 12.6kJ/mol, respectively. Nevertheless, it is clear that the conformations having 1,3-diaxial H–H interactions are avoided.

Grein and Deslongchamps (163) suggested that the large equatorial (or pseudoequatorial) preference of a pyridinium group regarded as being due to the reverse anomeric effect is simply rationalized by the fact that there is maximum electrostatic attraction between the ring oxygen lone pairs and the (pseudo) equatorially oriented nitrogen. This explanation, however, neglects the fact that the actual positive charge on the pyridinium nitrogen is smaller than the formal one, due to the influence of the π system of the ring (Figure 12a). In the case of the imidazolium group this positive charge must

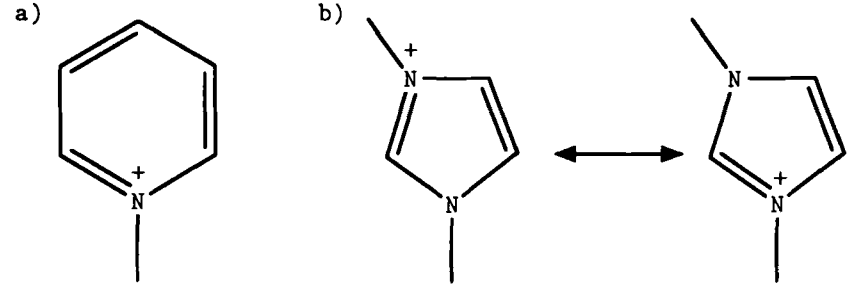
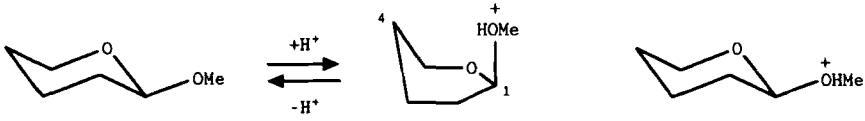


Figure 12. Resonance structures of (a) pyridinium and (b) imidazolium group.

even be smaller (162) owing to much more effective resonance delocalization (Figure 12b), and therefore the electrostatic explanation seems to be invalid. The latter conclusion seems to be supported by the fact that the equatorial preference of pyridinium- and imidazolium-substituted pyranosides is very similar (161) despite the difference in positive charge on nitrogen.

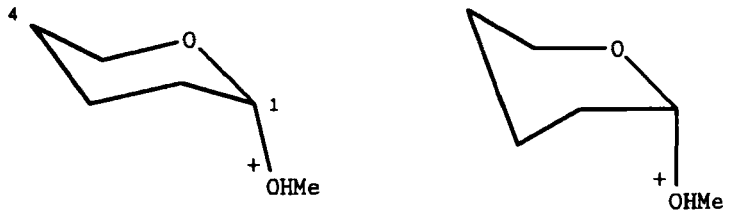
Deslongchamps (7c) suggested that the protonation of one of the alkoxyl groups in an acetal affords an alkyloxonium RO^+H group that is involved in a classical $n_O-\sigma^*_{C-O^+}$ interaction (cf. calculations on $H_nXCH_2Y^+H_n$, *vide supra*). This interaction may be responsible solely for the generalized anomeric effect. Such point of view has been supported by *ab initio* studies (165) on acid-catalyzed C—O bond cleavage in β-glycosides. The ground-state conformation of the protonated β-glycoside **81e** (Scheme 25) was found (165) to



39e ^4E sofa 81e $^4C_1$ chair

Scheme 25

be ^4E sofa (ca. 25 kJ/mol more stable than the appropriate $^4C_1$ chair). This result stands in flat contradiction to the idea of the reverse anomeric effect, according to which positively charged substituents are expected to exhibit strong preference for the equatorial or pseudoequatorial position in the pyranose ring. Protonation of axial 2-methoxytetrahydropyran **39a** was shown (165) to produce as the lowest energy species either $^4C_1$ flattened chair (calculation at the 6–31G*/3–21G level) or $^4H_3$ half-chair (calculation at the



flattened $^4C_1$ chair $^4H_3$ half-chair

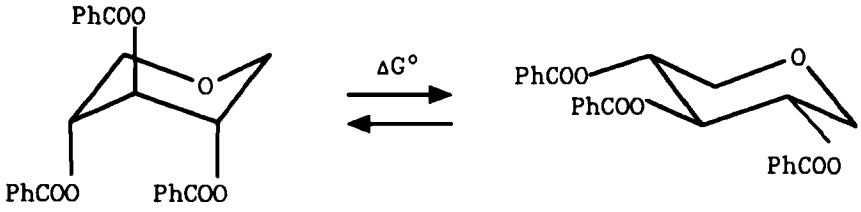
81a

6–31G*/6–31G* level) of **81a**. In both of these conformations the position of the $^+$OHMe moiety is axial or pseudoaxial, and the arrangement of the endocyclic oxygen π-type lone electron pair is optimal for the n_O–$\sigma^*_{C-O^+}$ interaction. In other words, the $^+$OHMe group does not exhibit behavior typical of the reverse anomeric effect. It must be added that the ^4E sofa conformer of **81e** also creates a very good opportunity for overlap between the π-lone pair of the *endo* oxygen O1 and the σ^* orbital of the C1—OMe bond. This should result in concommitant maximum lengthening of the C1—OMe bond and maximum shortening of the endocyclic O1—C1 bond, as was indeed found (165).

Very recently cations **77**, **80**, and 2-ammoniotetrahydropyran (**2**, X = NH_3^+; see Scheme 1a) have been extensively studied by Cramer (166a) at *ab initio* (MP2/6-31G**//HF/6-31G**) and semiempirical (AM1) levels of theory. In the case of acyclic compounds the most stable conformers at both levels of theory were found to be **77b** and **80b** having oxygen lone electron pair adequately oriented to permit n-σ^* delocalization. This suggested to Cramer (166a) that the anomeric effect is present, in contrast to what has been claimed by Grein and Deslongchamps (163) and Woods et al. (164). Additional support to this conclusion Cramer (166a) based on analysis of geometric changes inherent in rotation about the C—O bond in **77** and **80**. Geometric differences between **2e** and **2a** (X = NH_3^+; see Section IV.B.1) have been considered by this author (166a) to be indicative of the n_O-$\sigma^*_{C-N^+}$ delocalization responsible for the anomeric effect in **2** (X = NH_3^+). In his opinion this anomeric effect may be opposed by solvation which, according to the semiempirical calculations performed (166a), may drive the equilibrium toward the equatorial conformer. Steric and local dipole effects may additionally lead to preference for **2e** (X = NH_3^+) (166a).

In the opinion of Kirby (6c), steric requirements of the heterocyclic ring do not change on going from **74** to **75** (Scheme 22). Juaristi and Cuevas (18) claimed that "the preference for the equatorial conformation (of the imidazole

ring in **75**) is stronger than the normal steric preference found in cyclohexane (represented by *A*-value). This is the reverse anomeric effect". To the best of our knowledge nobody has studied the appropriate cyclohexane derivatives in order to determine the relevant *A* values, and so the opinion maintained by Kirby, and Juaristi and Cuevas is risky. The latter authors (18) considered the equatorial preference of the imidazolyl group as being increased upon protonation to an unexpectedly large degree, since three acetoxy groups are forced into the axial orientation. However, the equatorial preference need not be very large since the free energy difference ΔG° (Scheme 26) between



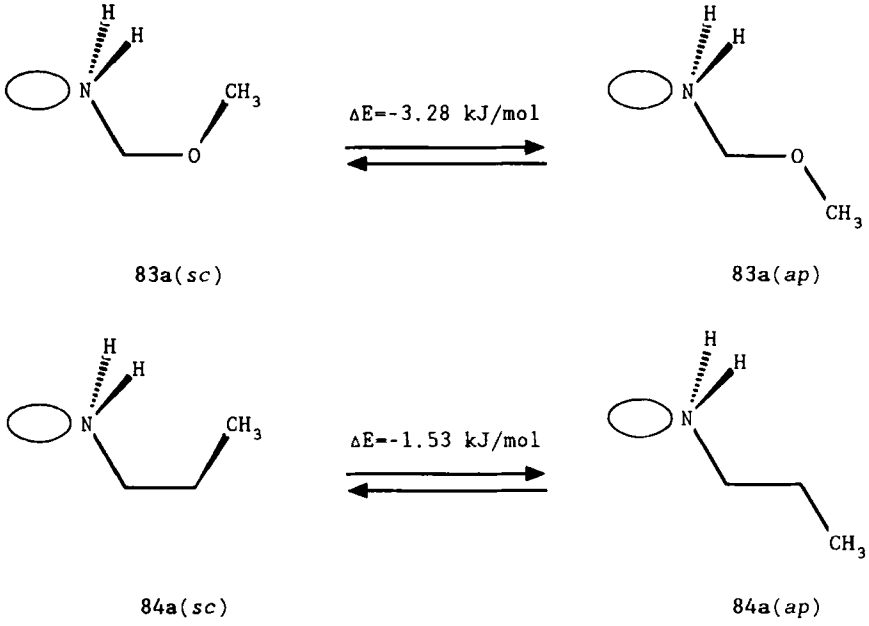
82a **82e**

Scheme 26

the conformations with three benzoyloxy groups axial (in **82a**) and equatorial (in **82e**) is only 3.5 kJ/mol (166b). Consequently, the ordinary steric requirements of the imidazolium group may well account for such a shift in the equilibrium. The observed behavior could thus be attributed to the disappearance of the anomeric effect of the imidazolyl group and/or the overwhelming increase of steric interactions on going from an imidazolyl to an imidazolium group. It is usually assumed (6c, 18, 161) that the steric requirements of imidazolyl and imidazolium groups are very similar, if not identical. However, this point of view may be erroneous since, in the opinion of Manoharan and Eliel (167a) and Abraham et al. (167b), conformational equilibria in amines and their salts are often quite different. Though the energies of geminal groups are not fully additive, Geneste et al. (168) showed that the equatorial preference of a positively charged piperidinium moiety attached to a cyclohexane ring is very large and can exceed that of the phenyl group by 18.4 kJ/mol!

The reverse anomeric effect was postulated for the carboalkoxy group (29, 37, 42) in an O—C—COOR system, but it was proved (38) (see also Table 4) that in fact one deals here with a normal anomeric effect. Recent calculations by Altona's group (72) on the conformation of molecules of the type $X—CH_2—OCH_3$ ($X = COOH, COO^-, C{\equiv}N, C{\equiv\equiv}CH$) revealed that the changes in bond lengths on going from the *ap* to the *sc* conformation

agree with the anticipated n_O–σ^*_{C-X} negative hyperconjugation. However, they suggested operation of the reverse anomeric effect for methoxymethylamine (**83a**) having a nitrogen lone pair antiperiplanar to the C—O bond (Scheme 27), and for cation **88** (*vide infra*). An estimate of the magnitude of



83a(*sc*) 83a(*ap*)

84a(*sc*) 84a(*ap*)

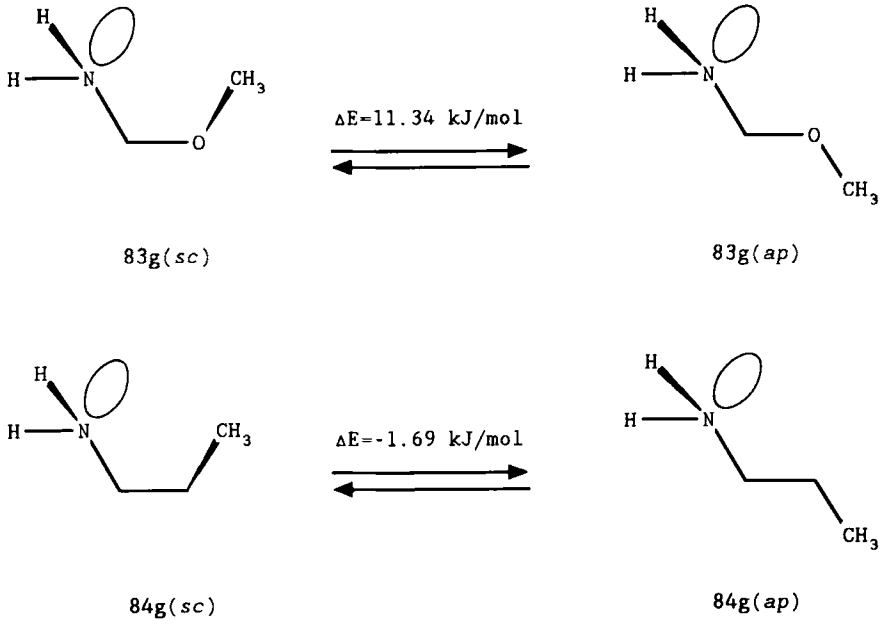
Scheme 27

the anomeric effect ΔE_{AE} in **83a** according to Franck's methodology (Eqs. [4] and [5]; $\Delta E = -3.28$ kJ/mol from ref. 72) using $\Delta E = -1.53$ kJ/mol for the relevant carbon analogue, that is, *n*-propylamine (**84a**) (169), and $F = 1.7$[†] affords $E_{AE} = -3.28 - 1.7 \times (-1.53) = -0.68$ kJ/mol. Therefore, the observed effect, if any, is negligible.

Analogous treatment of the anomeric effect in **83g**,[‡] however, affords a substantial anomeric effect $\Delta E_{AE} = -11.34 - 1.58 \times (-1.69) = 14.0$ kJ/mol

[†]Factor F_G, derived from the free energy difference $\Delta G^\circ_C = 6.07$ kJ/mol (170) for the NH_2 group in cyclohexane, according to the interpolation procedure shown in Sections II.C and II.D, should be equal to 1.58 (assuming $F_G = 1.7$ for the Me group, see Section II.D). One should note, however, that the nitrogen lone pair does not participate in the actual steric interactions in **83a**. Therefore, the NH_2 group behaves as CH_3, and the methyl factor $F = 1.7$ has been used for **83a**.

[‡]Conformers of **83** (and **84**) which have a nitrogen lone pair synperiplanar or synclinal (*gauche*) to the C—O bond are denoted as **83s** and **83g** (**84s** and **84g**), respectively.



83g(*sc*) 83g(*ap*)

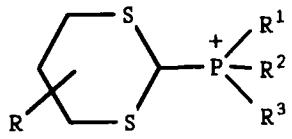
84g(*sc*) 84g(*ap*)

Scheme 28

(Scheme 28: $\Delta E = 11.34$ kJ/mol for **83g** and $\Delta E = -1.69$ kJ/mol for **84g** taken from refs. 72 and 169, respectively). Therefore, the lack of the anomeric effect in **83a** is the result of weak acceptor properties of the σ^*_{C-N} orbital and strong competition between anomeric interactions (the lone pair of nitrogen is antiperiplanar to the C—O bond) (72).

The presence of a reverse anomeric effect was suggested (29) for chloromethyl, $ClCH_2$—, and bromomethyl, $BrCH_2$—, groups located at the anomeric carbon atom of a 1,3-dioxane ring. This claim was based on the observed reversed dependence of axial preference on solvent polarity, that is, more polar solvents increased the population of axial conformers. This observation is in line with the fact that α-glucopyranosylimidazoles in water (very polar solvent) do not change conformation on protonation (162).

In fact, however, more polar solvents may enhance axial preferences without the intervention of a reverse anomeric effect, as was shown by Lemieux (27), Fuchs et al. (129), Zefirov and Fedorovskaya (171), and Giralt et al. (172). In the course of our studies on the conformation of 2-phosphonio-1,3-dithianes **85** we also found (173) that the axial preference may increase with increasing solvent polarity, as expected based on the concept of the reverse anomeric effect. However, 2-phosphonio-1,3-dithianes **85** do not exhibit the reverse but the generalized anomeric effect (see Section V.A). Since the axial



85

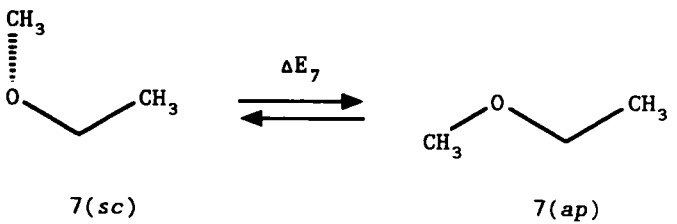
preference in **85** depends also on the counterion, the above findings could, perhaps, be attributed to the more tight character of an ion pair in nonpolar media, which might result in (1) a larger effective "size" of the phosphonium group and (2) a smaller net charge at phosphorus and hence less effective n_S–σ^*_{C-P} negative hyperconjugation. These factors would lead to a decreased axial preference. With increasing polarity of the medium, the interaction between cation and anion decreases, the effective size of the phosphonium group decreases, the net charge at phosphorus increases, and consequently, the axial preference increases. Therefore, the conformational behavior of charged systems cannot be interpreted solely in terms of electrostatic interactions; many other phenomena must also be taken into account. Hence, solvent studies cannot be used as a test for the reverse anomeric effect (see also Section II.G).

Amino groups attached at C(2) to a tetrahydropyran ring were suspected to exhibit the reverse anomeric effect (8, 50, 70) for the reasons discussed in Section II.E. Wolfe et al. (70) also postulated a reverse anomeric effect for aminomethanol (**86**), ethanol (**9**), and ethanethiol (**87**) after redefinition of

$H_2N—CH_2—OH$ $CH_3—CH_2—SH$

86 **87**

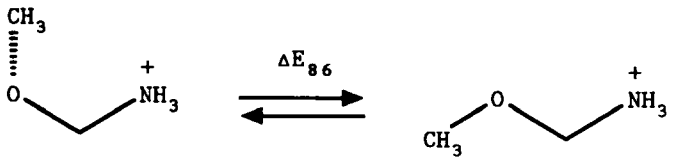
this term on theoretical grounds. Hosie et al. (174) pointed out, however, that this approach is wholly without experimental foundation, as is the explanation of the reverse anomeric effect given by David et al. (175). Nevertheless, the *phenomenological* sense of this effect has been overlooked by theoretical chemists, and Tvaroška and Bleha (9), basing themselves on MO calculations, suggested the presence of a reverse anomeric effect for ethyl methyl ether (**7**). Surprisingly, they found that for the cation **88**, conformer *sc* is less stable than *ap* (rotation about C—O bond; Scheme 29) by 3.8 kJ/mol [5.6 kJ/mol according to Krol et al. (72)], about the same value as that for **7** [3.1 kJ/mol (9); 8.0 kJ/mol according to Allinger et al. (64)]. Hence, though **7** is not a



7(*sc*) 7(*ap*)

ΔE_7=-3.1 kJ/mol (Ref.9)

-8.0 kJ/mol (Ref.64)

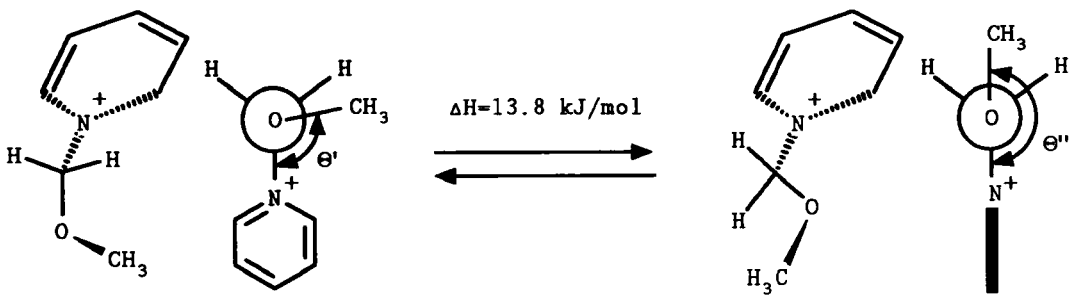


88(*sc*) 88(*ap*)

ΔE_{86}=-3.8 kJ/mol (Ref.9)

-5.6 kJ/mol (Ref.72)

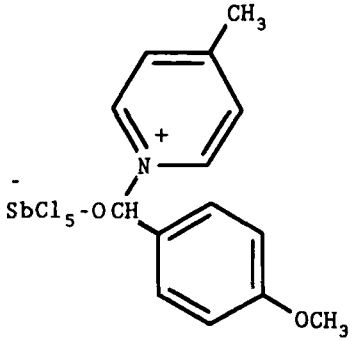
Scheme 29



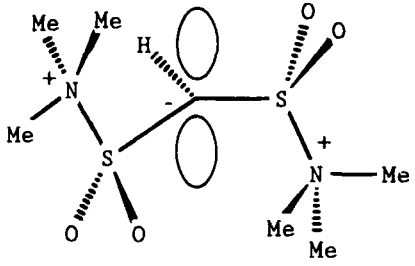
Scheme 30

classical reference system,† no increased preference for **88** (*ap*) is observed, in contrast to expectation based on the reverse anomeric effect.

It should be noted that semiempirical MNDO calculations (176) of the conformation of various *N*-alkylpyridinium compounds indicate an increased preference of $\Delta H = 13.8$ kJ/mol for the *og* ($\Theta' = 106.1°$) over the *ap* conformation about the C—O bond in **89** (Scheme 30). For **90** the appropriate angle Θ was found (176) in the crystal state to be 109.7°. These data are in disagreement with expectations based on observations (106–162, 174) of sugar derivatives where the reverse anomeric effect is manifested in enhanced preference of a pyridinium group for the *ap* arrangement in the C—O—C—N^+ system.



90



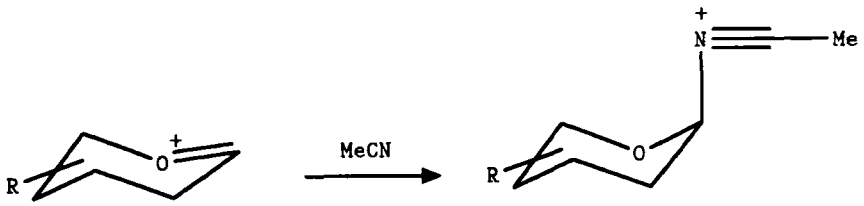
91

X-ray analysis of the tetraphenylborate of cation **91** revealed that its conformation is determined by the n_C–$\sigma^*_{S-N^+}$ negative hyperconjugation (177). No features characteristic of the reverse anomeric effect were observed.

Recently, Ratcliffe and Fraser-Reid (178) have shown that the formation of α-D-glucopyranosylacetonitrilium ions **93** from the appropriate oxocarbenium ion **92** and acetonitrile occurs highly stereoselectively (Scheme 31). This result is in contrast to that predicted by the reverse anomeric effect as applied to the stability of the appropriate transition state. On the other hand, such behavior is anticipated based on the n_O–$\sigma^*_{C-N^+}$ interaction. It must be added that the application of the concept of the reverse anomeric effect to stability of transition states, presented by Sinnott (11), has recently been criticized by Deslongchamps et al. (179, 180) (see also the footnote on p. 288).

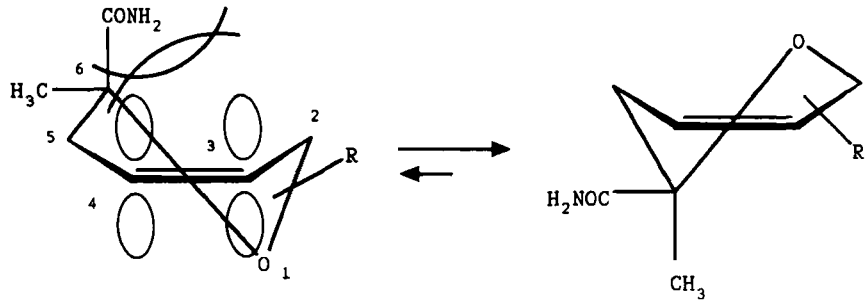
Chmielewski et al. (181) studied the conformational equilibrium of the

†A reference system for **88** should be $CH_3CH_2CH_2NH_3^+$, but the detailed conformational energetics of this molecules is not available.



92 93

Scheme 31



94a 94e

Scheme 32

6-carbamoyl group in a 5,6-dihydro-2*H*-pyran ring (Scheme 32). They found the magnitude of the respective equatorial preference of the $CONH_2$ group much larger than that of a 6-methyl group in **94**. Since ΔG_C° values describing the preference of $CONH_2$ and Me groups in a cyclohexane ring should be quite similar, they concluded (181) that a strong reverse anomeric effect must be operative. In our opinion, however, the relation between ΔG_C° values of $CONH_2$ and Me groups in cyclohexane is not informative. Rather, the appropriate relation in cyclohexene should be taken into account, since conformational behavior of the carbamoyl group there may be different from that observed in the saturated system. In particular, nonbonding repulsions between the carbamoyl group (e.g., carbonyl oxygen lone electron pairs) and the π-electrons of the C=C double bond in cyclohexene might destabilize the axial disposition of the carbamoyl group, and thereby be responsible for a much larger equatorial preference of a $CONH_2$ as compared to a Me group (cf. **94a**). Furthermore, the anomeric effect of the $CONH_2$ group (if any) must

be smaller than that of a COOH group owing to the smaller positive charge at the carbonyl carbon atom and the less effective n_O–σ^*_{C-C} negative hyperconjugation. The latter factor might perhaps be responsible for the observed differences between the conformations of $CONH_2$ and COOMe derivatives both in 5,6-dihydro-2*H*-pyran (181) and in hexapyranose (182) systems. It must be added that according to Franck's approach, a normal anomeric effect of about 0.4 kJ/mol is exhibited by the $CONH_2$ group attached to C(2) in a tetrahydropyran ring (13).

It should be mentioned that the inverse (reverse?) anomeric effect has been postulated (183) recently for propanedinitrile $CH_2(CN)_2$ (**95**) and its derivatives, based on a synergistic destabilization by two geminal cyano substituents. The authors assumed that the anomeric effect always implies a stabilizing interaction between two substituents at an anomeric center (this assumption is not justified, see Section II.H) and a destabilizing interaction must therefore correspond to an inverse effect. However, such an assumption does not correspond to the definition of the anomeric (and reverse anomeric) effects, which is based on the relation between energies of conformers, not on the energy of interaction between substituents at an anomeric center.

III. ORIGIN OF ANOMERIC EFFECT

Interpretations of the anomeric effect depend on the theory that is applied, and only within a given theory can their correctness be checked. Hence, the number of explanations of the anomeric effect is quite large. They can be divided (23) into two basic groups: classical structural theory supplemented with electronic effects (Section III.A) and quantum chemistry (Section III.B).

The quality of rationalization provided by a given theory can be evaluated with relative ease by its applicability to explain *all* phenomena caused by the anomeric effect and its ability (if possible) to afford quantitative predictions of conformational equilibria. Following this approach, the description of the most important interpretations of the anomeric effect will be presented.

A. Classical Approaches

1. Electrostatic Interactions

The first attempt, in 1955, to explain the increased stability of axial alkoxyl groups at the anomeric carbon atom of a pyranose ring is due to Edward (184). He considered the anomeric effect to arise from the destabilization of the equatorial RO— group in **96e** by repulsive interactions between two dipoles connected with the oxygen atoms, that is, the C(2)—OR dipole and

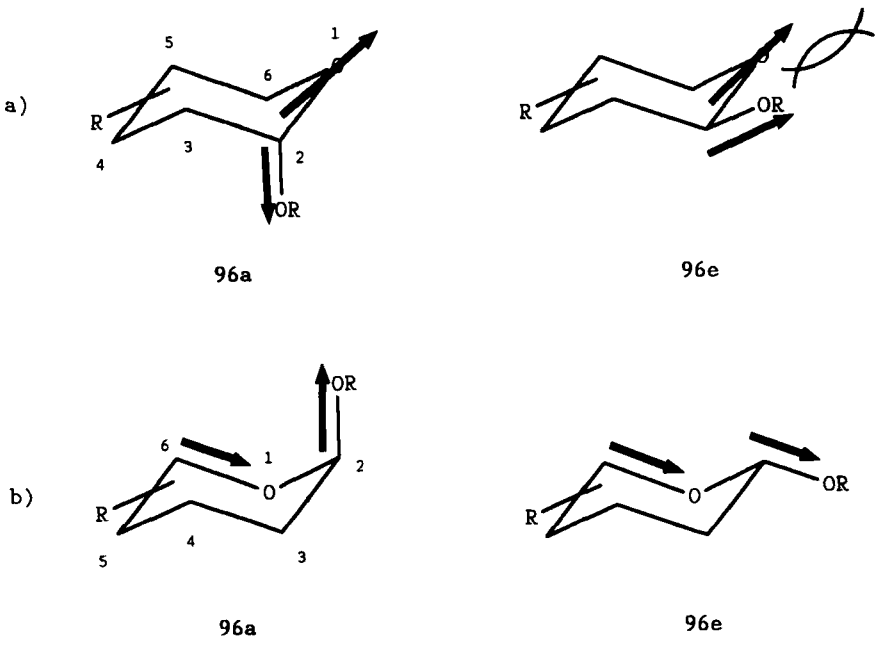
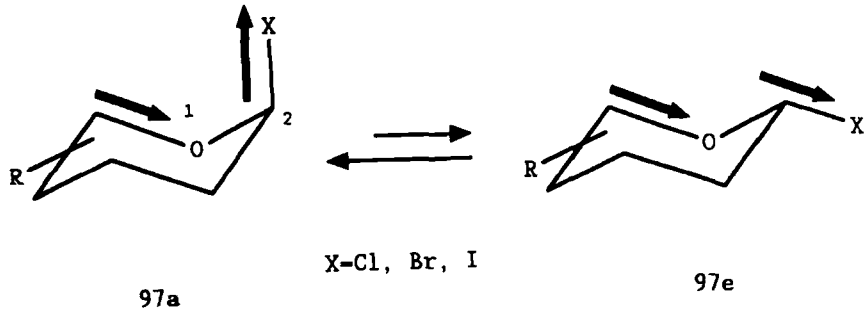


Figure 13. Dipole–dipole interactions in 2-alkoxytetrahydropyrans **96** according to (a) Edward (184) and (b) Lemieux and Chü (24, 185).

the resultant of the C(6)—O(1) and C(2)—O(1) dipoles as shown in Figure 13a.

Four years later, the anomeric effect was more simply attributed, by Lemieux and Chü (24, 185), to interactions between the dipoles of the C(6)—O(1) and C(2)—OR bonds in **96** (Figure 13b). This approach enabled Anderson and Sepp (125) to find a qualitative explanation of the observed axial preference in 2-halotetrahydropyrans **97** (Scheme 33) for it allowed one



Scheme 33

to expect smaller axial preferences of less electronegative substituents (e.g., X = I) as is usually observed (6). Nevertheless, they encountered considerable difficulty in accounting for the larger axial preference of bromine versus chlorine.

The main advantage of this rationalization relates to solvent effects. In polar media electrostatic interactions are reduced, and hence destabilization of the equatorial conformer (in Figure 13a) or stabilization of the axial one (in Figure 13b) is attenuated. The same conclusion may be drawn if the polarity (representd by dipole moments) of the two conformers is scrutinized (cf. Section II.G). Such solvent trends have generally been assumed to be indicative of the electrostatic etiology of the anomeric effect.

It should be pointed out, however, that the increased equatorial preference in more polar media may be attributed to other factors. For instance, ΔG_C° for the hydroxyl group in cyclohexane decreases by 1.4 kJ/mol on passing from aprotic solvents to water (186). This behavior was ascribed to tighter solvation in hydrogen-bonding solvents resulting in an increase in size of a hydroxyl group. Although the importance of dipole–dipole interactions in the conformational behavior of the C—O—C—O—C moiety has been supported by perturbational molecular orbital (PMO) calculations (187) (see Section III.B.4), these calculations were based on arbitrary partitioning of the total energy into its component parts and arbitrarily attributing the dipole–dipole interactions to the V_1 coefficient of the Fourier expansion (see Section III.B.2).

The electrostatic interpretation of the anomeric effect has generally been regarded as incomplete because it does not lead to quantitative agreement with experiment (188) and does not account for the observed geometries. In particular, dipole–dipole repulsive interactions have been criticized from the theoretical point of view on the basis of *ab initio* (189) and semiempirical EHMO and CNDO/2 calculations (190) and recently (191) based on the decreased barrier to ring inversion in 2,2-dimethoxyoxane (**98**, see Section IV.A.2). Perrin and Nuñez (191) analyzed the possible dipole–dipole repulsions in this compound and suggested that they would increase in the transition state; thus the barrier would increase, contrary to observation. Nevertheless, the role of the electrostatic attraction between a terminal atom in the R—O—C—X—R′ moiety [e.g., C(6) in Figure 13] and the heteroatom X (e.g., exocyclic oxygen atom) was suggested to be worth reevaluating (192).

Sometimes (9, 60, 84, 187, 193) the anomeric effect is discussed in terms of *both* dipole–dipole interactions, being a part of classical structural theory, *and* quantum chemistry based on n–σ^* overlap, with variable *relative* importance. This problem is related to the partitioning of total energy via Fourier expansion and will be discussed in Section III.B.2.

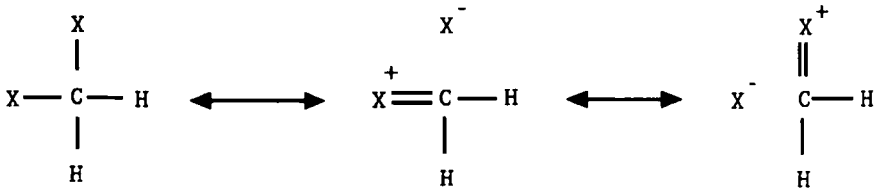


Figure 14. Double bond–no bond resonance.

2. *Solvent-induced Anomeric Effect*

The destablization of more polar equatorial conformers in nonpolar solvents (see Section II.G) is supposed to enhance the anomeric effect (71). It should, however, be pointed out that the influence of solvent is always reflected in a decrease of the anomeric effect already present in an isolated molecule.

3. *Double Bond–No Bond Resonance*

In order to explain the shortening of carbon–halogen bonds in polyhalogenomethanes as compared with methyl halides, in 1937 Brockway (194) postulated *double bond–no bond resonance*, pictured schematically in Figure 14. The changes in bond length with X are related to a progressive increase in the C—X bond energy. On the basis of this point of view, it was easy to explain the electrical properties of the trifluoromethyl group (195).

This concept was not at first accepted universally because averaging the structures shown in Figure 14 suggests that no change in bond length should occur. Moreover, contrary to observation, it suggested larger than tetrahedral X—C—X (X = F) bond angles.

Lucken (196) seems to be the first to hint at a molecular orbital counterpart of double bond–no bond resonance, which will be discussed in Section III.B.3.

4. *Rabbit Ear Effect*

In 1958 Kabayama and Patterson (197) suggested that the instability of equatorial glycosyl halides **97e** may arise from repulsions between lone pairs of electrons in the aglycon X with those of the ring oxygen (Figure 15a). This concept was extended by Hutchins et al. (198) to all systems in which unshared electron pairs on nonadjacent atoms are parallel or synaxial; they termed this the *rabbit ear effect*. The relevant interactions for the R′—Y—C—X—R″ system **14** are schematically presented in Figure 16 using sp^3 hybrid orbitals. It is clear that the *ap, ap* conformation is destabilized by two interactions, but the *ap, sc* by only one. A slight increase in the Y—C—X—R″

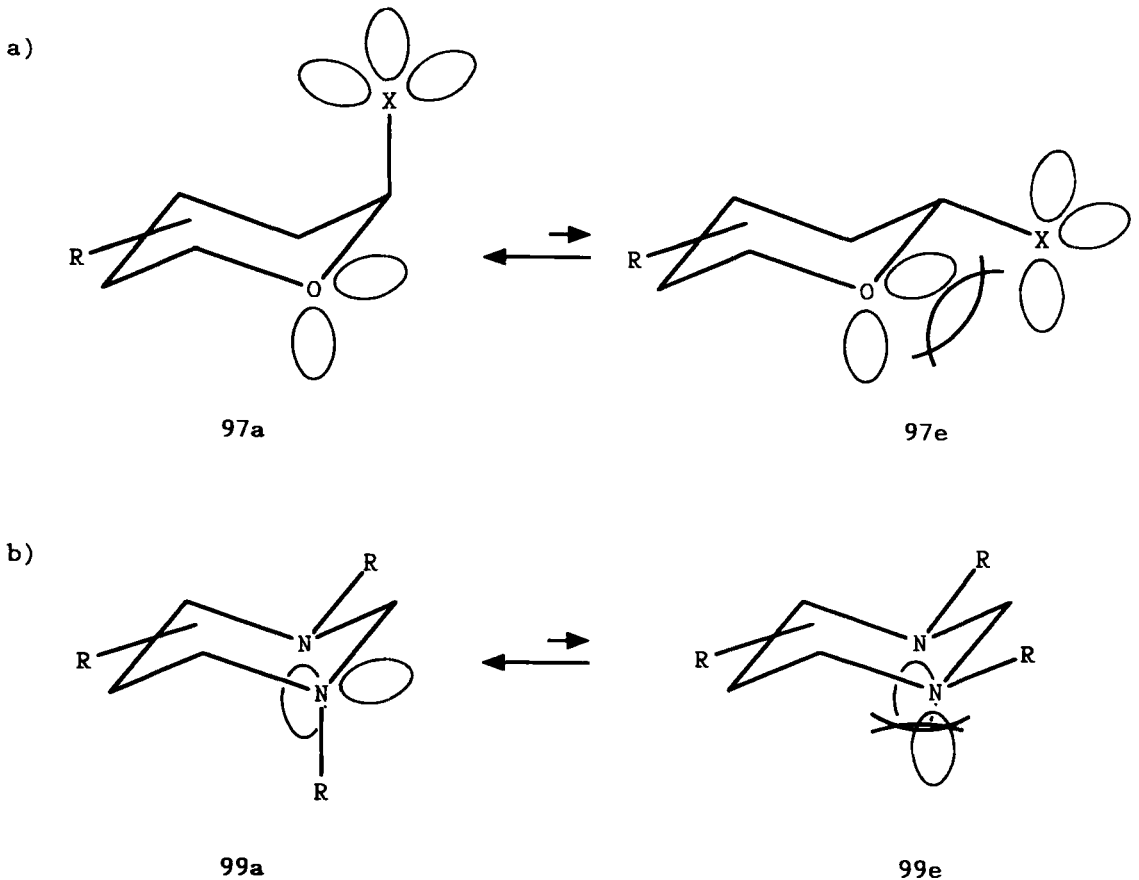


Figure 15. Rabbit ear effect in (a) 2-halogenotetrahydropyrans **97** and (b) 1,3-diazane derivatives **99**.

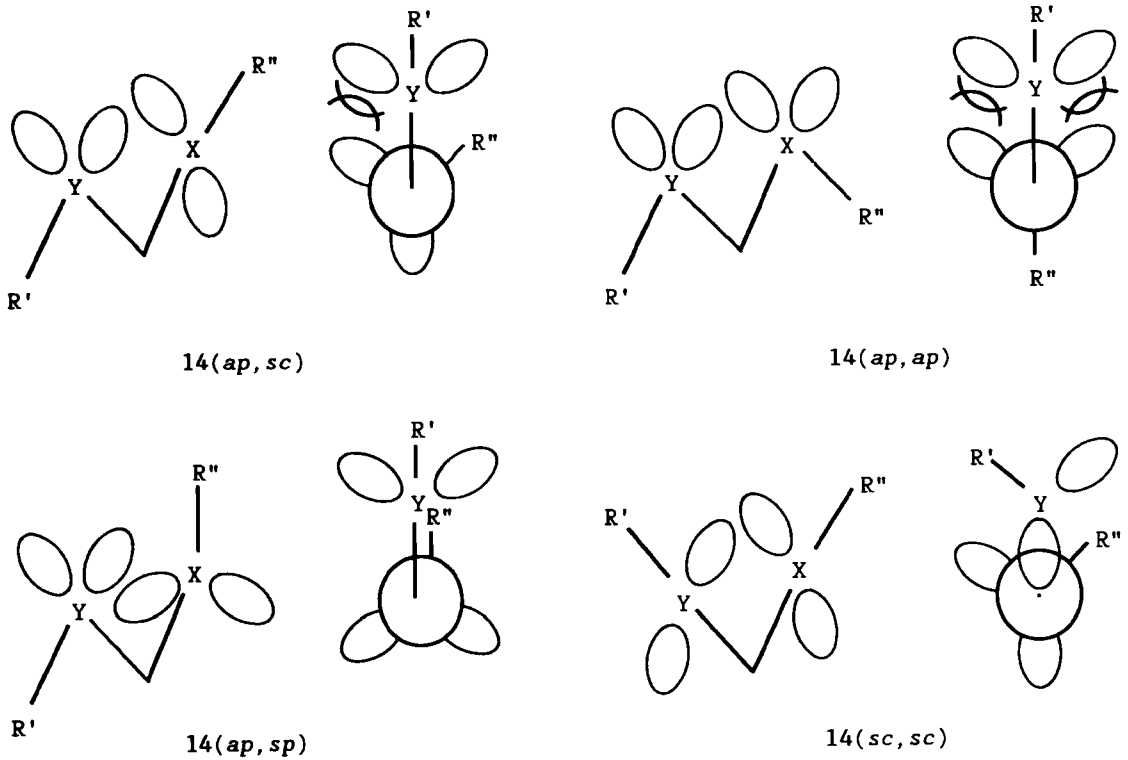
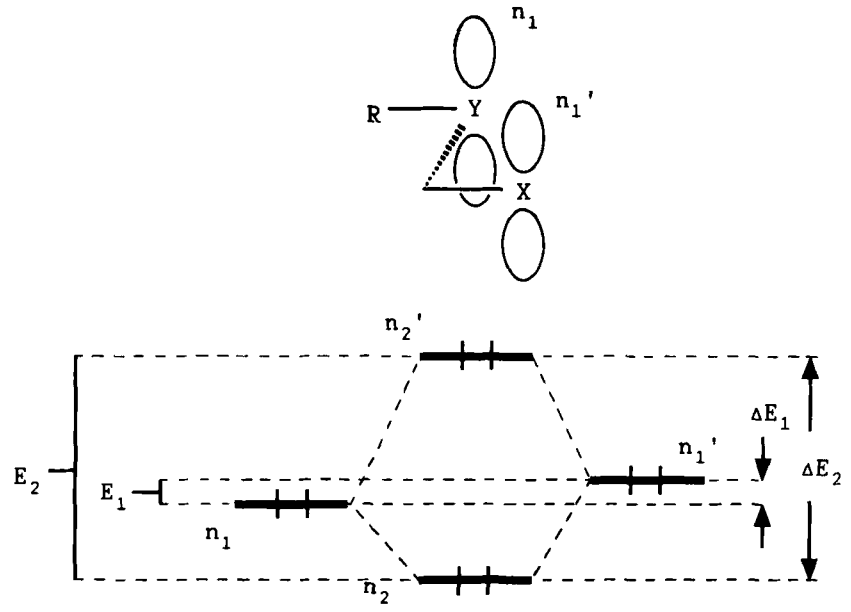
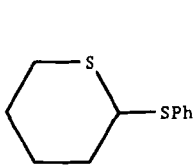


Figure 16. Rabbit ear effect in R′—Y—C—X—R″ system **14**.

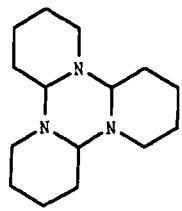


Scheme 34

torsion angle can further minimize the latter interaction (a decrease in this angle to 0° could minimize the repulsion even better, but the resulting *ap, sp*, conformation is disfavored on steric grounds). The *sc, sc* conformer is not destabilized (the use of nonequivalent lone electron pairs leads to similar conclusions, cf. Scheme 34 and Figure 19). With the aid of this concept, the authors (198) explained the tendency of various 1,3-diazanes **99** to avoid a conformation **99e** in which both nitrogen lone pairs are located axially (Figure 15b). Subsequently, the term rabbit ear effect has been applied to account for the relative stability of conformers of, for example, 2-alkoxytetrahydropyrans **96** (28, 126) (Figure 13), 2-phenylthiothiane (**100**) (111), dimethoxymethane (**11**) (6d, 199), cyclic oligomers of formaldehyde (199), and tripiperideines **101** (200).



100



101



102

In the initial publications (28, 198) concerning the rabbit ear effect, its electrostatic nature was emphasized, since electric dipoles were attributed to the atom–lone pair systems. Such point of view encouraged and enabled other workers to criticize this concept rather successfully (see Section III.B.1).

Nevertheless, classical electrostatic interaction has been invoked (9) as being in the nature of destablizing interactions between lone electron pairs. This perhaps need not be true. Eisenstein et al. (201) pointed out that two types of interactions between lone electron pairs, namely *Coulomb repulsion*, and *exchange repulsion*, should be taken into account. A good example is provided by the enthalpy ΔH°_{IS} of the isodesmic reaction for diiodomethane (**64**) discussed in Section II.H. It is clearly seen that the geminal arrangement of two iodine atoms is accompanied by sizable destabilization. This observation may perhaps be attributed to the rabbit ear effect. Strong repulsive interaction of relevant dipoles is improbable in this case since electrons are expected to be disposed almost symmetrically around C—I bonds and to some extent around iodine atoms. Therefore, dipole moments should be too small to be responsible for the observed effect. Perhaps the nature of the phenomenological rabbit ear effect could be accounted for in terms of a molecular orbital description (Section III.B) as an *n*-orbital 2*n*-electron destabilizing interaction, pictured in Scheme 34 (only π-type lone pairs are shown) for two-orbital four-electron destabilizing interaction [*overlap repulsion*; sometimes regarded (202) as the MO counterpart of a "steric effect"]; for the sake of simplicity only π-type orbitals are taken into account. The overlap between filled orbitals n_1 and n'_1 leads to two new orbitals, n_2 and n'_2, the mean energy of which, E_2, is larger than the starting one, E_1. Thus, this process is accompanied by an overall increase in energy, which is responsible for the instability of the *anti* arrangement of the R—Y— C—X system.

These interactions can probably play an important role as far as the anomeric effect of second- and third-row elements is concerned (see Section II.H and especially footnote 44 in ref. 203). But even for the first-row atoms, in the opinion of Box (8, 14, 15), the predominant role of the destabilizing interactions, with a minor contribution from the n–σ^* interactions, is a better model for rationalizing the chemistry of simple acetals. This point of view seems to be strongly supported by the work (204) of Jorgensen and Norskov-Lauritsen. By means of photoelectron spectroscopy they showed that the energy separation of the nonbonding orbitals in dioxadecalin **102** of β-anomeric-like arrangement is 0.85 eV, while in the *sc,sc* conformer of dimethoxymethane (**11**) only 0.02 eV [calculated (204); for *ap,ap* 0.69 eV]. The results were interpreted (14) in terms of strong interactions of the nonbonding oxygen orbitals in the dioxadecalin molecule. Such destabilizing interactions should lead to the observed increase in the energy separation between the orbitals involved from ΔE_1 to ΔE_2, as shown in Scheme 34.

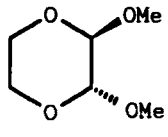
5. *Energy Decomposition Scheme*

An energy decomposition scheme in terms of classical theory proposed by Grein and Deslongchamps (163) is discussed in Section II.I.

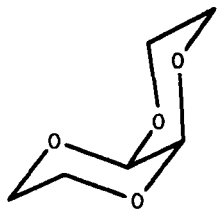
6. *Molecular Mechanics Calculations*

The anomeric effect seems to be not solely due to the interplay of simple van der Waals repulsions and electrostatic interactions. Therefore, molecular mechanics (MM) force field calculations are not expected to reproduce it unless the effect is deliberately included. Hence it has long been recognized that considerable difficulties may appear in proper description of a molecule by the MM method when two heteroatoms are geminally bonded (48, 205, 206).

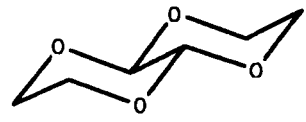
The most popular and useful force field has undoubtedly been Allinger's MM2 program. Its original version MM2-77 (48) was initially parametrized in terms of torsional energy and dipole–dipole interactions to afford the energies of conformers of a R—O—C—O—R system, in reasonable agreement with experiment. The energetic aspect of the anomeric effect was also introduced into the 1974 version of Allinger's previous MM force field by Burkert (207, 208). This parametrization was satisfactorily tested in calculations of carbohydrates (117, 209), 1,4-dioxane **103** (210), and two isomeric tetraoxadecalins **104** and **105** (210).



103



104

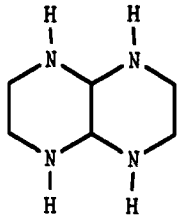


105

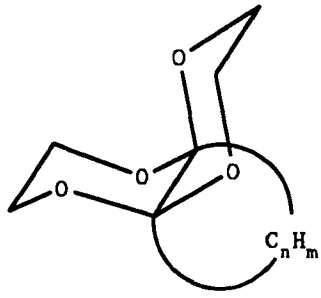
The MM2-80 version was recently shown to reproduce *ab initio* high-level energetics of systems even as complicated as $C(O—R)_4$ (R = H, Me, Ph) (155). However, since the anomeric interactions are reflected not only in energies but also in structure (see Section IV.B), it was necessary to extend the parametrization so as to include the changes in bond lengths and angles. The first attempt in this regard was made by Jeffrey and Taylor (206); a general approach to the problem was later provided by Allinger's group (211)

and incorporated into MM2-82. They showed a parametrization scheme involving a redetermination of l_0 ("natural" C—O bond length used in MM2) for the O—C—O bonds as a function of the torsion angles around them. The changes in bond angles with changes in the C—O bond lengths of the R—O—C—O—R system were included in MM2 by reparametrization of a stretch-bend term.

Comparison of a considerable body of calculated and experimentally determined structures showed, however, that while the calculated O—C—O bond lengths matched the experimental ones well, agreement for the R—O (outer) bond lengths was not satisfactory (211). Inspection of the data revealed that the outer C—O bond gets longer when its adjacent inner C—O bond gets shorter and vice versa. To remedy this situation, the parametrization scheme was extended by Aped et al. in the so-called MM2-AE force field for R—O—C—O—R (192) and for R—N—C—N—R (156) systems. It should be stressed that in the latter case the parametrization of the MM2-80 force field was performed by Aped et al. (156) using *ab initio* conformations of methylenediamine (**73**) and its *N*-methyl derivative. This approach seems to be very promising since *ab initio* MO calculations are prohibitive for molecules of moderately large size [e.g., they are so far limited to analogues of monosaccharides such as **39** (165)]. On the other hand, the MM2 force field thus obtained was used for calculations of large molecules containing a C—N—C—N—C system [e.g., including derivatives of 1,4,5,8-tetraazadecalin (**106**)], with satisfactory reproduction of relative energies and molecular geometries. Recently, Senderowitz et al. (212) improved the parametrization of the N—C—N system based on higher level *ab initio* (6–31G* and MP3/6–31G*) computations and X-ray structural–statistical study.



106

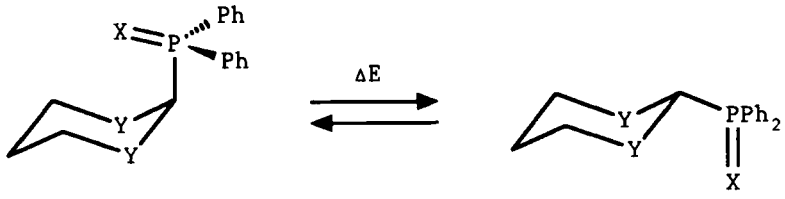


107

The MM2-AE force field was also applied by Aped et al. (192) to conformational study of a series of trimethylsilyloxy- and *t*-butoxy-substituted 1,4-dioxanes **54**. Consideration of MM2-AE-derived data and MO *ab initio*

calculations enabled these investigators to explain the alleviation of the anomeric effect in the compounds under investigation in terms of strong attractive nonbonded O—Si···O interactions within the R—O—C—O—Si system and inductive electron donation by the $SiMe_3$ (or CMe_3) group, which lowers the electronegativity of the O—R ($R = SiMe_3$, CMe_3) substituent. Steric factors were found to be negligible. Recently, this research group applied MM2-AE to conformational studies on 9,10-annellated-1,4,5,8-tetraoxadecalins **107** (213) and some orthoesters containing $C(O—C)_3$ grouping (214). Good agreement was obtained between MM2-AE-derived geometries and X-ray structural data. On the other hand, the fit of the MM2-AE with the *ab initio* (3–21G) results for trimethyl orthoformate (**71**) was very good for the bond lengths and bond angles, but only moderately so for the dihedral angles (214).

Results of molecular mechanics calculations were also used by us to explain the source of the anomeric effect in the Y—C—P=X (X, Y = O, S) system (79). As model compounds we chose **55**, **108**, and **109** (Scheme 35).



55a, X=Y=S — 55e

108a, X=Y=O — 108e

109a, X=O, Y=S — 109e

Scheme 35

The energy minimization of the 2-phosphoryl-substituted 1,3-dioxane **108** showed that the chair conformation **108e** with an equatorial phosphoryl group is more stable than the axial conformer by about 7 kJ/mol [experiment (78) gives $\Delta G^{\circ}_{296} = -8.3$ kJ/mol]. The primary reasons for the lower stability of the axial conformer **108a** are, as expected, repulsive nonbonding 1,3-synaxial interactions between the phosphoryl group and the methylene groups in the ring. These interactions, reflected in the nonbonding interaction term E^{ax}_{nb}, are stronger than the repulsive interactions (given by the lone-pair interaction term E^{eq}_{lep}) between the lone electron pairs on endocyclic oxygens and the phosphoryl oxygen atom in the equatorial conformation **108e** (see Figure 17; for the sake of simplicity lone pairs of X are not shown). In the

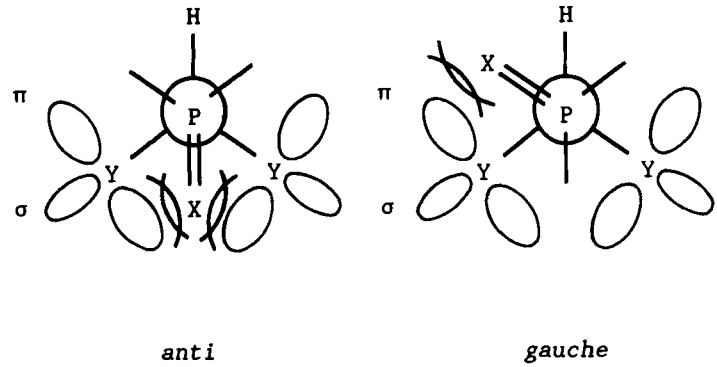


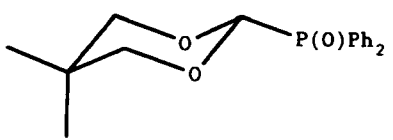
Figure 17. Destabilization of *anti* and *gauche* rotamers [about C(2)—P bond] in equatorial conformers of **55**, **108**, and **109**.

case of the 1,3-dithiane derivative **109** 1,3-synaxial interactions are weaker and the axial conformer predominates by $\Delta E = 5.5$–8.0 kJ/mol [$\Delta G^\circ = 4.1$–4.4 kJ/mol by an experiment (54)]. The calculation for **55** leads to approximately the same population of both conformers, in excellent agreement with experiment (54, 97, 136).

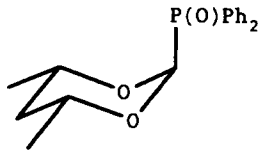
The destabilizing interactions between lone electron pairs play a decisive role as far as conformation about the equatorial C(2)—P bond is concerned. In the *gauche* rotamer, with phosphoryl oxygen (X = O) located *anti* to one of the endocyclic oxygen atoms (Y = O), two repulsive interactions between the lone electron pairs on P=O oxygen and ring oxygen atom are avoided (Figure 17). The energy difference between *anti* and *gauche* rotamers of the equatorial conformer of **108** was calculated as 5.5 kJ/mol (79). Such *gauche* arrangement is indeed observed in the solid-state structures of 1,3-dioxanes **110e** (215) and **111e** (78). In 1,3-dithianes **112e** the preferred conformation about the equatorial C(2)—P bond for X = O should be *anti* due to longer C—Y bonds and a larger Y—Y distance, as observed (54) (see also Figure 62).

A molecular orbital counterpart of the lone electron pair repulsions, n_S–n_Y, will be discussed in Section V.B. The X-ray data support this mechanism for 1,3-dithiane derivatives (see Section V.B.3). However, in the case of 1,3-dioxane **111a** the n_O–σ^*_{C-P} interaction, not reproduced by molecular mechanics calculations, seems to be of greater importance (78) (see Sections V.B.3 and V.B.4).

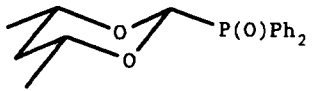
Recently, based on *ab initio* calculations, the MM2-85 force field was modified by Fernandez et al. (216) to linear and cyclic compounds containing N—C—O units. The results calculated for derivatives of **113** (217), **114** (218), **115** (219), **116** (219), **117** (218), and **118** (218) with regard to energetic stabilities and geometries of the different conformers were consistent with



110e



111a

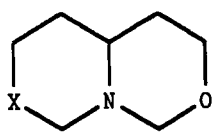


111e

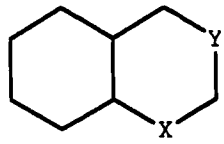


R^1, R^2=Ph, OMe, OCH_2CF_3

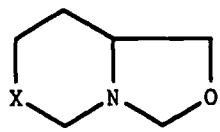
112e



113, X=CH_2
114, X=O



115, X=N, Y=O
116, X=O, Y=N



117, X=CH_2
118, X=O

the available experimental data (NMR, X-ray, infrared spectra, and dipole moments).

Analogous agreement between calculation and experiment (NMR) as far as the preferred conformation of the acetal grouping is concerned was found by Anderson et al. (58) for some simple acyclic acetals.

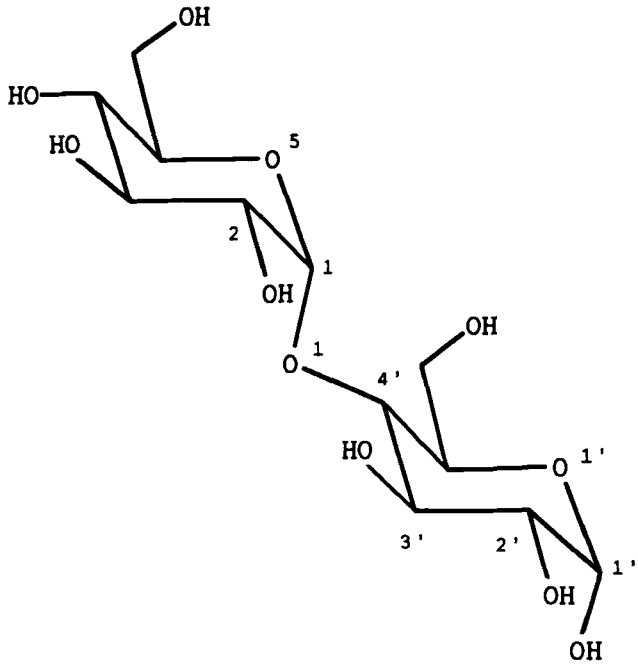
Navio and Molina (105) evaluated the applicability of different versions of MM2 [MM2-77, Jaime and Osawa version (220), and MM2-85 (221)] to structure calculations for twelve 2-alkoxytetrahydropyran derivatives. The calculations were performed using different effective dielectric constants. As expected, the axial conformers were 4–7 kJ/mol more stable than the equatorial ones, and the energetic preference for the axial position decreased with increasing solvent polarity. The calculated populations of the axial conformers were found to be in fairly good agreement with those based on NMR data. The *exo*-anomeric effect could also be predicted. As far as the O–C–O angle is concerned, the tendencies apparent in MO calculations and experimental data (see Section IV.B.1) were well reflected. However, the MM2-77 force field (unlike MM2-85) did not describe geometry well, since bond lengths at the anomeric carbon were the same and did not depend on conformation.

It should be noted that an O—H···O hydrogen bond potential function was developed for the MM2 force field by Kroon-Batenburg and Kanters (222). However, Aped et al. (156) found it inadequate for the proper description of "classic" hydrogen bonds and therefore took refuge in a modification of the existing van der Waals potential function. Recently the treatment of hydrogen bonding was refined (226). This version was applied by Liu and Waterhouse (224) to obtain a relaxed energy map of levanbiose. The authors compared the results with those obtained by other computational methods, namely MM3 (*vide infra*), three methods in MOPAC (225), AM1, MNDO, and MINDO/3. While the MM2 and MM3 methods gave comparable torsion angles for the global minimum structure, the semiempirical methods afforded rather scattered values ranging, for example, from 48.81° (AM1) to 85.23° (MINDO/3) when MM2 and MM3 gave 65.37° and 66.62° for the O5–C5–C6–O2′ torsion angle. MM2-85 was also favorably compared with other

molecular mechanics models (Sybyl 5.1, Sybyl 5.21, and ChemX) and with semiempirical methods by Guntertofte et al. (226) However, Woods et al. (164) found semiempirical methods [MNDO, AM1, and PM3 (227)] also capable of reproducing the trends in geometries, conformational energies, and proton affinities associated with the anomeric and related effects.

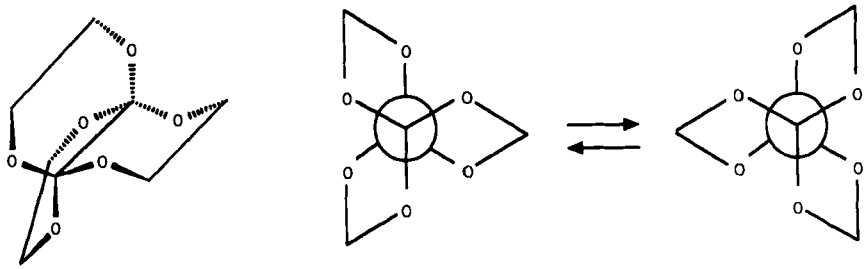
Recently, Allinger et al. (228) have developed a new force field, MM3. They found that the various reasons for inserting lone pairs into the calculation in MM2 are no longer pertinent with MM3, and hence lone pairs are omitted. The authors (64) applied MM3 to the calculation of energy, structure, heats of formation, and vibrational spectra (the latter not accessible by MM2) of alcohols, ethers, and simple acetals. They concluded that MM3 permits one to calculate them with experimental accuracy. Limited accuracy was, however, found for vibrational spectra. Also an inspection of MM2 and MM3-derived outer C—O bond lengths in dimethoxymethane (**11**) revealed that they were too short, though a parametrization analogous to that presented by Aped et al. (192) was expected (64) to be useful in overcoming this difficulty.

The MM3 program was applied by Dowd et al. (229) to compute energy surfaces for relative orientations of the relaxed pyranosyl rings of the two



anomeric forms of such disaccharides as kojibiose, nigerose, and maltose. The authors found similar overall characteristics of the maps. However, within the low-energy region (<33 kJ/mol above the global minimum), the maps exhibit differences which were related to the positioning of the glycosidic bonds relative to the anomeric region and relative to the hydroxymethyl group. The results for maltose were compared with the available crystallographic data on maltosyl-containing molecules. The MM3-predicted bond lengths and valence angles were in good agreement with those found from crystallography. However, the C1–O1–C4′ glycosidic valence angle in α-maltose **119** was underestimated [113.7° in MM3 and 120.1° in the crystallographic structure (230)]. Interestingly, MM3 reproduced the O2 to O3′ intramolecular hydrogen bond, which for α-maltose is present in the global minimum conformation whereas for β-maltose it was found in the second lowest energy conformer. Similar results were also obtained by Dowd et al. (231) for sophorose, laminarabinose, and cellobiose.

Aped et al. (214) used the MM3 force field to calculate the minimum energy conformations of propellane **120** and the corresponding transition states on the inversion path (Scheme 36). A comparison of the inversion barriers calculated for the overall process (86 kJ/mol) and found experimentally by NMR measurements (49 kJ/mol) led the authors to the conclusion that it is difficult to obtain accurate results, since MM3 is currently not well parametrized for the *gauche* effect; also the solvent and entropy effects could not be properly assessed (214).



120

Scheme 36

B. Quantum Chemical Approaches

In principle, in order to solve a conformational problem, one must find a solution of the Schrödinger equation for a given system of nuclei and electrons to obtain the dependence of energy on geometry of this system. This solution

has rigorous (i.e., exact) meaning and tells *nothing* about the reason for the preferred arrangement of nuclei. As was pointed out by Zefirov (23), if the calculation for a given molecule is correct, one must get the description of the conformational behavior that conforms to the experimental data and the notion "conformational effect" does not emerge at all. However, since it is impossible to perform such calculations in most cases of interest, scientists have developed two simplified basic approaches to the quantum chemical description. Their purpose was to provide some sort of rationalization and to enable one to estimate conformational behavior without sophisticated calculations.

The first method is based on partitioning of the energy function into its component parts (23) (Sections III.B.1 and III.B.2). The second one uses sets of orbitals and evaluates their mutual interactions (Sections III.B.3–III.B.9).

1. *Energy Component Analysis*

Wolfe et al. (189) performed an *ab initio* SCF MO computation of the energy of fluoromethanol (**121**, cf. **14**, R′ = H, Y = O, X = F, Scheme 8) as a function of rotation about the carbon–oxygen bond assuming constant bond lengths and equivalence of oxygen lone pairs. They found a maximum of total energy E_T at $\Theta = 180°$ (cf. Scheme 1) and two equienergetic minima at $\Theta = 60°$ and $\Theta = 300°$. The differences in energy between the *sc* conformer ($\Theta = 60°$) and the *ap* and *sp* conformations (which are rotational transition states) were calculated to be 52.7 and 34.5 kJ/mol, respectively. Then they partitioned the E_T function according to Allen's (232) procedure into the following components:

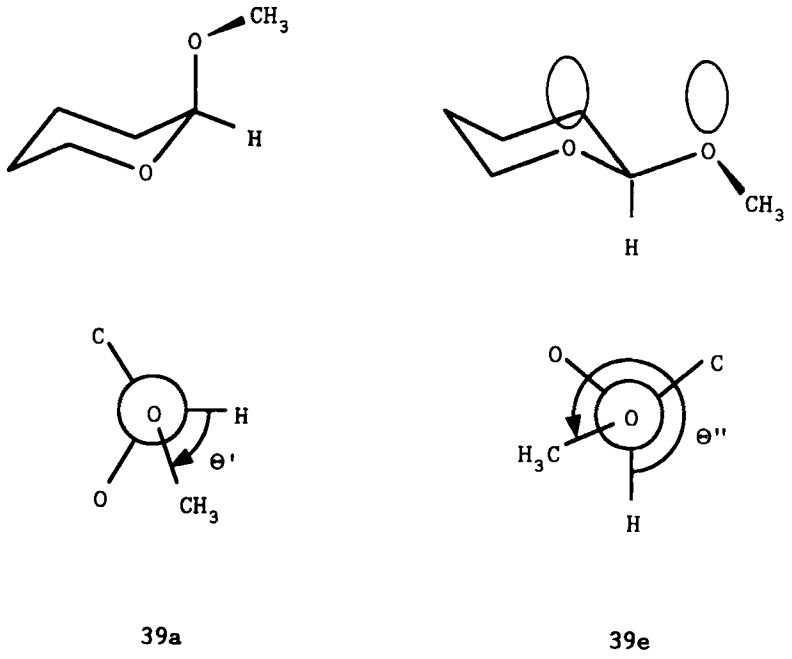
V_{nn} = nuclear–nuclear repulsion
V_{ee} = electron–electron repulsion
T = kinetic energy
V_{ne} = nuclear–electron attraction

Because the anomeric effect had been discussed at that time in terms of electrostatic interactions (cf. Section III.A.1), Wolfe et al. further separated the electron–electron repulsion term into coulombic V_{ee}^{coul} and exchange V_{ee}^{exch} terms. They assumed that V_{ee}^{coul} is the quantum mechanical counterpart of the classical electrostatic coulombic repulsions whose significance might thus be estimated.

Since the form of V_{ee}^{coul} as a function of Θ was not distinguishable from that of the other repulsive terms, namely V_{nn} and T, they concluded that the "physical origin of the Edward–Lemieux effect cannot be ascribed in any straightforward way to coulombic interactions. Consequently, analyses of

the phenomenon in terms of dipole–dipole repulsive interactions are without theoretical justification" (189).

Consideration of the magnitude of the rotational barriers showed that if two different barriers are present (as in the case of **121**, FCH_2OH), the lower barrier corresponds to the smaller number of bonded electron pair–bonded electron pair interactions, nonbonded electron pairs being of less importance. When polar bonds are in the *sp* arrangement, the repulsive $E_{rep} = T + V_{nn} + V_{ee}$ term outweighs the attractive one (V_{ne}). It results in a maximum E_T of 34.5 kJ/mol. In going to the *ap* conformer, both repulsions and attractions decrease (E_{rep} decreases, V_{ne} increases). For $\Theta = \pm 60°$ the sum of energies reaches a minimum. Since attractive interactions decrease (the V_{ne} term increases) faster than repulsions, the energy E_T at $\Theta = 180°$ is again at a maximum of 52.7 kJ/mol. Therefore, in the authors' opinion, the anomeric effect in fluoromethanol is the result of interactions of bonded electron pairs with each other and can be discussed in terms of a delicate balance between core-electron attractions and electron–electron and nuclear–nuclear repulsions. Moreover, the anomeric effect is a ground-state property only inasmuch as in the lowest lying singlet excited state the *ap* form is more



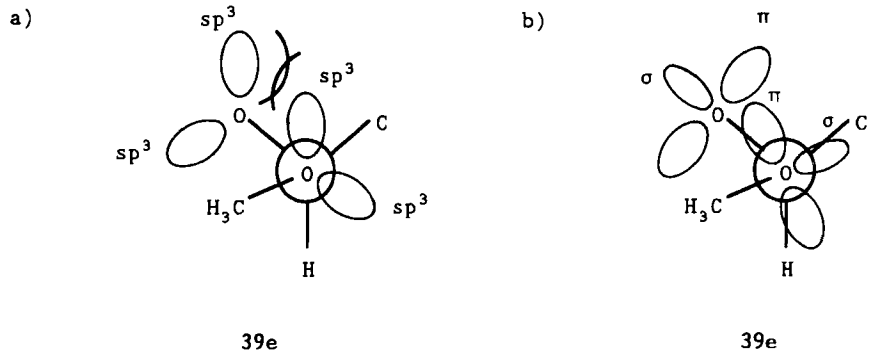
39a 39e

Figure 18. 2-Methoxytetrahydropyran conformers **39a** and **39e**.

stable that the *sc* one (233). Soon this interpretation was reconciled by Whangbo and Wolfe with a PMO-based interpretation (see Section III.B.3).

Related work concerning 2-methoxytetrahydropyran (**39**) (Figure 18) was subsequently published by Zhdanov et al. (190). Since this system is large, the energy calculations were performed by semiempirical EHMO and CNDO/2 methods without optimization of geometry. Fluoromethanol (**121**) was scrutinized in the same way to compare the results with those obtained by the *ab initio* method (189). Besides the total energy E_T of the system under investigation, Zhdanov et al. calculated the interaction energy E_{int} of unshared electrons on both heteroatoms. The repulsion energy E_μ of lone electron pairs in hybrid atomic orbitals was also estimated by dipole–dipole approximation. It was found that the total energy E_T of **39** is strongly dependent on rotational conformation about the exocyclic C—O bond (Figure 18; angles Θ' and Θ'' in **39a** and **39e**, respectively). The most stable axial (**39a**) and equatorial (**39e**) conformers were those with $\Theta' = 60°$ and $\Theta'' = 300°$, respectively, with the former more stable than the latter by 2.5 kJ/mol (with CNDO/2) or 13 kJ/mol (with EHMO); they are shown in Figure 18. Since in the most stable conformer of **39e** with $\Theta'' = 300°$, the axial lone pair located on the endocyclic oxygen is parallel to one of the equivalent nonbonding electron pairs on exocyclic oxygen (cf. Figure 18 with Figure 15a), Zhdanov et al. concluded that the *rabbit ear rule* does not operate. However, as discussed in Section III.A.4, this interaction normally occurs in the *ap*, *sc* conformer of the R′—O—C—O—R″ system (see Figure 16) and can be minimized by a slight increase in the O—C—O—CH_3 dihedral angle (see Figure 19a). Moreover, if one assumes nonequivalence of oxygen lone pairs, the relevant destabilizing interactions for **39e** will be rather small even at $\Theta'' = 300°$ (see Figure 19b).

The repulsion energy E_μ in **39e** depends on Θ'' and reaches a minimum



39e 39e

Figure 19. Interactions of (a) sp^3-type and (b) σ- and π-type lone electron pairs in **39e**.

value of -2.4 kJ/mol at $\Theta'' = 240°$ (synperiplanar conformation), as expected (see Section III.A.4). Nevertheless, since the minimum does not occur at $\Theta'' = 300°$, when **39e** is most stable, Zhdanov et al. (190) considered this finding as a significant piece of evidence that the dipole–dipole repulsion of lone electron pairs on hybrid orbitals is not the main reason for the anomeric effect in **39**. Also taking into account that the interaction energy of unpaired electrons E_{int} depends only to a small extent on the *exo* rotameric configuration, Zhdanov et al. concluded that their results support the previous suggestion by Wolfe et al. (189) that electrostatic interactions are not the main cause of the anomeric effect.

2. *Fourier Component Analysis of Potential Function*

The energy function $E_T = f(\Theta)$ for a molecule rotating around a single bond can be analyzed (23, 234) by a Fourier expansion $V(\Theta)$ given in Eq. [24]. The relation between $E_T = f(\Theta)$ and $V(\Theta)$ is expressed by Eq. [25] where the constant C is chosen in such a way that if $\Theta = 0°$, then $V = 0$. Of course, if rotation about two bonds is possible (as in dimethoxymethane), two dihedral angles Θ' and Θ'' are variable:

$$V(\Theta) = 0.5V_1(1 - \cos\Theta) + 0.5V_2(1 - \cos 2\Theta) + 0.5V_3(1 - \cos 3\Theta) + V'_1 \sin\Theta + V'_2 \sin 2\Theta \quad [24]$$

$$E_T(\Theta) = V(\Theta) + C \quad [25]$$

$$V(\Theta) = 0.5V_3(1 - \cos 3\Theta) \quad [26]$$

For each fixed Θ' one can obtain individual Fourier expansions $V(\Theta'')$ with respect to rotation described by the dihedral angle Θ''; this corresponds to a particular section through the energy surface $E_T = f(\Theta', \Theta'')$. If for $\Theta'' = 180°$ a molecule has a plane of symmetry, it suffices to consider only the first three terms of Eq. [24]. This is the case for fluoromethanol (**121**) (Figure 20) and dimethoxymethane (**11** with Θ' fixed at 180°). In addition, when one rotating alkyl group is of C_3 symmetry (as is, approximately, CH_3 in methanol), internal rotation may be adequately described by a simple threefold potential function expressed by Eq. [26].

Radom et al. (234) seem to have been the first to interpret internal rotation in molecules exhibiting the anomeric effect by means of a Fourier expansion of the potential function. They performed *ab initio* SCF MO calculations for a wide variety of molecules but without geometry optimization. It was found that internal rotation in ethane, propane, fluoroethane, and methylamine is

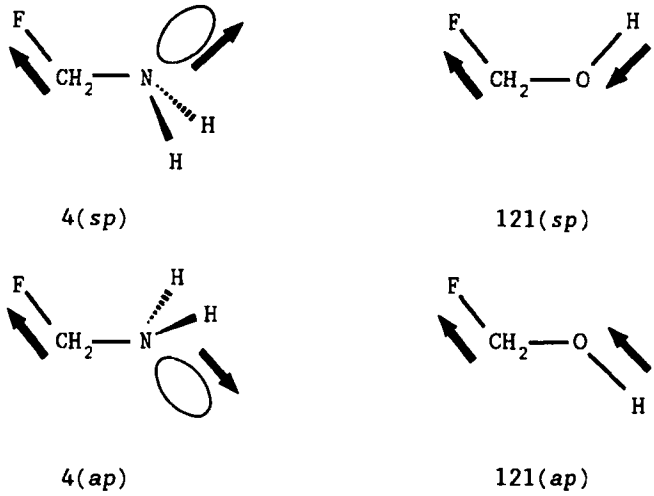


Figure 20. Intramolecular dipolar interactions in the *sp* and *ap* conformers of **4** and **121**.

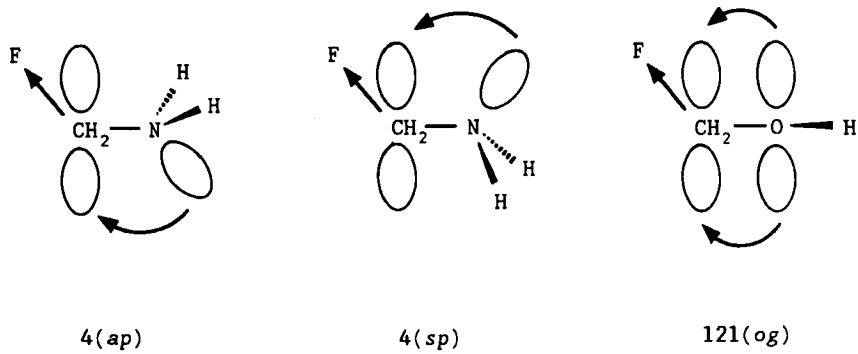
adequately described by (a negative) V_3 in Eq. [26]. Thus for $\Theta = 0°$, 120°, 240°, $V = 0$ ($E_T = -V_3$) and for $\Theta = 60°$, 180°, 300°, $V = V_3$ ($E_T = 0$ because $C = -V_3$ in Eq. [25]). It is clearly seen that for $\Theta = 0°$, 120°, 240° one has energetic maxima and for $\Theta = 60°$, 180°, 300° energetic minima corresponding to *eclipsed* and *staggered* conformations, respectively. For less symmetrical molecules [e.g., fluoromethylamine (**4**), ethylamine, fluoromethanol (**121**), or ethanol (**9**)] it was necessary to calculate V_1, V_2, and V_3 terms. But in all cases, the V_3 term was negative. This suggests that V_3 accounts for the usual preference for the staggered (*sc* or *ap*) over the eclipsed (*sp* or *ac*) conformation, possibly as a result of some form of bond–bond repulsion (234).

The V_1 constant is strongly negative ($V_1 = -20.3$ kJ/mol) for fluoromethylamine (**4**) but strongly positive ($V_1 = +21.9$ kJ/mol) for fluoromethanol (**121**). A negative V_1 constant indicates that the most stable conformation (from the V_1 term point of view) is *ap* and the least stable is *sp*. If V_1 is positive, on the other hand, the most stable conformation (from the V_1 term point of view) is *sp*. This finding is consistent with stabilization (or destabilization) of these molecules by intramolecular dipolar interactions as pictured in Figure 20. For **121**, the *ap* form is less stabilized (or more destabilized), whereas attractive, dipolar interactions in **121** are present predominantly in the *sp* conformation.†

† The difference in sign of the V_1 term between FCH_2OH and FCH_2NH_2 is of nomenclatural origin. If the dihedral angle Θ in FCH_2NH_2 were defined in such a way as to be zero for the *ap* or *anti* arrangement of the lone electron pair and the C—F bond (contrary to the Klyne–Prelog convention), the V_1 term for **4** would be of opposite sign, that is, positive.

Let us consider the V_2 term. Since it is modulated by $(1 - \cos 2\Theta)$, extrema appear at $\Theta = 0°$, 90°, 180°,⋯. If V_2 is positive, maxima of E_T appear at $\Theta = 90°$, 270° whereas minima are found at $\Theta = 0°$, 180°. This is the case for fluoromethylamine (**4**) ($V_2 = 17.9$ kJ/mol). For fluoromethanol (**121**) $V_2 = -9.2$ kJ/mol and the most stable form (taking only the V_2 term into account) should be the orthogonal (*og*, $\Theta = 90°$, 270°) one. Radom et al. (234) attribute the V_2 stabilization of the *sp* and *ap* conformations of **4** and of the *og* conformation of **121** to electron delocalization involving σ-electron withdrawal and *n*-electron donation (Figure 21). Electrons are donated from the nitrogen (oxygen) *p*-type pair into the partially emptied (due to the inductive effect of fluorine) carbon 2*p* orbital, thus leading to stabilization of the pertinent conformations. In the same paper (234), they suggest that the effect responsible for V_2 may be back donation from lone-pair *n* orbitals at one end of the molecule into antibonding σ^* orbitals at the other one. In our opinion, however, such interaction for **4** should be much greater in the *ap* than in the *sp* conformation (see Sections III.B.4 and III.B.5). This finding is in disagreement with the magnitude of the V_2 term, which has the same value at $\Theta = 0°$ and $\Theta = 180°$. Therefore, the fit between V_2 and the n–σ^* interaction seems to be purely fortuitous.

Since then the above approach has been applied to explain the conformational behavior of various systems by separating dipole–dipole (V_1), electron delocalization (V_2), and intrinsic (V_3) contribution to the anomeric effect in fluoromethylamine (**4**) (30), methanediol (**8**) (235), dimethoxymethane (**11**) (9, 236–238), methoxymethanol (**49**) (238), methoxymethylamine (**83**) (9), methoxymethylammonium cation (**88**) (9), flouromethanol (**121**) (9, 239), methoxymethyl chloride (**122**) (9, 236–238), methoxymethyl fluoride (**123**) (9, 238), methoxymethylthiomethane (**124**) (9), and some $XH_n—CH_2—OH$



4(*ap*) 4(*sp*) 121(*og*)

Figure 21. The σ-electron withdrawal and *n*-electron donation in **4** and **121**.

TABLE 11
Potential Constants V_1, V_2, and V_3 (kJ/mol) for Internal Rotation in **122** and **123**

Compound	V_1	V_2	V_3
122	−38.7	−46.6	−28.6
123	6.73	−17.3	−16.3

From ref. 238.

(X = F, O, N, C) systems (240):

$HO—CH_2—OH$ **8** $MeO—\mathbf{CH_2}—OMe$ **11** $MeO—CH_2—OH$ **49**

$MeO—CH_2—NH_2$ **83** $MeO—CH_2—NH_3^+$ **88** $ClCH_2OCH_3$ **122**

FCH_2OCH_3 **123** $MeSCH_2OMe$ **124**

Let us consider selected data calculated *ab initio* (RHF/4–31G level) by Jeffrey and Yates (238) (Table 11). These are quite reliable data, in contrast to data generated by lower level semiempirical methods (9, 236, 237, 239), which do not reproduce the anomeric effect very well (57, 211, 238). The constants V_1 for **122** and **123**, responsible for dipole–dipole interactions, have opposite signs. This means that dipolar interactions favor the *sp* conformation of **123** but the *ap* conformation of **122**. A negative V_1 term for methoxymethyl chloride (**122**) should be considered "abnormal" since it does not agree with the expected (cf. **121** in Figure 20) most effective attractive interaction between C—Cl and CH_3—O bond dipoles in the *sp* conformer of **122**.

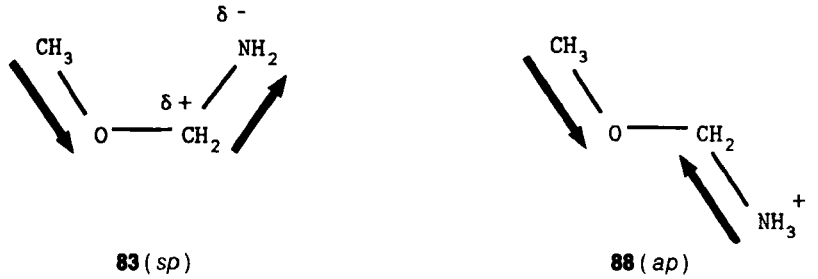
To avoid this inconsistency, Jeffrey and Yates (238) suggested that the V_1 term for **122** is underestimated as a result of underestimation of steric repulsions resulting from the use of a minimal STO-3G basis set. Consequently, V_1 would include some steric interactions which favor the *ap* conformation.

Similar conclusions may be drawn from the V_1 constants for some compounds listed in Table 12. For all compounds in Table 12, V_1 is negative and this implies that dipole–dipole interactions would favor the *ap* arrangement. This may be correct for ammonium cation **88**, which should favor the *ap* conformation both by dipole–dipole interactions and for steric reasons. However, for **83** one should anticipate the V_1 term to be considerably larger (i.e., more positive) than the V_1 term for **88** since (1) positive charge is located

TABLE 12
Potential Constants V_1, V_2, and V_3 for Internal Rotation about C—O Bond and *sc*, *ap* Conformational Energy Difference ΔE in $CH_3O—CH_2X$ Molecules

Compound	X	V_1	V_2	V_3	ΔE (kJ/mol)
7	CH_3	−6.18	0.05	3.77	−3.1
83	NH_2	−9.08	−6.25	−2.73	−2.1
88	NH_3^+	−9.96	−4.96	−6.17	−3.8

From ref. 9.

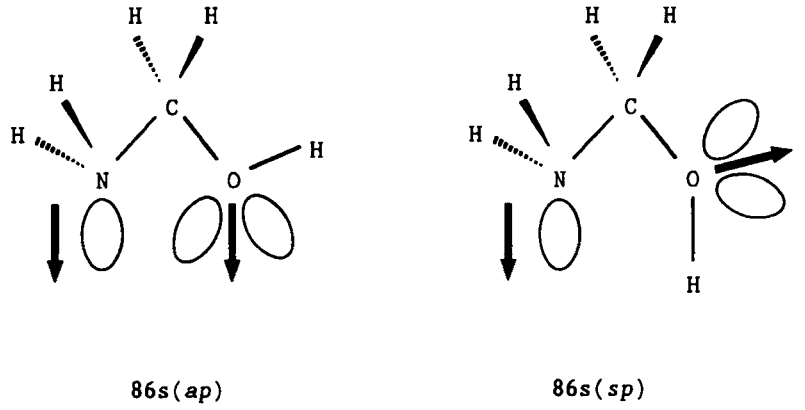


83 (*sp*) **88** (*ap*)

Figure 22. The most effective dipole–dipole interactions for nitrogen-containing compounds presented in Table 12 (X = $^+NH_3$, NH_2).

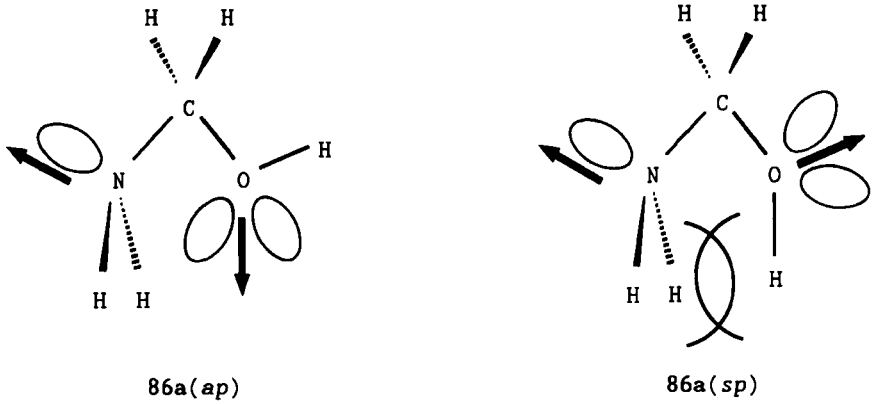
on the carbon of the CH_2NH_2 fragment, as shown in Figure 22, and (2) the steric requirements of the NH_2 group should be considerably smaller than that of NH_3^+. Interestingly, a negative V_1 term for **7** suggests a purely steric origin of this term.

An analogous inconsistency was encountered by Grein and Deslongchamps (240) in the case of aminomethanol (**86**). They studied rotation about the C—O bond in two conformers of **86**: **86s** with the nitrogen lone pair in the synperiplanar arrangement to the C—O bond (Figure 23) and **86a** having the nitrogen lone pair antiperiplanar to the C—O bond (Figure 24). They found the V_1 term equal to 20.6 and −4.0 kJ/mol [after correction of sign; note the opposite convention of signs of V_1 in this review (and, e.g., refs. 9, 234, 238) and the work of Grein and Deslongchamps (240)] for **86s** and **86a**, respectively. The former value agrees well with the dipole–dipole-determined preference for the *sp* arrangement of **86s**. On the other hand, a negative V_1 for **86a** would suggest that the dipole–dipole interaction favors the *ap* conformation of **86a**, which is impossible. Grein and Deslongchamps (240) proposed that a negative V_1 term for **86a** reflects also a strong repulsion



86s(*ap*) 86s(*sp*)

Figure 23. Dipole–dipole interactions in **86s**.



86a(*ap*) 86a(*sp*)

Figure 24. Dipole–dipole interactions in **86a**.

between the hydroxyl and amino hydrogens in the *sp* conformer of **86a** (see Figure 24). The authors (240) also faced difficulties in accounting for a negative V_2 term for **86a** and both eclipsed and staggered (rotation about the C—C bond) conformations of CH_3CH_2OH. Eventually, they attributed these difficulties to artifacts of the fitting formula.

For dimethoxymethane (**11**) with Θ' fixed at 60° the maximum destabilizing dipole–dipole interaction given by the V_1 term occurs (238) at $\Theta'' = 0°$. Simple consideration of possible dipole moments (125–128) implies that the maximum should not occur at $\Theta'' = 0°$. In Kirby's (6e) opinion the maximum dipole moment is at $\Theta'' = 120°$. His suggestion that dipolar interactions may

appear in other terms is unconvincing. Moreover, the physical sense of his V_4 and V_5 terms seems to be obscure.

The few examples discussed above show that analysis of a Fourier expansion of the potential function may sometimes lead to unexpected and rather improbable conclusions. This is not surprising because the decomposition of the potential function is less rigorous that the computation of total energy (70, 146). Fourier expansion almost *a priori* determines the physical sense of V_1, V_2, and V_3 by assuming periods of 360°, 180°, and 120°, respectively, for the modulating factors. There is no proof that V_1, V_2, and V_3 describe particular physical quantities. Radom et al. (234) and Grein and Deslongchamps (240) have suggested that the V_1 term may be responsible in part for steric interactions. On the other hand, when the latter authors obtained, for the $CH_2{=}OH^+$ cation, a steric term $V_3 = -3.4$ kJ/mol, they concluded that "due to the lack of threefold symmetry, V_3 is not meaningful" (240). Therefore, serious discussions concerning the importance of dipole–dipole versus hyperconjugative interactions as causes of the anomeric effect based solely on the magnitude of V_1 and V_2 constants are, in our opinion, inappropriate (54). Similar criticism concerning the assignment of dipole–dipole and hyperconjugative interactions to the origin of V_1 and V_2 constants, respectively, has been presented by Reed and Schleyer (146). Irwin et al. (30) pointed out that the interpretation of conformational behavior in FCH_2NH_2 (**4**) by a Fourier expansion is oversimplified, because it ignores the strong coupling between lone-pair orientation and pyramidality at nitrogen. Nevertheless, the validity of the Fourier component analysis of a potential function for understanding the conformational behavior of molecules exhibiting the anomeric effect seems still to be accepted (13, 18, 240).

Finally, it must be added that Tvaroška and Bleha, in order to support their V_1, V_2-based conclusion (9, 187, 236) concerning the prevailing importance of dipole–dipole or rabbit-ear-type electrostatic interactions in dimethoxymethane (**11**) took refuge in PMO calculations (187). They found (187) that the stabilization energy stemming from delocalization [lone pair, π^* (CH_2)] is large (about 37 kJ/mol) but its conformational dependence is not pronounced. The increase in energy of stabilizing interactions between lone pairs with σ^* orbitals on going from the *ap, ap* to the *ap, sc* conformation of **11** is only about 1 kJ/mol. It should be pointed out that the above authors' claim with regard to dipole–dipole interactions is in fundamental contradiction with studies (189, 190) presented in Section III.B.1.

3. *Initial MO-based Approach to Double Bond–No Bond Resonance*

In order to explain the anomalously low nuclear quadrupole resonance frequencies of ^{35}Cl in Y—C—Cl (Y = O, S, F, C=C, C≡C) systems, Lucken

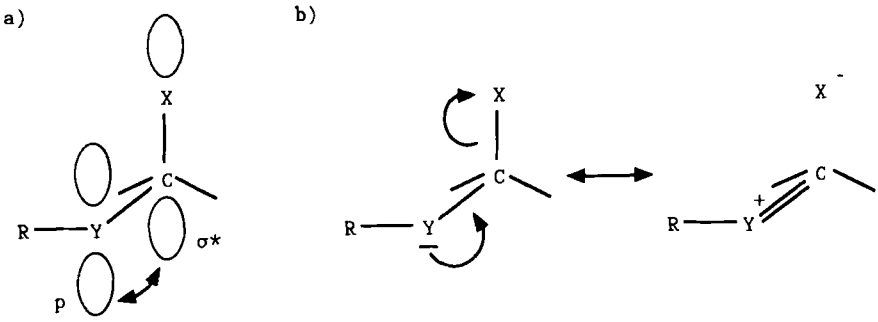


Figure 25. (a) Interaction between a p orbital of Y and the antibonding σ^*_{C-X} orbital of the C—X bond. (b) Classical double bond–no bond resonance structures.

(196), in 1958, proposed an interaction between a p-type orbital of the heteroatom Y (or group) and an antibonding orbital of the carbon–chlorine bond. This interaction was invoked by Altona (188, 241, 242) to account for the shortening of the Y—C (Y = O, S; Figure 25a) and the lengthening of the axial C—X (X = Cl) bonds in chlorinated 1, 4-dioxanes, dithianes, and thioxanes. Nonbonding electrons on Y are delocalized by mixing the p orbital of Y with a suitably oriented antibonding σ^* orbital of the C—Cl bond (188). This interaction should strengthen the Y—C bond and weaken the C—X bond, as may be easily concluded from classical double bond–no bond resonance structures shown in Figure 25b.

This explanation, though novel, was not without its critics (126, 127) since it did not account for the shortening of both bonds when Y and X were oxygen atoms.

A similar concept based on electron transfer from Y and X was proposed by Pople's group (139, 243) to explain bond separation energies of various Y—C—X systems (Figure 26). Thus σ withdrawal of electrons from carbon along the C—X bond decreases the occupancy of the carbon $2p_y$ orbital, which is then available in appropriate conformations of the —Y—C—X system to accept more electrons from the $2p_y$ (Figure 26a; Y = C, O, S, F) or sp^3 (Figure 26b; Y = N) lone pair on the atom Y. The interaction of the bonds in Y—C—X thus depends on both the π-electron-donating and σ-electron-accepting properties of Y and X. If Y is a strong π donor (e.g., NH_2 or OH) and X a strong σ acceptor (e.g., OH or F), the bond separation energy is large. When Y = CH_3 the energy ΔE_{IS} is relatively small due to the weak π-electron-donating ability of this group. If X is a σ donor (e.g., X = Li, Be) and Y a π acceptor (e.g., Y = Be, B), there should be stabilization (see Figure 26c) because of π donation from the highly populated carbon orbital of the C—X bond into the acceptor orbital on Y. Similarly, if X is a σ donor

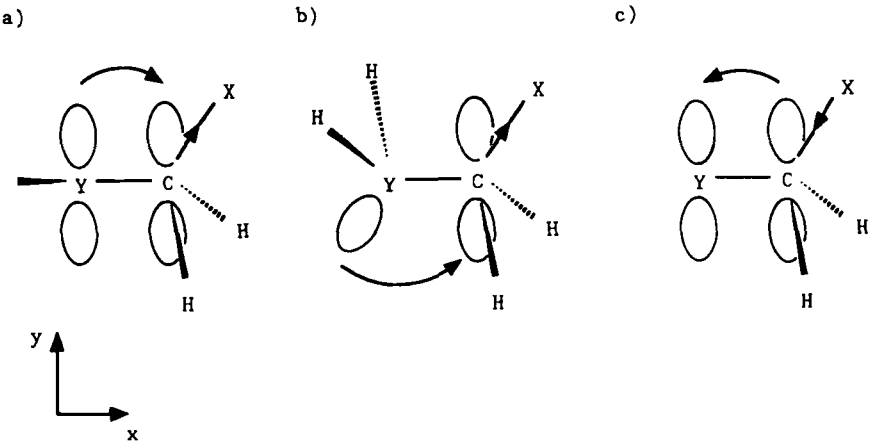


Figure 26. Electron transfer between Y and X according to Pople et al. (139, 243).

and Y a π donor, or if X is a σ acceptor and Y a π acceptor, the corresponding interaction will be destabilizing.

Soon this concept was connected (234) with the magnitude of the V_2 constant in a Fourier component analysis of internal rotation potential functions in molecules exhibiting the anomeric effect (see Section III.B.2). It was also used to account for bond lengths in methanediol (**8**) (235) and methoxymethanol (**49**) (244) (p. 196), but the authors claimed (235) that the shortening of the C—O bonds in the *ap, ap* conformers of **8** cannot be explained by the interaction pictured in Figure 26a.

This type of electron delocalization (represented by the V_2 term in Eq. [24]) suggests that in all cases conformer *og* should be preferred. However, it is not the only factor responsible for the actual stable conformation of a molecule. Since $V(\Theta)$ is dependent on V_1, V_2, and V_3, the behavior of a molecule exhibiting the anomeric effect should in the present authors' opinion (234, 235, 244) be considered in terms of *all* of the following: electron delocalization, dipole–dipole interactions, and steric effects (see Section III.B.2).

4. *Anomeric Effect in Light of Perturbational Molecular Orbital (PMO) Theory*

The PMO (245, 246) approach to the evaluation of structure and energy of molecules has raised new possibilities for the interpretation of preferred conformations in Y—C—X systems; initial studies dealt with cations **125**

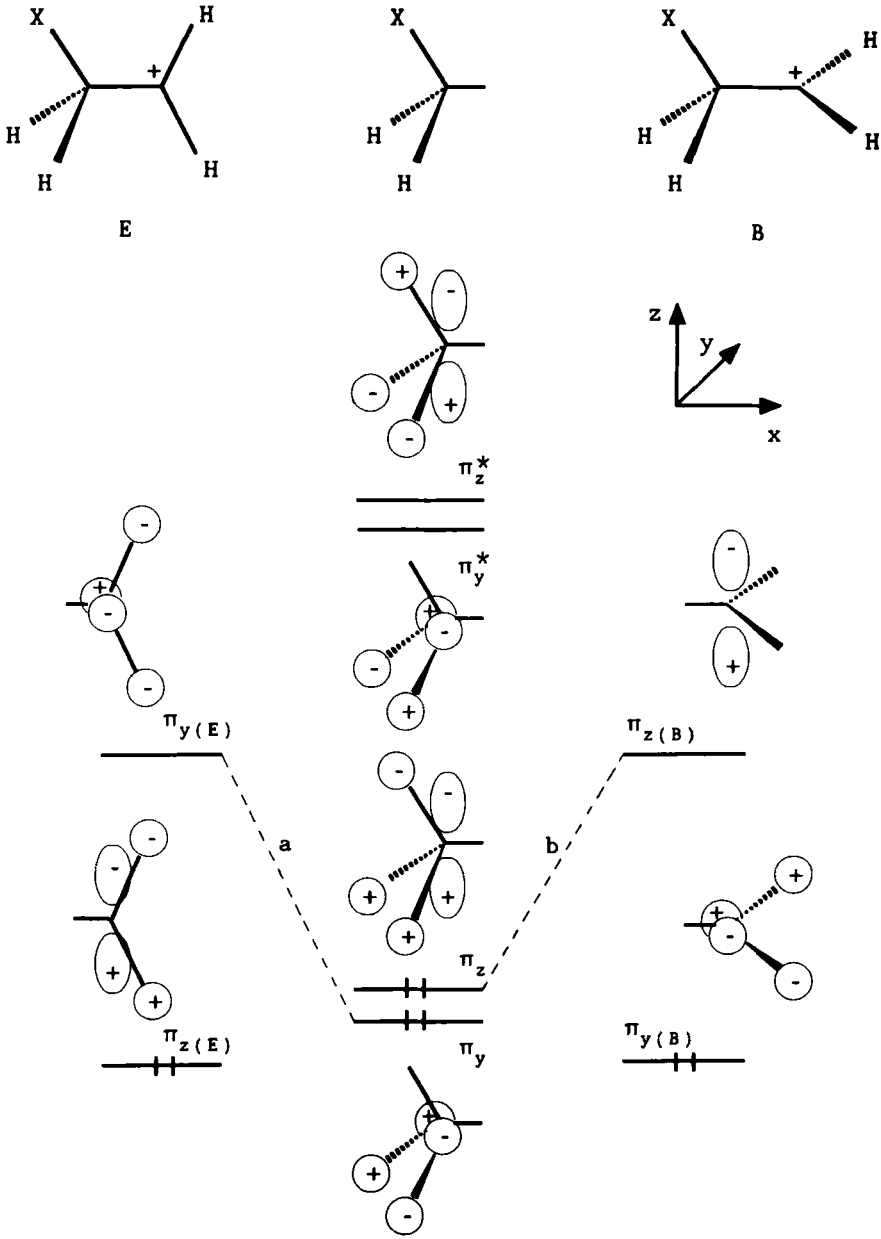


Figure 27. Orbital interaction diagram for $XCH_2CH_2^+$ cation (**125**).

and anions **126**,

$$\underset{\textbf{125}}{X{-}CH_2{-}CH_2^+} \qquad \underset{\textbf{126}}{X{-}CH_2{-}CH_2^-} \qquad \underset{\textbf{127}}{CH_3{-}CH_2{-}CH_2^+}$$

which may be related to anomeric-type molecules.

Let us consider first the $XCH_2CH_2^+$ system. In order to find the preferred arrangement of this cation, let us examine the interactions between XCH_2 and CH_2 group orbitals pictured in Figure 27. Two conformations need to be taken into account: *eclipsed* E and *bisected* B. Though other group orbitals are also present, those for which x is a symmetry axis are not influenced by rotation around the x axis and therefore are not shown. If X = H, π_z and π_y, π_z^* and π_y^* are rigorously degenerate (247a). Because the two-electron two-orbital stabilization energy ΔE_{ij} is (Eq. [27]) (248) inversely proportional to the energy separation of the two molecular orbitals i and j of energy E_i and E_j, respectively, and directly proportional to the square of their resonance integral H_{ij}, interaction a (Figure 27) between π_y and empty $\pi_{y(E)}$ involves two electrons and is as stabilizing as interaction b between π_z and $\pi_{z(B)}$:

$$\Delta E_{ij} = \frac{2(H_{ij} - E_i S_{ij})^2}{E_i - E_j} \qquad [27]$$

where S_{ij} is an overlap integral. Interactions $\pi_{z(E)}$–π_z^* and $\pi_{y(B)}$–π_y^* are not so important owing to the large energy difference between interacting orbitals. Thus one should expect that the stabilization of E and that of B are identical, barring differences due to molecular distortions. The situation is different if X = H is replaced by a more electronegative (26) substituent. The orbitals π_y and π_y^* are practically unaffected for symmetry reasons (X lies in a nodal plane). Since the electronegativity of X is greater than that of H, the π_z (as well as π_z^*) orbital will decrease in energy. The energy gap corresponding to interaction b will increase and interaction a should become more stabilizing than b. This will favor the eclipsed conformation E, as was shown by Hoffmann et al. (249).

It should be noted that though CH_3 has been suggested (250) to be more electronegative than H, the *n*-propyl cation (**127**) favors the bisected conformation B. Jorgensen and Salem (247b) rationalized this finding in terms of higher energy of the C—H compared to the C—C bond, thus leading to the increase in π_z energy on going from X = H to X = CH_3.

Whangbo and Wolfe (251), in the case of **127**, considered the highest occupied orbitals of the ethyl group as a whole, namely σ_{CC} and π_{CC}^-, instead of orbitals of a substituted methylene group (Figure 28, cf. Figure 27). The energies of orbitals σ_{CC} and π_{CC}^- are nearly the same and from this point

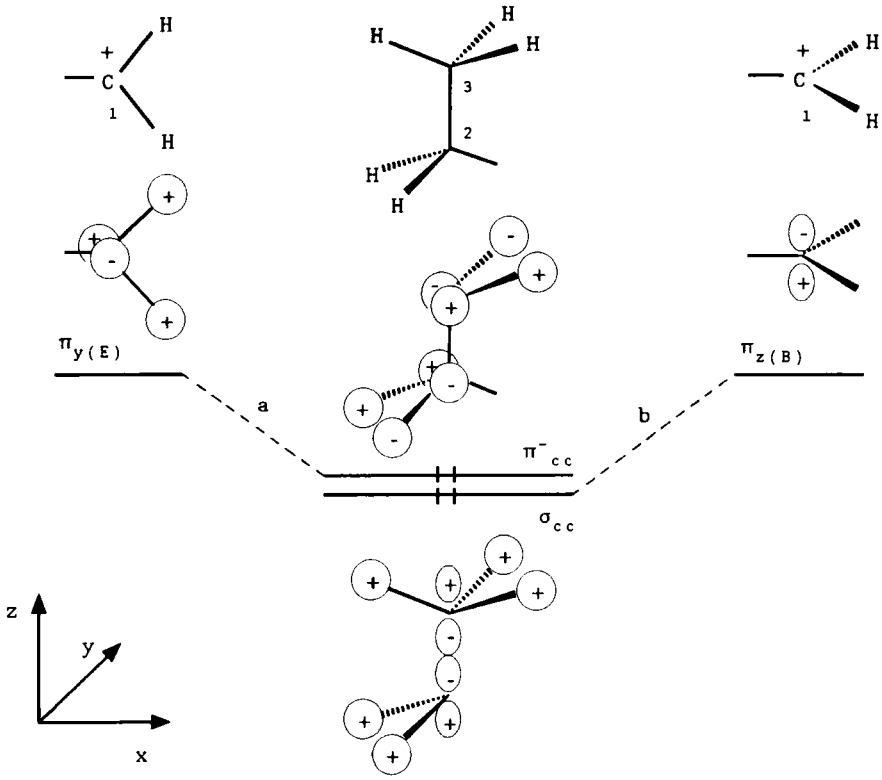


Figure 28. Orbitals interaction diagram for *n*-propyl cation (**127**).

of view interactions *a* and *b* should be equally stabilizing. While interaction *a* leads to π bonding with C(2) and antibonding with C(3), interaction *b* leads to bonding with both C(2) and C(3). Therefore *b* will be more stabilizing than *a* and thus the bisected conformation B will be favored for **127**.

The conformation of anions **126** was examined by Hoffmann et al. (249) in analogy with that of cations. The interaction diagram is very similar to that given in Figure 27 but now $\pi_{y(E)}$ and $\pi_{z(B)}$ are filled (each with two electrons) and the anions are not planar but pyramidalized at the carbanion end. Let us assume that X is more electronegative than H. The relevant energy diagram is shown in Figure 29. Because of the high electronegativity of X, π_z and π_z^* are lowered in energy. Hence stabilizing interaction *b* is more effective than *a* due to a smaller energy gap. On the other hand, destabilizing interaction *d* is less effective than *c* because of the smaller mean energy of the orbitals involved. Therefore, when X is more electronegative than H, conformation B containing a lone pair antiperiplanar to the C—X

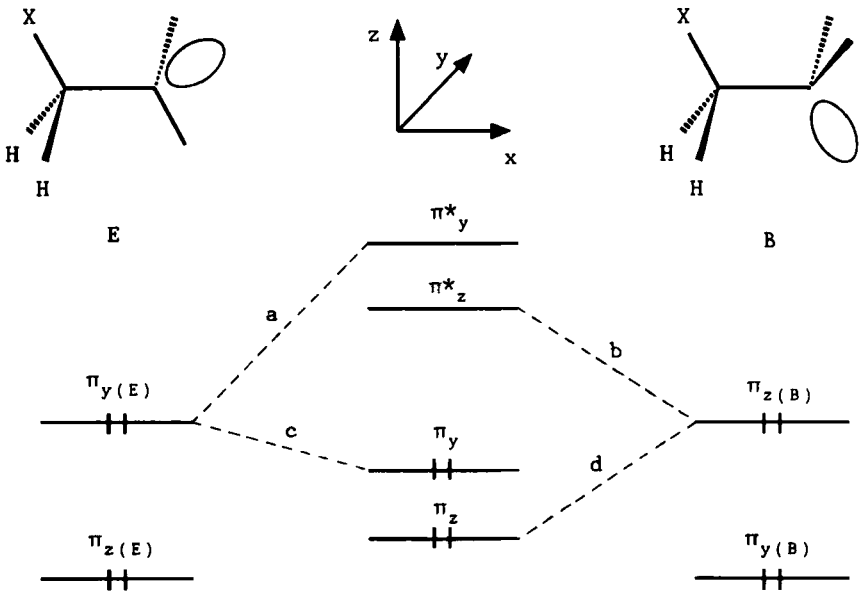


Figure 29. Energy diagram for orbital interaction in the $XCH_2CH_2^-$ anion (**126**).

bond will be preferred for both the aforesaid reasons. A similar conclusion can be readily drawn from a simple perturbation treatment of charge densities in substituted ethane molecules as shown by Zefirov (23, 252). Let us exchange X = H in the ethane molecule (Figure 30a) for a group more electronegative than hydrogen. The lowest and highest occupied molecular orbitals (LUMO, HOMO) of ethane are shown in Figures 30b and c, respectively. This perturbation will not affect orbitals antisymmetric with respect to the *xz* plane and therefore they are not pictured. Such replacement may be described as a perturbation leading to the mixing of HOMO (c) and LUMO (b) to give the molecular orbital presented in Figure 30d, and it will result in an increase in electron density at X and C(2) and a decrease at C(1) at H_a. Therefore, electropositive ligands (including lone electron pairs) attached to C(2) in place of a hydrogen will prefer to be antiperiplanar to the electronegative substituent X. However, such a simple treatment based only on the electronegativity of X does not account for the geometric changes involved. Moreover, the π orbitals of the X group may play a significant role, as shown above for the *n*-propyl cation where the electronegativity of X (= CH_3) is not the sole factor determining the preferred conformation. We will return to this problem later.

Obviously, the approach presented above for anions **126** can be applied to molecules with heteroatoms containing lone electron pairs, for example,

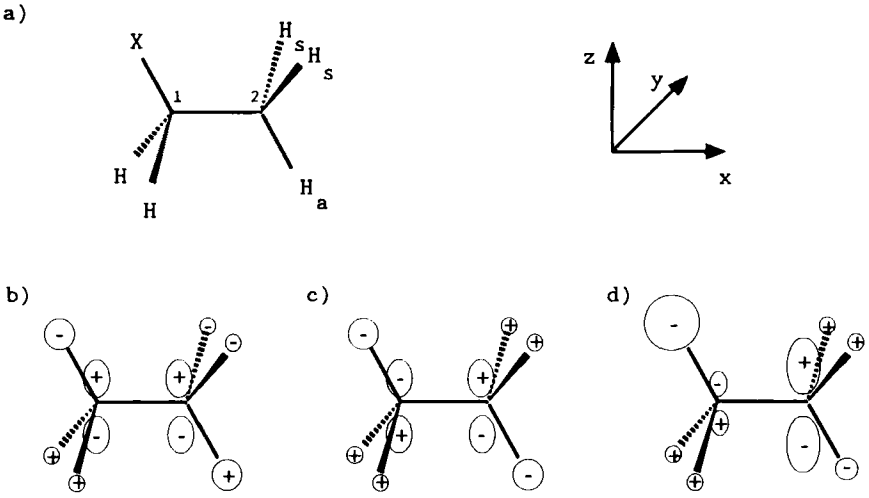


Figure 30. Substituted ethane molecule: (a) staggered ethane derivative, (b) LUMO for X = H, (c) HOMO for X = H, and (d) the result of perturbation for X more electronegative than hydrogen.

:N—CH_2—X. For X = F it may be readily predicted that the nitrogen lone electron pair will tend to be situated antiperiplanar to the fluorine atom. The situation is more complicated when the heteroatom placed in the β position has two lone pairs, as in the case of oxygen (e.g., —O—CH_2—X). These two pairs are not energetically equivalent, as was found by molecular orbital calculations for water (253, 254) and for tetrahydropyran (**70**) by means of photoelectron spectroscopy (255). The energy of a σ-type lone pair is about 1.35 eV below the energy of a π-type lone pair (175). The photoelectron spectrum (256) of water shows four ionization bands at 12.6, 13.7, 17.2, and 32 eV, which could be ascribed to the *p*-type oxygen lone pair, two O—H bonding molecular orbitals, and the *s*-type lone pair, respectively. Although it was suggested by Kirby (6f) that the use of equivalent sp^3 hybrid lone pairs in discussing the anomeric and kinetic anomeric effects is justified, this is not valid for the photoelectron spectra, since in such a case only two bands should be expected (due to bonding orbitals and equivalent lone pairs).

Soon, it was pointed out by Fuchs et al. (89) that the equivalence of oxygen lone electron pairs is not consistent with X-ray structures of carbohydrates. They scrutinized 111 structures and found torsion angles Θ in O_{endo}—C—O—R fragments appreciably larger than 60°. If lone pairs were equivalent, one might expect $\Theta = 60°$ to be preferred whereas nonequivalence implies $\Theta > 60°$. Indeed, Cosse-Barbi et al. (69, 257) have recently shown that the *endo* anomeric effect is stronger in furanoses than in pyranoses. They

attributed this finding to more favorable orientation of the π-type endocyclic oxygen lone pair with respect to the polar C—X bond (and σ^*_{C-X} orbital) in furanose than in pyranose rings (see Section II.E, Figure 4). If both *endo* oxygen lone pairs were equivalent, sp^3-type, the n_O–σ^*_{C-X} negative hyperconjugation should be stronger in the pyranose ring because of collinearity of the σ^*_{C-X} antibonding orbital and one sp^3 oxygen lone pair in the tetrahydropyran system (see also Section IV.B.1). The nonequivalence of oxygen lone pairs was also supported by infrared studies of tetrahydropyrans (86) (see Section IV.B.3.c).

Thus, if the energy levels of the two oxygen lone pairs are different, their interaction with low-lying antibonding orbitals should be different also. Following this idea David et al. (175) considered the conformational equilibrium in the C—O—CH—X system qualitatively. For the sake of simplicity, they replaced the appropriate π^*-group orbital with a σ^*_{C-X} hybrid orbital and examined its interaction with two nonequivalent oxygen lone pairs in two possible conformations, as shown in Figure 31. They assumed constant overlap and postulated that repulsion energy need not be considered since it is independent of the energy gap between orbitals. Thus, the interaction energies in the *sc* and *ap* conformations, E_{a-d}, are due almost entirely to

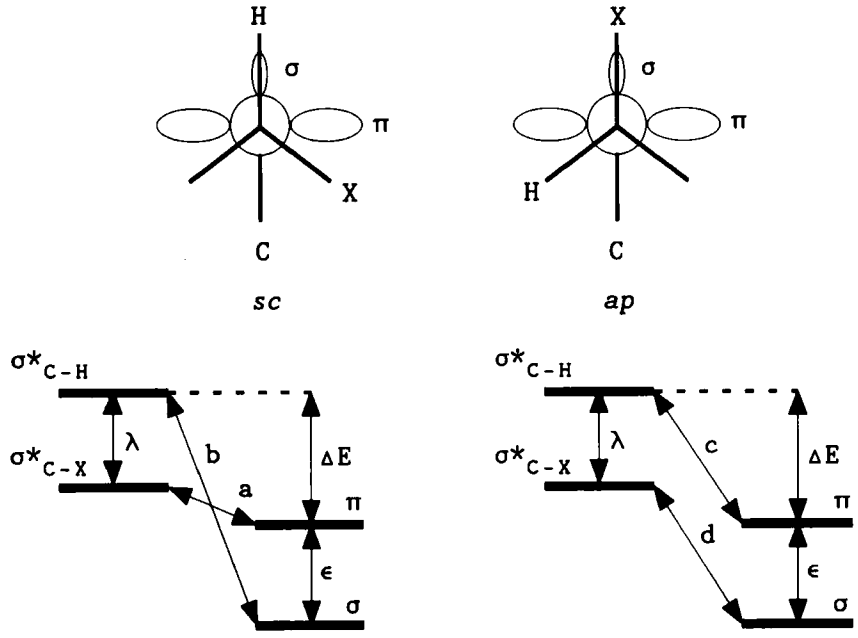


Figure 31. Energy diagram for orbital interaction in C—O—CH—X system.

stabilizing interactions between lone pairs of the π or σ type and antibonding orbitals of C—X (σ^*_{C-X}) and C—H (σ^*_{C-H}) bonds, which are given by Eqs. [28]–[31]. The energetic preference for the *sc* conformation is the difference $(E_c - E_d) - (E_a - E_b) = 4h^{*2}\lambda\varepsilon/\Delta E^3$:

$$E_a = \frac{-2h^{*2}}{\Delta E - \lambda} \qquad [28]$$

$$E_b = \frac{-2h^{*2}}{\Delta E + \varepsilon} \qquad [29]$$

$$E_c = \frac{-2h^{*2}}{\Delta E} \qquad [30]$$

$$E_d = \frac{-2h^{*2}}{\Delta E + \varepsilon - \lambda} \qquad [31]$$

The authors (175) estimated this preference to be about 13.8 kJ/mol for X = Cl. For X *less* electronegative than hydrogen, they expected enhanced preference for the *ap* arrangement, thus suggesting the rationalization for the reverse anomeric effect.

Since the stablest conformation of compounds of this type (as well as anions) is determined by a stabilizing interaction between a nonbonding HOMO level and a *superjacent* (LUMO) level, David et al. (175), to describe such interaction, proposed the term *superjacent orbital control.*

This explanation of the anomeric and reverse anomeric effects has been criticized from various standpoints. First, as far as the reverse anomeric effect is concerned, X was experimentally shown to be more electronegative than hydrogen (as should be expected for ammonium cations), and Hosie et al. (174) pointed out that David's hypothesis is without experimental foundation. Second, the above-presented arguments depend, in Dewar's (142) opinion, on assessments of the energies of the orbitals involved. He stated that "this explanation like other similar explanations is unsatisfactory in the sense that the arguments used would not have led to a convincing prediction of the phenomenon in question, had it not already been known" (142). Finally, the neglect of repulsive energies need not be appropriate for all systems exhibiting an anomeric effect, especially when X bears lone electron pairs [David et al. (175) neglected such pairs]. In the case under scrutiny the energy gap independence of the repulsive energy is not sufficient to justify neglect of destabilizing interactions since the latter may be overlap controlled (*vide infra* and Eq. [1] in ref. 175). As discussed in Section III.B.2, Tvaroška and Bleha (187) actually excluded the n_Y–σ^*_{C-X} mechanism as responsible for the

conformational preference when X = OMe. Destabilizing interactions in the F—CH_2—X system were recognized by Eisenstein et al. (201), who ascribed the influence of X (X = Cl, C=C) on the CH_2F fragment to a delicate balance of destabilizing and stabilizing interactions of the *bisecting* (orthogonal to X–C–F plane) lone pair of fluorine.

However, the stabilization of molecules exhibiting the anomeric effect may arise not solely from the n_Y–σ^*_{C-X} interaction, as was shown by Whangbo and Wolfe (251) for fluoromethanol (**121**). The relevant orbital diagram is pictured in Figure 32 for the interaction between the CH_2F and OH groups. One can find six possible two-electron–two-orbital stabilizing interactions, namely *a*, *b*, *c*, *d*, *e*, and *f*. Since interaction *b* is less stabilizing than *d* due to a larger energy gap, conformer *sc* should be preferred. On the other hand, stabilizing interaction *c*, which leads to preference of the *ap* arrangement, is more effective than *e*. Therefore, the interactions of n_π and n_σ have opposite conformational consequences. Whangbo and Wolfe (251) evaluated this problem by taking into account that the rotational dependence of the FCH_2OH HOMO level parallels that of the total energy. Since the HOMO level should be lower in the *sc* conformation, interactions with n_σ can be neglected. The synclinal conformation of **121** is also preferred in a positive fashion by interactions *a* and *f* involving the antibonding σ^*_{O-H} orbital. The authors stressed that *a* and *f*, where oxygen and fluorine lone electron pairs are not important, refer to interactions between polar C—F and O—H bonds and are the group molecular equivalent of their (189) quasi-spherical lone-pair interpretation (see Section III.B.1).

Let us come back to Figure 32 and concentrate our attention on the *destabilizing* interactions *g*, *h*, *i*, and *j* present in **121**. It seems reasonable to suspect that interactions in *xz* and *xy* planes are overlap differentiated. Orbitals π_z and π_y (Figure 27) are rigorously degenerate. Since the barrier to internal rotation in the $CH_3CH_2^+$ cation is sixfold and very small (249), one may conclude that there should not be any essential difference between overlap integral S_z for the π_z–$\pi_{z(B)}$ interaction occurring in the *xz* plane and overlap integral S_y for the π_y–$\pi_{y(E)}$ interaction taking place in the *xy* plane. The replacement of H, lying in the *xz* plane, by the more electronegative fluorine should not influence π_y and π^*_y for X lies in their nodal planes. On the other hand, in the CH_2F moiety π_z becomes more localized on fluorine and less on adjacent carbon (249, 252). Thus, overlap integrals S_z and S_y will be different and $S_y > S_z$. One may expect that the same conclusion will be valid in a more exact treatment of the CH_2F orbitals as pictured in Figure 32.

The four-electron destabilization energy ΔE_{kl} for the interaction of orbitals *k* and *l* is given (248) by

$$\Delta E_{kl} = \frac{-4S_{kl}H_{kl} + 2S^2_{kl}(E_k + E_l)}{1 - S^2_{kl}} \qquad [32]$$

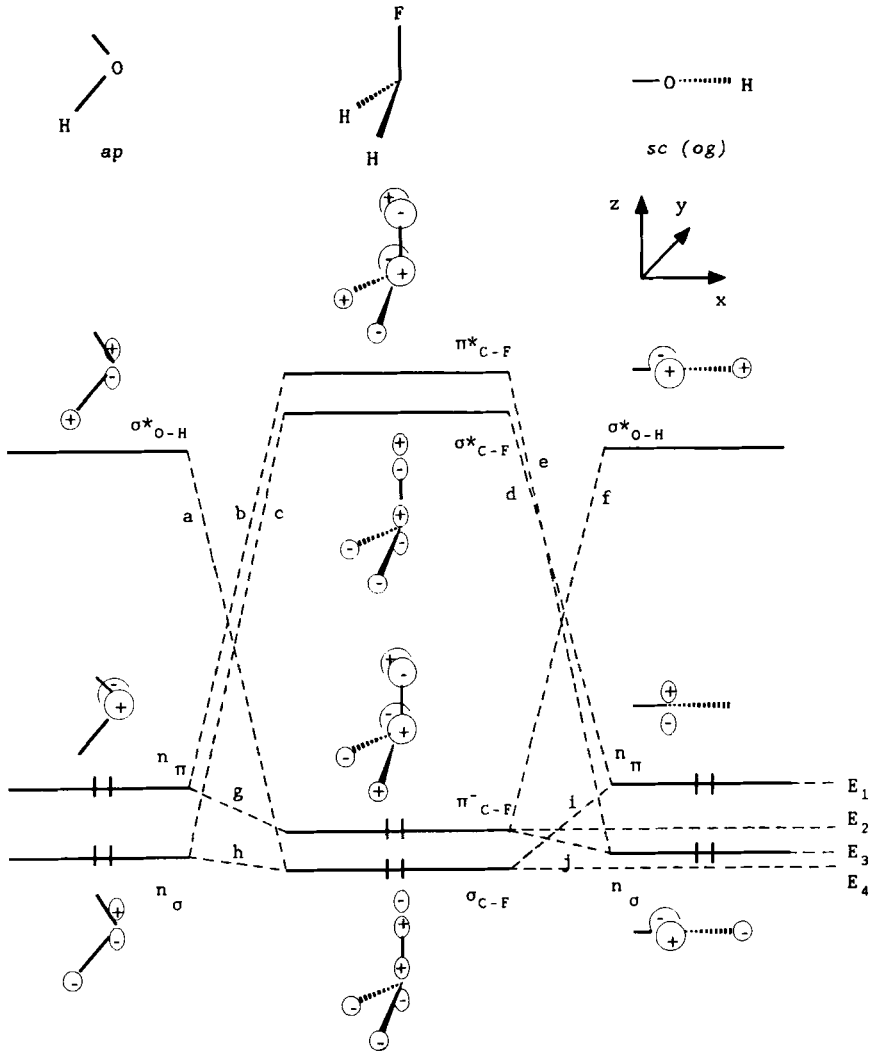


Figure 32. Orbital interaction diagram for fluoromethanol (**121**).

where

S_{kl} = overlap integral
E_k = energy of orbital k
E_l = energy of orbital l
H_{kl} = resonance integral of orbitals k and l

For interactions g, h, i, and j (Figure 32), the destabilizing energies are expressed by Eqs. [33]–[36]. It seems justified to assume that overlap

integrals S_g and S_j for interactions g and j are close, for they occur in the same plane and are equal to S_y. Similarly, S_h and S_i are equal to S_z. Consequently, let us assume that $H_g \cong H_j \cong H_y$ and $H_h \cong H_i \cong H_z$. Then one can estimate the difference in energies between conformers *ap* and *sc* of fluoromethanol due to destabilizing interactions (*overlap repulsion*) $E_{ap(\text{dest})} - E_{sc(\text{dest})}$ according to Eq. [37]:

$$E_g = \frac{-4S_gH_g + 2S_g^2(E_1 + E_2)}{1 - S_g^2} \qquad [33]$$

$$E_h = \frac{-4S_hH_h + 2S_h^2(E_3 + E_4)}{1 - S_h^2} \qquad [34]$$

$$E_i = \frac{-4S_iH_i + 2S_i^2(E_1 + E_4)}{1 - S_i^2} \qquad [35]$$

$$E_j = \frac{-4S_jH_j + 2S_j^2(E_2 + E_3)}{1 - S_j^2} \qquad [36]$$

$$E_{ap(\text{dest})} - E_{sc(\text{dest})} = E_g + E_h - E_i - E_j \qquad [37]$$

Taking into account that

$$S_g \cong S_j \cong S_y \qquad S_h \cong S_i \cong S_z$$
$$H_g \cong H_j \cong H_y \qquad H_h \cong H_i \cong H_z$$

one obtains

$$E_{ap(\text{dest})} - E_{sc(\text{dest})} = 2(E_1 - E_3)\left(\frac{S_y^2}{1 - S_z^2} - \frac{S_z^2}{1 - S_z^2}\right) \qquad [38]$$

Since $S_y > S_z$ and $E_1 > E_3$ (cf. Figure 32),

$$E_{ap(\text{dest})} - E_{sc(\text{dest})} > 0$$

Thus the synclinal conformer of fluoromethanol (**121**) appears to be preferred due to overlap repulsion as well. This conclusion is of significance, since it provides additional proof for the role of destabilizing interactions in the origin of the anomeric effect. Though the importance of destabilizing interactions involving lone electron pairs seems to be well established even in the

case of first-row elements (202, 258), perhaps for **121** they are not so important as stabilizing ones.

Soon after a rigorous quantitative PMO analysis of *ab initio* SCF MO wavefunctions had been performed (259), Wolfe et al. (70) presented a quantitative PMO treatment of various $X—CH_2—YH$ ($X = NH_2$, CH_3, OH, F, and Cl; Y = O, S) systems in order to (1) establish the importance of stabilizing orbital interactions as an origin of the anomeric effect, (2) determine orbital interactions responsible for bond length changes (they will be discussed in Section IV.B.1), (3) compare calculated trends in energies and geometric changes with those found experimentally, and (4) find a connection (if any) between their study and alternative descriptions of the anomeric effect.

They found that one of the six possible orbital interactions in difluoromethane (**61**) (fragmentation mode: FCH_2–F), namely p_z–σ_3^* (cf. interaction *d* in Figure 32), is equivalent to Lucken and Altona's n–σ^* mixing between a lone pair and an antibonding orbital of an adjacent polar bond. On the other hand, the authors claimed that "the rationalization of the behavior of the total molecular wavefunction in terms of specific orbital interaction would thus seem to constitute an arbitrary and incomplete description of the problem" (70). Since stabilizing orbital interaction energies for CH_nF_{4-n} are linear functions of the number of traditional double bond–no bond resonance structures, Wolfe et al. neglected analysis of destabilizing interactions, the more so because it was difficult to relate the destabilizing orbital interaction energies to some more traditional concept. Nevertheless, it should be noted that for the compounds under investigation, the calculated difference in the magnitude of stabilizing orbital interactions (p_z–σ_3^* and p_y–π_3^*; cf. interactions *d* and *b*, respectively in Figure 32) in the *sc* and *ap* conformers is close to the difference ΔE_T in their total energies, thus supporting the assumption of the predominant role of stabilizing orbital interactions (cf. discussion on negative hyperconjugation in methanediselenol, Section III.B.5).

Wolfe et al. (70) found that the preference for the *sc* arrangement for oxygen $HOCH_2X$ (X = F, Cl) compounds (**121** and **128**, respectively) is larger than for sulfur derivatives $HSCH_2X$ (**129** and **65**, respectively), contrary to anticipation based solely on the relative energies of the n_O and n_S lone pairs (n_S lies higher in energy than n_O):

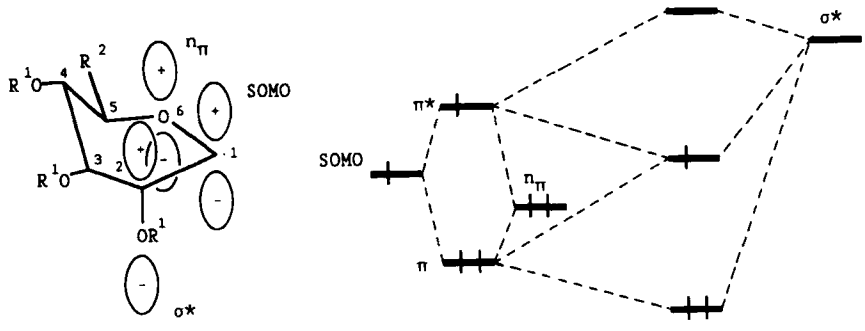
$Cl—CH_2—OH$	$F—CH_2—SH$	$HSe—CH_2—SeH$
128	**129**	**130**

They explained this behavior as due to different overlap. Because of the difference in the C—Y (Y = O, S) bond lengths, the overlap of σ_{C-X}^* or π_{C-X}^* (X = F, Cl) to n_S is less than the overlap to n_O. Since this factor predominates

over the larger energy difference of interacting orbitals (see Eq. [27]), the preference is overlap controlled.

It is interesting to compare the results obtained by Wolfe et al. (70) for methanediol (**8**) with those presented by Tvaroška and Bleha (187) for dimethoxymethane (**11**). This is permissible because the energies of these compounds should not be significantly influenced by the presence of the methyl groups on oxygen, as was shown by Jeffrey et al. (260) (the differences are below 6 kJ/mol). Tvaroška and Bleha (187) found that the magnitude of the stabilizing interactions of lone oxygen pairs with σ^*_{C-O} is almost constant during the rotation around the C—O bond (about 1 kJ/mol larger for *ap, sc* than for *ap, ap*). Moreover, the total stabilization due to orbital interactions is also constant 34–37 kJ/mol), while Wolfe et al. (70) suggest that it is much greater and strongly depends on conformation: 93 kJ/mol for the *sc, sc*, 85 kJ/mol for the *ap, sc*, and 70 kJ/mol for the *ap, ap* conformers [cf. methanediselenol (**130**), Section III.B.5]. Perhaps one reason for this discrepancy lies in the different methods of calculation used by the two groups. However, the problem of rotational dependence of stabilizing orbital interactions should be clarified, in view of its importance for the understanding of the role of stabilizing orbital interactions.

It should be noted that the frontier molecular orbital picture can be applied to explain the conformation of radicals, as was shown by Korth et al. (261) for the sofa conformation of pyranosyl radicals **131**. The relevant interaction diagram is presented in Figure 33. A maximum energy gain arising from the interaction between the SOMO (*single occupied molecular orbital* at the anomeric carbon atom), n_π (the π-type lone electron pair at oxygen), and the antibonding σ^* orbital of the C2—O bond (*quasi-homo-anomeric stabilization effect*) should be expected, for overlap reasons, when the O6—C1—C2 region



131

Figure 33. Orbital interaction in pyranosyl radicals **131**.

is flat, as it is in the sofa conformation. The extra stabilization of radicals of this type is in accord with the calculation performed by Irwin et al. (30) for the homolytic breaking of the C—F bond in fluoromethylamine (**4**). This work showed easier homolysis of the C—F bond antiperiplanar to the nitrogen lone electron pair.

In the molecular orbital approach to conformational problems one finds various types of *conjugation*, for example, σ conjugation, π conjugation, hyperconjugation, negative (positive) hyperconjugation, and anionic (cationic) hyperconjugation. Hyperconjugation involves the interaction of orbitals of π symmetry (antisymmetric with regard to a defining plane) present both in unsaturated and in saturated groups (262). If the second orbital is *p*, filled with two electrons or empty, respectively, one deals with negative or anionic or positive or cationic hyperconjugation, respectively. The case of π–π^* interaction has been named π conjugation (263). The problem of σ conjugation will be discussed in Section III.B.6.

Since the stabilization of the *sc* conformers of various first-row R—Y—C—X systems was shown (*vide supra*) to arise mainly from the interaction of a *p* lone pair on a heteroatom Y with an antibonding orbital (of π symmetry) of the C—X bond, the anomeric effect has been generally regarded as being due to negative hyperconjugation (138, 262). It must be pointed out, however, that negative hyperconjugation (n–π^*) also stabilizes the *ap* conformation but usually to a lesser extent than the *sc* conformation (70). Nevertheless, negative hyperconjugation has been identified with the anomeric effect (262, 264) and vice versa. This may, however, be incorrect because other mechanisms (of stabilizing or destabilizing character, see Sections II.H and III.B.6) can operate when two heteroatoms are geminally bonded, as will also be shown in the next paragraph.

The use of negative hyperconjugation as a "key" to conformational problems has been criticized by Epiotis (see Section III.B.8) and Box (14–16). The latter author based his reasoning on the analysis of X-ray data (see Section IV.B.1) and the chemistry of monosaccharides.

5. *Interpretation of Anomeric Effect with the Aid of Natural Bond Orbital Analysis*

Natural bond orbital (NBO) analysis is a quantitative method for representing *ab initio* wavefunctions in terms of localized Lewis structures (143). In the PMO description (Section III.B.4) of negative hyperconjugation in fluoromethane, for example, the two degenerate π_F orbitals (cf. $\pi_{z(B)}$ in Figure 27 is one of them) interact with two degenerate π^*_{Me} molecular orbitals (π^*_z and π^*_y in Figure 27) of the methyl fragment. This interaction is mathematically equivalent to the NBO description, wherein the π_F orbitals delocalize into the

three σ^*_{C-H} orbitals (143). Therefore, NBO analysis is quite suitable for the study of hyperconjugative interactions. It was applied by Reed and Schleyer (143), for instance, to the analysis of the interaction energies ΔE_{IS} and bond length and bond angle effects which result when the central atom A (A = Be, B, C, N, O, Mg, Al, Si, and P) in X—A—Y is bonded to more than one fluorine. Interaction energies ΔE_{IS} were determined according to the bond separation reaction given by Eq. [39]:

$$F_nAH_m + (n-1)AH_{m+n} \rightleftharpoons nFAH_{m+n-1} + \Delta E_{IS} \qquad [39]$$

$$\Delta E_{IS} = \Delta E_L + \Delta E_D \qquad [40]$$

(cf. Eq. [19]). The authors found ΔE_{IS} for $n = 2$ (Eq. [39]) decreasing in the order F_2PH (69.0 kJ/mol), F_2S (67.8 kJ/mol), F_2CH_2 (65.0 kJ/mol), F_2NH (54.0 kJ/mol), F_2O (37.3 kJ/mol), and F_2SiH_2 (32.3 kJ/mol) at the MP2/6–31G* level. Similarly, for F_3P, $\Delta E_{IS} = 197.6$ kJ/mol (!) exceeded that for F_3CH (168.7 kJ/mol). Bond separation energies for electropositive A's were either close to zero (e.g., F_2AlH) or strongly negative (e.g., for F_2Be, $\Delta E_{IS} = -36$ kJ/mol). Thus, bond separation energies seem to be largest when the central atom A is of intermediate electronegativity [phosphorus, sulfur, carbon; in disagreement with molecular orbital valence bond (MOVB) theory, see Section III.B.8]. Reed and Schleyer (146) found similar trends in calculations performed for mono- and polyfluorinated first- and second-row amines $F_nAH_mNH_2$ (A, central first- or second-row atom), though the ΔE_{IS} peaked near A = C.

While considering bond separation energies ΔE_{IS} in terms of NBO analysis Reed and Schleyer (143) presented a very informative breakdown of ΔE_{IS} into the change of energy of the localized NBO Lewis structure ΔE_L and the change in net delocalization energy ΔE_D (Eq. [40]). Let us examine polyfluoromethanes. The reactions shown in Table 13 correspond to the loss of

TABLE 13
Decomposition of Stabilization Energies by NBO Energetic Analysis of Polyfluoromethanes

Reaction	ΔE_{IS} (kJ/mol)	ΔE_L (kJ/mol)	ΔE_D (kJ/mol)
$CH_2F_2 + CH_4 \rightarrow 2CH_3F$	58.5	−65.2	123.7
$CHF_3 + CH_3F \rightarrow 2CH_2F_2$	35.5	−94.0	129.6
$CF_4 + CH_2F_2 \rightarrow 2CHF_3$	−4.6	−176.6	171.8

From ref. 143.

two n_F–σ^*_{C-F} stabilizing interactions. This is reflected in strongly positive ΔE_D values. These values suggest that stabilization by negative hyperconjugation is very strong (above 100 kJ/mol) and increases with increasing numbers of fluorine atoms. On the other hand, the change in energy of the Lewis structure, ΔE_L, is *negative*, in agreement with the destabilizing character of geminal F–F interactions. Such destabilizing interactions increase rapidly with the number of fluorine atoms and play a predominant role in tetrafluoromethane (**68**), where they are sufficiently large to render $\Delta E_{IS} < 0$. It may be expected that for larger halogen atoms (Cl, Br, and I), for which stronger geminal destabilizing interactions may be anticipated, the absolute value of ΔE_L will exceed ΔE_D even in less substituted methanes. As was seen in Section II.H, this is true for diiodomethane (**64**) for which $\Delta H^\circ_{IS} = -15.2$ kJ/mol (calculated from experimental data). In Reed and Schleyer's opinion destabilizing factors for the polyfluorides may be either purely electrostatic interaction or exclusion repulsion (see Eq. [32]).

It would be very interesting to obtain ΔE_L and ΔE_D values for, for example, O—C—O, S—C—S, and Se—C—Se anomeric interactions as a function of appropriate torsion angles so as to establish the relative importance of stabilizing and destabilizing interactions as a source of the observed anomeric effects. So far, NBO analysis has been applied to the elucidation of anomeric effects involving silicon centers (145) (see ref. 144 for a PMO approach), to Se—C—Se anomeric interactions (148), and to the study of fluorinated amines (146) $F_nAH_mNH_2$. The amine study showed that due to the two opposing factors of energy and overlap, the n_N–σ^*_{S-Cl} interaction in **132** is roughly of the same energy as the n_N–σ^*_{S-F} interaction in **133**:

Cl—S—NH_2	F—S—NH_2	Cl—CH_2—NH_2
132	**133**	**134**

The most stable conformation of XCH_2NH_2 (X = F, Cl; **4** and **134**, respectively) is one having the lone pair of nitrogen antiperiplanar (*ap*) to the C—X bond. The orthogonal (*og*) conformation is a transition state with energy 76 kJ/mol (X = F) or 67 kJ/mol (X = Cl) above the minimum (*ap*).

The predominance of n_N–σ^*_{C-F} delocalization stands out in the NBO analysis of **133** containing a *planar* SNH_2 fragment with the lone pair of nitrogen and the S—F bond lying in the same plane. The n_N and σ^*_{S-F} NBO occupancies were found to be 1.890 and 0.094 e, respectively. These are the orbitals in the NBO analysis whose occupancies deviate by far the most from the ideal Lewis values of 2.0 for bonds and 0.0 for antibonds (see Section IV.B.2).

Reed and Schleyer (146) found the energy of Lewis structure E_L of **133** (with planar SNH_2 as before, *vide supra*) higher by 100 kJ/mol than the total

energy E_T. Interactions other than n_N–σ^*_{C-F} were insignificant, and the energy of 100 kJ/mol could be regarded as a trustworthy estimate of the strength of the n_N–σ^*_{C-F} interaction. The application of NBO analysis to the geometry of the $FSNH_2$ system will be described in Section IV.B.1.

It is interesting to consider stabilizing hyperconjugative interactions in methanediselenol (**130**) (148). Two interactions need to be taken into account: $3p_{Se}$–σ^*_{C-Se} and $3p_{Se}$–σ^*_{C-H}. The former, in the *sc,sc*, $+sc$, $-sc$, and *ap,ap* conformers, respectively, are 35.4, 38.7, and 0 kJ/mol, whereas the latter interactions amount to 9.2, 7.8, and 13.9 kJ/mol, respectively (148). Thus, the total stabilizations owing to these two types of hyperconjugation in *sc,sc*, $+sc$, $-sc$, and *ap,ap* conformations are equal to 44.6, 46.5, and 27.8 (two such interactions) kJ/mol. The relative energies of these conformations calculated from the point of view of negative hyperconjugation, E_{hyp}, and total energies, E_T (148), are given in Table 14. It is seen clearly that negative hyperconjugation is more favorable for $+sc$, $-sc$ as compared to *sc, sc*. Therefore, the observed greatest stability of the *sc, sc* conformation must be attributed to destabilization of the $+sc$, $-sc$ conformation from other causes. In addition, the *ap, ap* conformation, which is a transition state on the (rotational) potential energy surface, is not as unstable (9.8 kJ/mol) as might be expected on the basis of negative hyperconjugation [18.7 kJ/mol, cf. methanediol (**8**) in Section III.B.4]. Perhaps additional destabilization of the *sc, sc* and $+sc$, $-sc$ conformations with regard to the *ap, ap* one or stabilization of the *ap, ap* conformer might be responsible for this finding. The possibility of the involvement of Se—H bonds in these interactions seems to have been disregarded by the authors (148). Nevertheless, Salzner and Schleyer (148) unequivocally showed that the hyperconjugative stabilizing interaction n_Y–σ^*_{C-X} (here Y = X = Se) is only one of several factors that may influence the actual conformation of the larger systems. In fact, the common

TABLE 14
Relative Energies of $CH_2(SeH)_2$ Based on Magnitude of Hyperconjugative Interactions E_{hyp} and Total Energies E_T[a]

Conformer	E_{hyp} (kJ/mol)	E_T (kJ/mol)
sc, sc	1.9	0
$+sc$, $-sc$	0	3.1
sc, ap	—	2.8
ap, ap	18.7	9.8

[a]Based on data from ref. 148.

belief in the predominant role of negative hyperconjugation has been questioned (see the end of Section III.B.4).

Recently, Wiberg and Rablen (157b) criticized attributing the off-diagonal elements between the lone pairs and the partially occupied σ^*_{C-F} localized orbitals in polyfluoromethanes to negative hyperconjugation, as has been done by Schleyer's group in order to obtain, for instance, ΔE_D (Eq. [40], Table 13). In the opinion of Wiberg and Rablen (157b) it is difficult to localize the bonds perfectly in any molecule. "If one wishes to attribute this difficulty in localization to hyperconjugation, then the latter will be found everywhere" (157b).

6. *Anomeric Effect in Terms of σ Conjugation*

It is usually assumed that orbitals that are mutually orthogonal do not interact with each other. Thus, for a tetrahedral atom CR_4 the bonds are formed by interactions between four sp^3 orbitals and four atomic orbitals of the ligands. The proper representation of the molecule should be a wavefunction corresponding to pairs of electrons localized in two-center bonds. However, as was pointed out by Dewar (142), the resonance integral between two mutually orthogonal hybrid atomic orbitals (AOs) does not vanish. He found that the resonance integral between two *sp* hybrids of a carbon atom exceeds 480 kJ/mol and is about five times greater than that between adjacent 2*p* AOs in a conjugated hydrocarbon. For the combination sp^2–sp^3, it is about 240 kJ/mol, still large enough to abandon the current distinction between conjugated π systems and nonconjugated σ ones.

If the interactions between different hybrid atomic orbitals of an atom are considered, each two-orbital CH_2 unit in an *n*-alkane is seen to play the same role as a two-orbital =CH—CH= unit in a conjugated polyene (142). Thus, the ethane molecule is *isoconjugate* with butadiene (see Figure 34a). Since the 1,4 bond order p_{1-4} in butadiene is negative (265), the same should be true for ethane and its derivatives $Y—CH_2—CH_2—X$ (Figure 34b and c). The energy contribution ΔE_{1-4} arising from this interaction is given by

$$\Delta E_{1-4} = 2pH_{1-4} \qquad [41]$$

where

p = bond order

H_{1-4} = resonance integral

It can be proved (142) that the resonance integral H_{1-4} is always negative, being most negative (or least positive) at an Y–C–C–X torsion angle of $\Theta = 0°$ (*sp* conformation) and least negative (or most positive) at $\Theta = 180°$ (*ap* conformation). Therefore the ΔE_{1-4} value is least positive at $\Theta = 180°$, indicating

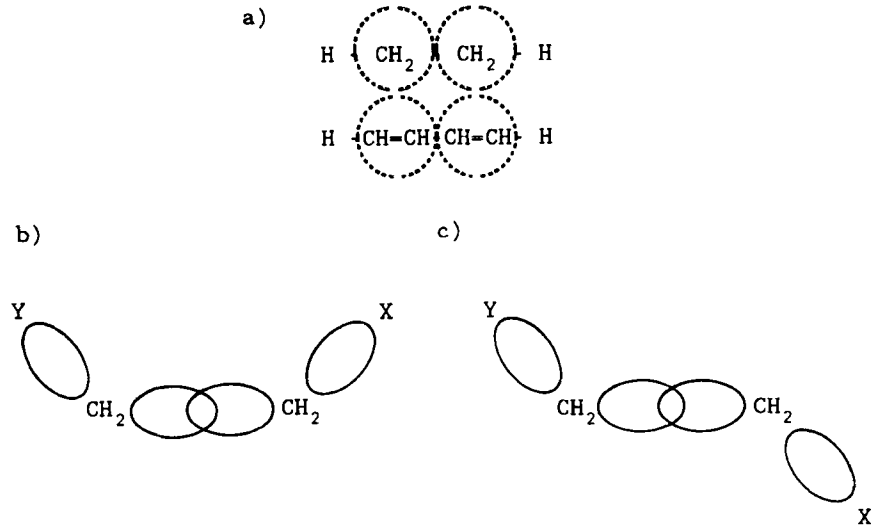


Figure 34. σ Conjugation in (a) ethane and (b) *sp* and (c) *ap* conformers of its derivatives.

that in the least unstable conformation C—Y and C—X bonds are located in antiperiplanar positions, provided their interaction is more important than the interaction between *vicinal* C—X (or Y) and C—H bonds. If Y is a lone electron pair, it can interact σ conjugatively with adjacent σ bonds and hyperconjugatively with appropriate antibonding orbitals (see Section III.B.4, cf. Figure 29). Thus, σ conjugation will reinforce hyperconjugation if the latter involves the bond *trans* to the lone pair. Dewar (142) suggests that this treatment will be applicable to systems exhibiting an anomeric effect. Moreover, σ conjugation might account for the anomalous stability of polyfluoromethanes. However, these conclusions have not been supported by quantitative calculations. In particular, the relative importance of σ conjugation versus hyperconjugation for geometry (bond lengths, torsion angles) and energy (e.g., stability of conformers and bond separation energies) has not been established.

7. *Anomeric Effect as a Result of σ-Electron Delocalization Controlled by Orbital Phase*

In 1986 Inagaki et al. (266, 267) suggested that *gauche* and anomeric effects (antiperiplanar effects) are brought about by the interaction of three bonds *A*, *B*, and *C* (see Figure 35) represented by appropriate bonding *a*, *b*, and *c* and antibonding a^*, b^* and c^* orbitals which are linear combinations of relevant

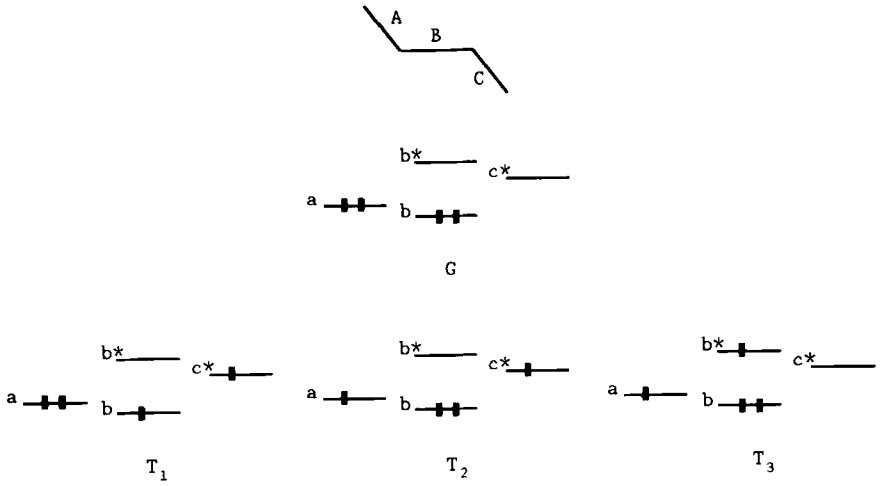


Figure 35. σ-Electron delocalization modes for three-bond system.

hybrid atomic orbitals. They assumed that A is a donor bond while C is an acceptor bond and hence a^* and c^* need not be taken into account. Ground-state configuration G (before any electron delocalization) and three bond-to-bond delocalization modes T_1, T_2, and T_3 are shown in Figure 35. The delocalization T_2 from the donor A to the acceptor bond C, believed to be responsible for the antiperiplanar effects, is termed *vicinal delocalization.* The delocalizations T_1 and T_3 are *geminal* ones.

Appropriate interactions leading to the three types of delocalization were estimated by Inagaki et al. (226, 267) in a perturbational approach. Whereas in the conventional orbital interaction geminal delocalization $b \rightarrow c^*$ (G–T_1) is independent of conformation, their approximation showed (when higher order terms of the orbital interactions were not neglected) that G–T_1 is under the influence of the orientation of the donor bond A, that is, dependent on conformation. The G–T_1 interaction involves the occupied orbital a of the donor bond, in addition to b and c^*.

As expected, the G–T_2 interaction responsible for vicinal delocalization is dependent on conformation. However, relevant calculations reveal that the vicinal delocalization involves the bonding orbital b of the intervening bond B. Inagaki et al. (266, 267) found in addition that the interactions are controlled by orbital phase continuity, namely $a \rightarrow b$ out of phase, $b \rightarrow c^*$ and $a \rightarrow c^*$ in phase. These requirements were found to be simultaneously satisfied for the *ap* arrangement, as shown in Figure 36a. In the synperiplanar conformation at least one requirement cannot be met, for example, orbitals a and c^* are out of phase (Figure 36b).

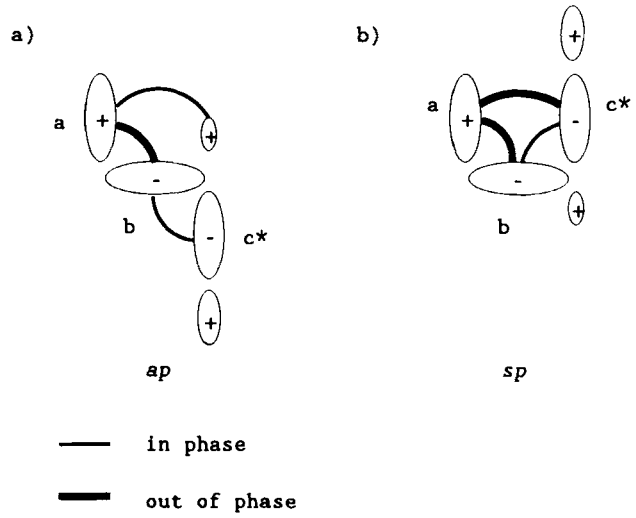


Figure 36. Orbital phase continuity control in (a) *ap* and (b) *sp* arrangement of three-bond system.

Quantitative calculations revealed that without the intervening bond *B* not all models did exhibit the antiperiplanar effect. Thus, the geminal delocalization from the intervening bond *B* and the involvement of this bond are of great importance. However, while orbital *b* is essential, the effect of *b** is negligible. For instance, if orbitals *a*, *b*, *b**, and *c** are taken into account, the *ap* conformation of the $CH_2^-—CH_2F$ anion is more stable than the *sp* one by 15.74 kJ/mol. If only *a*, *b*, and *c** are involved, the difference in energies is little changed: 14.31 kJ/mol. But if orbital *b* is neglected, the *sp* conformation becomes surprisingly more stable than the *ap* one, by 7.80 kJ/mol.

The authors scrutinized bond-to-bond delocalizations in four compounds, namely fluoromethylamine (**4**), chloromethylamine (**134**), anion **135**, and phosphine **136**. The lone electron pair was considered as a donor bond *A*:

$F—CH_2—NH_2$	$Cl—CH_2—NH_2$	$F—CH_2—CH_2^-$	$H_2P—CH_2—F$
4	**134**	**135**	**136**

The preference of both geminal and vicinal delocalizations for the *ap* over the *sp* arrangement of donor and acceptor bonds was confirmed for all models examined. In the first three compounds, the change in geminal delocalization by the $sp \rightarrow ap$ conversion is larger than in the vicinal one. Inagaki et al. attributed this finding to the predominant role of geminal delocalization in stabilizing the *ap* versus the *sp* arrangement. On the other hand, if the *sc* to

ap conformational change is taken into account, the increase in vicinal delocalization is larger than in the geminal case. For **136** both delocalizations are less pronounced since phosphorus is a poorer π donor, in agreement with the conclusion by Schleyer et al. (141).

The concept of orbital phase as an important factor controlling the bond-to-bond delocalization of σ electrons, presented by Inagaki et al. (267), seems to fit well with phase continuity conditions deep rooted in organic chemistry (e.g., the Woodward–Hoffmann rules). Unfortunately, the geometric consequences (e.g., changes in bond lengths) inherent in relevant delocalizations were not brought out in a quantitative way.

8. *Other General Explanations of Anomeric Effect*

Alternative rationalizations of the anomeric effect have been presented by Ponec and Chvalovsky (268), by Smits et al. (269–272), and by Epiotis (203, 273–279).

Ponec and Chvalovsky (268) stressed that an equilibrium conformation of a molecule is the result of competition of two effects: electronic stabilization and core repulsion (cf. Section III.B.1). Therefore, explanations based solely on analysis of electronic interactions would seem to be incomplete. They found that the effect of core symmetry can be included through a Jahn–Teller second-order effect. The predicted preferred conformations of fluoromethylamine (**4**) and $CH_3CH_2NH_2$ are correct, but no quantitative data were presented.

Smits and Altona (269–272) have described intramolecular interactions using a method involving nonorthogonal, strictly local molecular orbitals (NOLMOs). They developed an energy decomposition scheme in terms of quasi-classical (overlap-independent), interference (overlap-dependent), and charge transfer components. They found (272) that the quasi-classical component stabilizes the *gauche* conformation of systems $X—CH_2—OH$ ($X = CH_3$, NH_2, OH, F). This stabilization becomes *less* important at high values of electronegativity of the substituent X (and thus opposes the anomeric effect). Interference energy stabilizes the *trans* conformer at low electronegativity of X, but with an increase in electronegativity, the stabilization of the *guache* conformer becomes predominant. The effect of charge transfer was found to contribute only to a minor degree to the stabilization of the *gauche* conformer. Thus, the anomeric effect is caused by an attenuation of the destructive CX–CO interference as the electronegativity of the substituent increases. This finding remains in contradiction to other calculations (143, 280) in which negative hyperconjugation is taken to be the main source of the anomeric effect. In the model of Smits et al. (272), in which a determinant of standard NOLMOs is used as an approximation to the HF-SCF

wavefunction, the anomeric effect is present without admitting charge transfer into virtual NOLMOs.

Epiotis (203), while considering the case of polyfluoromethanes, labeled the concept of hyperconjugation as a "nominal fallacy" or as a "poor algorithm". He emphasized that "the idea that we can interact bond molecular orbitals and hope to understand stereoselection is false because all bond orbitals within a molecule interact even if they are orthogonal" (203) (cf. Section III.B.6). The assumption that orthogonal orbitals do not interact is based on chemists' erroneous belief that interaction is equivalent to overlap. While the overlap intergral of two *sp* hybrids of a given atom is indeed zero, the resonance integral can be nonzero. The mere fact that hybrid atomic orbitals interact with each other virtually eliminates, in Epiotis's opinion, any possibility of understanding what goes on even in a system as simple as methane. If one says that the isodesmic reaction between CH_2F_2 and CH_4 (Eq. [21]; Tables 8 and 13) is endothermic because of negative hyperconjugation [as is maintained by Reed and Schleyer (143)], this is, according to Epiotis, essentially a restatement of the fact that the substrates have stronger bonds than the products (203). Smart (281) and Liebman and Greenberg (282) have reviewed various conflicting models for bond contraction and bond strengthening in fluoromethanes and have concluded that the matter remains unresolved. However, according to very recent calculations by Wiberg and Rablen (157b) of various polysubstituted methanes, simple consideration of electrostatic interactions may well account for the trends in energy and geometry of polyfluoromethanes. Interestingly, the energetic superiority of $CF_2{=}CH_2$ over $CHF{=}CHF$ is maintained in calculations (274) in which fluorine lone pairs are artificially deleted. Epiotis (203) claims that both energy and geometry of polyfluoromethanes have nothing to do with lone pairs (cf. Section III.B.V). Both problems should be considered in terms of bonds and symmetry. This is impossible using valence bonds (VBs) (283) or resonance theories (284) because of neglect of symmetry problems. On the other hand, Hückel MO theory (248) has many limitations owing to the neglect of interelectronic repulsion (275). To avoid all these deficiencies, Epiotis (203, 273–279) proposed a new theory intended to couple the strong points of MO and VB theories, namely MOVB theory. This theory represents an attempt to adapt quantum mechanics to the chemist's mind and was constructed with total disregard for its computer implementation potentiality (203).

According to the MOVB theory, anomeric interactions in lower row anomeric atoms must be accompanied by a decrease of ΔE_{IS} (Eq. [19]). Such a statement stands in contrast to calculations performed by Reed and Schleyer (143), who found the strongest anomeric interactions at atoms of intermediate electronegativity (see Section III.B.V). Nevertheless Epiotis (203) was not

discouraged and eventually claimed that better computations would reveal that he had been right.

Recently, Epiotis (279) has criticized the art of "arrow pushing" (the art that expresses the mechanism of electron delocalization within a molecule) and negative hyperconjugation as an example of this art. In his opinion, while the MOVB theory is able to account for a negative ΔH_{IS} for the isodesmic reaction presented in Eq. [42] (cf. Eq. [19], Section II.H), the concept of negative hyperconjugation is not:

$$F_2C{=}O + CH_3COCH_3 \rightarrow 2CH_3(CO)F + \Delta H_{IS} \qquad \Delta H_{IS} = -33.5\,\text{kJ/mol} \qquad [42]$$

According to Epiotis (279), the insensitivity of ΔH_{IS} for the isodesmic reaction involving methylenediamine (**73**, Eq. [43]) to a conformation about both C—N bonds in **73** should be regarded as an unambiguous evidence against the model of negative hyperconjugation:

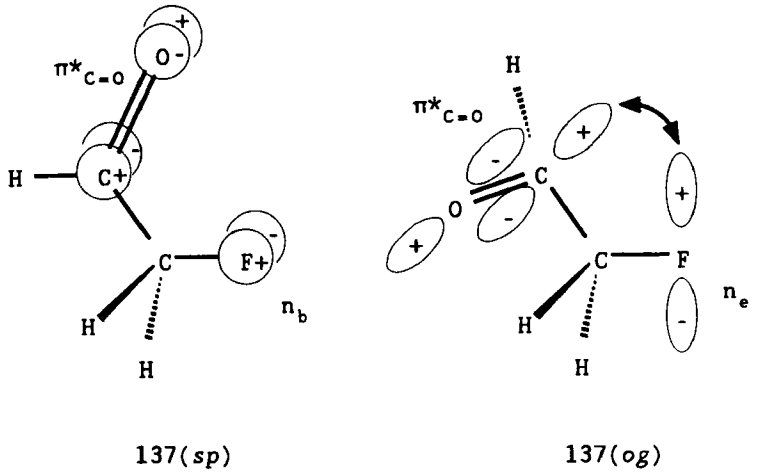
$$\underset{\mathbf{73}}{H_2N{-}CH_2{-}NH_2} + H{-}CH_2{-}H \rightarrow 2H{-}CH_2{-}NH_2 + \Delta H_{IS} \qquad [43]$$

However, in our opinion, this reasoning is based on a neglect of destabilizing interactions, which may accompany the negative hyperconjugation and may decrease ΔH_{IS} (see Section II.H). Epiotis also claims (279) that the negative hyperconjugation is not able to explain the shortening (with respect to methanol CH_3OH) of *both* C—O bonds in the *ap, sc* conformer of methanediol (**8**, cf. however, Section IV.B.1). He presented (279) an explanation for these phenomena as well as for the rotaional behavior of various X—A—A—X molecules (A = O, S, Se; X = H, F, Cl).

9. *Special Cases*

Sometimes one faces the situation where none of the explanations presented in Sections III.B.1–III.B.8 is sufficient to account for the observed conformational preference. Then, additional interactions need to be taken into account. They are usually discussed in terms of stabilizing two electron–two orbital interactions. Some of these, which may be useful in discussions of the anomeric effect, are presented below.

a. n_F–$\pi^*_{C=O}$ and n_F–n_O Interactions. Such interactions were considered by Eisenstein et al. (201) to explain the conformational behavior of halogenoaldehydes and ketones. In α-fluoroacetaldehyde (**137**), for example, two con-



137(*sp*) 137(*og*)

Figure 37. Overlap between fluorine lone pair and carbonyl $\pi^*_{C=O}$ orbital in *sp* and *og* conformers of fluoroacetaldehyde (**137**).

formations need to be examined: synperiplanar, **137** (*sp*), and orthogonal, **137** (*og*) (Figure 37). It can be proved that the strength of the n_F–$\pi^*_{C=O}$ stabilizing interaction is overlap controlled. Therefore, the *og* conformation, which ensures better overlap, should be preferred. In contrast, the *through-bond* (23) stabilizing interaction between oxygen n_O and fluorine n_e lone pairs was shown to favor the *sp* conformation. The n_O–n_e and n_O–n_b destabilizing *through-space* (23) interactions are in the authors' opinion very similar in the two conformations. The observed conformational behavior of the molecule will thus be determined by a balance of these effects. Eisenstein et al. (201) predicted that the replacement of F by Cl, Br, and I should favor the *og* conformation because of stronger n_X–$\pi^*_{C=O}$ (X = Cl, Br, I) interactions. It seems, however, doubtful that the increase in the length of the carbon–halogen bond resulting in diminished overlap with $\pi^*_{C=O}$ (cf. Section III.B.4, the work of Wolfe et al. (70)] can be neglected. Indeed, for cyclic α-halogenoketones Cantacuzène (285) observed an increase in the axial preference (analogous to the preference for the *og* conformation) in the series F, Cl, Br, I. However, the assumption of similarity of repulsive through space interactions in the *sp* and *og* conformers may be questioned, particularly in the case of lower row elements. In our opinion, since carbonyl oxygen lone electron pairs are located in the C–C–O plane (6g), there should be clear distinctions between through-space interactions in the *sp* and *og* conformers. Therefore, the increasing preference for the *og* arrangement in going from F to I may be attributed at least in part to increasing destabilizing through-space interactions between oxygen and halogen lone pairs in the *sp* conformation.

b. $3p$–$3d$ Interaction. It has generally been accepted that back donation of electrons from adequately oriented p orbitals of oxygen to vacant d orbitals on sulfur can occur in the S—O bond of the sulfinyl group. This type of interaction was invoked by Brunet et al. (286) and Alcudia et al. (287) to account for the preferred conformation of compounds containing the O—C—C—S—O system. Since d orbitals lying in the plane that contains the S—O bond are involved in the interaction between sulfur and sulfinyl oxygen, the only available d orbital to interact with the C—O oxygen is that lying in the plane perpendicular to the S—O bond, as shown in Figure 38. This conformation corresponds to the *gauche* (*sc*) arrangement of the O—S—C—C fragment.

The p–d donation from endocyclic sulfur to exocyclic phosphorus has been considered by Juaristi et al. (12, 18, 56, 135) to explain the axial preference of the diphenylphosphinoyl group ($Ph_2P{=}O$) bonded to the anomeric carbon atom of a 1,3-dithiane ring (e.g., in **109**, Scheme 35). However, we cannot see any reason why p–d interaction should be (overlap) favored in the axial conformation to such an extent as to provide an effect of magnitude of almost 16 kJ/mol (135). Moreover, the conformational preference during rotation about the anomeric carbon–phosphorus bond in the equatorial isomer should be dependent on p–d interaction in such a way as to prefer the P=O to be placed between two sulfur atoms, as shown in Figure 17 (rotamer *anti*). If p–d interactions were strong enough to create an anomeric effect of magnitude 16 kJ/mol, the replacement of P=O by P=S (or P=Se) should not change the preferred conformation, contrary to the observation (54) (see also Section V.B.3). Finally, let us assume that (1) the p–d interaction involves π-type lone electron pair of sulfur, (2) the S–S and S–P nonbonding distances are equal to about 3.00 Å (173), and (3) the maximum radial extent of the phosphorous $3d$ orbital is 2.43 Å (288). In that case no (or negligible) $3p$–$3d$

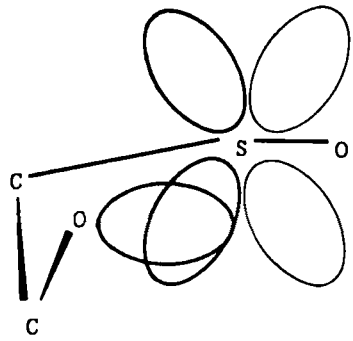
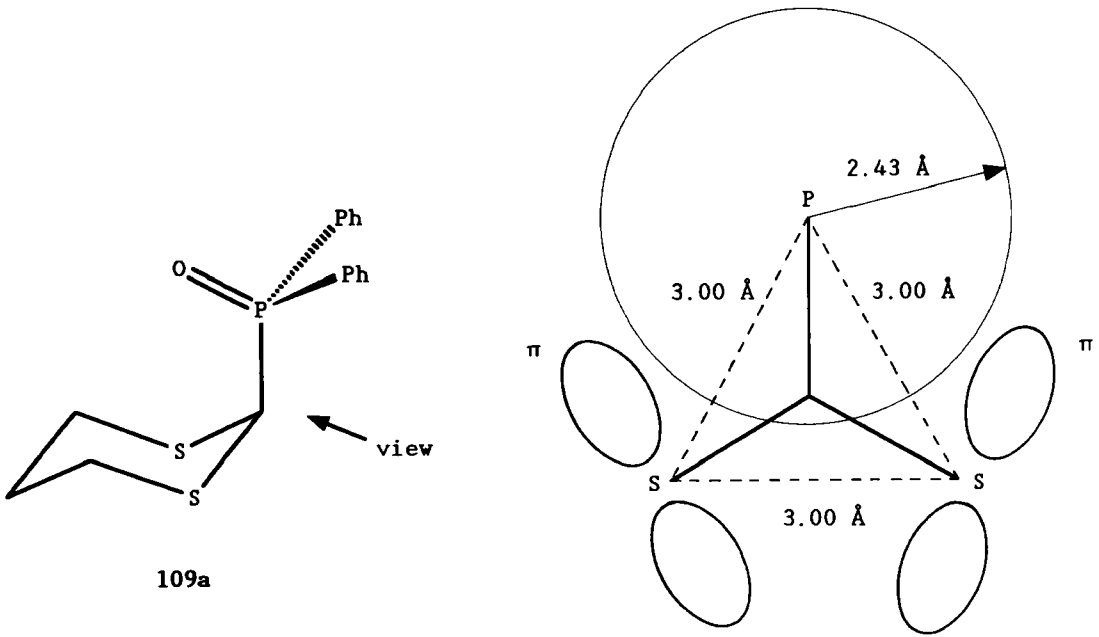


Figure 38. Favored conformation of O—S—C—C—O system for the p_O–d_S interaction.



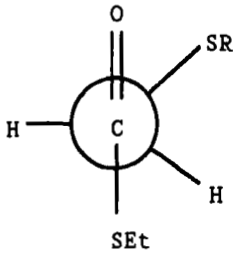
109a

Figure 39. Section through S—P—S plane in **109a**.

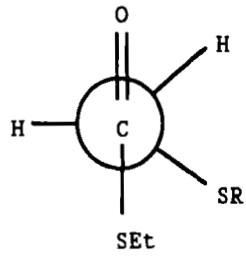
overlap is possible in **109a**, as shown in Figure 39. If one uses hybrid sp^3 orbitals of sulfur, the overlap will even be smaller.

It must be noted that the importance of p–d bonding with d orbitals of second-row atoms has been questioned on theoretical grounds (146).

c. $\pi_{C=O}$–$3d_S$ Interaction. Olivato et al. (289) explained the preference for the *cis* over the *trans* conformer of α-(alkylthio)thioacetates **138** as being due to the stabilizing interaction between the $\pi_{C=O}$ orbital as donor and the 3*d* orbital of sulfur (SR) as an acceptor. This concept has recently been applied by Tschierske et al. (38) to account for the rotational preference of a carboethoxy group attached axially to the anomeric carbon atom of a 1,3-oxathiane ring in **52**.

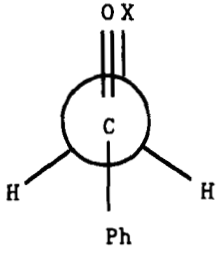


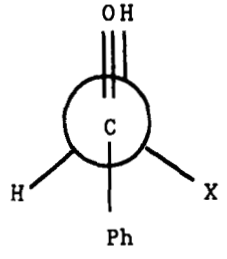
cis-138



trans-138

d. σ_{C-X}–$\pi^*_{C=O}$ and $\pi_{C=O}$–σ^*_{C-X} Interactions. A σ_{C-X}–$\pi^*_{C=O}$ hyperconjugative interaction was suggested by Olivato et al. (290) to be responsible for the increasing stabilization of the *gauche* rotamers of **139** in going from





X=F, Cl, Br, I

cis-139

gauche-139

ω-fluoro- to ω-iodoacetophenone, since the donor ability of C—X bond should increase in that order (cf. the n_F–$\pi^*_{C=O}$ interaction). However, when X = SEt, the stability of the *gauche* conformation is larger than expected on the basis of only the σ_{C-S}–$\pi^*_{C=O}$ interaction. The carbonyl force constant is also smaller than anticipated. Thus, the operation of the second mechanism, namely $\pi_{C=O}$–σ^*_{C-S} was suggested (290).

It should be pointed out that Juaristi et al. (113) have questioned the importance of a $\pi_{C=O}$–σ^*_{C-S} stabilizing interaction associated with the anomeric effect of a carbonyl substituent in the 5-methyl-5-aza-1,3-dithiacyclohexane ring.

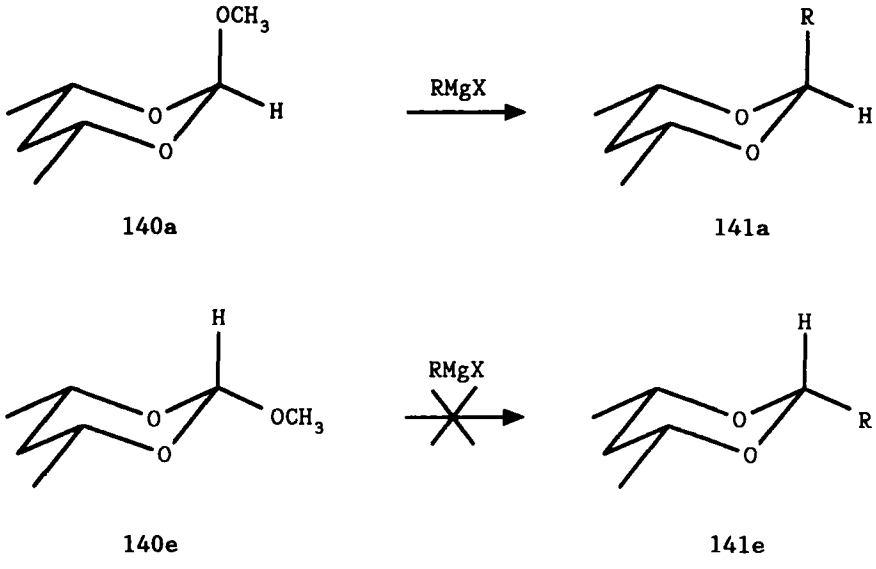
IV. CONSEQUENCES OF THE ANOMERIC EFFECT

There are two main manifestations of the anomeric effect: concerning energy (Section IV.A) and concerning structure (Section IV.B). In this section, however, the energies of ground states are not considered further since they are an essential part of the *definition* of the anomeric effect. We shall deal here only with energies of transition states, in particular with transition states of chemical reactions (bond breaking) and transition states for rotation about bonds to an anomeric atom.

A. Anomeric Effect and Energy

1. *Kinetic Anomeric Effect*

As far as chemical reactions are concerned, such consequences are reflected in the rate of the C—X bond breaking insofar as they depend on the conformation of the R—Y—C—X moiety. A pioneering observation in this area is due to Eliel and Nader (291), who showed the lack of reactivity of equatorial 2-alkoxy-1,3-dioxanes **140e** toward Grignard reagents, in contrast to axial derivatives **140a** (Scheme 37). Such striking behavior has been called the *kinetic anomeric effect* (6, 292). The kinetic anomeric effect is one of the most studied (174, 178, 179, 293–302) and reviewed (6, 7, 10, 11, 13, 180, 303) phenomena in organic chemistry. Its explanation in terms of the *theory of stereoelectronic control* (7) is an extension of the interpretation of the ground-state behavior of molecules R—Y—C—X based on the n_Y–σ^*_{C-X} negative hyperconjugation (see Figure 40a). Recently, this theory has been suggested (11) to be called the *antiperiplanar lone-pair hypothesis* (ALPH) since *stereoelectronic control* [or *stereoelectronic effect* (304)] is far too general a term. This theory predicts that C—X cleavage occurs readily only when a lone

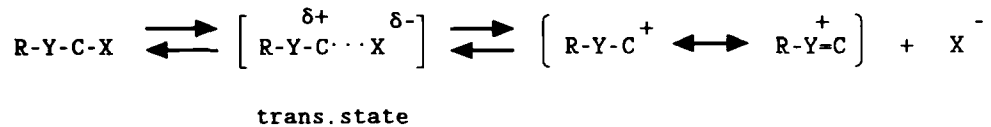


Scheme 37

electron pair of Y is antiperiplanar to the C—X bond being broken, as shown in Figure 40.

First, however, one should provide an answer to a question: Which is the best way of bond breaking in such systems: homo- or heterolysis? The work of Irwin et al. (30) on fluoromethylamine (**4**) showed that the C—F bond stretching should lead preferably to radicals $H_2NCH_2^{\cdot}$ and $F^{\cdot}$ rather than to the methyleneiminium cation $H_2NCH_2^+$ and fluoride anion F^- because the calculated dissociation energy according to the latter, heterolytic mechanism is at least 380 kJ/mol larger than that according to the former, homolytic one. The usually observed heterolytic cleavage of the R—Y—C—X systems in a solution could be, in our opinion, attributed to much more effective solvation of ions than that of radicals. Since solvation energies are of the order of hundreds or thousands of kilojoules per mole, the actual preferred pathway of a bond breaking can be different from that calculated for gas phase conditions.

The second question that might arise for the reaction in a R′—Y—C—X—R″ system is: Which bond will be broken, C—Y or C—X? If the properties of Y and X are very different, an intuitive treatment can usually provide the answer, as for methoxymethanol, $CH_3O—CH_2—Cl$ (**122**), for instance. When X = Y, the situation is not so clear. This problem has been studied by McPhail et al. (302) for the acetolysis of methyl α- and β-glucopyranosides



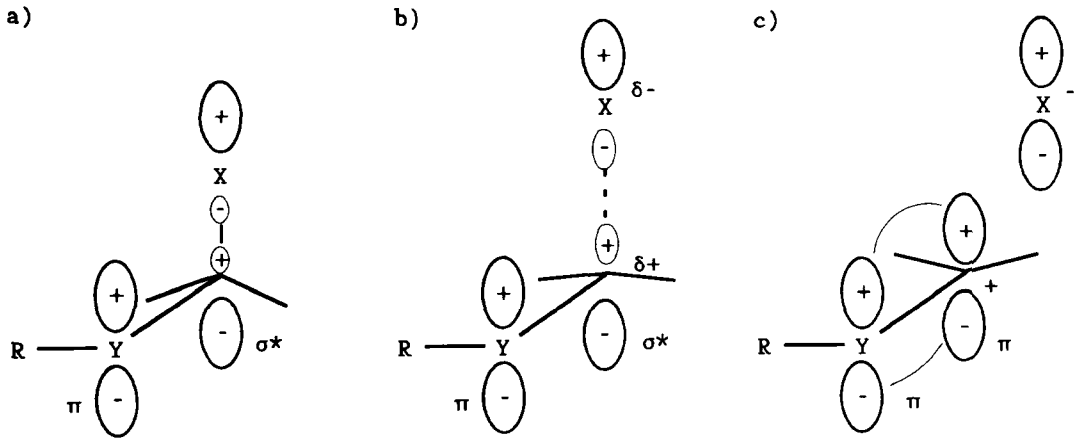
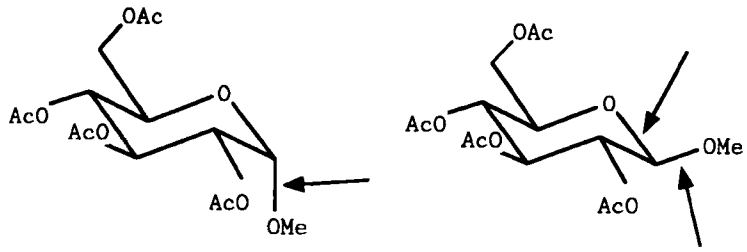


Figure 40. Negative hyperconjugation in (a) the *og* conformer of R—Y—C—X, (b) a transition state during heterolysis of the C—X bond, and (c) planar cation R—Y—C^+.



142a 142e

Figure 41. Preferred cleavage of C—O bonds in **142a** and **142e**.

142a and **142e**, containing the R′—O—C—O—R″ grouping. In contrast to the anticipation based on the proton affinities of endo- and exocyclic oxygens (see Figure 3, Section II.E), it was shown that it is the β, **142e**, not the α, **142a**, anomer in which both bonds are likely to be cleaved (Figure 41). Thus, the relative basicities of oxygens have nothing to do with the predominant pathway of the reaction, as would also, in our opinion, be expected on the basis of the Curtin–Hammett principle (305), assuming rapid and reversible formation of appropriate protonated species. According to this principle, the relative amounts of products are completely independent of the relative populations of intermediates (protonated pyranosides) and depend only upon the difference in free energy of the respective transition states (for C—O^+ bond breaking). This cannot be related in any straightforward manner to oxygen basicities.

The third question is: How is one to account for a substantial rate of heterolysis of a C—X bond in R—Y—C—X systems that do not possess any lone pair being antiperiplanar to this bond (e.g., in the *ap* conformer)? At first sight this behavior could be regarded as an evidence against the antiperiplanar lone-pair hypothesis. An explanation presented by Deslongchamps (7d) is as follows: Let us assume that **143A**, **B**, **C**, **D**, and **E** (Figure 42) are chemical species involved in the transformations pictured (**143A** and **143D** may be epimers). Compounds **143A** and **143C** contain lone pairs antiperiplanar to the C—X bond whereas **143D** does not. The theory of stereoelectronic control implies that the activation energy for the heterolysis of the C—X bond in **143D**, $\Delta E^{\neq}_{\mathbf{D-E}}$, is much greater than that for compound **143A**, $\Delta E^{\neq}_{\mathbf{A-B}}$. Therefore the **143D** → **143E** reaction should not occur to a noticeable extent. If it occurs, such a situation can be attributed (7d) to a conformational flexibility of **143D** which enables the R—Y—C—X system to acquire a lone pair on Y antiperiplanar to the C—X bond by transformation to the higher energy conformation **143C**, provided $\Delta E^{\neq}_{\mathbf{D-C}} \ll \Delta E^{\neq}_{\mathbf{D-B}}$, to fulfill the requirements of the Curtin–Hammett principle (305). For instance (7d), if **143A** and

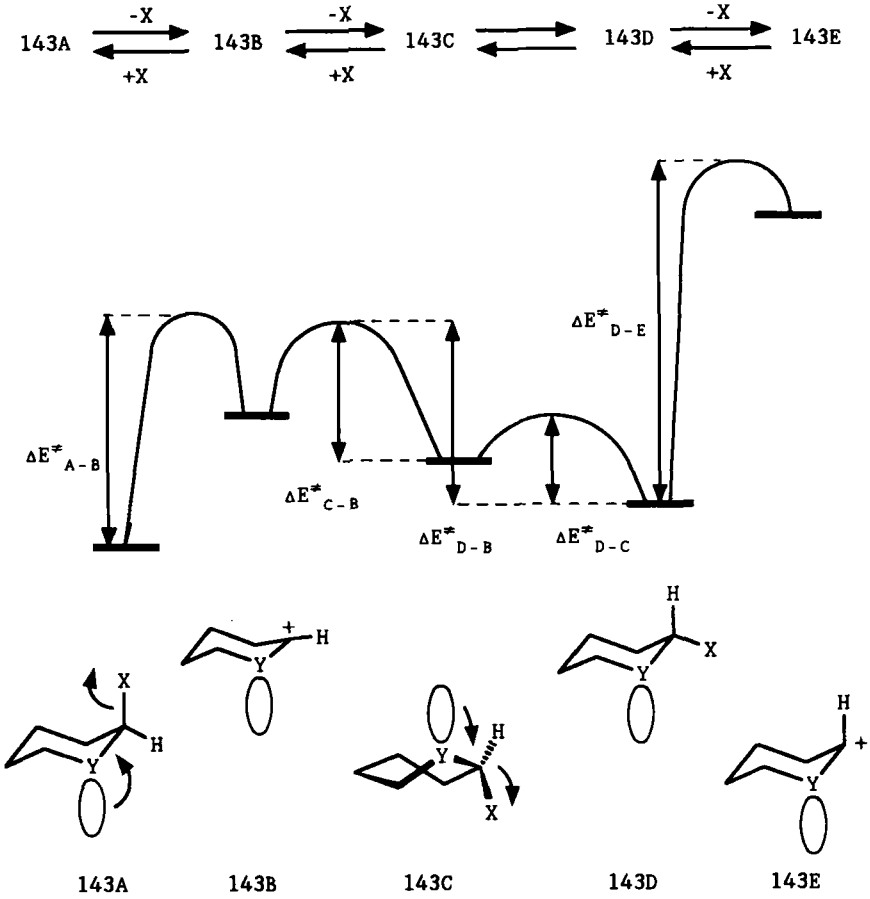


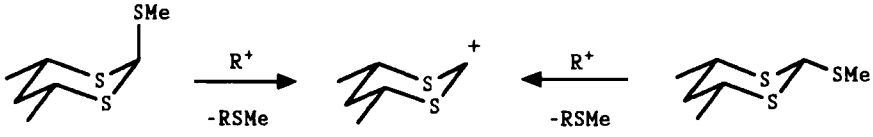
Figure 42. Transformations of chemical species **143A**, **B**, **C**, **D**, and **E** (see text).

143D are α- and β-anomers of aryl glycosides (Y = O, X = Ar) existing in chair forms, conformation **143C** may correspond to the relevant twist-boat conformation with a lone pair of the ring oxygen antiperiplanar to the pseudoaxial X group. Moreover, if the appropriate transition states for transformations **143A** → **143B** and **143C** → **143B** are late, they become close in energy and the relative reactivity of **143A** and **143D** is determined solely by a difference in their ground-state energies (179).

Though the stabilizing role of the lone electron pair of the oxygen atom (Figure 42; Y = O) on the resulting cationic intermediate **143B** (see also Figure 40c) has been supported both by experiment (306) and by calculation (307), the treatment of the ALPH as a dogma has been criticized from various

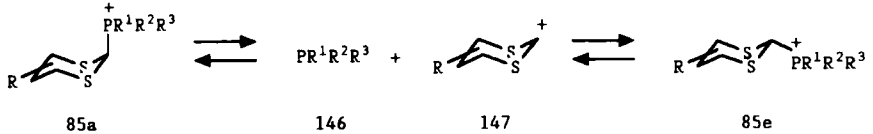
standpoints that emphasize the importance of least motion effects (11, 174) or destabilizing interactions (14). Recently, Ratcliffe et al. (308) proposed that the hydrolysis (or formation) of glycosides could take place in some cases by a synperiplanar rather than an antiperiplanar lone-pair pathway (*vide infra*). There is also a debate concerning the position of positively charged substituents X (e.g., OHR^+ in the acid hydrolysis of glycosides) in reactive species prior to the heterolysis of the C—OHR^+ bond. In the opinion of Sinnott (11), due to the operation of the reverse anomeric effect, such substituents must acquire equatorial or pseudoequatorial position prior to the cleavage of the C—X bond.

Recently, Caserio et al. (301) found almost equal rates of formation of the *cis*-4,6-dimethyl-1,3-dithian-2-yl cation (**144**) from the appropriate 2-methylthio derivatives **145a** and **145e** under FT-ICR conditions in the gas phase (Scheme 38). However, since phenomena occurring in gas phase and in liquid can differ markedly (309), the problem of applicability of the ALPH, when second-row atoms are involved in a reaction in solution, remained unresolved. In the course of our studies on the S—C—P system we found (310) that both the C—P bond breaking in 2-methylthiophosphonio-1,3-dithianes **85** (R^1 = SMe, R^2, R^3 = Ph; Scheme 39) and formation of 2-phosphonio-1,3-dithianes **85** (R^1, R^2, R^3 = Ph, Me, SMe) (from phosphine **146** and cation **147**) in solution do not fulfill the requirements of the ALPH. In particular, the results mitigate against the participation of higher energy intermediates **148** and **149** when the C—P bond in **85e** is formed or cleaved. In our opinion the processes shown in Scheme 39 are controlled by several factors, which *as a whole* are responsible for the *stereoelectronic control* of the C—P bond breaking and formation.



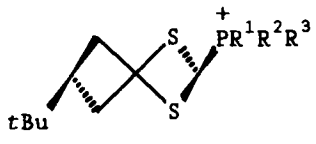
145a 144 145e

Scheme 38

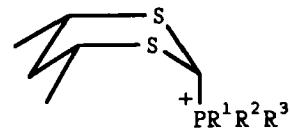


85a 146 147 85e

Scheme 39

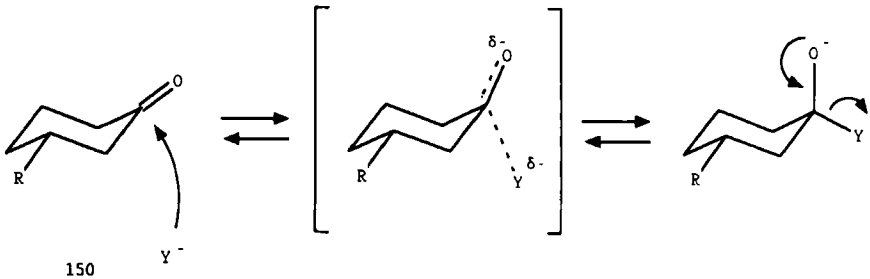


148



149

a. n_Y–σ^*_{C-X} Negative Hyperconjugation and Conformational Adjustment. This hyperconjugative interaction (Y = S, X = P), according to the ALPH, is operative only for derivatives with axial (or pseudoaxial) C—P bonds (e.g., **143A** and **143C** in Figure 42). While this may be true for ground-state phenomena, the situation on going to a transition state could, in our opinion, be quite different. Figure 43 shows possible steps during a heterolysis of the equatorial C—P bond in **85e**. With the lengthening of this bond, the C(2) atom becomes more and more planar (on going from *a* to *e*), and the n_S–σ^*_{C-P} hyperconjugative stabilization increases [note that the hyperconjugation intervenes significantly only after the C—P bond has been deformed beyond its "elastic limit" (15)]. Finally, when phosphorus is far enough away, the σ^*_{C-P} orbital is transformed into an empty π orbital of sp^2 carbon, which is situated adequately to overlap with the lone electron pair(s) of the endocyclic sulfur atom(s). This process, during which the H(2) hydrogen and nuclei of the S—C—S part of the ring change their respective position on going to the transition state, is called *conformational adjustment*. However, while conformational changes are accompanied by crossing of an energetic barrier, this process is similar to the vibrational movement of a ring and responds to monotonic movement through a potential energy surface toward the transition state. An analogous structural adjustment (in the reverse direction) has been considered (311, 312) for the equatorial attack of a nucleophile at 3-substituted cyclohexanones **150**, as shown in Scheme 40.



150

Scheme 40

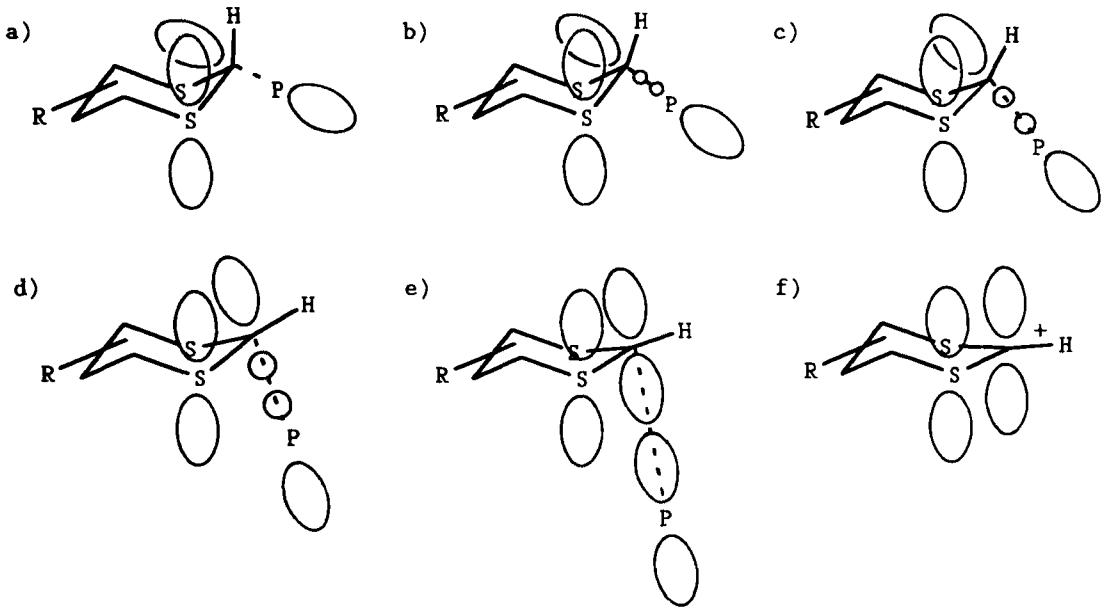
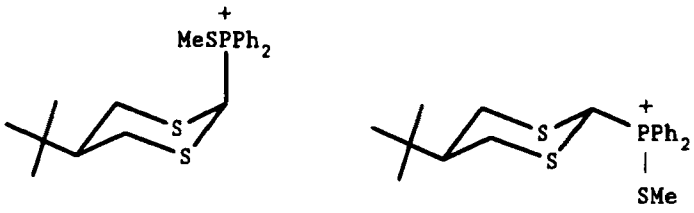


Figure 43. Conformational adjustment during heterolysis of C(2)—P bond in **85e**.

Late transition states are accompanied by significant secondary H/D isotope effects (293). This seems also to be the case for the heterolysis of the C(2)—P bond in **151a** and **151e** where H/D isotope effects are equal to 1.14 and 1.29, respectively (313). Hence, if situation *e* (Figure 43) corresponds to a transition state for **151e**, it will be stabilized in the same way as during the heterolysis of the axial C—P bond in **151a**. If both transition states were of the same energy, the difference in the rate of the heterolysis would arise from the difference in ground-state energies of the isomers [this conclusion is identical to that presented by Deslongchamps et al. (179), *vide supra*].



151a **151e**

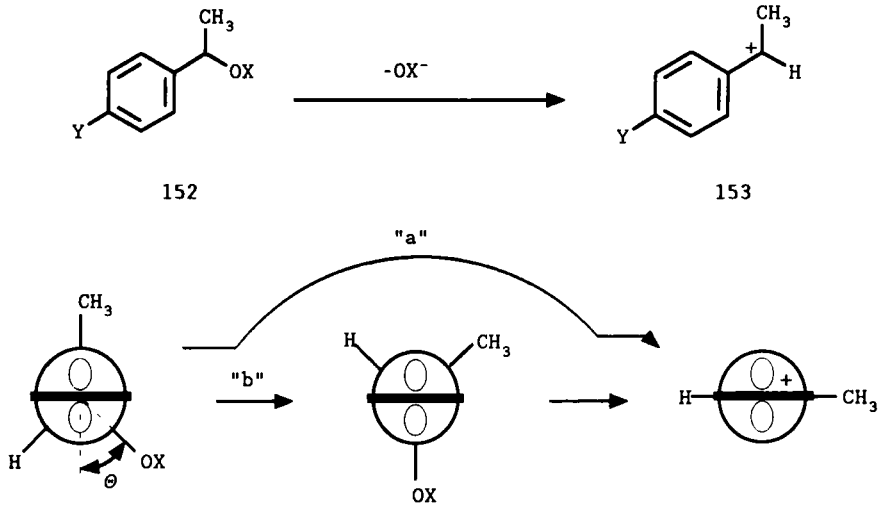
Analogous treatment of C—P bond formation, according to the principle of microscopic reversibility, shows that both isomers of **151**, when formed in comparable amounts, can arise from chairlike transition states.

The idea of conformational adjustment is strongly supported by an *ab initio* study (165) of the transition state in hydrolysis of the equatorial 2-methoxytetrahydropyran (**39e**) (Scheme 25). Andrews et al. (165) found that on going to the transition state the conformation of the possible reactive intermediates (derived from the protonated 2-methoxytetrahydropyran **81e**, Scheme 25) undergoes a change analogous to that shown in Figure 43. In particular, the C—OMe bond breaking occurs concurrently with ring flattening (165). The appropriate transition state for the protonated β-glycoside **81e** was found to be ^{4}E-*endo* sofa, which is close to the transition state *e* (Figure 43).† Hence, this process is always fast enough to follow the heterolysis of a bond. The influence of the conformational adjustment on the energy of a transition state is therefore dependent on its character and increases for systems where it is late. This would account for the observed (11) inapplicability of the ALPH for such systems. Moreover, it fits the observations of Kirby's group, who in a series of excellent studies (293–296) showed that the degree

†In contrast to what has been proposed by Sinnott (11), this *ab initio* study has shown the absence of the reverse anomeric effect in **81** (see Section II.I). Therefore, α-glycosides on protonation need not change their conformation toward the twist-boat to place the alkyloxonium group OHR^+ in the pseudoequatorial position prior to a heterolysis of the C(2)—$OHMe^+$ bond.

of "stereoelectronic control" decreases with later occurrence of the transition state. The importance of the lateness of the transition state for the stereochemical outcome of a reaction was also appreciated by Deslongchamps's group (179, 180). Nevertheless, they still maintain the existence of boat-type compounds as the reactive intermediates during hydrolysis of various β-glycosides.

The problem of participation of higher energy reactive conformers is not limited to derivatives of heteroanes. In particular, heterolytic cleavage of the C—OX (X = alkyl, acyl) bond in 1-arylethanol derivatives **152** (Scheme 41) to produce a cation **153** could serve as a good example. As was shown by Kirby's group (314), this heterolysis must be accompanied by an increase in the stabilizing π–σ^*_{C-OX} interaction which may occur independently (Scheme 41 and Figure 44, pathway *b*) or may be coupled with the conformational change **152a** → **152b** (Scheme 41 and Figure 44, pathway *a*). The coupled process, corresponding to the above-mentioned conformational adjustment, was assumed by the authors to be precluded by the much shorter time scale of a vibration (which leads to the bond breaking) compared with a rotation about the Ar—C bond (314). However, it seems to us that the rate of rotation about the Ar—C bond has nothing to do with the process *a* discussed by the authors. Obviously, the rate of rotation is related to a particular energetic barrier that is due to the eclipsing interactions of H and CH_3 with the phenyl ring (see Figure 44b, transition state TS). It is clear that on going from **152a** to



Scheme 41

153 via pathway *a* such interactions are avoided, and if they do appear, they appear in the final product, that is, **153**. This is in contrast to pathway *b*, where the benzylic hydrogen atom must first experience much stronger eclipsing interactions in the TS of going to **152b**. The movement of substituents connected with the benzylic carbon atom during process *a* is, therefore, best considered in terms of vibrations within the $-CH(CH_3)OX$ fragment. It must be added that X-ray data on various compounds **152** unequivocally showed (314) a linear decrease of dihedral angle Θ (see Scheme 41) with increase in the C—OX bond length. This may suggest monotonic increase of π–σ^*_{C-OX} interaction on going from **152a** to the transition state TS(*a*) (Figure 44a).

Now, consider in detail the appropriate reaction coordinates and conformational changes corresponding to pathways *a* and *b*, which are shown in Figure 44. Of course, the relative contribution of both pathways *a* and *b* depends on the relation between free energies G_{2a} and G_{4b} of transition states TS(*a*) and TS(*b*), respectively [Curtin–Hammett principle (305)]. If transition state TS(*a*) is early, its energy G_{2a} must be higher than G_{4b} owing to large Θ and inefficient π–σ^*_{C-OX} interaction.† In this case, and in the absence of other factors which might increase the energy of transition state TS(*b*), the reaction will proceed via pathway *b*. But if the transition states become later, they become similar and their energies G_{2a} and G_{4b} approach each other. According to the Curtin–Hammett principle (305), pathway *b* no longer predominates. The reaction will proceed mainly via pathway *a*, which represents the lowest lying way on the free energy surface (*there is no need to cross the transition state TS!*). In addition, since the free energy G_{1b} of **152b** is larger than that of **152a**, G_0, the transition state TS(*b*) should be, according to Hammond's postulate, somewhat earlier than TS(*a*). Therefore, the transition state TS(*a*) could be stabilized hyperconjugatively even better than TS(*b*), provided there are no overlap restrictions (i.e. $\Theta \cong 0$, Scheme 41; both transition states are late enough). Moreover, if transition state TS(*b*) were strongly destabilized due to steric reasons (as is, e.g., a boat conformation), the preference for pathway *a* might be even much greater. In our opinion, the involvement of two possible pathways—the first with conformational adjustment and the second via higher energy intermediates—must always be taken into account. So far, nobody has considered such a possibility.

The idea of conformational adjustment might explain the observed lack of stereoselectivity for the C(2)—OR bond breaking in orthoesters **140** in the gas phase (309) [in a solution the axial bond is much more easily cleaved

†Since the importance of entropic factors in the kinetics of reactions controlled by stereoelectronic interactions discussed in this chapter is well recognized now (6h, 10, 11, 315a), the influence of these interactions on the rates should preferably be discussed in terms of enthalpies of activation (cf. Section II.F). This seems to be especially important when stereoelectronic effects are deduced from rates of reactions of nonisomeric compounds.

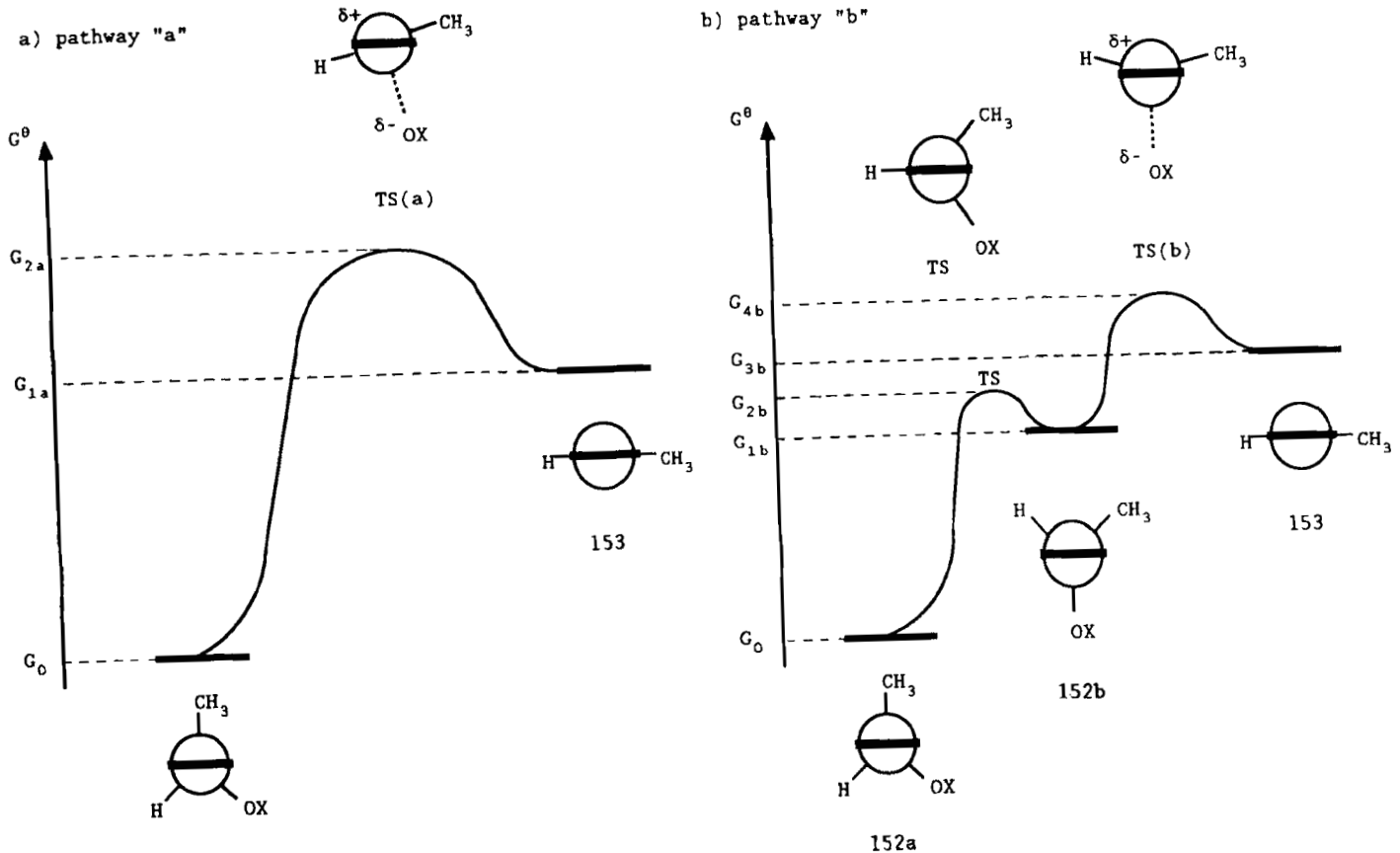


Figure 44. Heterolysis of C—OX bond in **152a:** (a) with conformational adjustment and (b) via conformation **152b**.

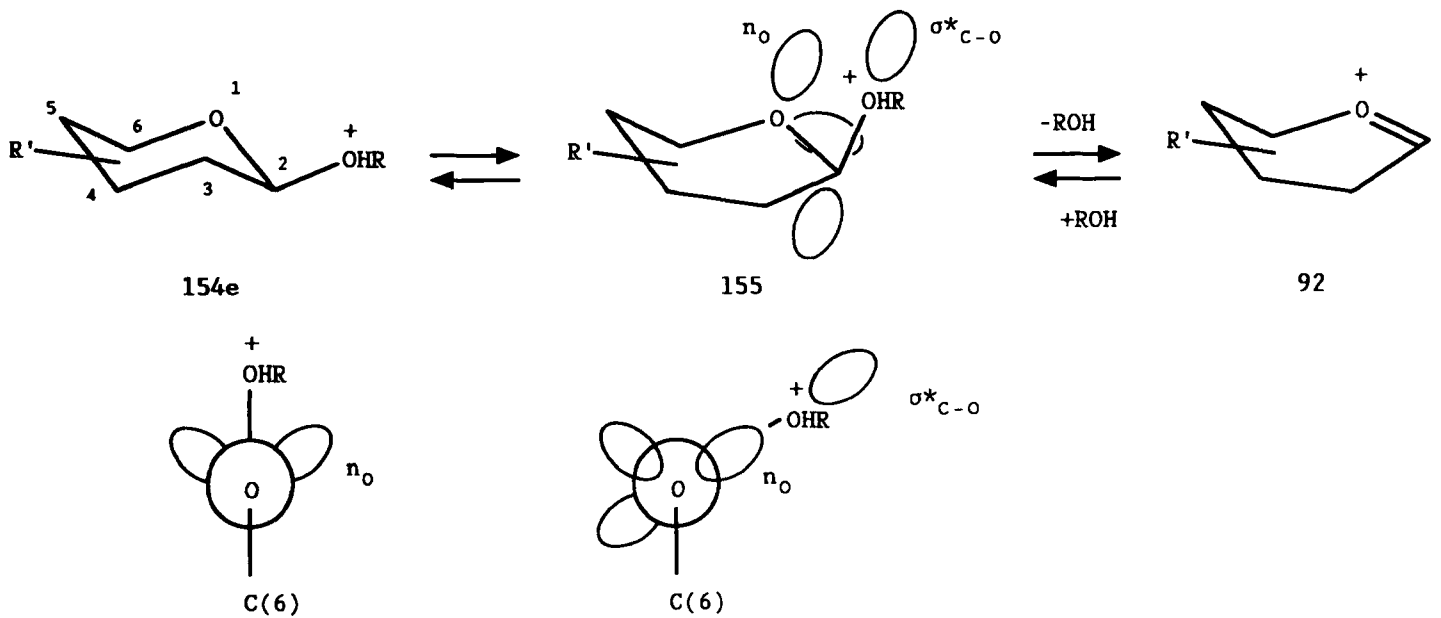
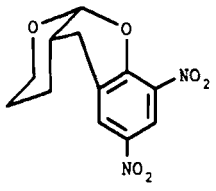


Figure 45. Synperiplanar pathway during the heterolysis of the equatorial C—$^+$OHR bond in **154e**.

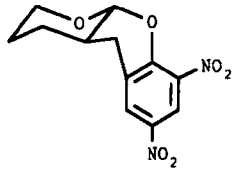
than the equatorial one (7e)]. In contrast to the situation in solution, both the substrate (large ion) and the products (neutral molecule and ion) resulting from the heterolysis are not solvated. The lack of solvation results in a much higher increase in energy of the products (which are smaller species) than of the substrate. According to Hammond's postulate, this would result in a much later transition state in the gas phase, much more effective conformational adjustment, and the disappearance of the stereoselectivity implied by ALPH. By the same token, solvent dependence of the reactions of cyclic orthoesters (315b) could be explained.

In the course of their studies on oxidative hydrolysis of conformationally restrained glycosides Ratcliffe et al. (308) found a similar rate of hydrolysis for α- and β-anomers. They concluded (308) that protonated β-anomers can react via half-chair (or sofa) conformers with *synperiplanar* arrangement of the endocyclic oxygen lone electron pair and antibonding σ^*_{C-O} orbital, as shown in Figure 45. In our opinion, the assumed relative arrangement of oxygen lone-pair and antibonding orbital *before the reaction* has nothing to do with the energy of the respective transition state, since the geometry of a molecule may change on going from the reactive ground state to the transition state. The results of Ratcliffe et al. (308) can be satisfactorily explained on the basis of conformational adjustment, which may easily occur in their system. Of course, the reasonable assumption of a late occurrence of the transition state is necessary.

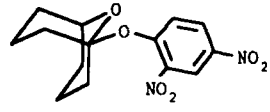
The possibility of conformational adjustment, though recognized by others (10, 13, 174, 293, 314, 316), has not been accepted so far. In particular, this possibility was studied by Kirby's group (293–296) based on a solvolysis of some acetals containing aryloxy groups linked to the anomeric carbon atom. In our opinion, their studies provide no unequivocal evidence to reject (with one exception, *vide infra*) the possibility of conformational adjustment. They strongly support the dependence of the degree of "stereoelectronic control" on the character of the transition state (293). The very small difference (by a factor of ca. 4.2) between the rate of spontaneous hydrolysis of two dinitrophenyltetrahydropyranyl acetals **156** and **157**, with the leaving group in **157** fixed equatorially by the *trans* ring junction (294), is not consistent



156



157



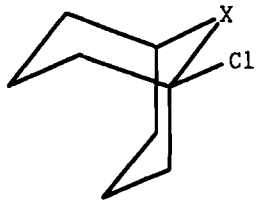
158

with the ALPH (the rate-determining steps for **156** and **157** must be the same as shown by a very similar deuterium solvent isotope effect). The possibility of conformational adjustment was indeed excluded by Kirby et al. (296) in bicyclic acetal **158**. However, this system was designed especially for this purpose, and the structural restrictions in **158** are not valid in other acetals studied by them.

The question of applicability of the ALPH discussed above is the problem of the relative magnitude of hyperconjugative and destabilizing interactions in appropriate transition states and the character of the latter.

b. $\sigma_{C(2)-Y}$–$\sigma^*_{C(2)-X}$ and $\sigma_{C(2)-X}$–$\sigma^*_{C(2)-Y}$ Hyperconjugations. As shown in Section IV.A.1.a, the importance of the n_Y–σ^*_{C-X} negative hyperconjugation for the stabilization of the relevant transition state (Figure 40b) is well accepted now. However, it is, in our opinion, of considerable concern that the donor abilities of σ orbitals of R—Y and C—X bonds (Figure 40) in σ_{R-Y}–σ^*_{C-X} and σ_{C-X}–σ^*_{R-Y} hyperconjugation, respectively, in the *ap* conformer of the R—Y—C—X system are usually overlooked, despite theoretical (317–319), spectroscopic (320) (for Y = S), and X-ray crystallographic [for Y = O (318, 321) and Si (318, 322)] support. While these donor abilities are of relatively small importance for first-row Y (e.g., Y = O), their role for second-row atoms is much greater. In 1987 Anet and Kopelevich (323) showed, for example, that the stretching frequencies of axial and equatorial C(2)—D bonds in a 1,3-dithiane ring are equal and that there is no isotope effect on the corresponding conformational equilibrium. Recent *ab initio* studies by Wolfe and Kim (324) on $CH_2(XH)_2$ (X = O, S) systems revealed the main factors responsible for such behavior, with the hyperconjugation involving σ_{S-H} orbitals as donors as one of them [the σ_{S-H} orbitals in $CH_2(XH)_2$ correspond to the $\sigma_{C(4,6)-S}$ orbitals in 1,3-dithiane; see also Section IV.B.3.c].

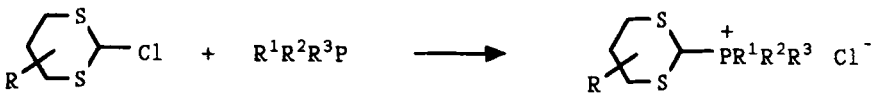
Hence, if the donor abilities of the $\sigma_{C(4,6)-S}$ orbitals in 1,3-dithiane can influence its ground-state energy, it seems quite possible that they may influence the energy of 2-P-substituted 1,3-dithiane derivatives during the heterolysis of the equatorial C(2)—P bond. It is probable that the $\sigma_{C(4,6)-S}$–$\sigma^*_{C(2)-P}$



159

interaction facilitates only initial heterolysis of the C(2)—P bond prior to the subsequent effective conformational adjustment. Indeed, Meyer and Martin (325) showed an important fractional contribution of the resonance stabilization by an α-heteroatomic substituent X of the resulting bridgehead cation resulting from the solvolysis of bicyclic chlorides **159**. Nevertheless, the overall rate of solvolysis was shown (326) to decrease in the series X = NMe, CH_2, O, S.

c. Overlap Repulsion. It must be noted that the importance of hyperconjugative interactions for ground-state behavior of molecules is not universally accepted (see Section III.B.4). In the opinion of Box (8, 14–16) and Tvaroška and Bleha (13) a source of ground-state preferences can rather be found in destabilizing interactions in *ap* conformations of C—O—C—O systems (rabbit ear effect, see Section III.B.4). Hence, if such interactions exist and if they can decrease in the transition state, they could influence the stereochemical course of a reaction. This suggestion is strongly supported by the results of the kinetically controlled reaction between 2-chloro-1,3-dithianes **160** and phosphines **146** (Scheme 42), which occurs according to an S_N1 mechanism (8, 310, 327, 328). For compound **160** (R = 5-*t*Bu or *cis*-4,6-Me_2), if $R^1 = R^2 = Me$ and $R^3 = Ph$ both diastereomers, **85a** and **85e**, are formed in almost equal amounts (54, 310). With an increase in the number of phenyl rings the amount of isomer containing an axial C—P bond increases up to 90% (54, 98). This result might be attributed to, among other factors, repulsive interactions between lone electron pairs π_S of endocyclic sulfur atoms and π electrons of phenyl ring(s) as well as the lone electron pair on phosphorus, which can destabilize the equatorial approach of a phosphine molecule (see Figure 46). This is why a large molecule such as Ph_3P prefers axial attack. Interestingly, the largest preference for axial approach is observed (54, 310) for Ph_2PSMe (93:7). It has been argued (*vide supra*) that, in the sense of C—P bond breaking, the appropriate transition state is late. Hence, ALPH cannot be expected to account for the observed stereoselectivity. On the other hand, the interactions discussed now constitute a very good explanation, with lone electron pairs on the MeS sulfur (Figure 46, X = S) being involved in repulsions with lone electron pairs of endocyclic sulfur atoms of the 1,3-dithianyl cation **147**.



160 **146** **85**

Scheme 42

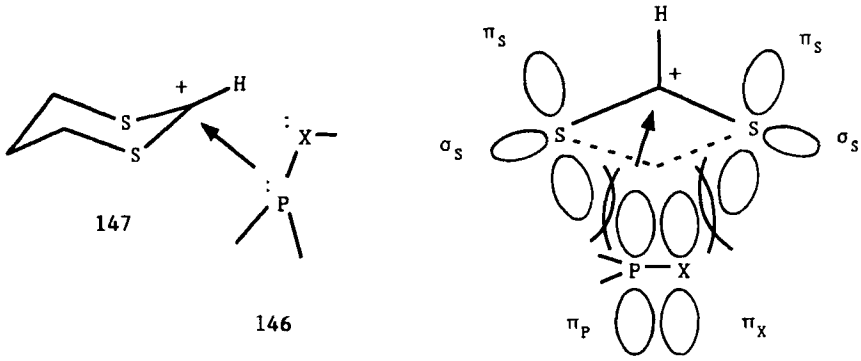
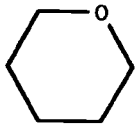


Figure 46. Repulsive interactions during equatorial approach of a phosphine **146** (X = C, S) to 1,3-dithianyl cation **147**.

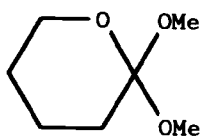
2. *Anomeric Effect and Rotational Barriers*

As expected on the basis of a PMO/NBO approach (Sections III.B.4 and III.B.5) to conformational equilibria in R—Y—C—X systems, hyperconjugative interactions are accompanied by a strengthening of the donor–anomeric carbon bond. Deslongchamps and Taillefer (329) were the first to suggest that this should result in an increase in the barrier for rotation about the Y—C bond. At the same time, if the C—X bond is weakened, the relevant barrier for rotation about C—X will be lowered.

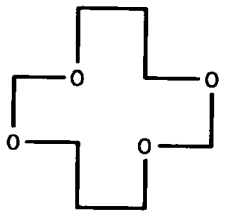
The latter hypothesis seems to be supported by reduced barriers to rotation about the C—N bonds in axial *N*-glycosides (330). The former postulate, however, is still a matter of controversy. Borgen and Dale (331) found that 1,3,7,9-tetraoxacyclododecane (**161**) has a much higher conformational barrier (46 kJ/mol) than comparable 12-membered rings such as cyclododecane (30 kJ/mol) (332) and 1,4,7,10-tetraoxacyclododecane (**162**, 23 and 28 kJ/mol) (333). On the other hand, Perrin and Nuñez (191), basing themselves on the value of $\Delta G^{\neq} = 36.3$ kJ/mol for ring inversion of 2,2-dimethoxyoxane (**98**), concluded that the anomeric effect does not raise but rather reduces the barrier to conformational change. Their argumentation was based on higher $\Delta G^{\neq}$ values for cyclohexane (43.9 kJ/mol), oxane (**70**, tetrahydropyran, 43.1 kJ/mol), and 1,1-dimethoxycyclohexane (**163**, 45.2 kJ/mol) and a similar low one for 2,2-dimethoxy-5,5-dimethyl-1,3-dioxane (**164**, 36 kJ/mol). Such reasoning, though seductive, would seem to be misleading from a methodological point of view. Even if no anomeric effect operated in **98**, $\Delta G^{\neq}$ for cyclohexane, **70**, and **163** would be larger than that for **98** because of smaller ground-state compression (40). In particular, the decrease in $\Delta G^{\neq}$ on going from **163** to **98**



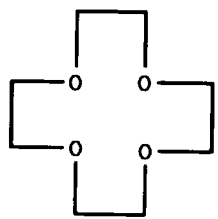
70



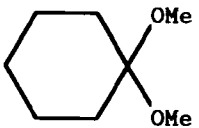
98



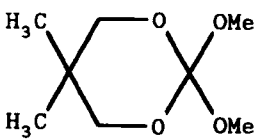
161



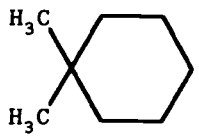
162



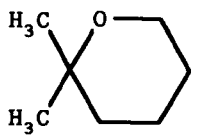
163



164



165



166

is expected as a result of the increase of the H—OMe 1,3-diaxial repulsions resulting from shorter C—O—C as compared to C—C—C bond distances.

In our opinion, the best way to probe the influence of the anomeric effect on $\Delta G^{\neq}$ in **98** would be to estimate a magnitude of the expected $\Delta G^{\neq}_{expd}$ in the absence of the anomeric effect and after correction for the ground-state compression effect. Let us examine $\Delta G^{\neq}$ for **165** and **166**, which can serve as reference systems, using modified Franck methodology (see Section II.C). First, the role of F in Eq. [3] ($C = 0$) will be played by a factor $\chi = \Delta G^{\neq}_{166}/\Delta G^{\neq}_{165}$ that will approximately correspond to a degree of decrease of $\Delta G^{\neq}$ (owing to the ground-state compression effect) on going from cyclohexane to tetrahydropyran rings substituted by two methyl groups and in the absence of the anomeric effect. Since the *endo* anomeric effect is not present in **163** (cyclohexane analogue of **98**), the expected inversion barrier in the absence of the anomeric effect in **98**, $\Delta G^{\neq}_{exp}$, will be given by

$$\Delta G^{\neq}_{exp} = \Delta G^{\neq}_{163} \times \chi \qquad [44]$$

It should be noted that the factor χ was based on dimethyl derivatives of cyclohexane and tetrahydropyran. As discussed for factor F_G in Section II.C, χ (like F_G) probably depends on the size of the substituent. Therefore, as shown in Section II.C, an adequate χ for the OMe group can be found by a linear interpolation of χ values found for H (unsubstituted cyclohexane and tetrahydropyran) and CH_3 (**165** and **166**) and assuming that the OMe group is of intermediate "size" (measured as ΔG°_{C}, Eq. [1]) between that of H and CH_3.

Nevertheless, the ground-state compression effect has been rejected by Ouedraogo and Lessard (76), who argued that the introduction of an oxygenated substituent in a cyclohexane ring has virtually no effect on the ring inversion barrier. Based on lower barriers to ring inversion in various 2-oxytetrahydropyrans (e.g., in **25**, **26**, and **28**, Table 3) than in unsubstituted tetrahydropyran **70** they concluded that the anomeric effect does lower the barrier to ring inversion of a tetrahydropyran ring. They rationalized their finding as being due to *exo* anomeric interactions, which can be maintained throughout the inversion process and thus impart some sp^2 character to the anomeric carbon atom. The barrier is low since methylenecyclohexane, which has one sp^2 carbon, has a lower inversion barrier than cyclohexane (76). However, in our opinion, the lack of a significant ground-state compression effect in cyclohexanes does not exclude such an effect in tetrahydropyran derivatives since the latter, due to shorter C—O—C versus C—C—C bonds, should be much more sensitive to steric interactions exerted by a substituent. (The question arises why the changes in the ring inversion barrier on going from tetrahydropyran to 2-methyltetrahydropyran were not taken into account). Moreover, we consider their explanation of the low inversion

barriers on the basis of sp^2 hybridization of the anomeric carbon as unconvincing.

The connection between anomeric effect and rotational barrier was found by Reed and Schleyer (146) for $FSNH_2$ (**133**) by an NBO approach. They studied the rotation around an N—S bond assuming rigid rotation and planarity of the SNH_2 fragment to avoid complications due to pyramidalization at nitrogen. The rigid rotation barrier ΔE was decomposed into two components: a change in energy of Lewis structure, ΔE_L, and a contribution ΔE_D from delocalization into appropriate antibonding orbitals (cf. Section III.B.5). The contributions of ΔE_L and ΔE_D to the rigid internal rotation barrier of the planar SNH_2 structure were found to be $\Delta E_L = -8.4$ kJ/mol and $\Delta E_D = 138$ kJ/mol. Therefore, the rotational barrier in **133** is due nearly entirely to the delocalization energy component ΔE_D. The largest contribution to ΔE_D comes from the n_N–σ^*_{S-F} interaction (100 kJ/mol), although other hyperconjugative interactions are also significant.

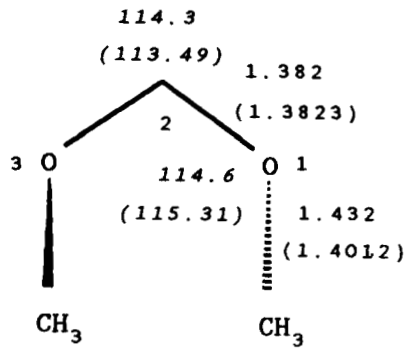
Considerably higher values (by more than 10 kJ/mol) of the rotational barriers for heteroatom derivatives of methanol, HCH_2—OX (X = F, Cl, O^-, OH, and OH_2^+), than for methanol itself were rationalized by Wu and Houk (334) in terms of the σ_{C-H}–σ^*_{O-X} hyperconjugation and π-type orbital interactions between $\pi^*_{CH_3}$ and π_{O-X} orbitals. Brunck and Weinhold (280) showed by semiempirical calculations that removal of the antibonding orbitals in FCH_2NH_2, $FNHNH_2$, and $FONH_2$ (which removal prevents hyperconjugation from occurring) resulted in almost complete disappearance of their internal rotation barriers. These findings additionally support the original suggestion by Deslongchamps and Taillefer (329) of the increase in rotational barrier for rotation around the Y—C bond in the R—Y—C—X system, as stemming from the n_Y–σ^*_{C-X} hyperconjugative interaction.

B. Anomeric Effect and Structure

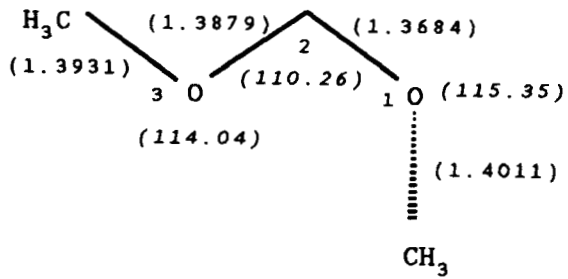
As one might expect, the anomeric effect may be accompanied by changes of structural parameters such as bond lengths, angles, electron density, and resultant spectral parameters. Such changes are thought to be connected with the origin of the anomeric effect, but as will be shown, this point of view may sometimes be erroneous. For example, it is often difficult to separate, at first sight, the purely inductive effects of electronegative Y and X ligands in the R—Y—C—X system from effects arising from an interaction between Y and X.

1. Bond Lengths and Angles

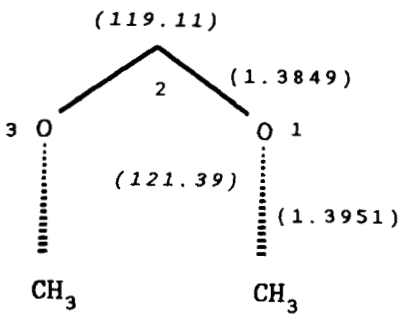
Let us first consider selected bond lengths and angles, found experimentally and calculated, for molecules exhibiting anomeric effects. They are shown in



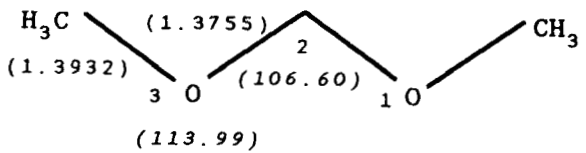
11(sc, sc)



11(ap, sc)

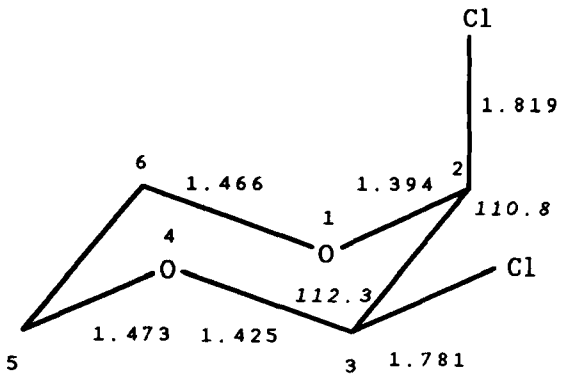


11(-sc, +sc)

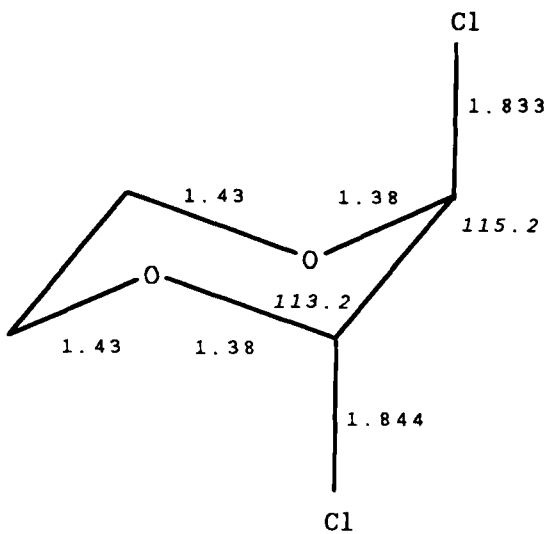


11(ap, ap)

Figure 47. Selected experimental (from ref. 335) and calculated (in parentheses; data from ref. 57) bond lenghts and angles (in italics) for dimethoxymethane (**11**).



167



168

Figure 48. Selected bond lengths and angles (O—C—C; in italics) in **167** and **168** (data from ref. 188).

Figures 47 and 48.† It is clear that in the *sc, sc* conformer of dimethoxymethane (DMM, **11**) the C(2)—O bond is much shorter (1.382 Å) than CH_3—O (1.432 Å). *Ab initio* high-level calculations (57) agree with this difference; however, the calculated CH_3—O bond length (1.4012 Å) is shorter than that found experimentally since *ab initio* geometry represents a minimum energy structure and fails to account for anharmonicity at the zero-point energy level (57). The calculated changes that occur during rotation about the C(2)—O bond starting from the *sc, sc* conformation are remarkable. While the C(2)—O(1) bond undergoes considerable shortening (by 0.0139 Å) in the *ap, sc* conformation, the C(2)—O(3) antiperiplanar bond is longer (by 0.0056 Å) than C(2)—O(3) in the *sc, sc* conformer. In going from the *ap, sc* to the $-sc$, $+sc$ conformation the C(2)—O(3) bond again becomes short (1.3849 Å), but not as short as it is in the *sc, sc* form. When both torsion angles refer to the antiperiplanar arrangement, both CH_2—O bonds are very short (1.3755 Å).

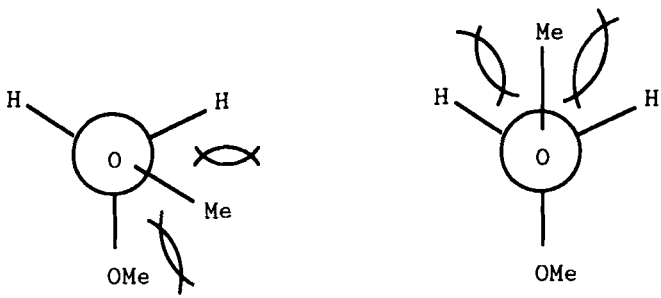
More remarkable data are provided by *cis-* and *trans*-2,3-dichloro-1,4-dioxanes (**167** and **168**, respectively; Figure 48). The axial C(2)—Cl bond in **167** is longer by 0.038 Å than the equatorial one. On the other hand, O(1)—C(2) is much shorter (by 0.031 Å) than O(4)—C(3). If both C—Cl bonds are axial, as in **168**, they are longer and the corresponding O—CH bonds are shorter compared to C(3)—Cl and O(4)—C(3), respectively in **167**.

Though *ab initio* MO calculations (57, 70, 90, 143–145, 153, 235, 238, 244, 260, 264) seem to reproduce bond length and angle changes rather well, the *rationalization* has been provided by PMO theory. Let us consider fluoromethanol (**121**) (Figure 32) as an example. In the *sc* conformation the only significant interaction is *d* (n–σ^*). Such interaction leads to an increase of the O—C bond order since the n_π oxygen lone pair is involved in bonding, and it results in the shortening of the O—C bond. On the other hand, the C—F bond is weakened and lengthened due to partial transfer of oxygen n_π electrons into an antibonding σ^*_{C-F} orbital. This is just the trend observed for the synclinal arrangement of C—O—C—Cl in **167** and **168** where axial C—Cl bonds are much longer than C—Cl in chloroalkanes [1.79 Å (188)]. If the antiperiplanar arrangement of H—O—CH_2—F is considered, one must take into account weaker interaction *b* (n–π^*) and to some extent *c*. This is why the C—O bond is also shortened, but to a much smaller degree than in the *sc* form. Therefore, one should expect the C—O bond to lengthen on going from the *sc* to the *ap* conformation, but C—O in *ap* should still be shorter than in simple ethers. Indeed, it is observed in **167** that the C(3)—O(4) is longer than the C(2)—O(1) bond and C(3)—O(4) is shorter than C(4)—O(5).

†In order to avoid confusion when bond lengths and angles are displayed or discussed simultaneously, the angstrom will be used instead of the picometer (1 Å = 100 pm).

The changes in the dimethoxymethane molecule are consistent with the participation of $n-\sigma^*$ and $n-\pi^*$ hyperconjugative interactions. In the *sc*, *sc* conformation two $n-\sigma^*$ interactions are present and there is a "competition" between them (see Section II.E). Thus, if one $n-\sigma^*$ interaction is removed in the *ap*, *sc* conformation, the second $n-\sigma^*$ interaction becomes stronger. Therefore the O(1)—C(2) bond becomes shorter than in the *sc*, *sc* form. The C(2)—O(3) bond would be short in *ap*, *sc* due to the $n-\pi^*$ interaction, but it is also involved in a $n-\sigma^*$ interaction as an acceptor bond. Since the latter interaction prevails, the bond is longer than in the *sc*, *sc* and *ap*, *ap* conformations. In the *ap*, *ap* form no $n-\sigma^*$ interaction occurs, and both bonds are short owing to $n-\pi^*$ interactions. One might ask: Why do C—O bonds tend to be always shorter in contrast to C—Cl bonds, which become longer? The answer lies in the relative donor and acceptor abilities. Since Cl is a good acceptor and a bad donor, it exhibits mainly properties connected with rendering the σ^*_{C-Cl} orbital accessible. Oxygen, in contrast, is both a good donor and a good acceptor, and therefore both interactions must be taken into account. The result, then, is the tendency of C—O bonds to be shortened.

Bond length changes in dimethoxymethane are accompanied by O—C—O angle variation. This angle is largest in $+sc$, $-sc$ and decreases on going to *sc*, *sc*, *ap*, *sc*, and *ap*, *ap* conformations. Whereas the concept of double bond–no bond resonance can account for an opening of the Y–C–X angle (cf. Figures 14 and 25b; the Y–C–X carbon is of partial sp^2 character), it completely fails to explain the less than tetrahedral (109.38°) O–C–O angle (106.60°) in the *ap*, *ap* conformation of dimethoxymethane. The rationalization here was provided by Gorenstein and Kar (336) (Figure 49). They suggested that in the *sc* conformation two repulsive interactions (H–Me and Me–Me)



11(*sc*) 11(*ap*)

Figure 49. Repulsive interactions in dimethoxymethane (**11**) according to Gorenstein and Kar (336).

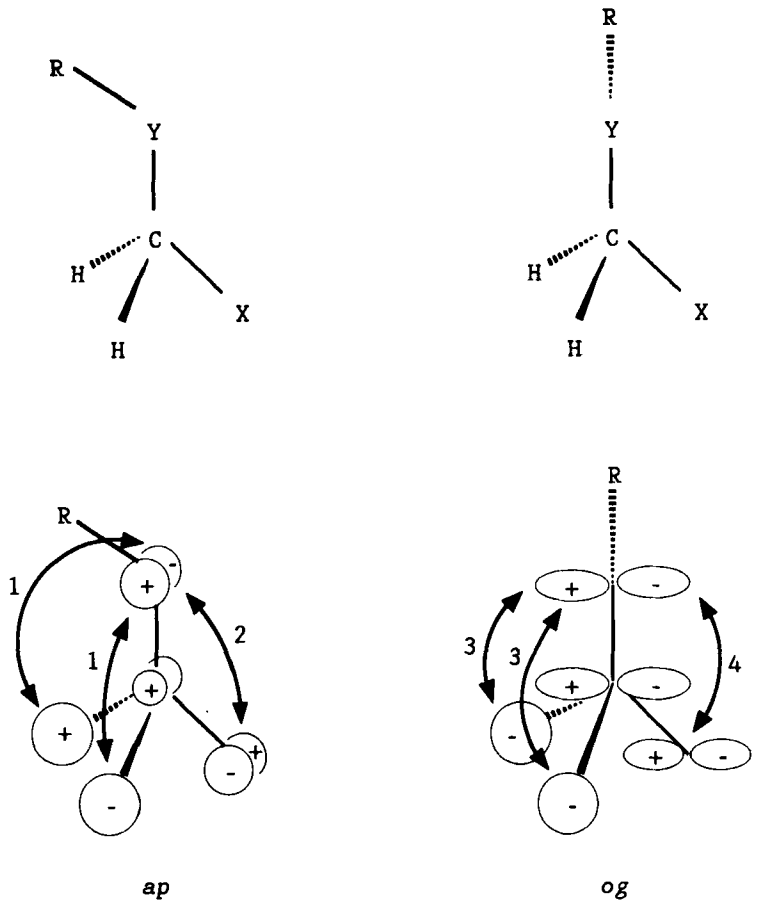


Figure 50. Secondary overlap in orbital interactions in R—Y—CH_2—X.

tend to open up the O–C–O angle whereas in the *ap* form two others (H–Me and Me–H) conspire to reduce it. An explanation on the basis of PMO theory was given by Pinto et al. (153) for the R—Y—CH_2—X system. The appropriate secondary interactions are pictured in Figure 50 (cf. Figure 32; OH = YR, F = X, relevant interactions: n_π–π^*_{C-F} in the *ap* conformation, n_π–σ^*_{C-F} in the *sc* conformation of $RYCH_2X$). Interactions 1 and 2 in the *ap* conformation are repulsive since secondary overlap occurs out of phase. Let us assume the CH_2X group to be rigid. Since the hydrogen atoms of $\pi^*_{CH_2}$ have larger coefficients than X, interactions 1 are more repulsive than 2. The R–Y–C angle increases while Y–C–X decreases.

In the *og* conformation there is competition between repulsive secondary

overlaps 3 and 4, but now 4 is more repulsive than 3. This results in an increase in the Y–C–X angle from the idealized tetrahedral one. It would seem then that this increase is steric in nature. This point of view has been a matter of controversy. Norskov-Lauritsen and Allinger (211), in their parametrization of MM2 for the anomeric effect, attributed the dependence of the Y–C–X angle on the conformation of a R—Y—C—X system to van der Waals repulsions, which implies a steric effect. Similarly, in Wiberg and Murcko's (57) opinion the changes in bond angles in dimethoxymethane are in large measure due to steric interactions; however, Salzner and Schleyer (148), basing themselves on NBO analysis, have attributed the Se–C–Se angle widening in methanediselenol (**130**) to a $3p\text{–}\sigma^*_{Se_C}$ hyperconjugative interaction.

Considerable effort has been devoted to the application of experimentally found geometric changes to the probing of anomeric effects, especially in O—C—O systems (60, 69, 88, 89, 153, 192, 214, 238, 257, 260, 321). In order to find regularities in the structure of C—O—C—O—C segments, large sets of crystallographic data were scrutinized statistically (60, 69, 88, 89, 257). The most exhaustive studies, based on 546 and 529 COCOC molecular fragments, are due to Cosse-Barbi and Dubois (60) and Schleifer et al. (88), respectively. Selected data from these papers are collected in Table 15. Indeed, in the *ap, sc* arrangement of the O(1)—C(2)—O(3) fragment, the length of the O(1)—C(2) bond is greater than that of C(2)—O(3). Moreover, the O(1)—C(2) bond in *ap, sc* seems to be longer than in the *sc, sc* conformation, while C(2)—O(3) in *ap, sc* is shorter than the relevant bond in the *sc, sc* conformation, in good agreement with the trend presented for dimethoxymethane (*vide supra*). Nevertheless, the shortest C(2)—O(1) and C(2)—O(3) bonds do not seem to appear in the *ap, ap* conformation, in contrast to the situation in dimethoxymethane.

Cosse-Barbi and Dubois (60) pointed out that the central angle, O(1)—C(2)—O(3), appears particularly sensitive to conformational variation. On going from the *sc, sc* to the *ap, ap* conformation, one observes a significant (about 12°) decrease of this angle, in rather good agreement with the reduction computed (57) for dimethoxymethane (8°).

While the torsion angle C—O(1)—C(2)—O(3), which relates to the *endo* anomeric effect, is predicated by the rigidity of the chair, the *exo* torsional angle, O(1)—C(2)—O(3)—C, can assume almost any value (neglecting steric effects). According to the structure correlation method (87), the mean *exo* torsional angles found for five- and six-membered rings (77° and 72°, respectively) may be treated as equilibrium values, and hence they have been attributed to the nonequivalence of oxygen lone electron pairs (60, 69, 89, 257). Such torsion angles for the *endo* arrangement can be accommodated more easily in the (flexible) five-membered rings. This is why the *endo*

TABLE 15
Selected Bond Lengths and Angles for C—O—C—O—C Systems[a]

Conformation[b]	Average Bond Length (Å)		Angle OCO (degrees)	Reference
	O(1)—C(2)	C(2)—O(3)		
sc, *sc*[c,f]	1.405	1.405	112.5	60
sc, *sc*[d,f]	1.420	1.420	111.5	60
sc, *sc*[e,g]	1.416	1.411	111.4	60
sc, *sc*[e,h]	1.418	1.408	111.0	60
sc, *sc*[g]	1.416	1.405	112.0	88
ap, *sc*[e,g]	1.423	1.394	107.4	60
ap, *sc*[c,g]	1.404	1.394	107.0	60
ap, $-sc$[g]	1.425	1.389	107.6	88
ap, *ap*[c,f]	1.421	1.421	100.6	60
ap, *ap*[g]	1.404	1.409	105.2	88
$+sc$, $-sc$[e,f]	—	—	107.2	60
$+sc$, $-sc$[c,h]	1.444	1.392	109.9	60
$+sc$, $-sc$[g]	1.421	1.416	108.5	88

[a]From refs. 60 and 88.
[b]Given in the order: torsional angle about O(1)—C(2) (endo) and C(2)—O(3) (exo) bonds, respectively.
[c]C(2) quaternary.
[d]C(2) secondary.
[e]C(2) tertiary.
[f]Acyclic structure.
[g]Six-membered ring.
[h]Five-membered ring.

anomeric effect in furanoses is stronger than in pyranoses (69, 257) (see Figure 4) and the equatorial position of the OR group in pyranose rings is statistically avoided (60).

The changes in bond lengths here presented are qualitatively consistent with a hyperconjugative explanation of the origin of the anomeric effect. This point of view has been strongly supported by the work of Briggs et al. (321) concerning the dependence of bond lengths in acetals and glucosides (**96**) (Figure 13) on the pK_a of the alcohol (ROH) corresponding to the exocyclic RO ligand. They found significant increases of axial exocyclic C(2)—OR and decreases of endocyclic O(1)—C(2) bond lengths with increasing acidity of ROH. Strongly electron-withdrawing OR groups should be weak donors in *exo* but good acceptors in *endo* negative hyperconjugation and thus lower the energy of the σ^*_{C-OR} orbital. This results in enhanced shortening of O(1)—C(2) and lengthening of C(2)—OR due to the stronger *endo* negative hyperconjuga-

tion. In equatorially substituted derivatives much less pronounced changes were observed. However, as in axial compounds, more electron-withdrawing OR groups are associated with longer exocyclic C(2)—OR bonds and shorter endocyclic O(1)—C(2) bonds. Though electron donation by endocyclic oxygen is prevented, Briggs et al. (321) attributed the above changes to hyperconjugation involving an electron-donating $\sigma_{C-O(1)}$ bonding orbital antiperiplanar to the C(2)—OR bond.

Krol et al. (72) studied the *ab initio* geometry of cation **88** (Figure 51). It is clearly seen that the CH_2—O bond undergoes shortening by 0.0211 Å and the O—N bond lengthening by 0.0426 Å on going from the *ap* to the *sc* conformer. These findings suggest a strong n_O–σ^*_{C-N} negative hyperconjugation, which is in contrast to expectations based on the idea of the reverse anomeric effect (Section II.I). Analogous observations concerning bond lengths in systems tested for the reverse anomeric effect were made by Grein and Deslongchamps (163) for protonated species $H_nXCH_2Y^+H_n$ (X and Y = O and/or N) **77**–**80** (Figure 10). Their *ab initio* calculations (at the 6–31G** level) revealed that when a lone pair of Y is antiperiplanar to the C—Y^+ bond, the C—X bond shortens, and the C—Y bond becomes much longer (and in some cases the tetrahedral species switch to a π complex). When a lone pair of X is *gauche* to the C—Y^+ bond, this bond does not become longer, as might be expected based on the n_X–σ^*_{C-Y} negative hyperconjugation. Recent *ab initio* and semiempirical calculations by Cramer (166a) on **77** and **80** (see Figure 10) have shown the same trends in geometric changes with rotation about the C—O bonds. Cramer (166a) also studied 2-ammoniotetrahydropyran (**2**, X = NH_3^+; see Scheme 1a) and found elongation of the C—N^+ bond (by 0.048 Å) and expansion of the O—C—N angle (by 5°) on going from **2e** to **2a** (X = NH_3^+), in agreement with n_O–$\sigma^*_{C-N^+}$-based anticipation.

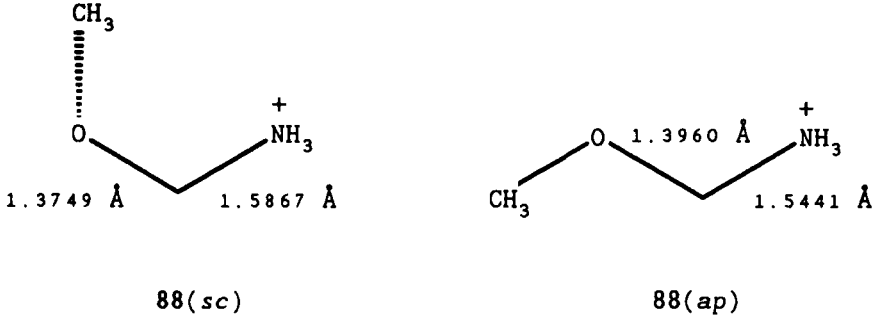


Figure 51. Selected bond lengths in methoxymethylammonium cation (**88**) calculated *ab initio* by Krol et al. (72).

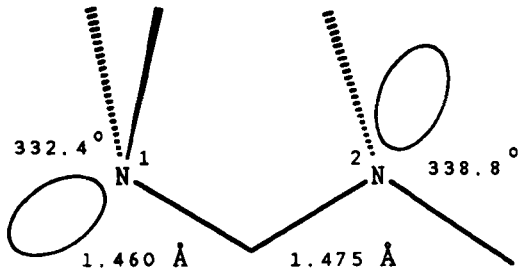


Figure 52. Selected geometric parameters for N—C—N system (taken from ref. 212).

It must be added that the hyperconjugative nature of the O—C—O anomeric interactions has recently been supported by X-ray data for ortho-esters containing $C(OC)_3$ (214) and $C(OC)_4$ (155) groups [see, however, below for compounds containing a $C(SC)_4$ group].

A structural-statistical study (212) performed by Fuchs's group for compounds containing N—C—N moiety supplemented their earlier *ab initio* and MM2 computation (156). The trends expected based on the n_N–σ^*_{C-N} negative hyperconjugation were followed (see Figure 52). In particular, the C—N(2) bond involved in this interaction as an acceptor was shown to be longer by 0.015 Å than the C—N(1) one. Interestingly, the pyramidality of nitrogen atom N(1) (332.4°; defined as the sum of the three valence angles around the nitrogen), which served as a donor, was *larger* than that of N(2) (338.8°). Similar, though less pronounced results were provided by an *ab initio* study (212) of H_2N–CH_2–NH_2 (327.3° vs. 328.9°, respectively). These findings parallel the observation of Irwin et al. (30) concerning pyramidality of nitrogen in F–CH_2–NH_2 [**4**, cf. results of Reed and Schleyer (141) for F–S–NH_2; *vide infra*]. Senderowitz et al. (212) interpreted the observed higher energy of species with lower pyramidality at the donor atom as a result of the overwhelming cost of planarization energy as compared to the energy gain from better n_π–σ^* than n_σ–σ^* overlap (n_π and n_σ denote lone pairs for planar and pyramidalized donor atoms, respectively).

Particularly strong hyperconjugation occurs in $FSNH_2$ (**133**) (146). The calculated F—S bond lengthening by 0.10 Å during internal rotation is associated with a barrier of 76 kJ/mol. Reed and Schleyer (146) reoptimized the geometry of $FSNH_2$ in terms of NBO analysis of its Lewis structure (hyperconjugation eliminated) in order to ascertain the full extent of the influence of the nitrogen lone-pair hyperconjugation on the molecular geometry. This approach resulted in a lengthening of the S—N bond by 0.077 Å, yielding a value of 1.692 Å (though still 0.006 Å less than that in the fully planar structure). Additionally, the S—F bond was shortened by

0.028 Å and the N–S–F angle decreased by 3°, in qualitative agreement with anticipation. However, the N–S–F angle could be widened by n_N–σ_{S-F} repulsive interaction, and the authors ascribed roughly half of the N–S–F angle increase in "real" $FSNH_2$ to the influence of negative hyperconjugation and the other half to other factors that might include n_N–σ_{S-F} repulsion.

Reed and Schleyer (144) pointed out that the shortening of the S—N bond by 0.083 Å is associated with a total increase of only 0.10 in the S—N π-bond order. They concluded that bond lengths are clearly not proportional to bond orders when strong hyperconjugation is present.

Applying an analogous procedure, Reed and Schleyer (144) found that n_N–σ^*_{S-F} interaction enforces greater planarity at the nitrogen atom. Different results were obtained by Irwin et al. (30), who studied the energy of conformers of fluoromethylamine (**4**) as a function of planarity at nitrogen. In the orthogonal conformation of the F—C—N—lp system ($\phi = 90°$), where the anomeric effect is switched off, the minimum energy was found for *N* nonplanar structures. For the nonorthogonal conformations minimum-energy species also contained pyramidalized nitrogen. The energy difference between N planar and N nonplanar structures was equal to ca. 19 kJ/mol [cf. the results of Senderowitz et al. (212) on **73**, *vide supra*]. The preference for structures stabilized by hyperconjugation involving a lone pair of predominating sp^3 character over structures stabilized by hyperconjugation with a lone pair of the *p* type as a donor has its consequences as far as the conformation of protonated methanediol molecule in concerned [see Section II.I, the results of Woods et al. (164)].

Bond length contraction in Y—C—X systems has been observed as a rule when Y and X are electronegative substituents. A good example is provided by polyfluoromethanes (cf. Section III.A.3). Brockway (194) observed that C—F bonds are shortened by about 0.06 Å on going from CH_3F to CF_4. Though stabilizing orbital interactions (6,70), or MOVB-based explana-

TABLE 16
Bond Length Contraction in Polyfluoromethanes in Terms of Lewis (L) and Full-Energy (F) Structures[a]

Molecules Compared	Bond Length Contraction (Å)	
	L	F
CH_3F, CH_2F_2	0.036	0.027
CH_2F_2, CHF_3	0.025	0.021
CHF_3, CF_4	0.011	0.015

[a]Based on data from ref. 143.

tion (203), have been offered to account (at least in part) for such bond shortening, it seemed clear that variations in the bond lengths of polyhalogenomethanes might originate (at least in part) from Coulomb attraction (70). On the other hand, increase in the C—X bond length in RYCX systems exhibiting an anomeric effect was regarded by Wolfe et al. (70) as the result of an overriding influence of hyperconjugation. A recent quantitative NBO approach (143) to this problem has revealed that the bond length shortening in the series CH_3F, CH_2F_2, CHF_3, and CF_4 is caused by the cumulative electrostatic effect of charge withdrawal from the carbon to the fluorines. This conclusion was based on the observation that the bond length contraction in the series occurring in terms of localized Lewis structure L (Table 16, cf. Section III.B.5) is about the same as in terms of full-energy (including delocalization) structure F. Similarly, Reed and Schleyer (143) found that 40% of the O—F contraction from FOH to F_2O is of electrostatic origin.

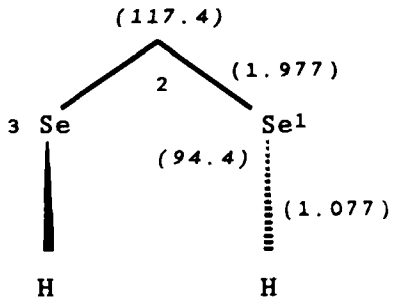
It should be added that electrostatic interpretation of bond lengths in polyhalogenomethanes has recently been advocated by Wiberg and Rablen (157b) based on results of high-level *ab initio* calculations for a large number of fluoro-, cyano-, chloro-, and silylmethanes. The authors (157b) noted, however, that another factor that operates in the same direction is hybridization. With increasing substitution in, for instance, fluoromethanes the fluorines compete for the carbon p-rich molecular orbital. With CF_4 each C—F bond is of 25% s character and, as a result, the C—F bond length is reduced.

It would seem interesting to consider bond length changes in systems where second- or third-row atoms are involved since the origin of the anomeric effect in such molecules is not so obvious. In *sc*, *sc* and $-sc$, $-sc$ fragments of 1,3,7,9,13,15-hexaselenacyclooctadecane (**169**) (Table 17), the Se—C bond lengths within the Se—C—Se system are about 0.012 Å shorter than the outer Se—C bond lengths. For methanediselenol (**130**) (Figure 53) the calculated difference in the two C—Se bond lengths in the *ap*, *sc*

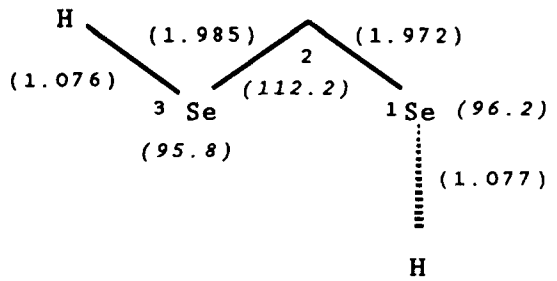
TABLE 17
Selected Bond Lengths (Å) and Bond Angles (degrees) (in parentheses) for 1, 3, 7, 9, 13, 15-Hexaselenacyclooctadecane (**169**)

Atoms	Arrangement	CH_2 — Se — CH_2 — S — CH_3			
18–4	$-sc$, $-sc$	1.967	1.947	1.946	1.953
			(94.6) (116.0) (96.0)		
6–10	$-sc$, $+sc$	1.955	1.932	1.944	1.937
			(100.4) (118.6) (100.0)		
12–16	$+sc$, $+sc$	1.951	1.946	1.939	1.955
			(98.3) (116.2) (98.8)		

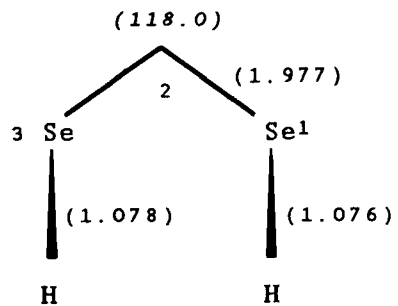
From ref. 83.



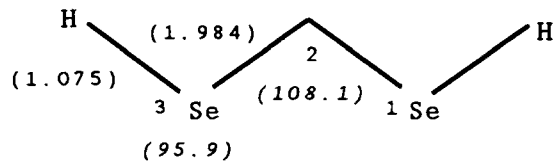
130(sc,sc)



130(ap,sc)

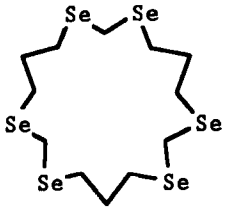


130(+sc,-sc)



130(ap,ap)

Figure 53. Calculated bond lengths (Å) and angles (degrees) (in italics) for methanediselenol (**130**) (data from ref. 148).

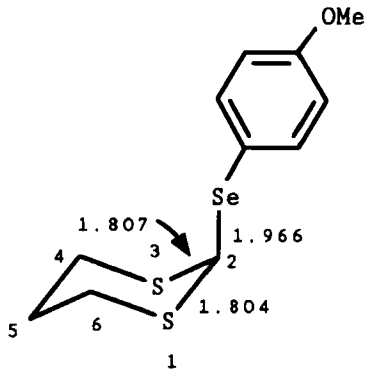


169

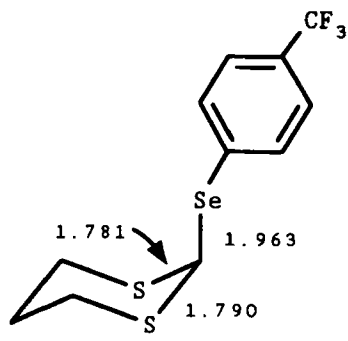
conformation is 0.013 Å, not much less than in corresponding C—O bonds of dimethoxymethane (**11**, 0.020 Å, Figure 47) despite the fact that the anomeric effect in **11** seems to be due to negative hyperconjugation (6, 70), whereas in **130** negative hyperconjugation is only one of many factors that determine conformation (148) (cf. Section III.B.5). Moreover, the C(2)—Se bond lengths in **170a** (Figure 54; cf. **37**, X = OMe) and **171a** (cf. **37**, X = CF_3, Scheme 13) are almost the same, in spite of the different electronegativities of the substituent aryl groups. If only negative hyperconjugation operated, different electronegativities of substituents should result in energy gap controlled differentiation of C(2)—Se bond lengths in **170a** and **171a** in such a way as to make the C(2)—Se bond longer in **171a**.

For a more exhaustive discussion concerning bond lengths in 2-P-substituted 1,3-diheteroanes see Section V.B.3.

All the above data indicate that geometric changes must be attributed to hyperconjugative interactions with great caution. While bond lengthening



170a

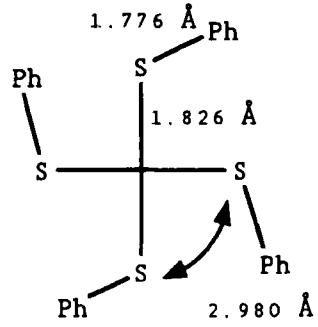


171a

Figure 54. Selected bond lengths in 2-arylseleno-1,3-dithianes **170a** and **171a** (data from ref. 83).

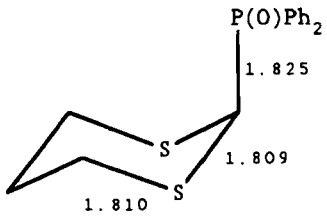
seems to be mainly of hyperconjugative character, the shortening can also be due to nonhyperconjugative (electrostatic) factors. Moreover, even for bond lengthening, one should consider other explanations as, for instance, nonbonded lone-pair repulsions (337) or strong steric interactions (20c, 338). The former possibility is not, in the opinion of Box (14), sufficiently appreciated in the chemical literature. In his review (14) devoted to the role of lone-pair interactions Box argued that a much more flexible approach is needed to the appreciation of "normal bond lengths." Bond lengths and angles of unusual magnitude are not necessarily the products of unusual stereoelectronic interactions operating on those bonds (14). The geometry of a molecule is established by the geometric adjustments required to minimize destabilizing interactions. In particular, X-ray data of the glycopyranosyl esters that have more than one ester group in a molecule showed that the length of the C1—OAc bond is fairly constant in value (covering a range of only 0.03 Å) regardless of the site, or stereochemical orientation, of the C—O bond in the molecule (14). Therefore, the putative predominant role of n–σ^* interaction is, in Box's opinion, of doubtful validity.

The importance of destabilizing interactions for the geometry of a molecule is best evidenced by X-ray data (151) for compound **172** containing the $C(S—C)_4$ fragment (Figure 55). In contrast to expectation based on stabilizing n_S–σ^*_{C-S} negative hyperconjugation, the outer C—S bonds are shorter than the inner ones. This finding can be attributed to destabilizing interactions between sulfur atoms (analogous to that between iodine atoms in CH_2I_2; see Sections II.H and III.A.4), which tend to elongate sulfur–sulfur distances. This conclusion is strongly supported by a small average S—S nonbonding

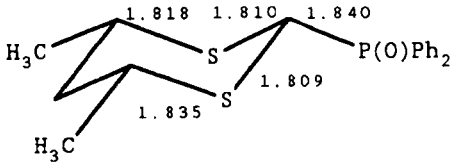


172

Figure 55. Average C—S bond lengths and nonbonding S—S distances in **172** (data taken from ref. 151).



109a



173e

Figure 56. Selected bond lengths in 2-diphenylphosphinoyl-1,3-dithianes **109a** and **173e** (data from refs. 135 and 340).

distance in **172** (2.980 Å), which is much smaller than the sum 1.80 + 1.80 = 3.60 Å of the sulfur van der Waals radii [1.80 Å (339)].

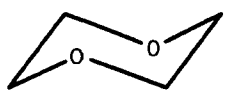
The magnitude of bond length variation in methanediselenol (**130**) and dimethoxymethane (**11**) (Figures 53 and 47) seems to be in line with differences in energies between the *ap*, *sc* and *ap*, *ap* conformers: in **130**, $\Delta E = 7.0$ kJ/mol (148); in **11**, $\Delta E = 13.5$ kJ/mol (57). One might think that though bond length variation cannot be connected with negative hyperconjugation in a straightforward way, it may be related to the magnitude of the synclinal preference of a substituent. The examples **109a** and **173e** presented by Juaristi (135, 340) (Figure 56) leave no doubt that this is not so. For the diphenylphosphinoyl group at the anomeric carbon atom in a 1,3-dithiane ring, in which a strong anomeric effect is observed (see Section V.A), one cannot find a palpable SC—P bond length difference between axial and equatorial isomers. Contrary to expectation, the equatorial C—P bond in **173e** actually seems to be longer (by 0.015 Å) than the axial one in **109a**. Thus, the bond length changes in this system suggested to Juaristi et al. (135, 340) that n_S–σ^*_{C-P} interaction is quite negligible (see, however, Section V.B.3). Moreover, this finding proves that there is no direct connection between bond length changes and the magnitude of the anomeric effect when different Y—C—X fragments are compared. Such connection may exist within a given Y—C—X system (e.g., O—C—O), but as Cosse-Barbi and Dubois (60) and Schleifer et al. (88) have recently shown, geometric parameters depend on a variety of factors, for example, alkyl substituents at the anomeric carbon atom, size of ring, and hybridization of the anomeric carbon.

2. *Anomeric Effect and Electron Density*

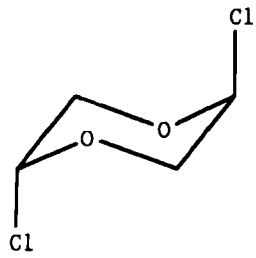
All explanations of the anomeric effect based on negative hyperconjugation involve charge transfer. This should result in a difference in electron density

distribution between synclinal and antiperiplanar conformations of anomeric molecules. Relevant *ab initio* calculations have been performed by Pichon-Pesme and Hansen (341) for CH_3OCH_2F (**123**) and $HO-CH_2-OH$ (**8**). Appropriate cuts for **123** through the deformation density did not show any clear evidence for back bonding (negative hyperconjugation) from the oxygen lone-pair orbital. However, in considering the quality of their 4–31G* calculations the authors could not be confident about differences of the order of 0.01 $eÅ^{-3}$ observed between *sc* and *ap* conformers. From an experimental point of view, variations of this size are presently unmeasurable and will, most likely, remain so (341). Pichon-Pesme and Hansen concluded that the electron density is rather insensitive to the conformation of molecules. They suggested, moreover, that another explanation for the anomeric effect, other than π back bonding, should be considered. However this proposal does not seem to be justified since Reed and Schleyer (143, 146) showed that negative hyperconjugation in CH_3F is accompanied by delocalization of only 0.023 e and usually results in total charge transfers of much less than 0.10 e. The latter authors claimed (143) that charge transfers of as little as 0.01 e can result in chemically significant energy stabilizations of the order of 24 kJ/mol.

Recently, Koritsánszky et al. (342) calculated the electron density distribution in 1,4-dioxane (**174**) and *trans*-2,5-dichloro-1,4-dioxane (**175**). The charge distribution in **174** served as a reference. They found that the electron density deformation caused by the substitution of a ring is localized on the first (carbon) and second (oxygen) neighbor atoms to the chlorine (342). The highly correlated orientation of the lobes at O, Cl, and the anomeric C indicated that the observed charge rearrangement is due to three-center interactions that take place through the O—C and C—Cl bonds. Density distribution also provided evidence in favor of mixing of lone-pair orbitals at both ends of the O—C—Cl system. However, the authors (342) were not able to attribute their observations to the $n_O-\sigma^*_{C-Cl}$ interaction which, in their opinion, might have only a secondary effect on the charge density.



174



175

3. *Spectroscopic Implications of Anomeric Effect*

Charge transfers that may accompany the anomeric effect, though unmeasurable by the X-ray diffraction method, may result in changes in spectral properties of molecules. It is probably impossible to relate a given spectral property directly to the anomeric effect in its phenomenological sense. An alternative approach should then be applied, namely to relate the spectral observation to negative hyperconjugation (as the most probable cause of the anomeric effect).

a. Chemical Shifts. David (343) rationalized the lower nuclear quadrupole resonance frequency of axial (*sc*) compared to equatorial (*ap*) ^{35}Cl in a Cl—C—O system as being due to n_O–σ^*_{C-Cl} negative hyperconjugation. The axial ^{35}Cl resonates at lower field, in accord with the more ionic nature of the axial C—Cl bond and the more symmetrical distribution of electrons around the Cl nucleus.

McKelvey et al. (344) observed that both *endo* and *exo* ^{17}O oxygen atoms in axial 2-alkoxytetrahydropyrans **96a** (Figure 13) are more shielded compared to those in the corresponding equatorial isomers **96e**. They attributed such observation to the participation of steric γ-*gauche* shielding and γ-*anti* deshielding effects on ^{17}O chemical shifts as well as to negative hyperconjugation. If the latter involves the lone pair of the *endo* oxygen and the σ^*_{C-O} orbital of the axial C—O bond, it may be demonstrated that the ring oxygen should be more shielded and the exocyclic oxygen less shielded in the axial isomers. However, owing to the presence of *gauche* carbons C(4) and C(6) (γ effect), the shielding of the axial oxygen is large enough to make the axial ^{17}O more shielded than the equatorial one. McKelvey et al. (344) claimed that the operation of the n_O–σ^*_{C-O} mechanism in 2-alkoxytetrahydropyrans **96** is consistent with the increase of chemical shift differences for both oxygens between anomers as one goes from hydrogen to methyl to *tert*-butyl in position 6 of the ring. With higher alkyl substitution the ionization potential of the ring oxygen decreases, the donating ability of the endocyclic oxygen increases, and negative hyperconjugation responsible for chemical shift differences becomes stronger.

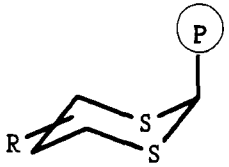
Similar observations concerning the order of resonances were made by Pinto et al. (84) for the S—C—Se system. They found that axial ^{77}Se in 2-arylseleno-1,3-dithianes **37** (Scheme 13) resonates at higher field than equatorial, just as in appropriate phenylselenocyclohexanes, thus suggesting the γ effect to be the most important factor.

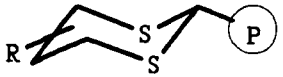
The ^{13}C chemical shifts for aromatic carbons are considered to be a sensitive probe in studies on polar and resonance effects of substituents (345). Thus, significant upfield ^{13}C chemical shifts for the *ortho* and *para* carbons

in the axial phosphinoyl $Ph_2P(O)$ (135), thiophosphinoyl $Ph_2P(S)$ (136), phosphinyl $Ph_2P(:)$ (346), and phosphinyl–borane $Ph_2P–BH_3$ (346) groups attached to a 1,3-dithiane ring at C(2) were interpreted by Juaristi et al. (135, 136, 346) to prove that some form of electron transfer occurs to the axially located substituent. They proposed (12, 56, 135) $3p–3d$ donation from sulfur to axial phosphorus as responsible for this effect. In our opinion, the increased electron density at the axial phosphorus may be due (among other factors; see Section V.B.4) to the $n_S–\sigma^*_{C-P}$ and $\sigma_{C(4,6)-S}–\pi^*_{P=Y}$ hyperconjugations (here Y = O, S), while the interaction suggested by Juaristi et al. (12, 56, 135) is not important (see Section III.B.9). We found (78) that the chemical shifts of *ortho* carbons are actually smaller for the axial $Ph_2P{=}O$ in 1,3-dioxane **111a** (p. 237) versus the equatorial $Ph_2P(O)$ in **111e**. However, the chemical shift of *para* carbons is almost the same for **111a** and **111e**. In 1,3-dithiane derivatives both *ortho* and *para* carbons resonate at higher field in axial $Ph_2P{=}O$, $Ph_2P{=}S$,

TABLE 18

Chemical Shifts of Aromatic Ortho and Para Carbons in ^{13}C NMR (75.47 MHz, CD_2Cl_2) spectra of some 5-*t*-Butyl- and *cis*-4,6-Dimethyl-1,3-dithiane Derivatives





Compound	Ⓟ	*R*	δ_{ortho} (ppm)	δ_{para} (ppm)	δ_{ortho} (ppm)	δ_{para} (ppm)
151	$^+PPh_2(SMe)$	*t*-Bu	135.07	136.77	134.68	136.68
176		Me_2	134.88	136.72	134.65	136.60
177	$^+PPhMe(SMe)$	*t*-Bu	133.96	136.73	133.36	136.62
178		Me_2	133.61	136.55	133.39	136.59
45	$Ph_2P(:)$	*t*-Bu	134.04	129.53	134.24	129.75
179		Me_2	133.91	129.45	134.36	129.74
180	PhMeP(:)	*t*-Bu	133.27	129.83	132.76	129.66
181		Me_2	133.15	129.75	132.82	129.62
182	$^+PPh_3$	*t*-Bu	135.23	135.16	135.38	135.67
183		Me_2	135.43	135.17	135.10	135.50
184	$^+PPh_2Me$	*t*-Bu	134.25	135.90	133.88	135.95
185		Me_2	134.04	135.84	133.71	135.87
186	$^+PPhMe_2$	*t*-Bu	133.22	136.04	132.66	135.78
187		Me_2	132.79	135.32	132.60	135.72

Data from ref. 54. *t*-Bu means 5-*t*-butyl-1,3-dithiane derivative, Me_2 means *cis*-4,6-dimethyl-1,3-dithiane derivative.

PhMeP=S, Ph_2P=Se, and Ph_2P(:) groups (54), which parallels Juaristi's observations (see Table 18). However, the opposite occurs (54) for Ph_2P^+SMe and PhMeP: substituents, where the *ortho* and *para* carbons resonate at the lower field in the axial isomers. An even more complicated situation exists in the Ph_2P^+Me derivatives **184** and **185** (see Table 18) since *para* carbons resonate at higher field and *ortho* ones at lower field when the phosphonium group is axial. Interestingly, the change of the chemical shift of the *para* carbon of the PhP^+Me_2 group on going from the equatorial to the axial position is opposite in two different anancomeric pairs **186** and **187**. Thus, the chemical shift of the *para* carbon increases by 0.26 ppm in **186** but decreases by 0.40 ppm in **187**. Analogous inconsistencies may be found for $PPhMe(SMe)^+$ and PPh_3^+ groups as far as the chemical shift of the *ortho* carbon is concerned. Therefore, the changes in chemical shifts should be interpreted with caution. They result, perhaps, from a much larger number of factors than those considered by Juaristi et al. (12, 56, 135). A similar warning with regard to ^{17}O chemical shifts [the work of McKelvey et al. (334), *vide supra*] has recently been presented by Booth et al. (112).

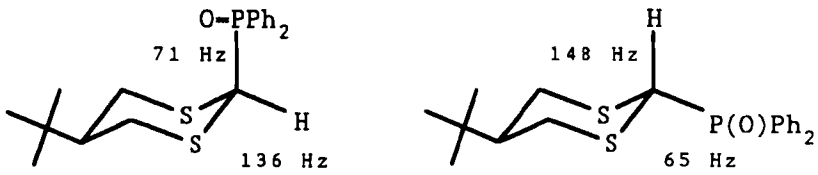
b. Coupling Constants. As far as the direct one-bond spin coupling constants through the C—H bond in R–CHXY systems are concerned, one can find a considerable body of experimental data (317, 320, 347) showing lower coupling constants $^1J_{C-H}$ for those bonds that possess *ap* orientation to a lone electron pair (for first-row atoms X and Y) or for donor bonds (when both X and Y are atoms below the first row), as would be expected based on hyperconjugation. This regularity has been reviewed, reproduced by the relevant *ab initio* calculations, and termed *Perlin effect* by Wolfe et al. (317). These authors performed the relevant calculations for X, Y = C, O, N, S. They found that the C—H bond length is the dominant factor that determines the magnitude of the $^1J_{C-H}$ coupling constant, and the constant decreases with increasing bond length. Therefore, the Perlin effect is the NMR counterpart of the changes in stretching frequencies ν_{C-H} (see Section III.B.3.c). The observed trend for $^1J_{C-H}$ in the O—CH systems has also been supported by semiempirical calculations (317, 348).

In the 1,3-dithiane system $^1J_{C-H}$ coupling constants through equatorial bonds were found (320) to be smaller than corresponding ones through axial ones, in contrast to what has been observed for 1,3-dioxane (349) and cyclohexane (350). This finding has been rationalized (317) in terms of dominant $\sigma_{C(4,6)-S}$–$\sigma^*_{C(2)-H}$ [over n_S–$\sigma^*_{C(2)-H}$] hyperconjugative interactions, which are responsible for the weakening of the equatorial C(2)—H bond in the 1,3-dithiane system. We found (54) that the introduction of a diphenylphosphinoyl group $Ph_2P(O)$ at C(2) of a 1,3-dithiane ring does not alter this regularity. In particular, one-bond coupling constants $^1J_{C-H}$ between the

anomeric carbon and proton in the ^{13}C NMR (75.47 MHz, $CDCl_3$) spectra of **188a** and **188e** were found to be 136 and 148 Hz, respectively (see Figure 57).

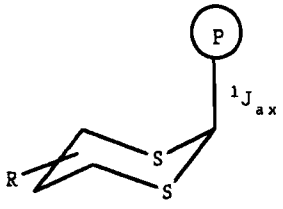
Interestingly, a relationship analogous to the Perlin effect can also be found for other coupling constants, namely ^{13}C–^{199}Hg in alkylmercurials (351) and ^{13}C–^{31}P in glycosylphosphonates (352) and cyclohexylphosphonates (353). Our work (78) showed that in 1,3-dioxanes **111a** and **111e** $^1J_{C-P}$ coupling constants between phosphorus and the anomeric carbon atom are 94.3 and 118.8 Hz, respectively, in agreement with the intuitive anticipation based on the n_O–σ^*_{C-P} interaction. In 1,3-dithiane derivatives the situation is not so clear (54). Only in phosphonium salts **85** (all types) is the $^1J_{C-P}$ coupling constant for isomers **85e** with phosphorus located equatorially larger than that for their epimers **85a** (see Figure 58). The difference between coupling constants is not so large as in 1,3-dioxanes **111** and varies in a range from 3.3 to 11.6 Hz (54, 98b). In nonionic 1,3-dithianes **189**, the $^1J_{C-P}$ coupling constant through the axial bond is always larger than the corresponding constant through the equatorial one, in disagreement with the intuitive expectation based on the n_S–σ^*_{C-P} interaction. The difference between constants is, as before, rather small, from 0.6–2.6 Hz for $Ph_2P{=}Se$ to 11.4–13.3 Hz for $(MeO)_2P{=}O$ derivatives (54). A similar relationship was found (173, 354) for 5-*t*-butyl-1,3-diselenanes **190** (Figure 59).

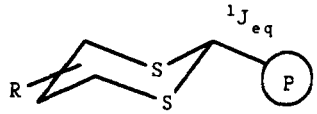
c. Stretching Frequencies and Conformational Equilibrium Isotope Effects. The change in bond order that usually accompanies hyperconjugation (see Section IV.B.1) may be reflected in the infrared spectra of relevant molecules. Stretching frequencies of axial halogens in halogenocycloalkanes are systematically lower than those of equatorial ones (355) because of σ_{C-H}–σ^*_{C-X} hyperconjugation. The n_O–σ^*_{C-H} negative hyperconjugation has long been invoked to explain the decrease in force constants of C—H bonds lying outside of the symmetry plane (C—O—C) of dimethyl ether (356) and



188a 188e

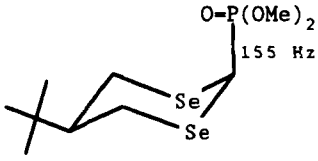
Figure 57. One-bond $^1J_{C-H}$ and $^1J_{C-P}$ coupling constants in **188** (data from ref. 54).



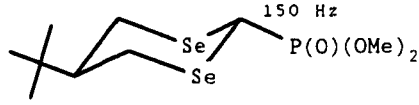


Comp.	P		
85	$^+PR^1R^2R^3$;	R^1,R^2,R^3=SMe, Me, Ph	$^1J_{ax}<^1J_{eq}$
189	$P(X)R^1R^2$;	X=lone pair, O, S, Se	$^1J_{ax}>^1J_{eq}$

Figure 58. Relationship between coupling constants in $^1J_{ax}$ and $^1J_{eq}$ through the axial and equatorial C—P bond, respectively, in **85** and **189**.



190a

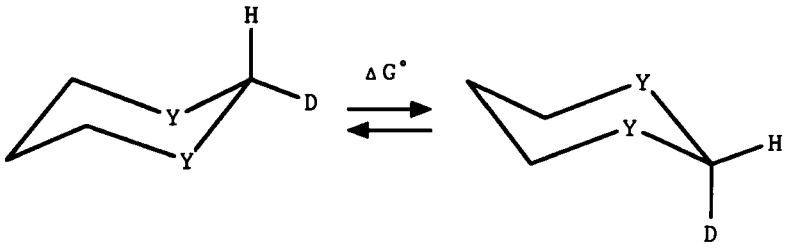


190e

Figure 59. One-bond coupling constants in **190** (data from refs. 173 and 354).

of methanol (357) (C—O—H) with regard to C—H bonds lying in the symmetry plane. Lower stretching frequency of C—H bonds that are *trans* to a nitrogen lone pair can be explained in terms of n_N–σ^*_{C-H} negative hyperconjugation (311, 358–365). The infrared spectral features associated with this lower stretching frequency have been called *Bohlmann bands* (361). It should be added that the decrease in stretching frequency for the acceptor bond has been experimentally (366) correlated with an increase in bond length and a decrease in bond dissociation energy.

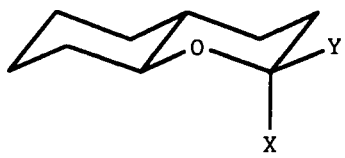
The larger donor ability of C—H versus C—C σ bonds (311) is enough to differentiate axial and equatorial positions in cyclohexane **191** (Scheme 43; $Y = CH_2$) as was found both by calculation (367) and experimentally



191e	Y = CH_2	191a
192e	O	192a
193e	NMe	193a
194e	S	194a

Scheme 43

(368–370). Williams (367) calculated *ab initio* stretching frequencies of 2873 and 2928 cm^{-1} for axial and equatorial C—H bonds in [$^2H_{11}$] cyclohexane. The corresponding C—D stretching frequencies were 2110 and 2151 cm^{-1}. The experiment gave 2884 and 2913 cm^{-1} for CH_{ax} and CH_{eq} (368) and 2144 and 2165 cm^{-1} for CD_{ax} and CD_{eq} (369), respectively. The smaller C—H_{ax} (and C—D_{ax}) than C—H_{eq} (C—D_{eq}) force constant is, in Williams's opinion, due to the more effective σ_{C-H}–$\sigma^*_{C-H(D)}$ than σ_{C-C}–$\sigma^*_{C-H(D)}$ hyperconjugation. One may expect that if the donor ability of Y increases, the axial bond becomes weaker as a result of more effective n_Y–σ^*_{C-D} negative hyperconjugation and the stretching frequency decreases. Experiment confirms such prediction. For **192** (Y = O) the stretching frequencies are 2086 and 2231 cm^{-1} for C—D_{ax} and C—D_{eq} (371) bonds, respectively. When Y is a much better donor, as for instance Y = NMe, the appropriate stretching frequencies in **193** are equal (323) to 1919 and 2166 cm^{-1}.



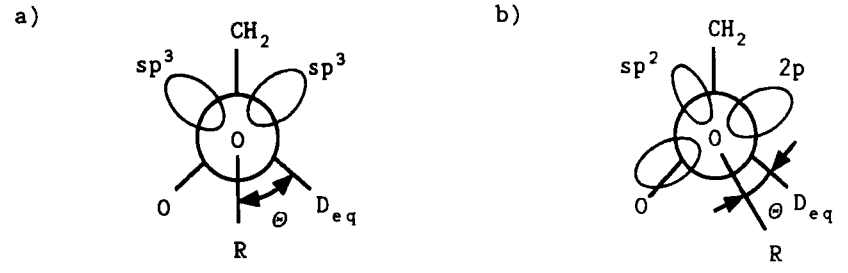
195, X=H, Y=D

196, X=D, Y=H

197, X=OR, Y=D

198, X=D, Y=OR

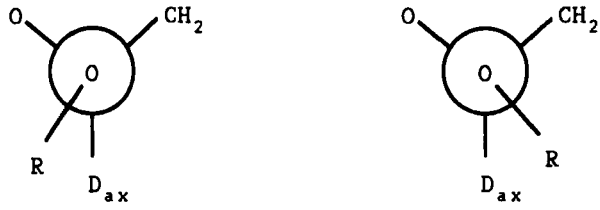
The importance of n_O–σ^*_{C-D} interactions for stretching frequencies in tetrahydropyran-C(2)-D derivatives **195–198** has recently been supported by Touboul and Dana (86). As expected based on the n_O–σ^*_{C-D} negative hyperconjugation, the stretching frequency ν_{C-D} of the axial C—D bond



197A 197B

Figure 60. Conformations **197A** and **197B** as a result of n_O–σ^*_{C-O} interactions involving (a) equivalent and (b) nonequivalent lone electron pairs of the exocyclic oxygen atom as donors.

in **196** ($2103\,cm^{-1}$) was lower than that of the equatorial one in **195** ($2185\,cm^{-1}$). The introduction of an alkoxyl in **197** and **198** led to an additional decrease $\Delta\nu$ in the ν_{C-D} frequency, both of axial and equatorial C—D bonds, as anticipated based on an additional n_O–σ^*_{C-D} negative hyperconjugation. Interestingly, this additional lowering $\Delta\nu$ depends on the size of the alkyl R group and is small for large R ($\Delta\nu = -15/-25\,cm^{-1}$ for R = Ph, *t*-Bu; $\Delta\nu \cong -30/-50\,cm^{-1}$ for R = Me, $PhCH_2$). This finding was explained in terms of nonequivalence of oxygen lone pairs. In conformation **197A** (Figure 60a), where both lone pairs on exocyclic oxygen are in sp^3 orbitals, the angle Θ is about 60° and steric interactions between R and D_{eq} are rather small. Hence, this conformation is not expected to be very sensitive to steric hindrance exerted by R, in contrast to the conformation **197B** (Figure 60b), where Θ is much smaller ($\Theta \cong 30°$) and where the increase in size of R is accompanied by an increase of Θ. The changes of Θ must result in changes in strength of the n_O–σ^*_{C-D} hyperconjugative interactions and in ν_{C-D}, as observed. Analogous reasoning applies to **198**. It must be added, however, that two rotamers (**198C** and **198D**, analogous to the *ap*, *ap* and *ap*, $-sc$



198C 198D

conformers of 2-alkoxytetrahydropyran **38**; see Section II.E), containing nonequivalent oxygen lone pairs, should be taken into account in the latter case, since supplementary multiplicity due to C—D stretching is observed (86).

Since the heavier isotope (e.g., D vs. H) tends to accumulate in the site where it experiences a larger force constant (370, 372), it may be expected that the equilibrium depicted in Scheme 43 for cyclohexane **191** [$Y = CH_2$, $\nu_{C-D} = 2144$ and $2165\,cm^{-1}$ for CD_{ax} and CD_{eq} (369), respectively] will be shifted toward the left side (neglecting bending contributions). Indeed, Anet and Kopelevich (370) found $\Delta G^\circ = 25 \pm 5$ J/mol. One may expect that if the donor ability of Y increases, the equilibrium will be more shifted toward the left side (**e**) as a result of more effective n_Y–σ^*_{C-D} negative hyperconjugation involving the axial C—D bond. In line with the above, Anet and Kopelevich (371) found $\Delta G^\circ = 205 \pm 15$ J/mol for 1,3-dioxane **192** (Y = O; stretching frequencies are 2086 and $2231\,cm^{-1}$ for $C—D_{ax}$ and $C—D_{eq}$, respectively). Further increase in the donor ability in **193** (Y = NMe) resulted in an increase in ΔG° to 420 ± 30 J/mol (appropriate stretching frequencies are 1919 and $2166\,cm^{-1}$) (323). The increase of ΔG° paralleled by the decrease of ν_{C-D} for an axial C—D bond with increasing donor ability of Y is in line with the assumption of a predominant role of negative hyperconjugation, at least as far as first-row elements are concerned.

Based on indentical stretching frequencies for axial and equatorial C—D bonds ($\nu_{C-D} = 2145\,cm^{-1}$) and the absence of an isotope effect ($\Delta G^\circ = 0 \pm 5$ J/mol, by NMR measurments) on the conformational equilibrium in the 1,3-dithiane system **194**, Anet and Kopelevich (323) concluded that the lone electron pairs on sulfur are not involved in the n_S–$\sigma^*_{C-H(D)}$ negative hyperconjugation, in disagreement with the opinion expressed by Pinto et al. (45, 82–84, 152) (see Sections II.H and III.B.5). As was proposed by us (54b) and found in *ab initio* studies by Wolfe et al. (317, 324), the observed differences in stretching frequencies between 1,3-dioxane, 1,3-dithiane, and cyclohexane systems result from an interplay of several factors, with n_Y–$\sigma^*_{C-D(H)}$ and $\sigma_{C(4)-Y}$–$\sigma^*_{C-D(H)}$ hyperconjugation in 1,3-dioxane and 1,3-dithiane (Y = O, S) and σ_{C-H}–$\sigma^*_{C-D(H)}$ and σ_{C-C}–$\sigma^*_{C-D(H)}$ hyperconjugation in cyclohexane among the most important interactions. In particular, the n_S–$\sigma^*_{C-D(H)}$ and $\sigma_{C(4)-S}$–$\sigma^*_{C-D(H)}$ hyperconjugation effects in 1,3-dithiane **194** are of similar magnitude, and therefore stretching frequencies for the axial and equatorial C(2)—D bonds are similar as well. As far as the H/D isotope effect on the conformational equilibrium in the 1,3-dithiane **194** is concerned, Wolfe and Kim showed (324) than an analysis that emphasizes C—H (C—D) stretching would not account for the observations. While the stretching contributions in $HO–CH_2–OH$ (**8**) and $HS–CH_2–SH$ (**66**) (which served as models for 1,3-dioxane and 1,3-dithiane systems, respectively) have the same sign, the

stretching and bending contributions to the free energy difference in methanedithiol have opposite signs, and the bending contributions dominate. The calculated (324) ΔG° values for methanediol and methanedithiol are -30 and 237 J/mol, respectively, and agree with those found by experiment (323), that is, $\Delta G^\circ = 0 \pm 5$ J/mol and 205 ± 15 J/mol for 1,3-dioxane and 1,3-dithiane, respectively.

Finally, it should be noted that the decrease of the carbonyl stretching frequency in *gauche* rotamers of α-heterosubstituted acetones (373) and acetophenones (290) with respect to unsubstituted acetone and acetophenone, respectively, has been considered to arise from $\pi^*_{C=O}$–σ_{C-X} hyperconjugative interactions (cf. Section III.B.9).

V. ANOMERIC EFFECT IN Y—C—P SYSTEMS (Y = O, S, Se)

A. Magnitude of Anomeric Effect

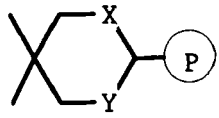
Several values of the magnitude of the anomeric effect, ΔG°_{AE}, based on Franck's methodology (Section II.C) and calculated by us (54, 78, 98, 173, 354) for 2-substituted 5, 5-dimethyl-1, 3-diheteroanes are collected in Table 19 (penultimate column) together with the appropriate values obtained by Juaristi's group (last column). The differences between these two sets of values can easily be explained as due to different methods of estimation of F_G factors (see Section II.C), different compounds studied, and different conformational probes applied. Nevertheless, except for dioxane derivative **110** (X = Y = O) the trends are the same.

Though the ΔG°_{AE} values can be treated only as an approximate measure of the anomeric effect, they undoubtedly indicate very strong anomeric interactions in the O—C—P system **110**. On passing down the periodic table with X and Y the anomeric effect becomes weaker and weaker (compounds **110**, **201**, and **206**). A replacement of the phosphoryl oxygen atom by sulfur also results in a decrease in ΔG°_{AE}. Interestingly, the anomeric effect in phosphonium salts (compounds **204** and **205**) is stronger than that in the relevant phosphines (compounds **202** and **203**), which is in contrast to anticipation based on the concept of the reverse anomeric effect (see Section II.I).

B. Nature of Anomeric Effect in Y—C—P System (Y = O, S, Se)

The nature of the anomeric effect operative in the S—C—P system will be considered taking into account (1) thermodynamic, (2) MM- and MO-based, (3) X-ray crystallographic, (4) spectroscopic, and (5) kinetic implications. It must be added that solvent studies were shown to be not useful to reveal

TABLE 19
Magnitude of Anomeric Effect ΔG°_{AE} in 2-P-substituted 5,5-Dimethyl-1,3-diheteroanes



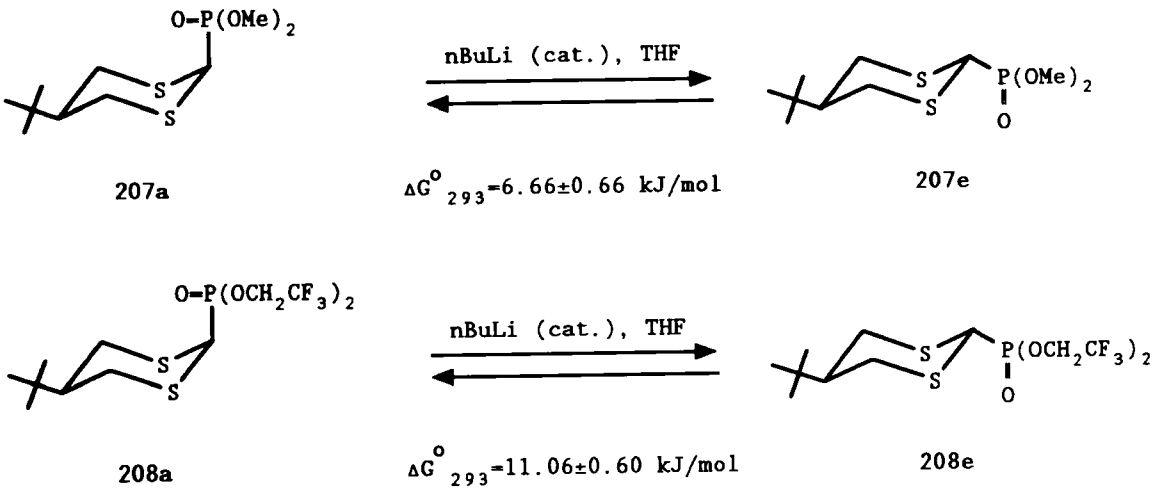
Compound	X	Y	P	ΔG°_{AE} (kJ/mol)	
110	O	O	$P(O)Ph_2$	19.7	11.7[a]
199	O	S	$P(O)Ph_2$	19.0	15.5[a]
200	S	S	$P(O)Ph_2$	14.3	11.0[b]
56	S	S	$P(S)Ph_2$	11.6	9.2[b]
201	S	S	$P(O)(OMe)_2$	15.1	
202	S	S	PPh_2	6.9	4.2[b]
203	S	S	PMe_2	5.9	
204	S	S	$^{+}PPh_3$	>8.5	
205	S	S	$^{+}PMe_3$	>9.8	9.2[c]
206	Se	Se	$P(O)(OMe)_2$	7.9	

[a]From ref. 375.
[b]From ref. 18.
[c]From ref. 374.

the nature of this effect [see Section II.G for thiophosphoryl **55–57** and Section II.I for phosphonium derivatives (**85**)].

1. *Thermodynamic Implications of Anomeric Effect in Y–C–P System (Y = O, S, Se)*

A dependence of the magnitude of the anomeric effect on the electronegativity of a substituent is usually regarded as a good test for its hyperconjugative nature (see Section II.E). Our results (54) show that the magnitude of the axial preference represented by ΔG° value for 1,3-dithiane derivative **207** containing the $(MeO)_2P{=}O$ group, is about 3 kJ/mol smaller than ΔG°_{exp} for **208** with the more electronegative (and undoubtedly larger) $(CF_3CH_2O)_2P{=}O$ group (Scheme 44). In addition, the anomeric effect in phosphonium salts **204** and **205** is stronger than that in the appropriate phosphines **202** and **203** (see Table 19). A positive charge at phosphorus in **204** and **205** should result in a decrease in the energy of the σ^{*}_{C-P} orbital. Thus, the findings presented above support the n_S–σ^{*}_{C-P} hyperconjugative mechanism.


O-P(OMe)2
S
S
nBuLi (cat.), THF
S
S
P(OMe)2
O
207a
ΔG°293=6.66±0.66 kJ/mol
207e
O-P(OCH2CF3)2
S
S
nBuLi (cat.), THF
S
S
P(OCH2CF3)2
O
208a
ΔG°293=11.06±0.60 kJ/mol
208e

Scheme 44

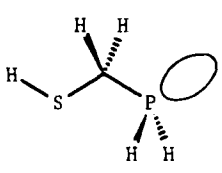
The stronger anomeric effect for the PPh_2 group (**202**; 6.9 kJ/mol) than for PMe_2 (**203**; 5.9 kJ/mol) is also consistent with the participation of π electrons of the phenyl rings in repulsive interactions with lone electron pairs of the endocyclic sulfur atoms, as shown in Figure 17. These interactions are expected to destabilize the equatorial arrangement of phosphorus and to increase the anomeric effect of the PPh_2 group, as observed. Nevertheless, a stronger electron-withdrawing effect of phenyl versus methyl groups, resulting in a decrease in energy of σ^*_{C-PPh} versus σ^*_{C-PMe} orbital, must also be taken into account.

A lack of manifestation of the *exo* anomeric effect in the S—C—P(:) system (see Section II.E) can be easily interpreted in terms of predominant steric over n_P–σ^*_{C-S} hyperconjugative interactions. This is in contrast to X—CH_2—H_2P(:) systems, for which the antiperiplanar arrangement of the C—X [X = F (267), Cl (141)] bond and phosphorus lone electron pair is preferred, perhaps due to much more effective n_P–σ^*_{C-X} hyperconjugation.

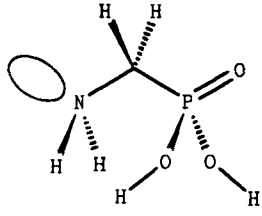
2. *Molecular Mechanics- and Molecular Orbital-derived Implications of Anomeric Effect in Y—C—P System (Y = O, S, Se)*

Molecular mechanics-derived implications were discussed in Section III.A.6.

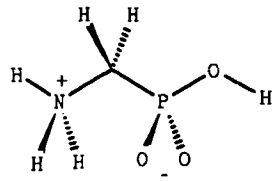
The *ab initio* calculations on **209** by Schleyer et al. (141) showed that the lowest energy species is **209a**, containing the phosphorus lone electron pair



209a



210a



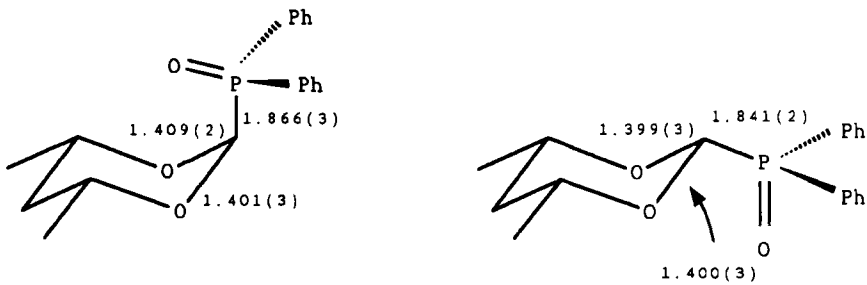
211

anti to the C—S bond. On the other hand, sulfur lone electron pairs are not involved in the n_S–σ^*_{C-P} interaction, thus suggesting that this interaction is less effective than the n_P–σ^*_{C-S} one. Since the n_P–σ^*_{C-S} interaction is not manifested in axial phosphines **44** (Scheme 15, Section II.A.2), one may conclude that the (*endo*) anomeric effect in **202** and **203** does not stem solely from the n_S–σ^*_{C-P} interaction and that other interactions, probably of destabilizing character (e.g., the rabbit ear effect), must also be taken into account.

Finally, it should be added that recent 3–21G* calculations (376) on two forms of aminomethylphosphonic acid, neutral **210** and zwitterionic **211**, showed that in the most stable conformation **210a** the nitrogen lone electron pair is antiperiplanar to the C—P bond. Since the C—N bond is considerably shorter in **210a** (1.477 Å) than in **211** (1.559 Å), it seems reasonable to consider the n_N–σ^*_{C-P} negative hyperconjugation in **210a** as responsible for this observation. However, the C—P bond in **210a** (1.779 Å) is shorter than that in **211** (1.838 Å), which is opposite to the trend expected on the basis of n_N–σ^*_{C-P} negative hyperconjugation.

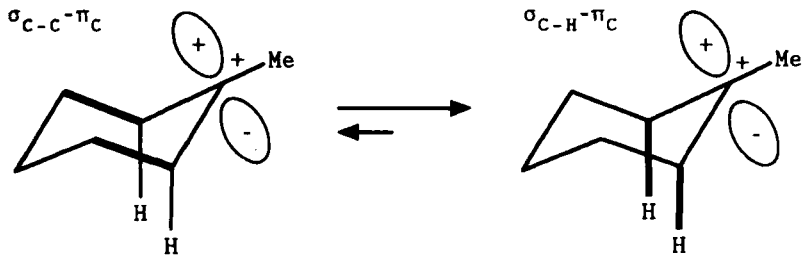
3. *X-Ray Crystallographic Implications of Anomeric Effect in Y—C—P System (Y = O, S, Se)*

In contrast to preliminary crystallographic data for 1,3-dithianes (377,378) (see also Section IV.B.1), which did not agree with n_Y–σ^*_{C-P}-based anticipations, the data (78) for 1,3-dioxanes **111a** and **111e** (Figure 61) provide more convincing arguments in favor of the n_Y–σ^*_{C-P} (Y = O) hyperconjugative interaction. The axial C(2)—P bond is longer by 0.025Å than the equatorial one. Moreover, while in **111e** both C(2)—O bond lengths are equal, they differ by 0.008 Å in **111a**, which could be interpreted in such a way that one endocyclic oxygen is involved in the n_O–σ^*_{C-P} interaction much more effectively than the other one. Analogous observations concerning the differentiation of the C(2)—Y bond lengths when phosphorus is situated axially were also made for Y = O and S (*vide infra*). It should be added that the presence of two possible donors (bonds) is known to lead to thermodynamic differentiation of chemical species which differ only in the donor involved in the hyperconjugation (379) (**212a** and **212b**, Scheme 45).



111a 111e

Figure 61. Bond lengths in dioxanes **111** (data from ref. 78).



212a **212b**

Scheme 45

Selected bond lengths in *cis*- and *trans*-2-phosphoryl-, 2-thiophosphoryl-, and 2-selenophosphoryl-5-*t*-butyl-1,3-dithianes are collected in Table 20. An inspection of these data reveals that the C(2)—P bond lengths in diastereomers are not characteristic for the position of phosphorus and, at first sight, are not consistent with n_S–σ^*_{C-P} negative hyperconjugation. While the axial C(2)—P bonds in **188** and **213** (Table 20) are longer than the equatorial ones (in agreement with the n_S–σ^*_{C-P} interaction), the opposite relationship occurs for **207** and **57**. Similarly, the endocyclic C(2)—S bond lengths practically do not depend on the configuration at the anomeric carbon atom.

Nevertheless, a comparison of the structural data between **207a** and **208a** (Table 20) supports n_S–σ^*_{C-P} negative hyperconjugation as a source of the

TABLE 20
Selected Bond Distances (Å) in Diastereomeric 2-P-substituted 5-*t*-Butyl-1,3-dithianes

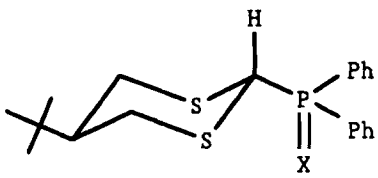


Compound	P	C(2)—P	C(2)—S	C(2)—P	C(2)—S
57	$P(S)Ph_2$	1.817(5)	1.803(4); 1.817(5)	1.831(3)	1.809(4); 1.814(5)
188	$P(O)Ph_2$	1.834(4)	1.805(5); 1.803(5)	1.821(2)	1.807(3); 1.799(2)
207	$P(O)(OMe)_2$	1.782(5)	1.811(6); 1.812(5)	1.798(4)	1.796(4); 1.791(5)
208	$P(O)(OCH_2CF_3)_2$	1.794(3)	1.796(4); 1.814(4)	1.794(3)	1.806(3); 1.815(3)
213	$P(Se)Ph_2$	1.855(4)	1.801(5); 1.807(5)	1.841(3)	1.804(3); 1.810(3)

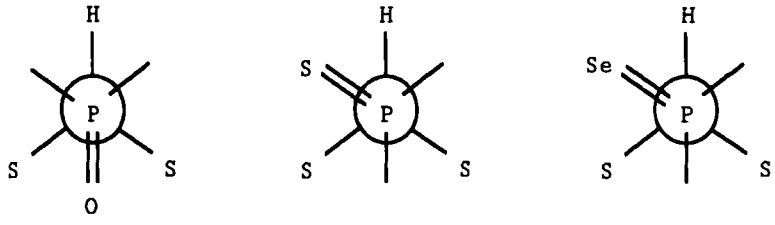
From ref. 54.

anomeric effect in the S—C—P=O system. In the latter compound, which contains the more electron-withdrawing $(CF_3CH_2O)_2P(O)$ group, the C(2)—P bond is longer than that in the former one containing a $(MeO)_2P{=}O$ group (1.794 vs. 1.782 Å, respectively), as expected based on more effective negative hyperconjugation in **208a** (cf. Section V.B.1). This conclusion is additionally supported by a more definitive difference between the two C(2)—S bond distances of 0.018 Å in **208a**, while in **207a** they are equal.

Interestingly, the equatorial C(2)—P bond lengths increase (54) in the order **188e**, **57e**, **213e** (1.821, 1.831, and 1.841 Å, respectively; see Figure 62). This observation cannot be easily accounted for in terms of hyperconjugative interactions. In particular, the $\sigma_{C(4,6)-S}$–$\sigma^*_{C(2)-P}$ hyperconjugation which could lengthen the C(2)—P bond must not be considered as an important factor. The positive charges at phosphorus, which could increase the acceptor ability of the $\sigma^*_{C(2)-P}$ orbital, decrease on going from **188** to **57** to **213**, in contrast to what is needed to explain the increasing bond length [in $H_3P{=}O$, $H_3P{=}S$, and $H_3P{=}Se$ these charges are equal to 0.805, 0.403, and 0.378, respectively (288)]. On the other hand, these findings are consistent with the increasing 1,4-intramolecular repulsions n_S–n_X (X = O, S, Se) between lone pairs of the endocyclic sulfur atoms and nonbonding electron pairs of phosphoryl heteroatom X [repulsive interactions are known (143) to be accompanied



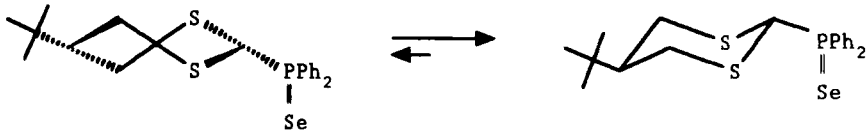
Comp.	C(2)-P [Å]
188e, X=O	1.821 (2)
57e, X=S	1.831 (3)
213e, X=Se	1.841 (3)



188e 57e 213e

Figure 62. Equatorial C(2)—P bond lengths in **57e**, **188e**, and **213e**, and the preferred rotamers about the C(2)—P bond (data form ref. 54).

by bond lengthening]. Increasing dipole moments on going from $H_3P{=}O$ to $H_3P{=}S$ to $H_3P{=}Se$ (288) are also consistent with this interpretation. This n_S–n_X repulsive interaction, which is a molecular orbital counterpart of lone electron pair–lone pair repulsions proposed by us (79) on the basis of molecular mechanics calculations (see Section III.A.6; Figure 17), destabilizes the equatorial position of phosphorus and determines the conformation about the exocyclic C(2)—P bond. While in **188e** the phosphoryl oxygen, in the solid state, is located between two endocyclic sulfur atoms (the H–C–P–O angle is 170.4°), in **57e** and **213e** the system H—C(2)—P—X (X = S, Se) is in the *gauche* conformation (see Figure 62). This finding agrees very well with the increasing n_S–n_X repulsions† on going from X = O to X = S to X = Se. It must be added that the strongest n_S–n_{Se} repulsions in **213e** contribute, in solution, to the largest (as compared to **188e** and **57e**) amount of twist-boat conformer of **213e** (Scheme 46), where these repulsions are minimized (137).



213e(TB) 213e(C)

Scheme 46

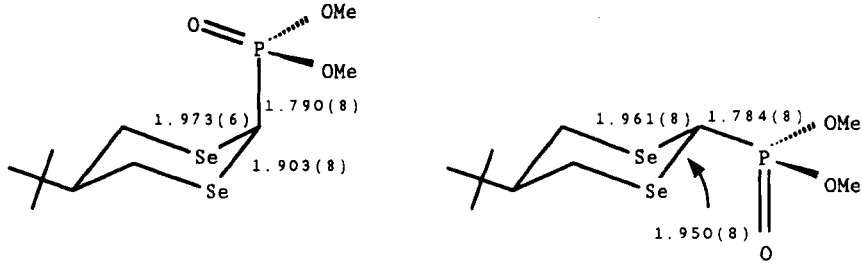
One should explain also why the equatorial C(2)—P bonds can be longer than the axial ones. A possible explanation involves the $\sigma_{C(4,6)-S}$–$\sigma^*_{C(2)-P}$ hyperconjugative interaction. This interaction should tend to lengthen the C(4, 6)—S and the equatorial C(2)—P bonds and to shorten the C(2)—S bond. The C(4, 6)—S bonds are, in fact, longer in **213e** than in **213a** (by 0.020 Å) and in **208e** than in **208a** (by 0.016 Å) (54). The differences in **188** and **57** are not so distinct because of the opposite influence of the $\sigma_{C(4,6)-S}$–$\pi^*_{P=X}$ interaction in the **a** isomers, which is more effective for P=O and P=S than for P=Se (*vide infra*). The phosphoryl group in **208a** is, perhaps, not able to participate effectively in a $\sigma_{C(4,6)-S}$–$\pi^*_{P=O}$ interaction, as a result of the greater distance from the axial H(4, 6) hydrogens and hence from the C(4, 6) carbons (overlap control). Interestingly, the C(4, 6)—S bonds in **208e** are long, even if compared to those in other e isomers, as would be expected based on the strong electron-withdrawing properties of the $(CF_3CH_2O)_2P{=}O$ group. Presumably, the $\sigma_{C(4,6)-S}$–$\sigma^*_{C(2)-P}$ interaction is responsible, in part, for the lack of differences in axial and equatorial C—P

†Interestingly, 1,4-intramolecular interactions of divalent sulfur (and selenium) with C—O—C oxygen can be either attractive (380) or repulsive in character (381).

bond lengths as well as for the lack of correlation between the position of phosphorus and C(2)—S bond lengths in 1,3-dithiane derivatives as a whole.

The $\sigma_{C(4,6)-S}$–$\pi^*_{P=X}$ (X = O, S, Se) interaction mentioned above is possible only if the P=X (X = O, S, Se) group is located axially and *endo* over the 1,3-dithiane ring, and it is expected to stabilize the axial position of phosphorus and to lengthen the C(4,6)—S bonds. Since the energy of the $\pi^*_{P=Se}$ orbital is high due to low electronegativity of selenium, this interaction should be negligible for **213a**. This is the case because the C(4,6)—S bond length differences between **213a** and **213e** imply that these bonds are involved only in the $\sigma_{C(4,6)-S}$–$\sigma^*_{C(2)-P}$ interaction (*vide supra*). It should be added that the $\sigma_{C(4,6)-S}$–$\pi^*_{P=O}$ interaction could synergize the formation of the appropriate H···O=P hydrogen bonds (see below), for example, by a transfer of electron density toward the P=O group. It should be added that the 3*p*–3*d* interaction proposed by Juaristi et al. (see Section III.B.9) is not supported by our X-ray data (54). It must be noted, however, that the unexpected structural pattern of 2-P-substituted 1,3-dithianes as compared with 1,3-dioxanes (*vide supra*) and 1,3-diselenanes (*vide infra*) [where features characteristic of the n_Y–$\sigma^*_{C(2)-P}$ (Y = O, Se) hyperconjugative mechanism may easily be recognized] may be due to variation in the magnitude of the $\sigma_{C(4,6)-Y}$–$\sigma^*_{C(2)-P}$ interaction. This interaction in 1,3-dioxanes is weak because of low donor ability of the σ_{C-O} orbital. In 1,3-diselenanes, the $\sigma_{C(4,6)-Se}$–$\sigma^*_{C(2)-P}$ interaction is unimportant because of overlap reasons. This is, perhaps, why 1,3-dioxanes and 1,3-diselenanes, unlike 1,3-dithianes, exhibit "normal" structures.

In the case of diselenane **190a** the difference between the two C(2)—Se bond lengths is very pronounced (0.07 Å), and the shortest selenium–carbon bond in this isomer is ca. 0.05 Å shorter than the two C(2)—Se bond distances in **190e**, which are almost equal (354) (Figure 63). Though the C(2)—P bond lengths are close in **190a** and **109e**, the difference in carbon–selenium distances



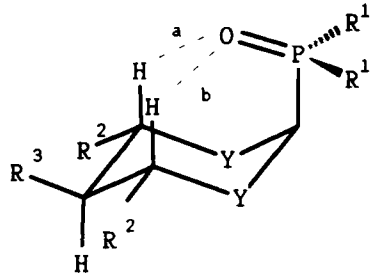
190a 190e

Figure 63. Selected bond lengths in diselenanes **190** (data from ref. 354).

is large enough to take the $n_{Se}-\sigma^*_{C-P}$ interaction into account as responsible for the shortening of C—Se bond in **190a** and for the anomeric effect observed in this system.

In the course of our studies (54, 78, 354) on 2-phosphoryl-1,3-diheteroanes we found also that the distances between axial hydrogens $H(4,6)_{ax}$ and the phosphoryl oxygen atom connected to axially located phosphorus are not equal (see Figure 64). Interestingly, the shorter H···O=P distance *a* for **111a**, **188a**, **190a**, **207a**, and **214a** is shorter than the sum of H and O van der Waals radii [H = 1.20 Å, O = 1.50 Å; sum 2.70 Å (140)], thus suggesting formation of a H···O hydrogen bond (140, 382). This hypothesis is strongly supported by the fact that the second, longer H···O distance *b* is larger than or equal to the sum of van der Waals radii of H and O, thus indicating attractive character of the H···O interaction. This effect may additionally stabilize the axial conformation of 2-phosphoryl-substituted 1,3-diheteroanes.

A comparison of appropriate shortest H···O distances in **207a** (2.49 Å and **208a** (2.72 Å) is very informative since the steric requirements of



111a,	Y=O,	R^1=Ph,	R^2=Me,	R^3=H	a=2.40Å,	b=2.53Å
188a,	Y=S,	R^1=Ph,	R^2=H,	R^3=*t*Bu	a=2.54Å,	b=2.76Å
190a,	Y=Se,	R^1=OMe,	R^2=H,	R^3=*t*Bu	a=2.55Å,	b=2.63Å
207a,	Y=S,	R^1=OMe,	R^2=H,	R^3=*t*Bu	a=2.49Å,	b=2.57Å
208a,	Y=S,	R^1=OCH_2CF_3,	R^2=H,	R^3=*t*Bu	a=2.72Å,	b=2.82Å
214a,	Y=S,	R^1=OMe,	R^2=Me,	R^3=H	a=2.54Å,	b=2.66Å

Figure 64. Selected nonbonded distances in 1,3-diheteroanes (data for Y = S, O, Se from refs. 54, 78, 354, respectively).

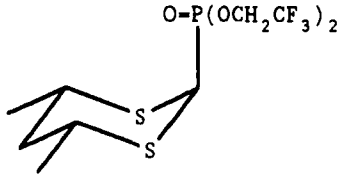
phosphoryl oxygen in $(MeO)_2P{=}O$ and $(CF_3CH_2O)_2P{=}O$ groups should be very similar [the P=O bond lengths in **207a** and **208a** are almost the same: 1.455 (3) and 1.457 (3) Å, respectively]. The longer (by 0.23 Å!) distance for **208a** can be easily explained on the basis of decreased electron density at the P=O oxygen in **208a** and hence a much smaller tendency to form the hydrogen bond in **208a** as compared to **207a**. The concept of hydrogen bond formation is also supported by infrared spectroscopic data (see Section V.B.4).

4. *Spectroscopic Implications of Anomeric Effect in Y—C—P System (Y = O, S, Se)*

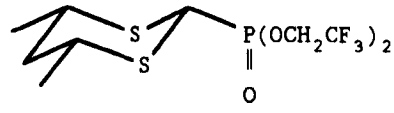
The chemical shift of the carbon nuclei of a phenyl group linked to phosphorus is not indicative of charge transfer to phosphorus (see Section IV.B.3.a).

The dependence of the magnitude of the coupling constant $^1J_{C-P}$ on the position of phosphorus in 2-P-substituted 1,3-diheteroanes was discussed in Section IV.B.3.b. While the argument supports n_Y–σ^*_{C-P} negative hyperconjugation as a source of the anomeric effect in 1,3-dioxane derivatives as well as in all phosphonium salts, the relationship between the $^1J_{C-P}$ coupling constant through the axial and equatorial C(2)—P bonds in nonionic 1,3-dithianes and 1,3-diselenanes does not agree with the intuitive expectation based on the n_Y–σ^*_{C-P} interaction. Thus, it seems reasonable to invoke the n_Y–n_X repulsions as responsible, at least in part, for the anomeric effect in Y—C—P=X (Y = S, Se; X = O, S, Se) systems.

The infrared spectra in the solid state (KBr) or compounds containing a phosphoryl group are very interesting with regard to the P=O stretching frequency. The corresponding $\nu_{P=O}$ values for **111a** (Figure 64) and **111e** are equal (78) to 1188 and 1196 cm^{-1}. The smaller force constant for the axial P=O group than for the equatorial one is consistent with the formation of a weak hydrogen bond with axial H(6) (the more so because the steric congestion in **111a** should act on $\nu_{P=O}$ in an opposite direction). In the case of 1,3-dithiane derivatives the decrease in the stretching frequency for axially situated P=O occurs (54) for **207a** versus **207e** (1222 vs. 1248 cm^{-1},



215a



215e

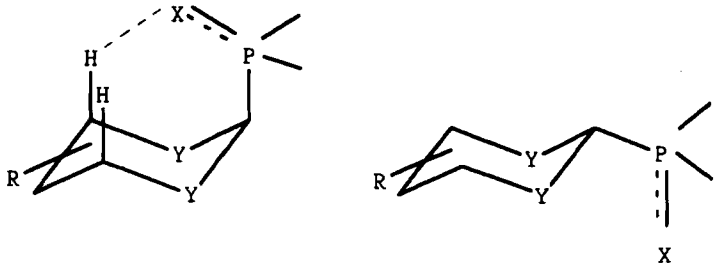
respectively); it may stem from hydrogen bond formation and/or $\sigma_{C(4,6)-S}-\pi^*_{P=O}$ hyperconjugation. Interestingly, for **208a** and **208e**, where, as suggested by X-ray data, a hydrogen bond is not formed, the appropriate stretching frequencies are close ($\nu_{P=O} = 1256$ and $1260\,cm^{-1}$, respectively), similarly as in **215a** and **215e** (1262 and $1256\,cm^{-1}$, respectively) (54).

5. *Kinetic Implications of Anomeric Effect in S—C—P System*

These were discussed in Section IV.A.1.

6. *Anomeric Effect in Y—C—P System (Y = O, S, Se): Summary (383)*

The conformational behavior of 2-P-substituted 1,3-diheteroanes is a result of interplay of several both stabilizing and destabilizing interactions depicted schematically in Figure 65. Their relative importance depends on a heteroane and on phosphorus-containing substituent. The $n_Y-\sigma^*_{C-P}$ negative hyperconjugation seems to be an important factor for Y = O. The conformation of 1,3-dithiane and 1,3-diselenane derivatives is a result of interplay of several factors. The $n_Y-\sigma^*_{C-P}$ hyperconjugative interactions are probably more important for 1,3-diselenanes and for phosphonium salts than for uncharged



Stabilizing	$n_Y-\sigma^*_{C-P}$	$\sigma_{C(4,6)-S}-\sigma^*_{C-P}$
interactions	$\sigma_{C(4,6)-S}-\pi^*_{P=X}$	
Destabilizing	1,3-*syn*-diaxial	rabbit ear effect
interactions		$n_S-\pi$
		n_Y-n_X

Figure 65. Stabilizing and destabilizing interactions in 2-P-substituted 1,3-diheteroanes.

1,3-dithiane derivatives. The axial preference resulting from this interaction may be enhanced by destabilizing interactions (overlap repulsion), which seem to play an important role for some phosphines (rabbit ear effect), phosphonium salts (n_S–π), and compounds containing a P=Se group (n_S–n_{Se}). The latter interaction, n_Y–n_X, is also responsible for the rotameric equilibria around the equatorial C—P(X) bond. The $\sigma_{C(4,6)—S}$–$\pi^*_{P=O}$ hyperconjugation is most effective in stabilizing the axial arrangement of the P=O group. The equatorial conformation is stabilized by the $\sigma_{C(4,6)—S}$–$\sigma^*_{C—P}$ hyperconjugation, which is responsible for the unexpected relations between bond lengths and coupling constants in axial and equatorial derivatives. The axial preference in 2-P-substituted 1,3-diheteroanes is additionally moderated by 1,3-diaxial repulsions, which are most important for 1,3-dioxane derivatives and decrease on going to 1,3-dithianes to 1,3-diselenanes.

SYMBOLS

ap	antiperiplanar conformation; appropriate torsion angle $\Theta \cong 180°$
ac	anticlinal conformation; appropriate torsion angle $\Theta \cong 120°$
C	chair conformer
C_A	axial chair conformer
C_E	equatorial chair conformer
δ	chemical shift in nuclear magnetic resonance spectra
ΔE	potential energy difference
ΔE_{st}	potential energy difference corresponding to steric interactions
ΔE_{AE}	magnitude of anomeric effect in terms of potential energy
ε	dielectric constant (except for Figure 31)
F	Franck's factor
ΔG°	standard free energy difference
ΔG°_C	standard free energy difference in cyclohexane
ΔG°_H	standard free energy difference in a heteroane
$\Delta G^\circ_{H(st)}$	standard free energy difference corresponding to steric interactions in a heteroane
ΔG°_{AE}	magnitude of anomeric effect in free energy terms
$\Delta G^{\neq}$	free energy of activation
$\Delta G^{\neq}_{expd}$	free energy of activation expected in absence of anomeric effect and after correction for ground-state compression effect
ΔH°	standard enthalpy difference
$\Delta H^\circ_{H(st)}$	standard enthalpy difference in heteroane corresponding to steric interactions
ΔH°_{AE}	magnitude of enthalpic anomeric effect
K	equilibrium constant for $sc \rightleftharpoons ap$ (axial$\rightleftharpoons$equatorial) equilibrium

og	orthogonal conformation; appropriate torsion angle $\Theta \cong 90°$
π	pi-type orbital (e.g., $\pi_{C=O}$ of C=O bond)
π^*	pi-type antibonding orbital
$\Delta S°$	standard entropy difference
sc	synclinal conformation; appropriate torsion angle $\Theta \cong 60°$
sp	synperiplanar conformation; the appropriate torsion angle $\Theta \cong 0°$
σ	sigma-type orbital (e.g., σ_{C-S} of C—S bond) or Hammett constant (e.g., σ_p)
σ^*	sigma-type antibonding orbital
TB	twist-boat conformer
Θ	R—Y—C—X torsion angle in R—Y—CH_2—X system

ABBREVIATIONS

ALPH	antiperiplanar lone pair hypothesis
AM1	Austin Model 1 (semiempirical quantum chemical method)
AO	atomic orbital
CNDO	complete neglect of differential overlap (semiempirical quantum chemical method)
DMM	dimethoxymethane
EA	electron affinity
EHMO	extended Hückel molecular orbital (quantum chemical method)
FT-ICR	Fourier transform ion cyclotron resonance
HF	Hartree-Fock (quantum chemical method)
HOMO	highest occupied molecular orbital
IP	ionization potential
IR	infrared
LUMO	lowest unoccupied molecular orbital
MINDO/3	modified intermediate neglect of differential overlap (semiempirical quantum chemical method)
MM	molecular mechanics
MNDO	modified neglect of differential overlap (semiempirical quantum chemical method)
MO	molecular orbital
MOPAC	semiempirical molecular orbital program
MOVB	molecular orbital valence bond (quantum chemical theory)
NBO	natural bond orbital (quantum chemical method)
NOLMO	nonorthogonal, strictly local molecular orbital
NMR	nuclear magnetic resonance
PMO	perturbational molecular orbital (quantum chemical method)
PM3	parametric method 3 (semiempirical quantum chemical method)

RHF	restricted Hartree-Fock (quantum chemical method)
SCF	self-consistent field (quantum chemical method)
SE	stabilization energy
SOMO	single occupied molecular orbital
STO	Slater-type orbitals
VB	valence bond

REFERENCES

1. Sachse, H. *Chem. Ber.* **1890**, *23*, 1363; *Z. Physik. Chem.* **1892**, *10*, 203.
2. Mizushima, S.; Morino, Y.; Higasi, K. *Sci. Pap. Inst. Phys. Chem. Res. Tokyo* **1934**, *25*, 159, as cited in Ref. 4.
3. Hermans, P. H. *Z. Physik. Chem.* **1924**, *113*, 337.
4. Eliel, E. L. *J. Mol. Struct.* **1985**, *126*, 385.
5. Barton, D. H. R. *Experientia* **1950**, *6*, 316.
6. Kirby, A. J. *The Anomeric Effect and Related Stereoelectronic Effects at Oxygen*; Springer-Verlag: Berlin, **1983**; (a) p. 18, (b) p. 24–26, (c) p. 17, (d) p. 38, (e) p. 68, (f) p. 79, (g) p. 43–44, (h) p. 90ff.
7. Deslongchamps, P. *Stereoelectronic Effects in Organic Chemistry*; Pergamon Press: Oxford, **1983**; (a) p. 30, (b) p. 5, (c) p. 31–32, (d) p. 35ff, (e) p. 77ff.
8. Box, V. G. S. *Heterocycles* **1984**, *22*, 891.
9. Tvaroška, I., Bleha, T. *Chem. Papers* **1985**, *39*, 805.
10. Gorenstein, D. G. *Chem. Rev.* **1987**, *87*, 1047.
11. Sinnott, M. L. *Adv. Phys. Org. Chem.* **1988**, *24*, 113.
12. Juaristi, E. *Acc. Chem. Res.* **1989**, *22*, 357.
13. Tvaroška, I., Bleha, T. *Adv. Carbohyd. Chem. Biochem.* **1989**, *47*, 45.
14. Box, V. G. S. *Heterocycles* **1990**, *31*, 1157.
15. Box, V. G. S. *Heterocycles* **1991**, *32*, 795.
16. Box, V. G. S. *Heterocycles* **1991**, *32*, 2023.
17. Juaristi, E. In *Reviews on Heteroatom Chemistry*; vol. 4; Oae, S., Ed.; MYU: Tokyo, **1991**; p. 47.
18. Juaristi, E.; Cuevas, G. *Tetrahedron* **1992**, *48*, 5019.
19. Eliel, E. L.; Allinger, N. L.; Angyal, S. J.; Morrison, G. A. *Conformational Analysis*; Wiley: New York, **1965**; (a) p. 42, (b) p. 46, (c) p. 377.
20. Anderson, J. E. In *The Chemistry of Alkanes and Cycloalkanes*; Patai, S.; Rappoport, Z., Eds.; Wiley: Chichester, 1992; Chapter 3 (a) p. 118ff and references therein, (b) p. 110 and references therein, (c) p. 101 and references therein.
21. Biali, S. E. *J. Org. Chem.* **1992**, 57, 2979.
22. Booth, H.; Everett, J. R. *Chem. Soc. Perkin Trans. 2* **1980**, 255.
23. Zefirov, N. S. *Tetrahedron* **1977**, *33*, 3193.
24. Lemieux, R. U.; Chü, N. J. *Abstracts of Papers*, 133rd National Meeting of the American Chemical Society, San Francisco, CA, April **1958**; American Chemical Society: Washington, D. C., **1958**; p. 31 N.

25. Lemieux, R. U. *Abstr. Papers Am. Chem. Soc.* **1959**, *135*, 5E.
26. Allen, L. C.; Knight, E. T. *J. Mol. Struct. (THEOCHEM.)* **1992**, *261*, 313 and references therein.
27. Lemieux, R. U. *Pure Appl. Chem.* **1971**, *25*, 527.
28. Eliel, E. L. *Angew. Chem. Int. Ed. Engl.* **1972**, *11*, 739, and references cited therein.
29. Bailey, W. F.; Eliel, E. L. *J. Am. Chem. Soc.* **1974**, *96*, 1798.
30. Irwin, J. J.; Ha, T. -K.; Dunitz, J. D. *Helv. Chim. Acta* **1990**, *73*, 1805.
31. Penner, G. H.; Schaefer, T.; Sebastian, R.; Wolfe, S. *Can. J. Chem.* **1987**, *65*, 1845.
32. Denmark, S. E.; Dappen, M. S. *J. Org. Chem.* **1984**, *49*, 798
33. Denmark, S. E.; Dappen, M. S.; Sear, N.; Jacobs, R. T. *J. Am. Chem. Soc.* **1990**, *112*, 3466.
34. Curran, D. P.; Suh, Y.-G. *Carbohyd. Res.* **1987**, *171*, 161.
35. Anderson, C. B.; Sepp, D. T. *Tetrahedron* **1968**, *24*, 1707.
36. Wolfe, S. *Acc. Chem. Res.* **1972**, *5*, 102.
37. Anderson, C. B.; Sepp, D. T. *J. Org. Chem.* **1968**, *33*, 3272.
38. Tschierske, C.; Köhler, H.; Zaschke, H.; Kleinpeter, E. *Tetrahedron* **1989**, *45*, 6987.
39. Eliel, E. L.; Giza, C. A. *J. Org. Chem.* **1968**, *33*, 3754.
40. Eliel, E. L.; Knoeber, Sr. M. C. *J. Am. Chem. Soc.* **1968**, *90*, 3444.
41. Eliel, E. L.; Hargrave, K. D.; Pietrusiewicz, K. M.; Manoharan, M. *J. Am. Chem. Soc.* **1982**, *104*, 3635.
42. Booth, H.; Dixon, J. M.; Khedhair, K. A. *Tetrahedron* **1992**, *48*, 6161.
43. Booth, H.; Everett, J. R. *J. Chem. Soc. Chem. Commun.* **1976**, 278.
44. Eliel, E. L.; Hutchins, R. O. *J. Am. Chem. Soc.* **1969**, *91*, 2703.
45. Pinto, B. M.; Johnston, B. D.; Nagelkerke, R. *Heterocycles* **1989**, *28*, 389.
46. Vijayalakshmi, K. S.; Rao, V. S. R. *Carbohyd. Res.* **1972**, *22*, 413.
47. Abe, A. *J. Am. Chem. Soc.* **1976**, *98*, 6477.
48. Allinger, N. L. *J. Am. Chem. Soc.* **1977**, *99*, 8127.
49. Franck, R. W. *Tetrahedron* **1983**, *39*, 3251.
50. Booth, H.; Khedhair, K. A. *J. Chem. Soc. Chem. Commun.* **1985**, 467.
51. Juaristi, E.; Tapia, J.; Mendez, R. *Tetrahedron* **1986**, *42*, 1253.
52. Höfner, D.; Lesko, S. A.; Binsch, G. *Org. Magn. Res.* **1978**, *11*, 179.
53. Juaristi, E.; López-Núñez, N. A.; Glass, R. S.; Petsom, A.; Hutchins, R. O.; Stercho, J. P. *J. Org. Chem.* **1986**, *51*, 1357.
54. (a) Mikołajczyk, M. *Pure Appl. Chem.* **1987**, *59*, 983. (b) Graczyk, P. Ph. D. Dissertation, Łódź, 1991.
55. Juaristi, E.; Cuevas, G. *Tetrahedron Lett.* **1992**, *33*, 2271.
56. Juaristi, E. *Heteroatom Chem.* **1990**, *1*, 267.
57. Wiberg, K. B.; Murcko, M. A. *J. Am. Chem. Soc.* **1989**, *111*, 4821.
58. Anderson, J. E.; Heki, K.; Hirota, M.; Jörgensen, F. S. *J. Chem. Soc. Chem. Commun.* **1987**, 554.
59. Abe, A.; Inomata, K.; Taniswa, E.; Ando, A. *J. Mol. Struct.* **1990**, *238*, 315.
60. Cosse-Barbi, A.; Dubois, J.-E. *J. Am. Chem. Soc.* **1987**, *109*, 1503.
61. Beckhaus, H.-D.; Dogan, B.; Verevkin, S.; Hädrich, J.; Rüchardt, C. *Angew. Chem.* **1990**, *102*, 313; *Angew. Chem. Int. Ed. Engl.* **1990**, *29*, 320.

62. Wiberg, K. B.; Murcko, M. A. *J. Am. Chem. Soc.* **1988**, *110*, 8029 and references cited therein.
63. Kitagawa, T.; Miyazawa, T. *Bull. Chem. Soc. Jpn.* **1968**, *41*, 1976.
64. Allinger, N. L.; Rahman, M.; Lii, J. -H. *J. Am. Chem. Soc.* **1990**, *112*, 8293.
65. Lemieux, R. U.; Koto, S.; Voisin, D. In *Anomeric Effect, Origin and Consequences*; Szarek, W. A; Horton, D., Eds.; American Chemical Society: Washington, D. C., 1979 (A. C. S. Symposium Series No 87, p. 21).
66. Praly, J.-P.; Lemieux , R. U. *Can. J. Chem.* **1987**, *65*, 213.
67. Andrews, C. W.; Bowen, J. P.; Freser-Reid, B. *J. Chem. Soc. Chem. Commun.* **1989**, 1913.
68. Booth, H.; Khedhair, K. A.; Al-Shirayda, H. A. R. Y. *Tetrahedron* **1988**, *44*, 1465.
69. Dubois, J. E.; Cosse-Barbi, A.; Watson, D. G. *Tetrahedron Lett.* **1989**, *30*, 167.
70. Wolfe, S.; Whangbo, M.-H.; Mitchell, D. J. *Carbohyd. Res.* **1979**, *69*, 1.
71. Booth, H.; Khedhair, K. A.; Readshaw, S. A. *Tetrahedron* **1987**, *43*, 4699.
72. Krol, M. C.; Huige, C. J. M.; Altona, C. *J. Comput. Chem.* **1990**, *11*, 765.
73. Alcaide, B.; Jimenez-Barbero, J.; Plumet, J.; Rodriguez-Campos, I. M. *Tetrahedron* **1992**, *48*, 2715.
74. Pierson, G. O.; Runquist, O. A. *J. Org. Chem.* **1968**, *33*, 2572.
75. Booth, H.; Readshaw, S. A. *Tetrahedron* **1990**, *46*, 2097.
76. Ouedraogo, A.; Lessard, J. *Can. J. Chem.* **1991**, *69*, 474.
77. Höfner, D.; Lesko, S. A.; Binsch, G. *Org. Magn. Res.* **1978**, *11*, 179.
78. Mikołajczyk, M.; Graczyk, P. P.; Wieczorek, M. W.; Bujacz, G. *Tetrahedron* **1992**, *48*, 4209.
79. Mikołajczyk, M.; Graczyk, P.; Kabachnik, M. I.; Baranov, A. P. *J. Org. Chem.* **1989**, *54*, 2859.
80. Köhler, H.; Tschierske, C.; Zaschke, H; Kleinpeter, E. *Tetrahedron* **1990**, *46*, 4241.
81. Bentrude, W. G.; Setzer, W. N.; Khan, M.; Sopchik, A. E.; Ramli, E. *J. Org. Chem.* **1991**, *56*, 6127.
82. Pinto, B. M.; Sandoval-Ramirez, J.; Dev Sharma, R. *Tetrahedron Lett.* **1985**, *26*, 5235.
83. Pinto, B. M.; Sandoval-Ramirez, J.; Dev Sharma, R.; Willis, A. C.; Einstein, F. W. B. *Can. J. Chem.* **1986**, *64*, 732.
84. Pinto, B. M.; Johnston, B. D.; Sandoval-Ramirez, J.; Dev Sharma, R. *J. Org. Chem.* **1988**, *53*, 3766.
85. Booth, H.; Dixon, J. M.; Khedhair, K. A.; Readshaw, S. A. *Tetrahedron* **1990**, *46*, 1625.
86. Touboul, E.; Dana, G. *Tetrahedron Lett.* **1990**, *31*, 3549.
87. Bürgi, H. B.; Dunitz, J. D. *Acc. Chem. Res.* **1983**, *16*, 153.
88. Schleifer, L.; Senderowitz, H.; Aped, P.; Tartakovsky, E.; Fuchs, B. *Carbohyd. Res.* **1990**, *206*, 21.
89. Fuchs, B.; Schleifer, L.; Tartakovsky, E. *Nouv. J. Chim.* **1984**, *8*, 275.
90. Garrett, E. C.; Serianni, A. S. *Carbohyd. Res.* **1990**, *206*, 183.
91. Wu, T.-C.; Goekjian, P. G.; Kishi, Y. *J. Org. Chem.* **1987**, *52*, 4819.
92. Goekjian, P. G.; Wu, T.-C; Kang, H.-Y.; Kishi, Y. *J. Org. Chem.* **1987**, *52*, 4823.
93. Babirad, S. A.; Wang, Y.; Goekjian, P. G.; Kishi, Y. *J. Org. Chem.* **1987**, *52*, 4825.
94. Goekjian, P. G.; Wu, T.-C.; Kishi, Y. *J. Org. Chem.* **1991**, *56*, 6412.
95. Goekjian, P. G.; Wu, T.-C.; Kang, H.-Y.; Kishi, Y. *J. Org. Chem.* **1991**, *56*, 6422.
96. (a) Deslongchamps, P.; Pothier, N. *Can. J. Chem.* **1990**, *68*, 597. (b) Graczyk, P. P; Mikołajczyk, M. *Tetrahedron Lett.*, **1993**, *34*, 1521.

97. Mikołajczyk, M.; Graczyk, P.; Bałczewski, P. *Tetrahedron Lett.* **1987**, *28*, 573.
98. (a) Mikołajczyk, M.; Graczyk, P.; Wieczorek, M. W.; Bujacz, G. *Angew. Chem.* **1991**, *103*, 604; *Angew. Chem. Int. Ed. Engl.* **1991**, *30*, 578–580. (b) Graczyk, P. P.; Mikołajczyk, M. *Phosphorus Sulfur and Silicon* **1993**, *78*, 313.
99. Pietrusiewicz, K. M. *Org. Magn. Res.* **1983**, *21*, 345.
100. Quin, L. D.; Caster, K. C.; Kisalus, J. C.; Mesch, K. A. *J. Am. Chem. Soc.* **1984**, *106*, 7021.
101. Quin, L. D.; Bernhardt, F. C. *Magn. Res. Chem.* **1985**, *23*, 929.
102. Mitchell, T. N.; Heesche-Wagner, K.; Belt, H.-J. *Magn. Res. Chem.* **1991**, *29*, 78.
103. Aucar, G. A.; Giribet, C. G.; Ruiz de Azùa, M. C.; Diz, A. C.; Contreras, R. H. *J. Mol. Struct. (THEOCHEM)* **1988**, *164*, 1.
104 Contreras, R. H.; Giribet, C. G.; Ruiz de Azùa, M. C.; Cavasotto, C. N.; Aucar, G. A.; Krivdin, L. B. *J. Mol. Struct. (THEOCHEM)* **1990**, *210*, 175.
105. Navio, P. F.; Molina, J. M. *J. Mol. Struct.* **1990**, *222*, 387.
106. Allinger, N. L.; Hu, S.-E. *J. Am. Chem. Soc.* **1962**, *84*, 370.
107. Allinger, N. L.; Hu, S.-E. *J. Org. Chem.* **1962**, *27*, 3417.
108. Allinger, N. L.; Miller, M. A.; Van-Catledge, F. A.; Hirsch, J. A. *J. Am. Chem. Soc.* **1967**, *89*, 4345.
109. Allinger, N. L.; Hirch, J. A.; Miller, M. A.; Tyminski, I. J.; Van-Catledge, F. A. *J. Am. Chem. Soc.* **1968**, *90*, 1190.
110. Booth, H.; Grindley, T. B.; Khedhair, K. A. *J. Chem. Soc. Cummun.* **1982**, 1047.
111. Ōki, M.; Sugawara, T.; Iwamura, H. *Bull. Chem. Soc. Jpn.* **1974**, *47*, 2457.
112. Booth, H.; Dixon, J. M.; Readshaw, S. A. *Tetrahedron* **1992**, *48*, 6151.
113. Juaristi, E.; Gonzales, E. A.; Pinto, B. M.; Johnston, B. D.; Nagelkerke, R. *J. Am. Chem. Soc.* **1989**, *111*, 6745.
114. Abraham, R. J.; Bretscheider, E. In *Internal Rotation in Molecules*; Orville-Thomas, W. J., Ed., Academic Press: New York, **1974**; Chapter 13, pp. 481–584.
115. (a) Abraham, R. J.; Hudson, B. D.; Kermode, M. W., Mines, J. R. *J. Chem. Soc. Faraday Trans. 1* **1988**, *84*, 1911. (b) Ha, S.; Gao, J.; Tidor, B.; Grady, J. W.; Karplus, M. *J. Am. Chem. Soc.* **1991**, *113*, 1553. (c) Wong, M. W.; Frisch, M. J.; Wiberg, K. B. *J. Am. Chem. Soc.* **1991**, *113*, 4776. (d) Montagnani, R.; Tomasi, J. *Int. J. Quantum Chem.* **1991**, *39*, 851.
116. Mayer, U. *Pure Appl. Chem.* **1979**, *51*, 1697.
117. Burkert, U. *J. Comput. Chem.* **1980**, *1*, 192.
118. Reichardt, C. In *Molecular Interactions*; Vol. 3; Ratajczak, H.; Orville-Thomas, W. J., Eds., Wiley: New York.; **1982**, 241.
119. Abraham, M. H.; Grellier, P. L.; Abboud, J.-L. M.; Doherty, R. M.; Taft, R. W. *Can. J. Chem.* **1988**, *66*, 2673.
120. Drago, R. S. *J. Chem. Soc. Perkin. Trans. 2* **1992**, 1827 and references therein.
121. Walkinshaw, M. D. *J. Chem. Soc. Perkin. Trans. 2* **1987**, 1903.
122. Tvaroška, I.; Kozár, T. *Int. J. Quantum Chem.* **1983**, *23*, 765.
123. Tvaroška, I. *Chem. Papers* **1989**, *43*, 239 and references therein.
124. Kysel, O.; Mach, P. *J. Mol. Struct. (THEOCHEM)* **1991**, *227*, 285.
125. Anderson, C. B.; Sepp, D. T. *J. Org. Chem*, **1967**, *32*, 607.
126. de Hoog, A. J.; Buys, H. R.; Altona, C.; Havinga, A. *Tertrahedron* **1969**, *25*, 3365.
127. Zefirov, N. S.; Shechtman, N. M. *Usp. Khim.* **1971**, *40*, 593 and references therein; Engl. transl. p. 315.

128. Tvaroška, I.; Bleha, T. *Coll. Czech. Chem. Commun.* **1980**, *45*, 1883.
129. Fuchs, B.; Ellencweig, A.; Tartakovsky, E.; Aped, *P. Angew. Chem.* **1986**, *98*, 289; *Angew. Chem. Int. Ed. Engl.* **1986**, *25*, 287.
130. Zefirov, N. S.; Samoshin, V. V. *Tetrahedron Lett.* **1981**, *22*, 2209.
131. Hammarström, L.-G.; Berg, U.; Liljefors, T. *Tetrahedron Lett.* **1987**, *28*, 4883.
132. Ford, R. A.; Allinger, N. L. *J. Org. Chem.* **1970**, *35*, 3178.
133. Ouellette, R. J.; Williams, S. H. *J. Am. Chem. Soc.* **1971**, *93*, 466.
134. Eliel, E. L. *Chem. & Ind.* **1959**, 568.
135. Juaristi, E.; Valle, L.; Valenzuela, B. A.; Aguilar, M. A. *J. Am. Chem. Soc.* **1986**, *108*, 2000.
136. Juaristi, E.; López-Núñez, N. A.; Valenzuela, B. A.; Valle, L.; Toscano, R. A.; Soriano-Garcia, M. *J. Org. Chem.* **1987**, *52*, 5185.
137. Graczyk, P. P.; Mikołajczyk, M. *Magn. Res. Chem.* **1992**, *30*, 1261.
138. Hehre, W. J.; Ditchfield, R.; Radom, L.; Pople, J. A. *J. Am. Chem. Soc.* **1970**, *92*, 4796.
139. Radom, L.; Hehre, W. J.; Pople, J. A. *J. Am. Chem. Soc.* **1971**, *93*, 289.
140. Stull, D. R.; Westrum, E. F., Jr.; Sinke, G. C. *The Chemical Thermodynamics of Organic Compounds*; Wiley: New York, **1969**; pp. 636–637.
141. Schleyer, P. v. R.; Jemmis, E. D.; Spitznagel, G. W. *J. Am. Chem. Soc.* **1985**, *107*, 6393.
142. Dewar, M. S. J. *J. Am. Chem. Soc.* **1984**, *106*, 669.
143. Reed, A. E.; Schleyer, P. v. R. *J. Am. Chem. Soc.* **1987**, *109*, 7362.
144. Apeloig, Y.; Stanger, A. *J. Organomet. Chem.* **1988**, *346*, 305.
145. Reed, A. E.; Schade, C.; Schleyer, P. v. R.; Kamath, P. V.; Chandrasekhar, J. *J. Chem. Soc. Chem. Commun.* **1988**, 67.
146. Reed, A. E.; Schleyer, P. v. R. *Inorg. Chem.* **1988**, *27*, 3969.
147. Kumar, P. N. V. P.; Wang, D. -X.; Lam, B.; Albright, T. A.; Jemmis, E. D. *J. Mol. Struct.* **1989**, *194*, 183.
148. Salzner, U.; Schleyer, P. v. R. *J. Chem. Soc. Chem. Commun.* **1990**, 190.
149. Hati, S.; Datta, D. *J. Org. Chem.* **1992**, *57* 6056.
150. Arai, K.; Ōki, M. *Bull. Chem. Soc. Jpn.* **1976**, *49*, 553.
151. Kato, v. K. *Acta Crystallogr.* **1972**, *B28*, 606.
152. Batchelor, R. J.; Einstein, F. W. B.; Gay, I. D.; Gu, J.-H.; Johnston, B. D.; Pinto, B. M. *J. Am. Chem. Soc.* **1989**, *111*, 6582.
153. Vishveshwara, S.; Rao, V. S. R. *Carbohyd. Res.* **1982**, *104*, 21.
154. Pinto, B. M.; Schlegel, H. B.; Wolfe, S. *Can. J. Chem.* **1987**, *65*, 1658.
155. Narasimhamurthy, N.; Manohar, H.; Samuelson, A. G.; Chandrasekhar, J. *J. Am. Chem. Soc.* **1990**, *112*, 2937.
156. Aped, P.; Schleifer, L.; Fuchs, B.; Wolfe, S. *J. Comput. Chem.* **1989**, *10*, 265.
157. (a) Wu, Y.-D.; Kirmse, W.; Houk, K. N. *J. Am. Chem. Soc.* **1990**, *112*, 4557. (b) Wiberg, K. B.; Rablen, P. R. *J. Am. Chem. Soc.* **1993**, *115*, 614.
158. Pearson, R. G. *J. Am. Chem. Soc.* **1988**, *110*, 7684.
159. Leroy, G.; Sana, M.; Wilante, C. *J. Mol. Struct. (THEOCHEM)* **1991**, *234*, 303.
160. Lemieux, R. U.; Morgan, A. R. *Can. J. Chem.* **1965**, *43*, 2205; *Can. J. Chem.* **1965**, *43*, 2214.
161. Paulsen, H.; Györgydeak, Z.; Friedmann, M. *Chem. Ber.* **1974**, *107*, 1590.
162. Finch, P.; Nagpurkar, A. G. *Carbohyd. Res.* **1976**, *49*, 275.

163. Grein, F.; Deslongchamps, P. *Can. J. Chem.* **1992**, *70*, 1562.
164. Woods, R. J.; Szarek, W. A.; Smith, V. H., Jr. *J. Chem. Soc. Chem. Commun.* **1991**, 334.
165. Andrews, C. W.; Fraser-Reid, B.; Bowen, J. P. *J. Am. Chem. Soc.* **1991**, *113*, 8293.
166. (a) Cramer, C. J. *J. Org. Chem.* **1992**, *57*, 7034. (b) Luger, P.; Kothe, G.; Vangehr, K.; Paulsen, H.; Heiker, F. R. *Carbohyd. Res.* **1979**, *68*, 207.
167. (a) Manoharan, M.; Eliel, E. L. *Tetrahedron Lett.* **1984**, *25*, 3267. (b) Abraham, R. J.; Hudson, B. D.; Thomas, W. A. *J. Chem. Soc. Perkin Trans. 2* **1986**, 1635.
168. Geneste, P.; Kamenka, J. M.; Ung, S. N.; Herrmann, P.; Goudal, R.; Trouiller, G. *Eur. J. Med. Chem.* **1979**, *14*, 301.
169. Batista da Carvalho, L. A. E.; Amorim da Costa, A. M.; Teixeira-Dias, J. J. C. *J. Mol. Struct. (THEOCHEM)* **1990**, *205*, 327.
170. Booth, H.; Jozefowicz, M. L. *J. Chem. Soc. Perkin. Trans. 2* **1976**, 895.
171. Zefirov, N. S.; Fedorovskaya, M. A. *Zh. Org. Khim.* **1969**, *5*, 158; Engl. transl. p. 155.
172. Giralt, E.; Pericas, M. A.; Riera, A. *Tetrahedron* **1983**, *39*, 3959.
173. Unpublished results from this laboratory.
174. Hosie, L.; Mashall, P. J.; Sinnott, M. L. *J. Chem. Soc. Perkin Trans. 2* **1984**, 1121.
175. David, S.; Eisenstein, O.; Hehre, W. J.; Salem, L.; Hoffmann, R. *J. Am. Chem. Soc.* **1973**, *95*, 3806.
176. Anders, E.; Markus, F.; Meske, H.; Tropsch, J.; Maas, G. *Chem. Ber.* **1987**, *120*, 735.
177. Opitz, G.; Wiehn, W.; Ziegler, M. L.; Nuber, B. *Chem. Ber.* **1992**, *125*, 1621.
178. Ratcliffe, A. J.; Fraser-Reid, B. *J. Chem. Soc. Perkin. Trans 1* **1990**, 745.
179. Pothier, N.; Goldstein, S.; Deslongchamps, P. *Helv. Chim. Acta* **1992**, *75*, 604.
180. Deslongchamps, P. *Pure & Appl. Chem.*; **1993**, *65*, 1161. We would like to express our thanks for a preprint of this article.
181. Chmielewski, M.; Jurczak, J.; Priebe, W.; Horton, D. *Magn. Res. Chem.* **1987**, *25*, 161.
182. Chmielewski, M.; BeMiller, J. N.; Cerretti, D. P. *J. Org. Chem.* **1981**, *46*, 3903.
183. Beckhaus, H. D.; Dogan, B.; Pakusch, J.; Verevkin, S.; Rüchardt, C. *Chem. Ber.* **1990**, 123, 2153.
184. Edward, J. T. *Chem. & Ind.* **1955**, 1102.
185. Chü, N. J. Ph.D. Thesis, University of Ottawa (Ontario, Canada), **1959**, p. 97.
186. Hirsch, J. A. *Top. Stereochem.* **1967**, *1*, 199.
187. Tvaroška, I.; Bleha, T. *Can. J. Chem.* **1979**, *57*, 424.
188. Romers, C.; Altona, C.; Buys, H. R.; Havinga, E. *Top. Stereochem.* **1969**, *4*, 39.
189. Wolfe, S.; Rauk, A.; Tel, L. M.; Csizmadia, I. G. *J. Chem. Soc. B* **1971**, 136.
190. Zhdanov, Yu. A.; Minyaev, R. M.; Minkin, V. I. *J. Mol. Struct.* **1973**, *16*, 357.
191. Perrin, C. L.; Nuñez, O. *J. Chem. Soc. Chem. Commun.* **1984**, 333.
192. Aped, P.; Apeloig, P.; Ellencweig, A.; Fuchs, B.; Goldberg, I.; Karni, M.; Tartakovsky, E. *J. Am. Chem. Soc.* **1987**, *109*, 1486.
193. Desilets, S.; St-Jacques, M. *J. Am. Chem. Soc.* **1987**, *109*, 1641.
194. Brockway, L. O. *J. Phys. Chem.* **1937**, *41*, 185.
195. Roberts, J. B.; Webb, R. L.; McElhill, E. A. *J. Am. Chem. Soc.* **1950**, *72*, 408.
196. Lucken, E. A. C. *J. Chem. Soc. III* **1959**, 2954.
197. Kabayama, M. A.; Patterson, D. *Can. J. Chem.* **1958**, *36*, 563.

198. Hutchins, R. O.; Kopp, L. D.; Eliel, E. L. *J. Am. Chem. Soc.* **1968**, *90*, 7174.
199. Dale, J. *Tetrahedron* **1974**, *30*, 1683.
200. Kessler, H.; Möhrle, H.; Zimmermann, G. *J. Org. Chem.* **1977**, *42*, 66.
201. Eisenstein, O.; Nguen Trong Anh; Jean, Y.; Devaquet, A.; Cantacuzène, J.; Salem, L. *Tetrahedron* **1974**, *30*, 1717.
202. Epiotis, N. D.; Yates, R. L. *J. Am. Chem. Soc.* **1976**, *98*, 461.
203. Epiotis, N. D. *J. Mol. Struct. (THEOCHEM)* **1988**, *169*, 289.
204. Jorgensen, F. S.; Norskov-Lauritsen, L. *Tetrahedron Lett.* **1982**, *23*, 5221.
205. Burkert, U.; Allinger, N. *Molecular Mechanics*, ACS Monograph 177, Am. Chem. Soc.: Washington, DC, 1982, p. 195.
206. Jeffrey, G. A.; Taylor, R. *J. Comput. Chem.* **1980**, *1*, 99.
207. Burkert, U. *Tetrahedron* **1977**, *32*, 2237.
208. Burkert, U. *Tetrahedron* **1979**, *35*, 1945.
209. Burkert, U. *Carbohyd. Res.* **1980**, *85*, 1.
210. Fuchs, B.; Ellencweig, A.; Burkert, U. *Tetrahedron* **1984**, *40*, 2011.
211. Norskov-Lauritsen, L.; Allinger, N. L. *J. Comput. Chem.* **1984**, *5*, 326.
212. Senderowitz, H.; Aped, P.; Fuchs, B. *Tetrahedron* **1992**, *48*, 1131.
213. Aped, P.; Fuchs, B.; Goldberg, I.; Senderowitz, H.; Schleifer, L.; Tartakovsky, E.; Anteunis, M.; Borremans, F. A. M. *Tetrahedron* **1991**, *47*, 5781.
214. Aped, P.; Fuchs, B.; Goldberg, I.; Senderowitz, H.; Tartakovsky, E.; Weinman, S. *J. Am. Chem. Soc.* **1992**, *114*, 5585.
215. Mikołajczyk, M.; Graczyk, P.; Wieczorek, M. W.; Bujacz, G.; Struchkov, Y. T.; Antipin, M. Y. *J. Org. Chem.* **1988**, *53*, 3609.
216. Fernandez, B.; Rios, M. A.; Carballeira, L. *J. Comput. Chem.* **1991**, *12*, 78.
217. Fernandez, B.; Carballeira, L.; Rios, M. A. *J. Mol. Struct.* **1991**, *245*, 53.
218. Fernandez, B.; Carballeira, L.; Rios, M. A. *J. Mol. Struct.* **1991**, *263*, 157.
219. Fernandez, B.; Rios, M. A.; Carballeira, L. *J. Mol. Struct.* **1991**, *246*, 301.
220. Jaime, C.; Osawa, E. *Tetrahedron* **1983**, *39*, 2769.
221. Liljefors, T.; Tai, J.; Li, S.; Allinger, N. L. *J. Comput. Chem.* **1987**, *8*, 1051.
222. Kroon-Batenburg, L. M. J.; Kanters, J. A. *J. Mol. Struct. (THEOCHEM)* **1983**, *105*, 417.
223. Allinger, N. L.; Kok, R. A.; Imam, M. R. *J. Comput. Chem.* **1988**, *9*, 591.
224. Liu, J.; Waterhouse, A. L. *Carbohyd. Res* **1992**, *232*, 1.
225. Stewart, J. J. P. *QCPE* **1989**, *9*, 99.
226. Guntertofte, K.; Palm, J.; Pettersson, I.; Stamvik, A. *J. Comput. Chem.* **1991**, *12*, 200.
227. Stewart, J. J. P. *J. Comput. Chem.* **1989**, *10*, 221.
228. Allinger, N. L.; Yuh, Y. H.; Lii, J.-H. *J. Am. Chem. Soc.* **1989**, *111*, 8551.
229. Dowd, M. K.; Zeng, J.; French, A. D.; Reilly, P. J. *Carbohyd. Res.* **1992**, *230*, 223.
230. Takusagawa, F.; Jacobson, R. A. *Acta Crystallogr., Sect. B.* **1976**, *32*, 155.
231. Dowd, M. K.; French, A. D.; Reilly, P. J. *Carbohyd. Res.* **1992**, *233*, 15.
232. Allen, L. C. *Chem. Phys. Lett.* **1968**, *2*, 597.
233. Wolfe, S.; Tel, L. M.; Haines, W. J.; Robb, M. A.; Csizmadia, I. G. *J. Am. Chem. Soc.* **1973**, *95*, 4863.
234. Radom, L.; Hehre, W. J.; Pople, J. A. *J. Am. Chem. Soc.* **1972**, *94*, 2371

235. Jeffrey, G. A.; Pople, J. A.; Radom, L. *Carbohyd. Res.* **1972**, *25*, 117.
236. Tvaroška, I.; Bleha, T. *Tetrahedron Lett.* **1975**, *4*, 249.
237. Tvaroška, I.; Bleha, T. *J. Mol. Struct.* **1975**, *24*, 249.
238. Jeffrey, G. A.; Yates, J. H. *J. Am. Chem. Soc.* **1979**, *101*, 820.
239. Zhdanov, Yu. A.; Minyaev, R. M.; Minkin, V. I. *Dokl. Akad. Nauk USSR. Ser. Khim.* **1973**, *211*, 343; Engl. transl. p. 563.
240. Grein, F.; Deslongchamps, P. *Can. J. Chem.* **1992**, *70*, 604.
241. Altona, C. Ph. D. Thesis, University of Leiden, **1964**.
242. de Wolf, N.; Romers, C.; Altona, C. *Acta Crystallogr.* **1967**, *22*, 715.
243. Dill, J. D.; Schleyer, P. v. R.; Pople, J. A. *J. Am. Chem. Soc.* **1976**, *98*, 1663.
244. Jeffrey, G. A.; Pople, J. A.; Radom, L. *Carbohyd. Res.* **1974**, *38*, 81.
245. Dewar, M. S. J.; Dougherty, R. C. *The PMO Theory of Organic Chemistry*; Plenum Press: New York, **1975**; (a) p. 63, Eq. 2.8.
246. Herndon, W. C. *J. Chem. Educ.* **1979**, *56*, 448.
247. Jorgensen, W. L.; Salem, L. *The Organic Chemist's Book of Orbitals*; Academic Press: New York, 1973; (a) p. 33 (b) p. 34.
248. Epiotis, N. D.; Cherry, W. R.; Shaik, S.; Yates, R. L.; Bernardi, F. *Top. Curr. Chem.* **1977**, *70*, 1.
249. Hoffmann. R.; Radom, L.; Pople, J. A.; Schleyer, P. v. R.; Hehre, W. J.; Salem, L. *J. Am. Chem. Soc.* **1972**, *94*, 6222.
250. Wells, P. R. *Prog. Phys. Org. Chem.* **1968**, *6*, 111.
251. Whangbo, M.-H.; Wolfe, S. *Can. J. Chem.* **1976**, *54*, 963.
252. Zefirov, N. S. *Zh. Org. Khim.* **1974**, *10*, 1124; Engl. Transl. p. 1137.
253. Ellison, F. O.; Shull, H. *J. Chem. Phys.* **1955**, *23*, 2348.
254. Dunning. T. H.; Pitzer, R. M.; Aung, S. *J. Chem. Phys.* **1972**, *57*, 5044.
255. Sweigart, D. A.; Turner, D. W. *J. Am. Chem. Soc.* **1972**, *94*, 5599.
256. Laing, M. *J. Chem. Educ.* **1987**, *64*, 124.
257. Cosse-Barbi, A.; Watson, D. G.; Dubois, J. E. *Tetrahedron Lett.* **1989**, *30*, 163.
258. Van-Catledge, F. A. *J. Am. Chem. Soc.* **1974**, *96*, 5693.
259. Whangbo, M. H.; Schlegel, H. B.; Wolfe, S. *J. Am. Chem. Soc.* **1977**, *99*, 1296.
260. Jeffrey, G. A.; Pople, J. A.; Binkley, J. S.; Vishveshwara, S. *J. Am. Chem. Soc.* **1978**, *100*, 373.
261. Korth, H. G.; Praly, J.-P.; Somsak, L.; Sustmann, R. *Chem. Ber.* **1990**, *123*, 1155.
262. Schleyer, P. v. R.; Kos, A. J. *Tertrahedron* **1983**, *39*, 1141.
263. Epiotis, N. D.; Yates, R. L.; Larson, J. R.; Kirmaier, C. R.; Bernardi, F. *J. Am. Chem. Soc.* **1977**, *99*, 8379.
264. Carballeira, L.; Fernandez, B.; Rios, M. A. *J. Mol. Struct. (THEOCHEM)*; **1990**, *209*, 201.
265. Dewar, M. S. J. *The Molecular Orbital Theory of Organic Chemistry*; McGraw-Hill: New York, **1969**; pp. 212, 217.
266. Inagaki, S.; Iwase, K.; Mori, Y. *Chem. Lett.* **1986**, 417.
267. Inagaki, S.; Mori, Y.; Goto, N. *Bull. Chem. Soc. Jpn.* **1990**, *63*, 1098.
268. Ponec, R.; Chvalovsky, V. *Coll. Czech. Chem. Commun.* **1974**, *39*, 2613.
269. Smits, G. F.; Altona, C. *Theor. Chim. Acta* **1985**, *67*, 461.
270. Smits, G. F.; Krol, M. C.; van der Hart, W. J; Altona, C. *Mol. Phys.* **1986**, *59*, 209.

271. Smits, G. F.; Krol, M. C.; Altona, C. *Mol. Phys.* **1988**, *63*, 921.
272. Smits, G. F.; Krol, M. C.; Altona, C. *Mol. Phys.* **1988**, *65*, 513.
273. Epiotis, N. D.; Larson, J. R.; Eaton, H. *Lect. Notes. Chem.* **1982**, *29*, 1.
274. Epiotis, N. D. *Lect. Notes Chem.* **1983**, *34*, 1. (p. 263)
275. Epiotis, N. D. *Nouv. J. Chem.* **1983**, *8*, 11.
276. Epiotis, N. D. *New J. Chem.* **1987**, *11*, 303.
277. Epiotis, N. D. *J. Mol. Struct.* **1987**, *153*, 1.
278. Epiotis, N. D. *Top. Curr. Chem.* **1988**, *150*, 47.
279. Epiotis, N. D. *J. Mol. Struct. (THEOCHEM)* **1991**, *229*, 205.
280. Brunck, T. K.; Weinhold, F. *J. Am. Chem. Soc.* **1979**, *101*, 1700.
281. Smart, B. E. In *Molecular Structure and Energetics*; Vol. 3; Liebman, J. F.; Greenberg, A., Eds.; VCH: Dearfield Beach, FL, 1986, pp. 141–148.
282. Liebman, J. F.; Greenberg, A. unpublished results; 1978, as cited in Ref. 203.
283. Pauling, L. *The Nature of the Chemical Bond*; 3rd ed.; Cornell University Press: Ithaca, NY, 1960.
284. Wheland, G. W. *Resonance in Organic Chemistry*; Wiley: New York, 1955.
285. Cantacuzène, J.; Jantzen, R.; Ricard, D. *Tetrahedron* **1972**, *28*, 717.
286. Brunet, E.; Garcia Ruano, J. L.; Martinez, M. C.; Rodriguez, J. H.; Alcudia, F. *Tetrahedron* **1984**, *40*, 2023.
287. Alcudia, F.; Campos, A. L.; Llera, J. M.; Zorrilla, F. *Phosphorus Sulfur* **1988**, *36*, 29.
288. Yang., C.; Goldstein, E.; Breffle, S.; Jin, S. *J. Mol. Struct. (THEOCHEM)* **1992**, *259*, 345.
289. Olivato, P.; Wladislaw, B.; Guerrero, S. A.; Russovsky, D. *Phosphorus Sulfur* **1985**, *24*, 225.
290. Olivato, P. R.; Guerrero, S. A.; Hase, Y.; Rittner, R. *J. Chem. Soc. Perkin. Trans. 2* **1990**, 465.
291. Eliel, E. L.; Nader, F. W. *J. Am. Chem. Soc.* **1970**, *92*, 584.
292. Petrzilka, M.; Felix, D.; Eschenmoser, A. *Helv. Chim. Acta* **1973**, *56*, 2950
293. Chandrasekhar, S.; Kirby, A. J.; Martin, R. J. *J. Chem. Soc. Perkin. Trans. 2* **1983**, 1619.
294. Kirby, A. J.; Martin, R. J. *J. Chem. Soc. Perkin. Trans. 2* **1983**, 1627.
295. Kirby, A. J.; Martin, R. J. *J. Chem. Soc. Perkin. Trans. 2* **1983**, 1633.
296. Briggs, A. J.; Evans, C. M.; Glenn, R.; Kirby, A. J. *J. Chem. Soc. Perkin. Trans. 2* **1983**, 1637.
297. Chiodini, L.; Malatesta, V.; Fusco, R.; Ranghino; G.; Scordamaglia, R.; Tosi, C. *J. Mol. Struct. (THEOCHEM)* **1986**, *138*, 51.
298. Clennan, E. L.; L'Esperance, R. P.; Lewis, K. K. *J. Org. Chem.* **1986**, *51*, 1440.
299. Khouri, F. F.; Kaloustian, M. K. *J. Am. Soc. Soc.* **1986**, *108*, 6683.
300. Huber, R.; Vasella, A. *Tetrahedron* **1990**, *46*, 33.
301. Caserio, M. C.; Shih, P.; Fisher, C. L. *J. Org. Chem.* **1991**, *56*, 5517.
302. McPhail, D. R.; Lee, J. R.; Fraser-Reid, B. *J. Am. Chem. Soc.* **1992**, *114*, 1905.
303. Sinnott, M. L. *Chem. Rev.* **1990**, *90*, 1171.
304. Berson, J. E. *Acc. Chem. Res.* **1991**, *24*, 215.
305. Seeman, J. I. *Chem. Rev.* **1983**, *83*, 83.
306. Lustgarten, R.; Brookhart, M.; Winstein, S. *Tetrahedron Lett.* **1971**, 141.
307. Fărcaşiu, D.; Horsley, J. A. *J. Am. Chem. Soc.* **1980**, *102*, 4906.
308. Ratcliffe, A. J.; Mootoo, D. R.; Andrews, C. W.; Fraser-Reid, B. *J. Am. Chem. Soc.* **1989**, *111*, 7661.

309. Caserio, M. C.; Souma, Y.; Kim, J. K. *J. Am. Chem. Soc.* **1981**, *103*, 6712.
310. Graczyk, P. P.; Mikolajczyk, M. Third International Congress on Heteroatom Chemistry; 1992; Riccione, Italy; communication P-44.
311. Cieplak, A. S. *J. Am. Chem. Soc.* **1981**, *103*, 4540.
312. Coxon, J. M.; McDonald, D. Q. *Tetrahedron* **1992**, *48*, 3353.
313. Graczyk, P.; Mikolajczyk, M. *Tetrahedron Lett.* **1991**, *32*, 7329.
314. Edwards, M. R.; Jones, P. G.; Kirby, A. J. *J. Am. Chem. Soc.* **1986**, *108*, 7067.
315. (a) Taillefer, R. J.; Thomas, S. E.; Nadeau, Y.; Beierbeck, H. *Can. J. Chem.* **1979**, *57*, 3041. (b) Croteau, A.; Bailey, W. F. 178th National meeting of the American Chemical Society; Washington, D. C.; Sept. **1979**, Org. 105.
316. Ahmad, M.; Bergstrom, R. G.; Cashen, M. J.; Chiang, Y.; Kresge, A. J.; McClelland, R. A.; Powell, M. F. *J. Am. Soc. Soc.* **1979**, *101*, 2669.
317. Wolfe, S.; Mario Pinto, B.; Varma, V.; Leung, R. Y. N. *Can. J. Chem.* **1990**, *68*, 1051 and references therein.
318. Amos, R. D.; Handy, N. C.; Jones, P. G.; Kirby, A. J.; Parker, J. K.; Percy, J. M.; Der Su, M. *J. Chem. Soc. Perkin. Trans. 2* **1992**, 549.
319. Coxon, J. M.; McDonald, D. Q. *Tetrahedron Lett.* **1992**, *33*, 651.
320. Juaristi, E.; Cuevas, G. *Tetrahedron Lett.* **1992**, *33*, 1847.
321. Briggs, A. J.; Glenn, R.; Jones, P. G.; Kirby, A. J.; Ramaswamy, P. *J. Am. Chem. Soc.* **1984**, *106*, 6200.
322. White, J. M.; Robertson, G. B. *J. Org. Chem.* **1992**, *57*, 4638.
323. Anet, F. A. L.; Kopelevich, M. *J. Chem. Soc. Chem. Commun.* **1987**, 595.
324. Wolfe, S.; Kim, C.-K. *Can. J. Chem.* **1991**, *69*, 1408.
325. Meyer, W. P.; Martin, J. C. *J. Am. Chem. Soc.* **1976**, *98*, 1231.
326. Krabbenhoft, H. O.; Wiseman, J. R. Quinn. C. B. *J. Am. Chem. Soc.* **1974**, *96*, 258.
327. Jonas, J.; Kratochvíl, M.; Mikula, J.; Pichler, J. *Coll. Czech. Chem. Commun.* **1971**, *36*, 202.
328. Sugawara, T.; Iwamura, H.; Ōki, M. *Tetrahedron Lett.* **1975**, *11*, 879.
329. Deslongchamps, P.; Taillefer, R. J. *Can. J. Chem.* **1975**, *53*, 3029.
330. Depmeier, W.; v. Voithenburg, H.; Jochims, C. J. *Chem. Ber.* **1978**, *111*, 2010.
331. Borgen, G.; Dale, J. *J. Chem. Soc. Chem. Commun.* **1974**, 484.
332. Anet, F. A. L.; Cheng, A. K.; Wagner, J. J. *J. Am. Chem. Soc.* **1972**, *94*, 9250.
333. Anet, F. A. L.; Krane, J.; Dale, J.; Daasvatn, K.; Kristiansen, P.O. *Acta Chem. Scand.* **1973**, *27*, 3395.
334. Wu, Y.-D.; Houk, K. N. *J. Phys. Chem.* **1990**, *94*, 4856.
335. Astrup, E. *Acta Chem. Scand.* **1973**, *27*, 327.
336. Gorenstein, D. G.; Kar, D. *J. Am. Chem. Soc.* **1977**, *99*, 672.
337. Palenik, G. J.; Koziol, A. E.; Katritzky, A. R.; Fan, W.-Q. *J. Chem. Soc. Chem. Commun.* **1990**, 715.
338. Rüchardt, C.; Beckhaus, H.-D. *Angew. Chem.* **1985**, *97*, 531; *Angew. Chem. Int. Ed. Engl.* **1985**, *24*, 529.
339. Taylor, R.; Kennard, O. *J. Am. Chem. Soc.* **1982**, *104*, 5063.
340. Juaristi, E.; Valenzuela, B. A.; Valle, L.; McPhail, A. T. *J. Org. Chem.* **1984**, *49*, 3026.
341. Pichon-Pesme, V.; Hansen, N. K. *J. Mol. Struct. (THEOCHEM)* **1989**, *183*, 151.
342. Koritsánszky, T.; Strumpel, M. K.; Buschmann, J.; Hansen, N. K.; Pichon-Pesme, V. *J. Am. Chem. Soc.* **1991**, *113*, 9148.

343. David, S. in Ref. 65, p.1.
344. McKelvey, R. D.; Kawada, Y.; Sugawara, T.; Iwamura, H. *J. Org. Chem.* **1981**, *46*, 4948.
345. Levy, G. C.; Nelson, G. L. *Caron-13 NMR for Organic Chemists*; Wiley-Interscience: New York, **1972**; Chapter 4.
346. Juaristi, E.; Aguilar, M. A. *J. Org. Chem.* **1991**, *56*, 5919.
347. Jennings, W. B.; Boyd, D. R.; Watson, C. G.; Becker, E. D.; Bradley, R. B.; Jerina, D. M. *J. Am. Chem. Soc.* **1972**, *94*, 8501.
348. Hricovini, M.; Tvaroška, I. *Magn. Res. Chem.* **1990**, *28*, 862.
349. Bailey, W. F.; Rivera, A. D.; Rossi, K. *Tetrahedron Lett.* **1988**, *29*, 5621.
350. Kalinowski, H.-O. In *Carbon-13 NMR Spectroscopy*; Berger, S.; Braun, S., Eds.; Wiley: New York, **1988**, p. 495.
351. Kitching, W.; Praeger, D.; Doddrell, D.; Anet, F. A. L.; Krane, J. *Tetrahedron Lett.* **1975**, 759.
352. Thiem, J.; Meyer, B.; Paulsen, H. *Chem. Ber.* **1978**, *111*, 3325.
353. Buchanan, G. W.; Bowen, J. H. *Can. J. Chem.* **1977**, *55*, 604.
354. Mikołajczyk, M.; Mikina, M.; Graczyk, P.; Wieczorek, M. W.; Bujacz, G. *Tetrahedron Lett.* **1991**, *32*, 4189.
355. Altona, C. *Tetrahedron Lett.* **1968**, 2325.
356. Allan, A.; McKean, D. C.; Perchard, J. P.; Josien, M. L. *Spectrochim. Acta Part A* **1971**, *27*, 1409.
357. Serrallach, A.; Meyer, R.; Günthard, Hs. H. *J. Mol. Spectrosc.* **1974**, *52*, 94.
358. (a) Bohlmann, F. *Angew. Chem*, **1957**, *69*, 641. (b) Bohlmann, F. *Chem. Ber.* **1958**, *91*, 2157.
359. Hamlow, H. P.; Okuda, S.; Nakagawa, N. *Tetrahedron Lett.* **1964**, *37*, 2553.
360. Krueger, P. J.; Jan, J.; Wieser, H. *J. Mol. Struct.* **1970**, *5*, 375.
361. Crabb, T. A.; Newton, R. F.; Jackson, D. *Chem. Rev.* **1971**, *71*, 109 and references therein.
362. Ernstbrunner, E. E.; Hudec, J. *J. Mol. Struct.* **1973**, *17*, 249.
363. Tamagake, K.; Tsuboi, M. *Bull. Chem. Soc. Jpn.* **1974**, *47*, 73.
364. Crabb, T. A.; Katritzky, A. R. *Adv. Heterocycl. Chem.* **1984**, *36*, 1.
365. Forsyth, D. A.; Prapansiri, V. *J. Am. Chem. Soc.* **1989**, *111*, 4548.
366. Mc Kean, D. C. *Chem. Soc. Rev.* **1978**, 7, 399.
367. Williams, I. H. *J. Chem. Soc. Chem. Commun.* **1986**, 627.
368. Wong, J. S.; MacPhail, R. A.; Moore, C. B.; Strauss, H. L. *J. Phys. Chem.* **1982**, *86*, 1478.
369. Langseth, A.; Bak, B. *J. Chem. Phys.* **1940**, *8*, 403.
370. Anet, F. A. L.; Kopelevich, M. *J. Am. Chem. Soc.* **1986**, *108*, 1355.
371. Anet, F. A. L.; Kopelevich, M. *J. Am. Chem. Soc.* **1986**, *108*, 2109.
372. Kreevov, M. M. *J. Chem. Educ.* **1964**, *41*, 636.
373. Guerrero, S. A.; Barros, J. R. T.; Wladislaw, B.; Rittner, R.; Olivato, P. R. *J. Chem. Soc. Perkin. Trans. 2* **1983**, 1053.
374. Juaristi, E.; Cuevas, G. *J. Am. Chem. Soc.* **1993**, *115*, 1313.
375. Juaristi, E.; Flores-Vela, A.; Labastida, V. *J. Org. Chem.* **1989**, *54*, 5191.
376. Latajka, Z.; Ratajczak, H.; Scheiner, S.; Barycki, J. *J. Mol. Struct. (THEOCHEM)* **1991**, *235*, 417.
377. Juaristi, E.; Valle, L.; Mora-Uzeta, C.; Valenzuela, B. A.; Joseph-Nathan, P.; Fredrich, M. F. *J. Org. Chem.* **1982**, *47*, 5038.

378. Mikolajczyk, M.; Balczewski, P.; Wróblewski, K.; Karolak-Wojciechowska, J.; Miller, A.; Wieczorek, M. W.; Antipin, M. Y.; Struchkov, Y. T. *Tetrahedron* **1984**, *40*, 4885.

379. Saunders, M.; Jiménez-Vázquez, H. A. *Chem. Rev.* **1991** *91*, 375.

380. Burling, F. T.; Goldstein, B. M. *J. Am. Chem. Soc.* **1992** *114*, 2313.

381. Santoyo-Gonzáles, F.; Molina-Molina, J.; Portal-Olea, D.; Vargas-Berenguel, A.; Martin-Ramos, J. D.; Romero-Garzón, J. *Tetrahedron* **1992**, *48*, 6839.

382. Desiraju, G. R. *Acc. Chem. Res.* **1991**, *24*, 290.

383. See also Mikołajczyk, M. *Phosphorus Sulfur and Silicon* **1993**, *74*, 311.

Unusual Saturated Hydrocarbons: Interaction between Theoretical and Synthetic Chemistry

HELENA DODZIUK

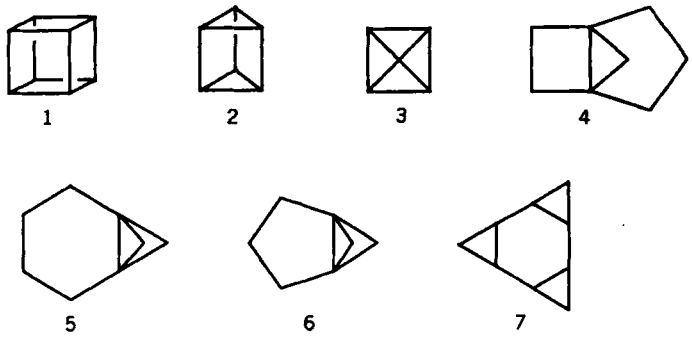
Institute of Organic Chemistry, Polish Academy of Sciences, Warsaw, Poland

I. Introduction
II. Molecules Possessing Inverted Carbon Atoms
III. Molecules with a Pyramidal Carbon Atom
IV. Molecules with a Planarized or Planar Cyclohexane Ring
V. Saturated Cage Compounds $C_{2n}H_{2n}$
  A. Tetrahedrane
  B. Triprismane
  C. C_8H_8-saturated Cage Compounds
    1. Cubane
    2. Octabisvalene **74a** and Cuneane **82**
  D. $C_{10}H_{10}$-saturated Cages: Pentaprismane **10** and diademane **57**
  E. $C_{12}H_{12}$-saturated Cage Molecules: Truncated Tetrahedrane **12**, Hexaprismane **13**, etc.
  F. [*n*]Prismanes and Higher Members of the $C_{2n}H_{2n}$ Family
VI. Future prospects
References

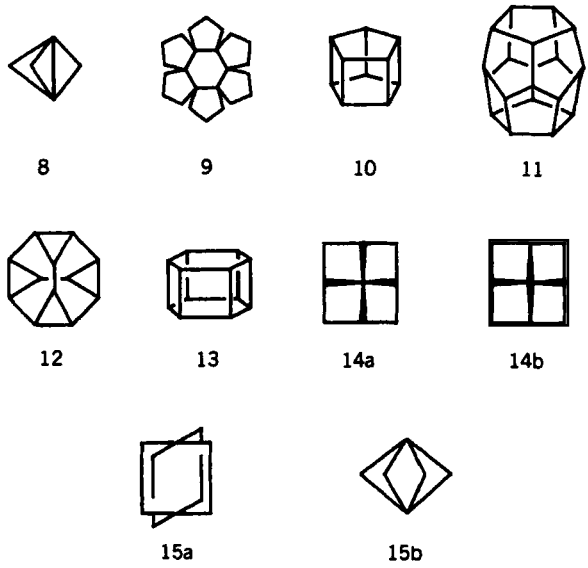
I. INTRODUCTION

From the time of van't Hoff (1) and Le Bel (2) the tetrahedral arrangement of substituents around a tetravalent carbon atom has been part of the foundation of organic stereochemistry. However, in the last 30 years, thanks to the rapid development of synthetic methods of organic chemistry as well as of experimental and theoretical methods of structure elucidation, many exciting saturated hydrocarbons with very unusual spatial structure have been synthesized. Cubane (1) was obtained as early as 1964 (3), triprismane (**2**) (4), a tetra-*t*-butyl derivative of tetrahedrane (**3**) (5), small-ring propellanes with structures involving inverted carbon atoms, **4**–**6** ([3.2.1], [4.1.1] and

Topics In Stereochemistry, Volume 21, Edited by Ernest L. Eliel and Samuel H. Wilen.
ISBN 0-471-52120-5 © 1994 John Wiley & Sons, Inc.



[3.1.1]) (6–8), and molecules possessing a planar cyclohexane ring such as *trans*-tris-σ-homobenzene (**7**) (9) were synthesized in the 1970s. During the 1980s, the search for new molecules possessing peculiar geometry continued with accelerating pace: the synthesis of small-ring propellanes reached its peak when [1.1.1]propellane (**8**) was obtained (10). [6.5]Coronane (**9**) (11), pentaprismane $C_{10}H_{10}$ (**10**) (12), and dodecahedrane $C_{20}H_{20}$ (**11**) (13) were synthesized and unsuccessful attempts at the synthesis of two interesting molecules of the same $C_{2n}H_{2n}$ group of saturated cage compounds, that is, of truncated terahedrane (**12**) (14) and of hexaprismane (**13**) (15) were reported. Many attempts have been also made to obtain [4.4.4.4] fenestrane (**14**) (16). The synthesis of this molecule and that of [2.2.2.2] paddlane (**15a**) seemed especially desirable since they were thought to possess a so-called planar



carbon atom, that is, an atom lying in the same plane with its four substituents (17b).

Why are such molecules worth studying? In addition to their aesthetic appeal and possible practical applications in the future, they are of great cognitive importance because of difficulties related to the definition of the chemical bond. Such a definition should cover not only standard bonds but should also describe H bonding (18), the bonding in supramolecular complexes (19), and that in van der Waals complexes (20), mesoionic compounds (21), and, last but not least, the highly distorted CC bonding in hydrocarbons with unusual spatial structure that are the subject of this short review. The question as to how far a bond can be distorted without being broken is fascinating and, in turn, evokes a second question as to the properties of such a distorted bond. These questions are not simple to answer since quantum chemistry (QC) correctly describes only the molecule as a whole. (Throughout this chapter QC will denote semiempirical and/or *ab initio* quantum chemical as opposed to molecular mechanics calculations.) The so-called Bader analysis (22) allows one to analyze the so-called bond path but does not resolve the difficulties in computing bond length. The difficulties with such a useful intuitive concept make studies of nonstandard molecules of great importance. The discussion concerning the strength, and even the existence, of the central bond in [1.1.1]propellane (**8**) (see Section II) illustrates serious conceptual problems, concerning the definition of a chemical bond, encountered when studying such unusual molecules. Publications dealing with these difficulties had a considerable impact on the theory of the chemical bond, showing ways to the solution of the problem. High symmetry and a well-defined, usually rigid structure also make studying such molecules expedient. For this reason they are well-suited both for theoretical calculations and for very accurate experimental measurements. In addition, such molecules provide an opportunity for checking empirical relations such as the Karplus equation (23).

As will be shown, theoretical calculations play an ever-increasing role in the quest for new and unusual systems. Elaborate quantum chemical *ab initio* calculations taking into account configuration interaction and involving big basis sets with full geometry optimization seem indispensable when accurate quantitative results are desired. Calculations for large and unusual molecules, such as those discussed in this chapter, are time consuming and beyond the possibility of most research groups. Moreover, it seems that even theoreticians having the appropriate *ab initio* computer programs and sufficient computational facilities at their disposal have not carried out calculations for this kind of molecule at sufficiently high levels of sophistication. On the other hand, the great importance of simpler theoretical studies cannot be overestimated. As will be shown in more detail, QC calculations for molecule **8**

(24, 28) can serve as a good example of the predictive power of theoretical studies. Similarly, numerous estimations of the energy required to planarize methane (17b, 35) triggered synthetic work in the field of [*k*, *l*, *m*, *n*] fenestranes (16) and paddlanes (25), despite the fact that a planar configuration at carbon atoms seems less stable than the pyramidal one and does not represent an energy minimum (17b). On the other hand, the existence and the properties of small-ring propellanes allowed one to check the predictive power of the theory. As mentioned earlier, the pertinent studies showed the conceptual limitations of interpreting quantum chemical results and of the definition of the chemical bond. The comparison of calculated results with experimental ones is crucial in the research under discussion; therefore, a few additional general comments may be of value:

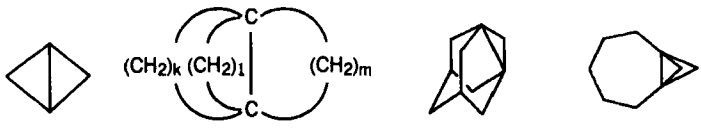
1. Experimental data for the molecules under investigation are often unavailable.
2. When available, these data sometimes refer not to the molecule of interest but to its derivatives (see below).
3. Experimental structure determinations are usually carried out by X-ray analysis in the solid state while the calculations usually refer to an isolated molecule.
4. The experimental results for bond lengths, bond angles, and so forth, depend on the technique [X-ray, microwave (MW), electron diffraction (ED) spectroscopy, etc.] used (26).

About 15 years ago Greenberg and Liebman published their extensive review article and book (27) on many unusual organic molecules. In their book *Nonclassical Structures of Organic Compounds*, Minkin et al. (17) discussed the results of quantum calculations for most of the molecules that are the subject of the present work as well as for many organic radicals and ions. Several review articles on the synthesis and properties of specific groups of compounds covered in this chapter have appeared. A few years ago a special issue of *Chemical Reviews* devoted to strained molecules appeared containing a review by Wiberg on small-ring propellanes (28), another one on cubane (29), another one dealing with the C_8H_8 family covering both saturated and unsaturated molecules of this general formula (30), and a review on bridged bicyclobutanes (31). Venepalli and Agosta (16) have discussed the syntheses of fenestranes, while Zipperer et al. (32) have summarized reactions of *cis*- and *trans*-tris-σ-homobenzenes, such as **7**, that possess planar cyclohexane rings. The synthetic routes to the aforementioned compounds have been discussed in these papers and their theoretical foundations described; but only in the Wiberg papers have the predictive power of QC calculations and the impact of theoretical considerations on the design and synthesis of an unsuaual

group of compounds (i.e., small-ring propellanes) been shown. Quantum chemical calculations were successfully used by him to predict the properties and the possibility of existence of [1.1.1]propellane **8**. The approach due to Wiberg is close to the one adopted in the present chapter, that is, the possibility of the existence of hydrocarbons possessing unusual spatial structure will be discussed on the basis of available experimental data and theoretical considerations. Contrary to the Wiberg work, our discussion will not be limited to quantum studies since recent molecular mechanics (MM) calculations by Dodziuk (33–37) summarized in a short review (38), as well as elegant studies by Osawa and co-workers (39–42), have revealed that the MM method (43) can also yield valuable information on the molecules under discussion. In addition to the influence of theory on the synthesis of molecules possessing unusual spatial structure, the impact of the existence and properties of these molecules on the development of theory, and in particular on the formulation of the concepts allowing one to describe and better understand chemical bonding in such systems, will be discussed. The interplay between theory and organic synthesis will be exemplified by the following groups of compounds molecules possessing inverted carbon atoms, "planar methane" molecules possessing pyramidal carbon atom, molecules possessing planarized and planar cyclohexane rings, and small saturated cage hydrocarbons of the general formula $C_{2n}H_{2n}$. Our aim is to show how synthetic work has stimulated theory, which, in turn, allows one today not only to rationalize existing experimental results but also to predict properties of hypothetical molecules and to propose plausible synthetic targets. In the presentation special emphasis will be placed on the MM method (43), whose predictive power appears not to have been sufficiently acknowledged. The domain of hydrocarbons with unusual three-dimensional structure is a rapidly growing field, and in spite of many partial reviews of relevant topics that have appeared recently, it is not possible to cover this topic exhaustively. Therefore, reactions of such molecules as well as the rapidly expanding domain of their noncarbon analogs will not be reviewed here.

II. MOLECULES POSSESSING INVERTED CARBON ATOM

According to Wiberg et al.'s definition (44), an inverted carbon atom is an atom having four of its substituents in one hemisphere. As pointed out by Dodziuk (35) in this definition no distinction was made between inverted and pyramidal atoms. To differentiate between them, inverted atoms should be defined as those having bond configuration obtained from the tetrahedral one by reversing the direction of one bond. Eight molecules of this type (**16**, **8**, **17a**, **17b**, **4**–**6**, and **18**) have been synthesized, [2.2.2]propellane (**17c**) being



16 17 a: k = 2, l = μ = 1 b: k = l = 2, m = 1 c: k = l = m = 2 18 19

the limiting case since its bridgehead atoms lie approximately in a plane with their three neighbors. In his latest review (28) Wiberg discussed the chemistry of small-ring propellanes and pointed out that the ease of formation, stability, structure, vibrational and photoelectron spectra, and enthalpy of formation of [1.1.1]propellane were all predicted prior to its preparation (10, 45). As stated earlier, the lack of a unique definition of a chemical bond in quantum mechanical descriptions of partial molecular properties resulted in vigorous discussions concerning the strength of the atypical central bond in **8** and even its existence was questioned on the basis of the calculations (46). The bond formed by two inverted atoms manifests its peculiarity in the lack of so-called deformation density (47) and the large difference in the out-of-plane component of the ^{13}C chemical shift of the methylene carbon atoms in comparison to bicyclobutane and cyclopropane (48). The analysis of charge density distribution in terms of bond and ring critical points (22), developed as a QC description of a chemical bond, allows one to understand better the unusual central bond in **8**. The evidence that this bond does exist is provided by Feller and Davidson's calculation (49) of the bridgehead C—H bond dissociation energy in bicyclopentane since the dissociation of the first bond requires 106 kcal/mol while for that of the second bond only 47 kcal/mol are needed.

Ab initio calculations using 6–31G* basis sets are thought to predict satisfactorily the geometries and enthalpies of formation of small-ring propellanes. d Orbitals on carbon are essential for proper description of such strained systems (22). But, despite remarkable achievements of such calculations (28), more experimental data to compare with are needed. In particular, experimental bond lengths in [2.2.2]propellane **17c** would be of interest as the corresponding QC values calculated at the SCF (self-consistent field) level exhibit a very unusual trend, the bridgehead–bridgehead bond being the shortest and the ethylene bridge bonds the longest (24). Molecular mechanics calculations (43) yielded the opposite, more plausible trend with the bridgehead–bridgehead carbons bond being longest. Among recent experimental studies of [1.1.1]propellane the analysis of its infrared intensities (50), that of ^{13}C–^{13}C coupling (51), and X-ray structure determination at 138 K (52) should be mentioned. Reactions of the molecule were discussed in (53).

Contrary to the results of earlier calculations cited in (28), a biradical character of [1.1.1]propellane was advocated by Murray et al. (54).

As stated earlier, in spite of considerable interest in hydrocarbons possessing inverted carbon atoms, only eight systems (**16**, **8**, **17a**, **17b**, **4**–**6**, and **18**) of this type are known. With the exception of bicyclobutane (**16**) they are all small-ring propellanes possessing symmetrical pairs of inverted atoms. In the course of the MM study of [*k.l.m*]propellanes (**17**), with *k*, *l*, *m* equal to 2–4 (55), four questions have arisen:

1. Are there propellanes possessing medium or large rings exhibiting inverted carbons?
2. Are there other types of molecules possessing inverted carbons?
3. Is there a possibility of existence of an asymmetric pair of inverted carbon atoms?
4. Is there a possibility of existence of an isolated inverted carbon in a molecule?

These questions have been discussed elsewhere (34). Simple stereometric consideration of the spatial relationships in [*n*.1.1]propellane ($n > 4$) using a few simplifying assumptions was used to show that such a molecule should possess inverted atoms independently on the value of *n*, and the MM calculation for [5.1.1]propellane (**19**) revealed that this molecule should not be excessively strained. Therefore, this molecule and higher [*n*.1.1]propellanes appear to be prospective synthetic targets yielding an infinite family of molecules with inverted carbons.

The extension of Paquette's idea (56) of fused bicyclics (called geminanes) to smaller molecules allowed Dodziuk (34) to propose a group of molecules **20**–**29** possessing inverted carbon atoms that differ from small-ring propellanes. Molecular mechanics calculations for the molecules revealed that molecules **20**–**23**, *cis*- and *trans*-**27**, the two stable *trans*-conformers of **28**, denoted as I and II, and the single conformer of *trans*-**29**, (denoted analogously as I) (57), should have inverted carbon atoms. There are symmetry related pairs of inverted carbons in molecules **21** and *cis*- and *trans*-**27**. The corresponding pairs in molecules **22**, **23**, and *trans*-**28**(I) are not symmetry related, and in molecules **20**, *trans*-**28**(I); *trans*-**29**(I) there is an isolated inverted carbon atom. In molecule **24** one of the bridgehead carbon atoms represents a limiting case similar to that found in molecule **17c**, that is, this atom and its three bridging neighbors lie approximately in a plane. The MM2 parametrization (58) used in the calculations (34) was developed on the basis of experimental results collected for hydrocarbons with standard spatial structure; nevertheless, the calculated values concerning energy and geometry apparently allow one to draw at least qualitative conclusions for the molecules under discussion.

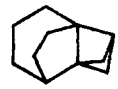

20

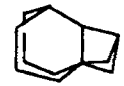
21

22

23


24

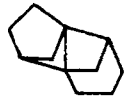

25


26


cis-27


trans-27


cis-28


trans-28


cis-29

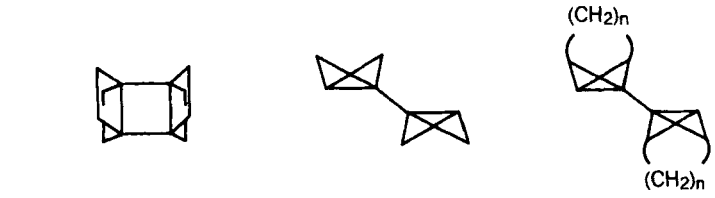

trans-29

In particular, they seem to indicate that the strain in molecules **20**–**29** is not large enough to preclude their synthesis. The synthesis of [1.1.1]geminane (**21**) and that of molecules **22**, **23**, and *trans*-**28**(I) would allow one to study the properties of a bond formed by inverted carbon atoms different from the central bond in small-ring propellanes while that of tricycloheptane **20** and *trans*-**28**(II) and *trans*-**29**(I) would provide the opportunity to analyze the bond between the carbon atoms with inverted and tetrahedral configuration of substituents, respectively.

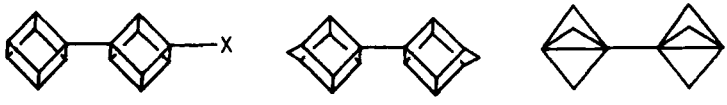
The possibility of the existence of a body-diagonal bond in 1,4-dehydrocubane (**50**), a prototype new molecule possessing inverted carbon atoms, has recently been discussed by Hassenrück et al. (59), Hrovat and Borden (60a), and Eaton and Tsanaktsidis (60b).

The existence of an interesting molecule (**30**) (61) with structure analogous to that of [2.2.2]propellane (**17c**) was proposed by Wiberg et al. (61), but in an attempted synthesis the authors were not able to detect it. Some other interesting propellanes without inverted carbon atoms will be mentioned in the next sections. Normal coordinate treatment with calculation of the infrared intensities of bicyclobutane (**16**) and of [1.1.1]propellane (**8**) was carried out

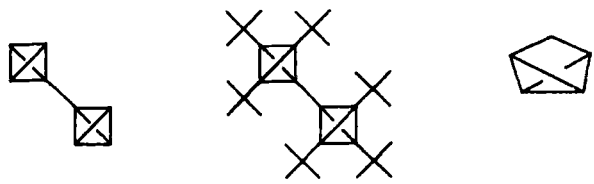
by Wiberg et al. (50). Among molecules having inverted carbon atoms, bicyclobutane (**16**) has attracted the least attention. Unusual contraction of the linking bond in the coupled bicyclobutanes **31** and **32**, analogous cubanes **33**, **34**, bicyclopentane **35**, and tetrahedranes **36**, **37** has been analyzed by Ermer et al. (62) and by Schleyer and Bremer (63).



30 31 32



33 a: X = H b: X = Br 34 35



36 37 38

The fact that bicyclobutane (**16**) also has an inverted carbon atom is sometimes overlooked, although its derivatives such as tricyclo[2.1.0.$0^{2,5}$]pentane (**38**) reviewed in (31) exhibit unusual patterns of electron density distribution analogous to that found in small-ring propellanes (47).

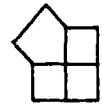
III. MOLECULES WITH A PYRAMIDAL CARBON ATOM

As already stated, Wiberg's definition of inverted carbon atoms is not limited to such atoms but includes also pyramidal ones. According to another concept by Minkin et al. (17) not only pyramidane (**39**) or pyramidal fenestrane (**14b**) but also cubane (**1**), triprismane (**2**), tetrahedrane (**3**), and the $(CH)_5^+$ cation

were treated as pyramidal structures. Dodziuk (35) has defined a pyramidal atom as one having pyramidal arrangements of bonds around it. No molecule with pyramidal or planar arrangement of bonds around a carbon atom is known, but the so-called planar methane problem has attracted considerable attention of both synthetic and theoretical organic chemists. Although calculations on methane varying from extended Hückel theory (EHT) (64a) to *ab initio* ones with basis set 6-31G* (65) and geometry optimization (discussed in 17b) as well as semiempirical calculations (64b) seemed to indicate that the pyramidal arrangement of bonds around a carbon atom was more stable than the planar one, most theoretical and experimental efforts in this domain were focused on molecules with the planar configuration at the carbon atom. Understandably, the results of the calculations for methane were limited both by the treatment of configuration interaction and by the quality of the basis sets used in the 1970s. Therefore, an extension of the Shavitt calculations (66) using 6-31G** and CI—so far carried out only for the planar configuration (which does not correspond to an energy minimum)—to the pyramidal configuration appears essential. Interesting studies of a molecule possessing the pyramidal configuration at a carbon atom were carried out by Minkin and Minayev (67) for pyramidane (**39**). The authors found that the pyramidal configuration of the central atom in the molecule should possess some kinetic stability. Its strain energy was calculated to be only 19 kcal/mol per C—C bond, thus, the molecule was considered a realistic synthetic target.



39



40



n = 10 – 14

41



42a



42b



42c

Although the estimates of the energy required to enforce planarity of tetrahedral methane differ from 95 to 250 kcal/mol (17b, 35), the theoretical discussion resulted in fruitful ideas concerning possible synthetic targets. The results of the calculations favoring pyramidal configuration at carbon over the planar one seems to have been overlooked, and the effort was focused mainly on obtaining the planar arrangement at a carbon atom. As a result, several exciting molecules have been synthesized, but none of them possessed either planar or pyramidal configuration at carbon.

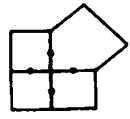
At first [4.4.4.4]fenestrane (**14**) was thought to possess a planar configuration at the central carbon atom and, as often happens, this erroneous idea inspired a lot of research on small-ring fenestranes. The calculations (STO-3G/6-31G* and 4-31G to second order in CI) by the Schulman group (68) revealed that out of two possible configurations at carbon, that is, the pyramidal one **14b** and the quasitetrahedral one **14a**, the former configuration is more stable by 48.3 kcal/mol. Despite massive synthetic efforts to synthesize [4.4.4.4]fenestrane (**14**) described in the Venepalli and Agosta review [16], [5.4.4.4]fenestrane (**40**) (69) is the smallest molecule synthesized in their series. In agreement with expectation, QC calculations by Würthwein, Schleyer et al. and by Wiberg (70) revealed that [1.1.1.1]- (**15b**) and [2.2.2.2]paddlane (**15a**) are prohibitively strained, and the smallest paddlanes known today are [n.2.2.2]paddlanes (**41**) with $n = 10, \ldots, 12$, synthesized by Eaton and Leipzig (25). Analyzing planarization at a tetravalent carbon atom and possible configurations of tetracyclo[4.2.1.$0^{2,9}$.$0^{5,9}$]nonane (**42**), Wiberg calculated [with a 3-21G basis set and full geometry optimization (71)] that the configuration with a pyramidal central atom, **42b**, is only 4 kcal/mol less stable than the most stable one. The calculated strain energies have been found to be quite large but somewhat smaller than that of [4.4.4.4]fenestrane (**14c**). Surprisingly, the author later only discussed possible synthetic routes to the most stable configuration **42a** and another one, **42c**, dismissing the pyramidal configuration **42b**, which was calculated by him to be 5 kcal/mol more stable than **42c**. It should be noted that the calculated energy differences between the isomers **42a, c** are certainly smaller than the limits of accuracy of the calculations. Therefore, the only practical conclusion of the calculations is that all three isomers are very close in energy, including **42b**—the one dismissed by Wiberg in spite of his belief in the predictive power of theoretical calculations.



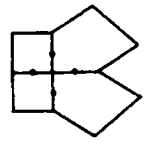
43



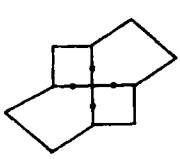
44



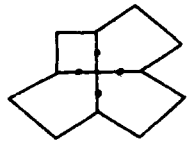
45



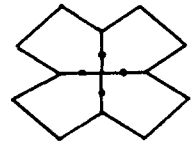
46



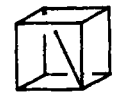
47



48



49

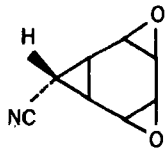


50

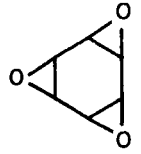
Bowlane (**43**) and some of its homologues **44**–**49** have been the first molecules possessing a pyramidal carbon atom in the ground state to be proposed as plausible synthetic targets on the basis of MM calculations (35). Work is in progress in this laboratory on other hypothetical molecules that should have pyramidal carbon atoms in the ground state.

IV. MOLECULES WITH A PLANARIZED OR PLANAR CYCLOHEXANE RING

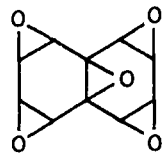
The tetrahedral arrangement of bonds around a tetravalent carbon atom implies chair or twist conformations for a cyclohexane ring; thus talking about molecules **51**–**53** and some complexes of **54** as having planar saturated six-membered rings (72–75) might make a student fail his exam! Cyclohexanes with flattened rings have been reviewed by Kellie and Riddell (76) and by Vereshchagin (77), but the existence of molecules with planar cyclohexane rings has been overlooked by stereochemists over many years. *trans*-Tris-σ-homobenzene (**55**) has been synthesized by Engelhardt and Lüttke (9) who claimed that the central ring in the molecule is planar. No sound argument in favor of this statement was given, but the nearly planar structure of its



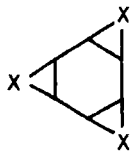
51



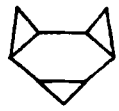
52



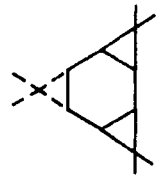
53



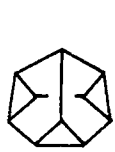
54



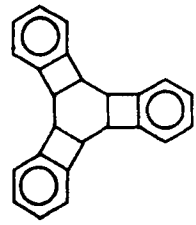
55



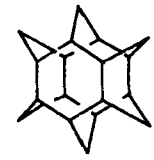
56



57



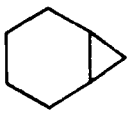
58



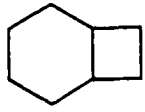
59

hexamethyl derivative **56** (78) seems to validate their claim. A planar cyclohexane ring was suggested by Spanget-Larsen and Gleiter (79) in their MNDO (minimum neglect of differential overlap) calculations and later in *ab initio* calculations by Schulman et al. (80) for diademane (**57**) (81, 82). Planar structures for the ring were also postulated, on the basis of molecular mechanics calculations, for hypothetical molecules **12** (37), **13** (83), and **59** (43b). As mentioned earlier, despite considerable synthetic efforts (14, 15), molecules **12** and **13** have not yet been synthesized; *ab initio* quantum calculations for them (84, 85) predict planar structures for the six-membered rings. Molecules **12**, **13**, and **57** belong to saturated cage compounds of the general formula $C_{2n}H_{2n}$ and, as such, will be discussed in the next section.

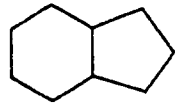
A planar central ring has also been found, by X-ray diffraction analysis, in the tribenzoderivative of tetracyclo[8.2.0^{2,5}.0^{6,9}]dodecane (**58**) (86). As will be shown, this result appears to be due to the action of crystal forces and not to reflect intrinsic properties of the system under investigation. The influence of *cis* fusion with a smaller ring on the planarization of a six-membered ring was systematically analyzed in (33) using molecular mechanics with MM2 parametrization (58). The sum of the absolute values of the torsion angles within the six-membered ring, $\sum\omega$, was chosen there as a measure of ring planarization. The calculation of steric energy and optimum



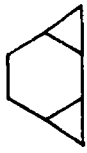
60



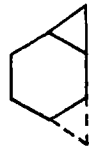
61



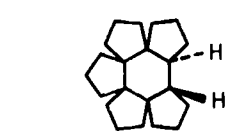
62



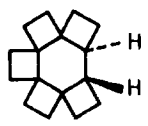
cis-63



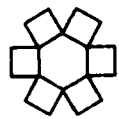
trans-63



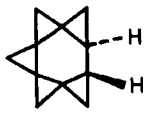
64



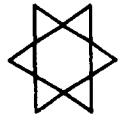
65



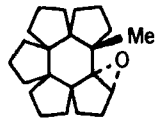
66



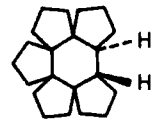
67



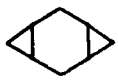
68



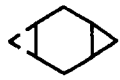
69



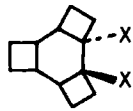
70



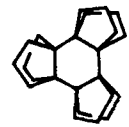
cis-71



trans-71



72a X = H
72b X = CN
cis
72c X = CN
trans



73

geometry was carried out for bicyclic molecules **60–62**, *cis-* and *trans*-tricyclooctane (**63**), for coronanes **9**, **66**, **68**, and their analogues lacking one ring: **64**, **65**, **67**. The dimethyl derivative **70** served as a model compound for **69**. The highly strained molecules **67** and **68** have been included in the series for the sake of completeness. Derivatives of incomplete coronanes **64**, **65** have been synthesized by Fitjer et al. (87) but, when the work (33) was started, [6.5]coronane (**9**) was not known. In the meantime, this molecule has been obtained by the same group (11), and its X-ray analysis has been carried out. Molecular mechanics calculations for some of these molecules had been performed earlier (88) but for different molecules using different force fields, therefore they had to be repeated for the sake of uniformity. On the other hand, the calculations for diademane (**57**) and *cis-* and *trans*-tricyclooctanes (**71**) have not been carried out in (33) since one of the torsional constants in the MM2 parametrization used seemed questionable (89).

As stated, the comparison of the calculated and experimental results is very difficult. Most of the molecules under investigation represent highly strained systems for which calculations parametrized for standard hydrocarbons might be of limited accuracy or even fail because minor inaccuracies in potential functions and/or parameters used, which do not impair results for less congested molecules, may influence those for highly strained systems.

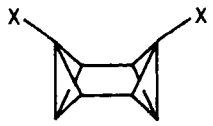
(Therefore, such calculations are also of value for detection of deficiencies and limitations of the method itself.) The problem of comparison is further complicated by the fact that the corresponding experimental data are scarce and often refer to solid-state X-ray measurements of derivatives of the molecules under investigation. This may be illustrated by the example of the experimental results for molecule **69**, which had to be compared with calculations for its simpler analog **70**. In cases where such a comparison could be carried out, the results of the calculations may be summarized as follows:

1. The method with MM2 parametrization yields reliable estimates of torsion angles and, therefore, seems suitable for the analysis of planarity of the cyclohexane ring.
2. MM2 performs poorly for bond lengths in highly congested systems.
3. Poor reproducibility of bond lengths and the condition for ring closure leads to incorrect values of bond angles.

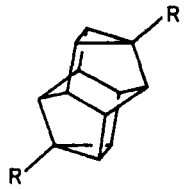
Therefore, the calculations called for a refinement of the MM2 force field, especially in the part describing the cyclopropane unit, and this gap has been filled recently by the Allinger group (89). The results of the calculations (33, 90) and the X-ray data for **72b** and **72c** (91a) strongly suggest that the central ring in **72a** must be flattened but is not planar. These results are in contradistinction to the planarity of the central ring in **58** established by X-ray analysis (86). The latter result can be understood only as the result of an imposition of crystal forces and not as a manifestation of the intrinsic properties of molecule **58**. X-ray analysis of the known molecule **72a** (91b) would be of value for clarification of the situation in **58**. Synthesis of an interesting molecule **73**, which according to MM2 calculations (11) should exhibit considerable planarization of the central ring ($\sum\omega = 232°$), is planned by Fitjer.

V. SATURATED CAGE COMPOUNDS $C_{2n}H_{2n}$

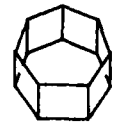
Discussion of $C_{2n}H_{2n}$ molecules leads back to the ancient Greeks since carbon skeletons of molecules **1**, **3**, and **11** (belonging to this group) are represented by ideal polyhedra: the cube, the tetrahedron, and the dodecahedron, respectively, discussed by Plato and Pythagoras (92). These molecules are formed by carbon atoms having three carbon and one hydrogen neighbor atoms. In spite of this restrictive condition, the number of isomers of such molecules rapidly grows with n. There is only 1 member of the group for $n = 2$ (**3**) and $n = 3$ (**2**), but there are 3 isomers for $n = 4$ (cubane (**1**), octabisvalene (**74a**), and cuneane (**82**)), 9 isomers for $n = 5$, 32 for $n = 6$, and



74a X = H
74b X = $SO_2C_6H_5$
74c X = Me



75a R = Me
75b R = H

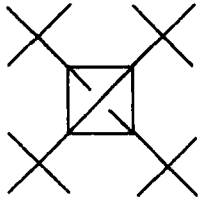


76

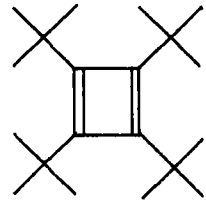
so on (93, 94). Only molecules **1** (3), **2** (4), **3** (5), **74** (94), **75** (95), **10** (12), and **11** (13) or their derivatives have been synthesized, and this group is a subject of constantly growing synthetic efforts. The possibility of the synthesis of **12**, **13**, and **76** has been intensely explored (14, 15, 37, 41, 84), and at the same time physicochemical studies of the known saturated cage molecules, especially cubane, are rapidly expanding. Within the group of compounds discussed one may consider a smaller group of [*n*]prismanes that has attracted considerable attention, the first members of which are triprismane (**2**), cubane (**1**), pentaprismane (**10**), hexaprismane (**13**), heptaprismane (**76**) ($n = 3, \ldots, 7$, respectively), and so on. There have been several studies of this group, which will be discussed in the following sections.

A. Tetrahedrane

Despite the highly unusual structure of tetrahedrane, **3**, the problem of its synthesis had been formulated more than 70 years ago (96). The first review article on tetrahedrane (97) appeared almost simultaneously with the paper describing the first synthesis of its tetra-*t*-butyl derivative **77** (5), which, until recently (98), remained the only tetrahedrane derivative known. On the basis of MM calculations using different force fields Hounshell and Mislow predicted *T* symmetry for **77** (99). Minkin et al. (17c) discussed the synthesis, reactions, and stability of **3** and **77** pointing out that high kinetic stability of the latter molecule is partly due to unfavorable steric repulsions in the



77



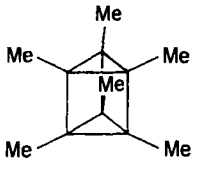
78

product of its rearrangement tetra-*t*-butyl-cyclobutadiene (**78**). Physicochemical studies of **77** have dealt with X-ray analysis of its crystal and molecular structure (100), spectral (101), and ^{13}C nuclear magnetic resonance (NMR) (102) studies. Numerous quantum chemical studies of **3** have ranged from MINDO/3 (103) to *ab initio* RMP2 calculations using a 6-31G* basis set (with full geometry optimization) by Schulman et al. (104). The latter authors have shown that for medium-sized hydrocarbons second-order correlation energies yield reasonable values of heats of formation (HOFs). Indeed, their calculated HOF value of 148.7 kcal/mol for cubane **1** is very close to the experimental one (as is the MM calculated value (36)], but calculated values for the most interesting molecules under study, that is, tetrahedrane **3** and dodecahedrane **11**, could not be checked against experiment because of the lack of the appropriate thermochemical data.

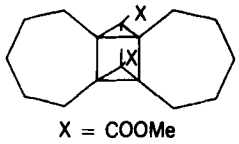
As mentioned earlier, coupled bicyclobutanes, bicyclocubanes, bicyclopentane, and bicyclotetrahedranes **31–37** analyzed by Ermer et al. and by Schleyer and Bremer (62, 63) exhibit remarkable shortening of the linking bond.

B. Triprismane

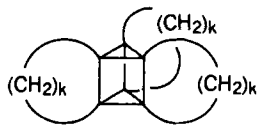
Known since 1973 (4), triprismane, also known as [3]prismane, (**2**) is the most stable of all valence isomers of benzene according to QC calculations by Schulman and Disch (105). The interaction diagram for molecular orbitals of **2** generated through π–π overlap of tangential σ-Walsh orbitals and through σ–σ overlap of π molecular orbitals of cyclopropenyl fragments calculated by the MINDO/3 method has been discussed by Minkin and Minayev (106, 17d). These authors considered this molecule and higher prismanes **1**, **10**, **13** as products of fusion of two identical annulene fragments and analyzed their stability. The molecules were found to exhibit high strain energy; nevertheless, high energy barriers for their transition to thermodynamically more stable isomers suggest that they should be quite stable. In spite of the relatively early synthesis of triprismane, it appears to have been little studied. Its geometry has not been determined, though that of its hexamethyl derivative **79** has been investigated (107). The extension of



79



80



81

the MM3 parametrization in molecular mechanics calculations to include the cyclopropane unit covered also the triprismane molecule (89). Gleiter and Treptow (108) have reported a synthesis of **80**, en route to propella[$\mathbf{n}_3$]prismanes (**81**).

C. C_8H_8-Saturated Cage Compounds

1. Cubane

Because of its high symmetry, cubane (**1**) has attracted great interest on the part of both theoreticians and experimentalists, and it is probably the most often studied molecule among those discussed in this review. Calculations on **1** (cited in ref. 29) have allowed one to better understand the remarkable stability of cubane (despite its unusually high strain). It is interesting that, in contrast to the results for other molecules discussed in this chapter, these theoretical studies [the MM studies by the Osawa group (39, 40) being an exception] had no immediate impact on synthetic work. The synthesis and chemistry of cubane has been recently reviewed by Griffin and Marchand (29). This review includes concise but very informative sections, "Spectral and Physical-Organic Studies of Cubanes" and "Theoretical Studies of Cubanes." Another recent review of consequences of strain in $(CH)_8$ hydrocarbons (30) covered both saturated and unsaturated molecules and dealt mainly with their reactivity. Therefore, in the following we shall limit the discussion to recent studies pertaining to the molecule and to the very interesting publications by the Osawa group (39, 40) mentioned earlier.

Hedberg et al. (109) combined an electron diffraction study of **1** in the gas phase at 77°C with microwave rotational constants (110) for cubane-d_1 to resolve the discrepancies between the equilibrium bond lengths in the molecule as determined by X-ray (111) and electron diffraction (ED) (112) and to determine a quadratic force field for the molecule. In the crystal the average C—C bond length was equal to 1.551(3) Å, the ED study yielded r_a(CC) value of 1.575(1) Å while the microwave (MW) spectrum of monodeuterated cubane led to the result r_0(CC) = 1.5708 Å. The corresponding r(CH) values are equal to 1.03(5), 1.100(6) and 1.097 Å. The discussion in the study by Hedberg et al. clearly illustrates the difficulties encountered in a comparison of experimental results obtained by modern experimental and theoretical methods (26). The use of combined ED–MW data with allowance for multiple scattering allowed the authors to estimate the equilibrium value r_e(CC) as 1.5618(40) Å and that of r(CH) as 1.0960(130) Å. A comparison of the equilibrium bond lengths (with estimated effects of molecular vibrations) with the calculation revealed that the r_e(CC) values from MINDO/3 (113) and from the *ab initio* studies with the 6-31G* and the STO-3G (114) basis sets

were in good agreement with this experimentally derived result for r_e(CC). Molecular mechanics calculations (36, 115) yielded reasonable values for the bond lengths and excellent agreement with the experimental value of the heat of formation [experimental, 148.7 kcal/mol (116); calculated, 148.9 kcal/mol].

An interesting study of the products of cubane hydrogenolysis was published by Stober, Musso and Ōsawa (39). In this reaction the authors found [2.2.2]bicyclooctane (**83**) to be the main product; tetracyclo[4.2.0.0^{2,5}.0^{3,8}]-octane (**84**) and tricyclo[4.2.0.0^{2,5}]octane (**85**) were identified as intermediates. The experimental findings have been rationalized by means of MM study of possible products of the reaction. It should be stressed that MM is mainly used to determine spatial structure and strain of organic molecules, and the method is seldom applied to explain the reactivity and course of reactions as has been done by the Osawa group.



82



83

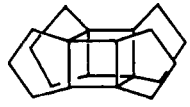


84

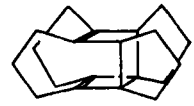


85

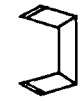
A combined AM1 (Austin Model 1) and MM study of an interesting cubane derivative, propella[3$_4$]prismane (**86**), was also carried out by Osawa's group (40). The molecule was synthesized by Gleiter and Karcher (117) by a $[\pi^2 + \pi^2]$ photochemical ring closure of *syn*-tricyclo[4.2.0.0^{2,5}]octa-3,7-diene (**87**). The course of the reaction was unclear in view of the failure of the same reaction on tricyclooctadiene **88** to give cubane (118). The analysis by Osawa's group (39, 40) revealed that the reaction **88** → **1** involves a prohibitively large increase in strain and that the ordering of the frontier molecular orbitals governed by the double bond–double bond distance is



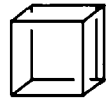
86



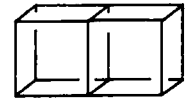
87



88



89



90

the most important factor in the reaction. Potential energy calculations by MM2 indicated that the trimethylene bridges in **86** are so flexible that they should appear flat on the NMR time scale. This is in accordance with the ^{13}C NMR spectra (117), which exhibit only 3 signals compatible either with D_{4h}, C_{4h}, and/or D_{2h} structures or an equilibrium mixture of low-energy conformers that averages to these symmetries. An X-ray analysis (59) of the 4-bromobicubyl structure **33b** [synthesized by Eaton's group (119)] indicates a very short length of the C—C bond linking the two cubane moieties, analogous to that found for dibicyclobutanes **31**, **32**, bitetrahedranes **36**, **37**, and the molecules **34**, **35** discussed earlier (62, 73). In references 59 and 60 the possibility of a diagonal bond in cubane yielding **50** with two pyramidal carbon atoms was studied. Cubene (**89**) lies outside the scope of this review, but its successful synthesis (120) merits acknowledgment. The possibility of a synthesis of the highly strained face-fused dicubane (**90**) was recently explored (121). The calculations on cubane have been also used for a study of new computational techniques by Stanton and co-workers (122). ^{1}H and ^{13}C NMR spectra of cubane derivatives have been recently reported by Axenrod et al. (123). Both *ab initio* (114) and MM calculations (36) with the MM2 parametrization (58) reproduced the experimental value of 148.7 kcal/mol (116) for the heat of formation of cubane very accurately.

2. *Octabisvalene* **74a** *and Cuneane* **82**

There are only a few studies of these molecules (30, 36, 124). They have been summarized in a review (30) together with those of unsaturated members of the C_8H_8 family. All but one of the semiempirical quantum chemical studies quoted in Table 1 of the review yielded cubane (which is [4] prismane) as the most strained member of the family. Except in ref 36, the existence of inverted carbon atoms (the bridgehead ones in the bicyclobutane units) in the octabisvalene molecule has been overlooked. There is no agreement in the literature concerning the relative stability of cuneane and octabisvalene. As mentioned earlier, the experimental determination and *ab initio* calculation have been carried out only for **1**; thus, more experimental measurements and further *ab initio* calculations for molecules **76a** and **83** are necessary.

D. $C_{10}H_{10}$-Saturated Cages: Pentaprismane 10 and Diademane 57

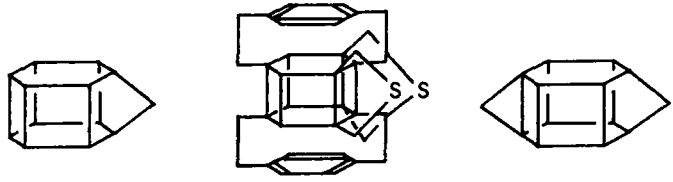
Only these two members out of nine possible saturated isomers of this family have been synthesized. Pentaprismane has been synthesized in the Eaton group (12). Its physicochemical studies have been limited to the measurements of photoelectron spectra (125). As mentioned earlier, the interaction diagrams for molecular orbitals of [3] prismane (**2**) and higher prismanes **1**, **10**, **13**

have been analyzed by Minkin et al. (106, 17d), while the results of theoretical calculations on the [*n*]prismane series will be discussed in the last section of this chapter. The synthesis of diademane has been described by Spielmann, de Meijere et al. (82) and that of this aza analog by Prinzbach's group (126). The parent molecule was foreseen to possess a planar cyclohexane ring by MINDO/3 calculations by Spanget-Larsen and Gleiter (79); it belongs to the group of molecules discussed in the next chapter of this volume. The same conclusion concerning planarity has been reached by Schulman et al. (80) (who overlooked that the molecule had been synthesized and studied prior to their work) on this basis of *ab initio* calculations.

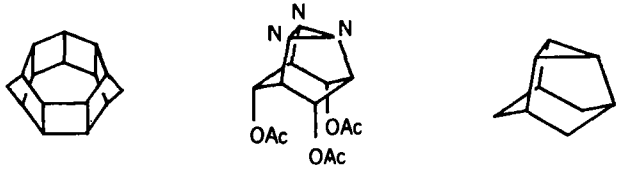
E. $C_{12}H_{12}$-Saturated Cage Molecules: Truncated Tetrahedrane 12, Hexaprismane 13, etc.

Both **12** and **13** have long been searched for; but no successful syntheses have been reported (14, 15a), and the synthesis of a derivative of another member of the $C_{12}H_{12}$ family, **75b** (95), has remained unnoticed. Ecohexaprismane (**91**) has been obtained by Mehta and Padma (127), but an attempt to synthesize hexaprismane as a part of a larger system **92** proved unsuccessful (15b). An MM study of the influence of strain energy on the photochemical $[\pi^2 + \pi^2]$ cage cyclization leading to hexaprisma ıe was published by Mehta et al. (41a). Analogous calculations on 1,4-bishomo[6]prismane (**93**) (42) allowed the authors to propose demethylenation of the latter molecule and of 1,4-bis-homo[7] prismane (**94**) as a potential synthetic route to [6] and [7] prismanes.

According to MM calculations (37, 41a, 128) **13** is expected to possess planar cyclohexane rings; thus it belongs also to the group discussed in the



91 92 93

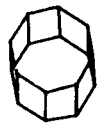


94 95 96

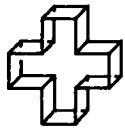
next section. On the other hand both MM (37) and QC calculation (85b) predict T_d symmetry for truncated tetrahedrane (**12**). Vibrational frequencies have been calculated in the latter study (85b) to confirm kinetic stability of this highly symmetrical form of the molecule under investigation. The agreement between the calculated values of heat of formation by two methods is satisfying [ca. 91 kcal/mol by QC calculations (85a) and ca. 87 kcal/mol by the MM method (37)]. Quantum chemical calculations on **13** (84, 129) have been carried out on the assumption of D_{6h} symmetry implying planarity of the six-membered rings. It should be stressed that not all saturated $C_{12}H_{12}$ isomers have been studied. Dodziuk and Nowinski (37) have studied several of them but have discussed only the results obtained for **12**, **13**, and **75b**. In addition to the QC calculations for unsaturated members of the $C_{12}H_{12}$ family, such calculations have been carried out for molecules **12**, **13** and **75b** by Schriver and Gerson (129). The same energy ordering was found by two groups, but the calculated energy difference between **75b** and **12** was larger in the QC calculations. The general conclusion of both calculations is that hexaprismane is the least stable of the molecules studied and heptacyclo[6.4.0.0^{2,4}.0^{3,7}.0^{5,12}.0^{6,10}.0^{9,11}]dodecane (**75b**) is the most stable one. Both groups have overlooked the reported synthesis of molecule **75a** and they predicted **75b** to be the most easily accessible synthetic target in the $C_{12}H_{12}$ family. According to the MM calculations (37), the latter molecule should exhibit considerable deformation of the central cyclohexane ring toward larger puckering with the value of the C–C–C–C torsional angles ϕ within the six-membered ring equal to 75.2°. The agreement between the experimental result for **95** (130) and the calculated MM value for the hydrocarbon analog **96** (131) support the calculated large value of the ω angle in **75b**. This result seems to indicate that the MM method is capable of reproducing not only the planarization of a six-membered ring (as shown in the next section) but also deformations of this ring toward greater puckering.

F. [*n*]Prismanes and Higher Members of the $C_{2n}H_{2n}$ Family

In addition to the information on specific lower prismanes, a few existing studies on higher prismanes and on the whole family should be mentioned. Photochemical reactions leading to [7]prismane analogues have been explored experimentally and by MM2 calculations by Mehta et al. (41b). A D_{4d} structure has been proposed for [8]prismane (**97**) by Reddy and Jemmis (128) while Jemmis et al. (132) and Miller and Schulman (84) on the basis of MNDO and AMI calculations argued at the semiempirical level that this structure is not a local minimum. The calculation of geometries and vibrational frequencies of [*n*]prismanes ($n = 3, \ldots, 9$) has been carried out by Disch and Schulman (84) under D_{nh} symmetry constraint using STO-3G, 3-21G, and 6-31G* basis



97



98



99

sets together with a RMP2 computation. Both heats of formation and strain energies yielded pentaprismane (**10**) as the most stable molecule within the series followed by triprismane (**2**) and cubane (**1**) (HOFs equal to 119.6, 136.4, and 148.5 kcal/mol, respectively). After that, the values increase considerably with increase of *n*. The values calculated for hexaprismane (**13**) by means of QM (84) and MM (37) methods differ considerably (153.1 kcal/mol by the former and 129.2 kcal/mol by the latter), but the direction of the differences underlines the conclusion based on the MM calculations (37) namely that, for a given *n*, [*n*]prismanes seem to be among the least stable isomers within a $C_{2n}H_{2n}$ family of saturated cage compounds. Dodecahedrane (**11**), which also belongs to the family, will not be covered here, but two highly hypothetical molecules, israelane (**98**) and helvetane (**99**), deserve mentioning. Following a jocular idea of A. Eschenmoser they were proposed by Ginsburg in the April 1 issue of the *Nouveau Journal de Chimie* (133). Nevertheless, some theoretical groups have studied them (134, 135) coming to the conclusion that helvetane, being only slightly less stable than [12]prismane, may be capable of existence. We believe, however, that QC calculations [84] and MM studies (36, 37) on prismanes suggest that higher prismanes are not promising synthetic targets and that the study of molecules **98** and **99** will probably remain a theoretician's exercise.

VI. FUTURE PROSPECTS

The domain of "unnatural chemistry" (136) will undoubtedly flourish in the future. Synthesis of molecules with a pyramidal carbon atom proposed in (17b, 35, 137) seems to be the greatest challenge in this field. Proposals of new types of molecules other than propellanes that should have inverted carbon atoms (34, 59, 60) seem promising. [6.4]Coronane (**66**), the fascinating tripropellacyclohexane (**73**), and other molecules having highly planarized cyclohexane ring still await their synthesis in the Fitjer group. Massive synthetical and theoretical efforts by Mehta, Osawa et al. (41) may eventually yield the highly desirable hexaprismane (**13**), but the synthesis of [7]prismane (**76**) appears less probable. Synthesis of new derivatives of tetrahedrane (**3**) and that of the highly symmetrical molecule of truncated tetrahedrane (**12**) will certainly be the subject of a large research effort. Hetero analogues of the

strained hydrocarbons have not been discussed in this study, but both theoretical and experimental studies of their properties will undoubtedly be carried out intensively as witnessed by recent publications (138). Physicochemical studies of most of the molecules discussed in this chapter are not known or are incomplete. In particular, experimental heat of formation values are missing for most (139) and experimental thermochemical studies are a must. The small usually highly symmetrical molecules discussed in this chapter are often used for parametrization purposes. They also provide a unique opportunity for comparison of the geometric parameters obtained by different experimental techniques, allowing one to derive equilibrium bond lengths and angles. Therefore, accurate structure determinations involving different experimental techniques such as the one recently carried out for cubane (109) will certainly follow for other molecules analyzed here. The rigid structure of $C_{2n}H_{2n}$ molecules will be especially useful for establishing and checking Karplus-type relations (23). The physicochemical studies will have to be accompanied by QC and MM calculations indispensable for hypothetical molecules especially those for which experimental results are very difficult or impossible to obtain. "Dry" chemistry, that is, computational chemistry, nowadays has enormous impact on "wet" chemistry. On the other hand, future syntheses of the aforementioned molecules and determination of their physicochemical properties will allow further development of theory. In particular, the MM parameters will be refined, thereby enabling quantitative studies of hydrocarbons with unusual three-dimensional structure. Further insight will undoubtedly be gained, making possible comparison of molecular parameters obtained by different experimental techniques and quantum chemical calculations. Even though many of the molecules discussed have presently no practical applications, their importance for theory and their interesting features foreshadow a rapidly growing development in the field of saturated hydrocarbons with unusual spatial structure in the future.

Compound **75b** has been synthesized recently (140) and its X-ray structure (141) yielded a value of 76° for the puckering angle in the central cyclohexane unit. This value is in good agreement with that predicted on the basis of the MM calculations discussed in this review. On the other hand, analogous calculations for tricyclo[4.1.0.$0^{1,3}$]heptane reported in ref. 89 yielded a pyramidal configuration of the central spiro atom. This result disagrees with the experimental finding (142).

REFERENCES

1. van't Hoff, J. H. *Arch. Nederl. Sci. Exactes Nat.* **1874**, 445, translated in *Classics in the Theory of Chemical Combinations*; Benfey, O. T.; Ed.; Dover: New York, 1963; pp. 151–157. The

van't Hoff idea was met with fierce opposition by many organic chemists as can be seen from the Kolbe statement: "A Dr J. H. van't Hoff, of the Veterinary School of Utrecht, has no liking, apparently, for exact chemical investigation. He has considered it more comfortable to mount Pegasus (apparently borrowed from the Veterinary School) and to proclaim in his *La Chimie dans l'espace* how the atoms appear to him to be arranged in space, when he is on the chemical Mt. Parnassus which he has reached by bold flight." (Kolbe, H. *J. Prakt. Chem.* **1877**, *15*, 473, cited in Riddell, F. G.; Robinson, M. J. T.) *Tetrahedron* **1974**, *30*, 2001–2007.

2. LeBel, J. A. *Bull. Soc. Chim. Fr.* **1874**, *22*, 337, translated in *Classics in the Theory of Chemical Combinations*, Benfey, O. T., Ed.; Dover: New York, 1963, pp. 151–157.
3. Eaton, P. E.; Cole, T. W. Jr. *J. Am. Chem. Soc.* **1964**, *86*, 962–964; 3157–3158.
4. Katz, T. J.; Acton, N. *J. Am. Chem. Soc.* **1973**, *95*, 2738–2739.
5. Maier, G.; Pfriem, S.; Schäfer, U.; Matusch, R. *Angew. Chem.* **1978**, *90*, 552–553; *Angew. Chem. Int. Ed. Engl.* **1978**, *17*, 520–521.
6. Wiberg, K. B.; Burgmaier, G. J.; Shen, K.; LaPlaca, J.; Hamilton, W. C.; Newton, M. D. *J. Am. Chem. Soc.* **1972**, *94*, 7402–7406.
7. Szeimies-Seebach, U.; Szeimies, G.; van Meersche, M.; Germain, G.; Declercq, J.-P. *Nouv. J. Chim.* **1979**, *3*, 357–358.
8. Declercq, J.-P.; Germain, G.; van Meersche, M. *Acta Crystallogr.* **1978**, *34B*, 3472–3474.
9. Engelhard, M.; Lüttke, W. *Angew. Chem.* **1972**, *84*, 346–347; *Angew. Chem. Int. Ed. Engl.* **1972**, *11*, 310–311.
10. Wiberg, K. B.; Walker, F. H. *J. Am. Chem. Soc.* **1982**, *104*, 5239–5240.
11. Wehle, D.; Schormann, N.; Fitjer, L. *Chem. Ber.* **1988**, *121*, 2171–2177.
12. Eaton, P. E.; Or, Y. S.; Branca, S. J. *J. Am. Chem. Soc.* **1981**. *103*, 2134–2136.
13. Ternansky, R. J.; Balogh, D. W.; Paquette, L. *J. Am. Chem. Soc.* **1982**, *104*, 4503–4504.
14. Brousseau, R. J. Ph.D. thesis, Harvard University, *Diss. Abstr. Int.* **1977**, *B37*, 6123b.
15. (a) Vedejs, E.; Shepherd, R. A. *J. Org. Chem.* **1976**, *41*, 742–743; Vedejs, E.; Wilber, W. R.; Twieg, R. *J. Org. Chem.* **1977**, *42*, 401–409. (b) Higuchi, H.; Kobayashi, E.; Sakata, Y.; Misumi, S. *Tetrahedron* **1986**, *42*, 1731–1739.
16. Venepalli, B. R.; Agosta, W. C. *Chem. Rev.* **1987**, *87*, 399–410.
17. (a) Minkin, V. I.; Minayev, R. M.; Zhdanov, Yu. A. *Nonclassical Structures of Organic Compounds*, Mir: Moscow, 1987. (b) Ref. 17a, p. 249. (c) Ref. 17a, p. 68. (d) Ref. 17a, p. 179.
18. Symposium; "Horizons in Hydrogen Bond Research 1989," *J. Mol. Struct.* **1990**, 237.
19. Vögtle, F. *Supramolecular Chemistry*, Wiley: New York, 1991.
20. Van der Avoird, A.; Wormer, P. E. S.; Mulder, F.; Berns, R. M. *Van der Waals Systems*; Top. Curr. Chem., Vol. 93; Springer-Verlag, Berlin, 1981, p. 1; Hobza, P.; Zahradník, R. *ibid.*, p. 53.
21. Newton, C. G.; Ramsden, C. A. *Tetrahedron* **1982**, *38*, 2965–3011.
22. Wiberg, K. B.; Bader, R. F. W.; Lau, C. D. H. *J. Am. Chem. Soc.* **1987**, *109*, 985–1000, *1001–1012*.
23. Karplus, M. *J. Chem. Phys.* **1959**, *30*, 11–15; *J. Phys. Chem.* **1960**, *64*, 1793–1798; *J. Am. Chem. Soc.*, **1963**, *85*, 2870–2871; Imai, K.; Osawa, E. *Tetrahedron Lett.* **1989**, *30*, 4251–4254.
24. Wiberg, K. B. *J. Am. Chem. Soc.* **1983**, *105*, 1227–1233.
25. Eaton, P. E.; Leipzig, B. D. *J. Am. Chem. Soc.* **1983**, *105*, 1656–1658.
26. Hargittai, I.; Hargittai, M. "The Importance of Small Structural Differences," In *Molecular Structure and Energetics*; Vol. 2; Liebman, J. F.; Greenberg, A. Eds.; VCH Publishers: New York, 1987, pp. 1–35.

27. (a) Liebman, J. F.; Greenberg, A. *Chem. Rev.* **1976**, *76*, 311–365. (b) Liebman, J. F.; Greenberg, A. *Strained Organic Molecules*, Academic Press: New York, 1978.
28. Wiberg, K. B. *Chem. Rev.* **1989**, *89*, 975–983.
29. Griffin, G. W.; Marchand, A. P. *Chem. Rev.* **1989**, *89*, 997–1010.
30. Hassenrück, K.; Martin, H.-D.; Walsh, R. *Chem. Rev.* **1989**, *89*, 1125–1146.
31. Dowd, P.; Irngartinger, H. *Chem. Rev.* **1989**, *89*, 985–996.
32. Zipperer, B.; Müller, K. H., Gallenkamp, B.; Hildebrand, R.; Fletschinger, M.; Burger, D.; Pillat, M.; Hunkler, D.; Knothe, L.; Fritz, H.; Prinzbach, H. *Chem. Ber.* **1988**, *121*, 757–780.
33. Dodziuk, H. *Bull. Chem. Soc. Jpn.* **1987**, *60*, 3775–3779.
34. Dodziuk, H. *Tetrahedron* **1988**, *44*, 2951–2955.
35. Dodziuk, H. *J. Mol. Struct.* **1990**, *239*, 167–172.
36. Dodziuk, H. *Bull. Pol. Acad. Scie., Chem.* **1990**, *38*, 11–15.
37. Dodziuk, H.; Nowinski, K. *Bull. Pol. Acad. Scie., Chem.* **1987**, *35*, 195–198.
38. Dodziuk, H. *Wiad. Chem.* **1991**, *45*, 667–687.
39. Stober, R.; Musso, H.; Ōsawa, E. *Tetrahedron* **1986**, *42*, 1757–1761.
40. Osawa, E.; Rudzinski, J. M.; Xun, Y.-M. *Struct. Chem.* **1990**, *1*, 333–344.
41. (a) Mehta, G.; Padma, S.; Ōsawa, E.; Barbiric, D. A.; Mochizuki, Y. *Tetrahedron Lett.* **1987**, *28*, 1295–1298. (b) Mehta, G.; Padma, S.; Jemmis, E. D.; Leela, G.; Osawa, E.; Barbiric, D. A. *Tetrahedron Lett.* **1988**, *29*, 1613–1616.
42. Ōsawa, E.; Barbiric, D. A.; Lee, O. S.; Kitano, Y.; Padma, S.; Mehta, G. *J. Chem. Soc. Perkin Trans. 2* **1989**, 1161–1165.
43. Allinger, N. L.; *Adv. Phys. Org. Chem.* **1976**, *13*, 1–82. (b) Osawa, E.; Musso, H. *Angew. Chem.* **1983**, *95*, 1–12; *Angew Chem. Int. Ed. Engl.* **1983**, *22*, 1–12.
44. Wiberg, K. B.; Hiatt, J. E.; Burgmaier, G. J. *Tetrahedron Lett.*, **1968**, 5855–5857.
45. Wiberg, K. B.; Dailey, W. P.; Walker, F. H.; Waddell, S. T.; Crocker, L. S.; Newton, M. *J. Am. Chem. Soc.* **1985**, *107*, 7247–7257.
46. Politzer, P.; Jayasuriya K. *J. Mol. Struct.* **1986**, *135*, 245–252; Pierini, A. B.; Reale, H. F.; Medrano, J. A. *J. Mol. Struct.* **1986**, *148*, 109–118.
47. Chakrabarti, P.; Seiler, P.; Dunitz, J. D.; Schlüter, A.-D.; Szeimies, G. *J. Am. Chem. Soc.* **1981**, *103*, 7378–7380.
48. Orendt, A. M.; Facelli, J. C ; Grant, D. M.; Michl, J.; Walker, F. H.; Dailey, W. P.; Waddell, S. T.; Wiberg, K. B.; Schindler, M.; Kutzelnigg, W. *Theor. Chim. Acta* **1985**, *68*, 421–430.
49. Feller, D.; Davidson, E. R. *J. Am. Chem. Soc.* **1987**, *109*, 4133–4139.
50. Wiberg, K. B.; Waddell, S. T.; Rosenberg, R. E. *J. Am. Chem. Soc.* **1990**, *112*, 2184–2194.
51. Jarret, R. M.; Cusumano, L. *Tetrahedron Lett.* **1990**, *31*, 171–174.
52. Seiler, P. *Helv. Chim. Acta* **1990**, *73*, 1574–1585.
53. Wiberg, K. B.; Waddell, S. T. *J. Am. Chem., Soc.* **1990**, *112*, 2194–2216.
54. Murray, J. S.; Seminario, J. M.; Politzer, P.; Sjoberg, P. *Int. J. Quant. Chem., Symp.* **1990**, *24*, 645–653.
55. Dodziuk, H. *J. Comput. Chem.* **1984**, *5*, 571–575.
56. Paquette, L. A.; Park, H. P.; King, P. F. *J. Chem. Res. (S)* **1980**, 296.
57. For the molecules *trans*-**28** and *trans*-**29** two stable conformers I and II, very close in energy, have been found.
58. Allinger, N. L.; Yuh, Y. H. "Operating Instructions to the MM2 and MMP2 Programs, updated as of January 1980," University of Georgia, Athens, GA.

59. Hassenrück, K.; Radziszewski, J. G.; Balaji, V.; Murthy, G. S.; McKinley, A. J.; David, D. E.; Lynch, V. M.; Martin, H.-D.; Michl, J. *J. Am. Chem. Soc.* **1990**, *112*, 873–874.
60. (a) Hrovat, D. A.; Borden, W. T. *J. Am. Chem. Soc.* **1990**, *112*, 875–876. (b) Eaton, P. E.; Tsanaktsidis, J. *J. Am. Chem. Soc.* **1990**. *112*, 876–878.
61. Wiberg, K. B.; Matturro, M. G.; Okarma, P. J.; Jason, M. E. *J. Am. Chem. Soc.* **1984**, *106*, 2194–2200.
62. Ermer, O.; Bell, P.; Schäfer, J.; Szeimies, G. *Angew. Chem.* **1989**, *101*, 503–506; *Angew. Chem., Int. Ed. Engl.* **1989**, *28*, 473–475.
63. Schleyer, P. v. R.; Bremer, M. *Angew. Chem.* **1989**, *101*, 1264–1266; *Angew. Chem., Int. Ed. Engl.* **1989**, *28*, 1226–1228.
64. (a) Hoffmann, R.; Alder, R. W.; Wilcox, C. F., Jr. *J. Am. Chem. Soc.* **1970**, *92*, 4992–4993. Minkin, V. I.; Minayev, R. M.; Zacharov, I. I. *J. C. S. Chemical Commun.* **1977**, 213–214. (b) Minkin, V. I.; Minayev, R. M.; Zacharov, I. I.; Avdeev, V. I. *Zh. Org. Khim.* **1978**, *14*, 3–15.
65. Kogh-Jespersen, M. B.; Chandrasekhar, J.; Würthwein, E.-U.; Collins, J. B.; Schleyer, P. v. R. *J. Am. Chem. Soc.* **1980**, *102*, 2263–2268.
66. Shavitt, I., work cited in Ref. 17, p. 251.
67. Minkin, V. I.; Minayev, R. M. *Zh. Org. Khim.* **1979**, *15*, 225–234. Minkin, V. I.; Minayev, R. M.; Orlova, G. V. *J. Mol. Struct. THEOCHEM* **1984**, *110*, 241–253.
68. Schulman, J. M.; Sabio, M. L.; Disch, R. L. *J. Am. Chem. Soc.* **1983**, *105*, 743–744.
69. Rao, V. B.; George, C. F.; Wolff, S.; Agosta, W. C. *J. Am. Chem. Soc.* **1985**, *107*, 5732–5739.
70. Würthwein, E.-U.; Chandrasekhar, J.; Jemmis, E. D.; Schleyer, P. v. R. *Tetrahedron Lett.* **1981**, *22*, 843–846. Wiberg, K. B. *Tetrahedron Lett.* **1985**, *26*, 5967–5970.
71. Wiberg, K. B. *J. Org. Chem.* **1985**, *50*, 5285–5291.
72. Kabuto, Ch.; Yagihara, M.; Asso, T.; Kitahara, Y. *Angew. Chem.* **1973**, *85*, 860–861; *Angew. Chem. Int. Ed. Engl.* **1973**, *12*, 836.
73. Littke, W.; Drück, U. *Angew. Chem.* **1974**, *86*, 557–558; *Angew. Chem. Int. Ed. Engl.* **1974**, *13*, 539–540.
74. Vogel, E.; Breuer, A.; Sommerfield, C.-D.; Davis, R. E.; Liu, L.-K. *Angew. Chem.* **1977**, *89*, 175–176; *Angew. Chem. Int. Ed. Engl.* **1977**, *16*, 169–170.
75. Schwesinger, R.; Piontek, K.; Littke, W.; Prinzbach, H. *Angew. Chem.* **1985**, *97*, 344–345; *Angew. Chem. Int. Ed. Engl.* **1985**, *24*, 318–319 and references cited therein.
76. Kellie, G. M.; Riddell, F. G. *Top. Stereochem.* **1974**, *8*, 225–269.
77. Vereshchagin, A. N. *Usp. Khim.* **1983**, *52*, 1879–1901; Chapters III, IV; Engl. transl. pp. 1081–1095.
78. Krüger, C.; Roberts, P. J. *Cryst. Struct. Commun.* **1974**, *3*, 459–462.
79. Spanget-Larsen, J.; Gleiter, R. *Angew. Chem.* **1978**, *90*, 471–472; *Angew. Chem. Int. Ed. Engl.* **1978**, *17*, 441–442.
80. Schulman, J. M.; Miller, M. A.; Disch, R. L. *J. Mol. Struct. THEOCHEM.* **1988**, *169*, 563–568.
81. de Meijere, A.; Kaufmann, D.; Schaller, O. *Angew. Chem.* **1971**, *83*, 404–405; *Angew. Chem. Int. Ed. Engl.* **1971**, *10*, 417–418.
82. Spielmann, W.; Fick, H.-H.; Meyer, L.-U.; de Meijere, A. *Tetrahedron Lett.* **1976**, 4057–4060; Kaufmann, D.; Fick, H.-H.; Schallner, O.; Spielmann. W.; Meyer, L.-U.; Gölitz, P.; de Meijere, A. *Chem. Ber.* **1983**, *116*, 587–609.
83. Allinger, N. L.; Eaton P. E. *Tetrahedron Lett.* **1983**, *24*, 3697–3700.
84. Disch, R. L.; Schulman, J. M. *J. Am. Chem. Soc.* **1988**, *110*, 2102–2105.

85. (a) Schulman, J. M.; Disch R. L.; Sabio, M. L. *J. Am. Chem. Soc.* **1986**, *108*, 3258–3260. (b) Disch, R. L. Schulman, J. M. *J. Am. Chem. Soc.* **1990**, *112*, 3377–3379.

86. Mohler, D. L.; Vollhardt, K. P.; Wolff, S. *Angew. Chem.* **1990**, *102*, 1200–1202; *Angew. Chem. Int. Ed. Engl.* **1990**, *29*, 1151–1154.

87. Fitjer, L.; Wehle, D.; Noltenmeyer, M.; Egert, E.; Sheldrick, G. H. *Chem. Ber.* **1984**, *117*, 203–221.

88. See references cited in Ref 33.

89. The V_3 torsional constant of the 22-1-22-1 type differed considerably from other constants in the MM2 parameterization. The value has been revised in the meantime: Aped P.; Allinger, N. L. *J. Am. Chem. Soc.* **1992**, *11*, 1–16.

90. Dodziuk, H. unpublished result.

91. (a) McMullen, G.; Lutterbeck, M.; Fritz, H.; Prinzbach, H.; Krüger, C. *Isr. J. Chem.* **1982**, *22* 19–26. (b) Mass, M.; Lutterbeck, M.; Hunkler, D.; Prinzbach, H. *Tetrahedron Lett.* **1983**, *24*, 2143–2146.

92. Heath, T. A. *A History of Greeek Mathematics*; Oxford University Press: London, 1976.

93. Banciu, M.; Popa, C.; Balaban, A. T. *Chem. Scr.* **1984**, *24*, 28–37.

94. Rücker, C. H.; Prinzbach, H. *Tetrahedron Lett* **1986**, *27*, 1565–1568.

95. Hirao, K.-I.; Ohuchi, Y.; Yonemitsu, O. *J. Chem. Soc., Chem. Commun.* **1982**, 99–100.

96. Beesly, R. M.; Thorpe, J. F. *J. Chem. Soc.* **1920**, 591; *Proc. Chem. Soc.* **1913**, *29*, 346, cited in Ref. 97.

97. Zefirov, I. S.; Koz'min, A. S.; Abramenkov, A. B. *Usp. Khim.* **1978**, *47*, 289–306; Engl. transl. pp. 163–171.

98. (a) Rauscher, G.; Clark, T.; Poppinger, D.; von Schleyer P. R. *Angew. Chem.***1978**, 90, 306–307; *Angew. Chem. Int. Ed. Engl.* **1978**, *17*, 276–277. (b) Maier, G.; Born, D. *Angew. Chem.* **1989**, *101*, 1085–1087; *Angew. Chem. Int. Ed. Engl.* **1989**, *28*, 1050–1052.

99. Hounshell, W. D.; Mislow, K. *Tetrahedron Lett.* **1979**, *14*, 1205–1208.

100. Irngartinger, H.; Goldmann, A.; Jahn R.; Nixdorf, M.; Rodewald, H.; Maier, G.; Malsch, K.-D.; Emrich, R. *Angew. Chem.* **1984**, *96*, 967–968; *Angew. Chem., Int. Ed. Engl.* **1984**, *23*, 993–994.

101. Maier, G.; Pfriem, S.; Malsch, K.-D.; Kalinowski, H.-O.; Dehnicke, K. *Chem. Ber.* **1981**, *114*, 3988–3996.

102. Loerzer, T.; Machinek, R.; Lüttke, W.; Franz, L. H.; Malsch, K.-D.; Maier, G. *Angew. Chem.* **1983**, *95*, 914–915; *Angew. Chem., Int. Ed. Engl.* **1983**. *22*, 878–879.

103. Bolotin, A. B.; Bolotin, V. A.; Shulksus, Yu. K.; Yarovoi, S. S. *Zh. Strukt. Khim.* **1984**, *25* (3), 161–164; Engl. transl. pp. 483–488.

104. Disch, R. L.; Schulman, J. M.; Sabio, M. L. *J. Am. Chem. Soc.* **1985**, *107*, 1904–1906.

105. Schulmann, J. M.; Disch, R. L. *J. Am. Chem. Soc.* **1985**, *107*, 5059–5061.

106. Minkin, V. I.; Minayev, R. M. *Zh. Org. Khim.* **1981**, *17*, 221–232; Engl. transl. pp. 175–186.

107. Karl, R. R.; Jr., Wang, Y. C.; Bauer, S. H. *J. Mol. Struct.* **1975**, *25*, 17–34.

108. Gleiter, R.; Treptow, B. *Angew. Chem.* **1990**, *102*, 1452–1454; *Angew. Chem., Int. Ed. Engl.* **1990**, *29*, 1427–1429.

109. Hedberg, L.; Hedberg, K.; Eaton, P. E.; Nodari, N.; Robiette, A. G. *J. Am. Chem. Soc.* **1991**, *113*, 1514–1517.

110. Hirota, E.; Endo, Y.; Fujitake, M.; Della, E. W.; Pigou, P. E.; Chickos, J. S. *J. Mol. Struct.* **1988**, *190*, 235–258.

111. Fleischer, E. B. *J. Am. Chem. Soc.* **1964**, *86*, 3889–3890.

112. Almenningen, A.; Jonvik, L. T.; Martin, H. D.; Urbanek, T. *J. Mol. Struct.* **1985**, *128*, 239–247.

113. Shatokhin, S. A.; Gribov, A.; Perelygin, I. S. *Zh. Strukt. Khim.* **1986**. *27* (2), 22–27; Engl. transl. pp. 194–199.

114. Schulman, J. M.; Disch, R. L. *J. Am. Chem. Soc.* **1984**, *106*, 1202–1204.

115. Allinger, N. L.; Yuh, Y. H.; Lii, J.-H. *J. Am. Chem. Soc.* **1989**, *111*, 8551–8566; Lii, J.-H.; Allinger, N. L. *J. Am. Chem. Soc.* **1989**, *111*, 8566–8575; Lii, J.-H.; Allinger, N. L. *J. Am. Chem. Soc.* **1989**, *111*, 8576–8582.

116. Kybett, B. D.; Carroll, S.; Natalis, P.; Bonnell, D. V.; Margrave, J. L.; Franklin, J. L. *J. Am. Chem. Soc.* **1966**, *88*, 626.

117. Gleiter, R.; Karcher, M. *Angew. Chem.* **1988**, *100*, 851–852; *Angew. Chem., Int. Ed. Engl.* **1988**, *27*, 840–841.

118. Criegee, R. *Angew. Chem.* **1962**, *74*, 703–730; *Angew. Chem. Int. Ed. Engl.* **1962**, *1*, 519–546.

119. Gilardi, R.; Maggini, M.; Eaton, P. E. *J. Am. Chem. Soc.* **1988**, *110*, 7232–7234.

120. Eaton, P. E.; Maggini, M. *J. Am. Chem. Soc.* **1988**, *110*, 7230–7232.

121. Seidil, E. T.; Schäfer, H. F. III, *J. Am. Chem. Soc.* **1991**, *113*, 1915–1917.

122. Stanton, J. F.; Gauss, J.; Watts, J. D.; Bartlett, R. J. *J. Chem. Phys.* **1991**, *94*, 4334–4345.

123. Axenrod, T.; Liang, B.; Bashir-Hashemi, A.; Dave P. R.; Reddy, D. S. *Magn. Res. Chem.* **1991**, *29*, 88–91.

124. Iwamura, H.; Morio, K.; Kunii, T. L. *J. Chem. Soc., D.*, **1971**, 1408–1409.

125. Honegger, E.; Eaton,P. E.; Shankar, B. K. R.; Heilbronner, E. *Helv. Chim. Acta* **1982**, *65*, 1982–1989.

126. Handreck, D.-R.; Hunkler D.; Prinzbach, H. *Angew. Chem.* **1989**, *101*, 1386–1388; *Angew. Chem. Int. Ed. Engl.* **1989**, *28*, 1351–1353.

127. Mehta, G.; Padma, S. *J. Am. Chem. Soc.* **1987**, *109*, 2212–2213.

128. Reddy, V. P.; Jemmis, E. D. *Tetrahedron Lett.* **1986**, *27*, 3771–3774

129. Schriver, G. V.; Gerson, D. J. *J. Am. Chem. Soc.* **1990**, *112*, 4723–4728.

130. Gleiter, R.; Sigwart, C.; Irngartinger, H.; Gries, S.; Martere, W.; Klinger, O.; Prinzbach, H. *Tetrahedron Lett.* **1988**, *29*, 185–188.

131. Dodziuk, H.; Nowinski, K.; unpublished result.

132. Jemmis, E. D.; Rudzinski, J. M.; Osawa, E. *Chem. Express*, **1988**, *3*, 109–112.

133. Dinsburg G. *Nouv. J. Chim.* **1982**, *6*, 175–177.

134. Miller, M. A.; Schulman, J. M. *J. Mol. Struct. THEOCHEM* **1988**, *163*, 133–134.

135. Li, W.-K.; Luh, T.-Y.; Chiu, S.-W. *Croat. Chim. Acta* **1985**, 1–3; Osawa, E.; Rudzinski, J. M.; Barbiric, A.; Jemmis, E. D. In *Strain and Its Implications in Organic Chemistry*; de Meijere, A.; Blechert, S., Eds.: Kluver Academic Publishers: Dordrecht, 1988; pp. 259–261.

136. We believe that, due to personal preferences, the importance of nonnatural target molecules such as those discussed here has been underestimated in a recent review on the perspectives of organic synthesis. Seebach, D. *Angew. Chem.* **1990**, *102*, 1363–1430; *Angew. Chem., Int. Ed. Engl.* **1990**, *29*, 1320–1367.

137. H. Dodziuk, to be published.

138. Sekiguchi, A.; Yatabe, T.; Kamatani, H.; Kabuto, C.; Sakurai, H. *J. Am. Chem. Soc.* **1992**, *114*, 6260–6262. Tesh, K. F.; Jones, B. D.; Hanussa, T. P.; Huffman, J. C. *J. Am. Chem. Soc.* **1992**, *114*, 6590–6591.

139. Liebman, J. F.; Greenberg, A. *Chem. Rev.* **1989**, *89*, 1225–1246.
140. Lee, C.-H.; Liang, S.; Haumann, T.; Boese, R.; de Meijere, A. *Angew. Chem.*, **1993**, *105*, 611–613; *Angew. Chem. Int. Ed. Engl.* **1993**, *32*, 559–561.
141. de Meijere, A., personal communication.
142. Smith, Z.; Andersen, B.; Bunce, S. *Acta Chem. Scand.* **1977**, *A31*, 557–562; Boese, R.; Bläser, D.; Gomann, K.; Brinker, U. H. *J. Am. Chem. Soc.* **1989**, *111*, 1501–1503.

Stereochemistry of Metabolic Reactions of Amino Acids

DOUGLAS W. YOUNG

School of Chemistry and Molecular Sciences, University of Sussex, Falmer, Brighton, United Kingdom

I. Introduction
II. Pyridoxal, Pyridoxamine, and Their Phosphates
III. Glycine
IV. Serine and Its Derivatives
V. Homoserine and Threonine
VI. Cysteine and Cystine
VII. Homocysteine, Methionine, and Related Compounds
VIII. Valine, Leucine, and Isoleucine
  A. Valine
  B. Leucine
  C. Isoleucine
  D. Biosynthesis
  E. Catabolism
IX. Aspartic Acid, β-Methylaspartate, and Asparagine
X. Glutamic Acid and Its Derivatives
XI. Proline
XII. α- and β-Lysine
XIII. Ornithine and Arginine
XIV. Histidine
XV. Phenylalanine, Tyrosine, and Tryptophan
  A. General
  B. Phenylalanine and Tyrosine
  C. Tryptophan
XVI. Other Amino Acids
  A. Aminocyclopropanecarboxylate
  B. Aminomalonic Acid
  References

Topics In Stereochemistry, Volume 21, Edited by Ernest L. Eliel and Samuel H. Wilen.
ISBN 0-471-52120-5 © 1994 John Wiley & Sons, Inc.

I. INTRODUCTION

The importance of stereochemistry in understanding the mechanism of biological processes has long been appreciated and, since Ogston's classic paper in 1948 (1), stereochemical studies have been extended to prochiral molecules normally thought of as symmetrical. Prochirality has been extensively reviewed, and the literature includes chapters in this series and elsewhere (2–4) and two books (5, 6). Extension of the concept to reactions at pro-prochiral centers has also been reviewed in this series (7).

In this review, we shall concentrate on the stereochemistry of enzymic reactions of amino acids, many of which involve transformations at prochiral centers. We shall use the nomenclature of Hanson (8) to specify the stereochemistry of prochiral atoms and groups as *pro-R* (H_R) and *pro-S* (H_S) and of prochiral faces as *Re* and *Si* and the nomenclature of Mislow and Raban (2) to describe prochiral groups as having *enantiotopic* or *diastereotopic* relationships. Reviews on the stereochemistry of enzymic reactions of amino acids were published in 1978 (9, 10), and since the seminal review by Dunathan in 1971 (11), several reviews comparing the stereochemistry of pyridoxal phosphate–catalyzed enzymic reactions have appeared (12–15).

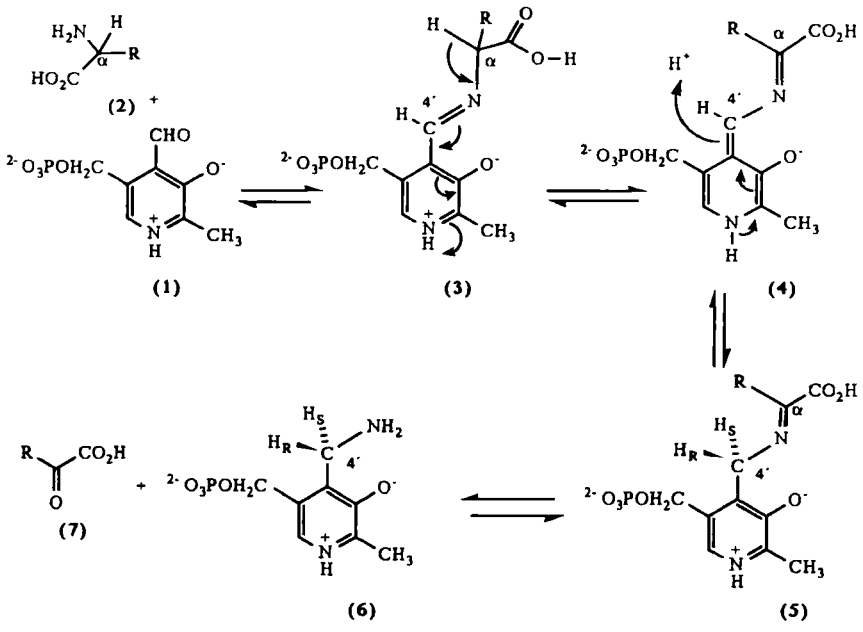
II. PYRIDOXAL, PYRIDOXAMINE, AND THEIR PHOSPHATES

A broad range of enzymic reactions of amino acids is mediated by pyridoxal phosphate (PLP), the cofactor form of vitamin B_6. The general mechanism of action of this cofactor was suggested independently by Braunstein and Shemyakin (16) and by Snell (17), and although a great deal of experimental work has been achieved since the Braunstein–Snell hypothesis was put forward, it still holds good today.

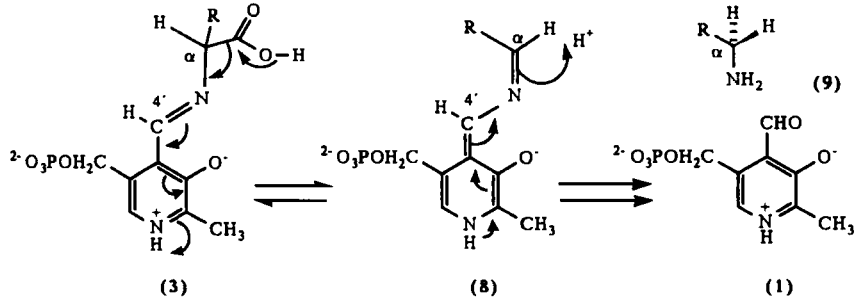
Pyridoxal phosphate **1** readily condenses with the amino group of an amino acid **2** to form a conjugated imine **3**, as shown in Scheme 1. The pyridine nitrogen will now act as an "electron sink", especially when protonated, and so α deprotonation will yield the imine **4**. Protonation at C-4′ in the imine **4** will yield the imine **5**, which on hydrolysis will give the ketoacid **7** and pyridoxamine-phosphate (PMP) **6**. This process is catalyzed by transaminases.

The intermediate **3** may also be decarboxylated, as shown in Scheme 2, and the decarboxylated imine **8**, on protonation followed by hydrolysis, will yield the amine **9** and PLP **1**. This process is catalyzed by amino acid decarboxylases. Retroaldol cleavage of a suitable β-hydroxy amino acid would be encouraged by the electron sink in a similar manner.

In addition to these reactions at the α-carbon of amino acids, pyridoxal phosphate catalyzes reactions at the β- and γ-carbon atoms of amino acids

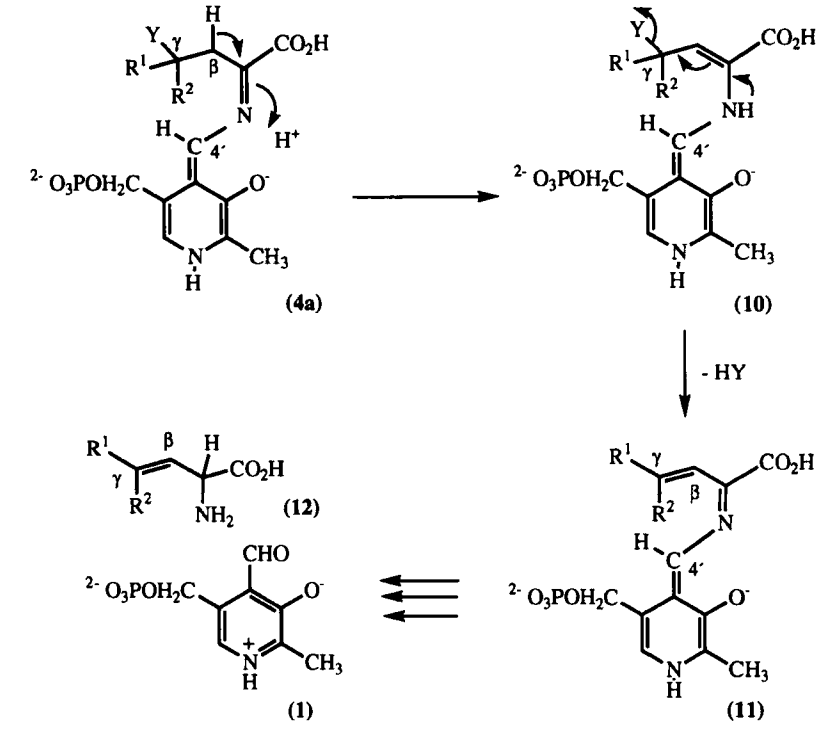


Scheme 1

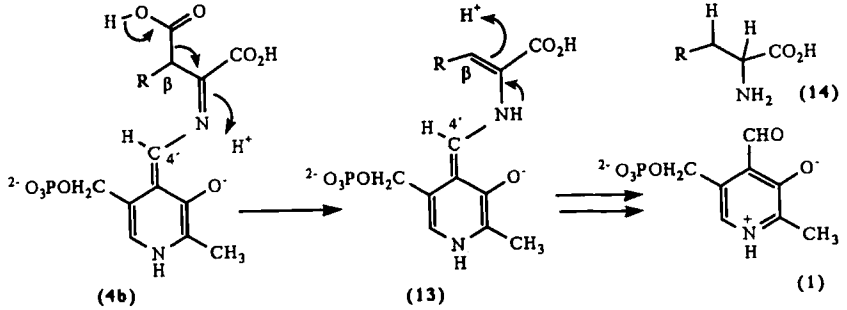


Scheme 2

as shown in Schemes 3–5. Just as the system **3** acted as an electron sink, so the imine **4a** or **4b** may act in similar fashion. Tautomerism in **4a** to the enamine **10** will allow elimination of a suitably disposed γ-functional group to yield the conjugated system **11**. A series of reactions similar to those outlined in Scheme 1 will then yield the amino acid **12** and PLP **1**. Also β decarboxylation can occur using **4b** as an electron sink, as shown in Scheme 4, yielding the product **14**. The fully conjugated system in **4c** will aid elimination

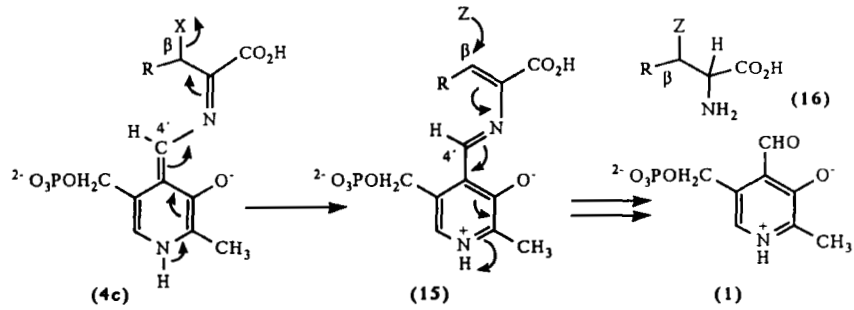


Scheme 3



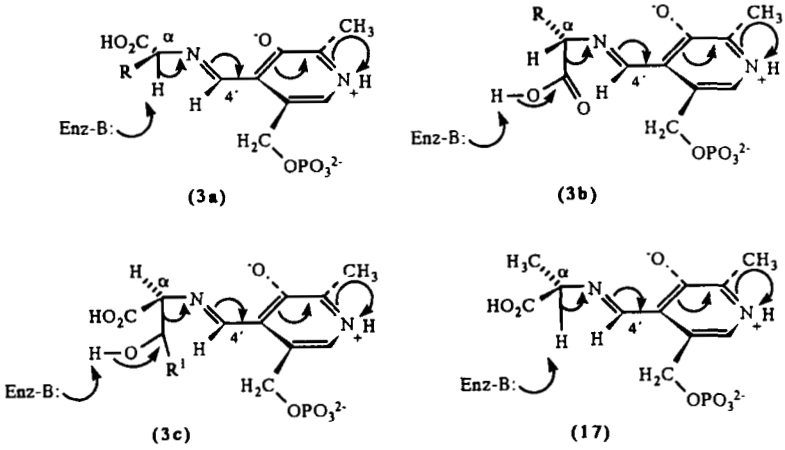
Scheme 4

of an electron-withdrawing group on the β-carbon atom of an amino acid to give the electrophilic species **15**. Addition of a suitable nucleophile may then occur, as shown in Scheme 5, to lead eventually to the β-substituted product **16**.



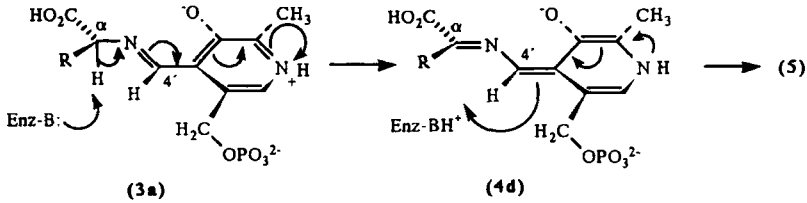
Scheme 5

In 1966 Dunathan (18) proposed that, in PLP-mediated reactions, the bond to be broken in the substrate–cofactor compound should be perpendicular to the plane of the extended conjugated system so that there would be maximum σ–π overlap between the breaking bond and the ring–imine π system. Thus **3a**, **3b**, and **3c** represent the conformations of the imine **3** best suited to achieve transamination reactions, decarboxylation reactions, and retroaldol reactions, respectively. The enzyme will be responsible for the orientation of the amino acid–PLP complex and thus dictate the nature of the resultant reaction. An example of an enzyme catalyzing two distinct reactions was found for serine hydroxymethyltransferase (EC 2.1.2.1), which normally catalyzes the retroaldol process outlined in **3c** when L-serine or L-threonine are substrates. When D-alanine was used as substrate, however, a slow transamination was observed (19). Comparison of the conformations of the amino acid–PLP complexes, **3c** and **17**, respectively, for the retroaldol and transamination reactions shows that both the proton removed from the



hydroxyl group in **3c** and the α-hydrogen removed in **17** take up similar environments in the active site of the enzyme, thus allowing the quite different reactions to occur.

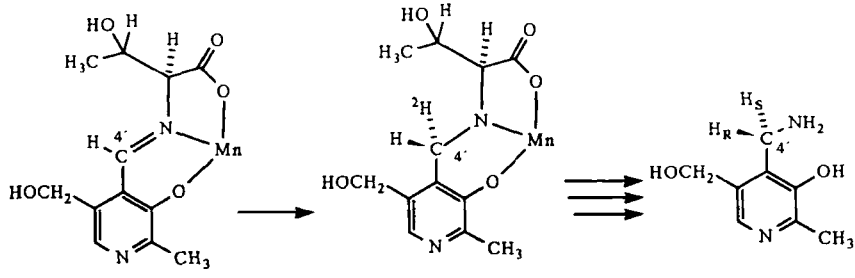
Transaminases will be specific for α-amino acids of one configuration and during the reaction (Schemes 1 and 6), conformation **3a** will be transformed to the imine **4**. This can be protonated either from the *Si* face (as in **4d**) or the *Re* face to give **5** and thence pyridoxamine **6**.



(3a) (4d)

Scheme 6

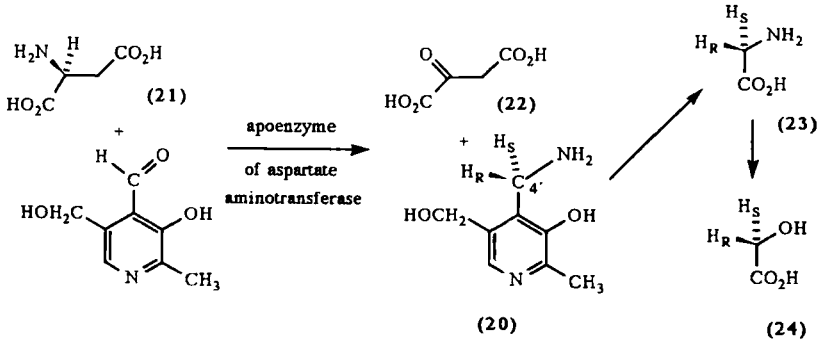
Dunathan et al. (20) and Besmer and Arigoni (21, 22) independently examined the stereospecificity of this process using the apoenzyme (23) of aspartate aminotransferase (EC 2.6.1.1) since this could be reconstituted with unphosphorylated pyridoxamine **20** and still show catalytic competence. Dunathan et al. (20) synthesized (4′*S*)-[4′-$^2H_1$]pyridoxamine **20**, $H_S = {}^2H$, by reduction of the manganese complex **18** from its less hindered side with NaB^2H_4 as in Scheme 7. Removal of the metal followed by periodate treatment then gave the stereospecifically labeled pyridoxamine **20**, $H_S = {}^2H$. Although this was not 100% enantiomerically pure, the kinetics of exchange with the apoenzyme and α-ketoglutarate were similar to those found for [4′,4′-$^2H_2$]pyridoxamine and not to those found for unlabeled pyridoxamine, suggesting that deprotonation of the unphosphorylated analog of **4d** had occurred from the *Si* face.



(18) (19) (20)

Scheme 7

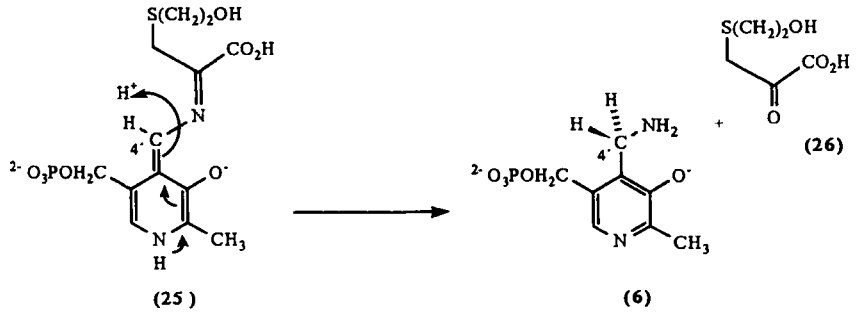
Besmer and Arigoni (21, 22) incubated the reconstituted apoenzyme with aspartic acid **21** in ^2H_2O as shown in Scheme 8. The resultant pyridoxamine **20**, $H_S = {}^3H$, was then degraded to (2*S*)-[2-$^3H_1$]glycine **23**, $H_S = {}^3H$. This could be converted to glycollic acid **24**, $H_S = {}^3H$, by nitrosation with retention of configuration. Since this acid is known (24, 25) to lose its 2-*pro-R* hydrogen on oxidation with glycollate oxidase (EC 1.1.3.1) and ^3H is retained, the stereochemistry of the glycine and hence the pyridoxamine could be assigned as being (*S*). Thus protonation of the unphosphorylated analogue of **4d** had occurred from the 4′-*Si* face.



Scheme 8

Subsequent to this work, apoaspartate transaminase was used to assay the stereospecificity of a variety of other transaminases, all of which were shown to involve protonation/deprotonation at the C–4′ *Si* face of the cofactor. These enzymes included pyridoxamine-pyruvate transaminase (EC 2.6.1.30) (26) and α-dialkylamino acid transaminase (27). L-Glutamate decarboxylase (EC 4.1.1.15) catalyzes an abortive transamination reaction when α-methylglutamate is used as substrate, and this too was shown to occur with protonation at the *Si* face of C-4′ in the intermediate **4d** (28) as was the abnormal transamination of D-alanine by serine hydroxymethyltransferase (29).

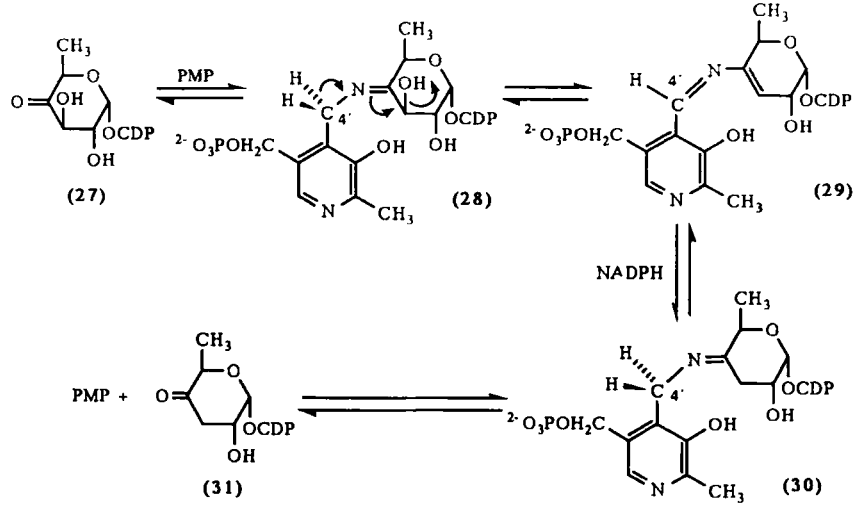
Tryptophan synthase (EC 4.1.2.20) normally catalyzes the synthesis of tryptophan from serine by the α,β elimination–addition reaction outlined in Scheme 5 where X = OH and Z = indole. The B protein of the oligomeric enzyme will catalyze the dehydration of serine, and in the presence of PLP and mercaptoethanol, the intermediate **15** will form adduct **25**. This will then react as in Scheme 9 to yield the ketoacid **26** and pyridoxamine-phosphate **6**. The net transamination has been shown to involve protonation at the 4′-*Si* face in yielding PMP (30). When the apoenzyme of tryptophan synthase is reconstituted with the unnatural substrates (4′*R*)- or (4′*S*)-[4-$^3H_1$]pyridoxamine-phosphate and indole-3-pyruvic acid, an unnatural transamination



Scheme 9

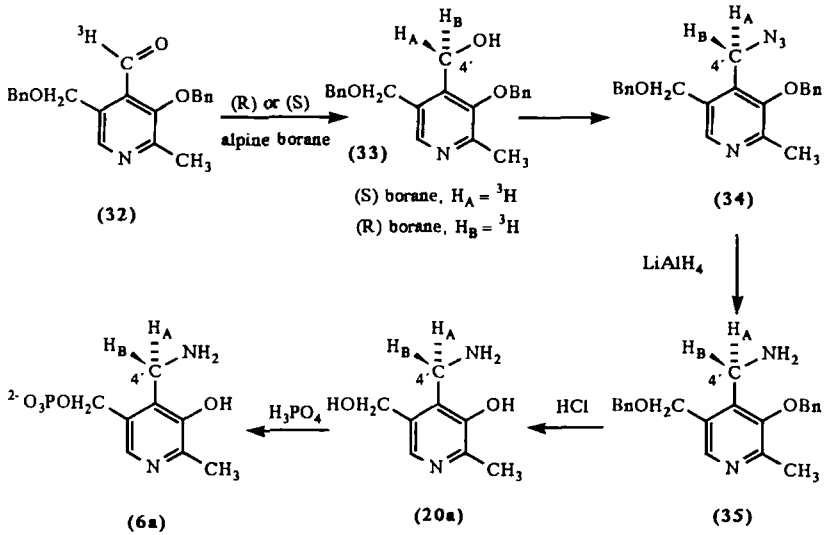
will result giving PLP and L-tryptophan. It was shown (31) that the PLP derived from the (4′*R*)-[4-$^3H_1$]-PMP retained tritium, whereas that derived from the (4′*S*)-isomer lost tritium.

Some amino sugar dehydratases use pyridoxamine phosphate **6** as a cofactor. The enzyme CDP-4-keto-6-deoxy-D-glucose reductase (EC 1.17.1.1) is one such enzyme, catalyzing the process shown in Scheme 10.



Scheme 10

Synthetic samples of (4′*S*)- and (4′*R*)-[4′-$^3H_1$]- and [4′-$^2H_1$]pyridoxamine **20a** were prepared by the route outlined in Scheme 11, the key step being reduction of the labeled pyridoxal derivatives **32** with alpine boranes (32).



Scheme 11

Unlike the earlier samples prepared by Dunathan (20), these were ca. 90% enantiomerically pure, and when they were converted to the phosphates **6a** and incubated with the enzyme CDP-4-keto-6-deoxy-D-glucose reductase, the (4′*S*)-labeled PMP preferentially lost tritium (33). Thus, in all of the enzymes studied so far, the 4′-*Si* face is the face at which reaction occurs. The most studied of these enzymes, aspartate aminotransferase (EC 2.6.1.1), has been shown to exchange the 4′-*pro-S* hydrogen in the absence of substrate, albeit at a slower rate than when the substrate is present (34, 35). The implication that the more reactive (4′-*Si*) face of the complex **3**⇌**4**⇌**5** (Scheme 1) would be more exposed than the less reactive (4′-*Re*) face was tested when the enzyme complex was reduced with NaB^3H_4. The reduced intermediate was degraded to show tritium in the 4′-*pro-S* hydrogen of the pyridoxamine and the (2*S*)-hydrogen of the amino acid (36). Thus reduction had occurred at the expected face. In the absence of substrate, however, the enzyme–lysine–pyridoxal phosphate Schiff base was shown to be reduced from the 4′-*Re* face (36, 37). When lysine 258 of the enzyme was carbamylated to prevent Schiff base formation, although pyridoxamine was formed in an irreversible transamination with 4′-*Si* protonation (38), NaB^3H_4 was shown to incorporate tritium at the 4′-*Re* face of the substrate–PLP imine (36). X-ray crystallographic studies of aspartate aminotransferase in unliganded form and in complexes with substrate analogues (39–41) suggest an explanation for these results

since the 4′-*Re* face is more exposed to solvent in the absence of substrate. Replacement of the amino group of lysine 258 by the α-amino group of the substrate allows the coenzyme to tilt by 30° and the lysine 258 is in a position to serve as a single-base proton acceptor/donor in the C-4′, C_α protonation. Site-specific mutagenesis of lysine 258 to alanine removes the catalytic competence of the enzyme (42).

Sodium borohydride reduction of the intermediates formed with other (nontransaminase) enzymes has given results very much in keeping with those found for aspartate aminotransferase. The tryptophan synthase (EC 4.2.1.20)/[4-^{3}H]pyridoxal-phosphate complex was reduced by $NaBH_4$, both in the presence of the substrate serine and in its absence (43). Degradation of the products to pyridoxamine showed that, in the presence of substrate, reduction was from the 4′-*Si* face, whereas in its absence, reduction of the PLP–lysine imine was from the 4′-*Re* face (43). Tyrosine decarboxylase (EC 4.1.1.25) in the presence of tyrosine is reduced with NaB^3H_4 from the 4′-*Si* face and in the absence of tyrosine from the 4′-*Re* face (44). Tryptophanase (EC 4.1.99.1) binds alanine as its Schiff base, which on reduction with NaB^3H_4 and degradation was shown to be attacked at the 4′-*Si* face and at the α-carbon to yield (2*S*)-[2-^{3}H]alanine (45).

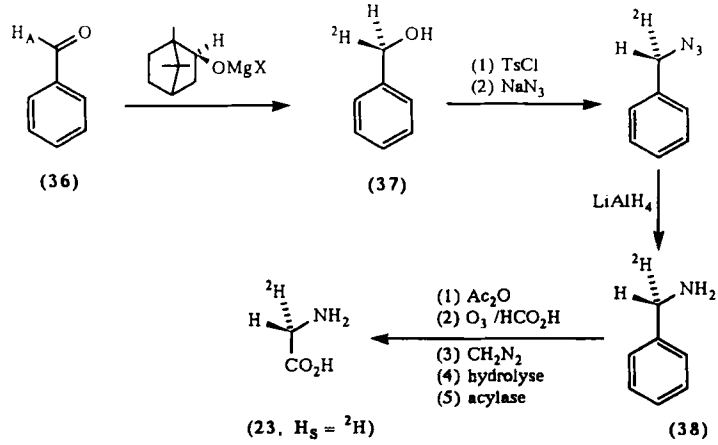
If a single base were to act as an intermediary in transferring a proton between C-4′ and C-α in the equilibrium 3⇌4⇌5 (Scheme 1), then this would imply suprafacial transfer. Such a single-base mechanism was indicated when Dunathan (26) incubated (2*S*)-[2-$^2H_1$]alanine with pyridoxamine-pyruvate transaminase (EC 2.6.1.30) for a short time, and the resultant pyridoxamine was shown to contain ca. 4% of deuterium by mass spectrometry. The pyridoxamine isolated after incubation of aspartate aminotransferase with [G-^{3}H]glutamate was shown to be radioactive and to have 82% of this activity in the 4′-*pro-S* hydrogen (46). Aspartate β-decarboxylase (EC 4.1.1.12) has been shown to catalyze decarboxylation–transamination at a rate of 0.005 of that of the normal β-decarboxylation process. The pyridoxamine phosphate from such an abnormal transamination of (2*S*)-[2-$^3H_1$]aspartate has been isolated and degraded showing that 17% of the original tritium was transferred to the 4′-*pro-S* position (47).

The suprafacial process in Scheme 6 is therefore indicated and the conformations shown in **3a** and **4d** would fit the results. The *syn* nature of the nitrogen and the phenolic OH can be inferred from nuclear magnetic resonance (NMR) (48, 49) and infrared spectroscopic (50) studies. These are in accord with electronic absorption spectra of constrained analogues and bound and unbound imines (51).

An enzyme responsible for recycling PLP from PMP, the flavin mononucleotide (FMN)-dependent pyridoxamine-5-phosphate oxidase (EC 1.4.3.5) has recently been shown to be nonstereospecific (52–54).

III. GLYCINE

Glycine **23**, the simplest of all amino acids, has no chiral center and yet enzymatic reactions can discriminate between the enantiotopic hydrogens H_R and H_S. This was first shown by Besmer and Arigoni (22, 55), who found that glycine could exchange ^2H_2O in the presence of L-alanine aminotransferase (EC 2.6.1.2). The resultant labeled glycine, 88% $^2H_1$ by mass spectrometry, was degraded to glycollic acid **24** by nitrosation with retention of configuration. The ORD (optical rotatory dispersion) spectrum of the [$^2H_1$]-glycollate obtained showed it to be (2*R*)-[2-$^2H_1$]glycollate **24**, $H_R = {}^2H$, and so the 2-*pro-R* hydrogen of glycine had been exchanged. An independent chemical synthesis of (2*S*)-[2-$^2H_1$]glycine **23**, $H_S = {}^2H$, was also achieved in this work (22). The key step was the asymmetric reduction of [$^2H_1$]benzaldehyde **36**, $H_A = {}^2H$, to the alcohol **37**, which was then converted to (2*S*)-[2-$^2H_1$]glycine **23**, $H_S = {}^2H$, as shown in Scheme 12.



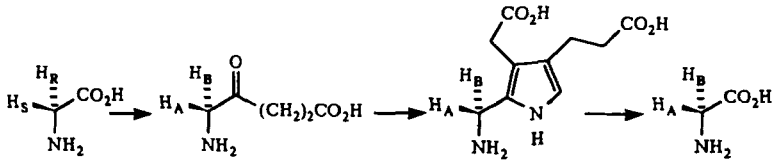
Scheme 12

When serine hydroxymethyltransferase (EC 2.1.2.1) was incubated with glycine and ^3H_2O in the absence of any other substrate, stereospecific exchange of tritium was observed (22, 56–59). The product was shown to be (2*S*)-[2-$^3H_1$]glycine **23**, $H_S = {}^3H$, by nitrosation to (2*S*)-[2-$^3H_1$]glycollic acid **24**, $H_S = {}^3H$, which retained tritium when oxidized with the *pro-R* specific enzyme glycollate oxidase (EC 1.1.3.1) (22). Alternatively, the *pro-S* specific D-amino acid oxidase (EC 1.4.3.3) was used to assay the stereochemistry (57, 58). Serine hydroxymethyltransferase therefore catalyzes exchange of a different hydrogen from that exchanged by L-alanine aminotransferase, and

both enzymes have been used to prepare samples of stereospecifically labeled glycine for metabolic studies.

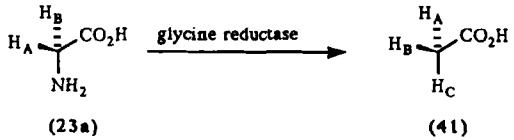
The (2*R*)- and (2*S*)-[2-$^3H_1$]glycines have been prepared by incubation of [2,2-$^3H_2$]glycine and unlabeled glycine in H_2O and ^3H_2O, respectively, with serine hydroxymethyltransferase (56–59). Use has been made of these compounds to assess stereochemical aspects of the metabolism of glycine. Thus feeding the labeled samples of glycine to 5-aminolevulinate synthase (EC 2.3.1.37), the first enzyme involved in the biosynthesis of porphyrins, showed that the 2-*pro-R* hydrogen of glycine was lost and the *2-pro-S* hydrogen was retained in the synthesis of 5-aminolevulinic acid **39** (60).

The full stereochemical implications of this enzymic condensation were assessed by coupling the synthase with 5-aminolevulinate dehydratase (EC 4.2.1.24), as shown in Scheme 13 so that the stereochemically labile 5-aminolevulinate **39** was converted directly to porphobilinogen **40** (61). Degradation of a sample of porphobilinogen **40** obtained from a sample of [2-^{3}H]glycine in a process involving oxidation of the pyrrole ring to a carboxyl group allowed glycine to be obtained. This lost tritium on treatment with the *pro-S* specific serine hydroxymethyltransferase. Thus, in aminolevulinic acid biosynthesis, the *2-pro-R* hydrogen of glycine is lost and the 2-*pro-S* hydrogen is incorporated as the *5-pro-S* hydrogen of 5-aminolevulinic acid **39** (61).



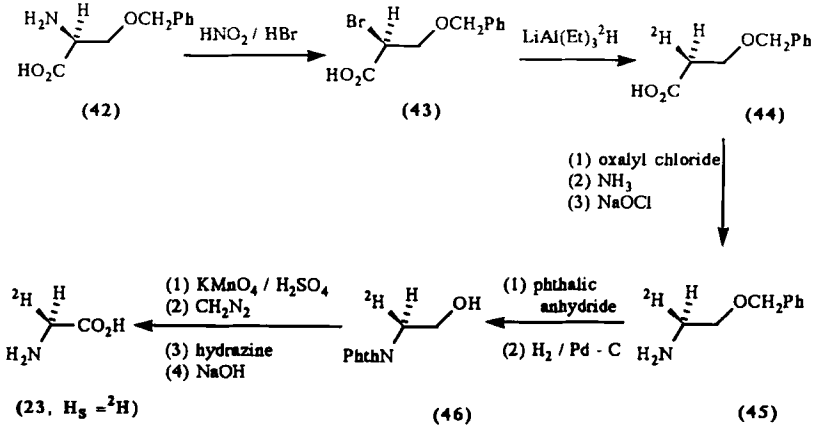
Scheme 13

Use of serine hydroxymethyltransferase with [2,2-$^2H_2$]glycine and ^3H_2O or [2,2-$^3H_2$]glycine and ^2H_2O gives (2*S*)- and (2*R*)-[2-$^2H_1$,2-$^3H_1$]glycines, respectively, and these were incubated with glycine reductase from *Clostridium sticklandii* to yield chirally labeled acetates (62) (Scheme 14). These acetates were assayed as described in references 3 and 7 to show that the reduction proceeded with inversion of configuration (62).



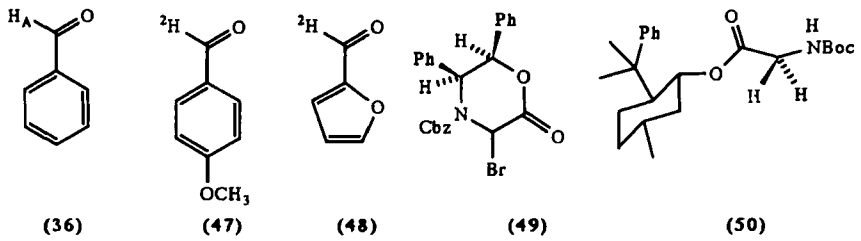
Scheme 14

Armarego et al. (63) sounded a warning on the use of serine hydroxymethyltransferase to prepare samples of stereospecifically labeled glycine, since they were able to obtain samples containing dideuterated glycine on incubation of glycine with this enzyme and ^2H_2O. They therefore devised a synthesis of (2*S*)- and (2*R*)-[2-$^2H_1$]glycines from (2*S*)- and (2*R*)-*O*-benzylserines, as shown in Scheme 15 for the (2*S*) series. The label was introduced by reduction of the bromide **43** with superdeuteride, which occurred, unusually, with retention of configuration, possibly due to an intramolecular effect.



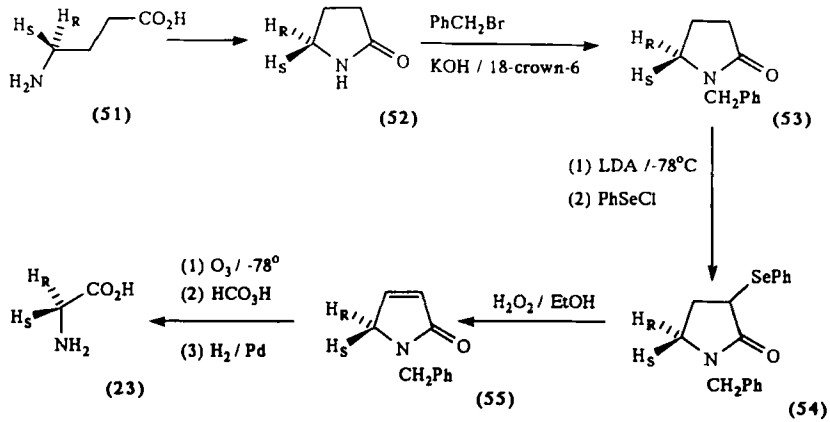
Scheme 15

Several other syntheses of stereospecifically labeled glycine have been devised, and some of these introduce chirality by reduction of a labeled aldehyde. Thus the *pro-R* specific horse liver alcohol dehydrogenase (EC 1.1.1.1) reduces the aldehydes **36**, $H_A = {}^2H$ or ^3H, to the corresponding (*S*)-alcohols (64); (*S*)- and (*R*)-alpine boranes reduce the aldehyde **47** to the corresponding (*R*)- and (*S*)-labeled alcohols, respectively (65), and *Saccharomyces cerevisiae* reduces the aldehydes **48**, $H_A = {}^1H$ or ^2H in ^2H_2O or H_2O, to the corresponding (*R*)- or (*S*)-labeled alcohols (66). In each of these syntheses, either tosylation with azide substitution (64) or phthalimide substitution in



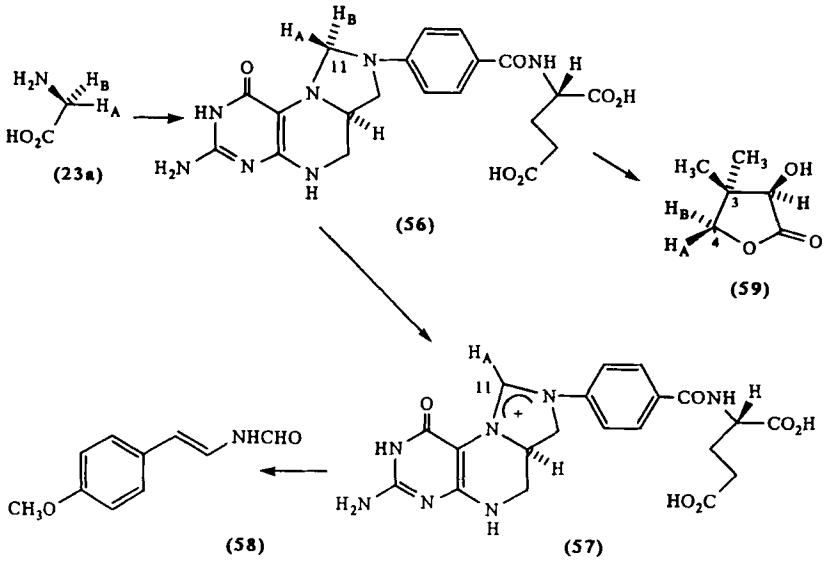
a Mitsunobu process (65, 66) is used to introduce the nitrogen. The carboxyl group of glycine is derived by oxidation of the aromatic ring.

Asymmetric induction using a transition metal complex (67), use of a carbohydrate template (68), and use of the chiral lactone **49** (69) or ester **50** (70) have all given effective syntheses of stereospecifically labeled samples of glycine. A further synthesis by Santaniello et al. (71, 72) has used glutamate decarboxylase to prepare labeled samples of γ-aminobutyric acid **51** (Scheme 16). On cyclization, protection, and oxidation, these gave the labeled enamides **55**, which were degraded to the labeled samples of glycine **23** (71, 72).



Scheme 16

The known 2-*pro-R* stereospecific exchange catalyzed by L-alanine aminotransferase (EC 2.6.1.2) (22, 55) has allowed this enzyme to be used to prepare stereospecifically labeled samples of glycine. We have used this enzyme to prepare (2*R*)- and (2*S*)-[2-$^2H_1$]glycines by exchanging unlabeled glycine in ^2H_2O and [2,2-$^2H_2$]glycine in H_2O, the ^1H and ^2H NMR spectra of the camphanoates indicating a high level of stereospecific exchange (73). Samples prepared in this way have been fed to *Streptomyces amakusaensis* (74). Isolation of the metabolite tuberin **58** and examination of the labeling of the *N*-formyl group allowed the stereochemistry of incorporation of glycine into the C-1 transfer coenzyme adduct 5,10-methylenetetrahydrofolate **56** to be assessed (Scheme 17) since the stereochemistry of the dehydrogenation of **56** to the methenyl adduct **57** was known (see Section IV). It was found that the 2-*pro-S* hydrogen of glycine **23** became the 11-*pro-S* hydrogen of 5,10-methylenetetrahydrofolate **56** (74). This stereochemistry was also confirmed when (2*R*)- and (2*S*)-[2-$^3H_1$]glycines **23** were fed to *Escherichia coli* and the product of C-1 transfer via **56**, pantolactone **59**, was isolated (75).



Scheme 17

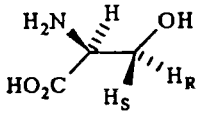
(2*R*)-[2-$^2H_1$]Glycine, prepared using L-alanine aminotransferase, was converted chemically to (2*R*)-[2-$^2H_1$]-2-fluorocitric acid for studies on the enzyme citrate synthase (EC 4.1.3.7) (76).

Doubly labeled glycines are required for studies in which a chiral methyl group is created and (2*R*)- and (2*S*)-[2-$^2H_1$,2-$^3H_1$]glycines **23**, $H_R = {}^3H$, $H_S = {}^2H$, and **23**, $H_R = {}^2H$, $H_S = {}^3H$, respectively, were prepared by exchange of [2-$^2H_2$]- and [2-$^3H_2$]glycines in ^3H_2O and ^2H_2O, respectively, using L-alanine aminotransferase (77).

The enzyme aspartate decarboxylase (EC 4.1.1.11) will decarboxylate aminomalonic acid in ^3H_2O to yield (2*S*)-[2-$^3H_1$]glycine and will also transaminate glyoxylic acid in ^3H_2O to yield (2*R*)-[2-$^3H_1$]glycine (78). The chirality of the product was assayed using the *pro-S* specific D-amino acid oxidase (EC 1.4.3.3).

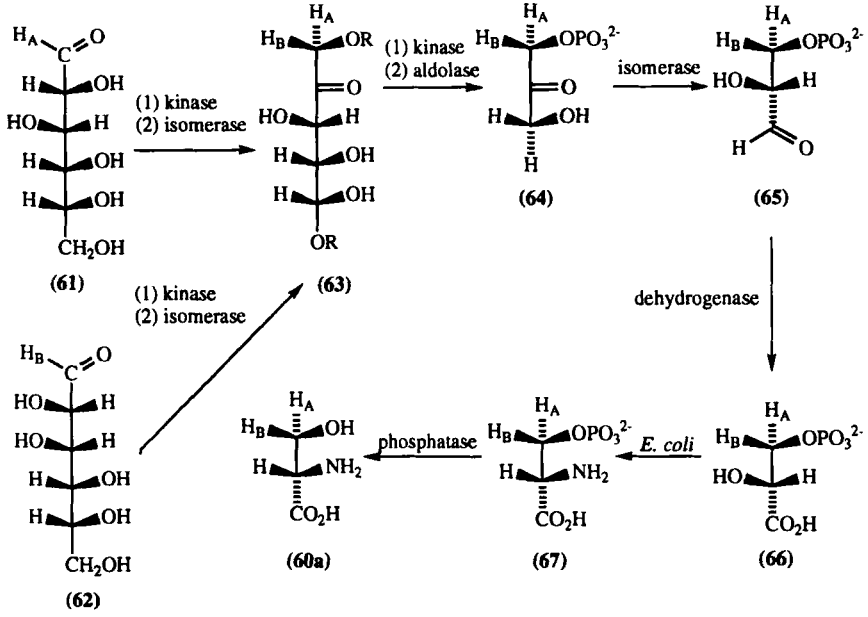
IV. SERINE AND ITS DERIVATIVES

The amino acid L-serine **60** and its derivatives, having a leaving group in the β position, are ideally situated for β-substitution reactions via the elimination–addition process outlined in Scheme 5, **4c**⇌**15**⇌**16**. The stereochemistry of such processes can be ascertained if samples of serine stereospecifically labeled at C-3 are available.



(60)

One of the most used syntheses of stereospecifically labeled serines was devised by Floss and co-workers using a mixture of enzymes of the glycolytic pathway to prepare (2*R*,3*R*)-, and (2*R*,3*S*)-[3-$^3H_1$]-3-phosphoglyceric acids **66**, $H_B = {}^3H$, and **66**, $H_A = {}^3H$, respectively, as in Scheme 18 (79–81). If [1-^{3}H]-D-glucose **61**, $H_A = {}^3H$, is incubated with a mixture of hexokinase, glucose-6-phosphate isomerase, phosphofructose kinase, aldolase, triosephosphate isomerase, and glyceraldehydephosphate isomerase, then (2*R*,3*S*)-[3-$^3H_1$]-3-phosphoglyceric acid **66**, $H_A = {}^3H$, is obtained. Incubation of [1^{3}H]-D-mannose **62**. $H_B = {}^3H$, with the same mixture but with mannose-6-phosphate isomerase replacing glucose-6-phosphate isomerase, gives (2*R*,3*R*)-[3-$^3H_1$]-3-phosphoglyceric acid **66**, $H_B = {}^3H$. The stereochemistry of these steps was well known (82), and so the chirality of labeling in the samples of 3-phosphoglyceric acid **66** was unambiguously defined. The samples of labeled 3-phosphoglyceric acid **66** were converted to 3-phosphoserines **67** using an

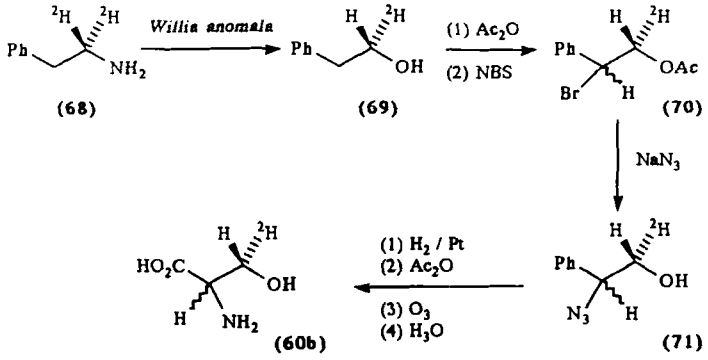


Scheme 18

E. coli enzyme preparation, and alkaline phosphatase then gave the labeled serines **60a** without the chirally labeled center being involved in the reaction (83, 84). The (2*S*, 3*R*)- and (2*S*, 3*S*)-[3-$^3H_1$]serines **60a**, $H_B = {}^3H$, and **60a**, $H_A = {}^3H$, were obtained from (2*R*, 3*R*)- and (2*R*, 3*S*)-[3-$^3H_1$]-3-phosphoglyceric acids **66**, $H_B = {}^3H$, and **66**, $H_A = {}^3H$, respectively. Confirmation of the final stereochemistry was given by conversion to tryptophan and thence indolmycin, as we shall see in Section XV.

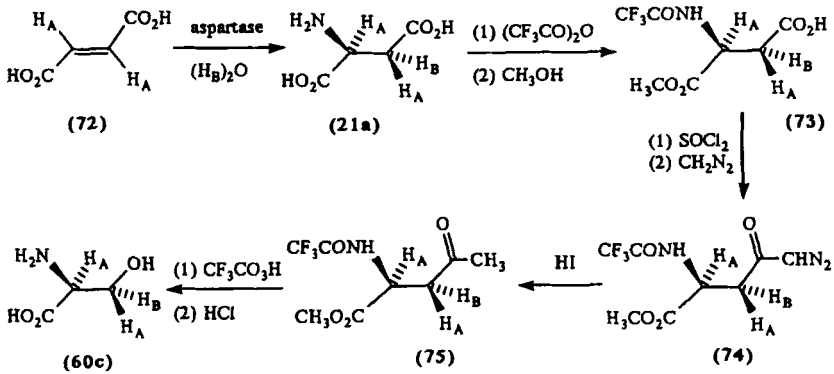
Use of ^2H_2O in the two isomerase steps leading to fructose-6-phosphate in this synthesis has allowed the doubly labeled (2*S*, 3*R*)- and (2*S*, 3*S*)-[3-$^2H_1$,3-$^3H_1$]serines **60a**, $H_A = {}^2H$, $H_B = {}^3H$, and **60a**, $H_A = {}^3H$, $H_B = {}^2H$, respectively, to be prepared (85–87).

Fuganti's synthesis of serine (Scheme 19) relied on the stereospecific conversion of [1,1-$^2H_2$]-2-phenylethylamine **68** to (1*S*)-[1-$^2H_1$]-2-phenylethanol **69** by *Willia anomala* (88). Acetylation, benzylic bromination, and



Scheme 19

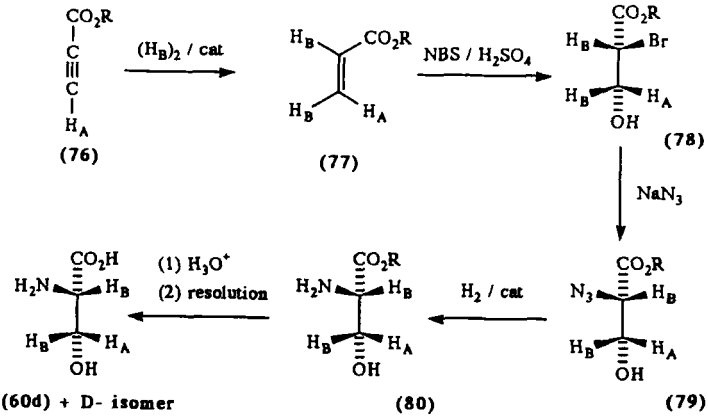
azide substitution then gave the azide **71**, which on reduction, acetylation, ozonolysis, and hydrolysis yielded (2*RS*, 3*S*)-[3-$^2H_1$]serine **60b** (88). This method relied on the use of a microorganism and so is rather specialized. Our method (89, 90) (Scheme 20) used the commercially available enzyme aspartase (EC 4.3.1.1) to add ammonia across the double bond of fumaric acid **72**. Since this is known to be an *anti* addition yielding (2*S*)-aspartic acid (see Section IX), use of [$^2H_2$]fumaric acid **72**, $H_A = {}^2H$, in H_2O gave (2*S*, 3*S*)-[2,3-$^2H_2$]aspartic acid **21a**, $H_A = {}^2H$, while use of fumaric acid **72** in ^2H_2O gave (2*S*, 3*R*)-[3-$^2H_1$]aspartic acid **21a**, $H_B = {}^2H$. Reaction with trifluoroacetic anhydride gave intermediate trifluoracetyl anhydrides that were opened regioselectively at the α-carbonyl group by methanol to give principally the esters **73**, $H_A = {}^2H$, and **73**, $H_B = {}^2H$. Conversion to the diazoketones **74** via the acid chlorides, followed by reduction with HI gave the methylketones **75**,



Scheme 20

$H_A = {}^2H$, and **75**, $H_B = {}^2H$. These underwent Baeyer–Villiger rearrangement with retention of configuration at C-3, and subsequent hydrolysis then gave samples of (2*S*, 3*S*)-[2,3-$^2H_2$]- and (2*S*, 3*R*)-[3-$^2H_1$]serines **60c**, $H_A = {}^2H$, and **60c**, $H_B = {}^2H$, respectively (89, 90).

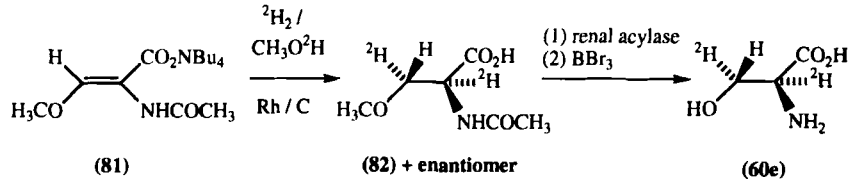
Two chemical syntheses of stereospecifically labeled serines (91, 92) relied on the stereospecific reduction of the acetylene **76** followed by *anti* addition of MeOBr (91) or HOBr (92) to the product **77**. The second of these syntheses (92) is shown in Scheme 21. It involved catalytic reduction of the anthracene adducts of the propiolates **76**, $H_A = {}^2H$, and **76** with hydrogen and deuterium, respectively, followed by a retro Diels–Alder reaction. The products were the (*Z*)-isomer **77**, $H_A = {}^2H$, and the (*E*)-isomer **7**, $H_B = {}^2H$, respectively. Reaction of these with *N*-bromosuccinimide in sulfuric acid gave three parts of the bromohydrins **78** together with one part of the alternative regioisomers.



Scheme 21

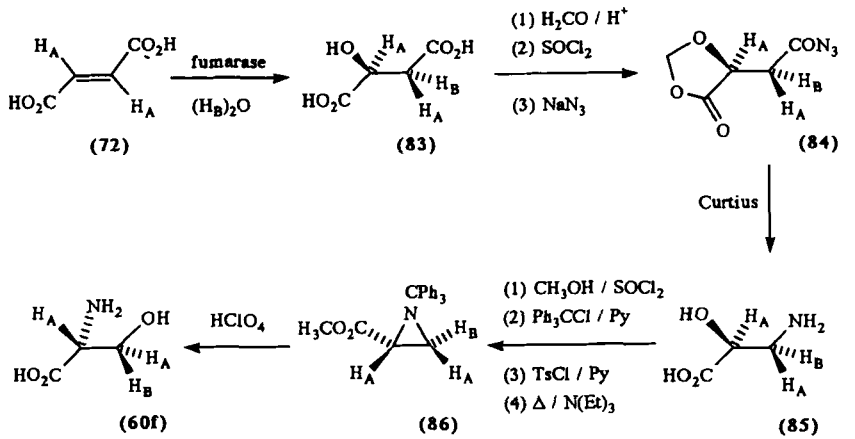
(The regioisomers were taken through the syntheses to yield isoserines and removed at that point.) Conversion of the bromohydrins **78** to the azides **79**, reduction, hydrolysis, and resolution gave (2*S*, 3*S*)-[3-$^2H_1$]- and (2*S*, 3*R*)-[2,3-$^2H_2$]serines **60d**, $H_A = {}^2H$, and **60d**, $H_B = {}^2H$, respectively. Samples of stereospecifically labeled D-serine were also obtained from these syntheses (91, 92).

A further chemical synthesis (93) (Scheme 22) relied on catalytic *cis* reduction of the (*Z*)-olefin **81**, yielding the protected serine **82**. This was resolved using hog renal acylase (EC 3.5.1.4), and BBr_3 treatment gave (2*S*, 3*R*)-[2,3-$^2H_2$]serine **60e** contaminated with (2*S*)-[2,3,3-$^2H_3$]serine. The (2*S*, 3*S*)-isomer could be obtained by a Mitsunobu reaction (93).



Scheme 22

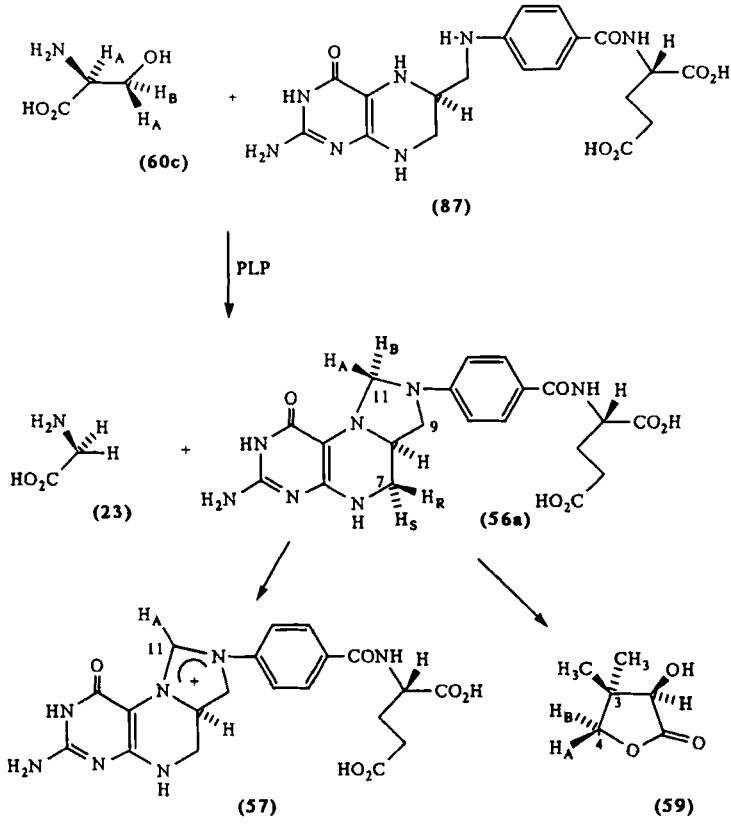
We have recently provided a stereospecific synthesis of samples of D-serine that are stereospecifically labeled at C-3 (94) (Scheme 23). This relies on the known (82) stereospecificity of the enzyme fumarase (EC 4.2.1.2) which adds water across the double bond of fumaric acid **72** with *anti* stereospecificity to give (2*S*)-malic acid **83**. Thus [$^2H_2$]fumaric acid, **72**, $H_A = {}^2H$, in H_2O yielded (2*S*, 3*S*)-[2,3-$^2H_2$]malic acid **83**, $H_A = {}^2H$, whereas fumaric acid **72**



Scheme 23

in ^2H_2O yielded (2*S*,3*R*)-[3-$^2H_1$]malic acid **83**, $H_B = {}^2H$. These samples of malic acid were converted to the protected azides **84**, $H_A = {}^2H$, and **84**, $H_B = {}^2H$, which underwent Curtius rearrangement with retention of configuration at the labeled carbon followed by deprotection to give the labeled samples of isoserine **85**. Esterification, N tritylation, O tosylation, and ring closure then led to the labeled aziridines **86** which underwent ring opening and deprotection in perchloric acid to yield (2*R*, 3*R*)-[2,3-$^2H_2$]- and (2*R*, 3*S*)-[3-$^2H_1$]serines **60f**, $H_A = {}^2H$, and **60f**, $H_B = {}^2H$, respectively (94).

The stereochemistry of many of the biological reactions involving serine and its derivatives has been studied using the labeled compounds prepared above. The carbon atom, C-3, of serine acts as a source of the one carbon unit transferred by the coenzyme tetrahydrofolic acid **87** (95) (Scheme 24). It is initially transferred to the coenzyme **87** to give 5,10-methylenetetrahydrofolic acid **56a** and glycine **23** in a reaction catalyzed by the enzyme serine



Scheme 24

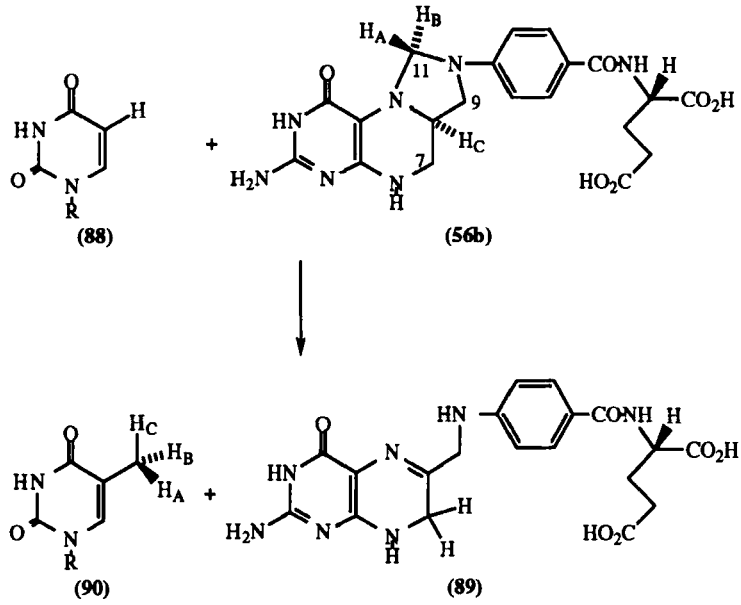
hydroxymethyltransferase (EC 2.1.2.1) and the coenzyme PLP as shown in Scheme 24. 5,10-Methylenetetrahydrofolate **56a** can then be oxidized to 5,10-methenyltetrahydrofolate **57** with the enzyme methylenetetrahydrofolate dehydrogenase (EC 1.5.1.5) and nicotinamide adenine dinucleotide phosphate (NADP). The one-carbon adduct **57** will then furnish formate and the coenzyme tetrahydrofolate **87**.

The stereochemistry of the reverse of this process was studied by Biellmann and Schuber (96, 97), who isolated [^{3}H]serine on feeding $^3HCO_2H$ to rat liver slices. The serine was degraded to [1-$^3H_1$]ethanol, which lost only ca. 30% of its tritium on oxidation to acetaldehyde with the *pro-R* specific enzyme yeast alcohol dehydrogenase (EC 1.1.1.1). The label lost was shown to be in the reduced NAD (NADH) formed by transfer to lactate using lactate dehydrogenase (96, 97). The label was therefore transferred to the 3-*pro-S* hydrogen of serine to the extent of ca. 70%. The groups of Benkovic and Floss (98) studied this reaction using samples of stereospecifically tritiated serine prepared as in Scheme 18. They showed that ca. 76% of the 3-*pro-S* hydrogen was lost in the overall C-1 transfer/dehydrogenation and that loss of stereospecificity was caused by nonenzymatic racemization of 5,10-methylenetetrahydrofolate **56**. Slieker and Benkovic were later able to prepare samples of (6*R*, 11*R*)- and (6*R*, 11*S*)-[9,9,11-$^2H_3$]-5,10-methylenetetrahydrofolate **56a**, $H_B = {}^2H$, and **56a**, $H_A = {}^2H$, respectively, proving the stereochemistry of labeling at C-11 by use of nuclear Overhauser enhancements between H-7*R* and one H-11 in the ^{1}H NMR spectrum (99). Use of (2*S*, 3*S*)- and (2*S*, 3*R*)-[3-$^2H_1$]serines **60**, $H_S = {}^2H$, and **60**, $H_R = {}^2H$, respectively, and isolation of the labeled adduct **56a** then showed that the 3-*pro-S* hydrogen of serine was incorporated as the 11-*pro-S* hydrogen of adduct **56a** and that the 11-*pro-R* hydrogen was lost on dehydrogenation of **56a** to **57**. In a recent reinvestigation of the coupled enzymes serine hydroxymethyltransferase and 5,10-methylenetetrahydrofolate dehydrogenase, only 10% racemization was observed (100).

Aberhart and Russell (101) have studied the stereochemistry of transfer of the carbon C-3 from serine via 5,10-methylenetetrahydrofolate **56** to yield D-pantolactone **59** using *E. coli*. Incubation with (2*S*, 3*S*)-[3-$^2H_1$]serine, prepared (91) by the method outlined in Scheme 21, gave D-pantolactone **59** labeled in the 4-*pro-S* hydrogen so that the overall stereochemistry of the process is as shown in Scheme 24.

In the biosynthesis of the deoxyribonucleic acid (DNA) base thymidine **90**, deoxyuridine monophosphate **88** reacts with the adduct **56b** to yield thymidine **90**. In this process, H_C of the adduct **56b** becomes the third hydrogen of the methyl group of thymidine, as shown in Scheme 25. When (2*S*, 3*R*)- and (2*S*, 3*S*)-[3-$^2H_1$,3-$^3H_1$]serines **60**, $H_R = {}^3H$, $H_S = {}^2H$, and **60**, $H_R = {}^2H$, $H_S = {}^3H$, respectively, prepared as in Scheme 18, were used as

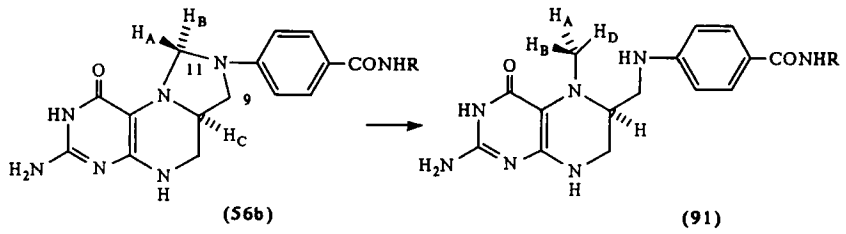
substrates for the coupled enzymes serine hydroxymethyltransferase and thymidylate synthase (EC 2.1.1.45), samples of thymidine **90** were obtained (85). These samples were degraded to acetate, which was assayed (3, 7) to show that the overall stereochemistry of the process was as outlined in Scheme 25 (85).



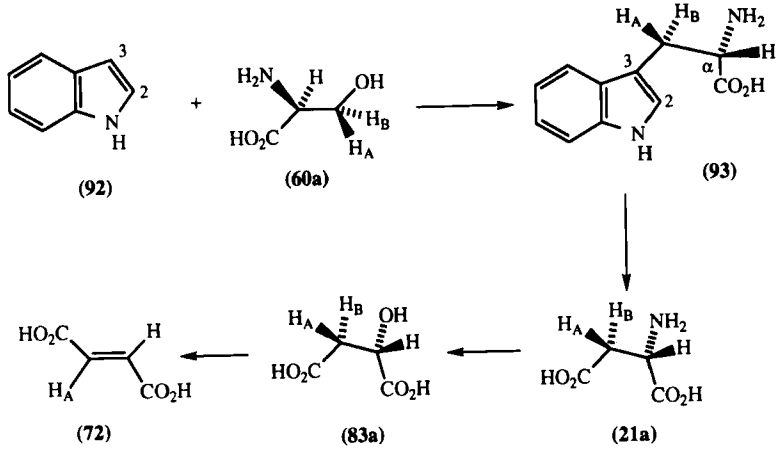
Scheme 25

The (3*R*)- and (3*S*)-[3-$^2H_1$,3-$^3H_1$]serines **60**, $H_R = {}^3H$, $H_S = {}^2H$, and **60**, $H_R = {}^2H$, $H_S = {}^3H$, respectively, were also used with the coupled enzymes serine hydroxymethyltransferase and methylenetetrahydrofolate reductase (EC 1.1.1.171) (100). Enzymic reduction of the labeled samples of the intermediate 5,10-methylenetetrahydrofolic acid **56b** gave samples of 5-methyltetrahydrofolic acid **91** (Scheme 26). These were degraded to acetate by a sequence that involved one inversion of configuration, and assay of the acetates showed that the overall stereochemistry of the reduction was as in Scheme 26 (100).

The enzyme tryptophan synthase (EC 4.2.1.20) catalyzes the reaction of serine **60** with indole **92** give the amino acid tryptophan **93** as shown in Scheme 27. Fuganti et al. (88) used this enzyme to convert samples of stereospecifically deuterated serine, prepared as in Scheme 19, to labeled samples of tryptophan **93**. These were shown to have the stereochemistry



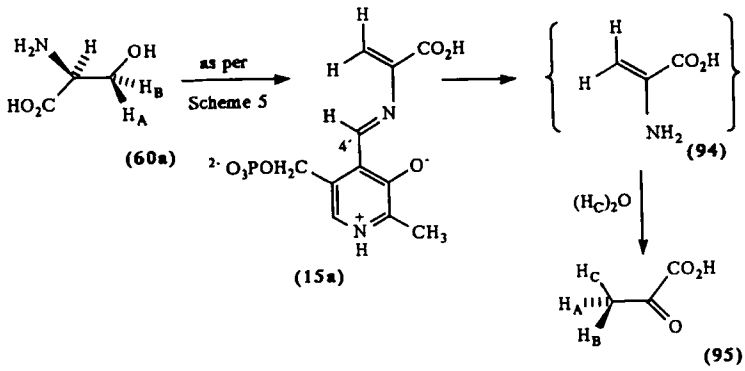
Scheme 26



Scheme 27

shown in Scheme 27 (88) by comparison of the ^{1}H NMR spectra of the *N*-benzoyl methyl esters with those of samples prepared by the method of Kirby and Varley (102) described in Section XV. The β-substitution reaction, occurring by the mechanism outlined in Scheme 5, had therefore taken place with retention of configuration (88). This result was also obtained by Floss et al. (83, 86, 103) using the tritiated serines prepared as outlined in Scheme 18. The resultant labeled samples of tryptophan were degraded to labeled samples of malate **83a** via the aspartates **21a** (Scheme 27). Use of the 3-*pro-R* specific enzyme fumarase (EC 4.2.1.2) then allowed the configuration of the product to be defined. Synthesis of tryptophan **93** from serine was catalyzed by the enzyme tryptophanase (EC 4.1.99.1) with the same stereochemical outcome (103).

Tryptophan synthase (EC 4.1.2.20) and tryptophanase also catalyze the dehydration of serine **60a** to pyruvate **95**, as shown in Scheme 28. Use of (2*S*, 3*R*)- and (2*S*, 3*S*)-[3-$^2H_1$,3-$^3H_1$]serines **60a**, $H_A = {}^2H$, $H_B = {}^3H$, and **60a**,

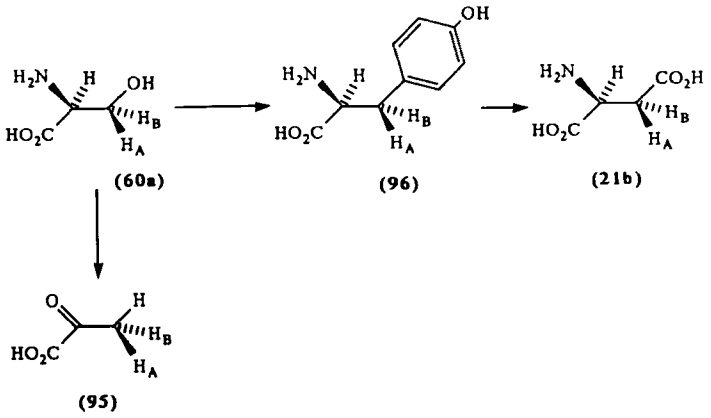


Scheme 28

$H_A = {}^3H$, $H_B = {}^2H$, respectively, in this process, followed by *in situ* enzymatic reduction to lactate of the pyruvate formed, gave samples that, on degradation to acetate, indicated that the proton had added to the β-carbon from the same side as the leaving hydroxyl group (45, 86, 103).

In the reverse reaction, the normal direction for tryptophanase, it has been shown that the hydrogen at C-3 of indole **92** comes directly from the C_α of tryptophan **93**, suggesting a single base at the active site and hence a *suprafacial* transfer (45, 103).

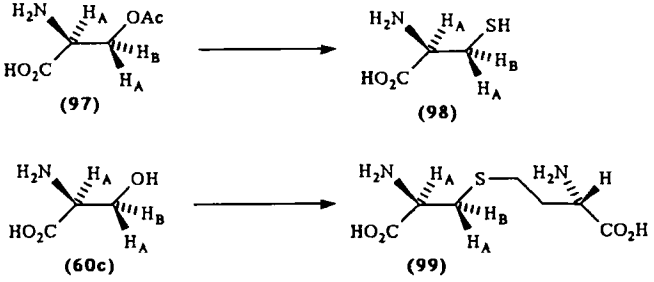
The reactions catalyzed by tyrosine phenol lyase (EC 4.1.99.2), shown in Scheme 29, are similar to those catalyzed by tryptophan synthase and tryptophanase. Fuganti et al. (104) incubated (3*R*)- and (3*S*)-[3-$^3H_1$]serines **60a**, prepared by the method in Scheme 19, with this enzyme. The resultant



Scheme 29

tyrosine **96**, on ozonolysis to aspartate and assay as in Scheme 27, was again shown to be formed with retention of configuration in the β-replacement reaction (104). Further, use of doubly labeled serines in the unusual dehydration to pyruvate **95** again showed that the hydroxyl group of serine was replaced by a proton with retention of configuration (105).

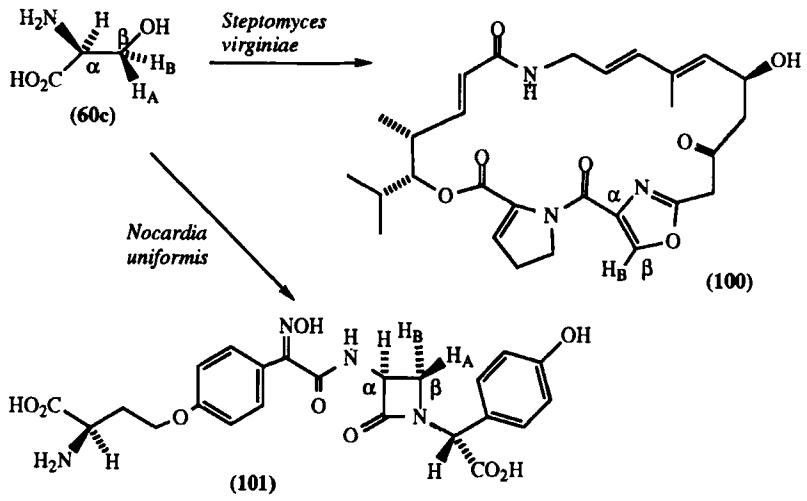
Further β-replacement reactions of serine and its derivatives have also been found to proceed with retention of stereochemistry. Thus *O*-acetylserine sulfydrase (EC 4.2.99.8) catalyzes the synthesis of cysteine **98** from *O*-acetylserine **97**, as shown in Scheme 30 (84) (see also p 414). Cystathione synthase (EC 4.2.1.22) catalyzes the condensation of serine **60c** with homocysteine to yield cystathione **99** (106). Both enzymes have a requirement for PLP.



Scheme 30

Serine is the precursor of several antibiotics. The oxazole ring of the antibiotic virginiamycin M_1 **100** (Scheme 31) is derived from serine; incubation of *Streptomyces virginiae* with samples of (2*S*, 3*R*)- and (2*S*, 3*S*)-[3-$^3H_1$]serine, derived as in Scheme 18, showed that the 3-*pro*-*S* hydrogen of serine is lost on formation of the double bond (107). This implies *anti* dehydrogenation, a process more commonly found to be *syn*. The β-lactam antibiotic nocardicin **101** is biosynthesized from serine, and incubation of *Nocardia uniformis* with stereospecifically deuterated serines, prepared by the method outlined in Scheme 21, has yielded samples of norcardicin, the ^2H NMR spectra of which indicated that β-lactam ring formation occurs with inversion of configuration (108, 109).

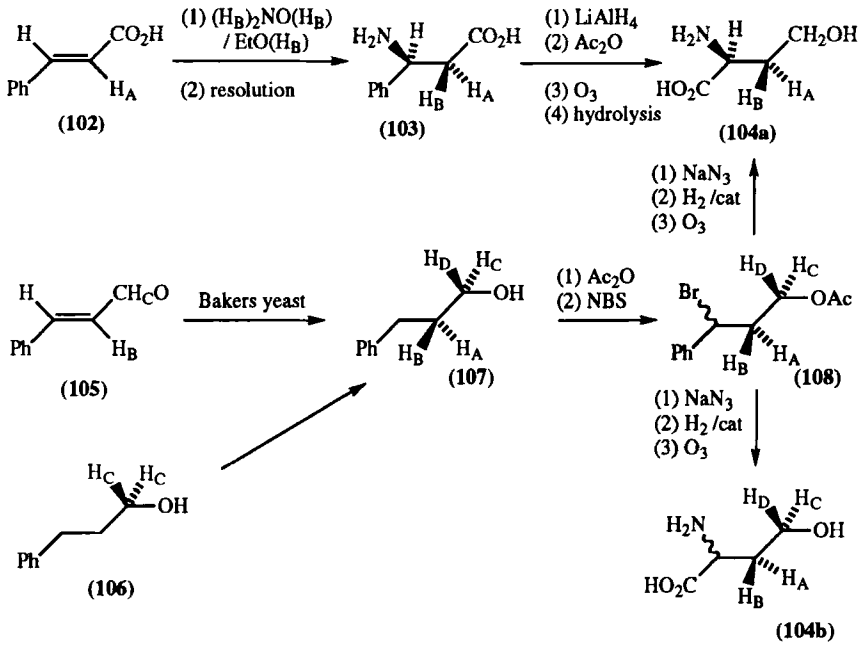
Decarboxylation of phosphaditylserine with phosphaditylserine decarboxylase (EC 4.1.1.65) in ^2H_2O gave [$^2H_1$]phosphatidylethanolamine (110). Conversion of this to [$^2H_1$]-2-aminoethanol using a phospholipase allowed comparison of the ^1H NMR spectra of camphanoates with those of authentic samples (73, 111). This showed that decarboxylation had occurred with retention of configuration (110).



Scheme 31

V. HOMOSERINE AND THREONINE

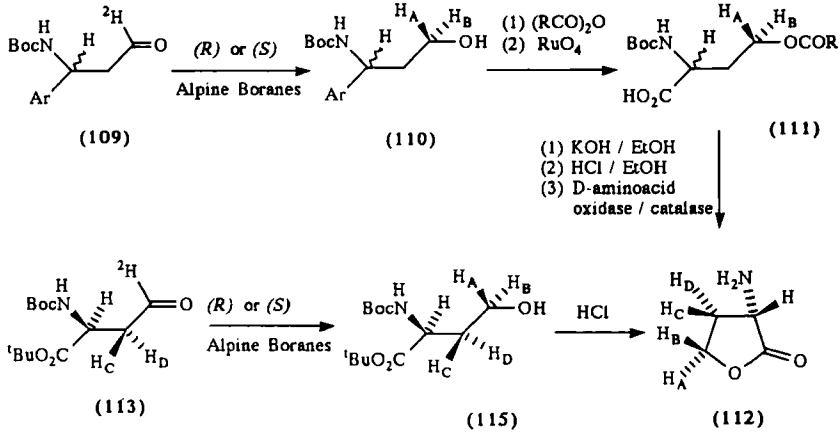
The first synthesis of samples of homoserine **104** that were stereospecifically labeled in the β and γ positions was achieved by Fuganti et al. (112, 113) as outlined in Scheme 32. Use of excess hydroxylamine in ethanol caused reductive *syn* addition of hydroxylamine to (*E*)-[2-$^2H_1$]cinnamic acid **102**, $H_A = {}^2H$. Resolution of the product gave the acid **103**, $H_A = {}^2H$, which was reduced to the alcohol. Acetylation, ozonolysis, and hydrolysis then gave (2*S*,3*R*)-[3-$^2H_1$]homoserine **104a**, $H_A = {}^2H$ (112). (2*S*,3*S*)-[3-$^2H_1$]Homoserine **104a**, $H_B = {}^2H$, was obtained by using unlabeled (*E*)-cinnamic acid and deuterated reagents, the addition of hydroxylamine to (*Z*)-cinnamic acid being only partially stereospecific (112). Since it had been shown (114) that reduction of (*E*)-cinnamaldehyde **105** by baker's yeast proceeded with addition of hydrogen to the *Re* face at C-2 of the double bond, reduction of [2-^{3}H]- and [2-^{2}H]cinnamaldehyde **105**, $H_B = {}^3H$, and ^2H, gave the alcohols **107**, $H_B = {}^3H$ and ^2H, which could be converted to (2*RS*,3*S*)-[3-$^3H_1$]- and [3-$^2H_1$]homoserines **104b**, $H_B = {}^3H$ and ^2H, respectively, as shown in Scheme 32 (112, 113). The aldehyde **105**, $H_C = {}^2H$, and the alcohol **106**, $H_C = {}^2H$, were used to prepare samples of homoserine stereospecifically labeled at C-4 (112, 115) with deuterium and tritium, baker's yeast (112), and yeast alcohol dehydrogenase (115) being used to effect reduction of **105** and exchange of **106**. The (4*R*)- and (4*S*)-[4-$^3H_1$,4-$^2H_1$]homoserines have been prepared in this way (115).



Scheme 32

Kalvin and Woodard (116) synthesized samples of homoserine labeled in all of the diastereotopic hydrogens. In their first synthesis, they used (*R*)- and (*S*)-alpine boranes to reduce the deuterated aldehyde **109**. (*R*)-Alpine borane gave the (*S*)-[$^2H_1$] alcohol **110**, $H_B = {}^2H$, (*S*)-alpine borane gave the corresponding (*R*)-alcohol **110**, $H_A = {}^2H$. ^1H NMR spectroscopic analysis of the mandelate esters indicated that the (*S*)-alcohol was present in an enantiomeric excess of 88% and that the (*R*)-alcohol was present in an enantiomeric excess of 76%. The lack of enantiomeric purity in the alcohols **110** was due to similar lack of purity of the commercial α-pinene used in the synthesis of the alpine boranes. The alcohols **110** were converted to the corresponding (2*S*,4*S*)- and (2*S*,4*R*)-[4-$^2H_1$]homoserine lactones, as shown in Scheme 33, resolution being effected by destruction of the (2*R*)-isomers using D-amino acid oxidase and catalase.

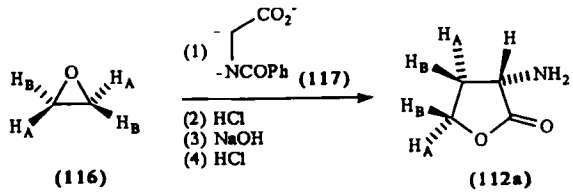
In Ramalingam and Woodard's synthesis (117) the protected aspartate semialdehyde **113** was synthesized from (2*S*)-aspartic acid and then converted to the labeled alcohols **115** using (*R*)- and (*S*)-alpine boranes (Scheme 33). Hydrolysis then led directly to (2*S*,4*R*)- and (2*S*,4*S*)-[4-$^2H_1$]homoserine lactones **112**. Since the enzyme aspartase may be used to prepare samples or (2*S*,3*R*)-[3-$^2H_1$]- and (2*S*,3*S*)-[2,3-$^2H_2$]aspartate (see Section IX), the synthesis, or a modification using more direct reduction methods, could be



Scheme 33

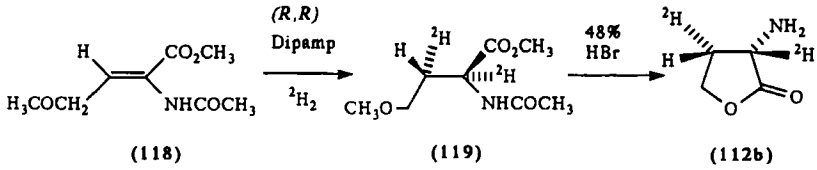
used to prepare the corresponding samples of homoserine lactone stereospecifically deuterated at C-3 (117, 118).

Schwab and Ho (119) have prepared the oxiranes **116**, $H_A = {}^2H$, and **116**, $H_B = {}^2H$, via a Sharpless reaction and found that the trianion **117** of hippuric acid would react with these to give products which, on deprotection, gave (2*RS*, 3*R*, 4*R*)- and (2*RS*, 3*S*, 4*S*)-[3,4-$^2H_2$]homoserine lactones **112a**, $H_A = {}^2H$, and **112a**, $H_B = {}^2H$, respectively (120, 121) (Scheme 34).



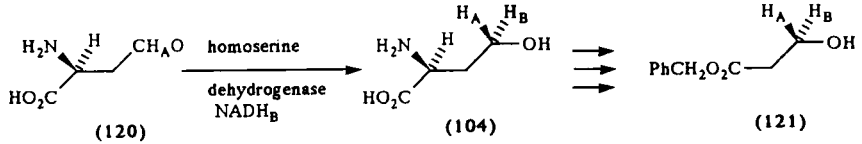
Scheme 34

A further synthesis (122) has used asymmetric reduction of the enamine **118** with deuterium and the chiral catalyst (*R*, *R*)-dipamp to obtain (2*S*, 3*R*)-[2,3-$^2H_2$]homoserine lactone **112b**, as in Scheme 35.



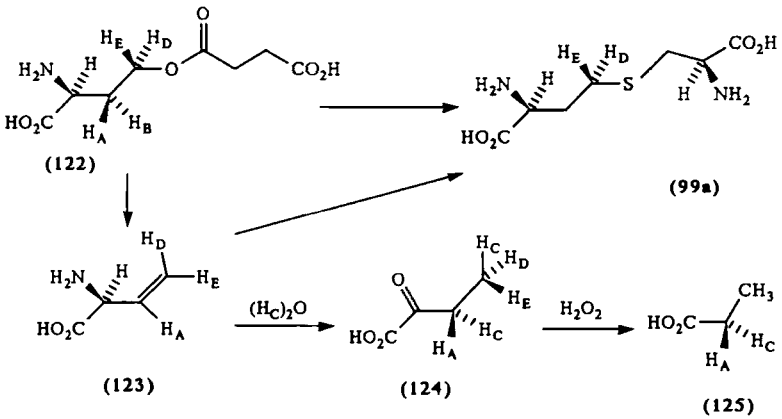
Scheme 35

The enzyme homoserine dehydrogenase (EC 1.1.1.3) catalyzes the reduction of L-aspartate semialdehyde **120** to L-homoserine **104** using the 4-*pro-S* hydrogen of reduced NADP (NADPH) (123) (Scheme 36). Chang and Walsh (123) reduced aspartate semialdehyde **120** using (4*S*)-[4-$^3H_1$]-NADPH and degraded the resultant homoserine **104** to the alcohol **121**. The tritium was retained in the aldehyde on oxidation of the alcohol **121** with *pro-R* specific alcohol dehydrogenase, thus showing the label to be *S*. The stereospecificity of labeling was thus proven, and the enzyme was used to prepare (4*R*)-[4-$^2H_1$]homoserine **104**, $H_A = {}^2H$, from [2-^{2}H]aspartate semialdehyde **120** $H_A = {}^2H$, and (4*S*)-[4-$^2H_1$]- and [4-$^3H_1$]homoserines **104**, $H_A = {}^2H$ and ^3H, respectively, from aspartate semialdehyde **120** and labeled NADH.



Scheme 36

The enzyme cystathione-γ-synthase (EC 4.2.99.9) catalyzes γ substitution of *O*-succinyl-L-homoserine **122** by L-cysteine **98** to yield cystathione **99a** by the mechanism shown in Scheme 3. It will also catalyze the dehydration to α-ketobutyrate **124** via vinylglycine **123** in the absence of L-cysteine. When the dehydration was conducted in ^2H_2O and the [^{2}H]-α-ketobutyrate was degraded to sodium propionate **125**, the specific rotation was in keeping with that of an authentic sample of (2*S*)-[2-$^2H_1$]propionate **125**, $H_C = {}^2H$ (124, 125) (Scheme 37). The proton had added to the intermediate **123** to



Scheme 37

give (3*S*)-[3-$^2H_1$]-α-ketobutyrate **124**, $H_C = {}^2H$. Fuganti and Coggiola, (126) used the samples of [3-$^2H_1$]homoserine, prepared as in Scheme 32, to show that the 3-*pro-R* hydrogen is lost on conversion to α-ketobutyrate **124**. They identified this hydrogen as the one that had been shown to exchange with ^2H_2O in ^1H NMR studies (125, 127) of exchange of *O*-succinylhomoserine **122** with this enzyme.

When Chang and Walsh (128, 129) prepared samples of (*Z*)-[4-$^2H_1$]- and (*E*)-[3,4-$^2H_2$]vinylglycines **123**, $H_D = {}^2H$, and **123**, $H_A = H_E = {}^2H$, respectively. and incubated them with the enzyme in ^3H_2O and in the absence of L-cysteine, they were able to isolate samples of α-ketobutyrate which, when subjected to Kuhn–Roth degradation, gave samples of [2-$^3H_1$,2-$^2H_1$]acetate. It was shown that the sample from (*Z*)-[4-$^2H_1$]vinylglycine **123**, $H_D = {}^2H$, gave (*S*)-acetate and that from (*E*)-[3,4-$^2H_4$]vinylglycine gave (*R*)-acetate, and so the stereochemistry of the process of C-4 was as indicated in **123** → **124**.

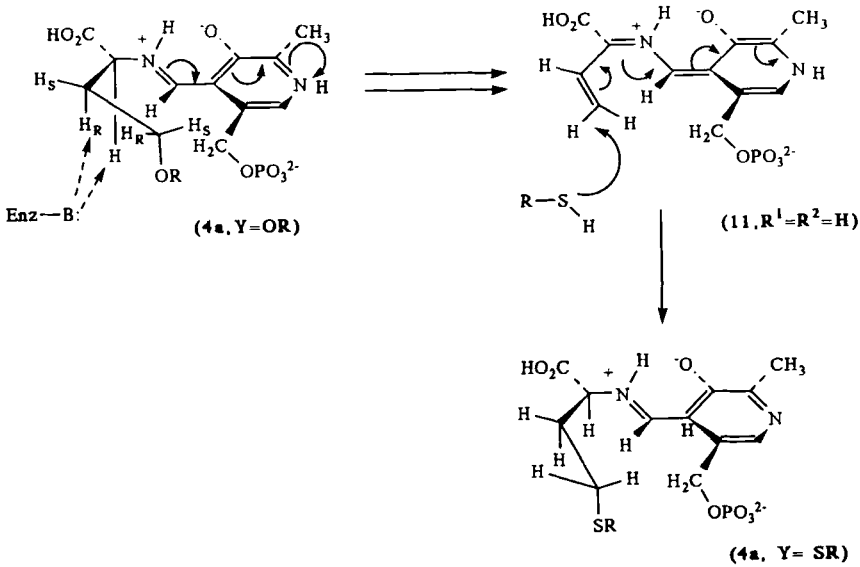
When the samples of labeled vinylglycine **123** were incubated with γ-cystathione synthase in the presence of cysteine, samples of labeled cystathione **99a** were obtained (128, 129). These were converted to samples of homoserine by a process involving one inversion of configuration, and these homoserine samples were subjected to the *pro-S* specific enzyme homoserine dehydrogenase (*vide infra*). In this way it could be shown that (*Z*)-[4-$^2H_1$]vinylglycine **123**, $H_D = {}^2H$, gave (4*S*)-[4-$^2H_1$]cystathione **99a**, $H_D = {}^2H$, and that the (*E*) compound **123**, $H_A = H_E = {}^2H$, gave the (4*R*)-isomer **99a**, $H_E = {}^2H$. The stereochemistry of the process was therefore as shown in Scheme 37.

Finally, synthetic samples of (4*R*)- and (4*S*)-[4-$^2H_1$]-*O*-succinylhomoserine **122**, $H_E = {}^2H$, and **122**, $H_D = {}^2H$, respectively, were incubated with the enzyme in the presence of L-cysteine (128, 129), and the ^1H NMR spectra of the resultant samples of cystathione **99a** were compared with those of the samples from the vinylglycine incubations. It was evident from these that the γ-substitution reaction had occurred with retention of configuration.

Elucidation of the stereochemistry of the reactions catalyzed by cystathione-γ-synthase has given a particularly detailed picture of the reactions. The γ-substitution reaction, previously shown in Scheme 3, can now be shown to take place at the active site of the enzyme with the stereochemistry outlined in Scheme 38 if we assume a *syn* conformation for the PLP–Schiff base.

The enzyme homoserine dehydratase (EC 4.4.1.1) catalyzes the conversion of L-homoserine **104** to α-ketobutyrate **124**. The stereochemistry of this reaction was shown (130) to be identical to that of the abnormal reaction of cystathione-γ-synthase, ^2H_2O being added as the 3-*pro-S* hydrogen of the α-ketobutyrate **124**.

The amino acid L-threonine **128** is synthesized in nature from L-homoserine **104** via the 3-phosphate **126**. Fuganti studied the stereochemistry of this

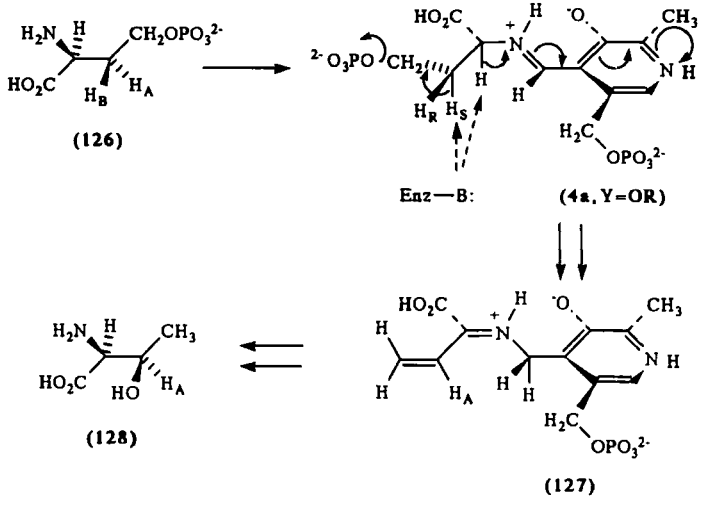


Scheme 38

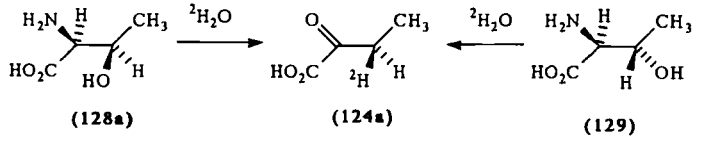
process by incubating synthetic samples of (3*R*)- and (3*S*)-[3-$^3H_1$]homoserine with yeast homoserine kinase (EC 2.7.1.39) and threonine synthase (EC 4.2.99.2) (113). The (3*R*)-[3-$^3H_1$] isomer gave a sample of L-threonine in which the label was shown to be retained at C-3, whereas the (3*S*)-[3-$^3H_1$]isomer gave a sample of L-threonine from which most of the tritium had been lost. The 3-*pro*-*S* hydrogen had been lost from the intermediate (**4a**, Y = OR), and assuming a single-base *suprafacial* mechanism, this would imply the stereochemistry shown in Scheme 39. The overall dehydration/hydration had occurred with retention of configuration at C-3.

The enzyme threonine dehydratase (EC 4.2.1.16) has been shown to dehydrate *both* L-threonine **128a** and L-allothreonine **129** in ^2H_2O to yield (3*R*)-[3-$^2H_1$]-α-ketobutyrate **124** (131) (Scheme 40), the configuration of which was proven by conversion to (2*R*)-[2-$^2H_1$]propionate and comparison of the ORD with that of an authentic sample. This implies either that the bound substrates **128a** and **129** dehydrate with different stereochemistries and protonate from the same side or that they dehydrate in identical fashion and protonate from different sides. Threonine dehydratase has an important role in the biosynthesis of valine, as we shall see in Section VIII.

Interestingly, D-threonine will act as a substrate for D-serine dehydratase (EC 4.2.1.4) and will yield (3*S*)-[4-$^2H_1$]-α-ketobutyrate **124**, $H_C = {}^2H$, in ^2H_2O (132).



Scheme 39

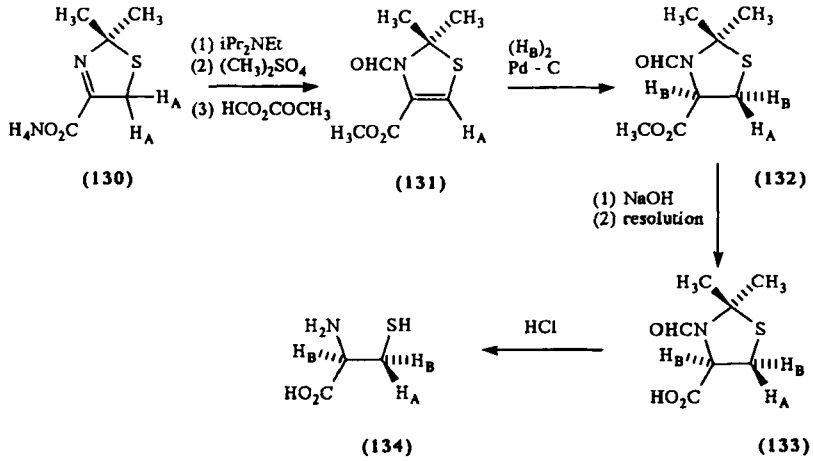


Scheme 40

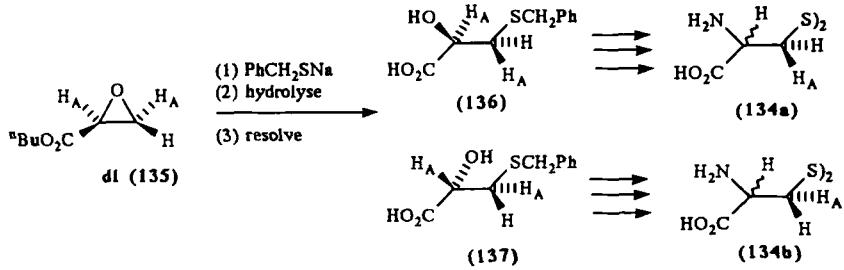
VI. CYSTEINE AND CYSTINE

Synthesis of samples of L-cysteine **134** stereospecifically labeled with tritium was first achieved by ourselves in connection with studies on the biosynthesis of the β-lactam antibiotics penicillin and cephalosporin (133, 134). The key steps in this synthesis were conversion of the imines **130** and **130**, $H_A = {}^3H$, to the acyl enamines **131** and **131**, $H_A = {}^3H$, respectively, as shown (Scheme 41). The tritiated compound **131**, $H_A = {}^3H$, was hydrogenated with *cis* addition of hydrogen to give **132**, $H_A = {}^3H$, while the unlabeled compound **131** was subjected to catalytic tritiation, giving **132**, $H_B = {}^3H$. Hydrolysis to the corresponding acids, resolution via the strychnine salts, and hydrolysis then gave the stereospecifically labeled samples of cysteine **134**.

Aberhart et al. (135) prepared the oxiranes **135**, $H_A = {}^2H$, and **135**, $H_A = {}^3H$, via reduction of anthracene adducts and epoxidation. These were readily ring opened with thiolate, and on hydrolysis, the products were resolved to yield the acids **136** and **137** in which the chirally labeled C-3 centers differed



Scheme 41

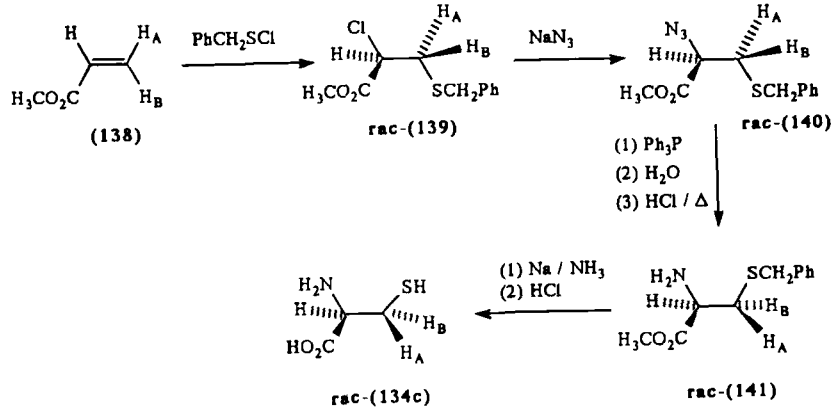


Scheme 42

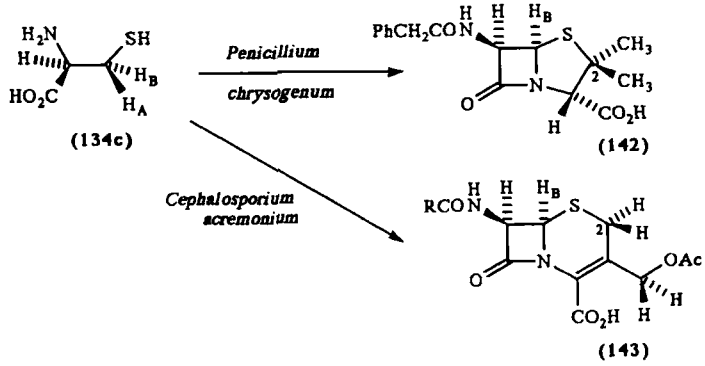
(Scheme 42). These were separately converted via the bromides, and amines to (2*RS*, 3*S*)- and (2*RS*, 3*R*)-[3-$^2H_1$] and [3-$^3H_1$]cystines, **134a** and **134b**, $H_A = {}^2H$ or ^3H, respectively.

More recently, Baldwin et al. (136) prepared samples of stereospecifically deuterated DL-cysteine by the method outlined in Scheme 43, and converted these to diastereomeric tripeptides that could be separated. It is of interest that the azide substitution **139** → **140** occurs with retention of configuration in this synthesis.

In our work (133, 134) and that of Aberhart et al. (135) and Baldwin et al. (136), the samples of cysteine were used to examine the biosynthesis of the β-lactam antibiotic penicillin **142**. All three groups found that the ring closure step that gave rise to the β-lactam in the antibiotic occurred with retention of configuration (Scheme 44). We have also shown (137) that the



Scheme 43

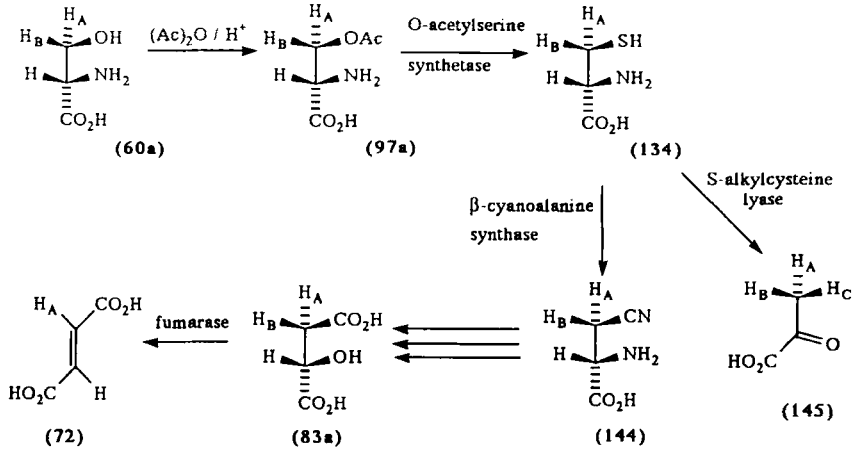


Scheme 44

ring closure that gives the β-lactam moiety of cephalosporin similarly occurs with retention of configuration.

The enzyme cysteine synthase (EC 4.2.99.8) catalyzes the last step in the biosynthesis of cysteine, converting serine acetate **97** to cysteine **134**. Floss et al. (84) studied this β-replacement reaction using stereospecifically tritiated serine acetates prepared from the labeled serines **60** synthesized as in Scheme 18 (Section IV). Assessment of chirality of the cysteine produced by degradation to serine and use of tryptophan synthase showed that the β-replacement reaction **97a → 134** had proceeded with retention of configuration (84) (Scheme 45).

Cysteine itself is the substrate for β-cyanoalanine synthase (EC 4.4.1.9) which catalyzes the β-replacement reaction yielding β-cyanoalanine **144**

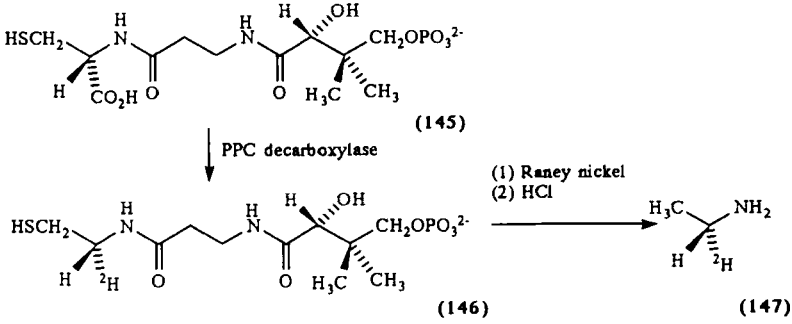


Scheme 45

(Scheme 45). When samples of (3*S*)- and (3*R*)-[3-$^3H_1$]cysteine **134**, $H_A = {}^3H$, and **134**, $H_B = {}^3H$, respectively, prepared using *O*-acetylserine sulfhydrase as above, were incubated with this synthase and the resultant samples of *β*-cyanoalanine **144** were degraded to malates **83a** via aspartates, the *pro-R* specific enzyme fumarase could be used to assess the stereochemistry, as shown in Scheme 45 (87). The *β* replacement **134** → **144** again occurred with retention of configuration (87).

The samples of (3*R*)- and (3*S*)-[3-$^3H_1$]cysteine were also incubated in ^2H_2O with *S*-alkylcysteine lyase (EC 4.4.1.6) to yield the [3-$^2H_1$, 3-$^3H_1$]pyruvates **145** (Scheme 45), which were converted *in situ* to lactates (87). Assessment of the chirality of the resultant lactates at C-3 indicated that the *β*-replacement reaction had again occurred with retention of configuration (87).

The cysteine moiety of phosphopantothenoylcysteine (PPC, **145**) can be



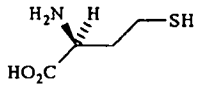
Scheme 46

decarboxylated by the enzyme PPC decarboxylase (EC 4.1.1.36) to yield pantotheine 4′-phosphate **146** (Scheme 46). This reaction was conducted in ^2H_2O, and the product **146** was degraded to [1-$^2H_1$]ethylamine **147**. Raney nickel treatment and hydrolysis followed by ^1H NMR spectroscopic analysis of the camphanamide showed that decarboxylation had occurred with retention of configuration (138, 139).

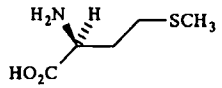
We have recently prepared samples of stereospecifically C-3 deuterated D-cystine by ring opening an aziridine related to **86** (Scheme 23) with benzyl mercaptan and subsequent deprotection and oxidation (94).

VII. HOMOCYSTEINE, METHIONINE, AND RELATED COMPOUNDS

The amino acid homocysteine **148** is obtained on treatment of cystathione **99** with the enzyme β-cystathionase (EC 4.4.1.8). Chang and Walsh (128) used the samples of (4*R*)- and (4*S*)-[4-$^2H_1$]cystathione **99a**, prepared as in Scheme 37, in this reaction and degraded the samples of homocysteine produced to labeled homoserinelactones. This indicated that, as expected, the chirally labeled center was not disturbed in the reaction.



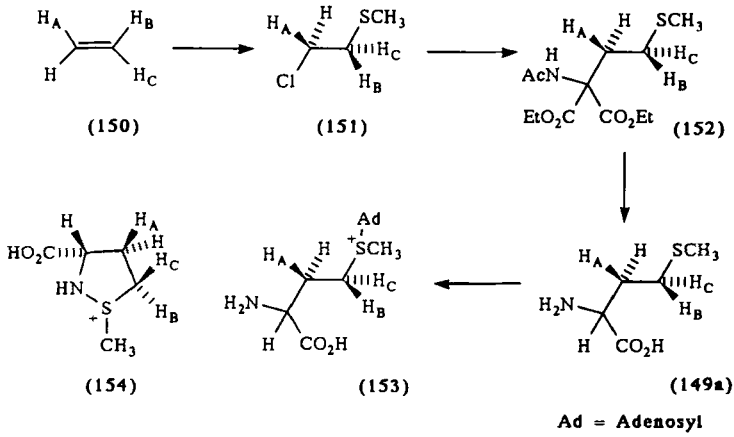
(148)



(149)

Methionine **149** is a very important amino acid, and several stereospecifically labeled samples have been prepared. Golding and others (140, 141) prepared samples of (*E*)- and (*Z*)-[1,2-$^2H_2$]ethylene **150**, $H_A = H_C = {}^2H$, and **150**, $H_A = H_B = {}^2H$, respectively, from [$^2H_2$]acetylene and converted these to the corresponding chlorides **151** by *anti* addition of methane sulfenyl chloride. Substitution by sodium acetylaminomalonate gave the products **152**, the reaction occurring with retention of configuration via a thiiranium ion intermediate (Scheme 47).

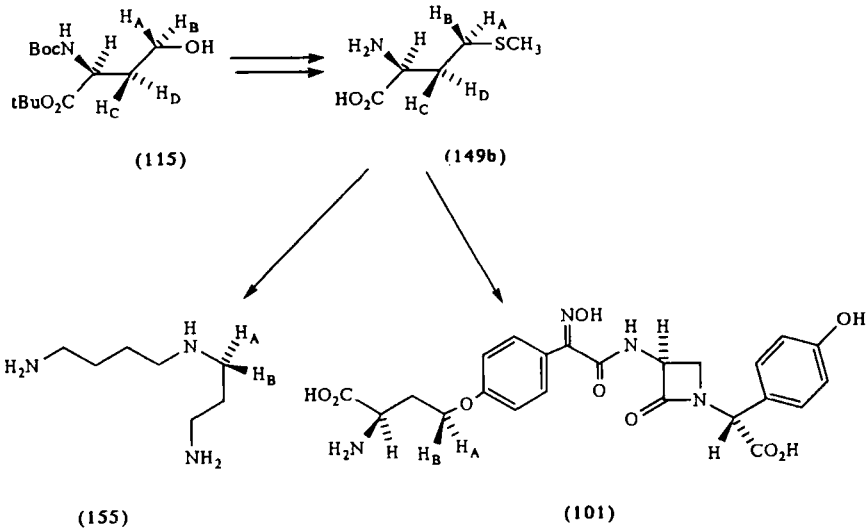
Hydrolysis then gave the [3,4-$^2H_2$]methionines **149a**. A mixture of the (2*R*,3*R*,4*S*)-, (2*R*,3*S*,4*R*)-, (2*S*,3*R*,4*S*)-, and (2*S*,3*S*,4*R*)-isomers was obtained starting from (*Z*)-[1,2-$^2H_2$] ethylene **150**, $H_A = H_B = {}^2H$, and a mixture of the (2*R*,3*R*,4*R*)-, (2*R*,3*S*,4*S*)-, (2*S*,3*R*,4*R*)-, and (2*S*,3*S*,4*S*)-isomers was obtained starting from (*E*)-[1,2-$^2H_2$]ethylene **150**, $H_A = H_C = {}^2H$. The stereochemistry was confirmed by ^1H NMR spectroscopic methods using the cyclic oxidation products **154**. Wiesendanger, Arigoni et al. (142) resolved the methionines **149a** by acylase hydrolysis of the *N*-acetamides, obtaining the



Scheme 47

(2*S*)-*threo* and (2*S*)-*erythro* pairs **149a**, $H_A = H_B = {}^2H$, and **149a**, $H_A = H_C = {}^2H$, respectively. They converted these to labeled samples of *S*-adenosylmethionine **153** by literature procedures (Scheme 47).

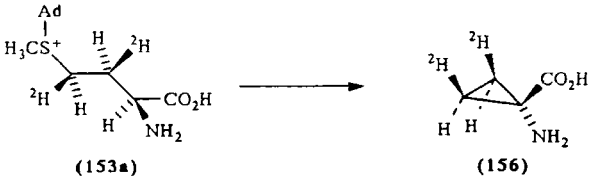
Two syntheses of (2*S*,4*R*)- and (2*S*,4*S*)-[4-$^2H_1$]methionine, **149b**, $H_B = {}^2H$, and **149b**, $H_A = {}^2H$, respectively, from the homoserine derivatives **115**, prepared as described in Section V, are shown in Scheme 48. These involved conversion of the samples of **115** to the tosylates (143) or the mesylates (144)



Scheme 48

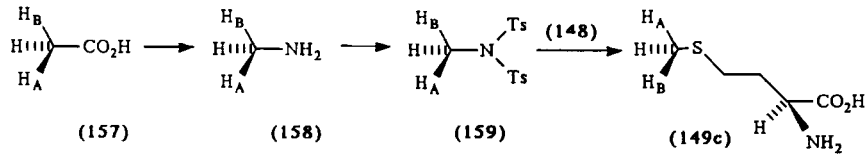
and nucleophilic substitution with inversion of configuration to obtain the samples of methionine **149b** (143, 144). These compounds were used to show that, in the biosynthesis of nocardicin A **101**, the methionine is incorporated with inversion of configuration (144). Labeled samples of methionine **149b** have also been incorporated into spermidine **155** by *E. coli* (141, 145, 146), and substitution of the intermediate decarboxylated *S*-adenosylmethionine was shown to occur with overall inversion of configuration (Scheme 48). This was shown independently (147) using the decarboxylated intermediate. Methionine decarboxylase (EC 4. 1. 1. 57) has been shown to decarboxylate methionine with retention of configuration (148).

S-Adenosylmethionine **153** is the precusor of the cyclic amino acid aminocyclopropanecarboxylate **156**. Ramalingam et al. (149) and Wiesendanger et al. (142) have investigated the stereochemistry of this process using similar methods, exemplified for the *threo* isomers **153a** in Scheme 49. Here (2*S*, 3*S*, 4*R*)-[3, 4-$^2H_2$]-*S*-adenosylmethionine **153a** and its (2*S*, 3*R*, 4*S*)-isomer were incubated with aminocyclopropanecarboxylate synthase from tomatoes and the cyclopropanes **156** were isolated. These were shown to be *meso* by ^1H NMR spectroscopy so that cyclization had taken place with inversion of configuration. *S*-Adenosylmethionine **153** is involved in a large number of methyl transfer reactions in nature, and Floss and co-workers (150–152) and Arigoni (153) have synthesized samples of methionine **149c** labeled stereospecifically in the methyl group by the method shown in Scheme 50. This involves Curtius rearrangement of (*R*)- and (*S*)-[2-$^3H_1$, 2-$^2H_1$]acetates **157**, $H_A = {}^3H$, $H_B = {}^2H$, and **157**, $H_A = {}^2H$, $H_B = {}^3H$, respectively, to yield the methylamines **158** with retention of configuration. Ditosylation followed by reaction with homocysteine **148** then gave (methyl-*S*)- and (methyl-*R*)-[methyl-$^3H_1$, $^2H_1$] methionies **149c**, $H_A = {}^3H$, $H_B = {}^2H$, and **149c**, $H_A = {}^2H$, $H_B = {}^3H$, respectively, with invension of configuration (Scheme 50).



(153a) (156)

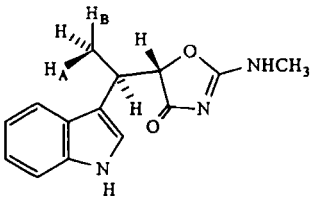
Scheme 49



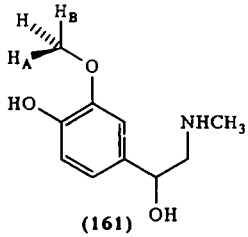
(157) (158) (159) (149c)

Scheme 50

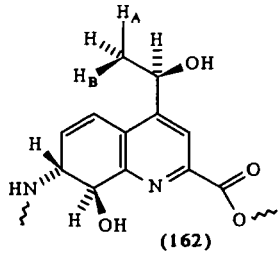
These samples of methionine were used to elucidate the stereochemical outcome of a number of biological methylation reactions. Thus incubation with *Streptomyces griseus* gave indolmycin **160**, which on Kuhn–Roth oxidation and assessment of configuration of the resultant acetate showed that C methylation had occurred with inversion of configuration (150–152). The O methylation catalyzed by catechol *O*-methyltransferase (EC 2. 1. 1. 6) yielding metanephrine **161** also occurred with inversion of configuration (152, 154), as did other O-methylation (153–155), S-methylation (153), and C-methylation (156) reactions. An apparent C methylation with retention of configuration has been found in the biosynthesis of the quinaldic acid residue **162** of the polypetide antibiotic thiostrepton (157), but the mechanism of the process may be more complex than a simple methyl substitution reaction.



(160)

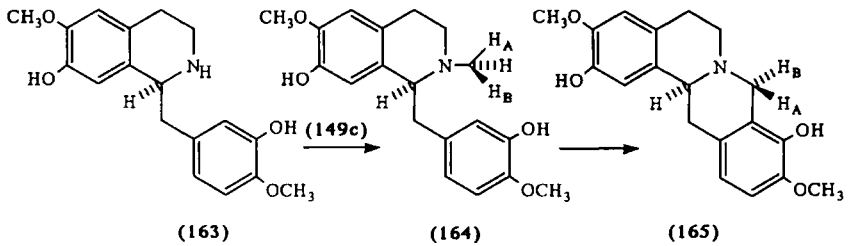


(161)



(162)

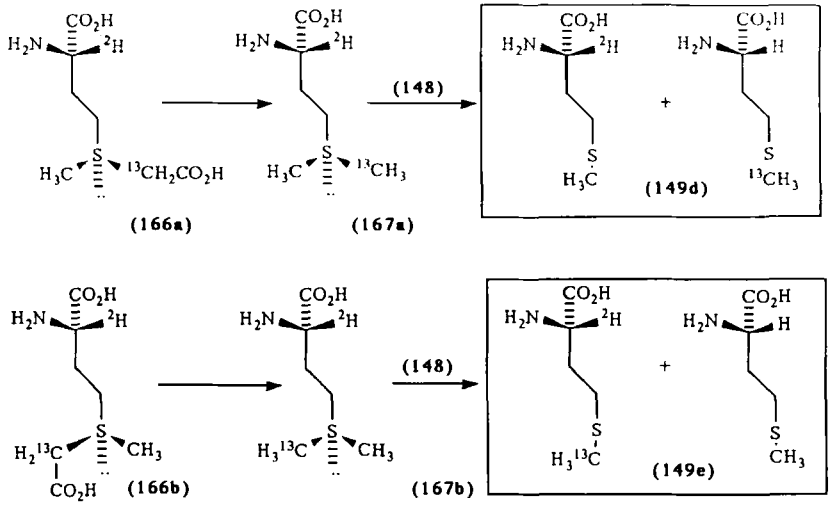
When (5*R*-methyl-$^3H_1$, $^2H_1$)- and (5*S*-methyl-$^3H_1$, $^2H_1$)-5-methyltetrahydrofolate **91**, $H_B = {}^3H, H_D = {}^2H$, and **91**, $H_B = {}^2H, H_D = {}^3H$, respectively, were prepared and incubated with the cobalamine-dependent methionine synthase (EC 2. 1. 1. 13) from *E. coli*, the degradation of the methionine produced showed that the overall two-step process had proceeded with net retention of configuration (158). Investigation of the N methylation/ring closure steps in the biosynthesis of the alkaloid scoulerine **165** showed that N methylation to reticuline **164** proceeded with inversion of configuration at the methyl group and that closure of the berberine bridge to **165** was also an inversion process (159) (Scheme 51).



(163) (164) (165)

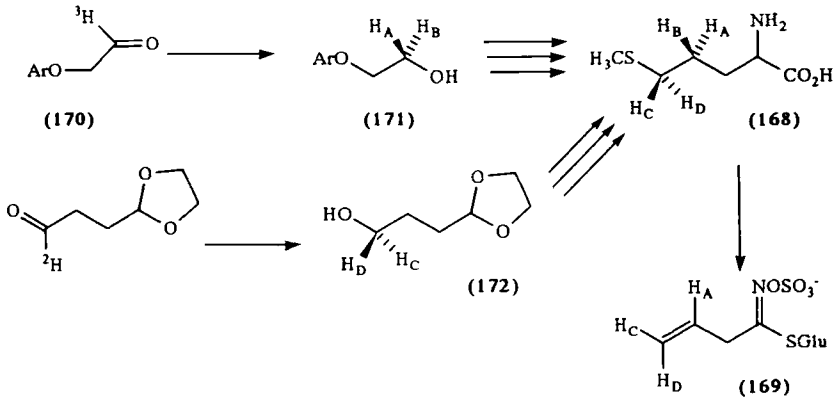
Scheme 51

An enzyme preparation from jack bean meal will transfer a methyl group from *S*-methylmethionine **167** to homocysteine **148** to yield 2 mol of methionine **149**. Use of the doubly labeled compounds **166a** and **166b**, separated by the method of Cornforth et al. (160), conversion to the (C_S, S_R)- and (C_S, S_S)-isomers of methylmethionine **167a** and **167b**, and incubation with the enzyme, allowed mass spectrometry to be used to show that the *pro-R* methyl group of *S*-methylmethionine is transferred to *L*-homocysteine **148** (161, 162), as shown in Scheme 52.



Scheme 52

The amino acid homomethionine **168** is involved in the biosynthesis of sinigrin **169** in horseradish (Scheme 53). Parry and Naidu (163) synthesised (4*R*)- and (4*S*)-[4-$^3H_1$]homomethionines **168**, $H_A = {}^3H$, and **168**, $H_B = {}^3H$, respectively, using the method outlined in Scheme 53. This relies on reduction of the aldehyde **170** with enantiomeric chiral boranes to give the alcohols **171**, $H_A = {}^3H$ or $H_B = {}^3H$, which are transformed by a series of steps to the amino acids **168**. They also prepared (5*R*)- and (5*S*)-[5-$^2H_1$]homomethionines **168**, $H_C = {}^2H$, and **168**, $H_D = {}^2H$, as shown (163). Feeding the labeled samples of homomethionine to horseradish showed that the 4-*pro-S* hydrogen was lost on incorporation into sinigrin **169**, isolated as an allyl isothiocyanate, and that the 5-*pro-R* hydrogen became the *cis*-5-hydrogen, H_C, and the 5-*pro-S* the *trans*-5-hydrogen, H_D, in sinigrin **169**. Thus *anti* elimination had occurred (163).



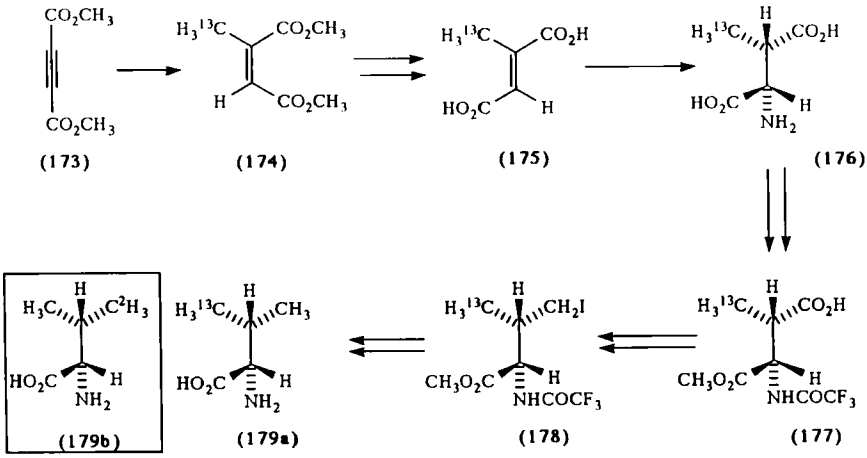
Scheme 53

VIII. VALINE, LEUCINE, AND ISOLEUCINE

The branched-chain amino acids valine, leucine, and isoleucine have very similar biosyntheses and catabolism. Valine **179** and leucine **205** have diastereotopic methyl groups and leucine **205** and isoleucine **212** have diastereotopic hydrogen atoms. These may be differentiated by labeling so that the stereochemistry of the biological processes involving these amino acids may be studied.

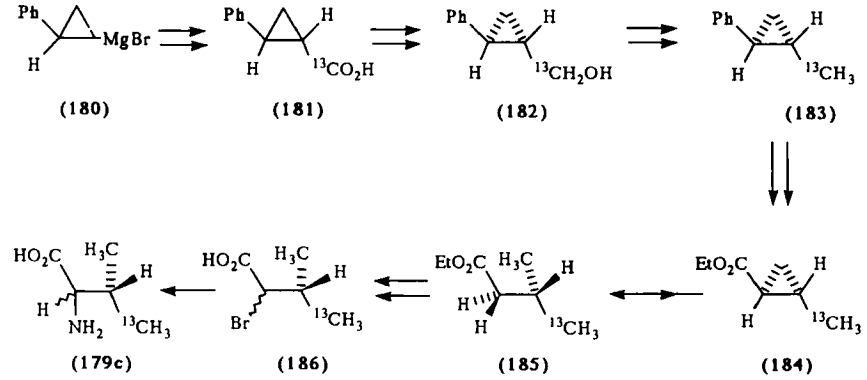
A. Valine

Syntheses of samples of valine **179** in which the diastereotopic methyl groups are differentiated by isotopic labeling have been achieved by several groups. In the synthesis shown in Scheme 54 (164) the ^{13}C-labeled diester **174** was prepared from the acetylene **173** by stereospecific addition of labeled dimethylcopper at $-78°C$. This was isomerized by light in the presence of a trace of bromine to the *trans* isomer, which was then hydrolyzed to the diacid **175**. The nonracemic chiral amino acid **176** was then obtained by ammonia addition using the enzyme β-methylaspartase (EC 4.3.1.2). Treatment of **176** with trifluoroacetic anhydride and regiospecific opening of the anhydride with methanol gave predominantly the α-ester β-acid **177**, which was reduced with diborane to the corresponding alcohol. This was converted via the iodide **178** to (2*S*, 3*S*)-[4-^{13}C]valine **179a** as shown in Scheme 54 (164). When C^2H_3I was used to prepare the dimethylcopper, (2*S*, 3*S*)-[4, 4, 4-$^2H_3$]valine was obtained using this synthesis (165). Reduction of the acid **177** with deutero-borane and further reduction of the iodide **178** with NaB^2H_4 allowed the synthesis to be used to prepare (2*S*, 3*R*)-[4, 4, 4-$^2H_3$]valine **179b** (165).



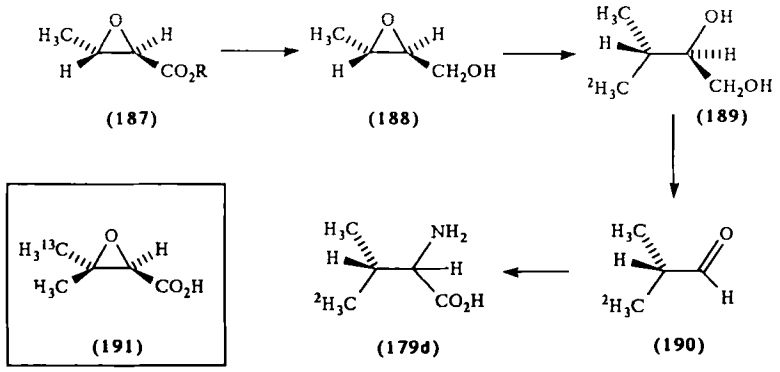
Scheme 54

Another synthesis of the stereospecifically ^{13}C-labeled valine **179c** (166) is shown in Scheme 55. The label was introduced by reaction of the Grignard reagent **180** with $^{13}CO_2$, and the resultant acid was esterified and isomerized to the thermodynamically more stable *trans* isomer. Hydrolysis to the acid **181**, resolution via the quinine salt, and reduction via the alcohol **182** then gave the cyclopropane **183**. Ozonolysis and esterification of **183** gave the ester **184**, which underwent regiospecific ring opening with lithium and ammonia to yield the product **185**. This was then converted to the labeled sample of valine **179c**, as shown (166).



Scheme 55

Ring opening of the enantiomerically pure epoxide **188** (from reduction of **187**) with labeled methyllithium has been used as the key step in a synthesis



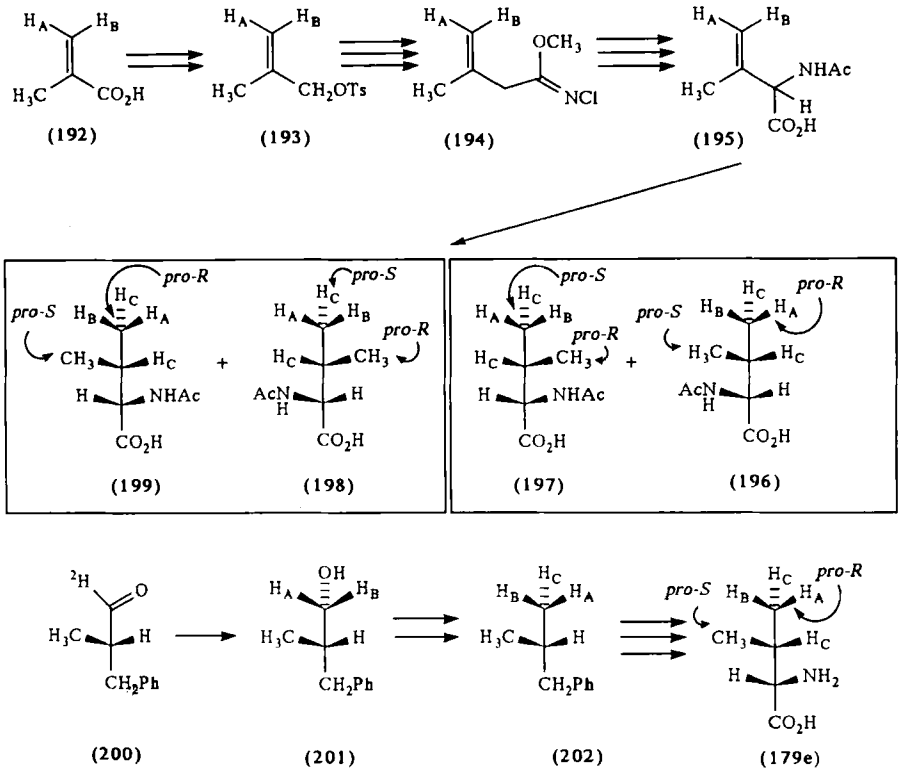
Scheme 56

of (2*RS*, 3*S*)-[4,4,4-$^2H_3$]- and [4-^{13}C]valines as summarized in Scheme 56 (167, 168). The enantiomeric epoxide was used to prepare the (3*R*)-isomers, and ring opening of the epoxide **191** with NH_4OH allowed stereospecifically labeled 3-hydroxyvalines to be prepared (169).

Samples of valine **179** in which one of the diastereotopic methyl groups is stereospecifically doubly labeled with the isotopes tritium and deuterium have been prepared. In the first such synthesis, Crout et al. (170, 171) prepared the (*E*)- and (*Z*)-[3-$^2H_1$]methacrylic acids **192**, $H_A = {}^2H$, and **192**, $H_B = {}^2H$, respectively, and converted them, as shown in Scheme 57, to the labeled derivatives **195** of dehydrovaline. Catalytic reduction using $^3H_2$ and Wilkinson's catalyst then proceeded with unexpected diastereoselectivity so that the *dl*-mixture **196** + **197** predominated over the *dl*-mixture **198** + **199** in a ratio of 19:1. The chirality of the product was assessed by ^3H NMR spectroscopy since it was known, from the synthetic samples already prepared, that the *pro-S* methyl group of (2*S*)-valine had the higher field chemical shift. Assuming *cis* catalytic tritiation, the product would have *R*-methyl in the 3-*pro-S* methyl, as in **197**, and *S*-methyl in the 3-*pro-R* methyl group, as in **196**, when the synthesis was conducted using (*E*)-[3-$^2H_1$]methacrylic acid **192**, $H_A = {}^2H$.

A second synthesis relying on reduction of the aldehyde **200** to the alcohol **201** by the *pro-R* specific horse liver alcohol dehydrogenase is also shown in Scheme 57. The alcohol **201** was converted via the compound **202** to (3*R*, 4*S*)-[4-$^2H_1$, 4-$^3H_1$]valine **179e** (172). The (3*R*, 4*R*)-isomer was obtained by inversion of the alcohol **201** by a Mitsunobu process and repetition of the synthesis (172).

Stereospecifically labeled samples of valine **179** have been used to examine the stereochemistry of the ring closure step, which leads to the non-β-lactam ring in penicillin **142** and cephalosporin **143** (see Scheme 44), NMR spectroscopic methods being used to assess the stereochemistry of the products. In



Scheme 57

this way, it was shown that the ring closure leading to penicillin **142** occurred with retention of configuration at the C-2 of penicillin (164, 168, 173, 174).

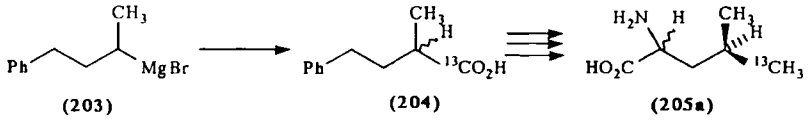
Further, the 3-*pro*-*S* methyl group of valine is incorporated as the ring carbon, C-2, of cephalosporin **143** (175) with loss of stereochemical integrity (176–178), although the exocyclic methylene group had evidently originated by stereospecific hydroxylation of the 3-*pro*-*R* methyl (176, 177).

The labeled samples of valine **179** have also been used to study the stereochemistry at C-3 of pantolactone **59** during the one-carbon transfer processes depicted in Schemes 17 and 24 (101, 179, 180). The one-carbon transfer occurred with retention of configuration at C-3 (101), although a previous misinterpretation (179) of the data had indicated an inversion process.

Since the major catabolic and biosynthetic pathways are similar for valine, leucine, and isoleucine, we shall consider these separately in Sections VIII.D and VIII.E.

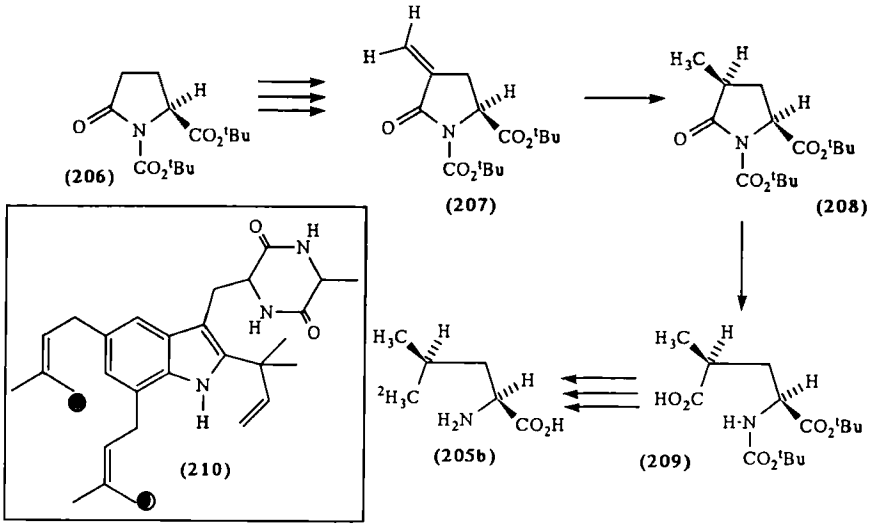
B. Leucine

Cardillo, Fuganti et al. (181) first synthesized samples of (2*RS*,4*R*)- and (2*RS*,4*S*)-[5-$^{13}C_1$]leucine **205** using the method outlined in Scheme 58, and this has been reinvestigated by Anastasis, Overton et al. (182). The label was introduced by reaction of the Grignard reagent **203** with $^{13}CO_2$, and the resultant (*RS*)-acids **204** were resolved. The synthesis was then completed using each of the isomers separately to yield the labeled samples of leucine.



Scheme 58

Aberhart and Weiller (183) used (2*RS*,3*S*)-[4-$^{13}C_1$]valine **179** prepared as described in the previous section to synthesize samples of (2*S*,4*S*)- and (2*R*,4*S*)-[5-$^{13}C_1$]leucine **205**. More recently, in need of a synthesis of large quantities of labeled leucine, we have devised a synthesis of (2*S*,4*R*)-[5,5,5-$^{2}H_3$]leucine **205b**, starting from the pyroglutamic acid derivative **206** (184). This is shown in Scheme 59, chirality being achieved by diastereoselective catalytic reduction **207** → **208**.

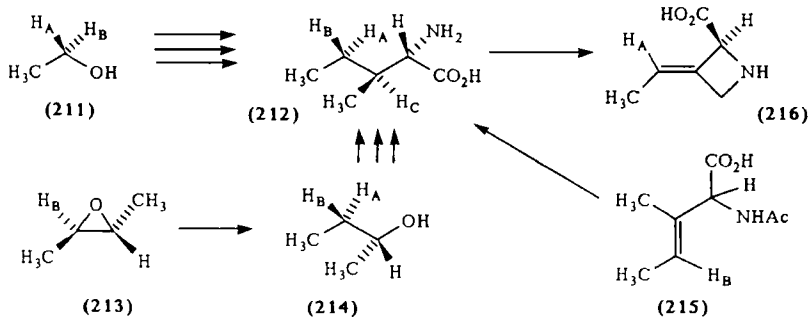


Scheme 59

Labeled samples of leucine **205** were fed to *Aspergillus amstelodami* to produce the metabolite echinulin **210**. The 4-*pro-S* methyl group of leucine was shown to be incorporated into the (*Z*)-methyl groups of the isoprenoid residues via catabolism to HMG–CoA (hydroxymethylglutaryl-coenzyme A) (see Section VIII.E) and mevalonic acid (181).

C. Isoleucine

Samples of isoleucine **212** stereospecifically labeled at C-4 with deuterium and tritium have been synthesized by the three routes shown in Scheme 60. Komatsubara, Crout et al. (185) converted the readily available (1*R*)-[1-$^2H_1$]ethanol **211**, $H_A = {}^2H$, via the tosylate and reaction with sodium acetylaminomalonate to DL-(3*S*)-[4$^2H_1$]2-aminobutanoic acid and thence biosynthetically to (2*S*, 3*S*, 4*S*)-[4-$^2H_1$]isoleucine **212**, $H_A = {}^2H$. Hill et al. (186, 187) used the biosynthetic method described in Section VIII.D to prepare **212**, $H_B = {}^3H$. They also used a method involving reduction of the epoxide **213** with lithium aluminum tritide to yield the alcohol **214**, $H_A = {}^3H$, in a synthesis of (2*RS*, 3*S*, 4*S*)-[4-$^3H_1$]isoleucine **212**, $H_A = {}^3H$, as shown in Scheme 60. (2*S*, 3*S*, 4*S*)-[3, 4-$^3H_2$]Isoleucine **212**, $H_A = H_C = {}^3H$, has also been prepared by reduction of the (*E*)-olefin **215** with [$^3H_2$]diimide followed by hydrolysis with renal acylase (188).

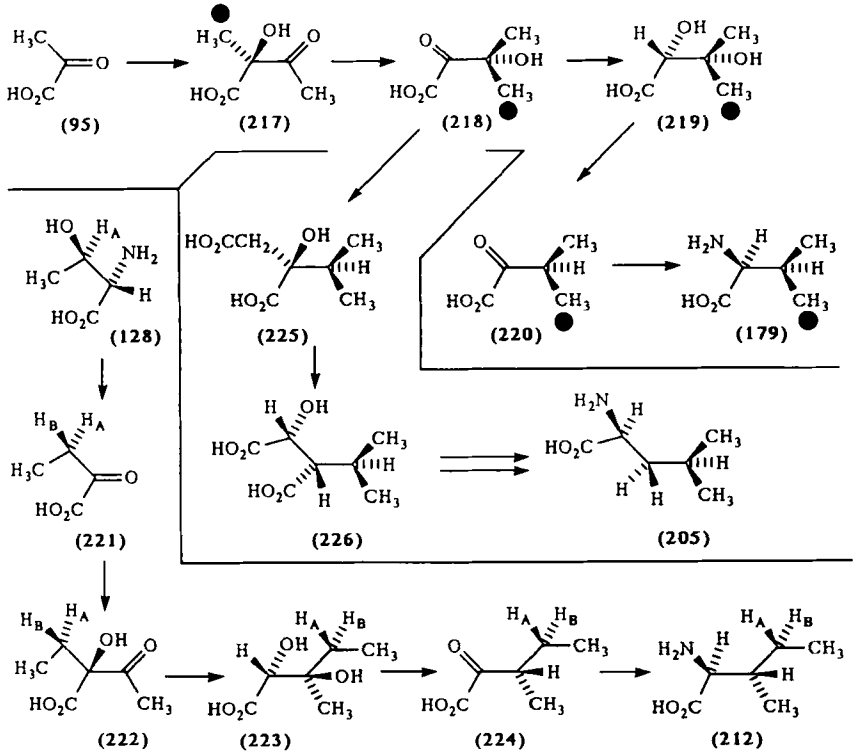


Scheme 60

Both synthetic and biosynthetically prepared samples of stereospecifically labeled isoleucine have been used to investigate the biosynthesis and catabolism of the amino acid described in Sections VIII.D and VIII.E. They have also been used to show that biosynthesis of 3-ethylidene-L-azetidine-(*Z*)-carboxylate **216** from isoleucine involves dehydrogenation with antiperiplanar elimination of H-3 and H-4*R* (187).

D. Biosynthesis

In the biosynthesis of valine **179** the first step is a benzoin condensation of 2 mol of pyruvate **95** to yield α-acetolactate **217**. A single enzyme, α-acetohydroxyacid reductoisomerase (EC 1.1.1.86), then catalyzes the rearrangement/reduction steps **217** → **218** → **219** (Scheme 61). The same enzyme catalyzes a similar sequence implied in **222** → **223** in the biosynthesis of isoleucine **212**. The substrates **217** and **222** for these reactions have been shown to have the (2*S*) configuration (189, 190), the product **223** to have the (2*R*, 3*R*) configuration (191–194), and the product **219** to have (2*R*) configuration (192, 193).



Scheme 61

The reduction step catalyzed by this enzyme has been shown to use the 4-*pro*-*S* hydrogen of NADPH (195), and when ^{13}C-labeled α-acetolactate **217** was used, it could be shown that the migrating methyl group eventually became the 3-*pro*-*S* methyl group of valine **179**. The migration thus has the

same stereospecificity as is found in isoleucine biosynthesis (196, 197). The stereochemistry of the subsequent dehydratase step **219** → **220** was discovered by synthesis of the (2*R*, 3*R*)- and (2*R*, 3*S*)-[3, 3, 3-$^2H_3$]diols **219** and conversion to valine **179** (198). The hydroxyl group was found to be replaced by hydrogen with retention of configuration (198).

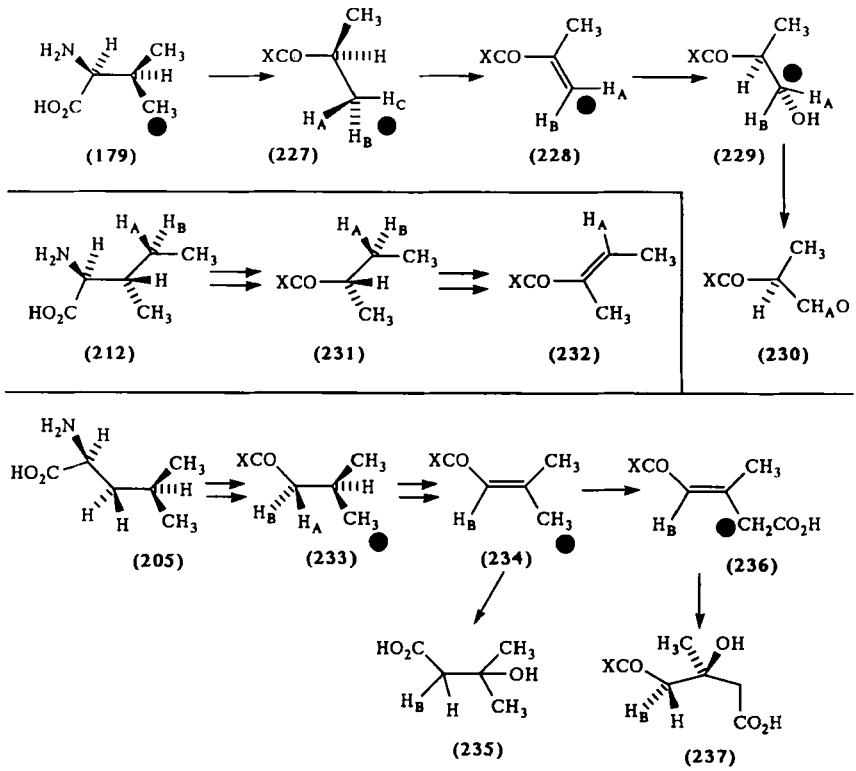
Use of DL-(3*S*)-[3-$^3H_1$]-2-aminobutanoic acid (188) and [3-$^2H_1$]-L-threonine **128**, $H_A = {}^2H$ (185, 199), with mutant strains of *Serratia marcescens* yielded (2*S*, 3*S*, 4*S*)-[4-$^3H_1$]- and [4-$^2H_1$]isoleucine **212**, $H_A = {}^3H$ or ^2H, indicating retention of configuration at the migrating center in the rearrangement **222** → **223**. Further, threonine dehydratase had evidently catalyzed the dehydration **128** → **221** with retention of configuration at C-3 (185, 188, 199) (Scheme 61).

In leucine biosynthesis, the intermediate **218** on the valine pathway reacts with acetyl-CoA to yield α-isopropylmalate **225** whose configuration has been shown to be *S* by X-ray crystallography (200). This reaction is analogous to that catalyzed by citrate synthase, and indeed the subsequent reaction, dehydration/rehydration giving β-isopropylmalate **226**, is analogous to the conversion of citrate to isocitrate. The configuration of β-isopropylmalate **226** had been shown to be 2*R*, 3*S* (201), and so the stereochemistry of the citrate and isopropylmalate reactions was identical. β-Isopropylmalate **226** was finally converted to leucine **205** by a 4-*pro-R* NADH specific dehydrogenase (EC 1.1.1.85) (202) and transamination (Scheme 61).

Use of [$^{13}C_6$]glucose mixed with nine equivalents of unlabeled glucose has allowed these biosynthetic processes to be used to prepare samples of protein containing valine **179** and leucine **205** in which the 3(4)-*pro-R* methyl group, being derived from C-4 of the intermediate **217**, will always contain an adjacent labeled carbon atom and show coupling. The 3(4)-*pro-S* methyl is derived from a different molecule of glucose from that of C-3 of valine (C-4 of leucine) and so will not show such coupling (203, 204).

E. Catabolism

Valine **179** is degraded in nature by transamination to the corresponding keto-acid which is decarboxylated to yield isobutyryl-CoA **227**, X = SCoA (Scheme 62a). Since it was found that stereospecifically labeled valine lost its stereochemical integrity in the process, possibly through racemization of the intermediate keto-acid, it was necessary to synthesize stereospecifically labeled isobutyric acid **227**, X = OH, to study the stereochemistry of the subsequent catabolic reactions (205). Thus (2*R*)- and (2*S*)-[3, 3, 3-$^2H_3$]isobutyric acid **227**, X = OH (205, 206), and (2*S*)-[3-^{13}C]isobutyric acid **227**, X = OH (207), have been prepared and used to show that it is the 2-*pro-S* methyl group that is "oxidized" on conversion to (2*S*)-2-hydroxymethylpropionic acid **229**,



Scheme 62

X = OH. The apparent oxidation in fact involves dehydrogenation to methacrylyl-CoA **228**, X = SCoA, and hydration, and when (*E*)- and (*Z*)-[$^2H_1$]methacrylic acids **228**, X = OH, $H_A = {}^2H$, and **228**, X = OH, $H_B = {}^2H$, respectively, were synthesized and incubated with *Pseudomonas putida*, the resultant (2*S*)-2 hydroxymethylpropionic acid **229** was compared to synthetic stereospecifically labeled samples to show that the hydration was a *syn* process, as in Scheme 62 (208), involving the 2-*Re* face.

The (*E*)- and (*Z*)-[$^2H_1$]methacrylic acids **228** were used as a starting point in a synthesis of (2*S*,3*R*)- and (2*S*,3*S*)-[3-$^3H_1$,3-$^2H_1$]isobutyric acids **227**, $H_A = {}^3H$, $H_B = {}^2H$, and **227**, $H_A = {}^2H$, $H_B = {}^3H$, respectively (209). These were fed to *P. putida*, and the ^3H NMR spectra of the labeled (2*S*)-hydroxymethylpropionates **229** obtained, coupled with a knowledge of the stereochemistry of the hydration reaction, allowed the dehydrogenation step to be assigned as an antiperiplanar elimination of hydrogen (209). Dehydrogenation of the hydroxymethylpropionate **229** to methylmalonate semialdehyde **230** has been shown to involve elimination of the 3-*pro*-*R* hydrogen, H_B (210).

Catabolism of isoleucine **212** follows an almost identical path of that of valine **179** above (211) (Scheme 62b). By incubating (4*R*)- and (4*S*)-[4-$^3H_1$]isoleucines prepared as in Section VIII.C above and isolation of tiglic acid **232**, X = OH, it was shown (186) that the 4-*pro-R* hydrogen was lost, and so the dehydrogenation was antiperiplanar, as had been shown for the corresponding dehydrogenation **227** → **228** in valine catabolism.

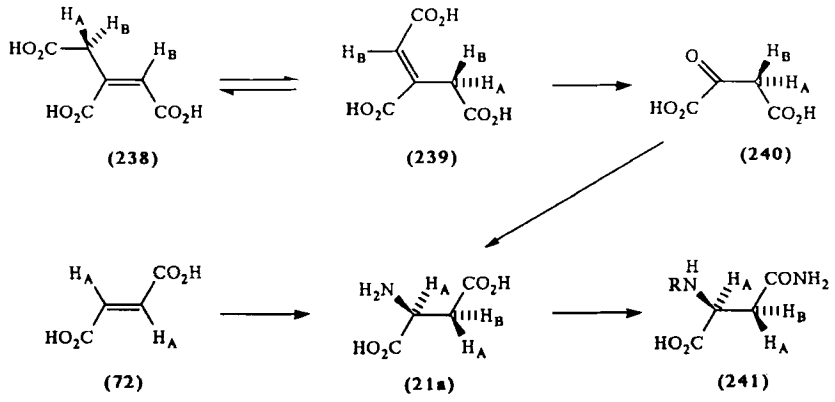
In leucine catabolism (Scheme 62c), the first steps leading to isovaleryl-CoA **233**, X = CoA, are similar to those in the catabolism of valine **179** and isoleucine **212**. When samples of (2*R*)- and (2*S*)-[2-$^3H_1$]isovaleric acid **233**, X = OH, were fed to biotin-deficient rats, β-hydroxyisovalerate **235** was isolated and shown to have lost the 2-*pro-R* hydrogen (212), thus indicating that the dehydrogenation step **233** → **234** had occurred with loss of this hydrogen. The hydration step **234** → **235** proved to be nonstereospecific for both C-2 and C-3 (213). The complete stereochemistry of the dehydrogenase step **233** → **234** was elucidated using a sample of (3*S*)-[4-$^{13}C_1$]isovalerate **233**, X = OH, prepared from the corresponding sample of valine (214). The product **234**, X = OH, showed ^{13}C enrichment in the (*E*)-methyl group so that the dehydrogenation was antiperiplanar, like the corresponding reactions in the catabolism of valine **179** and isoleucine **212** (214).

After dehydrogenation to **234**, X = SCoA, the catabolism of leucine **205** (Scheme 62c) differs from that of the other branched-chain amino acids. A biotin-dependent carboxylation leads to the acid **236**, X = SCoA, which is hydrated to HMG–CoA **237**, a compound involved in isoprenoid biosynthesis. Feeding stereospecifically labeled samples of leucine in studies of terpenoid biosynthesis indicated that the (*E*)-methyl group was carboxylated without isomerization of the double bond (181, 182). Messner, Cornforth et al. (215) investigated the hydration **236** ⇌ **237** catalyzed by the enzyme 3-methylglutaconyl-CoA hydratase (EC 4. 2. 1. 18) and showed that the reversible reaction had *syn* stereospecificity.

IX. ASPARTIC ACID, β-METHYLASPARTATE, AND ASPARAGINE

The enzyme aspartase (EC 4.3.1.1.) has long been known to catalyze stereospecific addition of ammonia across the double bond of fumaric acid (216–218), and after the original assignment of stereochemistry to this reaction was corrected, it was realized that addition of ammonia was *anti* (82). Since the enzyme is commercially available, reaction of fumaric acid **72** in $^2H_2O/N^2H_3$ readily affords (2*S*, 3*R*)-[3-$^2H_1$]aspartic acid **21a**, $H_B = {}^2H$, whereas addition of ammonia to [$^2H_2$] fumaric acid **72**, $H_A = {}^2H$, yields (2*S*, 3*S*)-[2,3-$^2H_2$] aspartic acid **21a**, $H_A = {}^2H$ (218–221). Recently, aspartase in immobilized

E. coli has been used in an improved synthesis of these compounds (118). The enzyme β-methylaspartase (EC 4.3.1.2) also adds ammonia across the double bond of fumaric acid in the same way as aspartase (222), and so an alternative synthesis is available. When [$^2H_2$]fumaric acid **72**, $H_A = {}^2H$, was incubated with aspartase in ^3H_2O, (2*S*,3*R*)-[2,3-$^2H_2$, 3-$^3H_1$]aspartic acid **21a**, $H_A = {}^2H$, $H_B = {}^3H$, was obtained (47) (Scheme 63).



Scheme 63

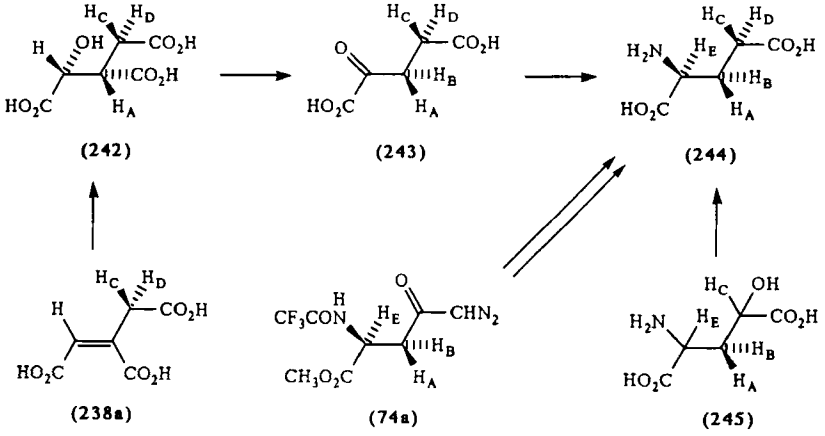
A further synthesis of labeled aspartic acids **21a** used the enzyme aconitate isomerase (EC 5.3.3.7). This enzyme interconverts *cis*- and *trans*-aconitates **238** and **239**, respectively, with exchange of the *4-pro-S* hydrogen. The (4*S*)-[4-$^3H_1$]-*trans*-aconitate **239**, $H_A = {}^3H$, produced in ^3H_2O could be ozonized and then converted *in situ* with sodium periodate and glutamic oxaloacetic transaminase (EC 2.6.1.2) to (3*S*)-[3-$^3H_1$]aspartic acid **21a**, $H_A = {}^3H$ (223). This process involves (3*S*)-[3-$^3H_1$]oxaloacetic acid **240**, $H_A = {}^3H$, as an intermediate.

Conversion of stereospecifically labeled samples of aspartic acid **21a** to the corresponding asparagine derivatives **241** has been achieved by ourselves (224) and others (225). The enzyme β-methylaspartase has been used to prepare (2*S*,3*S*)-[3-$^2H_1$]-3-methylaspartate and (2*S*,3*S*)-[3-$^2H_1$]-3-ethylaspartate (222, 226, 227).

It is of interest to note that incubation of labeled aspartate with aspartate β-decarboxylase (EC 4.1.1.12) resulted in decarboxylation to L-alanine with inversion of configuration (47). This differs from most PLP-mediated α-decarboxylation reactions that catalyze decarboxylation with retention of configuration.

X. GLUTAMIC ACID AND ITS DERIVATIVES

An early synthesis of labeled samples of glutamic acid involved the use of the citrate cycle enzyme isocitrate dehydrogenase (EC 1.1.1.41), which catalyzes the decarboxylation of isocitric acid **242** to yield α-ketoglutaric acid **243** (Scheme 64). It will also catalyze exchange of the hydrogen H_B from α-ketoglutarate **243.** Thus decarboxylation of isocitrate in ^3H_2O followed by transamination gave (3*S*)-[3-$^3H_1$]glutamic acid **244**, $H_B = {}^3H$, whereas exchange of [3,3-$^3H_2$]-α-ketoglutarate **243**, $H_A = H_B = {}^3H$, gave the (3*R*)-[3-$^3H_1$] isomer **243**, $H_A = {}^3H$ (228). These samples of α-ketoglutarate were converted to (2*S*, 3*S*)- and (2*S*, 3*R*)-[3-$^3H_1$]glutamic acids **244**, $H_B = {}^3H$, and **244**, $H_A = {}^3H$, respectively, using the enzyme glutamate dehydrogenase (EC 1.4.1.2). The stereochemistry of labeling was confirmed by degradation to aspartic acid **21a** and use of the 3-*pro-R* specific enzyme aspartase (see Section IX) (228). This sequence is generally used to prepare (3*S*)- and (3*R*)-[3-$^3H_1$]glutamates, although it is more usual to use [3-$^3H_1$]isocitrate **242**, $H_A = {}^3H$, prepared from *cis*-aconitate **238a** using aconitase (EC 4.2.1.3) and ^3H_2O for preparation of the (3*R*)-isomer (229–233).



Scheme 64

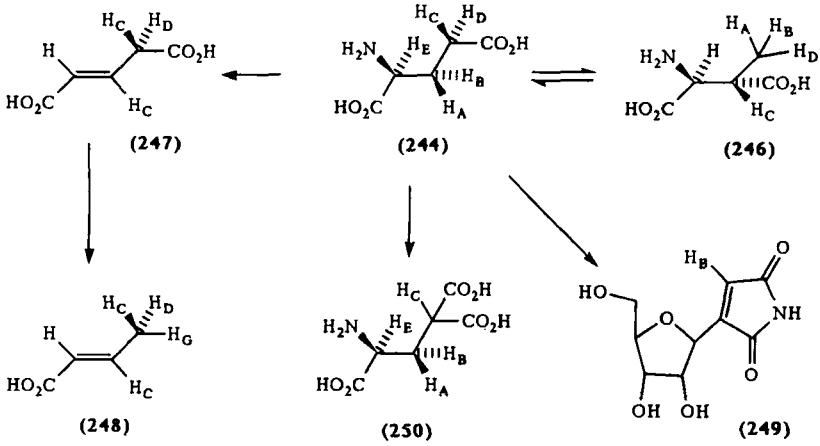
When (4*S*)-[4-$^3H_1$]isocitrate **242**, $H_D = {}^3H$, was prepared from stereospecifically labeled succinate using the enzyme isocitrate lyase (EC 4.1.3.1), this could be used in Scheme 64 to prepare (2*S*, 4*S*)-[4-$^3H_1$]glutamic acid **243**, $H_D = {}^3H$ (234).

Use of the isocitrate dehydrogenase/glutamate dehydrogenase system with isotopically labeled medium and labeled α-ketoglutarate **243** has allowed (2*S*, 3*R*)- and (2*S*, 3*S*)-[3-$^2H_1$, 3-$^3H_1$]glutamates **244**, $H_A = {}^3H$, $H_B = {}^2H$, and

244, $H_A = {}^2H$, $H_B = {}^3H$, respectively, to be prepared (235). The (2*S*,4*R*) and (2*S*,4*S*)-[4-^{3}H, 4-$^2H_1$] derivatives **244**, $H_C = {}^3H$, $H_D = {}^2H$, and **244**, $H_C = {}^2H$, $H_D = {}^3H$, were prepared from labeled samples of acetate using mixed enzymes of the citrate cycle (236). A synthesis of samples of glutamic acid stereospecifically labeled at C-4 has been achieved by a method involving nonstereospecific functionalization at C-4, separation, and resolution (234, 237, 238).

We have prepared (2*R*,3*R*)- and (2*S*,3*S*)-[3-$^2H_1$]glutamic acids **244** by Wolff rearrangement of the diazoketones **74a** (prepared as in Scheme 20) and deprotection (239, 240). When the Wolff rearrangement step was conducted in the presence of ^3H_2O, nonstereospecific labeling at C-4 was achieved in addition to the stereospecific labeling at C-3 (239, 240).

Glutamic acid **244** is involved in many biological processes, and several of these involve reaction at the prochiral atoms C-3 and C-4. The coenzyme B_{12}–mediated reaction catalyzed by the enzyme glutamate mutase (EC 5. 4. 99. 1) causes the reversible migration of hydrogen from the C-3 of glutamate **244**, to C-4 and of the carboxyl from C-4 to C-3, yielding β-methylaspartic acid **246**, (Scheme 65). When [3-$^2H_1$]-β-methylaspartate **246**, $H_C = {}^2H$, prepared using the enzyme β-methylaspartase as described in Section IX, was used in this rearrangement, the glutamic acid **244**, $H_C = {}^2H$ produced was degraded to succinic acid, shown to be (2*R*)-[2-$^2H_1$]succinate by comparison of the ORD with that of an authentic sample (241–243). Thus the migration was entirely stereospecific at the C-4 of glutamate, the 4-*pro*-*R* hydrogen being involved. When (3*S*)- and (3*R*)-[3-$^3H_1$, 3-$^2H_1$]glutamic acids **244**, $H_A = {}^3H$, $H_B = {}^2H$, and **244**, $H_A = {}^2H$, $H_B = {}^3H$, respectively, were used



Scheme 65

in the reaction and the β-methylaspartate **246**, produced was degraded to acetate, the results indicated that the reaction was nonstereospecific with respect to the methyl group of β-methylaspartate (235). This was in keeping with results obtained with ethanolamine ammonia lyase (EC 4.3.1.7), another vitamin B_{12}–mediated enzyme (77).

Use of the (2*S*,4*R*)- and (2*S*,4*S*)-[4-$^3H_1$, 4-$^2H_1$]glutamic acids **244**, $H_C = {}^3H$, $H_D = {}^2H$, and **244**, $H_C = {}^2H$, $H_D = {}^3H$, respectively, with the organism *Acidaminococcus lermentans* has shown that the decarboxylation **247** → **248** proceeds with retention of configuration (236). Feeding (2*S*,3*R*)- and (2*S*,3*S*)-[3-$^2H_1$]glutamates **244**, $H_A = {}^2H$, and **244**, $H_B = {}^2H$, respectively, to *Streptomyces showdoensis* has shown that the 3-*pro-R* hydrogen, H_A, is lost in the biosynthesis of the nucleoside antibiotic showdomycin **249** (244).

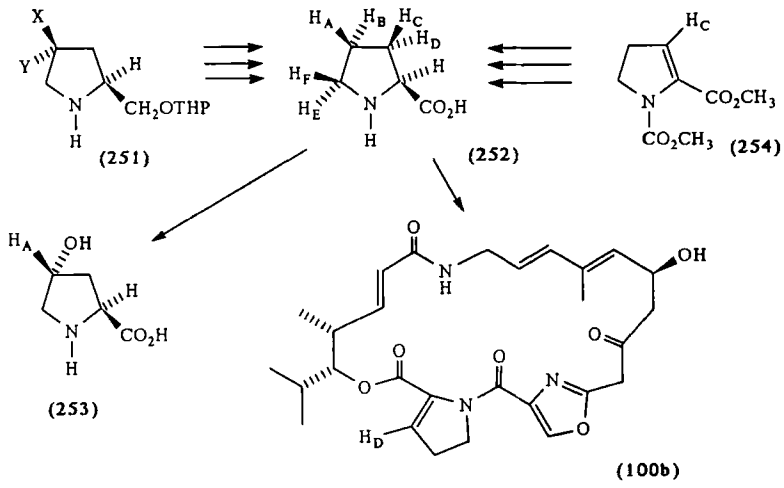
The vitamin K–mediated carboxylation of protein-bund glutamate residues to γ-carboxyglutamate residues **250** has been shown to exhibit a small isotope effect when the 4-*pro-S* hydrogen H_D is labeled and none when the 4-*pro-R* hydrogen H_C is labeled, indicating that the 4-*pro-S* hydrogen is lost in the process (234, 238, 245). This result is in keeping with findings from incubation of stereospecifically fluorinated glutamates (246).

The decarboxylation of glutamic acids to the neuronal transmitter γ-aminobutyric acid (GABA) has been much studied, and since the original discovery that the reaction occurred with retention of configuration (247), the process has been used to prepare labeled samples of GABA (248–255).

XI. PROLINE

The cyclic amino acid proline **252** is converted to both 4-hydroxyproline and 3-hydroxyproline in collagen synthesis. Fujita, Witkop et al. (256) provided (2*S*,4*S*)- and (2*S*,4*R*)-[4-$^2H_1$]- and [4-$^3H_1$]prolines **252**, $H_A = {}^2H$ or ^3H, and **252**, $H_B = {}^2H$ or ^3H, respectively, by a synthesis in which the key step was reduction of the protected tosylates **251**, X = H, Y = Ts, and **251**, X = Ts, Y = H, respectively, with $LiAl^2H_4$ or $LiAl^3H_4$ (Scheme 66). The ^1H NMR spectra of the deuterated compounds were different, and when the tritiated compounds were fed to chick embryos, the (2*S*,4*S*)-4-hydroxyproline **253** obtained from the collagen had lost the 4-*pro-R* hydrogen and retained 4-*pro-S* hydrogen of the proline (256). Hydroxylation had, therefore, occurred with retention of configuration. The samples of [4-$^3H_1$]proline used in the above study were also used to show that hydroxylation of the proline residues in the antibiotic actinomycin occurred with retention of configuration (257).

Prockop and others (258, 259) prepared a sample of [3,4-$^3H_2$]proline **252**, $H_B = H_D = {}^3H$, by catalytic tritiation of 3, 4-dehydroproline, and while acknowledging that some randomization of label might occur in this process,



Scheme 66

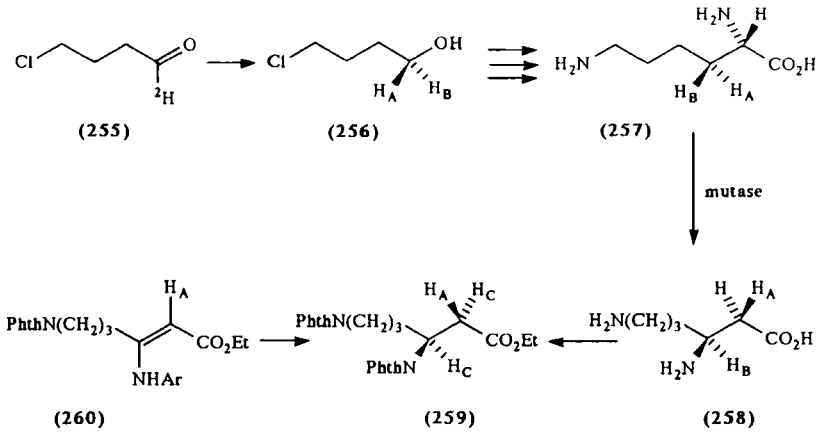
they indicated that one tritium was lost on 4-hydroxylation by chick embryos. ^3H NMR spectroscopy has recently revealed that [3, 4-$^3H_2$] proline prepared in this way has ca. 5% ^3H at C-5, 45% at C-3*S*, and 49% at C-4*R* with considerable monotritiation at C-3α and C-4α accompanying the expected *cis* ditritiation (260).

The sample of (2*S*, 3*S*, 4*R*)-[3, 4-$^3H_2$]proline **252**, $H_B = H_D = {}^3H$, was incorporated into virginiamycin *M* **100b** (Scheme 66) with retention of all tritium (261). A sample of (2*S*, 3*R*)-[3-$^3H_1$]proline **252**, $H_C = {}^3H$, was prepared in a synthesis involving reduction of the dehydroproline derivative **254**, $H_C = {}^3H$, and this lost tritium on incorporation into virginiamycin M **100b** (261).

The (5*R*)- and (5*S*)-[5-$^2H_1$]prolines **252**, $H_E = {}^2H$, and **252**, $H_F = {}^2H$, respectively, have been prepared from the labeled intermediates **52**, $H_R = {}^2H$, and **52**, $H_S = {}^2H$, respectively, in Scheme 16 (72, 255).

XII. α- AND β-LYSINE

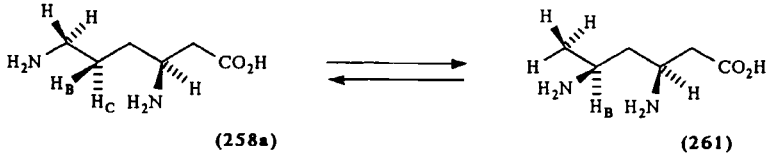
A chemical synthesis of (2*RS*, 3*R*)- and (2*RS*, 3*S*)-[3-$^2H_1$]lysines **257**, $H_A = {}^2H$, and **257**, $H_B = {}^2H$, respectively, has been achieved as outlined in Scheme 67 using the, by now familiar, reduction of a [^2H]aldehyde with chiral boranes (262, 263). Thus reduction of the chloroaldehyde **255**, with chiral boranes gave the alcohols **256**, $H_A = {}^2H$, and **256**, $H_B = {}^2H$. The chirality of these compounds was verified by ^1H NMR spectroscopic methods, and mesylation and further elaboration, involving inversion of the labeled center, gave the



Scheme 67

lysines **257**, $H_A = {}^2H$, and **257**, $H_B = {}^2H$. These compounds were then incubated with lysine 2,3-aminomutase (EC 5.4.3.2), which caused rearrangement of the (2*S*)-isomer to 3*S*-β-lysine **258** with rearrangement of the 3-*pro*-*R* hydrogen to C-2 (262, 263). The stereochemistry of labeling at C-2 was proven by converting the labeled β-lysine **258** to the diphthaloyl ethyl ester **259**, a racemic sample of which had been synthesized by catalytic deuteration of the (*Z*)-olefin **260** and further elaboration. ^1H NMR spectroscopy then indicated that the mutase caused replacement of the 2-amino group by the 3-*pro*-*R* hydrogen with inversion at C-2 (262, 263). A similar result has been observed for a lysine 2,3-aminomutase involved in the biosynthesis of the metabolite streptothricin (264).

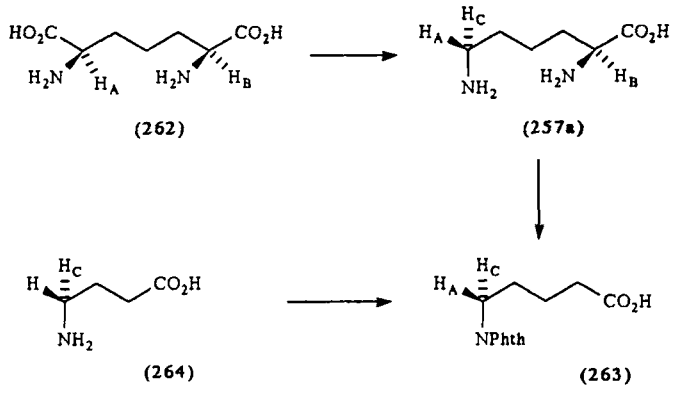
Lysine 2,3-aminomutase is not coenzyme B_{12} dependent, but a further lysine mutase, β-lysine mutase (EC 5.4.3.3), catalyzes the coenzyme B_{12}-dependent rearrangement shown in Scheme 68, the product 3,5-diaminohexanoic acid **261** having been shown (265) to have the (3*S*, 5*S*) configuration. When the reaction was conducted in the presence of [5′-^3H] coenzyme B_{12} and the β-lysine **258a** was degraded to succinic acid, assay with succinate dehydrogenase showed the latter to be (2*S*)-[2-$^3H_1$] succinate (266). Thus



Scheme 68

the labeled β-lysine was (3*S*, 5*S*)-[5-$^3H_1$]-β-lysine **258a**, $H_C = {}^3H$ (266). The amino group had therefore been replaced by hydrogen with inversion of configuration.

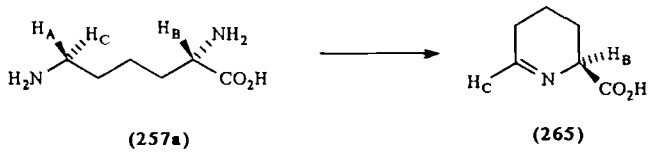
The enzyme α, ε-diaminopimelate decarboxylase (EC 4.1.1.20) decarboxylates the (*R*) center of (2*S*, 6*R*)-*meso*-diaminopimelic acid **262** to give lysine **257a** (Scheme 69). When this reaction was conducted in ^2H_2O and (2*S*, 6*R*)-[2, 6-$^2H_2$]-α, ε-diaminopimelic acid **262**, $H_A = H_B = {}^2H$, was decarboxylated in H_2O, samples of [6-$^2H_1$] lysine **257a**, $H_C = {}^2H$, and [2, 6-$^2H_2$] lysine **257a**, $H_A = H_B = {}^2H$, respectively, were obtained (267). These were converted to samples of [5-$^2H_1$]-*N*-phthaloyl-5-aminovaleric acid **263**, $H_C = {}^2H$, and **263**, $H_A = {}^2H$, respectively. An authentic sample of (5*R*)-[5-$^2H_1$]-*N*-pathaloyl-5-aminovaleric acid **263**, $H_C = {}^2H$, was obtained via an Arndt–Eistert synthesis from (4*R*)-[4-$^2H_1$]-γ-aminobutyric acid **264**, $H_C = {}^2H$, prepared as in Section X, and this sample had the same optical rotation as the corresponding sample prepared using α, ε-diaminopimelate decarboxylase. The decarboxylation had, uniquely for a PLP-mediated decarboxylation, occurred with *inversion* of configuration at the (6*R*) center (267). The result was so unusual that an alternative assay was used to confirm it. Here decarboxylation of the [^{2}H]lysine **257a** produced by decarboxylation of **262** in ^2H_2O yielded a sample of cadaverine **266** (Scheme 71) that retained the label on oxidation with the *pro-S* specific diamine oxidase (EC 1.4.3.6) (267). It was shown that α, ε-diaminopimelate from *Bacillus sphaericus* and from wheat germ also catalyzed decarboxylation with inversion of configuration (268).



Scheme 69

Samples of (2*S*, 6*R*)-[6-$^3H_1$]- and (2*S*, 6*S*)-[2, 6-$^3H_2$]lysine **257a**, $H_C = {}^3H$, and **257a**, $H_A = H_B = {}^3H$, have been prepared using α, ε-diaminopimelate decarboxylase and tritium in place of deuterium in the synthesis described

above for the deuterated analogues (269). These were used to assess the stereochemistry of L-lysine-6-aminotransferase (EC 2.6.1.36). The aldehyde product from the reaction catalyzed by this enzyme formed Δ^1-piperideine-6-carboxylate **265** (Scheme 70), in which the 6-*pro-R* hydrogen was retained and the 6-*pro-S* hydrogen was lost (269). This *S* stereospecificity was in keeping with that found for GABA aminotransferase and, as we shall see in Section XIII, for ornithine δ-aminotransferase.

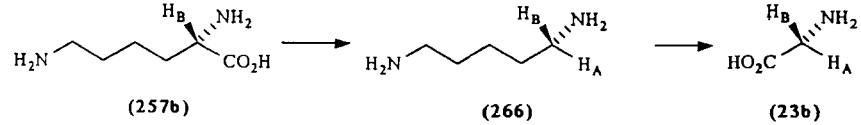


(257a) **(265)**

Scheme 70

L-Lysine-ε-dehydrogenase (EC 1.4.1.15), an enzyme specific for the 4-*pro-R* hydrogen of NADPH (270), has been incubated with (2*S*,6*R*)- and (2*S*,6*S*)-[6-$^3H_1$]lysines **257a**, $H_C = {}^3H$, and **257a**, $H_A = {}^3H$, respectively, and shown to be converted to Δ^1-piperideine-6-carboxylate **265** with loss of the 6-*pro-R* hydrogen (271). The stereochemistry is very different from that exhibited by the ε-aminotransferase, but it is in keeping with that of a D-amino acid dehydrogenase.

Decarboxylation of lysine **257b** gives the important biosynthetic intermediate cadaverine **266** (Scheme 71). This reaction is catalyzed by L-lysine decarboxylase (EC 4.1.1.18), decarboxylation in ^2H_2O or ^3H_2O, giving (1*R*)-[1-$^2H_1$]- and [1-$^3H_1$]cadaverines **266**, $H_A = {}^2H$ or ^3H, and decarboxylation of (2*S*)-[2-$^2H_1$]- or [2-$^3H_1$]lysines in H_2O, giving (1*S*)-[1-$^2H_1$]- and [1-$^3H_1$]cadaverines **266**, $H_B = {}^2H$ or ^3H. The stereochemistry of the process was shown by oxidation of the samples of [$^3H_1$]cadaverine **266**, $H_A = {}^3H$ and $H_B = {}^3H$, to glycine **23b**, which was then incubated with the *pro-S* specific *D*-amino acid oxidase and the *pro-R* specific L-alanine aminotransferase (272). The reaction was shown to occur with retention of configuration, although there was a suggestion that an enzyme from *Sedum* might follow a different path (273).



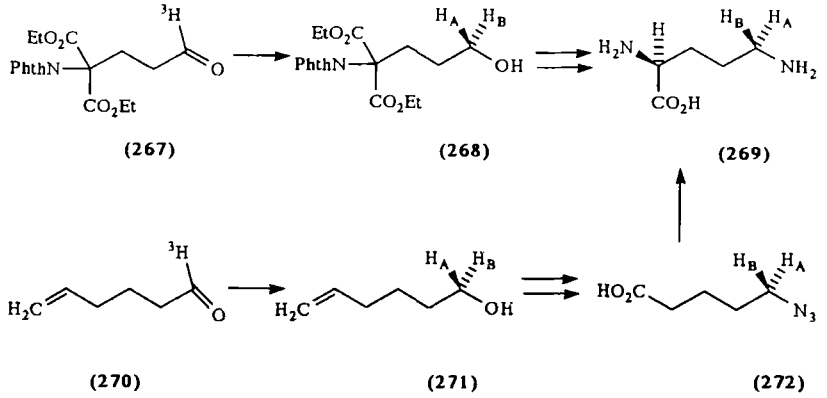
(257b) **(266)** **(23b)**

Scheme 71

L-Lysine decarboxylase has been used extensively to prepare stereospecifically labeled samples of cadaverine for use in biosynthetic studies (274–280).

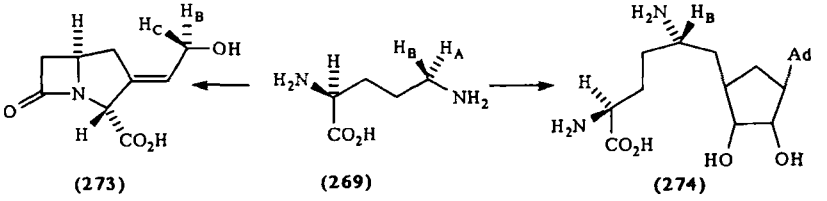
XIII. ORNITHINE AND ARGININE

Two chemical syntheses of stereospecifically labeled ornithine **269** rely on reduction of a labeled aldehyde with a chiral borane. The (2*RS*, 5*R*)- and (2*RS*, 5*S*)-[5-$^3H_1$]ornithines **269**, $H_B = {}^3H$, and **269**, $H_A = {}^3H$, respectively, were obtained via reduction of the aldehyde **267** to the alcohols **268**, $H_B = {}^3H$, and **268**, $H_A = {}^3H$, and were converted to the desired products via an azide with inversion at C-5 (281). A second synthesis involved reduction of the aldehyde **270**, as shown in Scheme 72 (282).



Scheme 72

When the labeled samples of ornithine were fed to *Streptomyces clavuligerus* it was shown that the 5-*R* label was retained and 5-*S* label was lost on incorporation into clavulanic acid **273** (281) (Scheme 73). Degradation of



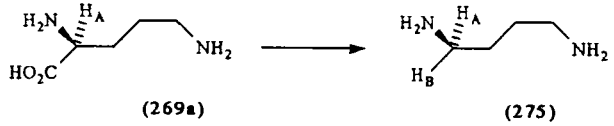
Scheme 73

clavulanic acid to glycollic acid **24** and use of the *pro-R* specific glycollate oxidase showed the stereochemistry of the label to be (9*S*). Thus oxidation to a hypothetical aldehyde intermediate might be followed by reduction from the *Re* face. There was net inversion at C-9 of clavulanic acid **273** in the process (281).

On feeding stereospecifically tritiated samples of ornithine to *Streptomyces griseolus*, it was found that the 5-*pro-S* hydrogen was lost on incorporation into sinefungin **274** so that bond formation was accompanied by inversion of configuration (282).

ω-Transamination may be achieved with L-ornithine aminotransferase (EC 2.6.1.13), and when this reversible reaction was conducted in ^2H_2O and the [$^2H_1$] ornithine was isolated and degraded to 4-phthalimidobutyrate, the rotation was equal but opposite to that of an authentic sample prepared from (4*R*)[4-$^2H_1$]-GABA (269). This reaction, as that of other ω-aminotransferases, was therefore *pro-S* specific.

Decarboxylation of ornithine **269a** gives the diamine putrescine **275** (Scheme 74) which is used in the biosynthesis of many alkaloids. *L*-Ornithine decarboxylase (EC 4.1.1.17) catalyzes this reaction, and when unlabeled ornithine is decarboxylated in ^2H_2O and [2-$^2H_1$]ornithine is decarboxylated in H_2O, samples of (1*R*)- and (1*S*)-[1-$^2H_1$]putrescine **275**, $H_B = {}^2H$, and **275**, $H_A = {}^2H$, respectively, are obtained (283). The configuration of these samples was assessed by conversion to [$^2H_1$]-*N*-phthalimidobutyrate of known chirality (283) or by ^1H NMR spectroscopic techniques (277, 284). The enzyme has been used extensively to prepare stereospecifically labeled samples of putrescine **275** for biosynthetic studies (278, 285–290).

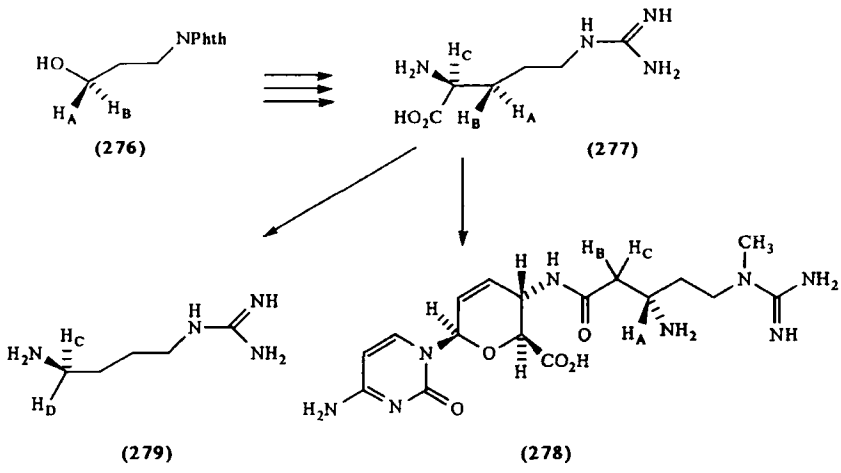


(269a) (275)

Scheme 74

The amino acid arginine **277** resembles ornithine, and samples of (3*R*)- and (3*S*)-arginine **277**, $H_B = {}^2H$, and **277** $H_A = {}^2H$, respectively, have been synthesized using the labeled alcohols **276** (291) (Scheme 75). When these were fed to *Streptomyces griseochromagenes* and samples of blasticidin S, **278** were isolated, it was evident that the 3-*pro-R* hydrogen had migrated in a reaction catalyzed by an aminomutase (291). The stereochemistry is similar to that found for lysine 2,3-aminomutase (see Section XII).

Arginine decarboxylase (EC 4.1.1.19) has the same stereospecificity as lysine and ornithine decarboxylases, and samples of (1*R*)- and (1*S*)-[1-$^2H_1$]-



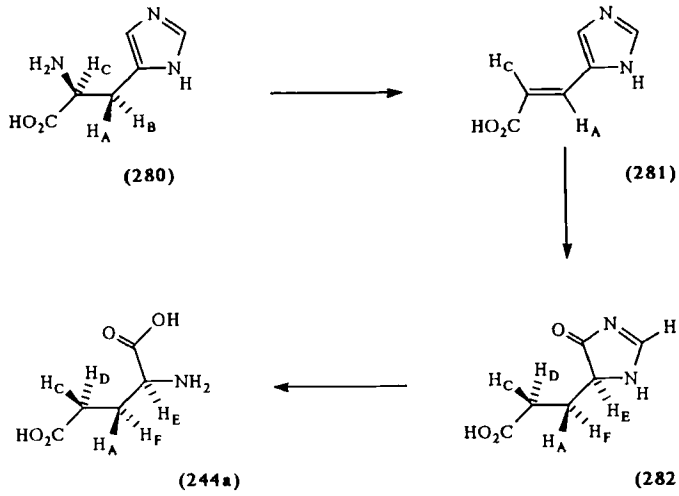
Scheme 75

and [1-$^3H_1$]agmatine **279** may be prepared in this way for biosynthetic studies (277, 278, 283, 287) (Scheme 75).

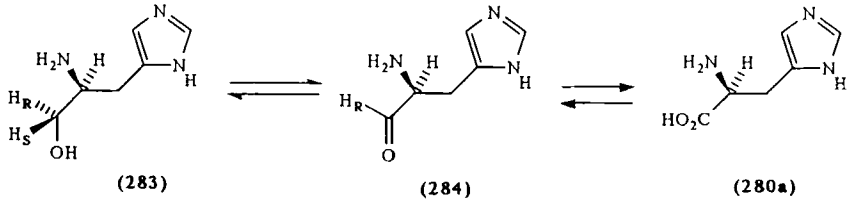
XIV. HISTIDINE

Histidine **280** is catabolized by first losing ammonia to yield urocanic acid **281**. The enzyme catalyzing this process is histidine ammonia lyase (EC 4.3.1.3), and the process being reversible, it will also exchange one of the C-3 protons in the process. Givot, Abeles et al. (292) degraded histidine, prepared using the enzyme and ^3H_2O, to aspartic acid **21** and assessed the stereochemistry using the *pro-R* specific enzyme aspartase. Rétey et al. (293) used degradation to succinate and chirality assessment with succinate dehydrogenase. The stereochemistry of the label was found to be (3*R*) by both groups. Since it had been shown that the hydrogen that was exchanged was the hydrogen eliminated on conversion to urocanate **281** (294), the elimination was evidently an *anti* process (Scheme 76).

The next step in the catabolism of histidine **280** is conversion of urocanate **281** to the compound **282**, a reaction without analogy. In a final step, **282** is converted to glutamic acid **244a**. Kaeppeli and Rétey (295) used a cell-free extract of *P. putida* in ^2H_2O to convert urocanic acid **281** to glutamic acid **244a**. This proved to be (2*S*,3*R*,4*R*)-[2,3,4-$^2H_3$]glutamic acid **244a**, $H_E = H_F = H_D = {}^2H$, by degradation to succinate and comparison of mass spectral and ORD data with expected values. Both hydrogens had added to the *Re* face of the double bond in urocanic acid.



Scheme 76



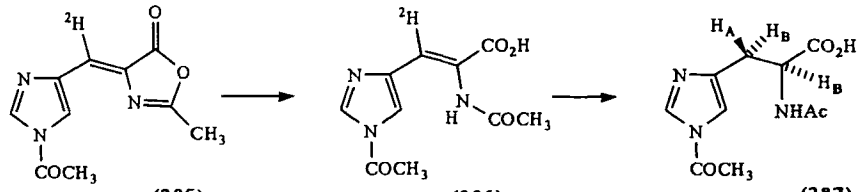
Scheme 77

Histidinol dehydrogenase (EC 1.1.1.23) reduces histidine **280a** to histidinol **283** using the 4-*pro-R* hydrogen of NADH (296) (Scheme 77). An exchange is catalyzed by the enzyme and NADH using the reversible step **283**⇌**284**, and ^{1}H NMR spectroscopic arguments have been used to show that the intermediate aldehyde **284** is reduced with [4-^{2}H]-NADPH to give (1*S*, 2*S*)-[1-$^2H_1$] histidinol **283**, $H_S = {}^2H$. This was confirmed by oxidation with the *pro-R* specific horse liver alcohol dehydrogenase (296).

Histamine *N*-methyltransferase (EC 2.1.1.8) catalyzes the N methylation of the imidazole ring of histamine. *S*-Adenosylmethionine is the methylating agent, and methods outlined in Section VII have shown that the methylation occurs with inversion of configuration (297).

Bacterial histidine decarboxylase (EC 4.1.1.22) is unique among bacterial amino acid decarboxylases in not requiring PLP. Mammalian histidine decarboxylase does have a PLP requirement. Battersby et al. (298, 299)

showed that the decarboxylation of histidine **280** to histamine catalyzed by the bacterial enzyme did so with retention of configuration, a conclusion tentatively made earlier by Chang and Snell (300). Battersby et al. prepared [2-^{3}H]histidine and decarboxylated it to (1*S*)-[1-$^3H_1$]histamine, which lost tritium on incubation with diamine oxidase, known to be specific for the *pro-S* hydrogen of amines (298, 299). They also presented a synthesis of stereospecifically labeled samples of histidine in this work. This is outlined in Scheme 78, the key step being *cis*-catalytic hydrogenation of the (*Z*)-olefin **286** (299). Resolution was effected by acylase I, and (2*S*,3*S*)- and (2*S*,3*R*)-[3-$^2H_1$]histidines were obtained from the (2*S*)-acetate **287** and its (2*R*)-enantiomer. The stereochemistry of the histidine decarboxylase catalyzed reaction has been confirmed more recently using deuterium labeling (301).



Scheme 78

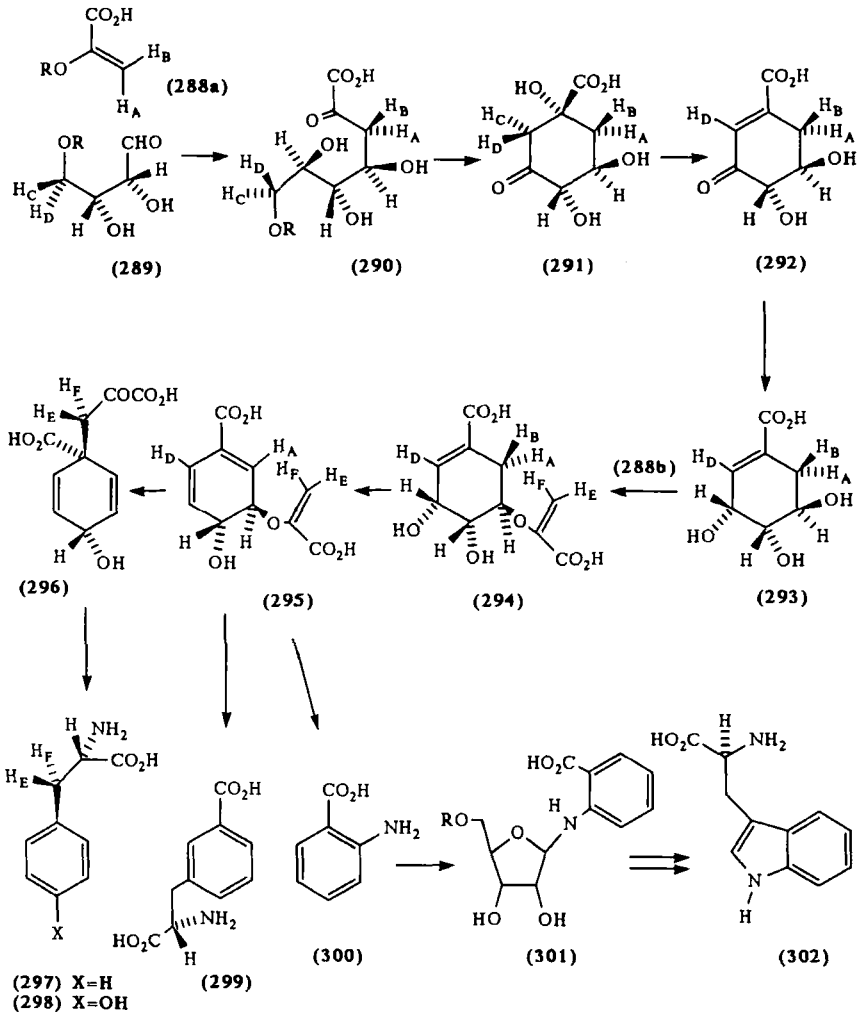
XV. PHENYLALANINE, TYROSINE, AND TRYPTOPHAN

A. General

The three aromatic amino acids that are biosynthesized in the shikimic acid pathway have much in common. The many stereochemical events occurring between the condensation of compounds **288a** and **289** derived from carbohydrates to the formation of prephenic acid **296** have been extensively reviewed including a recent review by ourselves (82), and so we have summarized the stereochemistry of the biosynthesis in Scheme 79. Prephenic acid **296** leads to phenylalanine **297** and tyrosine **298**. The *meta*-substituted amino acids **299** are derived from chorismate **295**, as is tryptophan **302**, as shown.

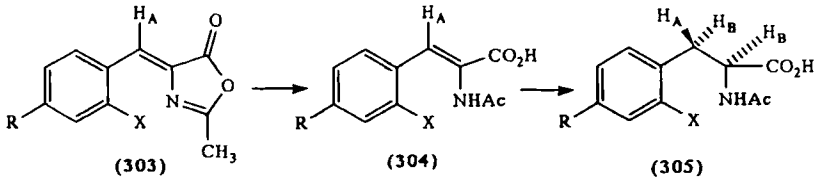
B. Phenylalanine and Tyrosine

The groups of Kirby (302–304) and Battersby (305–307) developed the "oxazolone" synthesis for preparation of samples of phenylalanine **297** and tyrosine **298** stereospecifically labeled at C-3. The oxazolones **303**, of well-



Scheme 79

defined configuration, could readily be prepared from benzaldehyde, substituted benzaldehydes, or [$^2H_1$]- or [$^3H_1$]benzaldehydes **306**. These were hydrolyzed to the (Z)-olefins **304**, $H_A = H$, ^2H, or ^3H, R = H, CH_3O, or $PhCH_2O$. Catalytic hydrogenation of the labeled compounds gave the products **305**. $H_A = {}^2H$ or ^3H, and catalytic tritiation of the unlabeled compounds gave **305**, $H_B = {}^3H$ (Scheme 80). Resolution and deprotection could be effected, and the configuration was verified by degradation to aspartic acid **21** and malic acid **83** for enzymic assay or to [$^2H_1$]succinic acid for assay

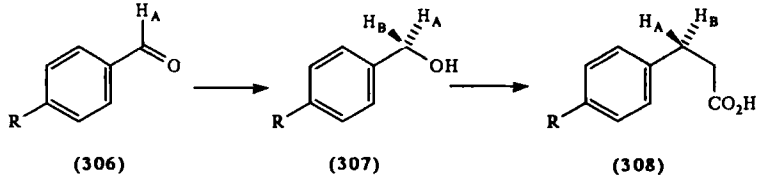


(303) (304) (305)

Scheme 80

by ORD. Battersby et al. racemized the (2R)-isomers from their resolution to obtain the C-3 epimers of the labeled amino acids. Kirby's group applied this synthesis to the preparation of (2*S*, 3*R*)-[3-$^2H_1$]-*ortho*-tyrosine **305**, X = OH, $H_A = {}^2H$ (308), by using the oxazolone **303**, X = $PhCH_2O$, $H_A = {}^2H$.

In a second synthesis of labeled phenylalanine Battersby et al. (305, 306) used the *pro-R* specific enzyme horse liver alcohol dehydrogenase to reduce [$^2H_1$]benzaldehyde **306**, $H_A = {}^2H$. The (1*S*)-[1-$^2H_1$]benzyl alcohol **307** obtained was converted via tosylation and reaction with malonate anion to the acid **308** (Scheme 81), which, on bromination and ammonolysis, gave (2*RS*, 3*R*)-[3-$^2H_1$]phenylalanine **297**, $H_E = {}^2H$. Ife and Haslam (309) used the more direct replacement of the tosylates of the alcohol **307** with acetamidomalonic ester in a similar synthesis of (3*R*)- and (3*S*)-[3-$^2H_1$]phenylalanines. Fermenting yeast replaced liver alcohol dehydrogenase in a further synthesis (310).

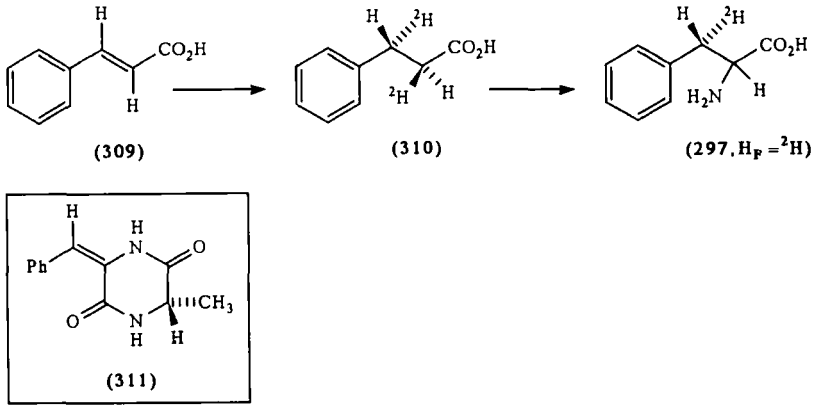


(306) (307) (308)

Scheme 81

Simon's *Clostridium kluyveri* system has been used to reduce *trans*-cinnamic acid **309** to (2*S*, 3*R*)-[2, 3-$^2H_2$]-3-phenylpropionic acid **310**, and this was converted by bromination and ammonolysis to (2*RS*, 3*S*)-[3-$^2H_1$]phenylalanine **297**, $H_F = {}^2H$ (311), as in Scheme 82. A Japanese group recently reduced the diketopiperazine **311** at the exomethylene group with asymmetric induction and obtained (2*R*, 3*R*)-[2,3-$^2H_2$]phenylalanine (312).

The enzyme phenylalanine ammonia lyase (EC 4.3.1.5) catalyzes elimination of ammonia from phenylalanine **297a** to yield (*E*)-cinnamic acid **309a**, X = H, and various research groups (303, 305, 306, 309) have shown that the 3-*pro-S* hydrogen, H_F, is eliminated in the process by using the synthetic samples of stereospecifically labeled phenylalanine. Elimination of ammonia is therefore



Scheme 82

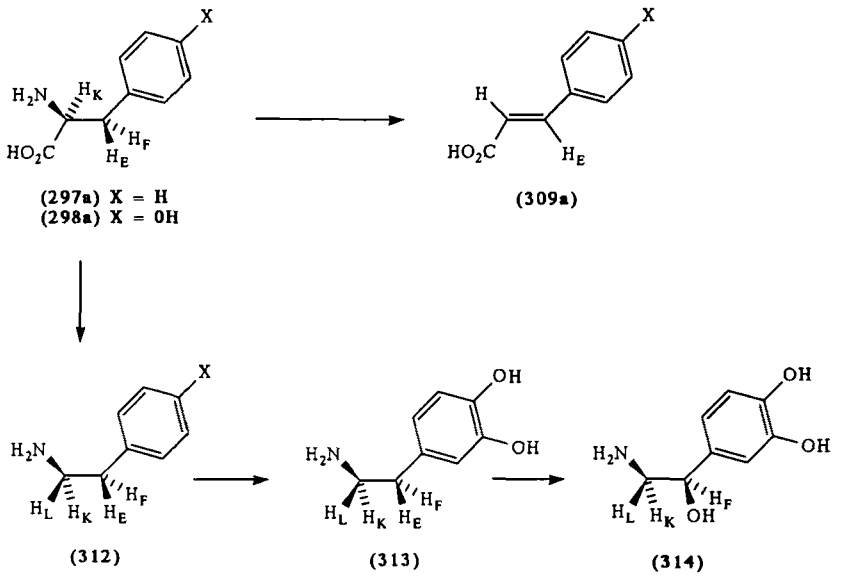
an *anti* process. Use of tyrosine **298a** as a substrate for this enzyme showed the same *anti* stereospecificity (313) as did the enzyme tyrosine ammonia lyase from maize cobs (307, 314) (Scheme 83).

Tyrosine decarboxylase (EC 4.1.1.25) was studied at a very early date by Belleau et al. (315, 316) and reinvestigated using more modern methods by Battersby et al. (317). These studies showed that decarboxylation to yield tyramine **312**, X = OH, occurred with retention of configuration. Later work (318) showed that aromatic L-amino acid decarboxylase (EC 4.1.1.28) from *Micrococcus percitreus* catalyzed decarboxylation of phenylalanine **297a** to phenylethylamine **312**, X = H, with retention of configuration.

Since the phenylethylamines **312** produced by these decarboxylases are substrates for systems containing dopamine β-hydroxylase (EC 1.14.17.1), the availability of 3*R* and 3*S* isotopically labeled samples of the aromatic amino acids has allowed the stereochemistry of the hydroxylation of dopamine **313** to yield norepinephrine **314** to be studied (Scheme 83). It was shown that the 3-*pro*-*S* hydrogen, H_E, was lost from phenylalanine **297a** in the process and that the hydroxylation yielding **314** therefore occurred with retention of configuration (319).

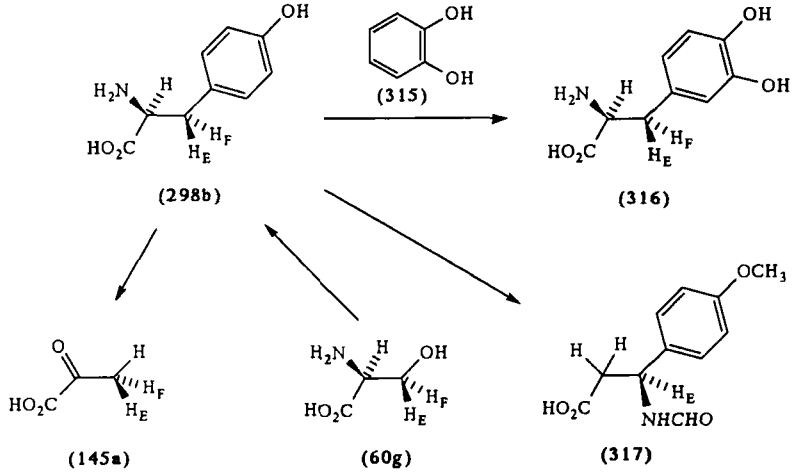
Phenylpyruvate tautomerase from beef kidney has been shown to cause preferential loss of the 3-*pro*-*R* hydrogen from phenylpyruvic acid using samples of stereospecifically labeled phenylalanine (320). This may explain some unusual 3-*pro*-*R* losses (321) in biosynthetic work.

Tyrosine phenol lyase (EC 4.1.99.2), which will reversibly break down tyrosine **298b** to phenol, pyruvate **145a**, and ammonia, also catalyzes the β-replacement reaction of tyrosine **298b** with pyrocatechol **315** to yield dihydroxyphenylalanine (DOPA) **316**. By using stereospecifically deuterated samples of tyrosine **298b** and assessing the configuration of the DOPA



Scheme 83

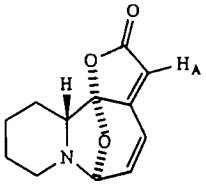
316 produced, it was shown that the reaction proceeded with retention of configuration at C-3 and loss of deuterium from C-2 (322), as shown in Scheme 84. This is in line with expectation for PLP-mediated β-replacement reactions which occur by the mechanism outlined in Scheme 5.



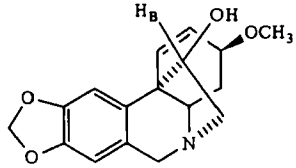
Scheme 84

The condensation of (3*R*)- and (3*S*)-[3-$^2H_1$]serines **60g**, $H_F = {}^2H$, and **60g**, $H_E = {}^2H$, respectively, to yield tyrosine **298b** using tyrosine phenol lyase as outlined in Scheme 84 was investigated using samples of labeled serine prepared as in Scheme 19. The tyrosine **298b** produced was degraded via aspartic acid **21** to malic acid **83** and the *pro-R* specific enzyme fumarase was used to assess the stereochemistry (104). Again β replacement occurred with retention of configuration. Breakdown of (2*S*, 3*R*)-[3-$^2H_1$]- and (2*SR*, 3*SR*)-[2,3-$^2H_2$]tyrosine **298b** in ^3H_2O using this enzyme gave samples of [3-$^2H_1$, 3-$^3H_1$]pyruvate **145a**, which were degraded to acetate and analyzed (105). Again the β replacement occurred with retention of configuration.

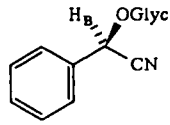
The recent use of stereospecifically C-3 tritiated samples of tyrosine **298b** in assessing the genesis of a β-tyrosine **317** unit in the peptide antibiotics edeines A and B produced by *Bacillus brevis* has shown loss of the 3-*pro-S* hydrogen and retention of the 3-*pro-R* hydrogen in the process **298b** → **317** shown in Scheme 84 so that migration of the amino group is accompanied by inversion of configuration (323). The 3-*pro-S* hydrogen is also lost in



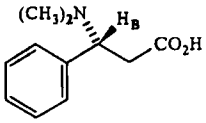
(318)



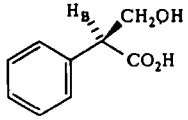
(319)



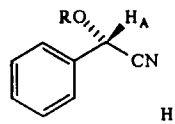
(320)



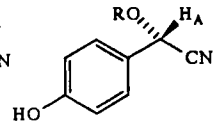
(321)



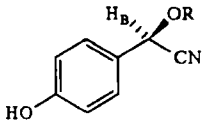
(322)



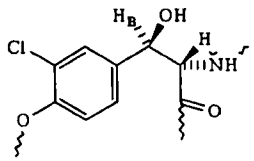
(323)



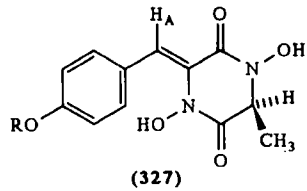
(324)



(325)



(326)



(327)

biosynthesis of the alkaloid securinine **318** (324). The loss of the 3-*pro-R* hydrogen when phenylalanine or tyrosine was fed to daffodils to produce the alkaloid haemanthamine **319** indicated retention of configuration during hydroxylation (302–304, 306, 325).

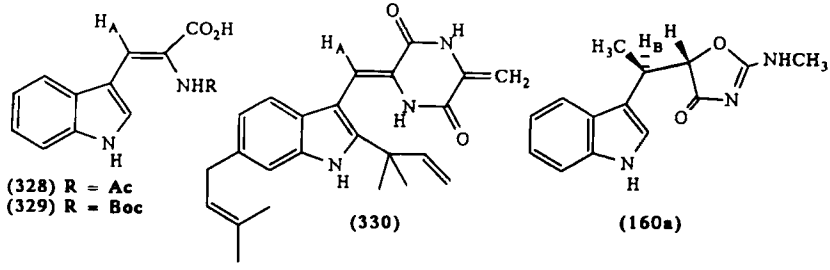
Platt, Haslam et al. (326) noted 3-*pro-R* loss on incorporation of labeled phenylalanines **297** into the metabolite prunacin **320**, Wintersteiner's acid **321**, and tropic acid **322**, whereas there was loss of the 3-*pro-S* hydrogen on incorporation into sombunigrin **323** (326). In keeping with these results was the finding that, in the biosynthesis of the epimeric cyanogenic glucosides dhurin **324** and taxiphillin **325**, the 3-*pro-S* hydrogen of tyrosine was specifically lost on formation of dhurin **324**, whereas the 3-*pro-R* hydrogen was specifically lost on formation of taxiphillin **325** (327). Hydroxylation of each epimer involved retention of configuration. The samples of labeled tyrosine **298** used in these experiments were obtained from samples of the corresponding phenylalanines using phenylalanine hydroxylase (EC 1.14.16.1) from rat liver (327).

The glycopeptide vancomycin has two *meta*-chloro-β-hydroxy-D-tyrosine residues **326**, and it was shown (328) that the 3-*pro-R* hydrogen was lost in the biosynthesis, indicating retention in the β-hydroxylation reaction. The 3-*pro-S* hydrogen was shown to be lost on formation of the olefin in the biosynthesis of mycelianamide **327** (329, 330).

C. Tryptophan

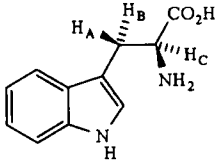
Although Kirby and Varley (102) prepared C-3 labeled tryptophan **331** via the "oxazolone route" (see Scheme 80) using the (*Z*)-olefin **328**, by far the most widely used source of (3*R*)- and (3*S*)-labeled tryptophans is the reaction of stereospecifically labeled samples of serine with indole, catalyzed by the enzyme tryptophan synthase (EC 4.2.1.20). This involves substitution at the β-carbon of serine with retention of configuration and has been discussed in Section IV (86, 88, 103).

These labeled samples of tryptophan have been used to show that, in the

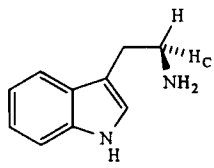


dehydrogenations leading to the metabolites **329** (331) and cryptoechinulin **330** (332), the 3-*pro-S* hydrogen is lost in a *syn* elimination. It was also shown that the 3-*pro-R* hydrogen was specifically lost on methylation in the biosynthesis of indolmycin **160a**, implying retention of configuration at C-3 during methylation (45, 83, 86, 333). We have seen in Section VII that this reaction involves inversion at the methyl carbon atom.

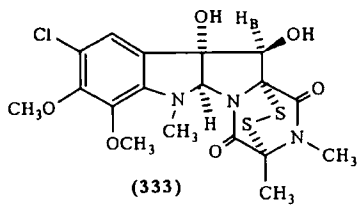
Tryptophan **331** is converted to tryptamine **332** by both aromatic L-amino acid decarboxylase (EC 4.1.1.28) and tyrosine decarboxylase (EC 4.1.1.25), and in both instances (334, 335) it was shown, either by use of the *pro-R* specific monoamine oxidase (335) or by degradation of the labeled tryptamines to glycine and use of the *pro-S* specific D-amino acid oxidase and *pro-R* specific glutamate pyruvate transaminase (334), that decarboxylation involved retention of configuration. Hydroxylation that leads to sporidesmin **333** has been shown to involve specific loss of the 3-*pro-R* hydrogen, and so again hydroxylation involves retention of configuration (102).



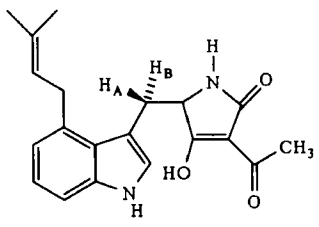
(331)



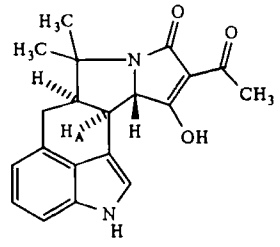
(332)



(333)



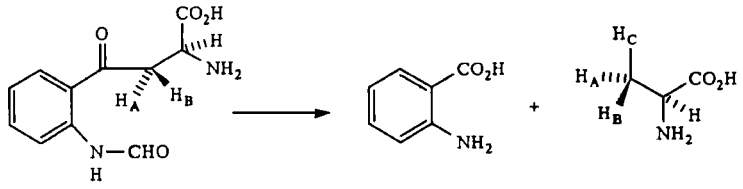
(334)



(335)

The cyclization **334** → **335** in ergot alkaloid biosynthesis has been shown to involve loss of the 3-*pro-S* hydrogen of tryptophan in the process, casting light on the stereochemistry of the ring closure step (336).

Samples of (3*R*)- and (3*S*)-[3-$^3H_1$]tryptophans **331** have been converted to the corresponding kynurenines **336** using the enzymes tryptophan dioxygenase (EC 1.13.11.11) and formylkynurenine formamidase (EC 3.5.1.9). These have been used to investigate the fission of kynurenine **336** to anthranilic acid **300** and alanine **337** in ^2H_2O (337) (Scheme 85). Conversion of the alanine to acetate and assessment of sense of chirality indicated that



(336) (300) (337)

Scheme 85

hydrogen replaced the anthranilate moiety with retention of configuration (337).

XVI. OTHER AMINO ACIDS

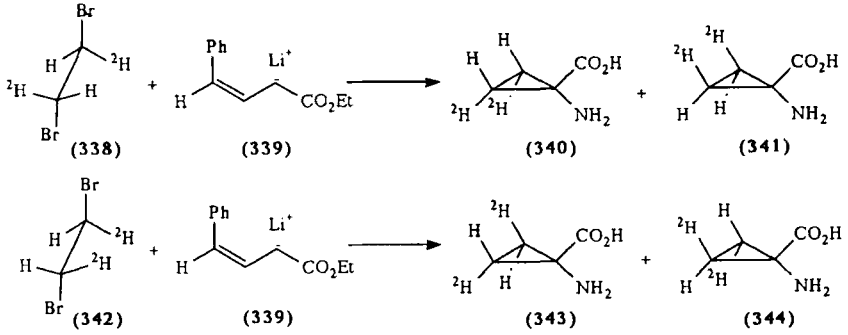
Most common amino acids have been given full or part sections in this review and less common amino acids (e.g., α,ω-diaminopimelic acid **262**) have been discussed where appropriate. However, two less common amino acids have been left to this section mainly because of the lack of opportunity to discuss them in one of the other sections of this chapter.

A. Aminocyclopropanecarboxylate

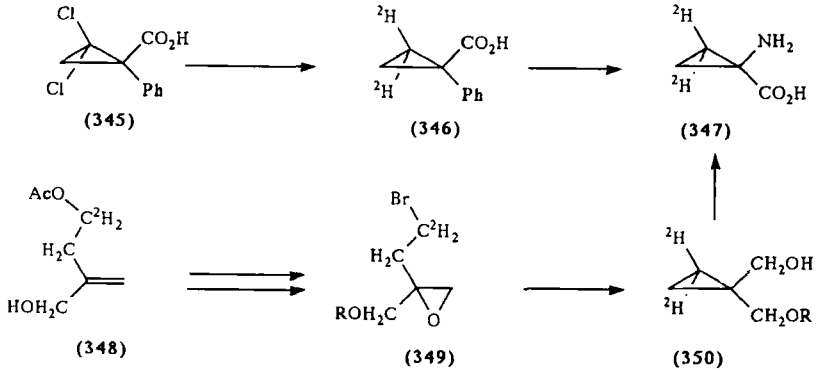
Aminocyclopropanecarboxylate (ACPC) provides an interesting problem, having a plane of symmetry through the α-carbon atom. Isotopic substitution on one of the β-carbon atoms will immediately provide a chiral molecule, and so labeling will allow us to see how enzymes can discriminate between the enantiotopic groups in the various reactions undergone by this compound.

Adlington et al. (338) first prepared *cis*- and *trans*-[2,3-$^2H_2$]-ACPC [**340** + **341**] and [**343** + **344**] from *trans*- and *cis*-[1,2-$^2H_2$]-ethylenes via *meso*- and *dl*-[1,2-$^2H_2$]-1,2-dibromoethanes **338** and **342**, respectively (Scheme 86). Reaction of these with the lithium salt **339** then gave the desired products. The stereochemistry was confirmed using computer-simulated ^1H NMR spectral comparison. The *cis*-isomer has also been prepared by Pirrung (339) using the *meso*-dibromide **338** in a method worked out by Schöllkopf. These methods have been used by Ramalingam et al. (340), who also used a similar technique to prepare [2,2-$^2H_2$]-ACPC.

Synthesis of (1*S*)-[2,2-$^2H_2$]-ACPC **347** was achieved independently by two groups in a joint publication (341) (cf. Scheme 87). The first synthesis confirmed the absolute configuration of the resolved dichloride **345** by conversion to a known compound. The chloride **345** was then converted to the acid **346** (Scheme 87). Curtius rearrangement converted the acid to an



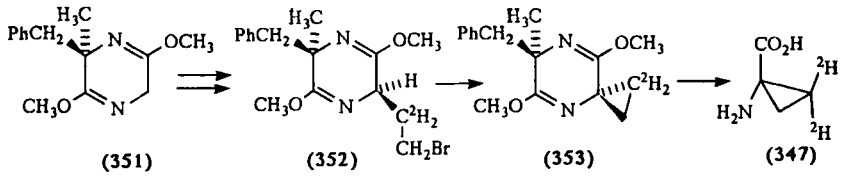
Scheme 86



Scheme 87

amine with retention of configuration, and oxidation of the phenyl ring then gave the desired product **347**. The second synthesis relied on Sharpless oxidation of the olefin **348** to achieve enantioselectivity, and the configuration of the resultant epoxide was correlated with that of (*S*)-citramalic acid. Further elaboration to the bromide **349**, reaction with lithium, accompanied by cyclization to **350** and an oxidation–Curtius–deprotection–oxidation sequence then gave the desired product **347** (341).

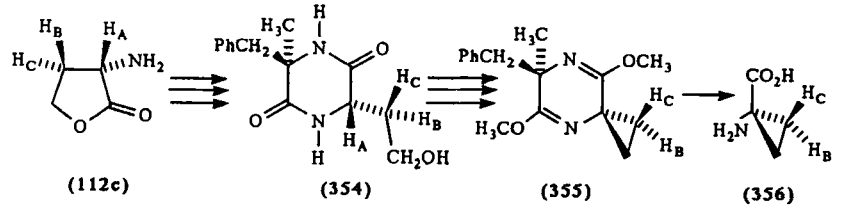
A Schöllkopf-type synthesis, used by Subramanian and Woodard (342) to prepare (1*S*)-[2, 2-$^2H_2$]-ACPC, is shown in Scheme 88. Initial alkylation of the anion of the bis(lactim ether) **351** occurred *cis* to the bulky benzyl group, in violation of observations by Schöllkopf. Both addition of $BrCH_2C^2H_2$-O-trifyl and the subsequent cyclization **352** → **353** were stereoselective reactions. The (2*R*)-isomer was obtained using $BrC^2H_2CH_2$-*O*-triflyl in the synthesis, and both isomers were obtained in enantiomeric excesses of ca. 44%.



(351) (352) (353) (347)

Scheme 88

(2*S*, 3*R*)-[2, 3-$^2H_2$]Homoserine lactone **112c**, $H_A = H_C = {}^2H$, prepared as in Section V, Scheme 35, was converted to the diketopiperazine **354** (Scheme 89). This was converted to the corresponding bromide and the bis(lactim ether) was cyclized to the spiro compound **355**, $H_C = {}^2H$. Although the cyclization was not entirely stereospecific, hydrolysis of **355**, $H_C = {}^2H$, gave (1*S*, 2*S*)-[2-$^2H_1$]-ACPC, **356**, $H_C = {}^2H$, contaminated with the (1*R*, 2*S*)-isomer (122). Synthesis of (1*S*, 2*R*)-[2-$^2H_1$]-ACPC **356**, $H_B = {}^2H$, contaminated with the (1*R*, 2*R*)-isomer, was achieved in the same way, starting from (2*R*, 3*S*)-[2, 3-$^2H_2$]homoserine lactone, prepared as in Section V, Scheme 35, but using (S, S)-DIPAMP in the reduction step (122).

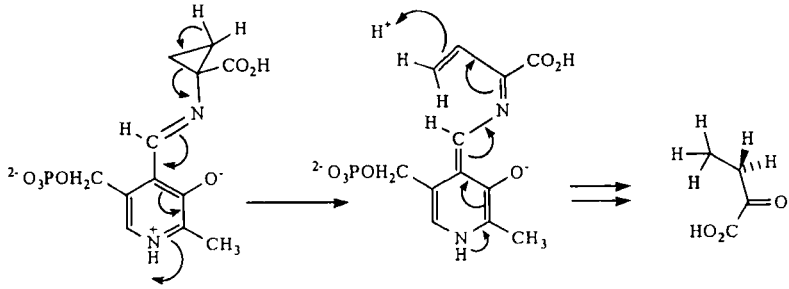


(112c) (354) (355) (356)

Scheme 89

We have seen in Section VII how ACPC is synthesised by cyclization of *S*-adenosylmethionine and how it was shown (142, 149) that the ring closure occurred with inversion at the γ-center. When Wiendanger, Arigoni et al. (343) conducted the cyclization using [4, 4-$^2H_2$]-S-adenosylmethionine, they were able to show that the product was (1*S*)-[2, 2-$^2H_2$]ACPC **347** by comparison of the ^2H NMR spectrum of a derivative with that of a synthetic sample. Cyclization was therefore accompanied by the comparatively rare inversion at the γ-center in the PLP-mediated reaction.

The ACPC deaminase (EC 4.1.99.4) converts ACPC to 2-oxobutyrate **124**, and incubation with (1*S*)- and (1*R*)-[2, 2-$^2H_2$]ACPC, which leads to labeling in the methyl and the C-3 positions, respectively, showed that it was the bond to the 2-*pro*-*S* carbon that was cleaved in the process (341). This is the bond made on biosynthesis of ACPC. A mechanism for the process is suggested in Scheme 90, and the indication of internal proton return suggests operation



(357) (358) (124)

Scheme 90

of a single base (344). Indications from feeding labeled alkylated derivatives of ACPC are that the *2-pro-R* hydrogen is removed in **357** and that this is returned at the *Si* face of the γ-carbon in **358** (344).

The ACPC is catabolized to ethylene in apples, and it has been shown that there is lack of stereochemical control in the process (338). Baldwin et al. have shown that a net stereochemical bias exists when 2-methyl-ACPC is used as substrate (345).

B. Aminomalonic Acid

Aminomalonic acid is a substrate for aspartate β-decarboxylase (EC 4.1.1.12). When (3*R*)- and (3*S*)-[3-^{14}C]aminomalonates were prepared from [3-^{14}C]- and [1-^{14}C]serines, respectively, and incubated with this enzyme, the *3-pro-R* carboxyl group was lost (346). Since the decarboxylation had been shown to incorporate label into the *2-pro-S* hydrogen of glycine (78), the decarboxylation was deemed to have occurred with retention of configuration.

The enzyme serine hydroxymethyltransferase will also catalyze this decarboxylation, but early work found apparent lack of stereospecificity in the process (347). Thomas, Gani et al. (348, 349) reinvestigated this reaction and overcame inherent racemization problems to show that the process is stereospecific and involves retention of configuration.

REFERENCES

1. Ogston, A. G. *Nature* **1948**, *162*, 963.
2. Mislow, K.; Raban, M. *Top. Stereochem.* **1967**, *1*, 1–38.
3. Arigoni, D.; Eliel, E. L. *Top. Stereochem.* **1969**, *4*, 127–243.
4. Eliel, E. L. *Top. Current Chem.* **1982**, *105*, 1–76.

5. Bentley, R. *Molecular Asymmetry in Biology*, Academic Press: New York; Vol. 1, 1969; Vol. 2, 1970.
6. Alworth, W. L. *Stereochemistry and Its Application in Biochemistry*, Wiley-Interscience: New York, 1972.
7. Floss, H. G.; Tsai, M.-D.; Woodard, R. W. *Top. Stereochem.* **1984**, *15*, 253–321.
8. Hanson, K. R. *J. Am. Chem. Soc.* **1966**, *88*, 2731–2742; Prelog, V.; Helmchen, G. *Helv. Chim. Acta* **1972**, *55*, 2581–2598; Hanson, K. R. *Ann. Rev. Biochem.* **1976**, *45*, 307–330.
9. Hill, R. K. In *Bioorganic Chemistry*; Vol. 2, *Substrate Behaviour*, van Tamelen, E. E., Ed; Academic Press: New York, 1978, pp. 111–151.
10. Parry, R. J. In *Bioorganic Chemistry*, Vol. 2, *Substrate Behaviour*, van Tamelen, E. E., Ed.; Academic Press: New York, 1978; pp. 247–272.
11. Dunathan, H. C. *Adv. Enzymol.* **1971**, *35*, 79–134.
12. Davis, L.; Metzler, D. E. *The Enzymes*, 3rd ed.; Vol. 7; Boyer, P. D., Ed. Academic Press: New York, 1972; pp. 33–74.
13. Vederas, J. C.; Floss, H. G. *Acc. Chem. Res.* **1980**, *13*, 455–463.
14. Floss, H. G.; Vederas, J. C. In *New Comprehensive Biochemistry*, Vol. 3, *Stereochemistry*, Tamm, C., Ed. Elsevier Biomedical Press: Amsterdam, 1982; pp. 161–199.
15. Akhtar, M.; Emery, V. C.; Robinson, J. A. In *New Comprehensive Biochemistry*, Vol. 6, Page, M. I., Ed. Elsevier: Amsterdam, 1984, pp. 303–372.
16. Braunstein, A. E.; Shemyakin, M. M. *Biokhimiya* **1953**, *18*, 393–411.
17. Metzler, D. E.; Ikawa, M.; Snell, E. E. *J. Am. Chem. Soc.* **1954**, *76*, 648–652.
18. Dunathan, H. C. *Proc. Natl. Acad. Sci., USA.* **1966**, *55*, 712–716.
19. Schirch, L.; Jenkins, W. T. *J. Biol. Chem.*, **1964**, *239*, 3797–3800.
20. Dunathan, H. C.; Davis, L.; Kury, P. G.; Kaplan, M. *Biochemistry* **1968**, *7*, 4532–4537.
21. Besmer, P.; Arigoni, D. *Chimia* **1969**, *23*, 190.
22. Besmer, P. Dissertation no. 4435, E. T. H., Zurich, 1970.
23. Wada, H.; Snell, E. E. *J. Biol. Chem.* **1962**, *237*, 127–132.
24. Rose, I. A. *J. Am. Chem. Soc.* **1958**, *80*, 5835–5836.
25. Johnson, C. K.; Gabe, E. J.; Taylor, M. R.; Rose, I. A. *J. Am. Chem. Soc.* **1965**, *87*, 1802–1804.
26. Ayling, J. E.; Dunathan, H. C.; Snell, E. E., *Biochemistry* **1968**, *7*, 4537–4542.
27. Bailey, G. B.; Kusamrarn, T.; Vuttivej, K. *Fed. Proc., Fed. Am. Soc. Exper. Biol.* **1970**, *29*, 857; abstract 3461.
28. Sukhareva, B. S.; Dunathan, H. C.; Braunstein, A. E. *F. E. B. S. Lett.* **1971**, *15*, 241–244.
29. Voet, J. G.; Hindenlang, D. M.; Blanck, T. J. J.; Ulevitch, R. J.; Kallen, R. G.; Dunathan, H. C. *J. Biol. Chem.* **1973**, *248*, 841–842.
30. Dunathan, H. C.; Voet, J. C., *Proc. Natl. Acad. Sci., USA.* **1974**, *71*, 3888–3891.
31. Miles, E. W. *Biochemistry* **1987**, *26*, 597–603.
32. Yang, D.; Shih, Y.; Liu, H. *J. Org. Chem.* **1991**, *56*, 2940–2946.
33. Shih, Y.; Yang, D.; Weigel, T. M.; Liu, H. *J. Am. Chem. Soc.* **1990**, *112*, 9652–9654.
34. Tobler, H. P.; Christen, P.; Gehring, H. *J. Biol. Chem.* **1986**, *261*, 7105–7108
35. Tobler, H. P.; Gehring, H.; Christen, P. *J. Biol. Chem.* **1987**, *262*, 8985–8989.
36. Austermühle-Bertola, E. Dissertation no. 5009, E. T. H., Zurich, 1973.
37. Zito, S. W.; Martinez-Carrion, M. *J. Biol. Chem.* **1980**, *255*, 8645–8649.

38. Martinez-Carrion, M.; Slebe, J. C.; Gonzalez, M. *J. Biol. Chem.* **1979**, *254*, 3160–3162.
39. Eichele, G.; Ford, G. C.; Glor, M.; Jansonius, J. N.; Mavrides, C.; Christen, P. *J. Mol. Biol.* **1979**, *133*, 161–180.
40. Ford, G. C.; Eichele, G.; Jansonius, J. N. *Proc. Nat. Acad. Sci., USA* **1980**, *77*, 2559–2563.
41. Kirsch, J. F.; Eichele, G.; Ford, G. C.; Vincent, M. G.; Jansonius, J. N.; Gehring, H.; Christen, P. *J. Mol. Biol.* **1984**, *174*, 497–525.
42. Kochhar, S.; Finlayson, W. L.; Kirsch, J. F.; Christen, P. *J. Biol. Chem.* **1987**, *262*, 11446–11448.
43. Miles, E. M.; Houck, D. R; Floss, H. G. *J. Biol. Chem.* **1982**, *257*, 14203–14210.
44. Vederas, J. C.; Reingold, I. D; Sellers, H. W. *J. Biol. Chem.* **1979**, *254*, 5053–5057.
45. Vederas, J. C.; Schleicher, E.; Tsai, M.-D.; Floss, H. G., *J. Biol. Chem.* **1978**, *253*, 5350–5354.
46. Gehring, H. *Biochemistry* **1984**, *23*, 6335–6340.
47. Chang, C.-C.; Laghai, A.; O'Leary, M. H.; Floss, H. G. *J. Biol. Chem.* **1982**, *257*, 3564–3569.
48. Tumanyan, V. G.; Mamaeva, O. K.; Bocharov, A. L.; Ivanov, V. I.; Karpeisky, M. Y; Yakolev, G. I. *Eur. J. Biochem* **1974**, *50*, 119–127.
49. Tsai, M.-D.; Byrn, S. R.; Chang, C.; Floss, H. G.; Weintraub, H. J. R. *Biochemistry*, **1978**, *17*, 3177–3182.
50. Pfister, K.; Kägi, J. H. R.; Christen, P. *Proc. Natl. Acad. Sci., USA* **1978**, *75*, 145–148.
51. Fisher, T. L.; Metzler, D. E. *J. Am. Chem. Soc.* **1969**, *91*, 5323–5328.
52. Bowers-Komro, D. M.; McCormick, D. B. In *Chemical and Biological Aspects of Vitamin B6 Catalysis, Part A*; Evangopoulos, A. E., Ed.; Alan Liss Inc.: New York, 1984; pp. 387–396.
53. Bowers-Komro, D. M.; McCormick, D. B. *J. Biol. Chem.* **1985**, *260*, 9580–9582.
54. McCormick, D. B.; Bowers-Komro, D. M. In *Mechanisms of Enzymatic Reactions–Stereochemistry*; Frey, P. A., Ed.; Elsevier: New York, 1986; p. 336.
55. Besmer, P.; Arigoni, D. *Chimia* **1968**, *22*, 494.
56. Akhtar, M.; Jordan, P. M. *J. Chem. Soc., Chem. Commun.* **1968**, 1691–1692.
57. Akhtar, M.; Jordan, P. M. *Tetrahedron Lett.* **1969**, 875–877.
58. Jordan, P. M.; Akhtar, M. *Biochem. J.* **1970**, *116*, 277–286.
59. Akhtar, M.; El-Obeid, H. A.; Jordan, P. M. *Biochem. J.* **1975**, *145*, 159–168.
60. Zaman, Z.; Jordan P. M.; Akhtar, M. *Biochem. J.* **1973**, *135*, 257–263.
61. Abboud, M. M.; Jordan, P. M.; Akhtar, M. *J. Chem. Soc., Chem. Commun.* **1974**, 643–644.
62. Barnard, G.; Akhtar, M. *J. Chem. Soc., Chem. Commun.* **1975**, 980–982.
63. Armarego, W. L. F.; Milloy, B. A.; Pendergast, W. *J. Chem. Soc., Perkin Trans. 1* **1976**, 2229–2237.
64. Kajiwara, M.; Lee, S.-F.; Scott, A. I.; Akhtar, M.; Jones, C. R.; Jordan, P. M. *J. Chem. Soc., Chem. Commun.* **1978**, 967–968.
65. Ramalingam, K.; Nanjappan, P.; Kalvin, D. M.; Woodard, R. W. *Tetrahedron* **1988**, *44*, 5597–5604.
66. Yamada, H.; Kurumaya, K.; Eguchi, T.; Kajiwara, M. *J. Labelled Compounds and Radiopharm.* **1987**, *24*, 561–575.
67. Belokon, Y. N.; Belikov, V. M.; Vitt, S. V.; Savel'eva, T. F.; Burbelo, V. M.; Bakhmutov, V. I.; Aleksandrov, G. G.; Struchkov, Y. T., *Tetrahedron*, **1977**, *33*, 2551–2564.
68. Kakinuma, K.; Imamura, N.; Saba, Y., *Tetrahedron Lett.* **1982**, *23*, 1697–1700.

69. Williams, R. M.; Zhai, D.; Sinclair, P. J. *J. Org. Chem.* **1986**, *51*, 5021–5022.
70. Hamon, D. P. G.; Razzino, P.; Massey-Westropp, R. A. *J. Chem. Soc., Chem. Commun.* **1991**, 332–333.
71. Santaniello, E.; Casati, R.; Manzocchi, A. *J. Chem. Soc., Perkin Trans. 1* **1985**, 2389–2392.
72. Santaniello, E.; Manzocchi, A., Casati, R. In *Mechanisms of Enzymatic Reactions–Stereochemistry*; Frey P. A., Ed.; Elsevier: New York, 1986; p. 346.
73. Gani, D.; Wallis, O. C.; Young, D. W. *Eur. J. Biochem.* **1983**, *136*, 303–311.
74. Cable, K. M.; Herbert, R. B.; Mann, J. *J. Chem. Soc., Perkin Trans. 1* **1987**, 1593–1598.
75. Aberhart, D. J.; Russell, D. J., *J. Am. Chem. Soc.* **1984**, *106*, 4907–4910.
76. Keck, R.; Haas, H.; Rétey, J. In *Enzyme Inhibitors*, Brodbeck, U., Ed.; Verlag Chemie: Berlin, 1980; pp. 213–222.
77. Rétey, J.; Suckling, C. J.; Arigoni, D.; Babior, B. M. *J. Biol. Chem.* **1974**, *249*, 6359–6360.
78. Palekar, A. G.; Tate, S. S.; Meister, A. *Biochemistry*, **1970**, *9*, 2310–2315.
79. Onderka, D. K.; Floss, H. G. *J. Am. Chem. Soc.* **1969**, *91*, 5894–5896.
80. Onderka, D. K.; Floss, H. G. *Biochem. Biophys. Res. Commun.* **1969**, *35*, 801–804.
81. Floss, H. G.; Onderka, D. K.; Carroll, M. *J. Biol. Chem.* **1972**, *247*, 736–744.
82. Young, D. W. In *Isotopes in Physical and Biomedical Sciences; Vol 1; Labelled Compounds (Part B)*; Buncel, E.; Jones, J. R., Eds.; Elsevier: Amsterdam, 1991; pp. 341–427.
83. Skye, G. E.; Potts, R.; Floss, H. G. *J. Am. Chem. Soc.* **1974**, *96*, 1593–1595.
84. Floss, H. G.; Schleicher, E.; Potts, R. *J. Biol. Chem.* **1976**, *251*, 5478–5482.
85. Tatum, C.; Vederas, J.; Schleicher, E.; Benkovic, S. J.; Floss, H. G. *J. Chem. Soc., Chem. Commun.* **1977**, 218–220.
86. Tsai, M.-D.; Schleicher, E.; Potts, R.; Skye G. E.; Floss, H. G. *J. Biol. Chem.* **1978**, *253*, 5344–5349.
87. Tsai, M.-D.; Weaver, J.; Floss, H. G.; Conn, E. E.; Creveling R. K.; Mazelis, M. *Arch. Biochem. Biophys.* **1978**, *190*, 553–559.
88. Fuganti, C.; Ghiringhelli, D.; Giangrasso, D.; Grasselli, P.; Amisano, A. S. *Chim. Indust. (Milan)* **1974**, *56*, 424.
89. Gani, D.; Young, D. W. *J. Chem. Soc., Chem. Commun.* **1982**, 867–869.
90. Gani, D.; Young D. W., *J. Chem. Soc., Perkin Trans. 1* **1983**, 2393–2398.
91. Cheung, Y.-F.; Walsh, C. *J. Am. Chem. Soc.* **1976**, *98*, 3397–3398.
92. Slieker, L.; Benkovic, S. J., *J. Label. Comp. Radiopharm.* **1982**, *19*, 647–657.
93. Ramer, S. E.; Moore, R. N.; Vederas, J. C. *Can. J. Chem.* **1986**, *64*, 706–713.
94. Axelsson, B. S.; O'Toole, K. J.; Spencer, P. A.; Young, D. W. *J. Chem. Soc., Chem. Commun.* **1991**, 1085–1086.
95. Young, D. W. In *Chemistry and Biology of Pteridines*, Blair, J., Ed.; Walter de Gruyter: Berlin, 1983; pp. 321–344.
96. Biellmann, J.-F.; Schuber, F. *Biochem Biophys. Res. Commun.* **1967**, *27*, 517–522.
97. Biellmann, J.-F.; Schuber, F. J. *Bull. Soc. Chim. Biol.* **1970**, *2*, 211–227.
98. Tatum, C. M.; Benkovic, P. A.; Benkovic, S. J.; Potts, R.; Schleicher, E.; Floss, H. G. *Biochemistry* **1977**, *16*, 1093–1102.
99. Slieker, L. J.; Benkovic, S. J. *J. Am. Chem. Soc.* **1984**, *106*, 1833–1838.
100. Vanoni, M. A.; Lee, S.; Floss, H. G.; Matthews, R. G. *J. Am. Chem. Soc.* **1990**, *112*, 3987–3992.

101. Aberhart, D. J.; Russell, D. J., *J. Am. Chem. Soc.* **1984**, *106*, 4902–4906.
102. Kirby, G. W.; Varley, M. J. *J. Chem. Soc., Chem. Commun.* **1974**, 833–834.
103. Schleicher, E.; Mascaro, K.; Potts, R.; Mann, D. R.; Floss, H. G. *J. Am. Chem. Soc.* **1976**, *98*, 1043–1044.
104. Fuganti, C.; Ghiringhelli, D.; Giangrasso, D.; Grasselli, P. *J. Chem. Soc., Chem. Commun.* **1974**, 726–727.
105. Kumagai, H.; Yamada, H.; Sawada, S.; Schleicher, E.; Mascaro, K.; Floss, H. G. *J. Chem. Soc., Chem. Commun.* **1977**, 85–86.
106. Borcsok, E.; Ables, R. H. *Arch. Biochem. Biophys.* **1982**, *213*, 695–707.
107. Purvis, M. B.; Kingston, D. G. I.; Fujii, N.; Floss, H. G. *J. Chem. Soc., Chem. Commun.* **1987**, 302–303.
108. Townsend, C. A.;Brown, A. M. *J. Am. Chem. Soc.* **1982**, *104*, 1748–1750.
109. Townsend, C. A.; Brown, A. M.; Nguyen, L. T. *J. Am. Chem. Soc.* **1983** *105*, 919–927.
110. No, Z.; Sanders, C. R.; Dowhan, W.; Tsai, M.-D. *Bioorg. Chem.* **1988**, *16*, 184–188.
111. Gani, D.; Wallis, O. C.; Young, D. W. *J. Chem. Soc., Chem. Commun.* **1982**, 898–899.
112. Coggiola, D.; Fuganti, C.; Ghiringhelli, D.; Grasselli, P. *J. Chem. Soc., Chem. Commun.* **1976**, 143–144.
113. Fuganti, C. *J. Chem. Soc., Chem. Commun.* **1979**, 337–339.
114. Fuganti, C.; Ghiringhelli, D.; Grasselli, P. *J. Chem. Soc., Chem. Commun.* **1975**, 846–847.
115. Fuganti, C.; Ghiringhelli, D.; Grasselli, P. *Experientia* **1978**, *34*, 297–298.
116. Kalvin, D. M., Woodard, R. W. *J. Org. Chem.* **1985**, *50*, 2259–2263.
117. Ramalingam, K.; Woodard, R. W. *J. Org. Chem.* **1988**, *53*, 1900–1903.
118. Lee, K.-M.; Ramalingam, K.; Son, J.-K.; Woodard, R. W. *J. Org. Chem.* **1989**, *54*, 3195–3198.
119. Schwab, J. M.; Ho, C.-K. *J. Chem. Soc., Chem. Commun.* **1986**, 872–873.
120. Schwab, J. M.; Ray, T. *J. Chem. Soc., Chem. Commun.* **1988**, 29–31.
121. Schwab, J. M.; Ray, T.; Ho, C.-K *J. Am. Chem. Soc.* **1989**, *111*, 1057–1063.
122. Subramanian, P. K.; Kalvin, D. M.; Ramalingam, K.; Woodard, R. W. *J. Org. Chem.* **1989**, *54*, 270–276.
123. Chang, M. N.; Walsh, C. *J. Am. Chem. Soc.* **1980**, *102*, 2499–2501.
124. Guggenheim, S.; Flavin, M. *J. Biol. Chem.* **1969**, *244*, 6217–6227.
125. Posner, B. I.; Flavin, M. *J. Biol. Chem.* **1972**, *247*, 6412–6419.
126. Fuganti, C.; Coggiola, D. *Experientia* **1977**, *33*, 847.
127. Posner, B. I.; Flavin, M. *J. Biol. Chem.* **1972**, *247*, 6402–6411.
128. Chang, M. N. T.; Walsh, C. *J. Am. Chem. Soc.* **1980**, *102*, 7368–7370.
129. Chang, M. N. T.; Walsh, C. T. *J. Am. Chem. Soc.* **1981**, *103*, 4921–4927.
130. Krongelb, M.; Smith, T. A.; Ables, R. H. *Biochim. Biophys. Acta* **1968**, *167*, 473–475.
131. Kapke, G.; Davis, L. *Biochemistry* **1976**, *15*, 3745–3749.
132. Yang, I. Y.; Huang, Y. Z.; Snell, E. E. *Fed. Proc., Fed Am. Soc. Exper. Biol.* **1975**, *34*, 496; abstract 1552.
133. Morecombe, D. J.; Young, D. W. *J. Chem. Soc., Chem. Commun.* **1975**, 198–199.
134. Young, D. W.; Morecombe, D. J.; Sen, P. K. *Eur. J. Biochem.* **1977**, *75*, 133–147.
135. Aberhart, D. J.; Lin, L. J.; Chu, J. Y.-R. *J. Chem. Soc., Perkin Trans. 1* **1975**, 2517–2523.
136. Baldwin, J. E.; Adlington, R. M.; Robinson, N. G.; Ting, H.-H. *J Chem. Soc., Chem. Commun.* **1986**, 409–411.

137. Huddleston, J. A.; Abraham, E. P.; Young, D. W.; Morecombe, D. J.; Sen, P. K. *Biochem. J.* **1978**, *169*, 705–707.

138. Aberhart, D. J.; Ghoshal, P. K.; Cotting, J.-A.; Russell, D. J. *Biochemistry* **1985**, *24*, 7178–7182.

139. Aberhart, D. J.; Ghoshal, P. K.; Cotting, J.-A.; Russell, D. J. In *Mechanisms of Enzymatic Reactions–Stereochemistry*, Frey, P. A., Ed.; Elsevier: New York, 1986; p. 319.

140. Billington, D. C.; Golding B. T. *J. Chem. Soc., Perkin Trans. 1* **1982**, 1283–1290.

141. Golding, B. T.; Nassereddin, I. K. *J. Am. Chem. Soc.* **1982**, *104*, 5815–5817.

142. Wiesendanger, R.; Martonini, B.; Boller, T.; Arigoni, D. *Experientia*, **1986**, *42*, 207–209.

143. Son, J.-K.; Woodard, R. W. *J. Am. Chem. Soc.* **1989**, *111*, 1363–1367.

144. Townsend, C. A.; Reeve, A. M.; Salituro, G. M. *J. Chem. Soc., Chem. Commun.* **1988**, 1579–1581.

145. Golding, B. T.; Nassereddin, I. K.; Billington, D. C. *J. Chem. Soc., Perkin Trans. 1* **1985**, 2007–2010.

146. Golding, B. T.; Nassereddin, I. K. *J. Chem. Soc., Perkin Trans. 1* **1985**, 2017–2024.

147. Orr, G. R.; Danz, D. W.; Pontoni, G.; Prabhakaran, P. C.; Gould, S. J.; Coward, J. K. *J. Am. Chem. Soc.* **1988**, *110*, 5791–5799.

148. Stevenson, D. E.; Akhtar, M.; Gani, D. *Tetrahedron Lett.* **1986**, *27*, 5661–5664.

149. Ramalingam, K.; Lee, K.-M.; Woodard, R. W.; Bleecker, A. B.; Kende, H. *Proc. Natl. Acad. Sci., USA* **1985**, *82*, 7820–7824.

150. Mascaro, L.; Hörhammer, R.; Eisenstein, S.; Sellers, L. K.; Mascaro, K.; Floss, H. G. *J. Am. Chem. Soc.* **1977**, *99*, 273–274.

151. Woodard, R. W.; Mascaro, L.; Hörhammer, R.; Eisenstein, S.; Floss, H. G. *J. Am. Chem. Soc.* **1980**, *102*, 6314–6318.

152. Floss, H. G.; Mascaro, L.; Tsai, M.-D.; Woodard, R. W. In *Transmethylation*; Usdin, E.; Borchardt, R. T.; Creveling, C. R., Eds; Elsevier: New York, 1979; pp. 135–141.

153. Arigoni, D., CIBA Foundation Symposium no. 60; *Molecular Interactions and Activity in Proteins*, Excerpta Medica: Amsterdam, 1978; pp. 243–261.

154. Woodard, R. W.; Tsai, M.-D.; Floss, H. G.; Crooks, P. A.; Coward, J. K. *J. Biol. Chem.* **1980**, *255*, 9124–9127.

155. Woodard, R. W.; Weaver, J.; Floss, H. G. *Arch. Bioch. Biophys.* **1981**, *207*, 51–54.

156. Lee, J. J.; Dewick, P. M.; Gorst-Allman, C. P.; Spreafico, F.; Kowal, C.; Chang, C.-J.; McInnis, A. G.; Walter, J. A.; Keller, P. J.; Floss, H. G. *J. Am. Chem. Soc.* **1987**, *109*, 5426–5432.

157. Zhou, P.; O'Hagan, D.; Mocek, U.; Zeng, Z.; Yuen, L.-D.; Frenzel, T.; Unkefer, C. J.; Beale, J. M.; Floss, H. G. *J. Am. Chem. Soc.* **1989**, *111*, 7274–7276.

158. Zydowsky, T. M.; Courtney, L. F.; Frasca, V.; Kobayashi, K.; Shimizu, H.; Yuen, L.-D.; Matthews, R. G.; Benkovic, S. J.; Floss, H. G. *J. Am. Chem. Soc.* **1986**, *108*, 3152–3153.

159. Frenzel, T.; Beale, J. M., Kobayashi, M.; Zenk, M. H.; Floss, H. G. *J. Am. Chem. Soc.* **1988**, *110*, 7878–7880.

160. Cornforth, J. W.; Reichard, S. A.; Talalay, P.; Carrell, H. L.; Glusker, J. P. *J. Am. Chem. Soc.* **1977**, *99*, 7292–7300.

161. Kjaer A.; Grue-Sorensen, G.; Kelstrup, E.; Madsen, J. O. *Pure & Appl. Chem.* **1979**, *52*, 157–163.

162. Grue-Sorensen, G.; Kelsturp, E.; Kjaer, A.; Madsen, J. O. *J. Chem. Soc., Perkin Trans. 1* **1984**, 1091–1097.

163. Parry, R. J.; Naidu, M. V. *J. Am. Chem. Soc.* **1982**, *104*, 3217–3219.

164. Kluender, H.; Bradley, C. H.; Sih, C. J.; Fawcett, P.; Abraham, E. P. *J. Am. Chem. Soc.* **1973**, *95*, 6149–6150.

165. Kluender, H.; Huang, F.-C.; Fritzberg, A.; Schnoes, H.; Sih, C. J.; Fawcett, P.; Abraham, E. P. *J. Am. Chem. Soc.* **1974**, *96*, 4054–4055.

166. Baldwin, J. E.; Löliger, J.; Rastetter, W.; Neuss, N.; Huckstep, L. L.; De LaHiguera, N. *J. Am. Chem. Soc.* **1973**, *95*, 3796–3797.

167. Aberhart, D. J.; Lin, L. J. *J. Am. Chem. Soc.* **1973**, *95*, 7859–7860.

168. Aberhart, D. J.; Lin, L. J., *J. Chem. Soc., Perkin Trans. 1.*, **1974**, 2320–2326.

169. Aberhart, D. J. *J. Label. Comp. Radiopharm.* **1983**, *20*, 605–610.

170. Crout, D. H. G.; Lutstorf, M.; Morgan, P. J.; Adlington, R. M.; Baldwin, J. E.; Crimmin, M. J. *J. Chem. Soc., Chem. Commun.* **1981**, 1175–1176.

171. Crout, D. H. G.; Lutstorf, M.; Morgan, P. J. *Tetrahedron* **1983**, *39*, 3457–3469

172. Townsend, C. A.; Neese, A. S.; Theis, A. B. *J. Chem. Soc., Chem. Commun.* **1982**, 116–118.

173. Baldwin, J. E.; Adlington, R. M.; Domayne-Hayman, B. P.; Ting, H.-H.; Turner, N. J. *J. Chem. Soc., Chem. Commun.* **1986**, 110–113.

174. Baldwin, J. E.; Adlington, R. M.; Crouch, N. P.; Turner, N. J.; Schofield, C. J. *J. Chem. Soc., Chem. Commun.* **1989**, 1141–1143.

175. Neuss, N.; Nash, C. H.; Baldwin, J. E.; Lemke, P. A.; Grunzer, J. B. *J. Am. Chem. Soc.* **1973**, *95*, 3797–3798.

176. Abraham, E.; Pang, C-P.; White, R. L.; Crout, D. H. G.; Lutstorf, M.; Morgan, P. J.; Derome, A. E. *J. Chem. Soc., Chem. Commun.* **1983**, 723–724.

177. Pang, C.-P.;White, R. L.; Abraham, E. P.; Crout, D. H. G.; Lutstorf, M.; Morgan, P. J.; Derome, A. E. *Biochem. J.* **1984**, *222*, 777–788.

178. Townsend, C. A.; Theis, A. B.; Neese, A. S.; Barrabee, E. B.; Poland, D. *J. Am Chem. Soc.* **1985**, *107*, 4760–4767.

179. Aberhart, D. J. *J. Am. Chem. Soc.* **1979**, *101*, 1354–1355.

180. Wasmuth, D.; Arigoni, D.; Seebach, D. *Helv. Chim. Acta* **1982**, *65*, 344–352.

181. Cardillo, R.; Fuganti, C.; Ghiringhelli, D.; Grasselli, P.; Gatti, G. *J. Chem. Soc., Chem. Commun.* **1977**, 474–476.

182. Anastasis, P.; Freer, I.; Overton, K. H.; Picken, D.; Rycroft, D. S.; Singh, S. B. *J. Chem. Soc., Perkin Trans. 1* **1987**, 2427–2436.

183. Aberhart, D. J.; Weiller, B. H. *J. Label. Comp. Radiopharm.* **1983**, *20*, 663–668.

184. August, R. A.; Khan, J. A.; Moody, C. M.; Young, D. W. *Tetrahedron Lett.*, **1992**, *33*, 4617–4620.

185. Komatsubara, S.; Kisumi, M.; Chibata, I.; Gregorio, M. M. V.; Muller, U. S.; Crout, D. H. G. *J. Chem. Soc., Chem. Commun.* **1977**, 839–841.

186. Hill, R. K.; Rhee, S.-W.; Leete, E.; McGaw, B. A. *J. Am. Chem. Soc.* **1980**, *102*, 7344–7348.

187. Hill, R. K.; Rhee, S.-W.; Isono, K.; Crout, D. H. G.; Suhadolnik, R. J. *Biochemistry* **1981**, *20*, 7040–7042.

188. Cahill, R.; Crout, D. H. G.; Mitchell, M. B.; Müller, U. S. *J. Chem. Soc., Chem. Commun.* **1980**, 419–421.

189. Armstrong, F. B.; Lipscomb, E. L.; Crout, D. H. G.; Mitchell, M. B.; Prakash, S. R. *J. Chem. Soc., Perkin Trans. 1* **1983**, 1197–1201.

190. Hill, R. K.; Sawada, S.; Arfin, S. M., *Bioorg. Chem.* **1979**, *8*, 175–189.

191. Hill, R. K.; Foley, P. J. *Biochem. Biophys. Res. Commun.* **1968**, *33*, 480–482
192. Hill, R. K.; Yan, S.-J. *Bioorg. Chem* **1971**, *1*, 446–456.
193. Armstrong, F. B.; Muller, U. S.; Reary, J. B.; Whitehouse, D.; Crout, D. H. G. *Biochim. Biophys. Acta* **1977**, *498*, 282–293.
194. Crout, D. H. G.; Whitehouse, D. *J. Chem. Soc., Perkin Trans. 1* **1977**, 544–549.
195. Arfin, S. M.; Umbarger, H. E. *J. Biol. Chem.* **1969**, *244*, 1118–1127.
196. Crout, D. H. G. In *Biosynthesis of Branch Chain Amino Acids*, Barak, Z.; Chipman, D. M.; Schloss, J. V., Eds.; VCH Publishers: New York, 1990; pp. 199–242.
197. Crout, D. H. G.; Hedgecock, C. J. R.; Lipscomb, E. L.; Armstrong, F. B. *Eur. J. Biochem.* **1980**, *110*, 439–444.
198. Hill R. K.; Yan, S.; Arfin, S. M. *J. Am. Chem. Soc.* **1973**, *95*, 7857–7861
199. Crout, D. H. G.; Gregorio, M. V. M.; Müller, U. S.; Komatsubara, S.; Kisumi, M.; Chibata, I. *Eur. J. Bioch.* **1980**, *106*, 97–105.
200. Cole F. E.; Kalyanpur, M. G.; Stevens, C. M. *Biochemistry* **1973**, *12*, 3346–3350.
201. Calvo, J. M.; Kalyanpur, M. G.; Stevens, C. M. *Biochemistry* **1962**, *1*, 1157–1161.
202. Yamada, T.; Kakinuma, K.; Endo, T.; Oshima, T. *Chem. Lett.* **1987**, 1749–1752.
203. Senn, H.; Werner, B.; Messerle, B. A.; Weber, C.; Traber, R.; Wüthrich, *K. F. E. B. S. Lett.*, **1989**, *249*, 113–118.
204. Neri, D.; Otting, G.; Wüthrich, K. *Tetrahedron* **1990**, *46*, 3287–3296.
205. Aberhart, D. J. *Tetrahedron Lett* **1975**, 4373–4374.
206. Amster, J.; Tanaka, K. *J. Biol. Chem.* **1980**, *255*, 119–120.
207. Aberhart, D. J., *Bioorg. Chem.* **1977**, *6*, 191–201.
208. Aberhart, D. J.; Tann, C.-H. *J. Chem. Soc., Perkin Trans. 1* **1979**, 939–942.
209. Aberhart, D. J.; Tann, C.-H. *J. Am. Chem. Soc.* **1980**, *102*, 6377–6380.
210. Aberhart, D. J.; Hsu, C.-T. *J. Chem. Soc., Perkin Trans. 1* **1979**, 1404–1406.
211. Metzler, D. E., *Biochemistry, the Chemical Reactions of Living Cells* Academic Press; New York, 1977; pp. 832–834.
212. Aberhart, D. J.; Tann, C.-H. *Bioorg. Chem.* **1981**, *10*, 200–205.
213. Aberhart, D. J.; Tann, C.-H. *Bioorg. Chem.* **1981**, *10*, 375–387.
214. Aberhart, D. J.; Finocchiaro, G.; Ikeda, Y.; Tanaka, K. *Bioorg. Chem.* **1986**, *14*, 170–175.
215. Messner, B.; Eggerer, H.; Cornforth, J. W.; Mallaby, R. *Eur. J. Biochem.* **1975**, *53*, 255–264.
216. Krasna, A. I. *J. Biol. Chem.* **1958**, *233*, 1010–1013.
217. Englard, S. *J. Biol. Chem.* **1958**, *233*, 1003–1009.
218. Englard, S.; Hanson, K. R. *Methods Enzymol.* **1969**, *13*, 567–601.
219. Kim, S. C.; Raushel, F. M. *Biochemistry* **1986**, *25*, 4744–4749.
220. Tamiya, N.; Oshima, T. *J. Biochem.* **1962**, *51*, 78–88.
221. Kainosho, M.; Ajisaka, K. *J. Am. Chem. Soc.* **1975**, *97*, 5630–5631.
222. Botting, N. P.; Akhtar, M.; Cohen, M. A.; Gani, D., *J. Chem. Soc., Chem. Commun.* **1987**, 1371–1373.
223. Klinman, J. P.; Rose, I. A. *Biochemistry* **1971**, *10*, 2259–2266.
224. Gani, D.; Young, D. W.; Carr, D. M.; Poyser, J. P.; Sadler, I. H. *J. Chem. Soc., Perkin Trans. 1* **1983**, 2811–2814.
225. Blattmann, P.; Rétey, J. *Eur. J. Biochem.* **1972**, *30*, 130–137.

226. Bright, H. J.; Lundin, R. E.; Ingraham, L. L. *Biochemistry* **1964**, *3*, 1224–1230.
227. Bright, H. J.; Ingraham, L. L.; Lundin, R. E. *Biochim. Biophys. Acta* **1964**, *81*, 576–584.
228. Lienhard, G. E.; Rose, I. A. *Biochemistry* **1964**, *3*, 185–190.
229. Rose, I. A.; O'Connell, E. L. *J. Biol. Chem.* **1967**, *242*, 1870–1879.
230. Englard, S.; Midelfort, C. F. *Fed Proc., Fed. Am. Soc. Exper. Biol.* **1978**, *37*, 1806; abstract 2943.
231. Blanchard, J. S.; Englard, S. *Biochemistry* **1983**, *22*, 5922–5929.
232. Englard, S.; Blanchard, J. S.; Midelfort, C. F. *Biochemistry* **1985**, *24*, 1110–1116.
233. Buckel, W. *Eur. J. Biochem.* **1980**, *106*, 439–447.
234. Ducrocq, C.; Righini-Tapie, A.; Azerad, R.; Green, J. F.; Friedman, P. A.; Beacourt, J.-P.; Rousseau, B. *J. Chem. Soc., Perkin Trans. 1* **1986**, 1323–1328.
235. Hartrampf, G.; Buckel, W. *F. E. B. S. Lett.* **1984**, *171*, 73–78.
236. Buckel, W. *Eur. J. Biochem.* **1986**, *156*, 259–263.
237. Ducrocq, C.; Decottignies-LeMaréchal, P.; Azerad, R. *J. Label. Comp. Radiopharm.* **1985**, *22*, 61–70.
238. Decottignies-LeMaréchal, P.; Ducrocq, C.; Marquet, A.; Azerad, R. *C. R. Acad. Sci., Paris* **1984**, *298* (Series II), 343–346.
239. Field, S. J.; Young, D. W. *J. Chem. Soc., Chem. Commun.* **1979**, 1163–1165.
240. Field, S. J.; Young, D. W. *J. Chem. Soc., Perkin Trans. 1* **1983**, 2387–2392.
241. Sprecher, M.; Sprinson, D. B., *Fed. Proc., Fed. Am. Soc. Exper. Biol.* **1963**, *22*, 361; abstract 1201.
242. Sprecher, M.; Sprinson, D. B. *Ann. New York Acad. Sci.* **1964**, *112*, 655–660.
243. Sprecher, M.; Switzer, R. L.; Sprinson, D. B. *J. Biol. Chem.* **1966**, *241*, 864–867.
244. Buchanan, J. G.; Kumar, A.; Wightman, R. H.; Field, S. J.; Young, D. W. *J. Chem. Soc., Chem. Commun.* **1984**, 1517–1518.
245. Decottignies-LeMaréchal, P.; Ducrocq, C.; Marquet, A.; Azerad, R. *J. Biol. Chem.* **1984**, *259*, 15010–15012.
246. Dubois, J.; Gaudry, M.; Bory, S.; Azerad, R.; Marquet, A. *J. Biol. Chem.* **1983**, *258*, 7897–7899.
247. Yamada, H.; O'Leary, M. H. *Biochemistry* **1978**, *17*, 669–672.
248. Burnett, G.; Walsh, C.; Yonaha, K.; Toyama, S.; Soda, K. *J. Chem. Soc., Chem. Commun.* **1979**, 826–828.
249. Bouclier, M.; Jung, M. J.; Lippert, B. *Eur. J. Biochem.* **1979**, *98*, 363–368.
250. Santaniello, E.; Kienle, M. G.; Manzocchi, A.; Bosisio, E. *J. Chem. Soc., Perkin Trans. 1* **1979**, 1677–1679.
251. Bosisio, E.; Santaniello, E.; Manzocchi, A.; Kienle, M. G. *Bioorg. Chem.* **1980**, *9*, 524–529.
252. Battersby, A. R.; Staunton, J.; Tippett, J. *J. Chem. Soc., Perkin Trans. 1* **1982**, 455–459.
253. Voss, D.; Gerdes, J.; Leistner, E. *Phytochemistry* **1985**, *24*, 1471–1473.
254. Pontoni, G.; Coward, J. K.; Orr, G. R.; Gould, S. J. *Tetrahedron Lett.* **1983**, *24*, 151–154.
255. Gramatica, P.; Manitto, P. *J. Label. Comp. Radiopharm.* **1980**, *18*, 955–962.
256. Fujita, Y.; Gottlieb, A.; Peterkofsky, B.; Udenfriend, S.; Witkop, B. *J. Am. Chem. Soc.* **1964**, *86*, 4709–4716.
257. Salzman, L. A.; Weissbach, H.; Katz, E. *Proc. Natl. Acad. Sci., USA* **1965**, *54*, 542–546.
258. Ebert, P. S.; Prockop, D. J. *Biochem. Biophys. Res. Commun.* **1962**, *8*, 305–309.

259. Prockop, D. J.; Ebert, P. S.; Shapiro, B. M. *Arch. Biochem. Biophys.* **1964**, *106*, 112–122.
260. Altman, L. J.; Silberman, N. *Anal. Biochem.* **1977**, *79*, 302–309.
261. Purvis, M. B.; LeFevre, J. W.; Jones, V. L.; Kingston, D. G. I.; Biot, A. M.; Gosselé, F. *J. Am. Chem. Soc.* **1989**, *111*, 5931–5935.
262. Aberhart, D. J.; Lin, H.-J.; Weiller, B. H. *J. Am. Chem. Soc.* **1981**, *103*, 6750–6752.
263. Aberhart, D. J.; Gould, S. J.; Lin, H.-J.; Thiruvengadam, T. K.; Weiller, B. H. *J. Am. Chem. Soc.* **1983**, *105*, 5461–5470.
264. Thiruvengadam, T. K.; Gould, S. J.; Aberhart, D. J.; Lin, H.-J. *J. Am. Chem. Soc.* **1983**, *105*, 5470–5476.
265. Kunz, F.; Rétey, J.; Arigoni, D.; Tsai, L.; Stadtman, T. C. *Helv. Chim. Acta.* **1978**, *61*, 1139–1145.
266. Rétey, J.; Kunz, F.; Arigoni, D.; Stadtman, T. C. *Helv. Chim. Acta* **1978**, *61*, 2989–2998.
267. Asada, Y.; Tanizawa, K.; Sawada, S.; Suzuki, T.; Misono, H.; Soda, K. *Biochemistry* **1981**, *20*, 6881–6886.
268. Kelland, J. G.; Palcic, M. M.; Pickard, M. A.; Vederas, J. C. *Biochemistry* **1985**, *24*, 3263–3267.
269. Tanizawa, K.; Yoshimura, T.; Asada, Y.; Sawada, S.; Misono, H.; Soda, K. *Biochemistry* **1982**, *21*, 1104–1108.
270. Hashimoto, H.; Misono H.; Nagata, S.; Nagasaki, S. *Agric. Biol. Chem.* **1989**, *53*, 1175–1176.
271. Misono, H.; Yoshimura, T.; Nagasaki, S.; Soda, K. *J. Biochem.* **1990**, *107*, 169–172.
272. Leistner, E.; Spenser, I. D. *J. Chem. Soc., Chem. Commun.* **1975**, 378–379.
273. Gerdes, H. G.; Leistner, E. *Phytochemistry* **1979**, *18*, 771–775.
274. Richards, J. C.; Spenser, I. D. *J. Am. Chem. Soc.* **1978**, *100*, 7402–7404.
275. Battersby, A. R.; Murphy, R.; Staunton, J. *J. Chem. Soc., Perkin Trans. 1* **1982**, 449–453.
276. Golebiewski, W. M.; Spenser, I. D. *J. Am. Chem. Soc.* **1984**, *106*, 7925–7927.
277. Orr, G. R.; Gould, S. J. *Tetrahedron Lett.* **1982**, *23*, 3139–3142.
278. Richards, J. C.; Spenser, I. D. *Tetrahedron* **1983**, *39*, 3549–3568.
279. Golebiewski, W. M.; Spenser, I. D. *J. Am. Chem. Soc.* **1984**, *106*, 1441–1442.
280. Golebiewski, W. M.; Spenser, I. D. *Can. J. Chem.* **1985**, *63*, 2707–2718.
281. Townsend, C. A.; Ho, M.; Mao, S. *J. Chem. Soc., Chem. Commun.* **1986**, 638–639.
282. Parry, R. J.; Arzu, I. Y.; Ju, S.; Baker, B. J. *J. Am. Chem. Soc.* **1989**, *111*, 8981–8982.
283. Richards, J. C.; Spenser, I. D. *Can. J. Chem.* **1982**, *60*, 2810–2820.
284. Orr, G. R.; Gould, S. J.; Pegg, A. E.; Seely, J. E.; Coward, J. K. *Bio-organic Chem.* **1984**, *12*, 252–258.
285. Wigle, I. D.; Mestichelli, L. J. J.; Spenser, I. D., *J. Chem. Soc., Chem. Commun.* **1982**, 662–664.
286. Rana, J.; Robins, D. J. *J. Chem. Soc., Chem. Commun.* **1983**, 1222–1224.
287. Robins, D. J. *Phytochemistry* **1983**, *22*, 1133–1135.
288. Rana, J.; Robins, D. J. *J. Chem. Soc., Chem. Commun.* **1984**, 517–519.
289. Asada, Y.; Tanizawa, K.; Nakamura, K.; Moriguchi, M.; Soda, K. *J. Biochem.* **1984**, *95*, 277–282.
290. Grue-Sorensen, G.; Spenser, I. D. *J. Am. Chem. Soc.* **1983**, *105*, 7401–7404.
291. Prabhakaran, P. C.; Woo, N.-T.; Yorgey, P. S.; Gould, S. J. *J. Am. Chem. Soc.* **1988**, *110*, 5785–5791.

292. Givot, I. L.; Smith, T. A.; Abeles, R. H. *J. Biol. Chem.* **1969**, *244*, 6341–6353.
293. Rétey, J.; Fierz, H.; Zeylemaker, W. P. *F. E. B. S. Lett.* **1970**, *6*, 203–205.
294. Peterkofsky, A. *J. Biol. Chem.* **1962**, *237*, 787–795.
295. Kaeppeli, F.; Rétey, J., *Eur. J. Biochem.* **1971**, *23*, 198–202.
296. Grubmeyer, C. T.; Insinga, S.; Bhatia, M.; Moazami, N. *Biochemsitry* **1989**, *28*, 8174–8180.
297. Asano, Y.; Woodard, R. W.; Houck, D. R.; Floss, H. G. *Arch. Biochem. Biophys.* **1984**, *231*, 253–256.
298. Battersby, A. R.; Joyeau, R.; Staunton, J., *F. E. B. S. Lett.* **1979**, *107*, 231–232.
299. Battersby, A. R.; Nicoletti, M.; Staunton, J.; Vleggaar, R. *J. Chem. Soc., Perkin Trans. 1* **1980**, 43–51.
300. Chang, G. W.; Snell, E. E. *Biochemistry* **1968**, *7*, 2005–2012.
301. Santaniello, E., Manzocchi, A.; Biondi, P. A. *J. Chem. Soc., Perkin Trans. 1* **1981**, 307–309.
302. Kirby, G. W.; Michael, J. *J. Chem. Soc. Chem. Commun* **1971**, 187–188 and 415–416.
303. Kirby, G. W.; Narayanaswami, S.; Rao, P. S. *J. Chem. Soc., Perkin Trans. 1* **1975**, 645–647.
304. Kirby, G. W.; Michael, J. *J. Chem. Soc., Perkin Trans . 1* **1973**, 115–120.
305. Hanson, K. R.; Wightman, R. H.; Staunton, J.; Battersby, A. R. *J. Chem. Soc., Chem. Commun.* **1971**, 185–186.
306. Wightman, R. H.; Staunton, J.; Battersby, A. R.; Hanson, K. R. *J. Chem. Soc., Perkin Trans. 1* **1972**, 2355–2364.
307. Strange, P. G.; Staunton, J.; Wiltshire, H. R.; Battersby, A. R.; Hanson, K. R.; Havir, E. A. *J. Chem. Soc., Perkin Trans. 1* **1972**, 2364–2372.
308. Kirby, G. W.; Michael, J.; Narayanaswami, S. *J. Chem. Soc., Perkin Trans . 1* **1972**, 203–205.
309. Ife, R.; Haslam, E. *J. Chem. Soc. (C)* **1971**, 2818–2821.
310. Nagai, U.; Kobayashi, J. *Tetrahedron Lett.* **1976**, 2873–2874.
311. Bartl, K.; Cavalar, C.; Krebs, T.; Ripp, E.; Rétey, J.; Hull W. E.; Günther, H.; Simon, H. *Eur. J. Biochem.* **1977**, *72*, 247–250.
312. Tanimura, K.; Kato, T.; Waki, M.; Lee, S.; Kodera, Y.; Izumiya, N. *Bull. Chem. Soc. Jpn.* **1984**, *57*, 2193–2197.
313. Sawada, S.; Kumagai, H.; Yamada, H.; Hill, R. K.; Mugibayashi, Y.; Ogata, K. *Biochim. Biophys. Acta* **1973**, *315*, 204–207.
314. Ellis, B. E.; Zenk, M. H.; Kirby, G. W.; Michael, J.; Floss, H. G. *Phytochemistry* **1973**, *12*, 1057–1058.
315. Belleau, B.; Burba, J. *J. Am. Chem. Soc.* **1960**, *82*, 5751–5752.
316. Belleau, B.; Fang, M.; Burba, J.; Moran, J. *J. Am. Chem. Soc.* **1960**, *82*, 5752–5754.
317. Battersby, A. R.; Chrystall, E. J. T.; Staunton, J. *J. Chem. Soc., Perkin Trans . 1* **1980**, 31–42.
318. Nakazawa, H.; Ajisaka, K.; Kainosho, M.; Sawada, S.; Yamada, H. *Agric. Biol. Chem.* **1981**, *45*, 2553–2557.
319. Bachan, L.; Strom, C. B.; Wheeler, J. W.; Kaufman, S. *J. Am. Chem. Soc.* **1974**, *96*, 6799–6800.
320. Rétey, J.; Bartl, J.; Ripp, E.; Hull, W. E. *Eur. J. Biochem.* **1977**, *72*, 251–257.
321. Johns, N.; Kirby, G. W.; Bulock, J. D.; Ryles, A. P. *J. Chem. Soc., Perkin Trans. 1* **1975**, 383–386.
322. Sawada, S.; Kumagai, H.; Yamada, H.; Hill, R. K. *J. Am. Chem. Soc.* **1975**, *97*, 4334–4337.
323. Parry, R. J.; Kurylo-Borowska, Z. *J. Am. Chem. Soc.* **1980**, *102*, 836–837.

324. Parry, R. J.; *J. Chem. Soc. Chem. Commun.* **1975**, 144–145.
325. Bettersby, A. R.; Kelsey, J. E.; Staunton, J. *J. Chem. Soc. Chem. Commun.* **1971**, 183–184.
326. Platt, R. V.; Opie, C. T.; Haslam, E. *Phytochemistry* **1984**, *23*, 2211–2217.
327. Rosen, M. A.; Farnden, K. J. F.; Conn, E. E.; Hanson, K. R. *J. Biol. Chem.* **1975**, *250*, 8302–8308.
328. Hammond, S. J.; Williamson, M. P.; Williams, D. H.; Boeck, L. D.; Marconi, G. C. *J. Chem. Soc., Chem. Commun.* **1982**, 344–346.
329. Kirby, G. W.; Narayanaswami, S. *J. Chem. Soc., Chem. Commun.* **1973**, 322–323.
330. Kirby, G. W.; Narayanaswami, S. *J. Chem. Soc., Perkin Trans. 1* **1976**, 1564–1567.
331. Gustafson, M. E.; Miller, D.; Davis, P. J.; Rosazza, J. P.; Chang, C.-J.; Floss, H. G. *J. Chem. Soc., Chem. Commun.* **1977**, 842–843.
332. Cardillo, R.; Fuganti, C.; Ghiringhelli, D.; Grasselli, P.; Gatti, G. *J. Chem. Soc., Chem. Commun.* **1975**, 778–779.
333. Zee, L.; Hornemann, U.; Floss, H. G. *Biochem. Physiol. Pflanzen* **1975**, *168*, 19–25.
334. Tsai, M.-D.; Floss, H. G.; Rosenfeld, H. J.; Roberts, J. *J. Biol. Chem.* **1979**, *254*, 6437–6443.
335. Houck, D. R.; Floss, H. G. *J. Nat. Products (Lloydia)* **1981**, *44*, 759–762.
336. Steyn, P. S.; Vleggaar, R.; Ferreira, N. P.; Kirby, G. W.; Varley, M. J. *J. Chem. Soc., Chem. Commun.* **1975**, 465–466.
337. Palcic, M. M.; Antoun, M.; Tanizawa, K.; Soda, K.; Floss, H. G. *J. Biol. Chem.* **1985**, *260*, 5248–5251.
338. Adlington, R. M.; Baldwin, J. E.; Rawlings, B. J. *J. Chem. Soc., Chem. Commun.* **1983**, 290–292.
339. Pirrung, M. C. *J. Am. Chem. Soc.* **1983**, *105*, 7207–7209.
340. Ramalingam, K.; Kalvin, D.; Woodard, R. W. *J. Label. Comp. Radiopharm.* **1984**, *21*, 833–841.
341. Hill, R. K.; Prakash, S. R.; Wiesendanger, R.; Angst, W.; Martinoni, B.; Arigoni, D.; Liu, H.-W. Walsh, C. T. *J. Am. Chem. Soc.* **1984**, *106*, 795–796.
342. Subramanian, P. K.; Woodard, R. W. *J. Org. Chem.* **1987**, *52*, 15–18.
343. Wiesendanger, R.; Martinoni, B.; Boller, T.; Arigoni, D. *J. Chem. Soc., Chem. Commun.* **1986**, 238–239.
344. Liu, H.; Auchus, R.; Walsh, C. T. *J. Am. Chem. Soc.* **1984**, *106*, 5335–5348.
345. Baldwin, J. E.; Adlington, R. M.; Lajoie, G. A.; Rawlings, B. J. *J. Chem. Soc., Chem. Commun.* **1985**, 1496–1498.
346. Palekar, A. G.; Tate, S. S.; Meister, A. *Biochemistry* **1971**, *10*, 2180–2182.
347. Paleker, A. G., Tate, S. S.; Meister, A. *J. Biol. Chem.* **1973**, *248*, 1158–1167.
348. Thomas, N. R.; Schirch, V.; Gani, D. *J. Chem. Soc., Chem. Commun.* **1990**, 400–402 and 724.
349. Thomas, N. R.; Rose, J. E.; Gani, D. *J. Chem. Soc., Chem. Commun.* **1991**, 908–909.

Searching Techniques for Databases of Three-Dimensional Chemical Structures

MARK G. BURES AND YVONNE C. MARTIN

Computer-Assisted Molecular Design Project, Abbott Laboratories, Abbott Park, Illinois

PETER WILLETT

Krebs Institute for Biomolecular Research and Department of Information Studies, University of Sheffield, Western Bank, Sheffield, United Kingdom

I. Introduction
II. Representation and Searching of Two-dimensional Chemical Structures
  A. Use of Graph Theory
  B. Structure Searching
  C. Substructure Searching
  D. Similarity Searching
III. Representation and Three-dimensional Substructure Searching
  A. Database Construction
  B. Screen Searching
  C. Geometric Searching
IV. Integration of Three-dimensional Substructure Searching and Molecular Modeling
V. Three-dimensional Similarity Searching
  A. Introduction
  B. Methods Based on Overlapping
  C. Use of Distance Information
  D. Organization of Search Output
  E. Use of Property Information
  F. Conclusions
VI. Current Research Areas
  A. Representation and Searching of Flexible Molecules
  B. *De Novo* Structure Generation
  C. Automated Generation of Pharmacophore Maps
VII. Conclusions
  References

Topics In Stereochemistry, Volume 21, Edited by Ernest L. Eliel and Samuel H. Wilen.
ISBN 0-471-52120-5 © 1994 John Wiley & Sons, Inc.

I. INTRODUCTION

Earlier this century crystallographers proved not only that molecules are three-dimensional (3-D) but also that small changes in chemical constitution often lead to subtle but real changes in 3-D structure (1). More recently, computerized *molecular modeling*, or *computer-aided molecular design*, has become a standard method to propose, visualize, and/or interpret 3-D molecular structures (2–8). As a key component of molecular modeling, computer graphics offers the advantages that molecular properties can also be displayed; the image can be as accurate as one knows the data and several 3-D structures can be compared by superposition. Because of both the growth in computer power and the perfection of experimental techniques, protein crystallography and nuclear magnetic resonance (NMR) are now able to produce atomic resolution 3-D structures of macromolecules, frequently bound to small molecules of biological interest (9, 10). The challenge is to use this 3-D information from molecular modeling or experiment to attempt to solve other problems. Searching databases of 3-D chemical structures, the subject of this review, is one of the tools being developed to utilize this information.

Pharmaceutical and chemical companies have invested millions of dollars in their corporate compound collections and are eager to capitalize on this proprietary resource by searching the 3-D structures of their existing molecules. For example, in a pharmaceutical company, a 3-D search might suggest a new biological property for some of its existing compounds, thus identifying possible candidates for clinical development or leads in subsequent molecular optimization programs. A complementary approach involves carrying out searches that are based on several 3-D hypotheses of pharmacological activity that cannot be distinguished with the available data: if active molecules are found in only one of these searches, then the other hypotheses can be discarded and interest focused more closely on the crucial structural features. A 3-D search of a database of existing compounds or of rigid 3-D partial structures can also form the basis for the *de novo* design of new compounds with a particular 3-D arrangement of key functionality. Special algorithms then transform or link the identified fragments into compounds that meet the original 3-D search criteria. Such 3-D searches can be made over many conformations of one, several, or many compounds to propose the conformation and intermolecular contacts in the complex that is formed when these compounds bind to a macromolecule of known 3-D structure. Finally, and alternatively, it is possible to search over many conformations of several molecules that exhibit strong binding to a particular biomacromolecule of unknown 3-D structure, with the resulting common structural features representing a *pharmacophore hypothesis*, that is, a set of proposed 3-D

requirements for binding. The above are just some of the applications of 3-D searching; these and many others are explored in the present review, which describes the wide range of techniques being developed for the representation and searching of databases of molecules in 3-D.

Computer techniques for searching chemical databases have been under active development since the early 1960s, and there is now a well-established body of theory and practice underlying the design and implementation of chemical structure retrieval systems. Almost without exception, these systems have been developed specifically for the storage and retrieval of information pertaining to two-dimensional, or 2-D, chemical structures, that is, the planar chemical structure diagrams that have provided the chemists' *lingua franca* for many years. Section II therefore provides a brief overview of the current state of development of 2-D structure handling systems, with special reference to the problems of representation and searching; the reader is referred to other reviews for more detailed accounts of 2-D structure handling techniques (11–15). Then, in Section III, we describe how these 2-D techniques can be extended to encompass the representation and searching of 3-D structures. Much of the material in this section is taken from a monograph by Willett, which provides a detailed review of the algorithms and data structures needed for efficient 3-D substructure searching (16). Other recent reviews are provided by Borman (17), Martin et al. (18), and Martin (19).

The 3-D database searching systems described in Section III are complementary in scope to the sophisticated techniques that have been developed for molecular modeling. The two approaches are complementary in that database searching provides an efficient means of scanning very large numbers of structures, as a precursor to the more detailed and computationally demanding processing required for molecular modeling. Additionally, 3-D searching normally requires that at least some modeling has been carried out so that it is possible to define a 3-D substructural query. The relationships between these two approaches to drug discovery are exemplified in Section IV, which details some recent studies on the integration of modeling and database searching.

Current 3-D searching systems focus upon *substructure searching* (as defined in Section II); in Section V, we present the first extended review of ongoing research to develop procedures for 3-D *similarity searching*, that is, the identification of those structures in a database that are most similar to an input target molecule. In Section VI we discuss three other areas that are the subject of much current research: (1) the development of techniques for the representation and searching of conformationally flexible 3-D molecules, rather than the rigid structures that have formed the basis for most work to date; (2) the development of methods for *structure generation*, the *de novo* design of molecules that will fit a known biological receptor site; and (3) the

automated generation of pharmacophore maps. Finally, in Section VII, we highlight areas that are in need of further research and development.

II. REPRESENTATION AND SEARCHING OF TWO-DIMENSIONAL CHEMICAL STRUCTURES

A. Use of Graph Theory

The primary means of representation for a 2-D chemical structure diagram is a *connection table.* A connection table contains a list of all of the atoms within a structure, together with bond information that describes the exact manner in which the individual atoms are linked together. Hydrogen atoms are often excluded since their presence or absence can be deduced from the bond orders and atomic types (although this may be difficult with organometallics and metal complexes, and in these cases it may not be possible to exclude the hydrogen atoms). Thus a complete and explicit description of the molecular topology is available for searching purposes, and connection tables now form the basis for most public and in-house chemical information systems. There are many ways in which a connection table can be represented in machine-readable form. However, it is generally very easy to convert from one form of connection table to another, and there is increasing interest in the use of standard formats that would lessen the need for such interconversions (20–22).

An important characteristic of a connection table is that it can be regarded as a *graph,* a mathematical construct that describes a set of objects (called *nodes* or *vertices*) and the relationships (called *edges* or *arcs*) that exist between pairs of the objects (13, 23–26). In fact, chemical graphs are examples of *labeled graphs,* since the atoms and bonds in a connection table are characterized by their elemental and bond types, respectively. A graph, G, consists of a set of nodes V, together with a set of edges E connecting pairs of nodes. Two nodes are said to be *adjacent* if they are connected by an edge. Two graphs, G_1 and G_2, are said to be *isomorphic* if they have the same structure, that is, if there is a correspondence or mapping between the nodes of G_1 and of G_2 such that adjacent pairs of nodes in G_1 are mapped to adjacent pairs of nodes in G_2. A *subgraph* of G is a subset, P, of the nodes of G together with a subset, F, of the edges connecting pairs of nodes in P. A *common subgraph* of two graphs G_1 and G_2 consists of a subgraph g_1 of G_1 and a subgraph g_2 of G_2 such that g_1 is isomorphic to g_2; the *maximal common subgraph* is the largest such common subgraph.

The presence or absence of isomorphism for a pair of graphs is determined by an isomorphism algorithm. Specifically, graph isomorphism, subgraph

isomorphism, and maximal common-subgraph isomorphism algorithms are computational procedures that, respectively, determine whether or not two graphs are identical; determine whether one graph is contained within another, larger graph; and determine the largest subgraph that is common to a pair of graphs. Reviews of isomorphism algorithms have been presented by Read and Corneil (27) and by Gati (28).

Graph-theoretical algorithms and data structures provide the basis for all modern 2-D chemical information systems, which offer three main types of searching facility. *Structure search* involves the search of a file of compounds for the presence or absence of a specified query compound. Such a search is required when there is a need to retrieve data associated with some compound or when a new molecule is to be added to a database and one needs to establish that it is not already present (a process that is normally referred to as *registration*). *Substructure search* involves the search of a file of compounds for all molecules containing some specified query substructure, irrespective of the environment in which the query substructure occurs. Finally, *similarity search* involves the search of a file of compounds for those molecules that are most similar to an input query molecule, using some quantitative definition of structural similarity. These three types of retrieval mechanism are considered now.

B. Structure Searching

Structure searching is the chemical equivalent of graph isomorphism, that is, the matching of one graph against another to determine whether they are identical. This can be carried out very rapidly if a unique structure representation is available, since a character-by-character match will then suffice to compare two structures for identity. However, connection tables are not necessarily unique since many different tables can be created for the same molecule, depending on the way in which the atoms in the molecule are numbered. Specifically, for a molecule containing N atoms, there are $N!$ different ways of numbering the atoms. The obvious algorithm for detecting the equivalence of two such variant representations involves the generation of all possible numberings of one molecule for comparison with the other; however, the factorial nature of this undertaking means that it is computationally infeasible for all but the smallest structures, unless some sort of heuristic procedure can be invoked to reduce the number of possible atom-to-atom equivalences that must be considered (27, 28). Two main approaches have been devised to overcome this problem in the chemical context, these being the use of *canonicalization* procedures, which produce a unique numbering of the set of atoms in a connection table (29, 30), and the use of arithmetic procedures, which permit the rapid generation of highly discriminating codes

that serve to eliminate all but a few molecules in a database from the detailed graph isomorphism search (31–33).

C. Substructure Searching

Substructure searching is the chemical equivalent of subgraph isomorphism, which is an example of an *NP-complete* problem (34, 35). This means that there is no algorithm known for which the running time is a simple polynomial function of the number of input records, that is, atoms in the structures under consideration; moreover, it is generally believed that such algorithms cannot, in fact, exist. Substructure searching involves determining the presence of a subgraph isomorphism between the query substructure and each and every one of the molecules in a database. It is thus highly demanding of computational resources, and efficiencies of operation are achieved by means of an initial *screen search*. This identifies that small fraction of the database that matches the query at the *screen* level, where a screen is a substructural feature, the presence of which is necessary but not sufficient for a molecule to contain the query substructure. These features are typically small, atom-, bond- or ring-centered fragment substructures that are algorithmically generated from a connection table when a compound is registered. The screen search checks each of the database structures for the presence of the screens that are present in the query substructure. Only those (hopefully) few molecules that match the query in the screen search are passed on for the final subgraph isomorphism, or *atom-by-atom*, search, which ensures that the features identified in the screen search are connected together in a database structure in the same way as they are connected in the query substructure.

The slowness of the atom-by-atom search means that the overall efficiency of a substructure searching system is crucially dependent on the *screenout*, that is, the fraction of the database that is eliminated by the screening search. There has accordingly been considerable interest in the development of algorithmic techniques for the selection of fragment screens that will give high screenout. These studies have suggested that the most generally useful fragments are those of intermediate, and approximately equal, frequencies of occurrence; in addition, the occurrences of the fragments that are chosen for inclusion in the *screen set* should, wherever possible, be statistically independent if high screenout is to be achieved (36–40).

The fragments that have been chosen to act as screens are listed in a fragment coding dictionary. When a query or a new molecule is to be processed, the corresponding connection table is analyzed to identify those screens from the coding dictionary that are present in the structure. A database structure or query substructure is then represented by a fixed-length bit string

in which the nonzero bits correspond to the screens that are present. The bit map is used for the first-stage search by checking for the presence of the bits that have been specified in the query bit string.

Once the screen search has been completed, the second stage, atom-by-atom search is carried out for those few molecules matching at the screen level; an atom-by-atom search will typically involve matching the query against less than 1% of the structures in a file. Screen searching can be implemented very rapidly indeed, with many thousands of structures per second being matched against a query, and thus the screen search stage of even a very large chemical database can be accomplished in a few tens of seconds. Conversely, the NP-complete nature of atom-by-atom searching means that only a few tens or hundreds of structures per second can be processed (depending on the hardware available), even when sophisticated heuristic procedures are used to minimize the number of possible query atom-to-database atom equivalences that need to be considered (41–43).

The simple, two-stage procedure described above characterizes many current 2-D substructure searching systems (15), and also forms the basis for the 3-D searching systems described later in this review; that said, the reader should note that other approaches to 2-D substructure searching are possible (see, e.g., refs. 44–46).

D. Similarity Searching

The last few years have seen substantial interest in the development of similarity searching systems (47, 48) in which the compounds in a database are ranked in order of decreasing similarity with an input query structure (rather than identifying those compounds that contain the query as in substructure searching). To implement similarity searching, one must provide an appropriate measure of intermolecular structural similarity, and many such measures are available (49).

A simple and obvious example of a measure of structural similarity is the *maximal common substructure* (MCS) where the MCS between a pair of molecules is the chemical equivalent of a maximal common subgraph (as defined previously in Section II.A). The MCS for a pair of molecules thus represents the maximal superimposition of one molecule upon the other, this providing a very precise measure of the degree of similarity between them. Maximal common substructure algorithms have, however, been little used for similarity searching in 2-D databases, owing to their computational requirements. The identification of the MCS for a pair of molecules is another NP-complete problem, and one that is even more demanding of computational resources, in practice, than is subgraph isomorphism; moreover, there

is no screening procedure that can be used to eliminate the great bulk of the definite nonhits prior to the MCS search. Accordingly, the main use of MCS algorithms in 2-D chemical structure handling has been in the context of reaction database systems; here, an MCS algorithm provides an effective means of identifying automatically those parts of the reacting molecules that are unchanged in the course of a reaction, and hence those parts that are changed, that is, the reaction center (50, 51). The MCS algorithms have also been used in spectral database systems (52, 53).

The most widely used approach to the measurement of intermolecular structural similarity involves determining the numbers of fragments common to a pair of molecules that is being compared, and then using this common-fragment information to calculate a similarity coefficient of some sort (47). Two main types of fragment have been used for similarity searching, these being fragments that describe the interatomic path lengths, that is, the numbers of bonds separating pairs of atoms in a molecule (54, 55), and the atom- and bond-centered fragments that are used for the screening stage of substructure searches (56). Whichever fragment definition is used, the similarity measure is obtained by comparing the fragments characterizing the query molecule and each database structure to determine the fragments in common, and then sorting the compounds into order of decreasing similarity with the query. Interesting compounds from this ranking can then be used as the basis for subsequent searches (47).

We have noted that there is no effective screening mechanism that can be used prior to an MCS search. This is true if one wishes to identify the largest substructure common to a pair of molecules, but alternative approaches are possible if the user is prepared to accept similarity rankings that are based on large, but not necessarily on the largest, common substructures. Such submaximal common substructures can be identified much more rapidly than the true MCS, and Hagadone (57) has recently described a similarity searching system based on this idea, in which an initial fragment-based search is used as a precursor to a fast, but approximate, MCS algorithm. With developments in computing power, it is likely that such systems will become widely used, with a consequent move from fragment-based to MCS-based 2-D similarity searching over the next few years.

Similarity searching involves matching a single target structure against each of the structures in a database. Clustering involves taking each member of the database in turn as the target structure, and then using all of the resulting pairwise similarities as the input to a clustering method to produce groups, or clusters, of structurally related molecules. A review of clustering methods that can be used for this purpose is presented by Willett (47), and there have been several reports of the use of clustered files for the selection of compounds for biological screening programs (58).

III. REPRESENTATION AND THREE-DIMENSIONAL SUBSTRUCTURE SEARCHING

The application to databases of 3-D chemical structures of the graph-theoretical methods of representation and searching that have been used previously for databases of 2-D chemical structures requires two things: techniques for representing a database of 3-D structures as chemical graphs, which implies the availability of the requisite 3-D coordinate data, and efficient and effective techniques for searching the resulting chemical graphs.

A. Database Construction

Gund (59) noted that the graph-based techniques described in Section II for the representation and searching of 2-D molecules are also applicable to the representation and searching of 3-D molecules. In a 2-D chemical graph, the nodes and edges of a graph are used to represent the atoms and bonds, respectively, of a molecule; Gund suggested that the nodes and edges in a 3-D chemical graph could be used to represent the atoms and interatomic distances, respectively. The edge labels in a 3-D chemical graph are thus real numbers, that is, distances in Angstrom, rather than the integer bondtype labels used to denote the edges of a 2-D chemical graph. Such a 3-D chemical graph is an example of a *fully connected* graph, that is, one in which there is an edge between every pair of nodes (since there is an interatomic distance between every pair of atoms in a molecule) so that the graph representing a structure that contains N atoms will contain $O(N^2)$ edges. This is in marked contrast to a 2-D chemical graph, where an individual node will typically be linked by an edge to only a small number of other nodes and there will thus be $O(N)$ edges. The chemical graphs considered in 3-D database systems are thus far more complex than those considered in 2-D systems; even so, graphs based on atoms and interatomic distances provide a simple and effective way of describing the geometries of small 3-D molecules, as is demonstrated in the remainder of this review.

Having identified a mechanism for the representation of 3-D structures as graphs, we must now consider how to obtain the coordinate data that are necessary for the creation of such graphs. There are two main sources of coordinate data: experimental coordinates or calculated coordinates. Experimental coordinates are usually obtained by X-ray crystallography; they can either be generated in-house or be accessed from one of the available databases of crystal coordinates, of which the best known is the Cambridge Structural Database, which is produced by the Cambridge Crystallographic Data Centre and which contains data for ca. 100,000 organic and organometallic compounds (60). Molecular modeling studies may also make use of

the crystallographic data in the Protein Data Bank, which is produced by the Brookhaven National Laboratory and which contains data for ca. 800 macromolecules (61).

Calculated 3-D structures are obtained from a range of computational techniques that include quantum mechanics (62), molecular mechanics (63), distance geometry (64), and symbolic logic (65–67). The most popular such technique for the creation of in-house databases of 3-D structures is the CONCORD program (68). This is a rule-based system that rapidly and automatically generates a single, high-quality, approximate 3-D conformation from a 2-D structure representation; a typical small molecule will require only one or two seconds of CPU time on a Unix workstation. This is one to three orders of magnitude faster than molecular or quantum mechanics, which also need an initial set of 3-D coordinates. The conformation that is produced by CONCORD is a low-energy one, although it is not guaranteed to be that of lowest energy, and the program can handle a large fraction of the compounds that might be expected to be encountered in a typical in-house corporate database. An example of the use of CONCORD to produce an in-house 3-D database from the corresponding set of 2-D structures is described by a group at Lederle Laboratories (69), who used CONCORD to produce 3-D coordinates for about a quarter of a million structures in their corporate database, to which were added ca. 30,000 sets of coordinate data from the Cambridge Structural Database. Other descriptions of the use of CONCORD to generate 3-D databases are provided by Henry et al. (70), Haraki et al. (71), and Fisanick et al. (72).

The expert system approach used in CONCORD provides one way of generating 3-D structures. Alternatively, 3-D structures can be rapidly built from 2-D connection tables by searching a database of 3-D structures for overlapping fragments that can be pieced together: this idea is the basis of the structure builders reported by Wipke and Hahn (67) and by Davies and Upton (73). More recently, Gasteiger et al. (74) have described an approach to the generation of 3-D coordinates that is based on the primary configurations that determine bond angles, for example, trigonal and tetrahedral geometries, and on the linking together of these primary units to yield acceptable bond lengths and torsion angles. Appropriate modifications are made for the deviations in standard bond lengths, bond angles and torsion angles that result from steric repulsion or ring formation. Particular attention is paid to rings, with the result that the program, which is called CORINA, can generate acceptable structures not just for simple cycles, but also for macrocyclic, polycyclic and macropolycyclic molecules, and for systems that contain small rings within larger rings. For flexible molecules, only a single, low-energy conformation is generated, but the basic approach can be extended to permit the generation of multiple conformations.

The contents of 3-D automatically generated databases have received little attention to date, a situation that is in marked contrast to the numerous studies that have been carried out on the Cambridge Structural Database. This is, however, beginning to change with the announcement by Chemical Abstracts Service (CAS) of CAST-3D, which contains ca. 370,000 CONCORD structures that have been identified as exhibiting limited conformational flexibility (72). Also, P. A. Bartlett et al. (unpublished) have systematically generated all the low energy conformations of all tricycles built from 4-, 5-, 6-, and 7-membered carbocycles, with the structures optimized using MMP2; this exhaustive database of conformations can then be searched for molecular templates using the CAVEAT program (75) that is discussed in Section III.B.

The availability of a graph-theoretical description of a 3-D molecule means that it is possible to carry out substructure searches using screening and subgraph-isomorphism techniques that are analogous to those presented in Section II. In the remainder of this section, we describe the implementation of these two techniques when they are used to access a database of 3-D molecules. Such a search is normally carried out to identify those molecules that contain a query *pharmacophoric pattern,* or *pharmacophore,* that is, the geometric arrangement of structural features that is necessary for biological activity, or to identify templates on which to build such molecules.

B. Screen Searching

Screens for 2-D substructure searching consist of patterns of connected or, less commonly, unconnected atoms and bonds. There are two obvious types of substructural feature that present themselves as screens for 3-D substructure searching, these being the distances and angles between atoms (or, more generally, points as discussed further below). The continuous natures of these two types of feature are very different from the simple, integer-valued fragment occurrence data that characterizes 2-D substructure searching system: this implies that screens for 3-D substructure searching must involve ranges of values, and there have been several reports of algorithmic procedures for the selection of screens for 3-D substructure searching. Distance screens are the most common and consist of a pair of (typically nonhydrogen) atoms together with an interatomic distance range. For example, a screen might be of the form C F 2.69–4.12, denoting the presence in a molecule or a query pharmacophore of a carbon atom and a fluorine atom separated by a distance, d, in Angstrom such that $2.69 \leqslant d \leqslant 4.12$. The elemental types may be augmented by additional information, such as the connectivities of atoms (76) or the numbers of π electrons (77).

The use of such screens requires the availability of methods for the selection of those pairs of atoms and those distance ranges that will maximize the

screenout for typical pharmacophoric patterns. The first screen set generation algorithm was described by Jakes and Willett (76), as part of their work on the SOLON system for 3-D substructure searching at Pfizer Central Research (U.K.) (78). The algorithm involved two main stages. In the first stage, a detailed analysis was made of the frequencies of occurrence of pairs of nonhydrogen atoms in the file that was to be searched (which was a subset of the Cambridge Structural Database). This analysis revealed a highly skewed distribution of atom-pair frequencies, with a few types of atom pairs occurring very frequently, but with the great bulk of the atom pairs occurring very infrequently; similar distributions are observed when fragments are selected for 2-D substructure searching (36, 37). The frequency data led to the identification of those atom pairs that occurred sufficiently frequently for them to be useful for screening. The second stage then involved a two-part analysis of the interatomic distances for the selected atom pairs, the distance ranges being chosen so that each screen occurred approximately the same number of times in the dataset that was being processed.

The algorithm of Jakes and Willett (76) was complex in operation and required the specification of several parameter values before a screen set could be generated that demonstrated the requisite equifrequency characteristics. It was, however, highly effective in that it produced screen sets that exhibited a high level of screenout in searches for pharmacophoric patterns from the literature (78). An alternative frequency-based selection algorithm was described later by Cringean et al. (79). This algorithm is markedly simpler in concept and gives the user a much greater degree of control over the size of the screen set that is produced, while still achieving high levels of screenout in pharmacophore pattern searches. The algorithm takes as input an alphanumerically sorted list of descriptor occurrences, for example, atom pairs and the associated interatomic distance, and can thus be applied to any type of descriptor that is to be used for indexing purposes, subject to the sole constraint that it is possible to create a sorted list; for example, Poirrette et al. (80) have reported its use for the selection of valence angle screens. The algorithm progressively subdivides the sorted list into a set of partitions such that each partition contains approximately the same number of fragment occurrences; each of the resulting partitions then defines a range of fragments that is characterized by the same screen (79).

The procedures described thus far have been developed to produce some small number of screens that can be encoded in a fixed-length bit string. An alternative, and simpler, selection procedure has been described by a group at Lederle Laboratories (77, 81). Their 3DSEARCH system uses an open-ended screen definition algorithm that results in the generation of over 13,000 distinct screens, as against just 1471 in the fixed-size screen sets used in the SOLON system. The screens again consist of pairs of atoms together with

an associated distance range, but the atom descriptors are defined in terms of no less than five characteristics: elemental type, connectivity, number of π electrons; calculated number of attached hydrogen atoms, and formal charge. The distance range screens are derived using a hashing-like scheme in which the bit that is to be set to represent some particular interatomic distance, d, is calculated from the expression $X \times \arctan[(d - 3.0)/2] + Y$, where X and Y are constants. This simple expression was found to provide a rough level of equifrequency without the need for the more sophisticated frequency-based procedures that are required to achieve nearequifrequency if small numbers of screens are to be used, as in SOLON. The distance ranges in 3DSEARCH are very narrow, and this, taken with the highly specific atomic types that are used, means that the screens are highly discriminating and provide a very high level of screenout in pharmacophore pattern searches (77). The same algorithm is used in the ChemDBS-3D system produced by Chemical Design Limited (73, 82).

The screen set selection procedures that are used in the MACCS-3D system involve both manual and automatic processing (83). MACCS-3D permits the specification of a range of geometrical objects in queries, including points (which can be either atoms or ring centroids), lines and planes (which are defined in terms of either two or three points, respectively), and normals (to planes or lines). Of these, 30 point types have been selected for inclusion in the screen set (with the other types of feature being searchable only in the final geometric search). A total of 32 ranges has been specified for interpoint distances (the lowest and highest ranges being 2.2–2.5 Å, and $\geqslant 30.0$ Å, respectively), and angles are quantized in ranges of 180/32, that is, 5.6° (with an angle being defined by sets of three points). There are ca. 2^{15} possible fragments that could be generated given these screen definitions, and ca. 20,000 of these have been manually selected for inclusion in the screen set; however, the screen set is much smaller than that used in 3DSEARCH since superimposed coding techniques are used to represent this set of screens by a bit string containing only some 2000 bits.

Two novel approaches to screening are described by Fisanick et al. (84) in exploratory work at Chemical Abstracts Service (CAS) on searching 3-D and related property data for CAS Registry substances, and by Bartlett et al. (75) in the CAVEAT program, which has been designed for the specific purpose of identifying ring systems that can fix functional groups in the correct relative positions for enzyme inhibitory activity.

The work at CAS has used conventional interatomic distance and valence and torsion angle screens, as well as the partially bonded angular screens described by Bartlett et al. (75) (*vide infra*), and a novel class of distance screens, which are based on information that can be calculated from triangles, that is, sets of three nonhydrogen atoms and the three corresponding inter-

atomic distances, in 3-D molecules. Specifically, Fisanick et al. (84) have used equifrequent sets of screens that define the areas, heights, perimeters, and inscribed circle radii of such triangles of atoms. The initial work (84) is concerned with 3-D similarity searching, as discussed further in Section V.E, but such screens are also clearly applicable to 3-D substructure searching.

The CAVEAT program uses a processed form of the Cambridge Structural Database (or of the exhaustive database of conformations mentioned in Section III.A) in which each molecule is characterized by the angular relationships between *substituent bonds*, where a substituent bond is a bond between an atom in a ring system (referred to as the *base atom*) and an atom that is not part of the same ring system (referred to as the *tip atom*). Note that this definition includes bonds to hydrogen atoms, which are often excluded in 2-D and 3-D substructure searching systems. Each substituent bond is considered as a vector of unit length and with an orientation defined by the base and tip atoms. A *vector pair* consists of two pairs of base and tip atoms (B_1, T_1) and (B_2, T_2), and is defined uniquely by four parameters: d, δ, α_1, and α_2. The distance d is the length of the line segment connecting B_1 and B_2; the dihedral angle, δ, is the absolute value of the two dihedral angles between the planes by the sets of atoms B_1–B_2–T_2 and B_2–B_1–T_1; the angle α_1 is the angle between the lines B_1–T_1 and B_1–B_2; and the angle α_2 is the corresponding angle between the lines B_2–T_2 and B_2–B_1 ($\alpha_1 \leqslant \alpha_2$). A detailed analysis of the statistical characteristics of such angle-based screens is presented by Poirrette et al. (80, 85).

Each of the molecules in a database is analyzed to identify their constituent vector pairs. The search file consists of the parameter values for each of these pairs, arranged as screens in which the distance and angular ranges are subdivided into 32 intervals. A search requires a user to specify the parameter values for a vector pair, together with any tolerances, and these are used to access the appropriate interval ranges in the search file. Bartlett et al. (75) give several examples of the use of CAVEAT to design peptide structural mimics, and Fisanick et al. (72) have reported initial experiments using vector-based searching of the CAST-3D file mentioned in Section III.A. More recent versions of CAVEAT allow searches for ring fragments, for example, for the purpose of linking a peptide into a macrocyclic structure, as well as the comparison of proteins to identify structural similarities that depend on side-chain orientations.

The screens that are used for 3-D substructure searching thus consist of two, three, or four points and an associated distance range or angular range. A database structure or query substructure is encoded when it is added to the database by generating each fragment (e.g., a pair of points and the interatomic distance) in turn, and then searching the screen set to identify a set of matching points and a range that includes the distance or angular

value in the fragment. Once the screen has been identified, the appropriate location is set in the bit string that is used for the screen search, which is implemented in much the same way as a 2-D substructure search with the bit string representing the query substructure being compared with the bit strings representing each of the database molecules; it should be noted that the keying of a database is a time-consuming process that can often use more computer time than the initial generation of the coordinates. An analogous screen assignment procedure is used to characterize query pharmacophores. The detailed subgraph isomorphism search, which is normally referred to as a *geometric search* to differentiate it from conventional, 2-D atom-by-atom searching, is then invoked only for those database structures that match the query at the screen level.

We have noted in Section II.C that atom-by-atom searching is needed in 2-D substructure searching since a molecule possessing all of the query screens might still not match the query because the substructural features corresponding to these screens were connected in a different way from the pattern of linkages in the query. There is a similar problem in 3-D searching since the screens describe only the fact the the query screens are present, without taking account of the relative geometric orientations of the sets of points in 3-D space. In fact, there is a further problem with 3-D screens in that they refer to ranges and not to precise values; a structure may thus well be assigned a query screen even though it does not contain the precise value (or range of values) for some distance or angle that has been specified in the query pharmacophore. The initial stage of a geometric search thus involves checking that the actual query values (to within any allowed tolerances) are present in the database structure that is under consideration. A molecule that passes this check then undergoes the final stage of a geometric search to determine whether or not the query pharmacophore is present; if a match is obtained, then the matching atoms (or sets of atoms if multiple isomorphisms are present) are noted, for example, for subsequent input to a structure display or modeling program.

C. Geometric Searching

The time-consuming character of geometric searching requires that the most efficient algorithms be used for the implementation of a 3-D substructure searching system. The early Pfizer work (78) used a modification of the well-known *set reduction* algorithm that had originally been described by Sussenguth for 2-D substructure searching (42). However, later comparative studies of the efficiencies of a range of subgraph isomorphism algorithms when they are used for geometric searching (86) demonstrated the general utility of the algorithm due to Ullmann (87); the general effectiveness of this

algorithm has been demonstrated by subsequent studies of substructure searching in 2-D molecules (88) and in 3-D macromolecules (89,90), and it is now used in both 3DSEARCH (77) and ChemDBS-3D (82).

The Ullmann algorithm operates by means of a backtracking tree search in which database atoms are tentatively assigned to query atoms and the match extended in a depth-first manner until a complete match is obtained or until a mismatch is detected; in this case the search then backtracks to the previous assignment. Ullmann noted that drastic increases in efficiency could be obtained by the use of a *refinement procedure*, which limits the number of levels of the search tree that have to be investigated before a mismatch is identified. Specifically, the algorithm makes use of the fact that, if some pharmacophore atom $P(X)$ has another atom $P(W)$ at some specific distance, and if some structure atom $S(Z)$ matches with $P(W)$, then there must also be some atom $S(Y)$ at the appropriate distance from $S(Z)$ that matches with $P(X)$: this is a necessary, but not sufficient, condition for a subgraph isomorphism to be present (except in the limiting case of all of the pattern atoms having been matched, when the condition is both necessary and sufficient). The refinement procedure is called before each possible assignment of a database atom to a query atom; and the matched substructure is increased by one atom only if the condition holds for all atoms W, X, Y, and Z. The refinement procedure seems to be particularly well suited to the processing of 3-D chemical structures since the graphs considered here are fully connected, with each atom being related to all of the other atoms by the interatomic distance. There is thus a large amount of information available to the refinement procedure and mismatches are detected very rapidly.

This brief description should serve to demonstrate that 3-D substructure searching is very similar in concept to 2-D substructure searching, and this has meant that it has been possible for systems to be developed very rapidly over the last few years. Systems have been developed in-house by fine-chemicals companies (77, 78, 91), by commercial software vendors (82, 83, 92, 93), and by academic research groups (60, 75): a review of the systems that were available as of mid-1992 is presented by Willett (94) and it is likely that other systems will be introduced over the next few years. The availability of such software has provided molecular modelers with new tools for the identification of novel active compounds. The results of combining modeling and database searching are discussed further in the next section.

IV. INTEGRATION OF THREE-DIMENSIONAL SUBSTRUCTURE SEARCHING AND MOLECULAR MODELING

The effectiveness of any 3-D searching program will be maximized if it is closely integrated with a molecular modeling and graphics program. There

are at least three reasons why 3-D searching and molecular modeling are complementary and why one might thus wish to integrate them. First, a 3-D search question is usually based on 3-D information that has been obtained from modeling or from experiment. It might be necessary to do extensive modeling before the search can be initiated; for example, the available conformations of several bioactive compounds might be compared to suggest the 3-D requirements for that activity, or an experimental protein–ligand complex might form the basis of a search. Second, if such a pharmacophore was used to search databases, molecular graphics comparison of each hit with the known actives might show that some of the hits contain unique features that could destroy bioactivity, for example, groups might protrude into regions in space different from those in the active compounds. If a search was based on the hydrogen-bonding geometry in a protein–ligand complex, molecular graphics might show that some of the compounds would not even fit into the binding site, or that electrostatic repulsion would disfavor the proposed binding mode. Such observations can help set priorities for testing such compounds and can suggest other analogs for synthesis that have a better chance for success. Third, molecular graphics studies can perform a useful validation function since they can often find errors in programs or search questions that are not obvious from tables of numbers or text. Access to energy calculations, conformational searching, and geometry optimization facilitates such error or concept checking.

An early example of a drug discovery application is described by Milne et al. (95). Protein kinase C is an enzyme that controls message transduction for many biologically active molecules. The natural product phorbol utilizes the active site in this enzyme and is known to be a powerful tumor promoter. Studies of the geometry of two inhibitors of this tumor-promoting activity suggested that the binding involves a carbon–carbon double bond at an appropriate distance from an oxygen atom; thus, searches for molecules containing this pharmacophore might be expected to identify further inhibitors of protein kinase C. Searches were carried out using the SOLON and 3DSEARCH systems that have been discussed previously in Section III.B. The query pattern consisted of three atoms C_1, C_2, and O with interatomic distances C_1–C_2, C_1–O and C_2–O of 1.33–1.37, 3.29–3.52, and 3.46–3.55 Å, respectively; searches for this pattern using the two systems resulted in the retrieval of some two dozen matching structures. One of the best fits to the query pharmacophore was the molecule neplanocin A, which was subsequently shown to exhibit antitumor activity.

The CAVEAT program (75) discussed in Section III.B has also found utility in compound design efforts. CAVEAT searches databases of 3-D cyclic structures for specified spatial arrangements of vector pairs, and the program can thus identify structures that contain bonds that match the orientation of bonds selected in the target. These structures are intended to serve as

templates in the design process. In one study, CAVEAT was used to help design potential inhibitors of α-amylase, based on a crystal structure of an inhibitor, tendamistat, bound to the enzyme (96). The target consisted of the key bonds in three or four of the enzyme residues that were involved in inhibitor binding. A search of ca. 36,000 structures from the Cambridge Structural Database identified several interesting compounds from which novel synthetic targets could be envisioned.

The next two examples in this section use the ALADDIN system, which has been developed at Abbott Laboratories (91,97). ALADDIN is based on an existing substructure query language, called GENIE, from Daylight Chemical Information Systems, that allows a user to carry out highly specific 2-D substructure searches. GENIE uses the SMILES linear notation (98) and an extension of SMILES, called SMARTS, for the specification of user-defined query patterns, for example, a phenolic oxygen connected to a six-membered aromatic carbocyclic ring with an acyclic saturated carbon attached to the para nitrogen atom. The user who wishes to carry out a search for a pharmacophoric pattern will first specify any topological structural characteristics by means of GENIE and then specify the topographic characteristics in terms of the bond angles, torsion angles, or distances between points, planes, or lines (in a manner that is analogous to the query definition facilities described for MACCS-3D). In contrast to MACCS-3D, ALADDIN can use any point, line, or plane that a user can describe, for example, the center of mass of an entire molecule is sometimes of interest. The GENIE search is carried out first and the geometric features are then searched for in each of the hits resulting from the initial search. The very wide range of query characteristics that can be specified makes it impracticable to carry out any sort of geometric screening and thus ALADDIN searches can be extremely time consuming, running for many CPU hours in some cases. However, this limitation is compensated for by the integration that has been achieved with molecular mechanics, quantum mechanics, and molecular graphics software as discussed above, and by the flexibility available in the search query.

An early ALADDIN investigation using 3-D searching and pharmacophore mapping (as discussed in Section VI.C) identified a potent D1 dopaminergic agonist, and traditional medicinal chemistry structural modifications based on this lead resulted in the most potent and selective D1 agonist known (99). We now present two more recent studies that exemplify the complementary natures of 3-D searching and molecular modeling.

The first study relates to the identification and design of novel herbicides and plant growth regulators that act by inhibiting polar transport of the plant hormone auxin (100). Previous studies (101) had identified seven auxin transport inhibitors, from which it was possible to describe a three-component

pharmacophore containing (1) an acidic functionality, for example, carboxylic acid or acid hydroxyl; (2) a tertiary, quarternary, or aromatic center; and (3) an aromatic system. The occurrences of each of these three components were identified in the seven selected compounds and their 3-D structures generated using Abbott Laboratories' molecular modeling package. The resulting structures were next overlaid to identify the maximum overlap of the chosen sets of pharmacophore points, so as to determine the geometric relationships between the points that were necessary for activity.

The pharmacophoric pattern that resulted from the modeling study was then used by ALADDIN to search the Abbott corporate database, which contains ca. 70,000 3-D structures that have been produced using the CONCORD program. In fact, three different searches were carried out, these differing in the precision with which the three components of the pharmacophore were characterized and in the distance tolerances that were allowed for a match to be detected with a structure in the database. For example, in the first search, the three points detailed above were defined to be (1) a carboxylic acid or hydroxyl group attached to an aromatic system; (2) a tertiary carbon center (but excluding an aromatic center); and (3) an aromatic atom. The distances between points 1 and 2, 2 and 3, and 1 and 3 were set to 2.7–3.7, 4.9–5.9, and 4.6–6.8 Å, respectively, these ranges coming from the minimum and maximum separations in the seven selected compounds with an additional tolerance of 0.2 Å. In all, the three searches identified 467 compounds; 77 of these underwent biological testing, of which 19 showed a moderate to good level of activity. These compounds were then used to develop a more refined pharmacophore than was available at the start of the search; some of them were also used to carry out searches of the Fine Chemicals Directory, which resulted in the identification of further active molecules. The study showed that several different classes of compounds, in addition to the traditional benzoic acid derivatives, can act as auxin transport inhibitors.

The second study (102) relates to the identification of novel, nonpeptidic inhibitors of human immunodeficiency virus 1 (HIV-1) protease, which is an important area of current research in the development of new agents for the treatment of the acquired immunodeficiency virus (AIDS). The query pharmacophore here was derived from an X-ray crystallographic study of the complex formed between the protease and a known inhibitor, and consisted of five points (a central hydroxyl group, two symmetrically opposed, hydrogen bond donating functionalities, a hydrogen bond accepting moiety, and a hydrophobic group) and five interpoint distances. Searches of the Abbott corporate database for this pattern retrieved some 600 structures; about 30 of these were chosen on grounds of sample availability, structural diversity, and comparison with the available crystallographic data for the active site of HIV-1 protease.

Subsequent testing revealed three hydroxy-substituted benzophenones that exhibited moderate levels of inhibition against HIV-1 protease and that could be used as leads for the design and synthesis of more potent inhibitors.

Research in the design of nonpeptidic inhibitors of HIV-1 protease has also been carried out by DesJarlais et al. (103), who used the DOCK program (104) (*vide infra*) to search for compounds that matched the shape of the active site of the enzyme. One of the compounds identified was bromperidol, an analog of the known antipsychotic haloperidol. The proposed binding orientation of bromperidol suggested that compounds of this class may have the ability to interact with the catalytic residues of the enzyme and show inhibition. Haloperidol was chosen for testing and exhibited weak levels of inhibition of HIV-1 and HIV-2 protease. Haloperidol, while not a useful therapeutic agent for AIDS, could serve as a lead for the design of useful inhibitors of HIV protease.

V. THREE-DIMENSIONAL SIMILARITY SEARCHING

A. Introduction

Similarity searching in databases of 2-D molecules has become well established since its introduction in the mid-1980s and now forms an important component of chemical information systems (47). With the introduction of 3-D substructure searching, it seems a natural development to consider approaches to 3-D similarity between searching. There are many ways in which one can determine the degree of resemblance between a pair of molecules (48). As noted in Section II, similarity searching in databases of 2-D structures generally involves fragment-based similarity measures. There is much less consensus as to what should form the basis for similarity searching in databases of 3-D structures, although most of the systems that have been described to date have considered either the steric or the electrostatic factors that are the most important determinants of biological activity (105).

There is generally a trade-off between the *effectiveness* of a similarity searching technique, that is, the extent to which the technique is able to identify structures that the chemist also perceives as resembling an input target molecule, and its *efficiency*, that is, the associated computational requirements. This trade-off means that many of the quantum mechanical and molecular modeling procedures that have been used for measuring molecular similarity are far too time consuming to be considered for use in a database searching environment, where a target molecule must be matched against many thousands of database structures. In what follows, we shall concentrate on methods that are sufficiently fast to be of potential use in the database context.

B. Methods Based on Overlapping

Steric similarities can be estimated using procedures based on the matching of atoms or of superimposed volumes. For example, Dean and co-workers have discussed the matching of pairs of atoms, one from a target structure and one from a database structure, so as to minimize the sum of the squared distance errors; both deterministic (106) and nondeterministic (107–110) algorithms have been reported, with run times of a few CPU seconds for a pair of structures. Meyer and Richards (111) measure the similarity of a pair of molecules by the extent to which their volumes overlap, and describe an efficient algorithm to obtain good, but not necessarily optimal, overlaps for pairs of structurally related molecules.

The molecular volume provides one direct, and readily calculable description of molecular shape. More sophisticated approaches to the quantification of molecular shape, and hence to the measurement of resemblance between pairs of structures, have been reported in a series of papers by Mezey and collaborators, who have developed a range of topological similarity measures; an overview of this work is presented by Mezey (112). Such approaches provide detailed insights into the similarity relationships that exist between pairs of structures, but their computational requirements are far too great for searching large databases. A much simpler approach involves characterizing molecular shape by a single number or ratio; examples of this have been described by Cano and Martinez-Ripoll (113) and by Petitjean (114), but there have not been any evaluations, to date, of their search effectiveness.

Carbo et al. (115) suggested that the similarity between a pair of molecules could be estimated by a similarity coefficient based on the overlap of the molecules' electron charge clouds. This idea has been taken up by several workers, using both electron densities and molecular electrostatic potentials (116–120). A molecule is positioned at the center of a 3-D grid and the electrostatic potential is calculated by taking the product of the potentials at each point in the grid. The similarity between a pair of molecules is then estimated by comparing the potentials at each grid point and summing over the entire grid, with a suitable normalizing factor to bring the similarities into the range -1.0 to $+1.0$. This numerical approach necessarily involves the matching of very large numbers of grid points, unless very coarse grids are to be used; Good et al. (121) have recently reported an alternative approach in which the potential distribution is approximated by a series of Gaussian functions that can be processed analytically, with a substantial increase in the speed of the similarity calculation and with only a minimal effect on its accuracy. This elegant idea removes one of the main limitations of field-based approaches to 3-D similarity searching but still requires

searching for the alignments of the two molecules that are being compared so as to ensure that analogous grid points are matched.

Field-based similarity searching in large databases will be feasible only with the identification of an appropriate alignment procedure. Exhaustive searching for alignments is completely infeasible unless extremely coarse grids are used, in which case the calculated similarities are unlikely to reflect accurately the true degree of resemblance of the molecules that are being compared. Even stochastic searching procedures can run for extended periods if one wishes to conduct a detailed examination of the alignment space. For example, Kearsley and Smith have described a method, called SEAL (Steric and Electrostatic Alignment), which uses a Monte Carlo procedure to optimize the alignment of two rigid 3-D molecules and that bases the matching on atomic partial charges and steric volumes (122). The method generates high quality alignments, but the comparison of a pair of molecules requires tens of minutes of CPU time on an IBM 3090 with a vector processing unit; an alternative alignment algorithm has been suggested recently by Kato et al. (123).

The most widely used method for processing field information is CoMFA, Comparative Molecular Field Analysis, which was pioneered by Cramer et al. (124) and which describes each (superimposed) molecule of a set on the basis of its steric and electrostatic fields at intersections of a lattice enclosing the compounds. Lin et al. (125) reduced the number of steric descriptors to 25 using principal components analysis. A complete-linkage cluster analysis based on the principal component scores successfully grouped similar molecules together. These groups could be used for initial screening by systematically selecting one compound from each cluster.

The procedures discussed above are all far too slow for database searching applications, unless coupled with an initial screening procedure that can eliminate the bulk of the database from this extremely time-consuming calculation; an example of such a two-stage approach is provided by the SPERM program of van Geerestein et al. (126), which is discussed in detail below. Future developments in computer hardware may enable similarity procedures such as these to be used for database searching; in the meanwhile, more efficient similarity algorithms are starting to be developed that use interatomic distance information. These distances provide a simple and obvious way of exploring the steric similarities between pairs of molecules: To date, four distance-based, similarity searching techniques have been reported, and all of these seem to be sufficiently fast in execution to be used on databases of nontrivial size and to provide effective measures of structural resemblance. There is also increasing interest in the use of calculated molecular properties as an alternative to the measurement of molecular similarity. These approaches are discussed further below.

C. Use of Distance Information

Pepperrell and Willett (127) have reported a detailed comparison of four different ways of calculating the similarity between pairs of interatomic distance matrices. The comparison involved structures for which both 3-D coordinate and biological activity data were available and suggested that the most effective similarity measure of those tested was the *atom-mapping* method, which is calculated in two stages. In the first stage, the geometric environment of each atom in the target molecule is compared with the corresponding environment of each atom in a database molecule to determine the similarity between each possible pair of atoms. The geometric environment of an atom is represented by the set of interatomic distances in which it is involved, and thus the calculated interatomic similarities reflect the extent to which a pair of atoms lies at the center of similar patterns of atoms and the extent to which they can be mapped onto each other (i.e., to be regarded as being geometrically equivalent). In the second stage, the similarity values associated with these atomic equivalences are used for the calculation of the overall, intermolecular similarity. Pepperrell and co-workers (128) have described a range of experiments that demonstrate the robustness and general effectiveness of this approach to the measurement of 3-D similarities.

The atom-mapping algorithm has a time complexity of order $O(N^3)$ for the matching of a pair of structures each containing N atoms (where the atoms can either include or exclude hydrogens). The run time requirements can be reduced by means of upperbound calculations that permit the elimination of many of the structures in a database from the full atom-mapping search (129); alternatively, parallel hardware can be used to enable a target structure to be matched against large numbers of database structures at the same time (130). A prototype search system has been implemented at ICI Agrochemicals, using the upperbound procedures on a file of 4500 structures. A typical search of this file for the 50 nearest neighbors of an input target structure requires about 60 s on a Unix workstation. Thus, similarity searches on a corporate database containing a quarter of a million structures would be expected to take about one hour using comparable equipment, the precise time depending on the target structure and the search parameters that are used. Pepperrell et al. (129) discuss the results of searches using this system and demonstrate the substantial differences that exist between the outputs of 2-D and 3-D similarity searches that are based on the same target molecules.

The second measure is that reported recently by Bemis and Kuntz (131). This again uses interatomic distance information, but in a rather different way in that a structure is decomposed into all possible three-atom substructures (so that a molecule containing N heavy atoms will produce $N(N-1)(N-2)/6$ such substructures). The procedure represents a molecule by a frequency

distribution, the 64 elements of which are initially set to zero. A three-atom substructure is selected, and the sum of the squared interatomic distances calculated over all of the pairs of atoms in the chosen substructure; this sum is then used to increment one of the elements of the frequency distribution. The procedure is repeated for all of the possible three-atom substructures, and the resulting frequency distribution is then used to provide a simple characterization of the shape of the chosen molecule. The similarity between a pair of molecules is obtained either by comparing numeric values that are derived from the elements of the corresponding frequency distributions or by comparing the distributions directly. The latter procedure is analogous to one of the similarity measures tested by Pepperrell and Willett (127); they found this approach to be less effective than atom mapping but considered only pairs of atoms, rather than the more discriminating three-atom substructures studied here.

Bemis and Kuntz note that an entirely comparable approach can be used to calculate measures of 2-D similarity using path lengths, rather than Euclidean distances, in the construction of the frequency distributions. They report an extended series of experiments to compare the two types of measure with each other and with a root-mean-square (RMS) fitting procedure derived from the DOCK program (104), which is used to dock ligands into macromolecular receptor sites and is described in detail later in this section. As described, the procedure is limited to the comparison of pairs of molecules that differ in size by one heavy atom, at most. However, the methodology would seem to be extendable to more disparate sets of structures and to be sufficiently fast in operation for searching large files (even if use is made of the full frequency distributions, rather than the hash codes used in Bemis and Kuntz's experiments).

The two similarity searching procedures discussed thus far in this section make no attempt to align the target molecule with each of the database structures; the elimination of this step is one of the main reasons why these programs are so fast in operation. The remaining procedures, called DOCK, CLIX, and SPERM, all consider the precise alignment of the target structure in the calculation of similarity.

The similarity searching methods of Pepperrell et al. (127–129) and of Bemis and Kuntz (131) have been developed as general-purpose tools for finding molecules that are sterically similar to a user-defined target structure. The DOCK program (104) is designed to retrieve those molecules from a database that are geometrically most complementary in shape to a protein binding site, and that might thus be putative ligands for this site. The approach assumes that the geometry of the binding site is known, typically from crystallographic or NMR analysis, so that it can be described by a set of spheres that are complementary to the grooves and ridges in the receptor's

surface and that fill the available binding site. The atoms comprising a putative ligand are represented by a similar set of spheres, and the shape similarity of the ligand to the site is then determined by the extent to which it is possible to overlap, or to dock, the two sets of spheres. The output from the program is a list of the best-matching equivalences, these being assumed to correspond with the preferred orientations of the ligand in the site; these orientations can then be checked by using crystallographic studies of the bound ligand.

The original DOCK program considered only the docking of a single ligand into a site (104), but the procedure was soon generalized to permit the searching of a whole database of 3-D structures (132). The docking is effected by matching subsets of the ligand interatomic distances with subsets of the receptor intersphere distances until the best fit has been obtained, and performing a least-squares superimposition of the resulting atom-sphere equivalences. The structures are then ranked in order of decreasing goodness of fit (103, 132–134) so that DOCK provides a means of identifying those structures in a database that are most likely to fit the receptor site on steric grounds. A detailed evaluation of the use of DOCK for this purpose has been reported recently by Stewart et al. (133), who docked 103 ligands that had been previously tested as inhibitors of α-chymotrypsin catalysis into the active site of the enzyme. A statistically significant relationship was found between the DOCK goodness of fit scores of the docked ligands and the observed inhibition strengths, with 8 of the 10 most active inhibitors appearing at the top of the DOCK ranking.

Lawrence and Davis (135) have recently reported a program, called CLIX, that performs a similar function to DOCK but that uses information from the GRID program of Goodford and co-workers (136, 137), which identifies regions of high affinity for chemical probes on the molecular surface of a bonding site. In CLIX one takes a 3-D structure from the Cambridge Structural Database and then exhaustively tests whether it is possible to superimpose a pair of the candidate's substituent chemical groups with a pair of corresponding favorable interaction sites proposed by GRID (only nonhydrogen atoms are considered). All possible combinations of ligand pairs and GRID binding site pairs are tested; if a match is obtained, then the candidate ligand is rotated about the two pairs of groups and checked for steric hindrance and coincidence of other candidate atomic groups with appropriate GRID sites. Lawrence and Davis demonstrate that the program is capable of predicting the correct binding geometry of sialic acid to a mutant influenza virus hemagglutin and also report the best-matching potential ligands resulting from a search of 29,720 3-D structures from the Cambridge Structural Database; this search took 33 CPU hours on a Silicon Graphics 4D/240 workstation.

The SPERM (Superpositioning by PERMutations) program has been developed by van Geerestein et al. (126) to provide a computationally efficient means of quantifying the degree of shape similarity between pairs of 3-D molecules (rather than the similarity between a pair of distance matrices, as in the case of the atom-mapping method). The work takes as its basis a series of studies by Dean and co-workers (138–140) that position a molecule at the center of a sphere and then characterize the molecule by a set of points on the surface of the sphere; the similarity between a pair of molecules may then be determined by a comparison of the corresponding sphere surfaces. The shape of a molecule in SPERM is described by mapping a specified property onto each of 32 points on a sphere surrounding the molecule, these points being the 12 vertices of an icosahedron and the 20 vertices of a dodecahedron oriented such that its vertices lie on the vectors from the center of the sphere through the midpoints of the icosahedral faces. In fact, not one but two properties are used to characterize a molecule, these being the distances from each hedral point to the nearest surface of the molecule and to the surface of the molecule along the vector linking that point to the center of the sphere.

A database molecule is matched with an input target molecule by orienting the sphere representing the former molecule so as to give the greatest degree of agreement between the two sets of property values, this orientation being obtained using an algorithm due to Bladon (141). The molecules in a database are ranked in decreasing order of the resulting similarities, and some number of the top-ranked molecules are then input to the similarity measure described by Hodgkin and Richards (116). This is based on the superposition of a pair of electron-density grids and is about three orders of magnitude slower than the sphere-matching procedure; it is thus typically applied to just the top 250 structures in the ranking. The orientation with the best Hodgkin–Richards score for a particular molecule is then taken to be the shape similarity for that molecule with the target structure.

Van Geerestein et al. (126) discuss the use of SPERM to search a 30,000-structure subset of the Cambridge Structural Database for molecules that are similar to the antitumor antibiotics netropsin and daunomycin, which bind to DNA. The best-matching molecules represented a wide range of structural types, included some known active compounds, and also suggested novel DNA-binding molecules. There was very little overlap either with 2-D similarity searches using fragment bit strings (as described in Section II.C) or with the outputs of DOCK searches for these two target molecules on a smaller subset of the Cambridge Structural Database. The search of the 30,000 Cambridge structures took about 24 h on a VAXstation 3100, although van Geerestein et al. (126) suggest this could be much reduced by the use of screening methods that could eliminate 80–90% of the file prior to the SPERM search with little effect on the quality of the final output.

D. Organization of Search Output

Another way to view similarity between 3-D structures is to focus on the pharmacophore atoms and the direction, or points, of their interaction with a target protein. The program FAMILY (142) assigns 3-D structures to families of compounds in which the variation in all distances between the points of interest are within a specified tolerance, usually 0.3–0.5 Å. FAMILY uses the Bron–Kerbosh clique detection algorithm (143, 144) to find these common 3-D substructures, and is rapid in execution since a typical test found that 384 compounds could be matched over seven points in under a minute on a VAX 9000. The points that are considered in the analysis are selected in an initial run of ALADDIN, and are typically the pharmacophore atoms and all heavy atoms that are attached to them. In a classification of dopaminergics, the atoms attached to these attached atoms were also used to increase the number of families found. In this example of compounds that met the pharmacophore requirements, it was shown that the set of computer-designed compounds (97) sorted itself into 36 families whereas compounds in a definitive review (145) sorted themselves into 15 families.

FAMILY provides a substructural measure of similarity that is useful for organizing hits from a 3-D search into subsets of more similar 3-D core. Such organization is helpful if the 3-D search identifies more existing compounds than can be easily assayed; in such a case one could select representatives from each family. If the 3-D search is used to suggest molecules for synthesis, the classification identifies redundant suggestions, that is, molecules that differ only in substituents remote from the pharmacophore atoms. The strategy in FAMILY is also useful for classifying multiple conformations of the same, or different, molecules as part of a molecular modeling investigation. Finally, its extension to automated pharmacophore mapping will be discussed in Section VI.C.

E. Use of Property Information

The descriptions of the similarity methods thus far have focused on the use of distance information; however, several of them can also be used to allow property-based similarity searching.

In atom mapping, pairs of atoms can be mapped to each other if they have comparable atomic properties (rather than the same elemental type, as in the basic form of the method). Specifically, an atom is described in terms of one or more of its hydrogen-bonding characteristics, its partial charge and its van der Waals radius, with each atom in a molecule being assigned an integer class number signifying the particular value(s) of the chosen characteristic(s) that is (are) associated with that atom. An analogous use of

atomic property values for characterizing atoms in 3-D substructure searching has been described by Guner et al. (146). It is also possible to specify weights so that the user can designate certain atoms as being of greater importance than others; for example, a greater degree of importance might be assigned to those atoms that can form hydrogen bonds than to those that cannot. If very high weights are assigned to some atoms, it is possible to obtain an output in which the top-ranked structures will contain all (or most) of the highly weighted atoms, so that one can execute a form of ranked 3-D substructure search. In the case of SPERM, the matching algorithm that lies at the heart of the program can be used with any property for which values can be calculated at the 32 vertices, for example, electrostatic or hydrophobic factors; indeed, searching using electrostatic potential is a standard option of the program that can be used instead of the distance criteria described in the previous section. The most recent version of DOCK augments the steric matching scores with electrostatic and molecular mechanics interaction energies for the ligand–receptor complex (147). The inclusion of the additional information provides more accurate dockings, but this is at the expense of considerably enlarged run times, which might be too great to allow rapid searching of a large database.

An alternative use of property-based searching has been reported recently by Fisanick et al. (72), who describe experiments using a set of 6000 3-D CONCORD structures for which molecular property data are available. Each structure is represented by a total of 29 computed properties; these including molar refractivity, logarithm of the partition coefficient, HOMO, LUMO, van der Waals surface area, dipole moment, heat of formation, and the mean atom charge, *inter alia*. The standard deviation across the whole database is calculated for each such property. The overall similarity between the target structure and a database structure is incremented by 1, 2, 3, or 4 if the property value for the target structure is within 1.0, 0.75, 0.5, or 0.25 standard deviations, respectively, of the corresponding value for the database structure; this simple matching procedure is repeated for some or all of the properties. Initial experiments suggest that the most similar structures resulting from a database search do, indeed, closely resemble the target molecule.

F. Conclusions

It will be clear that there is currently much interest in the development of measures of 3-D similarity, and this is expected to grow as users become fully conversant with the capabilities of 3-D substructure searching systems.

It is interesting to note that many of the most similar structures resulting from the property-based search described by Fisanick et al. (72) are very

different from those that are retrieved in a comparable, structure-based 2-D similarity search. Comparisons of 2-D and structure-based 3-D similarity searches have been described by Pepperrell et al. (127, 129), Bemis and Kuntz (131), and van Geerestein et al. (126), and all of them conclude that the outputs of the two types of search can be very different; it is likely that 2-D and 3-D clustering would also give very different sets of structurally related compounds. An integrated similarity searching system that uses the matching of both 2-D fragments and interatomic distances has been described by Mitchell et al. (148).

One obvious difference between 2-D and 3-D measures of molecular similarity is that the former are *global* in character, in that they return a number that describes the overall degree of similarity between a pair of objects. This number is a simple function of the number of fragments in common and provides no information as to which particular parts of the molecules that are being compared are responsible for the observed degree of similarity. Global measures are less appropriate in the context of 3-D similarity searching, since biological activity at a receptor site is determined by the presence of a particular set of atoms in a particular geometrical arrangement, that is, the pharmacophore. The DOCK method is global in nature since it provides a single, real-valued number that measures the overall degree of complementarity between the target and each of the database structures; however, it is inherently *local* in character since its primary purpose is to identify the local structural arrangements that are necessary for binding. Atom mapping is also global in character since it provides a real-number-based ranking of a dataset. However, it can also be regarded as a local similarity measure since the atom match matrix provides information about the structural equivalences that apply to individual pairs of atoms, and about the contribution of each of these pairs to the overall, global similarity. The first-stage, sphere-based component of SPERM is also global in character, but the subsequent grid calculation provides detailed information as to the most similar geometric regions of the two molecules that are being compared, and it also can thus be regarded as a local similarity measure.

VI. CURRENT RESEARCH AREAS

It will be clear from what has been said in this review that 3-D searching systems have developed with great rapidity since their introduction in the late 1980s and that they already provide a range of facilities that would have appeared quite remarkable only a few years ago. That said, there are still many areas where considerable research and development is needed if computational chemists are to be provided with appropriate tools to assist

them in the search for novel, biologically active molecules. In this section, we focus on three of these areas.

A. Representation and Searching of Flexible Molecules

A major limitation of the 3-D substructure searching systems that have been described thus far in this review is that they often take little account of conformational flexibility, storing only a single low-energy conformation for each molecule in a database (this typically being a CONCORD or X-ray crystal structure). However, biological molecules can exist in a variety of different conformations and can shift among these conformations, depending on energetic and environmental conditions. This fact has considerable implications for 3-D searching systems since, in general, there is no simple relationship between a single conformation of a molecule and the receptor-bound conformation sought when one searches for a pharmacophore (149). For example, acetylcholine bound to the nicotinic receptor is known to adopt a conformation that is distinctly different from that which it adopts in solution or in the crystal state (150). Accordingly, a search for molecules that can bind to the nicotinic receptor would be likely to miss acetylcholine unless some means can be found of both representing and searching this conformationally flexible molecule. In what follows, we shall refer to 3-D search systems that operate upon single conformations as *rigid searching systems* and those that encompass multiple conformations as *flexible searching systems.*

An obvious way to achieve flexible searching is to store not just a single structure for a flexible molecule but a whole set of representative low-energy conformations. The main problems with such an approach are, first, the large amount of storage that is required if many conformations are to be considered and, second, the impossibility of ensuring that the selected sample contains all of the important, biologically active conformations. Given the infeasibility of this approach, there has been some interest in developing techniques that permit the incorporation of flexibility information in the query. Flexible query search routines are now an established part of the MACCS-3D system; they involve a stepwise search procedure that results in an optimized query that will retrieve a high percentage of structures with the desired biological activity (151). An initial pharmacophoric pattern is obtained by taking a representative active molecule and then removing all parts of it that are not involved in the pharmacophore. The remaining features are categorized as rigid or flexible, and the positions of the flexible features are defined in terms of their distances from the rigid features. The resulting pattern is then used for a series of searches of a known database, in which the numbers of rigid points and the precise rigid-to-flexible distance ranges are varied so as to identify that query that gives the greatest ratio of known actives to known

inactives. Guner et al. (151) have suggested the use of the MDDR-3D database, which is based on the Prous journal *Drug Data Report*, but any file that contains both structural and activity data could be used. The optimized query that results from the set of searches is then used to search a database of rigid molecules of unknown activities, with those containing the optimized pharmacophore having a high *a priori* probability of exhibiting activity in the test system under investigation.

A second and more sophisticated strategy has been adopted in the ChemDBS-3D system (73,82). Here, a set of representative low-energy conformations for each structure is generated using a rapid, rule-based conformational expansion routine, and screens are assigned to each conformation in the normal way. The bit strings for the set of conformers are then merged using a Boolean OR operation to give a single bit string for each structure to be matched against the query in the screen search. Thus, while a flexible molecule is described by a single bit string, as with any molecule in a rigid searching system, this string summarizes not one but many low-energy conformations. The structures that match at the screen level are then subjected to a second conformational analysis, and a geometric search is carried out on each of the resulting conformations to determine which of them match the query. While this method obviates the need for storing a number of discrete conformations, there is still a reliance on the selection of some set of representative, low-energy conformations for the creation of the original bit strings. Even so, Haraki et al. have demonstrated that this approach can result in the retrieval of substantially larger numbers of active compounds than when only rigid structures are used in a pharmacophoric pattern search (71). Specifically, these workers carried out a series of searches on versions of the Derwent *Standard Drug File* that had been created using the single conformations produced by CONCORD and the multiple conformations produced by ChemDBS-3D. It is, however, worth noting that while the total number of retrieved active compounds was greater in the flexible searches, the number of retrieved inactive compounds was still larger (71). The rigid searches were thus more precise than the flexible searches, and a rigid search would hence seem to be the method of choice, in the first instance at least; only if this fails to retrieve sufficient material should a flexible search be carried out.

The ChemDBS-3D system provides a cost effective means of including flexibility information in a database, but it is still restricted to the set of conformations that is chosen for the generation of the fragment bit strings (and this set may not include the biologically important conformations that are necessary for binding to a receptor). This problem may be overcome if, and only if, techniques are available that can represent and can search the complete conformational space that is available to a flexible molecule. In a rigid 3-D molecule, the distance between each and every pair of atoms is a

single, fixed value, for example, 3.62 Å. This is not so in a flexible molecule, where the distance between a pair of atoms will depend on the particular conformation that is adopted. The separation of a pair of atoms is hence conveniently described by a *distance range*, the lower and upper bounds of which correspond to the minimum and maximum possible distances (though for some pairs of atoms, e.g., those within an aromatic ring system, these two distances will be the same whatever conformation is adopted by the molecule). The set of distance ranges for a molecule will contain all of the geometrically feasible conformations that molecule can adopt, and thus provides an obvious way of representing a flexible molecule. Martin et al. (18) noted that such sets of distance ranges could be generated using techniques derived from distance geometry (64, 152, 153), and this idea has formed the basis for an ongoing study in Sheffield (154, 155) that has further developed the graph-theoretical searching methods described in Sections II and III.

The distance ranges are generated using the *bounds smoothing* technique that forms an important component of the distance geometry approach to structure generation. Bounds smoothing starts with an initial interatomic distance matrix, which contains one upper and one lower bound for each interatomic distance. Some of these distance bounds can be set using considerations of molecular connectivity, together with lists of standard bond lengths and bond angles; the remainder are set to predetermined default values, typically the sum of the van der Waals radii and some arbitrarily large value for the lower and upper bounds, respectively. The initial bounds are then subjected to repeated application of the triangle inequality (64) to yield the final set of smoothed distances, which contain all of the geometrically feasible conformations for a molecule. It is possible to use higher-order inequalities, for example, the tetrangle and pentangle inequalities, in bounds smoothing, but these are very difficult to calculate and the resulting bounds are little better than those obtained using the much simpler triangle smoothing procedure (156).

The screening and geometric searching algorithms that are used for rigid 3-D searching operate on distance matrices where each element contains a single value; these algorithms require only minor modifications to enable them to process bounded distance matrices in which each element contains both a lower and an upper bound, thus allowing the retrieval of all molecules that could possibly adopt a conformation that contains a query pharmacophoric pattern (155). Indeed, it is possible to view the rigid searching algorithms described in Section III merely as a limiting case of the more general algorithms that are required for flexible searching. There is, however, one major difference between flexible 3-D and both 2-D and rigid 3-D substructure searching, in that those molecules that match the query in the

geometric search must then undergo a further, and final, check that uses some form of conformational searching procedure (157, 158); this is required since bounds smoothing is known to overestimate the true range of possible interatomic distances (because it takes no account of correlation effects) and since it gives no information regarding the energies of the possible conformations. The initial experiments in Sheffield have used the distance geometry technique known as embedding for this final search. Clark et al. (155) have demonstrated the effectiveness of this three-part retrieval algorithm (screening search, geometric search, and conformational search) and have shown that it can retrieve many more matching structures than can comparable rigid searches. However, these authors noted that flexible searching is extremely demanding of computational resources, being some two orders of magnitude slower than conventional 3-D substructure searching, and have suggested that flexible searching is unlikely to become routinely available without very substantial improvements in both software and hardware.

Conformational flexibility was added to the DOCK approach by Smellie et al. (159). Instead of using spheres to span the macromolecular binding site, they docked the hydrogen bond donor and acceptor atoms of ligands onto hydrogen bond donor and acceptor atoms in the protein. As with DOCK, the protein itself fixes the distances between these points in the protein. For the ligand, the distances between the points of interest were input not as single values but rather as the allowed range of distances, in all conformations, between the particular points. These could be derived by the simple distance-bounds calculations described above. If the distances between ligand atoms fall within hydrogen-bonding distance of the complementary distances in the protein, then there is a tentative match between the ligand and the protein site. Smellie et al. used distance geometry embedding to test if the proposed match could correspond to a real 3-D structure. They included, but kept rigid, all protein atoms within six atoms of the ligand, and found that only 20% of the matches that fell within the original distance bounds were consistent with a 3-D structure. This strategy is relatively fast since the distance-bounds calculation and matching algorithm take approximately one second on a low-end workstation, thus allowing a 60,000-compound database to be searched in about 20 h (and precalculation and screening approaches could be used to further reduce this timing requirement); however, the final, 3-D embedding stage is far slower.

Blaney (160) also used distance geometry for docking a flexible ligand into a rigid binding site. The docking points of the ligand–protein complex were found by the usual algorithm; then distance geometry embedding was used to generate several to many different conformations of the ligand with these points docked. For the distance matrices, the maximum distance between site points was used for the distance upper bounds. However, the allowed

distances between each pair of docked points was established by the distances between the corresponding spanning spheres. The method was tested by docking methotrexate to dihydrofolate reductase. Between 10 and 100 random fits were needed to find one that approximated the experimental binding conformation. One hundred fits of a ligand take about 3 min on a high-end workstation; however, this strategy again needs a final embedding and this is very slow with current algorithms.

B. *De Novo* Structure Generation

The techniques utilized in 3-D database searching are now being extended to the development of a methodology for the *de novo* generation of 3-D chemical structures. In this context, *de novo* structure design refers to the generation of molecules to fit a variety of spatial and chemical constraints using basic structural building blocks.

One approach to this problem follows naturally from 3-D database searching and involves the use of searching to find templates that can be converted into molecules that match the design criteria. Martin and co-workers used ALADDIN (91) to identify compounds that contain the appropriate geometric relationship between important functionality, but the atoms matched are more general precursors to the required atoms; these atoms are converted into the desired atoms using a program called MODSMI. This technique was used to develop a wide range of new classes of D2 agonists (97). Searching 3-D databases for templates used in structure generation has also been employed in a program called GROW (161), and Lewis et al. have used DOCK (104) to generate fragments for their approach to structure design, (*vide infra*).

Chau and Dean (162–164) have taken advantage of the wealth of information found in the Cambridge Structural Database (60) to generate a set of basic fragments for structure design. They began by constructing a large set of cyclic and acyclic aliphatic and aromatic fragments, consisting of H, C, N, O, P, S, F, or Cl atoms. The set was pruned by considering their frequency of occurrence in the database. Geometric data found in the database were used to determine a set of bond lengths for these fragments.

A second fundamental approach to this problem is the joining of small structural fragments into molecules that meet steric and chemical constraints (165–171) that are derived from consideration of the hydrophobic and electrostatic interactions found in ligand–receptor complexes. An example of this is the work of Danziger and Dean (172), who identify hydrogen-bonding interaction sites on the surface of binding regions. Lewis, Dean, and co-workers have published a series of papers on structure design based on information derived from binding sites (166–170). This method involves

building molecular graphs that fill a binding site and have appropriate functionality at vertices near site points. Fragments for structure design, called *spacer skeletons*, can be generated from the molecular graphs by taking the union of a set of subgraphs (166). Initially, the subgraphs used were planar four- to eight-membered rings. Molecular templates, from which potential ligands could be generated, are derived from the spacer skeletons. Distance matrix methods are used to fit atoms in the spacer skeletons to ligand points, in order to generate molecular templates that exhibit good complementarity to a binding region (167).

Recently, Lewis has extended this work from 2-D to 3-D (168). Here, a regular diamond lattice is used as a spacer skeleton in which each atom is sp^3 hybridized, and all torsion angles are staggered, and acyclic chains that span sets of site points are generated from this lattice. Lewis has also reported work on the formation of irregular linear chains of atoms using this methodology (170). This technique was used in the design of structures to fit the active site of HIV-1 protease (169). First, a DOCK search of a 3-D database was performed to find compounds that sterically matched the active site. Several interesting fragments derived from these searches were considered for joining into composite molecules. Both the regular and irregular lattice methods were used to generate chains of atoms to join these fragments into molecules that fitted the active site sterically.

Lewis and Dean (166) note that spacer skeletons are but one of several approaches that can be used to generate novel structures, and Gillet et al. (165) have recently discussed the use of one of these alternative strategies, which they refer to as *template joining*. The structure generation problem is formulated as a search of a space, the states of which correspond to molecules that can satisfy some or all of the steric, electrostatic, and hydrophobic constraints that define a binding site. A systematic exploration of this state space is totally infeasible, and thus the A* heuristic search algorithm is used [this algorithm has also been used for conformational analysis (173)]. The current version of the program results in structures that are based on hydrocarbon skeletons in which individual carbon atoms can be replaced by heteroatoms that have the same geometry. The program has been used successfully to design molecular skeletons that match the APPA (*p*-amidinophenylpyruvate) binding site of trypsin (165).

Several other researchers have reported on the development and use of computer programs that perform structure generation. One such effort is a program, developed by Moon and Howe, called GROW (161). In this approach, the building blocks used are a database of amino acid conformations and related fragments. Potential ligands are "grown" in a binding site starting from an amide group manually placed in the site. A simulated annealing approach, which considers steric fit, conformational energy, and

solvation, is used to place fragments in growing structures. In one test of the method, the program was able to duplicate the observed binding mode of an inhibitor of rhizopuspepsin, with an RMS deviation of only 0.6 Å. The program has recently been extended to allow the construction of nonpeptidic molecules (174).

Bohm is also developing a computer program, LUDI, for the *de novo* design of structures (171). This approach uses a large library of common molecular fragments, such as phenol, morpholine and acetic acid, and small bridging fragments such as $-CH_2-$, $-O-$, and $-NH-$. The program currently considers four types of interaction sites: lipophilic–aliphatic, lipophilic–aromatic, hydrogen donor, and hydrogen acceptor. Interaction sites can be generated based on a set of rules, based on a survey of nonbonded contacts found in the Cambridge Structural Database, or on the results of a GRID (136, 137) calculation. The interaction sites can be derived from a macromolecular binding site or from a set of superimposed ligands. LUDI searches the fragment library to find fragments that fit the interaction sites and the fragments are then bridged to form molecules. LUDI has been used to position several fragments that are known to bind to specificity pockets of trypsin like serine proteases.

De novo structure design is an exciting and dynamic area of research. A number of complementary approaches to tackle this problem are under continuing development. The importance of structure design in many aspects of chemistry ensures active work in this area for years to come.

C. Automated Generation of Pharmacophore Maps

Pharmacophore maps, that is, a representation of the 3-D chemical and spatial requirements for bioactivity, are now widely used in database searching and structure generation. An emerging research area is the development of software capable of automatically generating pharmacophore models for sets of biologically related compounds.

Important facets of pharmacophore modeling include the generation of pharmacophore maps, quantitative prediction of potency, and identification of structures that match the maps. Martin and co-workers recently reported on their developing approach to construct pharmacophore maps, implemented in a computer program called DISCO (DIStance COmparisons) (175). The program identifies a bioactive conformation and superposition rule for sets of active compounds. The points for superposition are typically the ligand hydrogen bond donor, hydrogen bond acceptor, and charged atoms; centers of ligand hydrophobic regions; and extensions of the hydrogen bonds and electrostatic interactions to binding sites in the receptor. Potential pharmacophore points, including hydrogen-bonding sites, are found with

ALADDIN (91). DISCO uses a rapid technique, clique detection, to identify maps from the set of all potential pharmacophore points. Typically, the maps are generated in a few minutes of CPU time and the results can be viewed in a variety of molecular modeling programs.

Two chemical software companies, BioCAD Corporation and Biosym Technologies, are developing integrated programs for pharmacophore modeling, including pharmacophore mapping and quantitative prediction. The approach adopted by BioCAD, implemented in their program called Catalyst (176), encompasses structure entry, conformational analysis, pharmacophore mapping, quantitative structure-activity modeling, and database searching. Pharmacophore maps, or *hypotheses*, in Catalyst consist of a small set of features important for bioactivity, such as hydrophobic groups, hydrogen bond donors and acceptors, and positive and negative charges, and distance ranges between these points. Quantitative structure-activity modeling is combined with pharmacophore mapping to provide a model that gives the best correlation between the geometric fit of each compound and its potency. The hypotheses can be used to estimate the activity of new compounds and to search 3-D databases from within Catalyst.

The system being developed by Biosym Technologies, Apex-3D (177), is based on the work of Golender, Rozenblit, and colleagues (178). Pharmacophore maps in Apex-3D, termed *biophores*, are generated by classifying compounds into active and inactive groups and identifying structural features common to the set of actives. The types of structural features considered include those involved in electrostatic, hydrophobic, and hydrogen-bonding interactions. Databases of generated biophores can be searched by Apex-3D to propose biological activities of new compounds. Apex-3D is integrated with the Insight II (179) molecular modeling package and can be used in conjunction with LUDI (171) for automated structure generation.

Methodologies for automated structure generation, pharmacophore mapping, and quantitative activity prediction are in the early stages of development. As more researchers report on the use of this technology, the utility and scope of the different approaches to these problems will become more evident.

VII. CONCLUSIONS

The first operational system for searching a 3-D database of nontrivial size was reported in 1987 (78); since then, the field of 3-D searching has been extremely rapid growth, and there are already several documented examples of the utility of 3-D searching in real research programs, as discussed in Section IV. This progress has occurred because of the converging interests

of many diverse groups in these techniques. Software companies, academic laboratories, and industrial users are presenting novel solutions to problems identified in the early systems and are also expanding the scope and breadth of the field. The rich mix of this growing field is also illustrated by the contributions of synthetic and medicinal chemists, structural chemists and biochemists, chemical information specialists, and molecular modelers. Each brings a unique viewpoint to the key problems to be solved and how this should be accomplished.

The progress that has been achieved to date can be illustrated by several specific statements. Originally, 3-D searching was based on structures derived from crystallography or careful molecular modeling and the databases were accordingly small; today, there are several options for converting 2D databases into 3-D in reasonable time. Originally, systems considered only a single stored conformation of the molecule; today, 3-D searching considering conformational flexibility is becoming a reality. Originally, 3-D searching identified molecules in a database that met search criteria; today, there are several programs that use 3-D searching to design totally new molecules that meet the users' 3-D criteria. Originally, 3-D searching of a database of a few thousands structures was a novel, exciting prospect; today, the concept of 3-D searching all or most of the molecules in CAS is a possibility. Originally, 3-D searching consisted of substructure matching using simple interatomic distances, angles, and torsions; today, the criteria for 3-D searching have been expanded to include shape, similarity in 3-D, and chemical and physical properties.

However, the successes that have been achieved have served only to identify new challenges. The first set of challenges, or opportunities if one is an optimist, arises from the fact that much more experimental 3-D information is being generated because of the revolutions that are taking place in molecular biology, protein crystallography, and macromolecular nuclear magnetic resonance spectroscopy. This increased amount of information puts pressure on those who aim to use such information to design better ligands to learn how to do so faster and more accurately. Are molecular graphics and human imagination the only tools available?

Other challenges arise from limitations in the computational methods themselves. *De novo* design based on a macromolecular binding site requires that we develop better methods for the calculation of interaction energies. Both the accuracy and the speed of the methods need improvement by at least an order of magnitude. *De novo* design also requires far more integration of synthetic knowledge into the design process that is suggested by a structure generation program (so that the proposed structures take account not only of complementarity with the site but also of whether the compound that is being suggested can be readily synthesized). There is hence substantial

scope for the integration of the new generation of programs for structure generation with those that have been developed over many years for computer-aided synthesis design (180, 181).

If the 3-D structure of the macromolecular binding site is not known, then in order to do a 3-D search one must infer key features of the structure from the structure-activity relationships of the ligands that bind to it. This field, pharmacophore mapping, is only now entering a more automated and objective phase. Better ways are needed to balance how closely structures should match in 3-D with how high in energy the proposed bioactive conformation can be. This strategy would benefit from the availability of better interaction energy calculations.

The challenges above all have to do with increasing the effectiveness of 3-D database searching systems. However, substantial problems of machine efficiency also need to be overcome. The computational requirements associated with rigid 3-D searching are substantially greater than those associated with 2-D database searching, and these requirements will undoubtedly increase still further with the development of techniques for flexible searching (155). There will thus be a continuing need for efficient algorithms and data structures and for the use of the most appropriate computer hardware if 3-D database searching is to be further developed as a potent tool for molecular design.

ACKNOWLEDGMENTS

PW thanks the Cambridge Crystallographic Data Centre, ICI Agrochemicals, ICI Pharmaceuticals, the Science and Engineering Research Council, Shell Research Centre, Tripos Associates, and Wellcome Laboratories for funding, and David Clark and Andrew Poirrette for a careful reading of an earlier draft of this chapter. The Krebs Institute for Biomolecular Research is a designated Centre for Molecular Recognition Studies under the Molecular Recognition Initiative of the Science and Engineering Research Council.

REFERENCES

1. Allen, F. H.; Kennard, O.; Taylor, R. *Acc. Chem. Res.* **1983**, *16*, 146.
2. Cohen, N. C.; Blaney, J. M.; Humblet, C.; Gund, P.; Barry, D. C. *J. Med. Chem.* **1990**, *33*, 883.
3. Fruhbeis, H.; Klein, R.; Wallmeier, H. *Angew. Chem. Int.* **1987**, *26*, 403.
4. Lipkowitz, K. B.; Boyd, D. B., Eds. *Reviews in Computational Chemistry Vols. 1–3*; VCH: New York, 1990–92.

5. Martin, Y. C.; Danaher, E. B. In *Receptor Pharmacology and Function*; Williams, M.; Glennon, R.; Timmermans, P., Eds.; Marcel Dekker: New York, 1988; p. 137.
6. Perun, T. J.; Propst, C. L., Eds. *Computer-Aided Drug Design*; Marcel Dekker: New York, 1989.
7. Tollenaere, J. P.; Janssen, P. A. J. *Med. Res. Rev.* **1988**, *8*, 1.
8. Richards, W. G., Ed.; *Computer-Aided Molecular Design*; IBC Technical Services: London, 1989.
9. Appelt, K.; Bacquet, R. H.; Bartlett, C. A.; Booth, C. L. J.; Freer, S. T.; Fuhry, M. A. M.; Gehring, M. R.; Herrmann, S. M.; Howland, E. F.; Janson, C. A.; Jones, T. R.; Kan, C.-C.; Kathardekar, V.; Lewis, K. K.; Marzoni, G. P.; Matthews, D. A.; Mohr, C.; Moomaw, E. W.; Morse, C. A.; Oatley, S. H.; Ogden, R. C.; Reddy, M. R.; Reich, S. H.; Schoettlin, W. S.; Smith, W. W.; Varney, M. D.; Villafranca, J. E.; Ward, R. W.; Webber, S.; Webber, S. E.; Welsh, K. M.; White, J. *J. Med. Chem.* **1991**, *34*, 1925.
10. Fesik S. W. *J. Med. Chem.* **1991**, *34*, 2937.
11. Ash, J. E.; Warr, W. A.; Willett, P., Eds. *Chemical Structure Systems*; Ellis Horwood: Chichester, 1991.
12. Figueras, J. In *Physical Methods of Organic Chemistry, Vol. 1: Components of Scientific Instruments and Applications of Computers to Chemical Research*; Rossitter, B. W., Ed.; Wiley: New York, 1986; p. 687.
13. Gray, N. A. B. *Computer-Assisted Structure Elucidation*; Wiley: New York, 1986.
14. Lipscombe, K. J.; Lynch, M. F.; Willett, P. *Ann. Rev. Inf. Sci. Tech.* **1989**, *24*, 189.
15. Barnard, J. M. *Perspec. Inf. Manage.* **1989**, *1*, 133.
16. Willett, P. *Three-Dimensional Chemical Structure Handling*; Research Studies Press: Taunton, 1991.
17. Borman, S. *Chem. Eng. News* **1992**, *August 10*, 18.
18. Martin, Y. C.; Bures, M. G.; Willett, P. In *Reviews in Computational Chemistry*; Lipkowitz, K.; Boyd, D. Eds.; VCH: New York, 1990; p. 213.
19. Martin, Y. C. *J. Med. Chem.* **1992**, *35*, 2145.
20. Bebak, H.; Buse, C.; Donner, W. T.; Hoever, P.; Jacob, H.; Klaus, H.; Pesch, J.; Roemelt, J.; Schilling, P.; Woost, B.; Zirz, C. *J. Chem. Inf. Comput. Sci.* **1989**, *29*, 1.
21. Barnard, J. M. *J. Chem. Inf. Comput. Sci.* **1990**, *30*, 81.
22. Dalby, A.; Nourse, J. G.; Hounshell, W. D.; Gushurst, A. K. I.; Grier, D. L.; Leland, B. A.; Lauffer, J. *J. Chem. Inf. Comput. Sci.* **1992**, *32*, 244.
23. Wilson, R. *Introduction to Graph Theory*; Oliver and Boyd: Edinburgh, 1972.
24. Trinajstic, N., Ed. *Chemical Graph Theory*; CRC Press: Boca Raton, FL, 1983.
25. McGregor, J. J. *Software—Pract. Exper.* **1982**, *12*, 23.
26. Tarjan, R. E. *Am. Chem. Soc. Symp. Ser.* **1977**, *46*, 1.
27. Read, R. C.; Corneil, D. G. *J. Graph Theory* **1977**, *1*, 339.
28. Gati, G. *J. Graph Theory* **1979**, *3*, 95.
29. Morgan, H. L. *J. Chem. Document.* **1965**, *5*, 107.
30. Wipke, W. T.; Dyott, T. M. *J. Am. Chem. Soc.* **1974**, *96*, 4834.
31. Bawden, D.; Catlow, J. T.; Devon, T. K.; Dalton, J. M.; Lynch, M. F.; Willett, P. *J. Chem. Inf. Comput. Sci.* **1981**, *21*, 83.
32. Freeland, R. G.; Funk, S. A.; O'Korn, L. J.; Wilson. G. A. *J. Chem. Inf. Comput. Sci.* **1979**, *19*, 94.

33. Wipke, W. T.; Krishnan, S. K.; Ouchi, G. I. *J. Chem. Inf. Comput. Sci.* **1978**, *18*, 32.
34. Garey, M. R.; Johnson, D. S. *Computers and Intractability: A Guide to the Theory of NP-Completeness;* W. H. Freeman: San Francisco, 1979.
35. Harel, D. *Algorithmics: The Spirit of Computing*; Addison-Wesley: Reading, MA, 1987.
36. Adamson, G. W.; Lambourne, D. R.; Lynch, M. F. *J. Chem. Soc. Perkin I* **1972**, 2428.
37. Adamson, G. W.; Clinch, V. A.; Lynch, M. F. *J. Chem. Document.* **1973**, *13*, 133.
38. Feldman, A.; Hodes, L. *J. Chem. Inf. Comput. Sci.* **1975**, *15*, 147.
39. Hodes, L. *J. Chem. Inf. Comput. Sci.* **1976**, *16*, 88.
40. Willett, P. *J. Chem. Inf. Comput. Sci.* **1979**, *19*, 159.
41. Figueras, J. *J. Chem. Document.* **1972**, *12*, 237.
42. Sussenguth, E. H. *J. Chem. Document.* **1965**, *5*, 36.
43. Von Scholley, A. *J. Chem. Inf. Comput. Sci.* **1985**, *25*, 235.
44. Attias, R. *J. Chem. Inf. Comput. Sci.* **1983**, *23*, 102.
45. Hicks, M. G.; Jochum, C.; Maier, H. *Anal. Chim. Acta* **1990**, *235*, 87.
46. Nagy, M. A.; Kozics, S.; Veszpremi, T.; Bruck, P. In *Chemical Structures. The International Language of Chemistry*; Warr, W. A., Ed.; Springer: Berlin, 1988; p. 127.
47. Willett, P. *Similarity and Clustering in Chemical Information Systems*; Research Studies Press: Letchworth, 1987.
48. Johnson, M. A.; Maggiora, G. M. *Concepts and Applications of Molecular Similarity*; Wiley: New York, 1990.
49. Johnson, M. A. *J. Math. Chem.* **1989**, *3*, 117.
50. Willett, P., Ed. *Modern Approaches to Chemical Reaction Searching*; Gower: Aldershot, 1986.
51. Barth, A. *J. Chem. Inf. Comput. Sci.* **1990**, *30*, 384.
52. Cone, M. M.; Venkataraghavan, R.; McLafferty, F. W. *J. Am. Chem. Soc.* **1977**, *99*, 7668.
53. Chen, L.; Robien, W. *J. Chem. Inf. Comput. Sci.* **1992**, *32*, 501.
54. Carhart, R. E.; Smith, D. H.; Venkataraghavan, R. *J. Chem. Inf. Comput. Sci.* **1985**, *25*, 64.
55. Klopman, G.; Raychaudhury, C. *J. Chem. Inf. Comput. Sci.* **1990**, *30*, 12.
56. Willett, P.; Winterman, V.; Bawden, D. *J. Chem. Inf. Comput. Sci.* **1986**, *26*, 36.
57. Hagadone, T. R. *J. Chem. Inf. Comput. Sci.* **1992**, *32*, 515.
58. Barnard, J. M.; Downs, G. M. *J. Chem. Inf. Comput. Sci.* **1992**, *32*, 644.
59. Gund, P. *Prog. Mol. Subcell. Biol.* **1977**, *5*, 117.
60. Allen, F. H.; Davies, J. E.; Galloy, J. J.; Johnson, O.; Kennard, O.; Macrea, C. F.; Mitchell, E. M.; Mitchell, G. F.; Smith, J. M.; Watson, D. G. *J. Chem. Inf. Comput. Sci.* **1991**, *31*, 187.
61. Abola, E. E.; Bernstein, F. C.; Bryant, S. H.; Koetzle, T. F.; Weng, J. In *Crystallographic Databases: Information Content, Software Systems, Scientific Applications*; Allen, F. H.; Bergerhoff, G.; Sievers, R., Eds.; Data Commission of the International Union of Crystallography: Chester, 1987; p. 107.
62. Richards, W. G. *Quantum Pharmacology*; Butterworths: London, 1983.
63. Burkert, U.; Allinger, N. L. *Molecular Mechanics*; American Chemical Society: Washington D. C., 1982.
64. Crippen, G. M.; Havel, T. F. *Distance Geometry and Molecular Conformation*; Research Studies Press: Letchworth, 1988.
65. Dolata, D. P.; Carter, R. E. *J. Chem. Inf. Comput. Sci.* **1987**, *27*, 73.

66. Leach, A. R.; Prout, K.; Dolata, D. P. *J. Computat. Chem.* **1990**, *11*, 680.
67. Wipke, W. T.; Hahn, M. A. *Tetrahedron Comput. Meth.* **1988**, *1*, 141.
68. Rusinko, A.; Skell, J. M.; Balducci, R.; McGarity, C. M.; Pearlman, R. S. *CONCORD: A Program for the Rapid Generation of High Quality Approximate 3-Dimensional Molecular Structures*; University of Texas at Austin and Tripos Associates: St Louis, Missouri, 1988.
69. Rusinko, A.; Sheridan, R. P.; Nilakantan, R.; Haraki, K. S.; Bauman, N.; Venkataraghavan, R. *J. Chem. Inf. Comput. Sci.* **1989**, *29*, 251.
70. Henry, D. R.; McHale, P. J.; Christie, B. D.; Hillman, D. *Tetrahedron Comput. Meth.* **1990**, *3*, 531.
71. Haraki, K. S.; Sheridan, R. P.; Venkataraghavan, R.; Dunn, D. A.; McCulloch, D. *Tetrahedron Comput. Meth.* **1990**, *3*, 565.
72. Fisanick, W.; Cross, K. P.; Rusinko, A. *Tetrahedron Comput. Meth.* **1990**, *3*, 635.
73. Davies, K.; Upton, R. *Tetrahedron Comput. Meth.* **1990**, *3*, 665.
74. Gasteiger, J.; Rudolph, C.; Sadowski, J. *Tetrahedron Comput. Meth.* **1990**, *3*, 537.
75. Bartlett, P. A.; Shea, G. T.; Telfer, S. J.; Waterman, S. In *Molecular Recognition: Chemical and Biochemical Problems*, Roberts, S., Ed.; Royal Society of Chemistry: Cambridge, 1989; p. 182.
76. Jakes, S. E.; Willett, P. *J. Mol. Graph.* **1986**, *4*, 12.
77. Sheridan, R. P.; Nilakantan, R.; Rusinko, A.; Bauman, N.; Haraki, K. S.; Venkataraghavan, R. *J. Chem. Inf. Comput. Sci.* **1989**, *29*, 255.
78. Jakes, S. E.; Watts, N. J.; Willett, P.; Bawden, D.; Fisher, J. D. *J. Mol. Graph.* **1987**, *5*, 41.
79. Cringean, J. K.; Pepperrell, C. A.; Poirrette, A. R.; Willett, P. *Tetrahedron Comput. Meth.* **1990**, *3*, 37.
80. Poirrette, A. R.; Willett, P.; Allen, F. H. *J. Mol. Graph.* **1991**, *9*, 203.
81. Sheridan, R. P.; Rusinko, A.; Nilakantan, R.; Venkataraghavan, R. *Proc. Nat. Acad. Sci. USA* **1989**, *86*, 8125.
82. Murrall, N. W.; Davies, E. K. *J. Chem. Inf. Comput. Sci.* **1990**, *30*, 312.
83. Christie, B. D.; Henry, D. R.; Wipke, W. T.; Moock, T. E. *Tetrahedron Comput. Method.* **1990**, *3*, 653.
84. Fisanick, W.; Cross, K. P.; Rusinko, A. *J. Chem. Inf. Comput. Sci.* **1992**, *32*, 664.
85. Poirrette, A. R.; Willett, P.; Allen, F. H. *J. Mol. Graph.* **1993**, *11*, 2.
86. Brint, A. T.; Willett, P. *J. Mol. Graph.* **1987**, *5*, 49.
87. Ullmann, J. R. *J. Assoc. Comput. Mach.* **1976**, *16*, 31.
88. Downs, G. M.; Lynch, M. F.; Willett, P.; Manson, G. A.; Wilson, G. A. *Tetrahedron Comput. Method.* **1988**, *1*, 207.
89. Brint, A. T.; Davies, H. M.; Mitchell, E. M.; Willett, P. *J. Mol. Graph.* **1989**, *7*, 48.
90. Mitchell, E. M.; Artymiuk, P. J.; Rice, D. W.; Willett, P. *J. Mol. Biol.* **1990**, *212*, 151.
91. Van Drie, J. H.; Weininger, D.; Martin, Y. C. *J. Computer-Aide Mol. Des.* **1989**, *3*, 225.
92. Hurst, T.; Smith, G. B.; Homer, R. W.; Epplin, J. L.; Soltanshahi, F. Paper presented at the 202nd National Meeting of the American Chemical Society, 1991.
93. Sprague, P. W. In *Recent Advances in Chemical Information*. Collier, H. R., Ed.; Royal Society of Chemistry: Cambridge, 1991; p. 107.
94. Willett, P. *J. Chemomet.* **1992**, *6*, 289.
95. Milne, G. W. A.; Driscoll, J. S.; Marquez, V. E. In *Proceedings of the Montreux 1989*

International Chemical Information Conference; Collier, H. R., Ed.; Infonortics: Calne, 1989; p. 19.

96. Lauri, G.; Shea, G. T.; Waterman, S.; Telfer, S. J.; Bartlett, P. A. *CAVEAT: A program to Facilitate the Design of Organic Molecules*; University of California: Berkeley, 1991.
97. Martin, Y. C. *Tetrahedron Comput. Meth.* **1990**, *3*, 15.
98. Weininger, D. *J. Chem. Inf. Comput. Sci.* **1988**, *28*, 31.
99. Martin, Y. C. In *Medications Development: Drug Discovery, Databases, and Computer-Aided Drug Design*; Rapaka, R. Ed., NIDA Research Monograph; U.S. Government Printing Office: Washington, D. C.; in press.
100. Bures, M. G.; Black-Schaefer, C.; Gardner, G. *J. Computer-Aided Mol. Des.* **1991**, *5*, 323.
101. Katekar, G. F.; Geissler, A. E. *Phytochemistry* **1981**, *20*, 2565.
102. Bures, M. G.; Hutchins, C. W.; Maus, M.; Kohlbrenner, W.; Kadam, S.; Erikson, J. W. *Tetrahedron Comput. Meth.* **1992**, *3*, 673.
103. DesJarlais, R. L.; Seibel, G. L.; Kuntz, I. D.; Furth, P. S.; Alvarez, J. C.; Ortiz De Montellano, P. R.; DeCamp, D. L.; Babe, L. M.; Craik, C. S. *Proc. Nat. Acad. Sci. USA* **1990**, *87*, 6644.
104. Kuntz, I. D.; Blaney, J. M.; Oatley, S. J.; Langridge, R.; Ferrin, T. E. *J. Mol. Biol.* **1982**, *161*, 269.
105. Dean, P. M. *Molecular Foundations of Drug-Receptor Interaction*; Cambridge University Press: Cambridge, 1987.
106. Danziger, D. J.; Dean, P. M. *J. Theor. Biol.* **1985**, *116*, 215.
107. Bakarat, M. T.; Dean, P. M. *J. Computer-Aided Mol. Des.* **1990**, *4*, 295.
108. Bakarat, M. T.; Dean, P. M. *J. Computer-Aided Mol. Des.* **1990**, *4*, 317.
109. Bakarat, M. T.; Dean, P. M. *J. Computer-Aided Mol. Des.* **1991**, *5*, 107.
110. Papadopoulos, M. C.; Dean, P. M. *J. Computer-Aided Mol. Des.* **1991**, *5*, 119.
111. Meyer, A. M.; Richards, W. G. *J. Computer-Aided Mol. Des.* **1991**, *5*, 426.
112. Mezey, P. G. *J. Chem. Inf. Comput. Sci.* **1992**, *32*, 650.
113. Cano, F. H.; Martinez-Ripoll, M. *J. Mol. Struct. (THEOCHEM)* **1992**, *258*, 139.
114. Petitjean, M. *J. Chem. Inf. Comput. Sci.* **1992**, *32*, 331.
115. Carbo, R.; Leyda, L.; Arnau, M. *Int. J. Quant. Chem.* **1980**, *17*, 1185.
116. Hodgkin, E. E.; Richards, W. G. *Int. J. Quant. Chem.: Quantit. Biol. Symp.* **1987**, *14*, 105.
117. Burt, C.; Richards, W. G.; Huxley, P. *J. Comput. Chem.* **1990**, *11*, 1139.
118. Hermann, R. B.; Herron, D. K. *J. Computer-Aided Mol. Des.* **1991**, *5*, 511.
119. Manaut, F.; Sanz, F.; Jose, J.; Milesi, M. *J. Computer-Aided Mol. Des.* **1991**, *5*, 371.
120. Richard, A. M. *J. Comput. Chem.* **1991**, *12*, 959.
121. Good, A. C.; Hodgkin, E. E.; Richards, W. G. *J. Chem. Inf. Comput. Sci.* **1992**, *32*, 188.
122. Kearsley, S. K.; Smith, G. M. *Tetrahedron Comput. Method.* **1990**, *3*, 615.
123. Kato, Y.; Inoue, A.; Yamada, M.; Tomioka, N.; Itai, A. *J. Computer-Aided Mol. Des.* **1992**, *6*, 475.
124. Cramer III, R. D.; Patterson, D. E.; Bunce, J. D. *J. Am. Chem. Soc.* **1988**, *170*, 5959.
125. Lin, C. T.; Pavlik, P. A.; Martin, Y. C. *Tetrahedron Comput. Method.* **1990**, *3*, 723.
126. van Geerestein, V.; Perry, N. C.; Grootenhuis, P. D. J.; Haasnoot, C. A. G. *Tetrahedron Comput. Method.* **1990**, *3*, 595.
127. Pepperrell, C. A.; Willett, P. *J. Computer-Aided Mol. Des.* **1991**, *5*, 455–474.
128. Pepperrell, C. A.; Poirrette, A. R.; Willett, P.; Taylor, R. *Pesticide Sci.* **1991**, *33*, 97–111.

129. Pepperrell, C. A.; Taylor, R.; Willett, P. *Tetrahedron Comput. Method.* **1990**, *3*, 575.
130. Artymiuk, P. J.; Bath, P. A.; Grindley, H. M.; Pepperrell, C. A.; Poirrette, A. R.; Rice, D. W.; Thorner, D. A.; Wild, D. J.; Willett, P. *J. Chem. Inf. Comput. Sci.* **1992**, *32*, 617.
131. Bemis, G. W.; Kuntz, I. D. *J. Computer-Aided Mol. Des.* **1992**, *6*, 607.
132. DesJarlais, R. L.; Sheridan, R. P.; Seibel, G. L.; Dixon, J. S.; Kuntz, I. D.; Venkataraghavan, R. *J. Med. Chem.* **1988**, *31*, 722.
133. Stewart, K. D.; Bentley, J. A.; Cory, M. *Tetrahedron Comput. Method.* **1990**, *3*, 713.
134. Grootenhuis, P. D. J.; Kollman, P. A.; Seibel, G. L.; DesJarlais, R. L.; Kuntz, I. D. *Anti-Cancer Drug Des.* **1990**, *5*, 237.
135. Lawrence M. C.; Davis, P. C. *Proteins: Struct. Func. Gen.* **1992**, *12*, 31.
136. Goodford, P. J. *J. Med. Chem.* **1985**, *28*, 849.
137. Boobbyer, D. N. A.; Goodford, P. J.; McWhinnie, P. M,; Wade, R. C. *J. Med. Chem.* **1989**, *32*, 1083.
138. Chau, P.-L.; Dean, P. M. *J. Mol. Graph.* **1987**, *5*, 97.
139. Dean, P. M.; Chau, P.-L. *J. Mol. Graph.* **1987**, *5*, 152.
140. Dean, P. M.; Callow, P.; Chau, P.-L. *J. Mol. Graph.* **1988**, *6*, 28.
141. Bladon, P. *J. Mol. Graph.* **1989**, 7, 130.
142. Martin, Y. C., DeLazzer, J. J. Computer-Aided Mol. Des., in press.
143. Bron, C.; Kerbosch, J. *Communications ACM* **1973**, *16*, 575.
144. Brint, A. T.; Willett, P. *J. Chem. Inf. Comput. Sci.* **1987**, *27*, 152.
145. Cannon, J. G. *Prog. Drug Res.* **1985**, *29*, 303.
146. Guner, O. F.; Hughes, D. W.; DuMont, L. M. *J. Chem. Inf. Comput. Sci.* **1991**, *31*, 408.
147. Meng, E. C.; Shoichet, B. K.; Kuntz, I. D. *J. Computat. Chem.* **1992**, *13*, 505.
148. Mitchell, E. M.; Allen, F. H.; Mitchell, G. F.; Rowland, R. S. in *Proceedings of the Second International Conference on Chemical Structures*; Warr, W. A., Ed.; Springer: Berlin, **1993**; p. 359.
149. Crippen, G. M. *J. Med. Chem.* **1979**, *22*, 988.
150. Behling, R. W.; Yamane, T.; Navon, G.; Jelinski, L. W. *Proc. Nat. Acad. Sci. USA* **1988**, *85*, 6721.
151. Guner, O. F.; Henry, D. R.; Pearlman, R. S. *J. Chem. Inf. Comput. Sci.* **1992**, *32*, 101.
152. Havel, T. F.; Kuntz, I. D.; Crippen, G. M. *Bull. Math. Biol.* **1983**, *45*, 665.
153. Wenger, J. C.; Smith, D. H. *J. Chem. Inf. Comput. Sci.* **1982**, *22*, 29.
154. Clark, D. E.; Willett, P.; Kenny, P. W. *J. Mol. Graph.* **1991**, *9*, 157.
155. Clark, D. E.; Willett, P.; Kenny, P. W. *J. Mol. Graph.* **1992**, *10*, 194.
156. Easthope, P. L.; Havel, T. F. *Bull. Math. Biol.* **1989**, *51*, 173.
157. Howard, A. E.; Kollman, P. A. *J. Med. Chem.* **1988**, *31*, 1669.
158. Leach, A. R. In *Reviews in Computational Chemistry II*; Lipkowitz, K. B.; Boyd, D. B., Eds.; VCH: New York, 1991; p. 1.
159. Smellie, A. S.; Crippen, G. M.; Richards, W. G. *J. Chem. Inf. Comput. Sci.* **1991**, *31*, 386.
160. Blaney, J. A. Paper presented at the 202nd National Meeting of the American Chemical Society; **1991**.
161. Moon, J. B.; Howe, W. J. *Tetrahedron Comput. Method.* **1990**, *3*, 697.
162. Chau, P.-L.; Dean, P. M. *J. Computer-Aided Mol. Des.* **1992**, *6*, 385.

163. Chau, P.-L.; Dean, P. M. *J. Computer-Aided Mol. Des.* **1992**, *6*, 397.
164. Chau, P.-L.; Dean, P. M. *J. Computer-Aided Mol. Des.* **1992**, *6*, 407.
165. Gillet, V. J.; Johnson, A. P.; Mata, P.; Sike, S. *Tetrahedron Comput. Method.* **1990**, *3*, 681.
166. Lewis, R. A.; Dean, P. M. *Proc. Roy. Soc. London, B* **1989**, *236*, 125.
167. Lewis, R. A.; Dean, P. M. *Proc. Roy. Soc. London, B* **1989**, *236*, 141.
168. Lewis, R. A. *J. Computer-Aided Mol. Des.* **1990**, *4*, 205.
169. Lewis, R. A.; Roe, D. C.; Huang, C.; Ferrin, T. E.; Langridge, R.; Kuntz, I. D. *J. Mol. Graph.* **1992**, *10*, 66.
170. Lewis, R. A. *J. Mol. Graph.* **1992**, *10*, 131.
171. Bohm, H.-J. *J. Computer-Aided Mol. Des.* **1992**, *6*, 61.
172. Danziger, D. J.; Dean, P. M. *Proc. Roy. Soc. London, B* **1989**, *236*, 115.
173. Leach, A. R.; Prout, K. *J. Computat. Chem.* **1990**, *11*, 1193.
174. Moon, J. B.; Howe, W. J. In *Trends in QSAR and Molecular Modelling '92. Proceedings of the 9th European Symposium on Structure-Activity Relationships: QSAR and Molecular Modelling, Strasbourg, France, 7–11 September, 1992*; Wermuth, C., Ed., ESCOM: The Netherlands, in press.
175. Martin, Y. C.; Bures, M. G.; Danaher, E. A.; DeLazzer, J.; Lico, I.; Pavlik, P. A. *J. Computer-Aided Mol. Des.* **1993**, *7*, 83.
176. Catalyst is developed by BioCAD Corporation, Mountain View, California, 94115.
177. Apex-3D was developed by DCL Systems International, Israel and is available from Biosym Technologies, San Diego, California, 92121.
178. Golender, V. E.; Rozenblit, A. B. *Logical and Combinatorial Algorithms for Drug Design*, Research Studies Press: Letchworth, 1983.
179. Insight II is developed by Biosym Technologies, San Diego, California, 92121.
180. Wipke, W. T.; Howe, W. J., Eds.; *Computer-Assisted Organic Synthesis*; American Chemical Society: Washington, D. C., 1977.
181. Loftus, F. In *Chemical Structure Systems*; Ash, J. E.; Warr, W. A.; Willett, P., Eds.; Ellis Horwood: Chichester, 1991; p. 222.

CUMULATIVE TITLE INDEX

	VOL.	PAGE
Absolute Configuration of Chiral Molecules, Crystals as Probes for the Direct Assignment of (*Addadi, Berkovitch-Yellin, Weissbuch, Lahav*, and *Leiserowitz*)	16	1
Absolute Configuration of Planar and Axially Dissymmetric Molecules (*Krow*)	5	31
Absolute Stereochemistry of Chelate Complexes (*Saito*)	10	95
Acetylenes, Stereochemistry of Electrophilic Additions (*Fahey*)	3	237
Acyclic Stereocontrol in Michael Addition Reaction of Enamines and Enol Ethers (*Oare* and *Heatcock*)	20	87
Aldol Condensations, Stereoselective (*Evans, Nelson*, and *Taber*)	13	1
Alkaloids, Asymmetric Catalysis by (*Wynberg*)	16	87
Aluminum Hydrides and Tricoordinate Aluminum Reagents, Asymmetric Reductions with Chiral Complex (*Haubenstock*)	14	231
Amino Acids, Stereochemistry of Metabolic Reactions of (*Young*)	21	381
Analogy Model, Stereochemical (*Ugi* and *Ruch*)	4	99
Anomeric Effect: Origin and Consequences (*Graczyk* and *Mikołajczyk*)	21	159
Asymmetric Catalysis by Alkaloids (*Wynberg*)	16	87
Asymmetric Reductions with Chiral Complex Aluminum Hydrides and Tricoordinate Aluminum Reagents (*Haubenstock*)	14	231
Asymmetric Synthesis, New Approaches in (*Kagan* and *Fiaud*)	10	175
Asymmetric Synthesis Mediated by Transition Metal Complexes (*Bosnich* and *Fryzuk*)	12	119
Atomic Inversion, Pyramidal (*Lambert*)	6	19
Atropisomerism, Recent Advances in (*Oki*)	14	1
Axially and Planar Dissymmetric Molecules, Absolute Configuration of (*Krow*)	5	31
Barriers, Conformational, and Interconversion Pathways in Some Small Ring Molecules (*Malloy, Bauman*, and *Carreira*)	11	97
Barton, D. H. R., and Hassel, O., Fundamental Contributions to Conformational Analysis (*Barton* and *Hassel*)	6	1
Bicyclic Compounds, Walk Rearrangements in [n.1.0] (*Kärner*)	15	1
Carbene Additions to Olefins, Stereochemistry of (*Closs*)	3	193
Carbenes, Structure of (*Closs*)	3	193
sp^2-sp^3 Carbon-Carbon Single Bonds, Rotational Isomerism about (*Karabatsos* and *Fenoglio*)	5	167
Carbonium Ions, Simple, the Electronic St Hydrogen Isotopes at Noncyclic Positions Chelate Complexes, Absolute Stereochemistry of (*Saito*)	10	95

	VOL.	PAGE
^{13}C Chemical Shielding Tensors Obtained from NMR, Molecular Structure and (*Facelli* and *Grant*)	19	1
^{13}C Chemical Shifts in Aliphatic Molecular Systems, Substituent Effects on. Dependence on Constitution and Stereochemistry (*Duddeck*)	16	219
Chirality Due to the Presence of Hydrogen Isotopes at Noncyclic Positions (*Arigoni* and *Eliel*)	4	127
Chiral Crown Ethers (*Stoddart*)	17	207
Chiral Homogeneity in Nature, Origins of (*Bonner*)	18	1
Chiral Lanthanide Shift Reagents (*Sullivan*)	10	287
Chiral Monolayers at the Air-Water Interface (*Stewart* and *Arnett*)	13	195
Chiral Organic Molecules with High Symmetry, The Synthesis and Stereochemistry of (*Nakazaki*)	15	199
Chiral Organosulfur Compounds (*Mikołajczyk* and *Drabowicz*)	13	333
Chiral Solvating Agents, in NMR (*Pirkle* and *Hoover*)	13	263
Classical Stereochemistry, The Foundations of (*Mason*)	9	1
Conformational Analysis, Applications of the Lanthanide-induced Shift Technique in (*Hofer*)	9	111
Conformational Analysis of Bicyclo[3.3.1]nonanes and Their Hetero Analogs (*Zefirov* and *Palyulin*)	20	171
Conformational Analysis, The Fundamental Contributions of D. H. R. Barton and O. Hassell (*Barton* and *Hassel*)	6	1
Conformational Analysis of Intramolecular Hydrogen-Bonded Compounds in Dilute Solution by Infrared Spectroscopy (*Ääron*)	11	1
Conformational Analysis of Six-membered Rings (*Kellie* and *Riddell*)	8	225
Conformational Analysis of Steric Effects in Metal Chelates (*Buckingham* and *Sargeson*)	6	219
Conformational Analysis and Torsion Angles (*Bucourt*)	8	159
Conformational Barriers and Interconversion Pathways in Some Small Ring Molecules (*Malloy, Bauman* and *Carreira*)	11	97
Conformational Changes, Determination of Associated Energy by Ultrasonic Absorption and Vibrational Spectroscopy (*Wyn-Jones* and *Pethrick*)	5	205
Conformational Changes by Rotation about sp^2-sp^3 Carbon-Carbon Single Bonds (*Karabatsos* and *Fenoglio*)	5	167
Conformational Energies, Table of (*Hirsch*)	1	199
Conformational Interconversion Mechanisms, Multi-step (*Dale*)	9	199
Conformations of 5-Membered Rings (*Fuchs*)	10	1
Conjugated Cyclohexenones, Kinetic 1,2 Addition of Anions to, Steric Course of (*Toromanoff*)	2	157
Crystals as Probes for the Direct Assignment of Absolute Configuration of Chiral Molecules, A Link Between Macroscopic Phenomena and Molecular Chirality (*Addadi, Berkovitch-Yellin, Weisbuch, Lahav*, and *Leiserowitz*)	16	1
Crystal Structures of Steroids (*Duax, Weeks*, and *Rohrer*)	9	271
Cyclobutane and Heterocyclic Analogs, Stereochemistry of (*Moriarty*)	8	271
Cyclohexyl Radicals, and Vinylic, The Stereochemistry of (*Simamura*)	4	1
Databases of Three-Dimensional Chemical Structures, Searching Techniques for (*Bures, Martin* and *Willett*)	21	467
Double Bonds, Fast Isomerization about (*Kalinowski* and *Kessler*)	7	295

	VOL.	PAGE
Electronic Structure and Stereochemistry of Simple Carbonium Ions, (*Buss, Schleyer,* and *Allen*)	7	253
Electrophilic Additions to Olefins and Acetylenes, Stereochemistry of (*Fahey*)	3	237
Enantioselective Synthesis of Non-Racemic Chiral Molecules on an Industrial Scale (*Scott*)	19	209
Enantioselective Synthesis of Organic Compounds with Optically Active Transition Metal Catalysts in Substoichiometric Quantities (*Brunner*)	18	129
Enzymatic Reactions, Stereochemistry of, by Use of Hydrogen Isotopes (*Arigoni* and *Eliel*)	4	127
Enzymology, Stereospecificity in: Its Place in Evolution (*Benner, Glasfeld* and *Piccirilli*)	19	127
1,2-Epoxides, Stereochemistry Aspects of the Synthesis of (*Berti*)	7	93
EPR, in Stereochemistry of Nitroxides (*Janzen*)	6	177
Ethylenes, Static and Dynamic Stereochemistry of Push-Pull and Strained (*Sandström*)	14	83
Five-Membered Rings, Conformations of (*Fuchs*)	10	1
Foundations of Classical Stereochemistry (*Mason*)	9	1
Geometry and Conformational Properties of Some Five- and Six-Membered Heterocyclic Compounds Containing Oxygen or Sulfur (*Romers, Altona, Buys,* and *Havinga*)	4	39
Hassel, O. and Barton, D. H. R., Fundamental Contributions to Conformational Analysis (*Hassel* and *Barton*)	6	1
Helix Models, of Optical Activity (*Brewster*)	2	1
Heterocyclic Compounds, Five- and Six-Membered, Containing Oxygen or Sulfur, Geometry and Conformational Properties of (*Romers, Altona, Buys,* and *Havinga*)	4	39
Heterocyclic Four-Membered Rings, Stereochemistry of (*Moriarty*)	8	271
Heterotopism (*Mislow* and *Raban*)	1	1
Hydrocarbons, Unusual Saturated: Interaction between Theoretical and Synthetic Chemistry (*Dodziuk*)	21	351
Hydrogen-Bonded Compounds, Intramolecular, in Dilute Solution, Conformational Analysis of, by Infrared Spectroscopy (*Aaron*)	11	1
Hydrogen Isotopes at Noncyclic Positions, Chirality Due to the Presence of (*Arigoni* and *Eliel*)	4	127
Infrared Spectroscopy, Conformational Analysis of Intramolecular Hydrogen-Bonded Compounds in Dilute Solution by (*Aaron*)	11	1
Intramolecular Hydrogen-Bonded Compounds, in Dilute Solution, Conformational Analysis of, by Infrared Spectroscopy (*Aaron*)	11	1
Intramolecular Rate Processes (*Binsch*)	3	97
Inversion, Atomic, Pyramidal (*Lambert*)	6	19
Isomerization, Fast, About Double Bonds (*Kalinowski* and *Kessler*)	7	295
Ketones, Cyclic and Bicyclic, Reduction of, by Complex Metal Hydrides (*Boone* and *Ashby*)	11	53

	VOL.	PAGE
Lanthanide-induced Shift Technique—Applications in Conformational Analysis (*Hofer*)	9	111
Lanthanide Shift Reagents, Chiral (*Sullivan*)	10	287
Mass Spectrometry and the Stereochemistry of Organic Molecules (*Green*)	9	35
Metal Chelates, Conformational Analysis and Steric Effects in (*Buckingham* and *Sargeson*)	6	219
Metal Hydrides, Complex, Reduction of Cyclic and Bicyclic Ketones by (*Boone* and *Ashby*)	11	53
Metallocenes, Stereochemistry of (*Schlogi*)	1	39
Metal Nitrosyls, Structures of (*Feltham* and *Enemark*)	12	155
Michael Addition Reaction, Stereochemistry of the Base-Promoted (*Oare* and *Heathcock*)	19	227
Michael Addition Reactions of Enamines and Enol Ethers, Acyclic Stereocontrol in (*Oare* and *Heathcock*)	20	87
Molecular Mechanics Calculations—Applications to Organic Chemistry (*Osawa* and *Musso*)	13	117
Molecular Modeling, Computer Graphics and, in the Analysis of Synthetic Targets (*Ripka* and *Blaney*)	20	1
Monolayers, Chiral, at the Air-Water Interface (*Stewart* and *Arnett*)	13	195
Multi-step Conformational Interconversion Mechanisms (*Dale*)	9	199
Nitroxides, Stereochemistry of (*Janzen*)	6	177
Non-Chair Conformations of Six-Membered Rings (*Kellie* and *Riddell*)	8	225
Nuclear Magnetic Resonance, ^{13}C Chemical Shifts in Aliphatic Molecular Systems, Substituent Effects on. Dependence on Constitution and Stereochemistry (*Duddeck*)	16	219
Nuclear Magnetic Resonance Chiral Lanthanide Shift Reagents (*Sulllivan*)	10	287
Nuclear Magnetic Resonance, ^{13}C Stereochemical Aspects of (*Wilson* and *Stothers*)	8	1
Nuclear Magnetic Resonance, Chiral Solvating Agents in (*Pirkle* and *Hoover*)	13	263
Nuclear Magnetic Resonance, for Study of Intra-Molecular Rate Processes (*Binsch*)	3	97
Nuclear Magnetic Resonance, Molecular Structure and Carbon-13 Chemical Shielding Tensors Obtained from (*Facelli* and *Grant*)	19	1
Nuclear Overhauser Effect, Some Chemical Applications of (*Bell* and *Saunders*)	7	1
Olefins, Stereochemistry of Carbene Additions to (*Class*)	3	193
Olefins, Stereochemistry of Electrophilic Additions to (*Fahey*)	3	237
Olefins, Strained: Structure and Reactivity of Nonplanar Carbon-Carbon Double Bonds (*Luef* and *Keese*)	20	231
Optical Activity, Helix Models of (*Brewster*)	2	1
Optical Circular Dichroism, Recent Applications in Organic Chemistry (*Crabbé*)	1	93
Optical Purity, Modern Methods for the Determinatin of (*Raban* and *Mislow*)	2	199

	VOL.	PAGE
Optical Rotary Dispersion, Recent Applications in Organic Chemistry (*Crabbé*)	1	93
Organic Solid-State, Stereochemistry and Reactions (*Green, Arad-Yellin,* and *Cohen*)	16	131
Organosulfur Compounds, Chiral (*Mikołajczyk* and *Drabowicz*)	13	333
Origins of Chiral Homogeneity in Nature (*Bonner*)	18	1
Overhauser Effect, Nuclear, Some Chemical Applications of (*Bell* and *Saunders*)	7	1
Phosphorus Chemistry, Stereochemical Aspects of (*Gallagher* and *Jenkins*)	3	1
Phosphorus-containing Cyclohexanes, Stereochemical Aspects of (*Maryanoff, Hutchins,* and *Maryanoff*)	11	186
Piperidines, Quaternization Stereochemistry of (*McKenna*)	5	275
Planar and Axially Dissymmetric Molecules, Absolute Configuration of (*Krow*)	5	31
Polymer Stereochemistry, Concepts of (*Goodman*)	2	73
Polypeptide Stereochemistry (*Goodman, Verdini, Choi,* and *Masuda*)	5	69
Pyramidal Atomic Inversion (*Lambert*)	6	19
Quaternization of Piperidines, Stereochemistry of (*McKenna*)	5	75
Radical Pair Reactions, Stereochemical Aspects of (*Porter* and *Krebs*)	18	97
Radicals, Cyclohexyl and Vinylic, The Stereochemistry of (*Simamura*)	4	1
Reduction, of Cyclic and Bicyclic Ketones by 3Sih and *Wu*)	19	63
Resolution, Kinetic (*Kagan* and *Fiaud*)	18	249
Resolving Agents and Resolutions in Organic Chemistry (*Wilen*)	6	107
Rotational Isomerism about sp^2-sp^3 Carbon-Carbon Single Bonds (*Karabatsos* and *Fenoglio*)	5	167
Silicon, Stereochemistry at (*Corriu, Guerin,* and *Mauman,* and *Carreira*)	11	97
Stereochemical Aspects of ^{13}C Nmr Spectroscopy (*Wilson* and *Stothers*)	8	1
Stereochemical Aspects of Phosphorus-containing Cyclohexanes (*Maryanoff, Hutchins,* and *Maryanoff*)	11	186
Stereochemical Aspects of Radical Pair Reactions (*Porter* and *Krebs*)	18	97
Stereochemical Aspects of Vibrational Optical Activity (*Freedman* and *Nafie*)	17	113
Stereochemical Nomenclature and Notation in Inorganic Chemistry (*Sloan*)	12	1
Stereochemistry, Classical, The Foundations of (*Mason*)	9	1
Stereochemistry, Dynamic, A Mathematical Theory of (*Ugi* and *Ruch*)	4	99
Stereochemistry of Biological Reactions at Proprochiral Centers (*Floss, Tsai,* and *Woodard*)	15	253
Stereochemistry of Chelate Complexes (*Saito*)	10	95
Stereochemistry of Cyclobutane and Heterocyclic Analogs (*Moriarty*)	8	271
Stereochemistry of Germanium and Tin Compounds (*Gielen*)	12	217
Stereochemistry of Linear Macromolecules (*Farina*)	17	1
Stereochemistry of Nitroxides (*Janzen*)	6	177
Stereochemistry of Organic Molecules, and Mass Spectrometry (*Green*)	9	35

	VOL.	PAGE
Stereochemistry of Push-Pull and Strained Ethylenes, Static and Dynammic (*Sandström*)	14	83
Stereochemistry of Reactions of Transition Metal-Carbon Sigma Bonds (*Flood*)	12	37
Stereochemistry at Silicon (*Corriu, Guérin*, and *Moreau*)	15	43
Stereochemistry of Transition Metal Carbonyl Clusters (*Johnson* and Benfield)	12	253
Stereoisomeric Relationships, of Groups in Molecules (*Mislow* and *Raban*)	1	1
Stereoisomerism, On Factoring Chirality and (*Hirschmann* and *Hanson*)	14	183
Stereoselective Aldol Condensations (*Evans, Nelson*, and *Taber*)	13	1
Stereospecificity in Enzymology: Its Place in Evolution (*Benner, Glasfeld*, and *Piccirilli*)	19	127
Steroids, Crystal Structures of (*Duax, Weeks*, and *Rohrer*)	9	271
Strained Olefins: Structure and Reactivity of Nonplanar Carbon-Carbon Double Bonds (*Luef* and *Keese*)	20	231
Torsion Angle Concept in Conformational Analysis (*Bucourt*)	8	159
Ultrasonic Absorption and Vibrational Spectroscopy Use of, to Determine the Energies Associated with Conformational Changes (*Wyn-Jones* and *Pethrick*)	5	205
Unusual Saturated Hydrocarbons: Interaction Between Theoretical and Synthetic Chemistry (*Dodziuk*)	21	351
Vibrational Optical Activity, Stereochemical Aspects of (*Freedman* and *Nafie*)	17	113
Vibrational Spectroscopy and Ultrasonic Absorption, Use of, to Determine the Energies Associated with Conformational Changes (*Wyn-Jones* and *Pethrick*)	5	205
Vinylic Radicals, and Cyclohexyl, The Stereochemistry of (*Simamura*)	4	1
Wittig Reaction, Stereochemistry of (*Schlosser*)	5	1
Wittig Reaction, Stereochemistry and Mechanism of the (*Vedejs* and *Peterson*)	21	1

SUBJECT INDEX

A* heuristic search algorithm, 501
Abbott Laboratories, 484, 485
(*R*)-[2-$^{3}H_1$, 2-$^{2}H_1$]-Acetate, 418
(*S*)-[2-$^{3}H_1$, 2-$^{2}H_1$]-Acetate, 418
[2-$^{3}H_1$,2-$^{2}H_1$]-Acetate, 410
ACC synthase, 418
α-Acetohydroxyacid reductoisomerase, 427
α-Acetolactate, 427
O-Acetylserine, 405
O-Acetylserine sulfydrase, 405, 415
cis-Aconitate, 432
(4*S*)-[4-$^{3}H_1$]-*trans*-Aconitate, 431
Aconitate isomerase, 431
Aconitates, 431
ACPC, *see* Aminocyclopropanecarboxylate
(1*S*,2*R*)-[2-$^{2}H_1$]-ACPC, 453
(1*S*,2*S*)-[2-$^{2}H_1$]-ACPC, 453
(1*R*)-[2,2-$^{2}H_2$]-ACPC, 453
(1*S*)-[2,2-$^{2}H_2$]-ACPC, 451–453
cis-[2,3-$^{2}H_2$]-ACPC, 451
trans-[2,3-$^{2}H_2$]-ACPC, 451
ACPC deaminase, 453
Actinomycin, 434
Activation energy, 283
Activation enthalpy, 138
Activation entropy, 138
Acyl silane olefinations, 120
S-Adenosylmethionine, 417, 418, 442
(2*S*,3*R*,4*S*)-[3,4-$^{2}H_2$]-*S*-Adenosyl-methionine, 418
(2*S*,3*S*,4*R*)-[3,4-$^{2}H_2$]-*S*-Adenosyl-methionine, 418
[4,4-$^{2}H_2$]-*S*-Adenosylmethionine, 453
Adjacent nodes, 470
ALADDIN, 484, 493, 500
Alanine, 390, 450
D-Alanine, 385, 387
L-Alanine, 431
(2*S*)-[2-$^{2}H_1$]-Alanine, 390
(2*S*)-[2-$^{3}H_1$]-Alanine, 390
L-Alanine aminotransferase, 391, 394, 395, 438
Alcohol dehydrogenase, 409
Aldolase, 396
Aldopyranoses, anomeric effect in, 196
Alkaline phosphatase, 397
(*E*)-Alkene selectivity, 34, 36, 50, 55, 76
(*E*)-Alkene selectivity, in Wittig reaction, 33
(*Z*)-Alkene selectivity, 55
Alkene, (*E*)-trisubstituted, formation, 104
  trisubstituted, synthesis, 38
Alkenes, (*E*)-selective synthesis, 55
  tetrasubstituted, synthesis, 106
  trisubstituted, 40
Alkenylphosphonium salts, 118
α-Alkoxyaldehydes, 81, 93
α-Alkoxyketones, 104, 142
α-Alkoxy ylides, 107, 142
Alkoxyphophines, 29
2-Alkoxytetrahydropyrans, 238
S-Alkylcysteine lyase, 415
α-Alkylthio ylides, 107, 142
L-Allothreonine, 411
Allylidene triphenylphosphorane, 17
Alpine boranes, 388, 393, 407
L-Aminoacid decarboxylase, 450
D-Aminoacid oxidase, 391, 395, 407, 438, 450
DL-(3*S*)-[3-$^{3}H_1$]-2-Aminobutanoic acid, 428
γ-Aminobutyric acid (GABA), 394, 434
(4*R*)-[4-$^{2}H_1$]-γ-Aminobutyric acid, 437
Aminocyclopropanecarboxylate (ACPC), 418, 451
[$^{2}H_1$]-2-Aminoethanol, 405
5-Aminolevulinate dehydratase, 392
5-Aminolevulinate synthase, 392
5-Aminolevulinate, 392
5-Aminolevulinic acid, 392
(3*R*)-[3-^{14}C]-Aminomalonate, 454
(3*S*)-[3-^{14}C]-Aminomalonate, 454
Aminomutase, 440
Aminotransferase, aspartate, 389, 390
Aminotransferase, GABA, 438

Aminotransferase, L-alanine, 391, 394, 395, 438
δ-Aminotransferase, ornithine, 438
Aminotransferase, L-ornithine, 440
Ammonia lyase, phenylalanine, 446
Ammonia lyase, tyrosine, 446
Angles, 477
  in MACCS-3D, 479
Anionic β-amido ylides, 107
Anionic sidechain substituents, 33
Anomeric effect and electron density, 314
Anomeric effect and structure, 299
Anomeric effect (AE), 208
Anomeric effect, 161, 163, 164, 167, 200, 270
  in aldopyranoses, 196
  anti-, 165
  benzylic, 165
  bidirectionality of, 174
  bond length and angles, 299
  calculated, 171
  competition, 179, 180, 182, 303
  σ-conjugation, 269
  dipole-dipole *vs* hyperconjugative interactions, 250
  due to negative hyperconjugation, 265
  electrostatic interactions, 241, 244
  electrostatic interpretation of, 227
  σ-electron delocalization, 270
  endo, 174, 176, 179, 180, 182, 183, 298, 305, 327
  enthalpic, 192
  exo, 174, 176, 178, 180, 186, 187, 189, 238, 327
  generalized, 163, 164, 214, 215, 219
  hyperconjugative explanation of the origin, 306
  hyperconjugative nature, 325
  hyperconjugative origin, 182, 199
  in ΔH^0_{AE} terms, 193
  interpretation of, 225
  interpretation, by Fourier expansion, 244
  inverse, 225
  kinetic, 257, 280
  magnitude of, 172, 178, 203, 206, 314, 324, 325
  magnitude of ΔE^0_{EA}, 166
  magnitude of ΔG^0_{AE}, 166
  magnitude of the generalized, 172
  nature of, 205
  nondirectional, 186
  one-directionality, 182
  origin of, 196, 225
  other general explanations of, 273
  partial, 175, 206
  reverse, 167, 180, 203, 209, 212, 214–220, 223, 259, 285, 288, 307, 324
  rotational barriers, 296
  saturation, 169
  solvent effects, 196, 197
  solvent-induced, 228
  source, 235
  spectroscopic implications of, 316
  syn-, 164, 167
  vinylogous, 165
  weak normal, 168
Anomeric interactions, 178, 183
  competition, 175, 219, 303
  competition of exo and endo, 197
  endo, 180, 182
  exo, 180, 181, 197, 298
  hyperconjugative origin, 183
  non-competitive hyperconjugative, 191
  one-directionality of, 183
Anomeric stabilization effect, quasi-homo, 264
Anthranilic acid, 450
Antiperiplanar lone pair hypothesis, 280
Apex-3D, 503
Apoaspartate transaminase, 387
Arcs, 470
Arginine, 439, 440
(3*R*)-[3-$^2H_1$]-Arginine, 440
(3*S*)-[3-$^2H_1$]-Arginine, 440
Arginine decarboxylase, 440
Arithmetic procedures, 471
Aromatic L-amino acid decarboxylase, 446
Arrow pushing, art of, 275
Art, of "arrow pushing", 275
Asparagine, 430, 431
Aspartase, 397, 407, 430, 432, 441
(2*S*)-[2-$^3H_1$]-Aspartate, 390
(2*S*,3*R*)-[3-$^2H_1$]-Aspartate, 407
(2*S*,3*S*)-[2,3-$^2H_2$]-Aspartate, 407
Aspartate aminotransferase, 386, 389, 390
Aspartate β-decarboxylase, 390, 431, 454
Aspartate decarboxylase, 395
Aspartate semialdehyde, 407
L-Aspartate semialdehyde, 409
Aspartates, 403, 415
Aspartic acid, 387, 407, 430–432, 441, 444, 448
(2*S*,3*R*)-[3-$^2H_1$]-Aspartic acid, 397, 430
(2*S*,3*S*)-[2,3-$^2H_2$]-Aspartic acid, 397, 430
(2*S*,3*S*)-[2,3-$^2H_2$, 3-$^3H_1$]-Aspartic acid, 431

(3*S*)-[3-$^3H_1$-Aspartic acid, 431
Asynchronous cycloaddition, 120
Asynchronous cycloreversion, 36
Atom-by-atom searching, 472, 473, 481
Atom mapping, 490, 495
Atom-mapping method, 489, 493
Automated generation of pharmacophore maps, 502
Automated structure generation, 503

Bader analysis, 353
Baker's yeast, 406
Barrier, to ring inversion, 227, 229, 296
Benzoic acid catalysis, effect on Wittig selectivity, 94
(1*S*)-[1-$^2H_1$]-Benzyl alcohol, 445
Benzylic anomeric effect, 165
Benzylidenetriphenylphosphorane, 61
Berberine bridge, 419
Betaine equilibration, 30
Betaine generation, 31
Betaine intermediate, 2
Betaine intermediates, probes for, 125
Betaine lithium halide adducts, 30, 42, 44, 53
Betaine lithium halide complexes, 32, 52
Betaine mechanism, 2
Betaine rationale, 2, 10
Betaine reversal, 6, 33
Betaine rotamers, 29
Betaine ylides, 38
Betaine-lithium halide aggregate, 38
Betaines, 29
  anti, 44
  salt-free, 121
  syn, 45, 127
Bibicyclobutanes, 358, 359, 370
Bicyclocubanes, 367
Bicyclopentane, 367
Bicyclotetrahedranes, 367
Bidirectionality, of the anomeric effect, 174
BioCAD Corporation, 503
Biophores, 503
Biosym Technologies, 503
1,4-Bishomo[6]prismane, 371
1,4-Bishomo[7]prismane, 371
Bit strings, 472, 497
Bitetrahedranes, 370
Blasticidin S, 440
Bohlmann bands, 320
Bond angle, double bond–no bond rationalization, 303
  NBO analysis, 305
  PMO rationalization, 304
Bond angle–NBO analysis, 305
Bond length, 302
Bond length–PMO rationalization, 302
Bond lengths and angles, anomeric effect, 299
Bond separation energies, 251, 266
Bond separation reaction, 266
Bond separation reactions, and "hardness", 207
  energy, 203
Bounds-smoothing technique, 498
β-Branched ylides, 50
Bron-Kerbosh clique-detection algorithm, 493
Brookhaven National Laboratory, 476
$Bu_3P^+CH{=}CH_2$, 118
$Bu_3P{=}CHC_3H_7$, 31
Butylidenetriphenylphosphorane, 22

Cadaverine, 437–439
(1*R*)-[1-$^2H_1$]-Cadaverine, 438
(1*R*)-[1-$^3H_1$]-Cadaverine, 438
(1*S*)-[1-$^2H_1$]-Cadaverine, 438
(1*S*)-[1-$^3H_1$]-Cadaverine, 438
Cage compounds, C_8H_8, saturated, 368
Cambridge Crystallographic Data Centre, 475
Cambridge Structural Database, 475, 477, 478, 480, 491, 492, 500, 502
Canonicalization, 471
Captodative substitution, 209
γ-Capture, 76
Carbon atoms, inverted, 355
Carbonyl-stabilized ylides, 2, 9, 31, 76
γ-Carboxyglutamate, 434
Carboxylation, 430, 434
CAS Registry substances, 479
CAS, 504
CAST-3D, 477, 480
Catalase, 407
Catalyst, 503
Catechol *O*-methyltransferase, 419
CAVEAT, 477, 479, 480, 483
  base atom, 480
  dihedral angles, 480
  substituent bonds, 480
  tip atom, 480
  vector pair, 480
CDP-4-Keto-6-deoxy-D-glucose reductase, 388, 389

2-Center pathways, in Wittig reaction, 120
4-Center pathways, in Wittig reaction, 120, 133
4-Center transition states, 134
Cephalosporin, 412, 414, 423, 424
Characterization of oxaphosphetanes, 19
ChemDBS-3D, 479, 482, 497
Chemical Abstracts Service, 477, 479
Chemical constraints, 500
Chemical Design Limited, 479
^{31}P Chemical shifts, 19
Chemical structure retrieval systems, 469
Chlorobenzaldehyde, in crossover experiments, 29
m-Chlorobenzaldehyde, 6, 9
m-Chloro-β-hydroxy-D-tyrosine, 449
2-Chloro-2-(triphenylphosphoranylidene)-acetophenone, 18
Chorismate, 443
[2-^{2}H]-Cinnamaldehyde, 406
[2-^{3}H]-Cinnamaldehyde, 406
(*E*)-[2-$^{2}H_{1}$]-Cinnamic acid, 406
Cis/trans equilibration, 55
Citrate, 428
Citrate synthase, 395, 428
Clavulanic acid, 439
Clique detection, 503
CLIX, 490, 491
Clostridium kluyveri, 445
Clustering, 474
CoMFA, *see* Comparative molecular field analysis
Common subgraph, 470
Comparative molecular field analysis (CoMFA), 488
Competition, between anomeric effects, 179, 180, 182
  between anomeric interactions, 175, 219
  of exo and endo anomeric interactions, 197
Computational methods, in Wittig reaction, 127
Computer graphics, 468
Computer-aided molecular design, 468
CONCORD, 476, 485, 494, 496, 497
Conformational adjustment, 286, 288, 289, 290, 294
Conformational analysis, 501
Conformational search, 499
Conformationally-flexible 3-D molecules, 469
Conformational-searching procedure, 499
Conformations, representative low energy, 497
π-Conjugation, 265
σ-Conjugation, 203, 265, 270
Connection table, 470
CORINA, 476
[6.4]Coronane, 373
[6.5]Coronane, 352, 364
Coronanes, 364
Coulomb attraction, 310
Coulomb repulsion, 232
^{13}C-^{31}P Coupling, 16
^{13}C-^{31}P Coupling constants, 22
Coupling constants, ^{13}C-^{31}P, 22
Crossover experiments, 29
  with ClC_6H_4CHO, 29
Crossover product, 6, 9
Crossover test, 9
Cryptoechinulin, 450
Crystal structures, of oxaphosphetanes, 19
  of ylides, 18
Crystallographic analysis, 490
Cubane, 351, 365, 366, 368
  ab initio calculations for, 368
Cubene, 370
Cuneane, 365, 368, 370
Curtin-Hammett principle, 283, 290
β-Cyanoalanine, 414
β-Cyanoalanine synthase, 414
Cycloaddition, 132
  2*s*+2*s*, 125
  asynchronous, in Wittig reaction, 120
  in Wittig reaction, 120
2*s*+2*s* Cycloaddition, 125
Cyclopentadienylidene, 18
Cyclopropylidene triphenylphosphorane, 18
Cycloreversion, asynchronous, 36
syn-Cycloreversion, 14
β-Cystathionase, 416
Cystathione, 405, 409, 410, 416
(4*R*)-[4-$^{2}H_{1}$]-Cystathione, 410, 416
(4*S*)-[4-$^{2}H_{1}$]-Cystathione, 410, 416
Cystathione synthase, 405
γ-Cystathione synthase, 409, 410
Cysteine, 405, 410, 412
L-Cysteine, 409, 410
Cysteine synthase, 414
Cystine, 412
(2*RS*,3*R*)-[3-$^{2}H_{1}$]-Cystine, 413
(2*RS*,3*S*)-[3-$^{2}H_{1}$]-Cystine, 413
[3-$^{3}H_{1}$]-Cystines, 413

(3*R*)-[3-$^3H_1$]-Cysteine, 414, 415
(3*S*)-[3-$^3H_1$]-Cysteine, 414, 415

Database construction, 475
Daylight Chemical Information Systems, 484
Decarboxylases, 382
Decarboxylation, 385, 432, 434, 437, 454
β-Decarboxylation, 383, 390
Decomposition, of oxasphosphetanes, 30, 34
Decomposition rate, of oxasphosphetanes, 36
Dehydrogenase, 430
ε-Dehydrogenase, L-lysine-, 438
Dehydrogenation, 405, 430, 450
3,4-Dehydroproline, 434
De novo design, 468, 469, 504
De novo structure generation, 500
Deoxyuridine monophosphate, 401
Destabilizing interactions, 143, 192, 204, 205, 207, 209, 211, 225, 232, 236, 252, 255, 259, 260, 262, 267, 275, 294, 295, 313, 335, 336
Deuterium incorporation, 42
Dhurin, 449
Diademane, 364, 370
  ab initio calculations for, 363
α,α′-Dialkoxyketone substrates, 104
α-Dialkylamino acid transaminase, 387
Diamine oxidase, 437, 443
3,5-Diaminohexanoic acid, 436
α,ε-Diaminopimelate decarboxylase, 437
(2*S*,6*R*)-*meso*-Diaminopimelic acid, 437
(2*S*,6*R*)-[2,6-$^2H_2$]-α,ε-Diaminopimelic acid, 437
Diamond lattice, 501
Diastereomers, equilibration, 23, 36
Dibenzophosphole derivatives, 34
Dibenzophopholes, 55
Dihydroxyphenylalanine (DOPA), 446
[$^3H_2$]-Diimide, 426
2,2-Dimethoxyoxane, 227
p-Dimethylaminopyridine (DMAP), 94
1,3,2-Dioxaphospholane derivatives, 11
2,3-Diphenylcyclopropanecarboxaldehyde, 50
Dipole moment, 196, 494
Dipole-dipole interactions, 200, 227, 247, 248, 250, 252
Dipole-dipole repulsion, 244
Dipole-dipole *vs* hyperconjugative interactions, and anomeric effect, 250
Diradical intermediates, 14
Diradicaloids, P–O bonded, 145
1,4-Diradicaloids, 121, 127
DISCO, 502
DIStance COmparisons, *see* DISCO
Distance distribution, 478
Distance geometry, 476, 498
Distance range, 498
  lower-bounds, 498
  upper-bounds, 498
Distance screens, 477
Distance-geometry embedding, 499
Distances, 477
cis-Disubstituted oxaphosphetanes, 34, 52
trans-Disubstituted oxaphosphetanes, 34
trans-Disubstituted oxaphosphetanes, thermodynamically more stable, 133
1,3-Dithianes, 190
DMAP, *see p*-Dimethylaminopyridine
DOCK, 486, 490, 492, 494, 495, 499–501
Docked ligands, 491
Dodecahedrane, 352
Dodecahedron, 492
p-d Donation, 277
Dopamine β-hydroxylase, 446
Double bond–no bond resonance, 228, 250, 303
Double bonds, trisubstituted, 95
Drug Data Report, 497

Echinulin, 426
Edeines, 448
Edges, 470, 475
Electron charge clouds, 487
σ-Electron delocalization, and anomeric effect, 270
Electron densities, 487
Electron density and anomeric effect, 314
Electron pair-lone pair repulsions, 331
Electron transfer (ET) pathway, in Wittig reaction, 121
Electron transfer, in Wittig reaction, 122
Electron-density grids, 492
Electronegativities, 181, 212, 254, 256, 267, 274, 325
Electronegativity, and anomeric effect, 273
  of OR substituents, 235
Electrostatic attraction, 214
Electrostatic effect, 310
Electrostatic interactions, 209, 267, 220, 225, 227, 250, 267, 500, 503

Electrostatic interactions (*Continued*)
in anomeric effect, 242, 244
Electrostatic interpretation, of the anomeric effect, 227
Embedding search, 499
Endo anomeric effect, 174, 176, 179, 180, 182, 183, 298, 305, 327
Endo anomeric interactions, 180–182
Energy component analysis, 241
Energy decomposition scheme, 212
classical theory, 233
Energy of bond separation reactions, 203
Enolizable ketones, 104
Enthalpic anomeric effect, 192
Equilibration, cis/trans, 55
diastereomer, 23, 36
oxaphosphetane, 36
Ergot alkaloids, 450
Ester stabilized ylide, 34
Esters, *Z*:*E* equilibration of α,β-unsaturated thiol, 94
$Et_3P{=}CHCH_3$, 31, 143
(1*R*)-[1-$^2H_1$]-Ethanol, 426
Ethanolamine ammonia lyase, 434
(2*S*,3*S*)-[3-$^2H_1$]-3-Ethylaspartate, 431
Ethylene, 454
cis-[2,3,-$^2H_2$]-Ethylene, 451
(*E*)-[1,2-$^2H_2$]-Ethylene, 416
trans-[2,3,-$^2H_2$]-Ethylene, 451
(*Z*)-[1,2-$^2H_2$]-Ethylene, 416
3-Ethylidene-L-azetidine-(*Z*)-carboxylate, 426
Ethylidenetriphenylphosphorane, 6, 9, 31
Ethyl *trans*-2-phenylglycidate, 6
2-Ethyltetrahydrofuran, 189
$EtPh_2P{=}CHCH_3$, 143
Euclidean distances, 490
Exchange repulsion, 232
Exo anomeric effect, 174, 176, 178–180, 183, 186, 187, 189, 191, 192, 194, 238, 327
Exo anomeric interactions, 180, 181, 197, 298
Exothermic oxaphosphetane formation, 12
[1-$^2H_1$]-Ethylamine, 416

FAMILY, 493
[4.4.4.4]Fenestrane, 361
[5.4.4.4]Fenestrane, 361
Field-based similarity searching, 488
Fine Chemicals Directory, 485
Flexible molecules, representation of, 496
searching of, 496
Flexible-query, 496
Flexible searches, 497
Flexible-searching systems, 496
Fluorenylidene ylides, 18
Fluorenylidenetriphenylphosphorane, 18
(2*R*)-[2-$^2H_1$]-2-Fluorocitric acid, 395
Formaldehyde, 40
Formylkynurenine formamidase, 450
2-Formyltetrahydropyran, 81
Four-center mechanisms, 13
Four-center process, 12
Four-center transition state, 11
Fourier component analysis, 252
of the potential function, 244
Fourier expansion, 227
Fragment, generation of, 480
Fragment screens, 472
Fragment substructures, 472
Fragment-based similarity measures, 486
Fragments, 474
for structure design, 500, 501
Franck's factor, 170
Franck's methodology, 167, 172, 298
Fully connected graph, 475
Fumarase, 399, 403, 415, 448

GABA, *see* γ-Aminobutyric acid
(4*R*)-[4-$^2H_1$]-GABA, 440
GABA-aminotransferase, 438
Gauche effect, 240, 270
Gaussian functions, 487
Geminal delocalization, 271, 272
Geminanes, 357
[1.1.1]Geminane, 358
General explanations, of the anomeric effect, 273
Generalized anomeric effect, 163, 164, 214, 215, 219
magnitude of, 172
GENIE, 484
Geometric screening, 484
Geometric searching, 481, 498, 499
Geometrical objects, specification, 479
Geometrically-feasible conformations, 498
[1-^{3}H]-D-Glucose, 396
Glucose-6-phosphate isomerase, 396
D-Glucose reductase, CDP-4-keto-6-deoxy-, 388, 389
(3*R*)-[3-$^3H_1$]-Glutamate, 432
(3*S*)-[3-$^3H_1$]-Glutamate, 432
(2*S*,3*R*)-[3-$^2H_1$, 3-$^3H_1$]-Glutamate, 432
(2*S*,3*S*)-[3-$^2H_1$, 3-$^3H_1$]-Glutamate, 432
(2*S*,4*R*)-[4-$^3H_1$, 4-$^2H_1$]-Glutamate, 433
Glutamate decarboxylase, 394

L-Glutamate decarboxylase, 387
Glutamate dehydrogenase, 432
Glutamate mutase, 433
Glutamate pyruvate transaminase, 450
(2*S*,3*S*)-[3-$^2H_1$]-Glutamates, 434
Glutamic acid, 432, 441
(2*S*,3*R*,4*R*)-[2,3,4-$^2H_3$]-Glutamic acid, 441
(3*S*)-[3-$^3H_1$]-Glutamic acid, 423
(3*R*)-[3-$^3H_1$, 3-$^2H_1$]-Glutamic acid, 433
(3*S*)-[3-$^3H_1$, 3-$^2H_1$]-Glutamic acid, 433
(2*R*,3*R*)-[3-$^2H_1$]-Glutamic acid, 433
(2*S*,3*R*)-[3-$^3H_1$]-Glutamic acid, 432
(2*S*,3*S*)-[3-$^3H_1$]-Glutamic acid, 432, 433
(2*S*,4*R*)-[4-$^3H_1$, 4-$^2H_1$]-Glutamic acid, 434
(2*S*,4*S*)-[4-^3H, 4-$^2H_1$]-Glutamate, 433
(2*S*,4*S*)-[4-$^3H_1$, 4-$^2H_1$]-Glutamic acid, 434
(2*S*,4*S*)-[4-$^3H_1$]-Glutamic acid, 432
Glutamic oxaloacetic transaminase, 431
Glyceraldehydephosphate isomerase, 396
Glycine, 387, 391, 450, 454
[2-$^2H_2$]-Glycine, 395
[2-$^3H_2$]-Glycine, 395
[2,2-$^2H_2$]-Glycine, 392, 394
[2,2-$^3H_2$]-Glycine, 392
(2*R*)-[2-$^2H_1$]-Glycine, 393–395
(2*S*)-[2-$^2H_1$]-Glycine, 391, 393, 394
(2*R*)-[2-$^3H_1$]-Glycine, 392, 394, 395
(2*S*)-[2-$^3H_1$]-Glycine, 387, 391, 392, 394, 395
(2*S*)-[2-$^2H_1$,2-$^3H_1$]-Glycine, 392, 395
(2*R*)-[2-$^2H_1$,2-$^3H_1$]-Glycine, 392, 395
[$^2H_1$]-Glycollate, 391
(2*R*)-[2-$^2H_1$]-Glycollate, 391
Glycollate oxidase, 391, 440
Glycollic acid, 387, 391, 440
(2*S*)-[2-$^3H_1$]-Glycollic acid, 391
Glycollic oxidase, 387
Glyoxylic acid, 395
Graph theory, use of, 470
Graph, 470
Graph, edges, 475
Graph, fully connected, 475
Graph, nodes, 475
Graphs, isomorphic, 470
Graphs, labelled, 470
GRID, 491, 502
Ground-state compression effect, 298
GROW, 500, 501

Haemanthamine, 449
2-Halotetrahydropyrans, 226
α-Halo-ylides, 142
Hammett σ,ρ correlations, 132
Hammond postulate, 290, 293
Hanson, nomenclature, 382
Hardness, and bond separation reactions, 207
Hashing-like scheme, 479
Heat of formation, 494
Helvetane, 373
Heptaprismane, 366
Hexafluoroacetone, 11
Hexaprismane, 352, 366, 371, 373
Hexokinase, 396
Histamine, 443
(1*S*)-[1-$^3H_1$]-Histamine, 443
Histamine *N*-methyltransferase, 442
Histidine, 441
(2*S*,3*R*)-[3-$^2H_1$]-Histidine, 443
(2*S*,3*S*)-[3-$^2H_1$]-Histidine, 443
Histidine ammonia lyase, 441
Histidine decarboxylase, 442, 443
Histidinol, 442
(1*S*,2*S*)-[1-$^2H_1$]-Histidinol, 442
Histidinol dehydrogenase, 442
Hog renal acylase, 399
HOMO, 494
Homo level, 16
trans-tris-σ-Homobenzenes, 354, 362
Homocysteine, 405, 416, 418, 420
L-Homocysteine, 420
Homomethionine, 420
(4*R*)-[4-$^3H_1$]-Homomethionine, 420
(4*S*)-[4-$^3H_1$]-Homomethionine, 420
(5*R*)-[5-$^2H_1$]-Homomethionine, 420
(5*S*)-[5-$^2H_1$]-Homomethionine, 420
Homoserine, 406, 417
(2*RS*,3*S*)-[3-$^2H_1$]-Homoserine, 406
(2*RS*,3*S*)-[3-$^3H_1$]-Homoserine, 406
(2*S*,3*R*)-[3-$^2H_1$]-Homoserine, 406
(2*S*,3*S*)-[3-$^2H_1$]-Homoserine, 406
(3*R*)-[3-$^3H_1$]-Homoserine, 411
(4*R*)-[4-$^2H_1$]-Homoserine, 409
(4*R*)-[4-$^3H_1$,4-$^2H_1$]-Homoserine, 406
(4*S*)-[4-$^2H_1$]-Homoserine, 409
(4*S*)-[4-$^3H_1$,4-$^2H_1$]-Homoserine, 406
(4*S*)-[4-$^3H_1$]-Homoserine, 409
Homoserine dehydratase, 410
Homoserine dehydrogenase, 409, 410
Homoserine kinase, 411
(2*R*,3*S*)-[2,3-$^2H_2$-Homoserine lactone, 453
(2*S*,3*R*)-[2,3-$^2H_2$]-Homoserine lactone, 408, 453
(2*RS*,3*R*,4*R*)-[3,4-$^2H_2$]-Homoserine lactone, 408

(2*RS*,3*S*,4*S*)-[3,4-$^{2}H_{2}$]-Homoserine lactone, 408
(2*S*,4*R*)-[4-$^{2}H_{1}$]-Homoserine lactone, 407
(2S,4S)-[4-$^{2}H_{1}$]-Homoserine lactone, 407
Horse liver alcohol dehydrogenase, 393, 423, 442, 445
Hydrocarbons, small saturated cage, 355
Hydrogen bonding, 196, 197, 212, 333, 334
Hydrogen bonds, in MM2, 238
in MM3, 240
Hydrogen-bonding geometry, 483
Hydrogen-bonding interations, 500, 503
Hydrogenolysis, of cubane, molecular mechanics study, 369
Hydrolysis, by synperiplanar pathway, 285
Hydrophobic interactions, 500, 503
β-Hydroxyamino acid, 382
α-Hydroxyketones, 104
Hydroxy-ylide, 30
β-Hydroxy-ylide, 42
γ-Hydroxyaldehydes, reactions, 93
β-Hydroxyisovalerate, 430
Hydroxylation, 446, 449, 450
4-Hydroxylation, 435
(2*S*)-Hydroxymethylpropionate, 429
(2*S*)-2-Hydroxymethylpropionic acid, 428
Hydroxymethyltransferase, serine, 387, 391, 392, 393, 401
β-Hydroxyphosphonium salts, 9, 23, 29, 30, 38, 42
3-Hydroxyproline, 434
4-Hydroxyproline, 434
(2*S*,4*R*)-4-Hydroxyproline, 434
3-Hydroxyvalines, 423
Hyperconjugation, negative, 164, 181, 203
Hyperconjugative anomeric interactions, non-competitive, 191
Hyperconjugative explanation, origin of the anomeric effect, 306
Hyperconjugative interactions, 197, 199, 212, 214
Hyperconjugative nature, of anomeric effect, 325
Hyperconjugative origin, of the anomeric effect, 182, 183, 199

(2*R*)-[3,3,3-$^{2}H_{3}$]-Isobutyric acid, 428
(2*S*)-[3,3,3-$^{2}H_{3}$]-Isobutyric acid, 428
(2*S*)-[3-^{13}C]-Isobutyric acid, 428
(2*S*,3*R*)-[3-$^{3}H_{1}$, 3-$^{2}H_{1}$]-Isobutyric acid, 429
(2*S*,3*S*)-[3-$^{3}H_{1}$, 3-$^{2}H_{1}$]-Isobutyric acid, 429
[3-$^{3}H_{1}$]-Isocitrate, 432
(4*S*)-[4-$^{3}H_{1}$]-Isocitrate, 432
(2*S*,3*S*,4*S*)-[3,4-$^{3}H_{2}$]-Isoleucine, 426
(2*S*,3*S*,4*S*)-[4-$^{2}H_{1}$]-Isoleucine, 426, 428
(4*R*)-[4-$^{3}H_{1}$]-Isoleucine, 430
(4*S*)-[4-$^{3}H_{1}$]-Isoleucine, 430
(2*RS*,3*S*,4*S*)-[4-$^{3}H_{1}$]-Isoleucine, 426
(2*S*,3*S*,4*S*)-[4-$^{3}H_{1}$]-Isoleucine, 428
(3*S*)-[4-$^{13}C_{1}$]-Isovalerate, 430
(2*R*)-[2-$^{3}H_{1}$]-Isovaleric acid, 430
(2*S*)-[2-$^{3}H_{1}$]-Isovaleric acid, 430
ICI Agrochemicals, 489
Icosahedron, 492
Independent betaine generation, 14
Indole, 449
Indolmycin, 397, 450
Initial screening procedure, 488
3*p*-3*d* Interaction, 277
Interactions, destabilizing, 192
1,2-Interactions, in Wittig reaction, 136
1,3-Interactions, in Wittig reaction, 136
Interatomic angles, 504
Interatomic distance information, 489
Interatomic distance matrices, 489, 498
Interatomic distances, 480, 482, 491, 504
Interconversion of pseudorotamers, 127
Inter-point distances, in MACCS-3D, 479
Interpretation, of the anomeric effect, 225
Inverse anomeric effect, 225
Inverted carbon atoms, 355
Ionic intermediates, 30
Ionic mechanisms, in Wittig reaction, 125
Isobutyric acid, 428
Isobutyryl CoA, 428
Isocitrate, 428
Isocitrate dehydrogenase, 432
Isocitrate lyase, 432
Isocitric acid, 432
Isodesmic equation, 203
Isodesmic reaction, 232, 274, 275, 204
Isoleucine, 421, 426, 427
Isomorphic graphs, 470
Isomorphism algorithm, 470
α-Isopropylmalate, 428
β-Isopropylmalate, 428
Isoserines, 399
Isovaleryl-CoA, 430
Israelane, 373

Jahn-Teller second-order effect, 273

α-Ketobutyrate, 410
(3*R*)-[3-$^{2}H_{1}$]-α-Ketobutyrate, 411
(3*S*)-[3-$^{2}H_{1}$]-α-Ketobutyrate, 410, 411

CDP-4-Keto-6-deoxy-D-glucose reductase, 388, 389
α-Ketoglutaric acid, 432
Ketones, α-alkoxy, 104, 142
  α,α′-dialkoxy substrates, 104
  α-hydroxy, 104
  enolizable, 104
  Wittig reactions, 95, 141
Kinetic anomeric effects, 257, 280
Kinetic control, 13, 23
  in Wittig reaction, 31, 92
  in Wittig synthesis, 38, 40
Kinetic isotope effects (KIE), 132
Kinetic oxaphosphetane ratios, 55
Kynurenines, 450

Labelled graphs, 470
β-Lactam, 405, 413
Lactate, 404
Lactate dehydrogenase, 401
Lederle Laboratories, 476, 478
Leucine, 421, 425, 427
(2*R*,4*S*)-[5-$^{13}C_1$]-Leucine, 425
(2*S*,4*S*)-[5-$^{13}C_1$]-Leucine, 425
(2*RS*,4*R*)-[5-$^{13}C_1$]-Leucine, 425
(2*RS*,4*S*)-[5-$^{13}C_1$]-Leucine, 425
(2*S*,4*R*)-[5,5,5-$^{2}H_3$-Leucine, 425
Lithium halide betaine adducts, 6
Lithium halide, effect on Wittig stereoselectivity, 50
  catalysis of Wittig reactions, 53
Lithium halides, 32
Lithium ion catalysis, of Wittig reactions, 70
Lithium ion concentration, 54
Lithium ion effects, in Wittig reaction, 143
LogP, 494
London attraction, 163
Lone electron pair-lone pair repulsions, 331
Lone electron pairs, oxygen, nonequivalence, 180
Lone pairs, nonequivalence of, 179
LUDI, 502, 503
LUMO, 494
(2*S*)-[2-$^{2}H_1$]-Lysine, 438
(2*S*)-[2-$^{3}H_1$]-Lysine, 438
(2*RS*,3*R*)-[3-$^{2}H_1$]-Lysine, 435
(2*RS*,3*S*)-[3-$^{2}H_1$]-Lysine, 435
(2*S*,6*S*)-[2,6-$^{3}H_2$]-Lysine, 437
(3*S*,5*S*)-[5-$^{3}H_1$]-β-Lysine, 437
(2*S*,6*S*)-[6-$^{3}H_1$]-Lysine, 438
(2*S*,6*R*)-[6-$^{3}H_1$]-Lysine, 437, 438
Lysine 2,3-aminomutase, 436
Lysine decarboxylase, 440
L-Lysine decarboxylase, 438, 439
β-Lysine mutase, 436
L-Lysine-6-aminotransferase, 438
L-Lysine-εε-dehydrogenase, 438
α-Lysines, 435
β-Lysines, 435
3*S*-β-Lysine, 436

MACCS-3D, 479, 484, 496
Macromolecular nuclear magnetic resonance spectroscopy, 504
Macromolecular receptor sites, 490
Magnitude ΔE_{AE} of the anomeric effect, 166
Magnitude of anomeric effect, 172, 178, 203, 206, 314, 324, 325
Magnitude of anomeric effect ΔG^0_{AE}, 166
Magnitude, of generalized anomeric effect, 172
Malic acid, 444, 448
(2*S*,3*R*)-[3-$^{2}H_1$]-Malic acid, 399
(2*S*,3*S*)-[2,3-$^{2}H_2$]-Malic acid, 399
Mandelate esters, 407
[1-^{3}H]-D-Mannose, 396
Mannose-6-phosphate isomerase, 396
Maximal common subgraph, 470
Maximal-common-subgraph-isomorphism, 471
Maximal common substructure (MCS), 473
Maximal common substructure (MCS) search, 474
MCS, *see* Maximal common substructure
MCS search, 474
Mean atom charge, 494
$MePh_2P{=}CHCO_2Et$, 92
$MePh_2P{=}CHPh$, 12
Metanephrine, 419
(*E*)-[$^{2}H_1$]-Methacrylic acid, 429
(*E*)-[3-$^{2}H_1$]-Methacrylic acid, 423
(*Z*)-[$^{2}H_1$]-Methacrylic acid, 429
(*Z*)-[3-$^{2}H_1$]-Methacrylic acid, 423
Methacrylyl-CoA, 429
Methionine, 416
(2*S*,4*R*)-[4-$^{2}H_1$]-Methionine, 417
(2*S*,4*S*)-[4-$^{2}H_1$]-Methionine, 417
Methionine decarboxylase, 418
Methionine synthase, 419
[3,4-$^{2}H_1$]-Methionines, 416
Methyl stabilization energy, 203, 208
β-Methylaspartase, 421, 430, 431
(2*S*,3*S*)-[3-$^{2}H_1$]-3-Methylaspartase, 431

[3-$^2H_1$]-β-Methylaspartate, 433
β-Methylaspartic acid, 433
2-Methylcyclohexanone, 104
2-Methylcyclopentanone, 104
5,10-Methylenetetrahydrofolate, 394, 401
(6*R*,11*R*)-[9,9,11-$^2H_3$]-5,10-Methylenetetrahydrofolate, 401
(6*R*,11*S*)-[9,9,11-$^2H_3$]-5,10-Methylenetetrahydrofolate, 401
5,10-Methylenetetrahydrofolate dehydrogenase, 401
Methylenetetrahydrofolate reductase, 402
5,10-Methylenetetrahydrofolic acid, 400, 402
3-Methyl-glutaconyl-CoA hydratase, 430
α-Methylglutamate, 387
Methylmalonate semialdehyde, 429
Methylmethionine, 420
(Methyl-*R*)-[methyl-$^3H_1$, $^2H_1$]-Methionine, 418
(Methyl-*S*)-[methyl-$^3H_1$, $^2H_1$]-Methionine, 418
(5*R*-Methyl-$^3H_1$, $^2H_1$)-5-methyltetrahydrofolate, 419
(5*S*-Methyl-$^3H_1$, $^2H_1$)-5-methyltetrahydrofolate, 419
5-Methyltetrahydrofolic acid, 402
Mevalonic acid, 426
MNDO, 127
Moderated ylides, 6, 9
MODSMI, 500
Molar refractivity, 494
3-D Molecules, conformationally-flexible, 469
Molecular biology, 504
Molecular electrostatic potentials, 487
Molecular graphics, 482
Molecular graphs, 501
Molecular mechanics, 355, 363–365, 476
  calculations, and anomeric effect, 233
  of cubane hydrogenolysis, 369
Molecular modelling, 468, 469, 482
Molecular shape, 487
Molecular similarity, molecular-modelling procedures, 486
  quantum-mechanical procedures, 486
Molecular templates, 501
Molecular topology, 470
Molecular volume, 487
Monoamine oxidase, 450
Monte-Carlo procedure, 488
MOVB theory, 274
Multiple isomorphisms, 481
Mycelianamide, 449

NADH, 442
NADPH, 427
Natural bond orbital (NBO) analysis, 265
NBO analysis, 305
Negative hyperconjugation, 164, 181, 203
NMR analysis, 490
  ^1H, 18
  ^{13}C, 16
  ^{31}P, 11, 22
NMR data, oxaphosphetanes, 22
Nocardicin, 405
Nocardicin A, 418
Nodes, 470, 475
  adjacent, 470
Nomenclature, of Hanson, 382
Non-competitive hyperconjugative anomeric interactions, 191
Nonequivalence, of lone electron pairs, 257
  of oxygen lone electron pairs, 180, 243, 257, 258, 305, 322
Nonstabilized ylide reactions, 2
Nonstabilized ylides, 9, 45, 55, 56
NP-Complete problem, 472
NP-Complete, 473
Nuclear magnetic resonance (NMR), 468

Octabisvalene, 365, 368, 370
Olefinations, acyl silane, 120
One-directionality, of anomeric effect, 182
  of anomeric interactions, 183
Origin of the anomeric effect, 196, 225
Ornithine, 439
(2*RS*,5*R*)-[5-$^3H^1$]-Ornithine, 439
(2*RS*,5*S*)-[5-$^3H_1$]-Ornithine, 439
L-Ornithine aminotransferase, 440
Ornithine δ-aminotransferase, 438
Ornithine decarboxylase, 440
L-Ornithine decarboxylase, 440
Overlap repulsion, 232, 262, 295, 336
(3*S*)-[3-$^3H_1$]-Oxaloacetic acid, 431
Oxaphosphetane, 2
Oxaphosphetane ratios, kinetic, 55
Oxaphosphetanes, 11
  characterization, 19
  cis-disubstituted, 34, 52
  crystal structures, 19
  decomposition, 10, 23, 29, 30, 34
  equilibration, 30, 36
  exothermic formation, 12

NMR data, 22
stable, 11, 19
trans-disubstituted, 34
Oxaphospholanes, 22
Oxido-ylides, 30, 40, 42, 44, 107
reactions, 38
β-Oxido-ylides, 38, 107
γ-Oxido-ylides, 33
Oxygen lone electron pairs, stabilizing interactions, 264
Oxygen lone pairs, nonequivalence, 243

[1.1.1.1]Paddlane, 361
[2.2.2.2]Paddlane, 352, 361
[n.2.2.2]Paddlanes, 361
Pantolactone, 394, 424
D-Pantolactone, 401
Pantotheine 4′-phosphate, 416
Partial anomeric effects, 175, 206
Path-lengths, 490
Penicillin, 412, 413, 423, 424
Pentacoordinated phosphorus, ^{31}P NMR, 19
Pentaprismane, 352, 366, 370, 373
Pentavalent phosphorus, 4, 22, 129
Pentylidenetriphenylphosphorane, 42
Peptide structural mimics, 480
Perlin effect, 318, 319
Perturbational molecular orbital (PMO) approach, 252
Pfizer Central Research, 478
$Ph_2MeP{=}CHPh$, 70
$Ph_3P^{(+)}$-CH_2Li, 17
$Ph_3P{=}C(CH_3)_2$8,132
$Ph_3P{=}C(CH_3)CO_2R''$, 93, 94, 141
$Ph_3P{=}CH_2$, 16–18
$Ph_3P{=}CHCH{=}CH_2$, 12, 118
$Ph_3P{=}CHCH_3$, 9, 12, 16, 38
$Ph_3P{=}CHCH_3$, *see also* Ethylidenetriphenylphosphorane
$Ph_3P{=}CHC_3H_7$, 50, 69
$Ph_3P{=}CHCH(OC_2H_5)$2, 118
$Ph_3P{=}CHCH_2N(CH_3)_2$, 118
$Ph_3P{=}CHCHO$, 94, 141
$Ph_3P{=}CHCN$, 92
$Ph_3P{=}CHC(O)CH_3$, 93, 94
$Ph_3P{=}CHC(O)R$, 14
$Ph_3P{=}CHCO_2CH_2CH_3$, 10, 14, 81, 92, 138
$Ph_3P{=}CHI$, 142
$Ph_3P{=}CHPh$, 12, 69, 132
$Ph_3P{=}CMe_2$, 16, 106
Pharmacophore hypothesis, 468
Pharmacophore mapping, 484, 503, 505
Pharmacophore maps, 470
automated generation of, 502
Pharmacophore modeling, 502
Pharmacophores, 477, 483, 481
Pharmacophoric pattern, 477, 478, 484, 496, 498
Pharmacophoric pattern search, 497
Phenol lyase, tyrosine, 448
Phenylalanine, 443
(2*R*,3*R*)-[2,3-$^2H_2$]-Phenylalanine, 445
(2*RS*,3*R*)-[3-$^2H_1$]-Phenylalanine, 445
(2*RS*,3*S*)-[3-$^2H_1$]-Phenylalanine, 445
(3*R*)-[3-$^2H_1$]-Phenylalanine, 445
(3*S*)-[3-$^2H_1$]-Phenylalanine, 445
Phenylalanine ammonia lyase, 445
Phenylalanine hydroxylase, 449
(1*S*)-[1-$^2H_1$]-2-Phenylethanol, 397
Phenylethylamine, 446
[1,1-$^2H_2$]-2-Phenylethylamine, 397
(2*S*,3*R*)-[2,3-$^2H_2$]-3-Phenylpropionic acid, 445
Phenylpyruvate tautomerase, 446
[$^2H_1$]-Phosphaditylethanolamine, 405
Phosphaditylserine, 405
Phosphaditylserine decarboxylase, 405
Phosphofructose kinase, 396
(2*R*,3*R*)-3-Phosphoglyceric acid, 396, 397
(2*R*,3*S*)-3-Phosphoglyceric acid, 396, 397
(2*R*,3*R*)-[3-$^3H_1$]-3-Phosphoglyceric acid, 396
(2*R*,3*S*)-[3-$^3H_1$]-3-Phosphoglyceric acid, 396
Phosphole reagents, 104
Phospholes, 92
Phosphonium salt pKas, 15
Phosphopantothenoylcysteine, 415
Phosphorus ligand effects, 54
Phosphorus, pentacoordinated, ^{31}P NMR, 19
Phosphorus ylides, 4
characteristics, 14
3-Phosphoserines, 396
Photoelectron ionization potentials of selected ylides, 15
Photoelectron spectra (PES), 15
(5*R*)-[5-$^2H_1$]-*N*-Phthaloyl-5-aminovaleric acid, 437
Δ^1-Piperideine-6-carboxylate, 438
pKa values, of phosphonium salts, 14, 15
Planar cyclohexane ring, 354, 362
"Planar methane" problem, 355, 360

PLP, *see* Pyridoxal phosphate
PMP, 387, 390
P-O bonded diradicaloids, 145
P-O bonded zwitterions, 121
Porphobilinogen, 392
Potential function, Fourier component analysis, 244
Potential ligands, 501
PPC decarboxylase, 416
Prephenic acid, 443
Principal components analysis, 488
[7]Prismane, 372, 373
[8]Prismane, 372
[12]Prismane, 373
[n]Prismanes, 366, 372
Proline, 434
(2*S*,3*R*)-[3-$^3H_1$]-Proline, 435
(2*S*,3*S*,4*R*)-[3,4-$^3H_2$]-Proline, 435
(2*S*,4*R*)-[4-$^2H_1$]-Proline, 434
(2*S*,4*S*)-[4-$^2H_1$]-Proline, 434
(2*S*,4*R*)-[4-$^3H_1$]-Proline, 434
(2*S*,4*S*)-[4-$^3H_1$]-Proline, 434
(5*R*)-[5-$^2H_1$]-Proline, 435
(5*S*)-[5-$^2H_1$]-Proline, 435
Propargylic ylides, 118
Propellane, 240
[1.1.1]Propellane, 352, 355, 356
[2.2.2]Propellane, 355
[2.2.2]Propellane, bond lengths in, 356
Propellanes, small-ring, 355
Propella[3_4]prismane, 369
(2*R*)-[2-$^2H_1$]-Propionate, 411
(2*S*)-[2-$^2H_1$]-Propionate, 409
Protein crystallography, 468, 504
Protein Data Bank, 476
Protic solvents, 12
Proton affinities, 198, 283
ab initio studies, 175
Prunacin, 449
Pseudorotamers, 42
Pseudorotamers, interconversion of, 127
Pseudorotation, 42, 127, 145
Putrescine, 440
(1*R*)-[1-$^2H_1$]-Putrescine, 440
(1*S*)-[1-$^2H_1$]-Putrescine, 440
Pyramidal carbon atom, 355, 359
Pyramidal inversion, 18
Pyramidane, 360
Pyridoxal phosphate (PLP), 382, 387, 390
Pyridoxal, 382
Pyridoxamine, 382, 386, 387, 389, 390
[4′,4′-$^2H_2$]-Pyridoxamine, 386
(4′*R*)-[4′-$^2H_1$]-Pyridoxamine, 388
(4′*S*)-[4′-$^2H_1$]-Pyridoxamine, 386
(4′*R*)-[4′-$^3H_1$]-Pyridoxamine, 388
(4′*S*)-[4′-$^3H_1$]-Pyridoxamine, 388
Pyridoxamine phosphate, 382, 388, 390
(4′*R*)-[4-$^3H_1$]-Pyridoxamine phosphate, 387
(4′*S*)-[4-$^3H_1$]-Pyridoxamine phosphate, 387
Pyridoxamine-5-phosphate oxidase, 390
Pyridoxamine-pyruvate transaminase, 387, 390
Pyrocatechol, 446
Pyruvate, 404
[3-$^2H_1$,3-$^3H_1$]-Pyruvate, 448
[3-$^2H_1$,3-$^3H_1$]-Pyruvates, 415

Quantitative activity prediction, 503
Quantum chemical approaches, to conformation, 240
Quantum mechanics, 476
Quasi-homo-anomeric stabilization effect, 264
Quinaldic acid, 419

Rabbit ear effect, 189, 205, 228, 232, 295, 336
Radical anion clock experiments, 133
Radical anion clocks, 125
Radical anion intermediates, in Wittig reaction, 123
Radical cation, 125
Radical ion pair collapse, rate-determining, 132
Radical ion pairs, 121
Rate-determining radical ion pair collapse, 132
Rationalization by PMO theory, 302
Reaction coordinate diagrams, 12
Reaction profile diagram, 2
Reaction-database systems, 474
Reactivity-selectivity principle (RSP), 133
Refinement procedure, 482
Registration, 471
Representation and searching of flexible molecules, 496
Representative low-energy conformations, 497
Repulsive interaction, of di, 235, 295, 303, 327, 330
Resonance, double bond-no bond, 228, 250
Reticuline, 419
Retrieval systems, for chemical structures, 469
Retro-Wittig cleavage, 9, 10, 33
Retro-Wittig process, 29
Retro-Wittig reaction, 34

Retroaldol cleavage, 382
Retroaldol reactions, 385
Reverse anomeric effect, 167, 180, 203, 209, 212, 214–220, 223, 259, 285, 288, 307, 324
Rigid 3-D searching, 498
Rigid searches, 497
Rigid-searching systems, 496
Ring inversion, barrier, 227
Rotamers, ylide, 141
Rotational barriers, 242
  and anomeric effect, 296
Rule-based conformational-expansion, 497

Saccharomyces cerevisiae, 393
Salt-free betaine intermediate, 121
Saturated cage compounds, C_8H_8, 368
Saturation, of anomeric effect, 169
Scoulerine, 419
Screen searching, 472, 477
Screen set, 472
Screen-set selection, 479
Screening search, 499
Screening, 477, 478, 498
Screenout, 472
Screens, 497
Search, similarity, 469, 471
Search, substructure, 469, 471
Secohexaprismane, 371
Securinine, 449
(*E*)-Selective alkene synthesis, 55
(*E*)-Selective reactions, 76
Z-Selective olefinations, 6
(*E*)-Selectivity, in Wittig reactions, 92
Serine, 387, 390, 395, 449
D-Serine, 399
L-Serine, 385
(2*R*,3*R*)-[2,3-$^2H_2$]-Serine, 400
(2*S*,3*R*)-[2,3-$^2H_2$]-Serine, 399
(2*S*,3*S*)-[2,3-$^2H_2$]-Serine, 398
(2*S*)-[2,3,3-$^2H_3$]-Serine, 399
(3*R*)-[3-$^2H_1$]-Serine, 448
(3*S*)-[3-$^2H_1$]-Serine, 448
(2*R*,3*S*)-[3-$^2H_1$]-Serine, 400
(2*S*,3*S*)-[3-$^2H_1$]-Serine, 399, 401
(2*RS*,3*S*)-[3-$^2H_1$]-Serine, 397
(3*R*)-[3-$^2H_1$,3-$^3H_1$]-Serine, 402
(3*S*)-[3-$^2H_1$,3-$^3H_1$]-Serine, 402
(2*S*,3*R*)-[3-$^2H_1$,3-$^3H_1$]-Serine, 397, 401, 403
(2*S*,3*S*)-[3-$^2H_1$,3-$^3H_1$]-Serine, 397, 401, 403
(3*R*)-[3-$^3H_1$]-Serine, 405
(3*S*)-[3-$^3H_1$]-Serine, 405
(2*S*,3*R*)-[3-$^3H_1$]-Serine, 397, 405
(2*S*,3*S*)-[3-$^3H_1$]-Serine, 397, 405
(2*S*,3*R*)-[3-$^2H_1$]-Serines, 398, 401
Serine acetate, 414
D-Serine dehydratase, 411
Serine hydroxymethyltransferase, 385, 387, 391, 392, 393, 401, 402, 454
Set-reduction algorithm, 481
Shikimic acid pathway, 443
Showdomycin, 434
Similarity searching, 469, 471, 473
  effectiveness of, 486
  efficiency of, 486
  field-based, 488
3-D Similarity searching, 486
Sinefungin, 440
Sinigrin, 420
Small saturated cage hydrocarbons, 355
Small-ring propellanes, 355
SMARTS, 484
SMILES, 484
Sodium diphenylphosphide, 9
SOLON, 478, 479, 483
Solvent compression effect, 199
Solvent dependence of *Z*:*E* ratios, 81
Solvent effects, 227
Solvent effects, in Wittig reactions, 11, 122, 140
Solvent polarity, 238
Solvent studies, 220, 324
Solvent-induced anomeric effect, 228
Sombunigrin, 449
Source, of the anomeric effect, 235
Spacer skeletons, 501
Spatial structures, unusual, 351
Spectral-database systems, 474
Spectroscopic implications of the anomeric effect, 316
SPERM, 488, 490, 492, 494, 495
Spermidine, 418
Spheres, representing ligands, 491
Sporidesmin, 450
Stability, of transition states, 223
Stabilization energy, methyl, 203
Stabilization energy, thermodynamic, 208
Stabilized ylides, 138
Stabilizing interactions, of oxygen lone electron pairs, 264
Stable oxaphosphetanes, 11, 19
Standard Drug File, 497
Stereochemical equilibration, 6
Stereochemical equilibration, of Wittig intermediates, 22
Stereoelectronic control, 280, 285, 289, 293
Stereoelectronic control, theory, 280

Stereoelectronic effect, 280
Stereospecific oxaphosphetane decomposition, 23
Steric constraints, 500
Steric similarities, 487
Strained hydrocarbons, synthesis, 351
Strained hydrocarbons, theoretical and experimental results, 354
Streptomyces amakusaensis, 394
Streptothricin, 436
Structure correlation method, 187, 305
Structure generation, 469
Structure search, 471
Structure searching, 471
Subgraph isomorphism algorithms, 481
Subgraph, 470
Subgraph, common, 470
Subgraph, maximal common, 470
Subgraph-isomorphism, 471, 472, 477, 481
Substructure searching, 469, 471, 472, 475, 496
Substructure searching, 3-D, 494
Succinate, 441
(2*R*)-[2-$^2H_1$]-Succinate, 433
(2*S*)-[2-$^3H_1$]-Succinate, 436
Succinate dehydrogenase, 441
Succinic acid, 433, 436
[$^2H_1$]-Succinic acid, 444
O-Succinyl-L-homoserine, 409
O-Succinylhomoserine, 410
(4*R*)-[4-$^2H_1$]-*O*-Succinylhomoserine, 410
(4*S*)-[4-$^2H_1$]-*O*-Succinylhomoserine, 410
Superjacent orbital control, 259
Superpositioning by PERMutations, *see* SPERM
Symbolic logic, 476
Syn betaines, 45
Synperiplanar lone pair pathway, 285
Synperiplanar pathway, 293

Taxiphillin, 449
Template-joining, 501
Tetracyclo[8.2.0^{2,5}.0^{6,9}]dodecane, 363
Tetrahedrane, 366
Tetrahydrofolate, 5,10-methylene, 394
Tetrahydrofolic acid, 400
  5,10-methylene, 402
  5-methyl, 402
Tetrahydrophospholes, 55
Tetrasubstituted alkene synthesis, 106
Theoretical considerations, in Wittig reaction, 127
Theory, of stereoelectronic control, 280
Thermodynamic stabilization energy (SE), 208, 209
Thiostrepton, 419
Threonine, 406
D-Threonine, 411
L-Threonine, 385, 410
[3-$^2H_1$]-L-Threonine, 428
Threonine dehydratase, 411, 428
Threonine synthase, 411
Through bond interactions, 276
Through space interactions, 191, 276
Thymidine, 401
Thymidylate synthase, 402
Tiglic acid, 430
Topological similarity measures, 487
Torsions, 504
Transaminase, α-dialkylamino acid, 387
  apoaspartate, 387
  pyridoxamine-pyruvate, 387, 390
Transaminases, 386
Transamination, 385, 387, 389, 390, 428, 432
Transient intermediates, 12
Transition state desolvation, 138
Transition states, stability of, 223
Triangle inequality, 498
syn-Tricyclo[4.2.0.0^{2,5}]octa-3,7-diene, 369
cis-Tricyclooctane, 364
trans-Tricyclooctane, 364
Trigonal bipyramid, 19
Trigonal bipyramidal phosphorus, 22
Triosephosphate isomerase, 396
Triphenylphosphine, 6
Trippett-Jones experiment, 12
Triprismane, 351, 366, 367
Triprismane, QC for, 367
Tripropellacyclohexane, 373
(*E*)-Trisubstituted alkene formation, 104
Trisubstituted alkenes, synthesis, 38, 40, 41
Trisubstituted double bonds, 95
Tropic acid, 449
Truncated tetradehrane, 371, 373
Tryptamine, 450
Tryptophan, 397, 402, 403, 443, 449
L-Tryptophan, 387, 388
(3*R*)-[3-$^3H_1$]-Tryptophan, 450
(3*S*)-[3-$^3H_1$]-Tryptophan, 450
Tryptophan dioxygenase, 450
Tryptophan synthase, 387, 390, 402–404, 414, 449

Tryptophanase, 390, 403, 404
Tuberin, 394
ω-Transamination, 440
Two-step mechanism, Wittig reaction, 12
Tyramine, 446
Tyrosine, 390, 405, 443
β-Tyrosine, 448
(2*S*,3*R*)-[3-$^{2}H_{1}$]-Tyrosine, 448
(2*SR*,3*SR*)-[2,3-$^{2}H_{2}$]-Tyrosine, 448
(2*S*,3*R*)-[3-$^{2}H_{1}$]-*ortho*-Tyrosine, 445
Tyrosine ammonia lyase, 446
D-Tyrosine, *meta*-chloro-β-hydroxy-, 449
Tyrosine decarboxylase, 390, 446, 450
Tyrosine phenol lyase, 404, 446, 448

Ugi turnstile mechanism, 127
Ullmann algorithm, 481
  refinement procedure, 482
α,β-Unsaturated thiol esters, Z:E equilibration, 94
Unusual spatial structure, 351
Urocanate, 441
Urocanic acid, 441

Valence-angle screens, 478
Valine, 411, 421, 427
[4-^{13}C]-Valine, 423
(2*RS*,3*S*)-[4-$^{13}C_{1}$]-Valine, 425
(2*S*,3*S*)-[4-^{13}C]-Valine, 421
(3*R*,4*R*)-[4-$^{2}H_{1}$,4-$^{3}H_{1}$]-Valine, 423
(3*R*,4*S*)-[4-$^{2}H_{1}$,4-$^{3}H_{1}$]-Valine, 423
(2*RS*,3*S*)-[4,4,4-$^{2}H_{3}$]-Valine, 423
(2*S*,3*R*)-[4,4,4-$^{2}H_{3}$]-Valine, 421
(2*S*,3*S*)-[4,4,4-$^{2}H_{3}$]-Valine, 421
van der Waals' radii, 498
van der Waals' surface area, 494
Vancomycin, 449
Vertices, 470
Vicinal delocalization, 271
Vinylglycine, 410
(*E*)-[3,4-$^{2}H_{2}$]-Vinylglycine, 410
(*E*)-[3,4-$^{2}H_{4}$]-Vinylglycine, 410
(*Z*)-[4-$^{2}H_{1}$]-Vinylglycine, 410
Vinylogous anomeric effect, 165
Virginiamycin *M*, 435
Virginiamycin M_{1}, 405
Vitamin B_{6}, *see* Pyridoxal phosphate, 382
Vitamin K, 434

Wintersteiner's acid, 449
Wittig intermediates, stereochemical equilibration, 22
Wittig reaction, computational methods in, 127
  effect of Lewis acids, 50
  electron transfer in, 121
  of ketones, 95
  kinetic control, 31
  Lewis acid catalysis, 143
  Li^{+} catalysis, 52
  mechanistic considerations, 120
  (*E*)-selectivity, 92
  transition state models, 145
  transition states, 132
Wittig stereoselectivity, effect of Lewis acids, 50

X-Ray crystal structure, 496
X-ray crystallography, 475
X-Ray data, for oxaphosphetanes, 19

Yeast alcohol dehydrogenase, 401, 406
Ylide, hydroxy, 30
  oxido, 30
Ylide bond lengths, 18
Ylide reactions, nonstabilized, 2
  with ketones, 95
Ylide rotamers, 141
Ylides, α-alkoxy, 107
  α-alkylthio, 107
  alkoxide, 107
  allylic, 61
  anionic β-amido, 107
  anionic carboxylate, 107
  benzylic, 61
  betaine, 38
  β-branched, 50
  carbonyl-stabilized, 2, 9, 31, 76
  crystal structures, 18
  ester stabilized, 34
  fluorenylidene, 18
  β-hydroxy, 42
  moderated, 6, 9
  nonstabilized, 9, 11, 45
  oxido, 38, 40, 42, 44, 107
  β-oxido, 107
  γ-oxido, 33
  propargylic, 118, 120
  stabilized, 138
Z:E Equilibration of α,β-unsaturated thiol esters, 94
Zwitterion, P–O bonded, 121
Zwitterionic intermediates, 14
Zwitterions, 42, 145